SIMULTANEOUS DESULPHURIZATION AND DENITRIFICATION OF DIESEL OIL USING IONIC LIQUIDS: QUANTUM CHEMICAL PREDICTIONS AND EXPERIMENTS

A Thesis Submitted

in Partial Fulfillment of the Requirements

for the Degree of

Doctor of Philosophy

by

ANANTHARAJ R

to the

DEPARTMENT OF CHEMICAL ENGINEERING

INDIAN INSTITUTE OF TECHNOLOGY GUWAHATI

May, 2011

C E R T I F I C A T E

It is certified that the work contained in this thesis entitled **"Simultaneous Desulphurization and Denitrification of Diesel oil using Ionic Liquids: Quantum Chemical Predictions and Experiments"**, by Anantharaj R, has been carried out under my supervision and that this work has not been submitted elsewhere for a degree.

Dr. Tamal Banerjee
Assistant Professor
Department of Chemical Engineering
Indian Institute of Technology Guwahati

May, 2011

Dedicated To

My

Parents and Teachers

Acknowledgement

I express my sincere thanks to my research supervisor **Dr.Tamal Banerjee** for his valuable guidance throughout my research work. I am indeed to him for giving me an opportunity to work in a very interesting area of research. His continuous encouragement, patience towards research and support gave me a lot of spirit in regard to research.
I would like to thank him for spending his precious time for discussion by which I have gained immense skills of knowledge in terms of research. I am fortunate to have him as a guide whose immense thinking and knowledge made my work fruitful without him this dissertation would not have been possible. I would like to express my deepest appreciation for his persistent guidance throughout my research work.

I would like to thank my doctoral committee members, **Dr.G. Pugazhenthi**, **Dr. Mahuya De**, Department of Chemical Engineering, and **Dr. Sandip Paul,** Department of Chemistry, for their valuable suggestion and effort which made my thesis successful.

I am also highly grateful to **Dr.Ramgopal Uppalari, Dr.P.Balasubramanian,** and **Dr. Kaustubha Mohanty** for their valuable suggestions during my course work**.** I should thank **Dr.Prabirkumar Saha**, Head, Department of Chemical Engineering, for providing me the necessary support throughout my work.

In addition, I thank **Dr.Pallab Ghoah** for his help in accessing Tensiometer for surface tension measurement.I extent my thanks to his student **Chenchaiah Sudulagunta** for his assistance in surface tension measurement.

I am thankful to **Central Instrument Facility**, for providing me the necessary support for sample analysis using Nuclear Magnetic Resonance **(NMR)** Spectrometer, Varian 400MHz FTNMR**.**

I must thank **Department of Science and Technology (DST),** India, for providing travel support to present the paper in 2nd Asia Pasicific Conference on Ionic Liquids and Green Processes, **Dalian, China.**

Helps done by my fellow research scholars, **Mr.S.Sakthivel and Mr. Prasenjit Saha,** Department of Chemistry for sharing them experience and their assistance in analyses have to be greatly acknowledged.

I am thankful to **Mr.Jayanta Kumar Mout**, Junior Technical Superintendent, Departement of Chemical Engineering, for his timely help both technical and personal, without any hesitation have been invaluable. I also thank all the non-teaching staffs for their contributions.

My sincere thanks to **Mr.Ananth Praveen Kumar**, research scholar of our research group, for his co-operative assistance in learning the basics of computational studies and provided me with a constant source of encouragement throughout my research carrier.

I gratefully remember the help of **Mr. N.R.Verma**, **Mr.S.Potdar**, and **S.P.Sing** for their support in computational and experimentation. I am also thankful to our present research group members **Mr.Saikiran Cheruku** and **Mr.Udaya Kiran**.

I also want to thank my labmates **Mr.Somen Jana**, **Mr.Venkadaswamy, Mr.Murugavelh, Mr.Manokar, Mr. Srinivas**, **Mr.Samanta**, **Mr.Sankar Chakma**, and **Mr.Hemant Kumar.**

I am thankful to my fellow research scholar **Mr.Anto Pradeep**, **Mr.Ashok Kumar**, **Mr. Shyam Anand, Mr.Ananthkumar, Mr.Eshwaran, Mr.Chokalingam, Mr.T.Kannan, Mr.Someswaran** and **Mr.Sathishkumar**, for their help, useful discussion and exchange their feelings.

I cannot forget to thank my friends **Dr.Gobi,Dr.Senthil,Dr.Perumal, Dr.Sathish, Dr.Santhosh, Mr.Monash, Mr.Subramaniyan, Mr.SanthoshKrishna, Mr.Unes, Mr.Thamaraiselvan, Mr.Arun, Mr.Sureshpandian, Ms.Kohila, Ms.Anjali dasari, Mr.Reddy, Mr.Anoop, Mr.Hari, Mr.Harsha**, **Mr.Laxmanan** and **Mr. Ravi**, for the lovely support in making my stay at IIT Guwahati memorable.

My whole hearted gratitude goes to my **father, mother, sister** and **brother** as well as **Dr.Tamal Banerjee** and **Dr.Pugazhenthi** family whose blessings and boundless patience have kept my morale high during the course of my study.

Above all I am thankful to God for giving me a wonderful and healthy life.

Date: May 2011 **Anantharaj R**

CONTENTS

List of Figures

Chapter 1

Introduction

Chapter 2

Experimental Techniques

Chapter 3

(Nd, K)-Mn-O Series

Chapter 4

(Nd, Na)-Mn-O Series

Chapter 5

Charge Order Suppression in $Nd_{0.8}Na_{0.2}MnO_3$

Chapter 6

Conclusions

1.1 Introduction

Diesel oil is one of the most important energy sources which is directly derived from crude oil by atmospheric distillation unit. The diesel oil is a complex mixture of several saturated, unsaturated and aromatic hydrocarbons. However the presence of pollutant contributors such as refractory sulphur and aromatic nitrogen compounds adds to environmental pollution. These compounds are difficult to remove because of its higher molecular weight and higher boiling point. Additionally these compounds are known to inhibit hydrodesulphurization process [Uday et al., 2003].

The sulphur species has been classified into non acidic and acidic sulphur compounds such as thioles (RSR), sulphides (RSR'), disulfides (RSSR'), cyclicsulfides (CS), thiophene (TS), benzothiophene (BTS) and dibenzothiophene (DBTS).These compounds are major pollutant contributor to the environment in the form of SO_X during combustion process. SO_X is the major contributor for acid rain and global warming [Shiraishi et al., 2001]. The commonly occurring sulphur compounds have a pungent odor and are highly flammable in nature [Wang et al., 2008]. The aromatic sulphur compounds tend to decompose on heating, producing toxic and irritating fumes. The sulphur content specifications in diesel oil are becoming increasingly stringent. The sulphur species, being the major pollutant to the environment are known to hinder hydrodesulphurization (HDS) by poisoning the catalyst at high operating temperature and pressure [Jeon et al., 2009]. Hence, a good knowledge of the inhibitory effect of the sulphur containing species in HDS process is essential [Song et al., 2006].The aromatic sulphur species are difficult to remove from diesel oil because of its lesser reactivity with the active catalyst [Zhang et al., 2001] and higher steric hindrance towards active sites of catalyst [Jeon et al., 2009].Till date the available catalyst is effective to remove thiols and sulphide through HDS process [Trakarnpruk et al., 2008]. There are several well established catalysts with HDS process [Li et al., 2003] which are employed for the removal of aromatic sulphur species with working temperature and pressure as high as

380^0C and 12 MPa respectively. Even processes conducted at high temperatures (>300^0C) [Li et al.,2003], high hydrogen pressures (20 to 100 atm of H_2), higher active catalyst, longer residence time and heavier hydrogen consumption has failed to remove the aromatic sulphur compounds.

The aromatic nitrogen compounds are classified into two different types such as non basic and basic nitrogen compounds. Non basic nitrogen compounds are: pyrrole (PYR), indole (IND), indoline (INDI), carbazole (CAR), benzocarbazole (BCAR), whereas the basic compounds are pyridine (PY), quinoline (QU) and benzoquinoline (BQU). NO_X is converted into nitrogen dioxide and is an important contributor for the troposphere ozone formation [Ferdous et al., 2003]. Nitrogen compounds having non-heteroaromatic or heteroaromatic structure with multiple ring adversely affect the stability of diesel oil during its storage [Yongtan et al., 2008].This reduces the efficiency of hydrodenitrification (HDN) process due to the poisoning of the catalyst. Thus it is important to reduce the nitrogen and sulfur level of the diesel oil with the ultimate goal of zero emissions. The maximum sulfur content is now limited to 10 – 15 ppm sulphur as compared to 350 -500 ppm presently [Yang et al., 2005], whereas the nitrogen content is also limited to < 0.1 ppm N [Jayaraman et al.,2006]. Uday et.al [2003] reported that a high sulfur removal will require knowledge of the influence of free nitrogen in diesel oil towards HDS process. The nitrogen based compounds has low reactivity and high refractoriness as compared to acidic and non acidic sulfur compounds in diesel oil. The nitrogen molecules also influence the formation of coke at specified and/or moderate operating conditions.

The elimination of nitrogen compounds from diesel oil and other liquid fuels by catalytic/non catalytic, ion exchange, alkylation, metalcomplexation and extraction process were reported earlier [Jayaraman et al.,2006] .Solvent extraction is a well known operation[Zhang et al.,2004] for removing nitrogen compounds both at ambient condition as well as moderate condition. However the operation fails to remove the aromatic nitrogen

compounds from diesel oil when the total nitrogen content is greater than 70 ppm [Sano et al., 2004]. Additionally the aromatic nitrogen compounds posses the most difficult challenge to HDS process [Jayaraman et al.,2006] because of its role in catalytic deactivation. In a recent work, Jiang et al.[1998] reported the solvent extraction for nitrogen compounds using carboxylic acid through π-complexation. A dinitrification study using methanol [Bogwon et al., 2002] presented the Liquid Liquid Equilibria (LLE) of aromatic nitrogen species with hydrocarbons.

1.2 Ionic Liquids

Before considering a new solvent for incorporation into an industrial application, a fundamental understanding must be established for the chemical and physical properties of the solvent. Ideally, if a new solvent is to be introduced as a 'green' solvent, it would be an improvement over the solvents currently available. Optimal physical properties would include low viscosity to facilitate mixing and a large density difference in comparison to other process fluids to hasten phase separation. Chemically, the solvent would have a high selectivity for the solute. To encourage widespread use of the solvent, it should be inexpensive to produce, recyclable, and robust to endure various processing environments. Of most interest to us at present are ionic liquids that are liquid at room temperature and represent potential replacements for traditional volatile organic solvents in separation processes [Brennecke et al., 2001].

Physical properties such as melting point, boiling point, density, and viscosity, are related to the mechanical and engineering aspects associated with a process. For example, densities, viscosities, and surface tensions will determine important parameters including rates of liquid–liquid phase separation, mass transfer, power requirements of mixing and pumping. Other physical properties, such as refractive index, are related to certain properties despite providing a bulk property description. Chemical properties such as the structure hardness, polarity, and relative hydrogen-bonding donating and accepting ability are related

to the molecular chemistry [Wasserchеid et al., 2003]. Due to the intermolecular interactions that these parameters measure, these chemical properties determine solubilities, partition constants, and reaction rates.

Figure 1.1: Structures of Cations and Anions in Ionic Liquids

In recent years there has been a significant increase in research into properties of ionic liquids; especially after having been proposed as reaction media for chemical reactions. Ionic Liquids have been successfully used for hydrogenations, hydroformylation, isomerization, dimerization and alkylations. It is used nowadays in fuel cell and electrolyte application because of its wide electrochemical window, high conductivity and low dielectric constant. They are also used as lubricants because of its high thermal stability and wide liquidus range [Brennecke et.al.,2001].Additionally they are good solvents for a wide range of metal catalysts as well as polar organic and aromatic liquids. Most of the studies were focussed on ionic liquids containing water and air stable anions like $[PF_6]$ and $[BF_4]$ with the 1-alkyl-3-alkylimidazolium cation. Few studies on pure 1-alkyl-3-alkylimidazolium hexafluorophosphates and their mixtures have been reported. [Rogers et al., 2001]

The term "ionic liquids" has been assigned to organic salts that are liquids at close to ambient conditions. Ionic liquids are normally composed of relatively large organic cations and inorganic or organic anions (Figure 1.1).Examples of cations are 1-alkyl-3-alkylimidazolium or 1-alkylpyridinium and examples of anions are hexafluorophosphate, tetrafluoroborate, aluminium(III) chloride and various organic ions based on fluorinated amides,imides,nitrides and methides. Ionic liquids have negligible vapor pressure at room temperature and are generally stable over a wide temperature range. They show considerable variation in their stability to moisture and their solubility in water, polar and nonpolar organic liquids.

1.3 Desulphurization and Denitrification of diesel oil using Ionic Liquids

Looking at the advantage of using IL as solvents, we would like to use it for desulphurization and denitrification studies. There are few reported work which discuses the

applications. Zhang et al., [2002] studied 1-ethyl-3-methylimidazolium tetrafluoroborate ([EMIM][BF_4]), 1-butyl-3-methylimidazolium hexafluorophosphate ([BMIM][PF_6]) and 1-butyl-3-methylimidazolium tetrafluoroborate ([BMIM][BF_4]) in the selective sulphur removal from fuels at room temperature. It was found that absorbtion capacity of the ionic liquids for sulphur containing compounds is sensitive to the structure of both the anion and cation of the ILs and alkyl substitution on the aromatic ring. Zhang et al.,[2004] showed that 1-alkyl-3-methylimidazolium tetrafluoroborate ([AMIM][BF_4]), 1-alkyl-3-methylimidazolium hexafluorophosphate ([AMIM][PF_6]) and 1-alkyl-3-methylimidazolium trimethylamine hydrochloride ([AMIM][$AlCl_3$-TMAC]) have remarkably high absorption capacities for aromatics. The absorption capacity were found to strongly depend on the cation and anion structure and its size in the ILs. Further the used ionic liquids were regenerated either by distillation or by water displacement of absorbed molecules.

Alonso et al., [2007] used 1-methyl-3-octylimidazolium tetrafluoroborate ([OMIM][BF_4]) to extract thiophene and dibenzothiophene from gasoline. A gasoline formulation was simulated as a mixture of n-hexane, cyclohexane, iso-octane and toluene with thiophene and dibenzothiophene as sulphur compounds. Further N-butylimidazole –derived dialkylphosphate ILs were demonstrated to be effective for the extractive removal of aromatic sulphur compounds from fuel oils. It showed strong preferential extraction for 3-methylthiophene, benzothiophene and dibenzothiophene from toluene. The selectivity of ILs were found to depend on the size and structure of both cation and anions of the ILs [Nie et al., 2008].Alonso et al.,[2008] also reviewed numerous attempts of using ILs for the separation of thiophene from alphatic and aromatic hydrocarbons via Liquid Liquid Extraction (LLE).A high solubility of thiophene in ILs and low solubility of ILs in aliphatic and aromatic hydrocarbons was observed in number of studies.

The use of 1-butyl-3-methylimidazolium chloride ([BMIM][Cl]) for the selective extraction of neutral nitrogen compounds from diesel feed was described by Xei et al.,[2008].The observed selectivity values were higher towards dibenzothiophene and carbazole. Alonso et al.,[2010] studied that the extraction ability of nitrogen containing compounds by using 1-ethyl-3-methylimidazolium ethylsulphate ([EMIM][$EtSO_4$]),1-octyl-3-methylimidazolium tetrafluoroborate and 1-octyl-3-methylimidazolium bis{(trifluoromethyl)sulfonyl}imide. Favourable values for the selectivity and distribution coefficient were found for the three ILs which implies that ILs are potential alternative solvent.

Currently there is no data for the simultaneous removal of aromatic sulphur and nitrogen compounds from diesel oil using ionic liquid. This is essential for future HDS and HDN process design with the view of severe environmental regulations since nitrogen compounds are the major inhibitors for HDS processes. However, for the effective removal of such compounds from diesel oil, the structural and theoretical information from micro to macro level is required for ionic liquid and its mixture with aromatic sulphur and nitrogen compound. This can be helpful in reducing the operating and investment cost of the simultaneous HDS and HDN process. To study chemical process involving ionic liquid with other compounds it is necessary to understand reactivity and stability of the interacting system *via Ab initio method*. The Higher Occupied Molecular Orbital (HOMO) and Lower Unoccupied Molecular Orbital (LUMO) energies with its energy gap can define the scalar properties of the mixture of ionic liquid and aromatic sulphur/nitrogen compounds at molecular level. The detailed examination of relative energies (LUMO/HOMO) and structural interaction can therefore be used to build up a picture of interactions occurring in ionic liquid and its complexes [Nishi et al., 2008]. Several studies have been done in the past for obtaining molecular orbital calculations such as heterocyclic cations [Natalia et al., 2008]. Angueira et al., [2005] studied the ionic liquid structure effects on the reactivity of toluene carbonylation. New application such as the design of task-specific ionic liquids for capturing

CO_2 using molecular orbital (MO) study were also been carried out [Yu et al., 2006]. Recently it was found that 1-butyl-3-methylimidazolium chloride([BMIM][Cl]) and 1-butyl-3-methylimidazolium bis(trifluoromethylsulfonyl)imide ([BMIM][$(CF_3SO_3)_2N$]) forms high and low network connectivity with its respective ions. The very fact that the coulombic attraction is the dominant stabilization force was demonstrated by the analysis of the charge distribution, molecular orbital and electron density for the dimer complex 1-butyl-3-methylimidazolium chloride [Hunt et al., 2007]. Since the coulombic forces are significant in an IL, charge distribution or point charges on the constituent ions are likely to be more significant than in liquid made up of neutral charges molecules.

Ionic Liquids based on imidazolium and pyridinium cations with $FeCl_4$ anions were recently screened via HOMO-LUMO energies [Murillo et al., 2009].The effect of activation energy of ionic liquids (ILs) over the thermal stability of heavy Mexican oil were subsequently obtained. In a recent study on a tetramethylguanidinium lactate ionic liquid it was found that the HOMO of anions interacts effectively with the LUMO of cation thereby increasing charge transfer. Cruz et al., [2007] predicted the proton affinities via HOMO/LUMO energies for a series of sulfur aromatic compounds. The proton activities were found to be an important descriptor for determining the activities of sulfur aromatic compounds towards hydrodesulphurization. However till date an approach based on simultaneous interaction has not been attempted.

The COSMO (**CO**nductor like **S**creening **Mo**del) [Klamt et al., 1993,1995,2005] in combination with **R**eal **S**olvents i.e. *COSMO-RS* could be used to compute the chemical potential and activity coefficient of any component in a mixture. Thus COSMO-RS is an effective way to screen the potential cations and anions for hydrodesulphurization, hydrodenitrification or the simultaneous removal of aromatic nitrogen and sulphur species are difficult by tuning the cations and anions. Kumar et al.,[2009] found that a smaller size cation

gave higher selectivity but lower capacity for theremoval of thiophene from simulated diesel oil at 298.15K .

1.4 Scope of present study

In this study we have used the three tier approach based on; (a) Ab initio method,(b) COSMO-RS and (c) Subsequent experimentation to study the flexibility of IL for desulphurization (DS) and denitrification (DN) studies. With this broad goal in view this thesis accomplishes the following objectives:

Estimate the Lower Unoccupied Molecular Orbital (LUMO) and Higher Occupied Molecular Orbital (HOMO) energy and global scalar properties of ILs with thiophene and pyridine molecules via *Ab initio method*. The scalar properties include chemical potential (μ), chemical hardness (η), chemical softness (S), electro negativity (χ) and electrophilicity index (ώ). Subsequently, the partial charges and interaction energy between ILs with thiophene and pyridine are evaluated using similar approach.

Use of COSMO-RS approach in predicting: An important advantage of the COSMO-RS model is that it predicts *a-priori* the liquid phase non-ideal activity coefficient of sulphur /nitrogen compound in IL. It uses the molecular structure of the solute/component as the only initial input. Thus it directly predicts the IDAC (**I**nfinite **D**ilution **A**ctivity **C**oefficient) values which are measurable and thereby used to calculate the selectivity and capacity at infinite dilution. Therefore, in this work we have used the COSMO-RS model for the *a-priori* prediction of IDAC values of the above mentioned nitrogen and sulphur species in both ionic liquid and diesel oil. With these measured values the judicious cation and anion combination is chosen.

Determination of physiochemical properties of 1-ethyl-3-methylimidazolium acetate ([EMIM][OAc]) 1-ethyl-3-methylimidazolium methylsulphonate ([EMIM][$MeSO_3$]),

1-ethyl-3-methylimidazolium ethylsulphate ([EMIM][$EtSO_4$]), Pyridine (PY), Quinoline (QU), Pyrrole (PYRR), Indoline (INDO),Thiophene (TS) and its mixtures at T=(298.15 to 323.15) K and atmospheric pressure were carried out. In addition their thermodynamic properties such as thermal exapansivity (α), excess molar volume ( ), deviation of surface tension ( ) and deviation of refractive index ( ) are calculated from the measured experimental data.

Obtain ternary Liquid Liquid Equilibria for the ternary system of imidazolium based ionic liquids with sulphur (benzothiophene) and diesel compound (n-hexane). The corresponding triangular diagram gives clear information of the change in the size and shape of the immiscibility region. Further prediction of functional group interaction parameters of the mixture containing IL, thiophene and diesel compounds using UNIFAC model via regression of experimental data is also accomplished. New group interaction parameters are regressed using GA from reported tie lines of liquid- liquid equilibrium data of three component systems.

To investigate the quaternary LLE phase behavior of [EMIM][OAc],[EMIM][$EtSO_4$] and [EMIM][$MesO_3$] for the simultaneous extraction of thiophene and pyridine from hydrocarbon stream. This LLE data will be essential for the design of the extraction equipment and also helps us to know the thermodynamic limit of separation. Therefore, the LLE diagram for quaternary mixture of [EMIM][OAc] + thiohphene + pyridine + diesel compounds,[EMIM][$EtSO_4$] + thiohphene + pyridine + diesel compounds and [EMIM][$MesO_3$] + thiohphene + pyridine + diesel compounds have been determined at ambient condition i.e. at 298.15K. From the experimental data, the extraction efficiency of thiophene and pyridine, the selectivity and the distribution coefficient have also been determined.

1.5 Thesis Organization

The thesis is organized into the following chapters

Chapter 2 presents a brief overview of the ab-initio quantum chemical calculations. It presents the different levels of theories, basis sets and the working of quantum chemistry programs. The procedure for geometry optimization for ionic liquids and the generation of COSMO file with Gaussian03 is also discussed.

Chapter 3 deals with the HOMO energy, LUMO energy, partial charges and interaction energy for the simultaneous interaction of IL with thiophene and pyridine molecules. Further the scalar properties are calculated from the predicted HOMO and LUMO energy.

Chapter 4 presents the values of infinite dilution activity coefficients (IDAC) using COSMO-RS model. It deals with the estimation of selectivity, capacity and performance index for the application of desulphurization, denitrification and simultaneous desulphurization and denitrification processes.

Chapter 5 reports the physiochemical properties of pure compounds including ILs, aromatic sulphur and nitrogen compound and its mixture. The corresponding thermodynamic properties calculated includes volume expansivity, excess molar volume, deviation of surface tension and deviation of refractive index.

Chapter 6 covers the experimental, NRTL and UNIQUAC model correlation as well as COSMO-RS prediction for the extraction of benzothiophene from diesel compound (n-hexane) using imidazolium based Ionic Liquids at 308.15K. In addition the estimation of functional group interaction parameters for the ternary system of IL+ Thiophene+Diesel compound is also carried out. New group interaction parameters are regressed through Genetic Algorithm (GA) via reported LLE data for the three component systems.

Chapter 7 presents the Liquid-Liquid Equilibria for the Quaternary Systems of Imidazolium based Ionic Liquid + Thiophene + Pyridine + Diesel compounds at 298.15K .From this measured data the selectivity and distribution coefficient values are calculated.

The experimental datas are correlated with the NRTL, UNIQUAC model and validated with COSMO-RS prediction. In addition the binary interaction parameter is also predicted for the quaternary systems that contain imidazolium ILs.

REFERENCES

Alonso, L.; Arce, A.; Francisco, M.; Soto, A.; Rodriguez.; O. Liquid-Liquid Equilibria for Systems Composed by 1-Methyl-3-octylimidazolium Tetrafluoroborate Ionic Liquid, Thiophene, and n-Hexane or Cyclohexane. *J.Chem. Engg. Data*. **2007**, 52, 1729-1732.

Alonso, L.; Arce, A.; Francisco, M.; Soto, Ana. Phase behaviour of 1-methyl-3-octylimidazolium bis[trifluoromethylsulfonyl]imide with thiophene and aliphatic hydrocarbons: The influence of n-alkane chain length. *Fluid Phase Equilibria.* **2008**, 263, 176-181.

Alonso,L.;Arce,A.;Francisco,M,Soto,A.Extraction ability of Nitrogen containing compounds involved in the Desulphurization of Fuels by using Ionic Liquids. *J.Chem. Engg. Data*. **2010**, 55, 3262-3267.

Angueira, E.J.; White. M.G. Super acidic ionic liquids for arene carbonylation derived from dialkylimidazolium chlorides and MCl_3 (M = Al, Ga, or In). *J. Mol. Cat A: Chem*.**2007**, 277, 164-170.

Bogwon, D.; Park, S.; Han, K.; Kim, C. Liquid-liquid equlibria for ethanol + hexadecane + heterocyclic nitrogen-containing compounds at298.15K. *Fluid phase Equilibria*.**2002**, 193,217-227.

Brennecke, F. J.; Magninn, J. E. Ionic liquids: Innovative Fluids for Chemical Processing *AIChEJ*, **2001,**47, 2384.

Cruz I.G, Valencia, D.; Klimova, T.; Roa, R.O.; Magadan,J.M.; Balderas,R.D.; Illas, F. Proton affinity of S-containing compounds: Implications for crude oil hydrodesulphurization. *J.Mol.Cat A: Chem*. **2008**, 281, 79-84.

Hunt, P.A.; Gould,I.R.,Kirchner,B.The structure of Imidazolium –Based Ionic Liquids: Insights from Ion Pair Interactions.*Aust.J.Chem*.**2007**,60,9-14

Jayaraman,A.; Yang,F.H.;Yang.R.T.Effects of Nitrogen Compounds and Polyaromatic Hydrocarbons on Desulfurization of Liquid Fuels by Adsorption via ∂-Complexation with Cu(I)Y Zeolite. *Energy & Fuels*. **2006**, 20, 909-914.

Jeon, H.J.; Hyun, K.C.; Kim, S.H.; Kim, J. N.; Removal of Refractory Sulfur Compounds in Diesel Using Activated Carbon with Controlled Porosity. *Energy & Fuels*. **2009**,23, 2537–2543.

Jiang .Q. Extraction of Nitrogen Compounds from Catalytically Cracked Diesel Oil with a Volatile Carboxylic Acid Based on Reversible Chemical Complexation. *Energy & Fuels*.**1998**, 12, 788-791.

Klamt, A. Conductor Like Screening Model for Real Solvents: A new Approach to the quantitative calculation of solvation phenomena. *J.Phy.Chem.***1995**, 99, 2224-2235.

Klamt, A. COSMO-RS: From Quantum Chemistry to Fluid Phase Thermodynamics and Drug Design. First Edition, Amsterdam: Elsevier, **2005**.

Klamt, A.; Schüürmann, G. COSMO: A New Approach to Dielectric Screening in Solvents with Explicit Expressions for the Screening Energy and its Gradient. *J. Chem. Soc. Perkin Trans*, **1993**, 2,799-805.

Kumar,A.P.;Banerjee, T. Thiophene Separation with Ionic Liquids for Desulphurization: A Quantum Chemical Approach. *Fluid Phase Equilibria*. **2009**,278, 1-8.

Li, W.; Liu, Q.; Xing, J.; Gao, H.; Xiong, X.; Li, Y.; Li, X.; Liu, H. High-Efficiency Desulfurization by Adsorption with Mesoporous Aluminosilicates. *AIChEJ*.**2003**,53, 3263-68.

Murillo, J. A.H; Lopez Ramirez, S.; Domínguez, J. M.; Duran-Valencia, C.; García-Cruz, I.; González-Guevara, J. A. *J. Ther. Anal. Cal*, **2009**,95, 173.

Natalia, V.P.; Seddon, K.R. Applications of ionic liquids in the chemical industry. Chem. Soc. Rev.**2008**, 37,123-150.

Nie, Y.; Li, C.; Meng, H.; Wang, Z.N. N-dialkylimidazolium dialkylphosphate ionic liquids: Their extractive performance for thiophene series compounds from fuel oils versus the length of alkyl group. Fuel Process. Tech.**2008**,89,978-983.

Nishi, T.; Iwahashi, T.; Yamane, H.; Ouchi, Y.; Kanai, K.; Seki,K. Electronic structures of ionic liquid $[C_n mim]^+$ BF_4 and $[C_n mim]^+$ PF_6 studied by ultraviolet photoemission inverse photoemission, and near edge X-ray absorption fine structure spectroscopies. *Chem. Phy. Lett*. **2008**, 455,213-217.

Rogers, R.D.; Huddleston, J.G.; Wilauer, H.D.; Swaltoloski, R.P.; Visser, A.E. Room Temperature Ionic Liquids as Novel Media for Clean Liquid-Liquid Extraction .*Chem. Comm*. **1998,** 36, 1765

Sano, Y.; Choi, K.; Korai, Y.; Mochida, I. Effects of nitrogen and refractory sulfur species removal on the deep HDS of gas oil. *Applied Catalysis B. Environmental*. **2004**, 53, 169–174.

Shiraishi, Y.; Taki, Y.; Hirai, T.; Komasawa, I. A Novel Desulfurization Process for FuelOils Based on the Formation and Subsequent Precipitation of S-Alkylsulfonium Salts.1. Light Oil Feedstocks. *Ind. Eng. Chem. Res* **2001**, 40, 1213-1224.

Song, T.; Zhang, Z.; Zbigniew, J.C.; Yang, H.; Zheng, Y. Effect of Aromatics on Deep Hydrodesulfurization of Dibenzothiophene and 4,6-Dimethyldibenzothiophene over NiMo/Al_2O_3 Catalyst. *Energy & Fuels*.**2006**, 20, 2344-2349.

Trakarnpruk, W.; Seentrakoon, B.; Porntangjitlikit, S. Hydrodesulphurization of Diesel Oils by MoS_2 Catalyst Prepared by in situ Decomposition of Ammonium Thiomolybdate. Silpakorn U *Science & Tech Journal*.**2008,**2,7-13.

Uday,T.; Xiaoliang Ma,T.; Song.C. Influence of nitrogen compounds on deep hydrodesulfurization of 4,6-dimethyldibenzothiophene over Al2O3- and MCM-41-supported Co-Mo sulfide catalysts. *Catalysis Today*.**2003**, 86, 265–275.

Wang, B.; Zhu,J.; Ma,H.. Desulfurization from thiophene by SO_42-/ZrO_2 catalytic oxidation at room temperature and atmospheric pressure. *J. Haz. Mat*.**2009**,164,256-264.

Wassercheid.P.; Welton.T. Ionic Liquids in Synthesis.Wiley-VCH.1st Edition.**2003**.

Xie, L.L.; Reguillon, A. F.; Rostaing, S.P.; Wang, X.X.; Fu, X.; Estager, J.; Vrinat, M.; Lemaire, M. Selective Extraction and Identification of Neutral Nitrogen Compounds Contained in Straight-Run Diesel Feed Using Chloride Based Ionic Liquid. *Ind. Eng. Chem. Res*. **2008**, 47, 8801–8807.

Yang, H.; Chen, J.; Briker, Y.; Szynkarczuk, R.; Ring, Z. Effect of nitrogen removal from light cycle oil on the hydrodesulphurization of dibenzothiophene, 4-methyldibenzothiophene and 4, 6-dimethyldibenzothiophene. *Catalysis Today*.**2005**, 109, 16–23.

Yongtan , Y. Determination of nitrogen compounds in catalytic diesel oil using gas chromatography. *Chin J Chromatogr* **2008**, 26, 478–483.

Yu, G.; Zhang, S.; Yao, X.; Zhang, J.; Dong, K.; Dai, W.; Mori, R. *Ind. Eng. Chem. Res*. **2006**,45,2875-2880.

Zhang, S.; Zhang, Q.; Conrad Zhang. Z. Desulfurization and Denitrogenation of Fuels Using Ionic Liquids. *Inorg. Chem*.**2001**, 40, 2298-2304.

Zhang, S.; Zhang, Q.; Zhang, Z.C. Extractive Desulfurization and Denitrogenation of Fuels Using Ionic Liquids. *Ind. Eng. Chem. Res*. **2004**, 43, 614-622.

Zhang,S.;Zhang,Z.C.Novel properties of ionic liquids in selective sulphur removal from fuels at room Temperature.*Green Chem*.**2002**,4,376-379.

2.1 Ab-initio Methods

Quantum theory is based on the Schrödinger equation:

(2.)

describes the state of the system as a function of coordinates. This function, called the *state function* or wave function, contains all the information that can be determined about the system. is the Hamiltonian (i.e., energy*) operator of the system; and* E *is the* energy of that particular state. Schrödinger equation for molecular systems can only be solved approximately. The approximation methods can be categorized as either ab initio or semi empirical. Semi empirical methods use parameters that compensate for neglecting some of the time consuming mathematical terms in Schrödinger equation, whereas ab initio methods include all such terms.

The term ab-initio implies a rigorous, non-parameterized molecular orbital treatment derived from first principles. However, this is not completely true. There are a number of simplifying assumptions in ab-initio theory, but the calculations are more complete, and therefore more expensive, than those of the semi-empirical methods. It is possible to obtain chemical accuracy via ab-initio calculations, and this approach is especially favored in situations in which little or no experimental information is available.

Ab-initio theory makes use of the Born-Oppenheimer [Born and Oppenheimer 1927] approximation that the nuclei remain fixed on the time scale of electron movement, that is, that the *electronic wave function* is unaffected by nuclear motion. It also assumes that *basis sets* adequately represent molecular orbitals. Each molecular orbital (one electron function) Ψ_i is expressed as a linear combination of *n* basis functions Φ_m.

(2.)

The coefficients c_{mi} are called molecular orbital expansion coefficients or simply *MO coefficients*. Usually these basis functions are located at the center of atoms and are therefore often called atomic basis functions. The basis functions used in molecular orbital calculations are usually described through an abbreviation or acronym such as "6-31G(d)".

2.2 Basis Sets

A basis set is essentially a finite number of *atomic-like functions* over which the molecular orbital is formed via *Linear Combination of Atomic Orbitals* (LCAO) methods, as summarized in Eq. (2.2).

The first stage of all ab-initio calculations is a single-determinant SCF (Self Consistent Field) calculation. Its quality depends on the basis set i.e LCAO used for the calculation and the computational method employed .Eq 2.1 is solved assuming the electron to move in a field of 'fixed' electrons and nuclei. First a set of trial solution ( ) is obtained which are used to calculate the Coulomb and Exchange operators. The Hartree Fock Equations are then solved giving a second set of solutions , which are used in the next iteration This approach i.e (SCF) continues till the energies for all the electrons remains unchanged. The object of all molecular orbital (MO) programs is to build a set of molecular orbitals to be occupied by the electrons assigned to the molecule. In principle this can be achieved by combining any number of different types of electron probability functions, or even by writing one extremely complex function to describe the electron density in each molecular orbital. A far more convenient way is to build up the molecular orbitals from sets of orbitals centered on the constituent atoms. The MO calculation then simply involves finding the combinations of these atomic orbitals that have the proper

symmetries and that give the lowest (most negative) electronic energy. This is the *linear combination of atomic orbitals* (LCAO) formalism.

There are many different possible choices of atomic orbitals (the *basis set*). The *Slater Type Orbitals* [Slater 1930] (STO's) have the following form in Cartesian coordinates:

(2.)

The *Gaussian Type Orbitals* [Boys 1950] (GTO's) have the following form in Cartesian coordinates:

(2.)

N is the normalization constant; a, b, c are non-negative integers which control the angular momentum $L = a + b + c$. When $a+b+c = 0$ (that is, $a = 0$, $b = 0$, $c = 0$), the Gaussian is called an s-type Gaussian; when $a+b+c = 1$, we have a p-type Gaussian, which contains the factor x, y or z. ς controls the width of the orbital – large ς gives tight function and small ς gives diffuse function.. Almost all modern ab-initio calculations employ Gaussian Type Orbital (GTO) basis sets. These bases, in which each atomic orbital is made up of a number of Gaussian probability functions, have considerable advantages over other types of basis sets for the evaluation of one- and two-electron integrals. They are much faster computationally than, for instance, equivalent Slater orbitals. The Gaussian series of programs deals exclusively with Gaussian type orbitals and includes several optional GTO basis sets of varying size. This is one of the main advantages of such a widely distributed program system - the methods and basis sets used become standard and a direct comparison with literature data is often possible.

The simplest of the optional basis sets in *Gaussian03* [Frisch et al., 2004] is the STO-3G [Hehre et al 1969, Collins et al 1976]. STO-3G is an abbreviation for *S*later-*T*ype-*O*rbitals *simulated* by *3* Gaussian functions each. This means that each atomic

orbital consists of *3* Gaussian functions added together. The coefficients of the Gaussian functions are selected so as to give as good a fit as possible to the corresponding Slater-type orbitals. STO-3G is a *minimal basis set*. This means that it has only as many orbitals as necessary to accommodate the electrons of the neutral atom. Because a complete basis set of *p-orbitals* must be added to maintain spherical symmetry, the elements boron to neon each have five atomic orbitals: 1*s*, 2*s*, $2p_x$, $2p_y$, and $2p_z$; for beryllium and lithium a minimal basis set actually requires only 1*s* and 2*s* orbitals. In STO-3G, however, the three 2*p*-orbitals are also included for these elements in order to give a consistent description across the periodic table. Because there is only one best fit to a given type of Slater orbital (1*s*, 2*p*, etc.) for each number of Gaussian functions, all STO-3G basis sets for any row of the periodic table are identical except for the *exponents* ς of the Gaussian functions. These are expressed as a *scale factor*, the square of which is used to multiply all exponents in the original best-fit Gaussian functions. In this way the ratios of the exponents of the individual Gaussians to each other remain constant, but the effective exponent of the entire orbital can be varied. The exponents, or scale factors, can be considered to be a measure of the extent of the orbital. A low exponent indicates a diffuse (and therefore relatively high energy) orbital; high exponents indicate compact orbitals close to the nucleus.

The STO-3G basis set is very economical, having only one basis function (or atomic orbital) per hydrogen as atom (the 1*s*), five per atom from Li to Ne (1*s*, 2*s*, $2p_x$, $2p_y$, and $2p_z$) and nine per atom for the second-row elements Na to Ar (1*s*, 2*s*, $2p_x$, $2p_y$, $2p_z$, 3*s*, $3p_x$, $3p_y$, and $3p_z$). Although STO-3G remained a standard basis set for ab-initio optimizations for several years, it has eventually been replaced by small split-valence basis sets and is now hardly used. Its weaknesses proved to be - overestimation of the stability of small rings; overemphasis of the π-acceptor characteristics of electropositive elements of the first row; and total failure for the second-row electropositive elements, especially sodium.

The greatest problem of any minimal basis set is its inability to expand or contract its orbitals to fit the molecular environment. One solution to the problem is to use either *split-valence* or *double zeta* basis sets. In these bases the atomic orbitals are split into two parts – a *compact inner orbital* and a more *diffused outer orbital*. The coefficients of these two types of orbitals can be varied independently during the molecular orbitals construction in the *self consistent field* SCF procedure. Thus the size of the atomic orbital that contributes to the molecular orbital can be varied within the limits set by the inner and outer basis functions (Figure. 2.1). Split-valence basis sets split only the valence orbitals in this way; whereas double zeta bases also have split core orbitals (double zeta implies two different exponents). The split –valence basis set most widely used for the early calculations was 4-31G [Ditchfield et al., 1971., Hehre et al., 1972, Hariharan and Pople,1974, Gordon et al., 1982]. This nomenclature means that the core orbitals consist of *4* Gaussian functions; inner valence orbitals have *3* Gaussian functions; and outer valence orbitals have 1 Gaussian function.

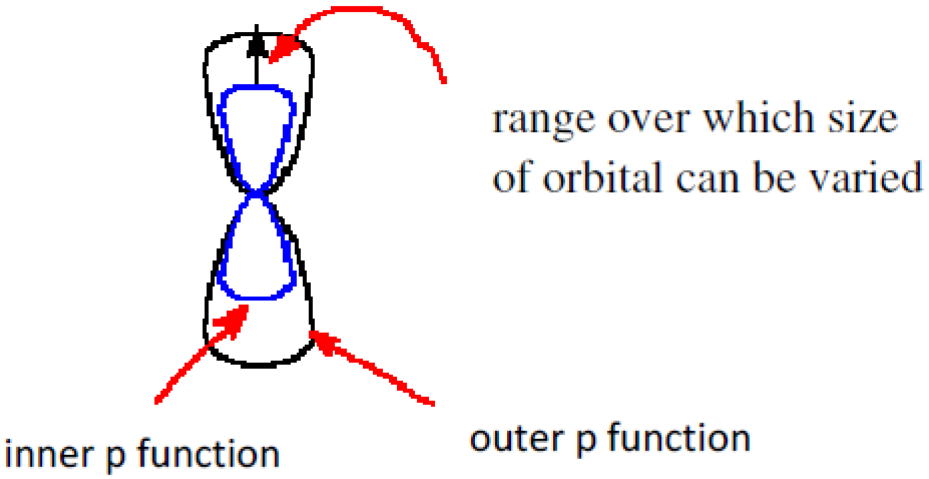

Figure 2.1: Split-valence p-orbital

The advent of optimization procedures that use analytical gradients led to the development of split-valence basis sets with fewer primitive Gaussians than 4-31G. 3-21G [Binkley et al., 1980, Gordon et al., 1982, Pietro et al., 1982, Dobbs and Hehre, 1986, 1987] became the basis set used most commonly for *geometry optimization*. It uses three primitive Gaussians for the core orbitals and a two/one split for the valence functions. Because the procedures used to calculate the atomic forces are very sensitive to the number of primitive Gaussians, a 3-21G optimization can be up to twice as fast as the same calculation with 4-31G, although the difference is not large for single point calculations.

The next step in improving a basis set is usually the addition of *d-orbitals* for all heavy (nonhydrogen) atoms. For most organic compounds these do not function as

d-orbitals in the normal sense of being involved in bond formation as in transition-metal compounds. Their purpose is far more to allow a shift off the center, for instance, a *p*-orbital away from the position of the nucleus. This *polarization* is illustrated in Fig. 2.2. Mixing the *d*-orbital, this has lower symmetry, with the p-orbital results in a deformation of the resulting orbital to one side of the atom. This adjustment is particularly important for small ring compounds and second-row elements. The most commonly used *polarization basis set* (i.e., one including *d*-orbitals) in the *Gaussian03* program is 6-31G*. This basis set uses six primitive Gaussians for the core orbitals, a three/one split for the *s*- and *p*-valence orbitals, and a single set of six *d*-functions (indicated by the asterisk). Six *d*-functions (equivalent to five *d*- and one *s*-orbital) are used for computational convenience, although Gaussian programs can also handle basis sets with five real *d*-orbitals. A further development is the 6-31G** basis, in which a set of *p*-orbitals has been added to each hydrogen in the 6-31G* basis set.

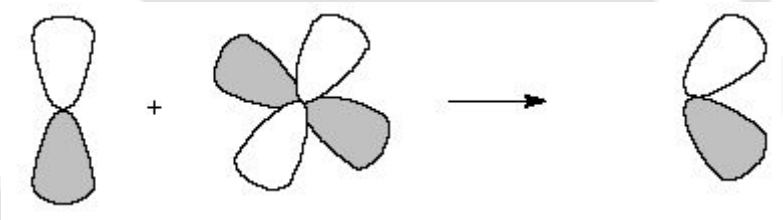

Figure 2.2: Polarization of a p-orbital by mixing with a d-orbital

The *diffuse function augmented* bases, is intended for use in calculations on anions or molecules that require very good descriptions of nonbonding electron pairs for e.g Ionic Liquids. These basis sets are obtained by adding a single set of very diffuse *s*- and *p*-orbitals (with exponents ς between 0.1 and 0.01) to the heavy atoms in a standard basis such as 6-31G*. This basis is then designated 6-31+G*, or 6-31++G* if diffuse functions are to improve the basis set at large distances from the nucleus and thus describe the high-energy electron pairs associated with anions better.

The split –valence basis sets are constructed by minimizing the energy of the atom at the HF level with respect to the contraction coefficients and exponents. The *correlation-consistent* basis sets are also used to extract the maximum electron correlation energy for each atom. The correlation consistent basis sets are designated as "*cc*-pVNZ", to be read as *correlation consistent polarized* split valence *N*-zeta, where *N* designates the degree to which the valence space is split. As *N* increases, the number of polarization functions also increases. Since a basis set must be of some limited size far short of the *HF limit*, their incompleteness can lead to a spurious result known as *basis set superposition error* (BSSE). The number of basis functions rises rapidly with increasing sophistication of the basis set, however the number of basis functions the program can handle is limited. The computer time required is roughly proportional to the fourth power of the number of basis functions. The List of basis sets in the order of their applicability and evolution is given in Table 2.1.

Table 2.1: List of Basis sets built in Gaussian 03.

Basis Set	**Applies to**	**Polarization Functions**	**Diffuse Functions**
STO-3G	H-Xe	*	
3-21G	H-Xe	* *or* **	+
6-21G	H-Cl	(d)	
4-31G	H-Ne	(d) *or* (d,p)	
6-31G	H-Kr	(3df,3pd)	++
6-311G	H-Kr	(3df,3pd)	++
D95	H-Cl *except Na and Mg*	(3df,3pd)	++
D95V	H-Ne	(d) *or* (d,p)	++
SHC	H-Cl	*	
CEP-4G	H-Rn	* *(Li-Ar only)*	
CEP-31G	H-Rn	* *(Li-Ar only)*	
CEP-121G	H-Rn	* *(Li-Ar only)*	
LanL2MB	H-Ba, La-Bi		
LanL2DZ	H, Li-Ba, La-Bi		
SDD, SDDAll	*all but Fr and Ra*		
cc-pV(DTQ5)Z	H-He, B-Ne, Al-Ar, Ga-Kr	*included in definition*	*added via* AUG-*prefix*
cc-pV6Z	H, B-Ne	*included in definition*	*added via* AUG-

			prefix
SV	H-Kr		
SVP	H-Kr	*included in definition*	
TZV and TZVP	H-Kr	*included in definition*	
MidiX	H, C-F, S-Cl, I, Br	*included in definition*	
EPR-II, EPR-III	H, B, C, N, O, F	*included in definition*	
UGBS	H-Lr	UGBS(1,2,3)P	
MTSmall	H-Ar		
DGDZVP	H-Xe		
DGDZVP2	H-F, Al-Ar, Sc-Zn		
DGTZVP	H, C-F, Al-Ar		

2.3 Calculation Methods

2.3.1 Hartree-Fock Theory

The molecular Hartree-Fock wave function is written as an antisymmetrized product (Slater determinant) of spin-orbitals, each spin-orbital ( ) being a product of a spatial orbital and a spin function (either α(spin up) *or* β(spin down)*). The* Slater determinant is given as:

Here indicates a function that depends on the space and spin coordinates of the spin orbital with electron labeled as '1'.The expression for the Hartree-Fock molecular electronic energy E_{HF} is given by the variation theorem as

(2.5)

where *D* is the Slater-determinant Hartree-Fock wave function and and are given by

(2.6)

(2.7)

Where is the sum of one-electron operators .The operator

and two-electron operators

(2.8)

where and , written in atomic units, are given by following expressions:

(2.9)

(2.10)

In the expression for E_{HF} ***bracket notation*** has been used. It is an abbreviated representation for the definite integral over all space of an operator sandwiched between two functions:

(2.11)

denotes the conjugate of . Since V_{NN} *does not involve electronic coordinates and* *D* is normalized, we have . The Hartree-Fock energy of a polyatomic molecule with *only closed subshells* is

(2.12)

(2.13)

The one-electron core Hamiltonian omits the interactions of electron i *with the* other electrons. The sums over *i* and *j* are over the *n*/2 occupied spatial orbitals of the *n*-electron molecule. In the Coulomb integrals J_{ij} and the exchange integrals K_{ij}, the integration goes over the spatial coordinates of electrons 1 and 2. The Hartree-Fock method looks for those orbitals that minimize the variational integral E_{HF}. The molecular orbitals (MOs) are taken to be normalized and mutually orthogonal. The closed-subshell orthogonal Hartree-Fock MOs satisfy

(2.14)

where ε_i is the orbital energy and where **(Hartree-) Fock operator is**

(2.15)

(2.16)

where the ***Coulomb operator*** and the exchange operator are defined by

(2.17)

(2.18)

where *f* is an arbitrary function and the integrals are definite integrals over all space. In our considerations *f* implies an orbital.

The first term on the right of Eq. (2.16) is the kinetic energy operator for one electron; the second term is the potential-energy operators for the attractions between one electron and the nuclei. The Coulomb operator is the potential energy of interaction between electron 1 and a smeared-out electron *j* with electronic density ; the factor 2 occurs because there are two electrons in each spatial orbit. The exchange operator has no simple physical interpretation but arises from the requirement that the wave function be antisymmetric with respect to electron exchange. The Hartree-Fock Hamiltonian operator is a one-electron operator (that is, it involves the coordinates of only one electron) and is peculiar in that it depends on its own eigen functions which are

not known initially. Hence the Hartree-Fock equations must be solved by an iterative procedure known as the *self-consistent field* (SCF) method in which the orbitals are improved from cycle to cycle until the electronic energy reaches a minimum value and the orbitals no longer change. This situation is described as "self-consistent."

In real systems the movements of the electrons are not independent of each other, as assumed in Hartree-Fock method, but are correlated to a certain extent so as to minimize repulsions as much as possible. This *electron correlation* means, in effect, that if electron A is at one end of the molecule, electron B prefers to be at the other end.

2.3.2. Koopmans theory

The Hartree Fock self consistent field (HF-SCF) equation

(:electronic Hamiltonian operator) imply that the orbital energies can be written as:

(2.19)

(2.20)

(2.21)

Where T+V represents the kinetic (T) ( ) and nuclear attraction (V) energies(is the average value of the kinetic energy plus), repectively. Thus,

Coulomb attraction to the nuclei for an electron in plus the sum over all the spin orbitals occupied in .

If is an occupied spin-orbital, the term i.e disappears in the above sum and the remaining terms in the sum represent the *Coulomb minus exchange interaction* of with all of the other occupied spin-orbitals. If is a virtual spin-orbital, this calculation does not occur because the sum over j does not include .So, one obtains the Coulomb minus exchange interaction of with all N of the occupied spin –orbitals in .Hence the energies of occupied orbitals pertain to interactions for a total of *N* electrons, whereas the energies of virtual orbitals pertain to a system with electrons. The model of detachment and attachment of an electron in an N-electron system can be used to understand the phenomena.

In this model, both the parent molecule and the species generated by adding or removing an electron are treated at the single-determining level. The Hartree-Fock orbitals of the parent molecule are used to describe both species. Such a model neglects "*orbital relaxation*" (i.e., the reoptimization of the spin-orbitals to allow them to become appropriate to the parent species).Within this model, the energy difference between two species can be written as follows (represents the particular spin-orbital that is added or removed):

For electron detachment /Ionization Potential (IP);

(2.22)

And for electron attachment/Electron Affinities (EA);

(2.23)

So, within the limitations of the HF *frozen orbital model*, the *ionization potentials* (IP) and *electron affinities* (EA) are given as the negative of the orbital energy of the *highest occupied molecular orbital* (HOMO) and virtual spin-orbital of the *lowest unoccupied molecular orbital energies* (LUMO),respectively. On the other hand the derivative of the total HF energy E, with respect to the occupation of a given orbital *n* is

equal to the corresponding orbital energy .This is known as Koopmans theorem [Koopmans, 1934] and it can be described as.

(2.24)

Therefore,

(2.25)

(2.26)

It is used extensively in quantum chemical calculations as a means of estimating global properties such as chemical potential , chemical hardness , chemical softness , electrophiliccity index and electronegaticvity for a system (Table 2.2). Some recent applications includes the study of HOMO and LUMO distribution on individual ligands in *mer*-Alq3 and its "CH"/N substituted derivatives [Irfan et.al.,2008].Other applications include the analysis of pericyclic reactions [Shaabani et.al.,2008] and reactivity of organic compounds [Zevatskii et.al.,2007]. The major advantages of HOMO/LUMO calculations is to study the selectivity and reactivity of ionic liquids and its complex without experimental data which thus yield results that are qualitatively correct .

Table 2.2: Scalar Quantities and its Definitions.

Properties name	**Empirical expression**	**Operational expression**	**Orbital Definition**
Chemical potential ( )			
Electronegativity ( )			-
Global Hardness ( )			
Global Softness (S)			

Electrophilicity index( )			

2.3.3 Møller-Plesset (MP) Perturbation Theory

Physicists and chemists have developed various perturbation-theory methods to deal with systems of many interacting particles (nucleons in a nucleus, atoms in a solid, electrons in an atom or molecule), and these methods constitute *many-body perturbation theory* (MBPT). [Møller and Plesset, 1934] proposed a perturbation treatment of atoms and molecules in which the unperturbed wave function is the Hartree-Fock function, and this form of MBPT is called Møller-Plesset (MP) perturbation theory.

For spin-orbitals u_i, the Hartree-Fock equations for electron m in an n-electron molecule have the forms

(2.27)

(2.28)

where and are defined by equations like (2.17) and (2.18) with spatial orbitals replaced by spin-orbitals and integrals over spatial coordinates of an electron replaced by integration over spatial coordinates and summation over the spin coordinate of that electron.

To do an MP electron-correlation calculation, one first chooses a basis set and carries out an SCF calculation to obtain the Hartree-Fock ground state function Φ_0, E_{HF}, and unoccupied orbitals. One then evaluates the second-order energy correction (and perhaps higher corrections) by evaluating the integrals over spin orbitals. The evaluation of higher order energy corrections is extremely time-consuming. To save time in MP2, MP3 and MP4 computations, the frozen-core approximation is often used. Terms involving excitations out of core orbitals are omitted.

Some recent applications includes the study of phenol-ammonia + hydrogen complexes [Pejov, 2002], isomers of C36 fullerene [Varganov et al.,2002] ,hydrogen bonded /stacked DNA base pairs [Jurecka et al.,2001] and the interactions of TMA-benzene and TMA-pyrrole systems [Liu et al.,2001]. A limitation of MP calculations is that although they work well near the equilibrium geometry, they do not work well at geometries far from equilibrium. Another limitation is that MP calculations are not generally applicable to excited electronic states.

2.3.4 Density Functional Theory

The electronic wave function of an *n*-electron molecule depends on 3*n* spatial and *n* spin coordinates. Since the Hamiltonian contains only one- and two-electron spatial terms, the energy can be written in terms of integrals involving only six spatial coordinates. In a sense, the wave function of a many-electron molecule contains more molecular orbitals than is needed and is lacking in direct physical significance. This has prompted the search for functions that involve fewer variables than wave function and that can be used to calculate the energy and other properties. The molecular energy can be expressed in terms of the first order spinless density matrix (which is a function of the spatial coordinates of one electron) and the second-order spinless density matrix (which is a function of the spatial coordinates of two-electrons). Unfortunately, no convenient principle (analogous to the variation principle used to calculate wave functions) has been developed that would allow direct calculation of these density matrices without first requiring calculation of the wavefunction.

[Hohenberg and Kohn 1964] proved that the ground state molecular energy, wave function, and all other molecular electronic properties are uniquely determined by the ground state electron probability density $\rho(x, y, z)$, a function of only three variables.The Hohenberg-Kohn theorem indicates that it is possible to calculate all the ground-state molecular properties from ρ, but does not tell us how to calculate the ground-state energy E_O from ρ or how to find ρ without first finding out the wavefunction ψ. Kohn and Sham 1965 showed that E_O of an n-electron molecule is given by

(2.29)

where $\Psi_i(1)$, $i = 1, 2, \ldots, n$ are the ***Kohn-Sham orbitals***, and $E_{xc}[\rho]$ is the ***exchange-correlation energy*** which is a functional of ρ. The Kohn-Sham orbitals are found by solving the one-electron equations

(2.30)

where the Kohn-Sham operator is

(2.31)

where the Coulomb operator is defined by Eq. (2.17) with replaced by $\Psi_j(2)$, and where ***exchange-correlation potential*** V_{xc} is found as the functional derivative of E_{xc}

(2.32)

If $E_{xc}[\rho]$ is known, its functional derivative is readily found, and V_{xc} is known. is like the Hartree-Fock operator, except that the exchange operators are replaced by V_{xc}, which handles the effects of both exchange (antisymmetry) and electron correlation.

Various approximate functionals $E_{xc}[\rho]$ have been used in molecular density functional (DF) calculations. Equation 2.32 is a first derivative of a function of a single position which depends both on the density and the gradient of the density. This is also called as the **G**eneralized **G**radient **A**pproximation (GGA). Functionals related to GGA are the [Becke,1986] abbreviated as B86, P due to [Perdew and Wang,1986]; PW91 due to [Perdew and Wang,1992], LYP due to [Lee,Yang and Parr,1992] and PBE due to [Perdew, Burke and Ernzerhof,1996;1997]. Pure DFT methods are defined by pairing an exchange functional with a correlation functional. For the well known B3LYP functional: Becke's (B) gradient corrected exchange functional is paired with the gradient functional correlation of Lee Yang and Parr (LYP), where 3 indicate it is a three parameter model. Most of the current DFT studies use either BP86, B3LYP or BPW91 functionals.

To investigate the accuracy of a particular approximate $E_{xc}[\rho]$, one uses it in DF calculations and compares the calculated molecular properties with their experimental values. The lack of a systemic procedure for improving $E_{xc}[\rho]$ and hence improving calculated molecular properties is the main drawback of the DF method. Some recent applications of DFT include the study of methylamines basicity in solvents [Safi et al., 1999],π-conjugated molecules in organic electronics [Sancho-Garcia, 2005] and atomic layer deposition of Al_2O_3 [Heyman and Musgrave, 2004] . Excellent reviews of the applications of DFT can be found in [Geerlings et al., 2003] and [Guner et al., 2003].

2.4. Interaction energy (IE)

The *interaction energy* (IE) is the contribution to the total energy that is caused by an interaction between the molecules or ion pair. It can be performed by Gaussian03 program with the appropriate level of theory and basis set choice such as HF/6-31G (d) or B3LYP/6-31G*. The interaction energy is evaluated as;

(2.33)

Where *a* refers to the basis set on cation C, *b* refers to the basis set on Anion A, and *ab* indicates the union of these two basis sets. For the combination of cation and anion in ionic liquid, the basis is used to (1) describe the electrons on C (cations),(2) describe ,in part, the electrons involved in the interaction between the cation and anions (Ionic liquids) ,and (3) aid in describing the electrons of A (anions).The same is true for the basis set b.Ionic liquids (IE) having larger basis set describe C or A individually, is therefore treated more completely ,and its energy is lowered ,relative to the energy of C or A. The interaction energy will therefore be larger (more negative).It implies that with the larger or more negative values of interaction energy implies more energy to disassemble the complex or compound. Recent applications include the structure of Imidazolium-Based ionic liquids where insights were obtained from ion pair interactions (Hunt et al., 2007).The interaction between thiophene and ionic liquids (Zhou et al.,2008) was also attempted recently.

2.5 Partial charges

In a molecule or ion pair, the bond formation takes place due to the redistribution of the valence electron density.This leads to regions where there is an imbalance between the ion core charges (the positive charge associated with the nucleus and the core electrons) and immediately surrounding valence electron charge. Thus that atoms in a molecule may have partial charges which can be one or lesser than that of charge of electron. The partial charge (PC) of atom can be calculated by

(2.34)

Where V_i is defined as the positive ion core charge which is equal to the net charge of the atom.c_i is the coefficient of the atomic orbital on this atom *i*.

The PC is calculated using CHELPG (**CH**arges from **EL**ectrostatic **P**otentials using a **G**rid based method) scheme (Breneman et.al., 1990) as given in Gaussian 03 program. The PC of atoms in molecules are fitted to reproduce the molecular electrostatic potential (MEP) at a number of points around the molecule. The MEP is calculated at a number of grid points spaced 3.0 pm apart and distributed regularly in a cube. Accordingly dimensions of the cube are chosen such that the molecule is located at the center of the cube, adding 28.0 pm headspace (Figure 2.3) between the molecule and the end of the box in all three dimensions. All points falling inside the van-der-Waals radius of the molecule are discarded from the fitting procedure. The following figure describes the PC for water:

The atomic charge for the oxygen atom in water (experimental gas phase structure with r(O-H) = 95.72 pm and a(H-O-H) = 104.52^{o}) has been calculated at several different levels of theory using the Mulliken as well as the **CHELPG** scheme. The Mulliken charge of the oxygen atom in water is calculated using two different level of theory such as B3LYP/cc-pVDZ and HF/6-31G (d). A large difference is observed in the PC i.e.-0.611 (between -0.255 and -0.866 respectively).The **CHELPG** charges obtained show much less differences i.e.-0.179 (between -0.694 and -0.873 respectively).Moreover, the **CHELPG** charges are often considered supperior to Mulliken charges as they depend much less on the fundamental theoretical method used to compute the wave function. Therefore, the **CHELPG** charges are practically constant at either HF or B3LYP level of theory provided that one of the correlation consistent basis sets is being used [http://www.cup.uni-muenchen.de/ch/compchem/pop/chelpg.html].

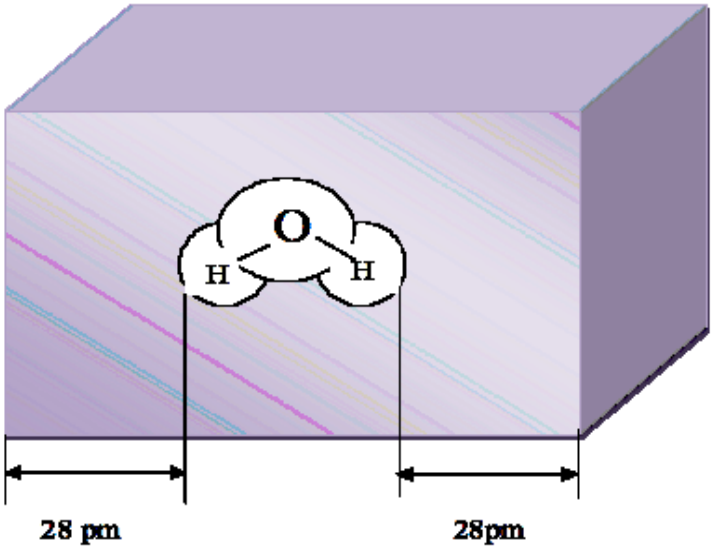

Figure 2.3:A functioning of **CHELPG** scheme for PC calculations.

2.6 Working of the *Gaussian* program

The first task is to determine the type of calculation required. The *Gaussian* program [Frisch et al., 2004] is usually controlled by specific *keywords*, which request given types of calculation. If the keywords are used, the program converts them to internal parameters, which then control the execution.

The various steps are summarized step by step:

1. The first step is to read in a title for the job plus molecular charge, multiplicity (singlet, triplet, etc.), molecular geometry in the form of a *Z-matrix*. This consists of atomic numbers, bond lengths, bond angles, dihedral angles from which the Cartesian (*x, y, z*) coordinates are calculated. The information from the Z-matrix is then used to work out electronic configuration and the orbital occupancies.

2. In the next step the nuclear repulsion energy which depends on the atomic numbers and the molecular geometry is calculated.
3. The atomic orbitals or basis sets are then assigned to each nucleus. *Ab-initio* programs use an internally stored standard set of coefficients and exponents that define the orbitals (the *basis set*).
4. *Ab-initio* programs next calculates the various one- and two-electron integrals required later in the calculation.
5. Ab-initio programs then produce an *initial guess* of molecular orbitals used as a starting point for the SCF calculations. The usual form of initial guess for ab-initio programs is that obtained from an extended Hückel calculation [Wolfsberg and Helmholz, 1952] on the molecule in question.
6. The solution to the SCF equations is iterated cycle by cycle until the electronic energy is at a minimum and the density matrix does not change. At this stage the calculation is said to be converged, or to have reached self consistency, and the program proceeds to the next step.
7. For a geometry optimization the atomic forces are then determined analytically and used to estimate the minimum-energy geometry for the molecular species being calculated.
8. The above process is repeated for each new geometry until the atomic forces are close to zero and the total energy does not change significantly from cycle to cycle.
9. The next stage of the calculation depends on the type of job to be performed. For a single point, the program may either move directly to the *population analysis*, which calculates the atomic charges, overlaps, dipole and higher moments. The correlation energy for DFT is then calculated using Eqn 2.32.

At this stage the optimization is complete and the program moves on to a population analysis of the optimized species. Figure. 2.4 shows the flow chart for the typical ab-initio job.

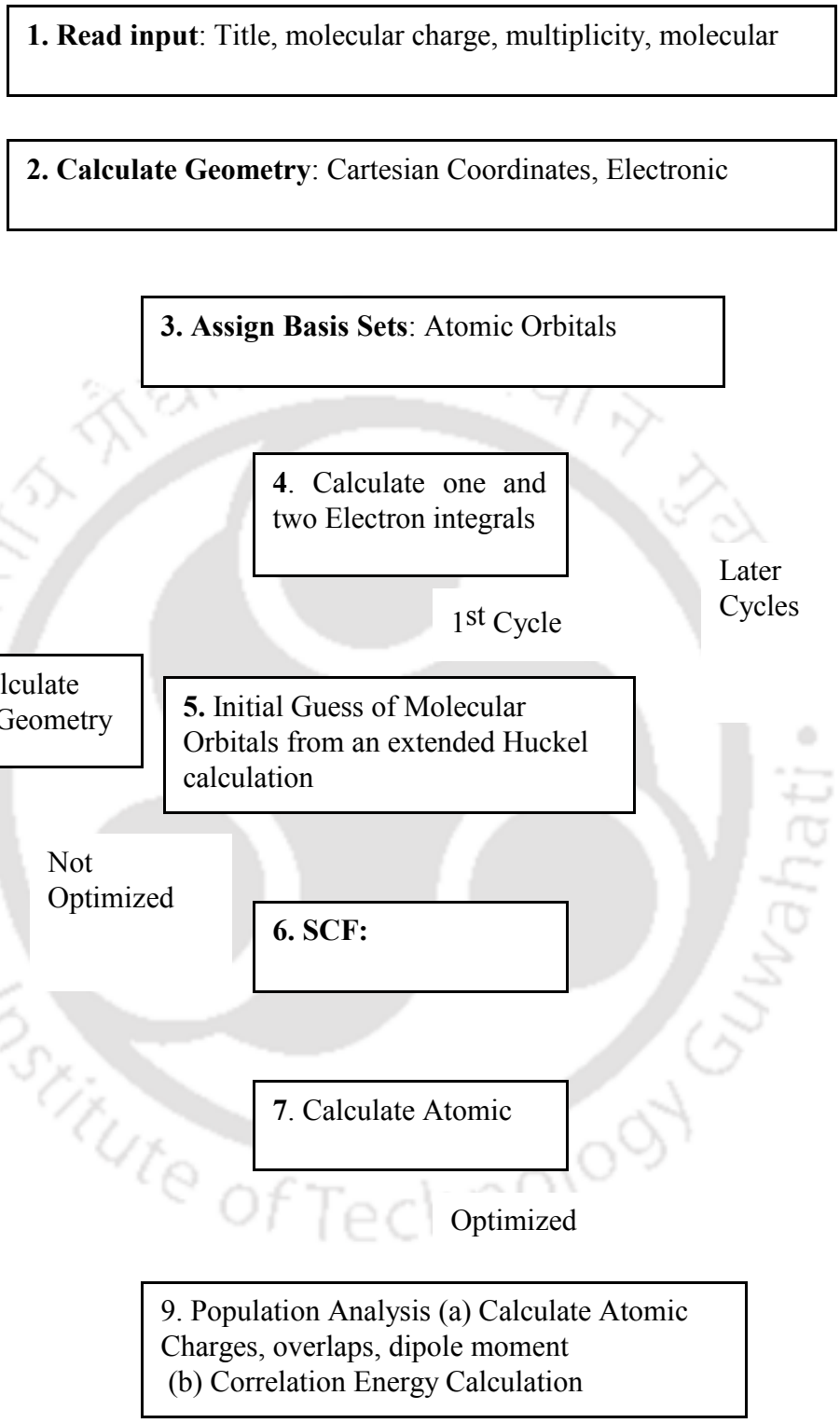

Figure 2.4: Typical flow chart for an ab-initio optimization

2.7 Geometry Optimization

Quantum chemical computation starts with an optimized structure of the molecule. Structural changes within a molecule produce differences in its energy and other properties. The way the energy of a molecular system varies with small changes in its structure is specified by its *potential energy surface*. Geometry optimization locates the minima on the potential energy surface, thereby predicting equilibrium structures. At both minima and saddle points, the gradient of the energy is zero. Since the gradient is the negative of the forces, the forces are zero at such a *stationary point*. At a minimum, any alteration of the geometry increases the energy and hence, all normal vibrations are *positive*. At a saddle point, displacement along a particular normal vibration decreases the energy and hence the vibration has a *negative frequency*, but all other displacements result in an energy increase. All optimizations can locate a stationary point, although not always a global minima.

2.8 Geometry optimization using *Gaussian03*

The structure of the molecule can be optimized using one of the several quantum chemistry packages. The most popular among them is *Gaussian03* [Frisch et al., 2004]. The next section discusses the steps, as shown in the form of a flowchart in Fig. 2.5, to be followed for carrying out geometry optimization in *Gaussian03*.

2.8.1 Input Specification

For doing a calculation in *Gaussian03*, an input file is required. The input file contains the *route section*, information about the molecular *charge* and *multiplicity*, and definitions of the molecular structure given in *Z-matrix*. All this information is used to calculate the total number of electrons and the orbital occupancies. Shown in Fig. 2.6 below is a sample input file for geometry optimization of water molecule.

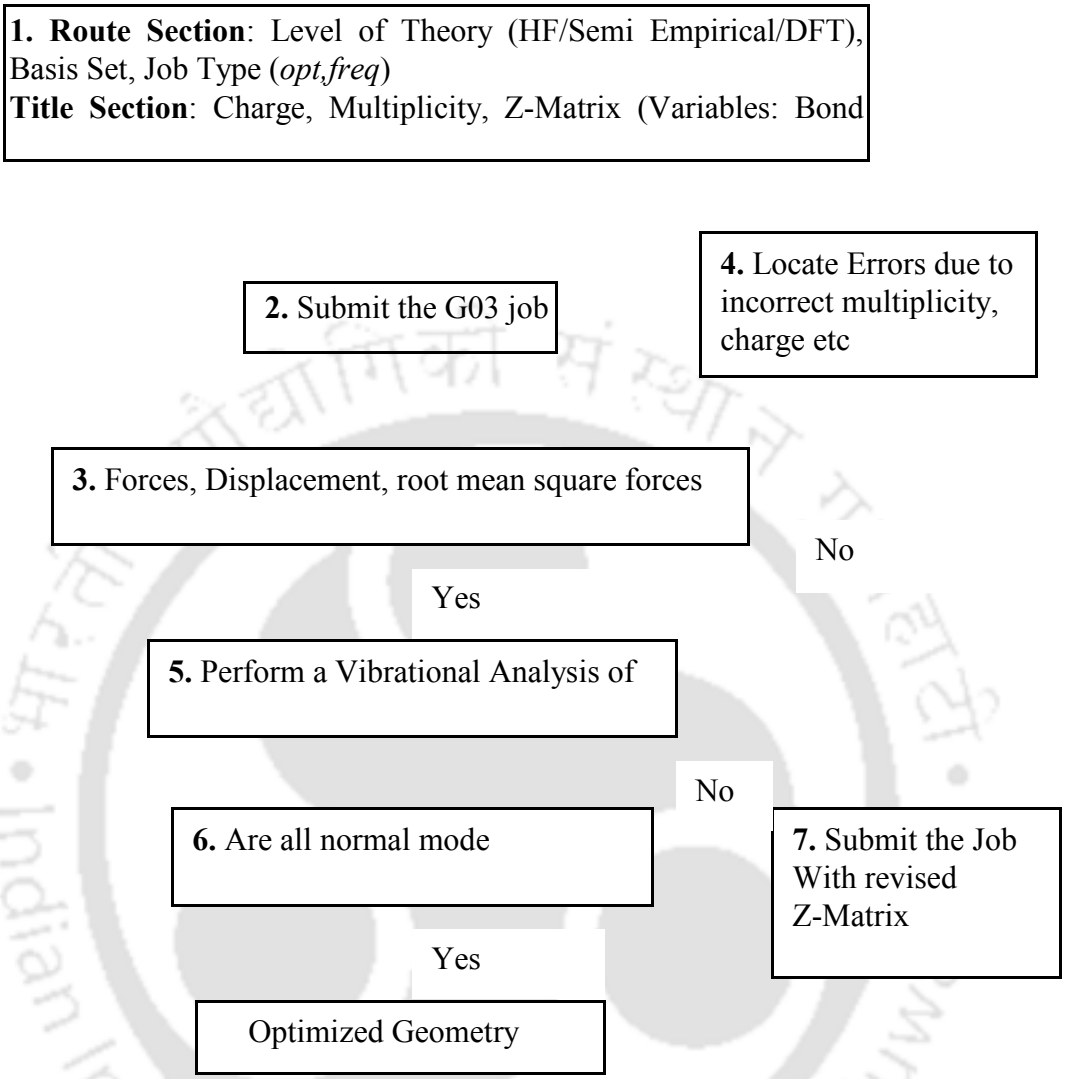

Figure 2.5: Procedure for geometry optimization

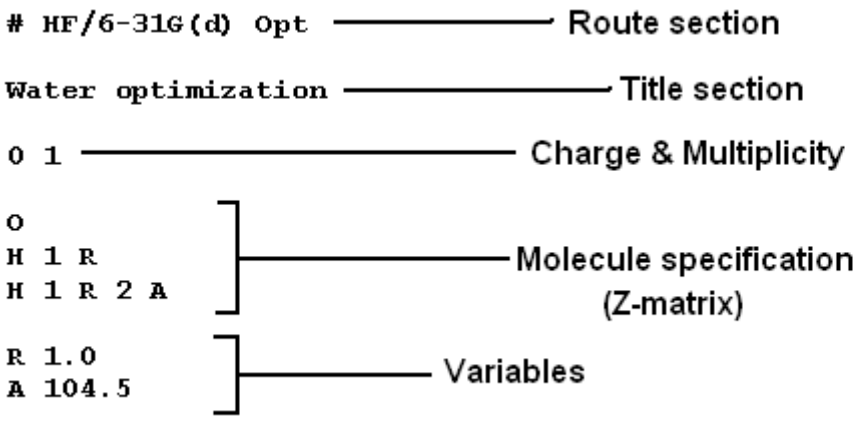

Figure 2.6: Sample input file for geometry optimization of water molecule

2.8.2 Route section

The route section of a Gaussian03 input file specifies the type of calculation to be performed. According to the Gaussian03 User's Reference [Frisch et al., 1999] there are three key components to this specification: - a) the job type, b) the method and c) the basis set. Optimization (**opt** keyword) and frequency calculation (**freq** keyword) are examples of job types. The combination of method and basis set specifies a model chemistry to Gaussian03, specifying a level of theory. HF (Hartree Fock), MPn (Moller Plesset Perturbation Theory), DFT (Density Functional Theory) are examples of methods. If no method keyword is specified, HF is assumed as a default. Most methods require a basis set. If no basis set keyword is specified then STO-3G basis will be used. STO-3G, 3-21G, 6-21G, and 6-31G are examples of basis sets. Single first polarization functions can also be requested using the usual * or ** notation. 6-31G* (or 6-31G(d)) is 6-31G with added d polarization functions on non-hydrogen atoms; 6-31G** (or 6-31G(d,p)) is 6-31G* plus p polarization functions for hydrogen. The + and ++ diffuse functions are available with some basis sets. 6-31+G is 6-31G plus diffuse s and p functions for non-hydrogen atoms;

6-31++G has diffuse functions for hydrogen also. For example, 6-31G(3df, 2p) designates the 6-31G basis set supplemented by diffuse functions, 3 sets of d functions and one set of f functions on heavy atoms, and supplemented by 2 sets of p functions on hydrogens. Which basis set to use is related to the objective of the calculation and the molecules to be studied. Even a large basis set is not always a guarantee for agreement with experimental data.

2.8.3 Z-matrix

The *molecular structure* given by Z-matrix definition contains information on the type of atoms used and their geometrical positions. *Z-matrix*, defines a molecule atom by atom in terms of *bond lengths*, *bond angles*, and *dihedral angles*. Z-matrix neither defines the bonds to be formed in the calculation nor represents a given electronic state. [Clark et al.,1985] discusses ways of efficiently writing the Z-matrix, the use of *symmetries* in the molecule and the use of *dummy atoms*. The text also contains an excellent explanation of how quantum chemical computational programs work.

For visualizing as well as specifying the Z-matrix MOLDEN [Schaftenaar 2000] visualization package can be used. It automatically assigns initial values to the bond lengths, bond angles, and dihedral angles.

2.8.4 Charge and Multiplicity

The charge is the *overall charge* (in atomic units) on the system specified in the Z-matrix. The individual *electronic spins add vectorially* to give a total electronic spin **S** whose magnitude has the possible values $[S(S+1)]^{1/2}\hbar$ with S = 0, ½, 1, ... The quantity $2S+1$ is called the multiplicity. The multiplicity is a measure of the number of unpaired electrons in the system. It is generally computed using the following thumb rule:

(2.34)

where, n_u is the number of unpaired electrons.

2.8.5 Submission of Job and Convergence Criteria

Gaussian03 may be run using the ***g03*** command. Ab-initio calculations are very time consuming and *Gaussian03* jobs may run for several hours or longer. So these jobs are forced to run in the background using ***&***.An optimization is complete when it has converged. *Gaussian03* uses the following criteria for convergence:

i. The forces must be 0. Specifically the maximum component of the force must be below the cutoff value of 0.00045 Hartree/Bohr.
ii. The root mean square of the forces must be below the defined tolerance of 0.0003 Hartree/Bohr.
iii. The calculated displacement for the next step must be smaller than the defined cutoff value of 0.0018 Bohr.
iv. The root mean square of the displacement for the next step must also be below the cutoff value of 0.0012 Bohr.

The presence of four distinct convergence criteria prevents a premature identification of the minimum. If all the above criteria are satisfied, a stationary point has been found and the program terminates normally. This is also indicated by the presence of a quotation at the end of the output file. At this point, one should proceed to carry out a vibrational analysis (Step 5 of Fig 2.5). If the program termination is not normal, the user should analyze the output files and look for the errors.

iv.9 Vibrational Analysis

After successful completion of an optimization job, *vibrational analysi*s (frequency calculation) is used in order to determine the nature of stationary points found by a geometry optimization as explained by [Foresman and Frisch 1996]. Geometry optimizations converge to a structure on the potential energy surface where the forces on the system are essentially zero. The final structure may correspond to a *minimum* on the potential energy surface, or it may represent a *saddle point*, which is a minimum with respect to some directions on the surface and a maximum in one or more others.

To carry out frequency calculation, ***freq*** keyword is used in place of ***opt***. The rest of the specifications are the same as discussed in Step 1.There are two pieces of

information from the output which are critical for characterizing a stationary point – (i) the number of imaginary frequencies and (ii) the normal mode corresponding to the imaginary frequency. Imaginary frequencies are listed in the output of a frequency calculation as negative numbers. By definition, a structure which has *n* imaginary frequencies is an n^{th} order saddle point. So if the frequency calculation found zero imaginary frequencies the structure is a minimum, else the structure is a saddle point. A point to note is that the frequency calculations should be done using same method and basis set as were used in the optimization calculations.

iv.10 Revised Z-matrix

Geometry optimization is easy for smaller molecules; larger molecules are usually difficult to optimize. For larger molecules [Höltje 1996] suggests a *stepping stone approach* - start with a lower level of theory and smaller basis set and sequentially optimize the geometry using the optimized geometry from the previous step as the initial geometry for the next step. Information from crystallographic databases can also be used to arrive at a better guess for Z-matrix.

2.11 Locating and Identifying Error(s)

If the program terminates abruptly, it writes the error messages in the output file. The crash could be attributed to errors in the input file. Some of the errors are – wrongly specified multiplicity (inconsistency with the charge), typographical errors in the route section, and use of integers in place of floating point numbers. Run-time errors can also occur, for example, when a bond angle reaches 180° during the optimization. To avoid such a runtime error use of *dummy atom(s)* is suggested. Dummy atoms are particularly useful for the study of ionic liquids where the cation and anion are initially connected together using a dummy atom. Then the molecule is geometrically optimized; in the final result the structure is without the dummy atom. This concept has been used by earlier work of [Meng et al., 2002] and [Turner et al., 2003] for ab-initio calculations on ionic liquids.

2.12 Benchmarking with Ionic Liquids

Geometry optimization procedure has been illustrated here for 1-ethyl-3-methyl imidazolium acetate ([EMIM][OAc] ($C_8H_{14}N_2O_2$)) which has the following structural formula as shown in Fig. 2.7.The *geometry optimization* of this IL was carried out by optimizing the cation and anion pair through dummy atom. MOLDEN [Schaftenaar 2000] was used to generate the initial structure of the ionic liquid (Figure 2.8). The corresponding Z-matrix was written to a file. The Z-matrix file was edited to specify the complete input. The charge is 0 and the multiplicity is 1. The **HF/6-31G* opt** route was used.

Figure 2.7: Molecular structure of [EMIM][OAc]

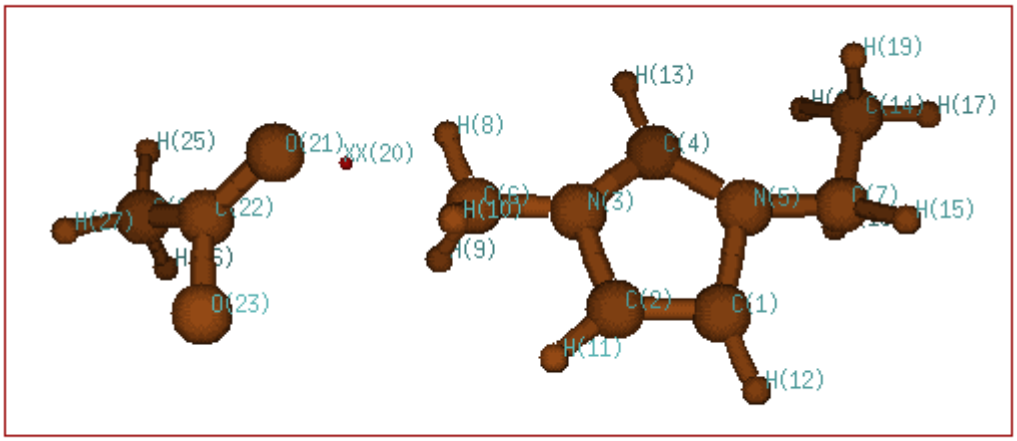

Figure 2.8: Input (starting) geometry for optimization of [EMIM][OAc]

XX denotes a dummy atom

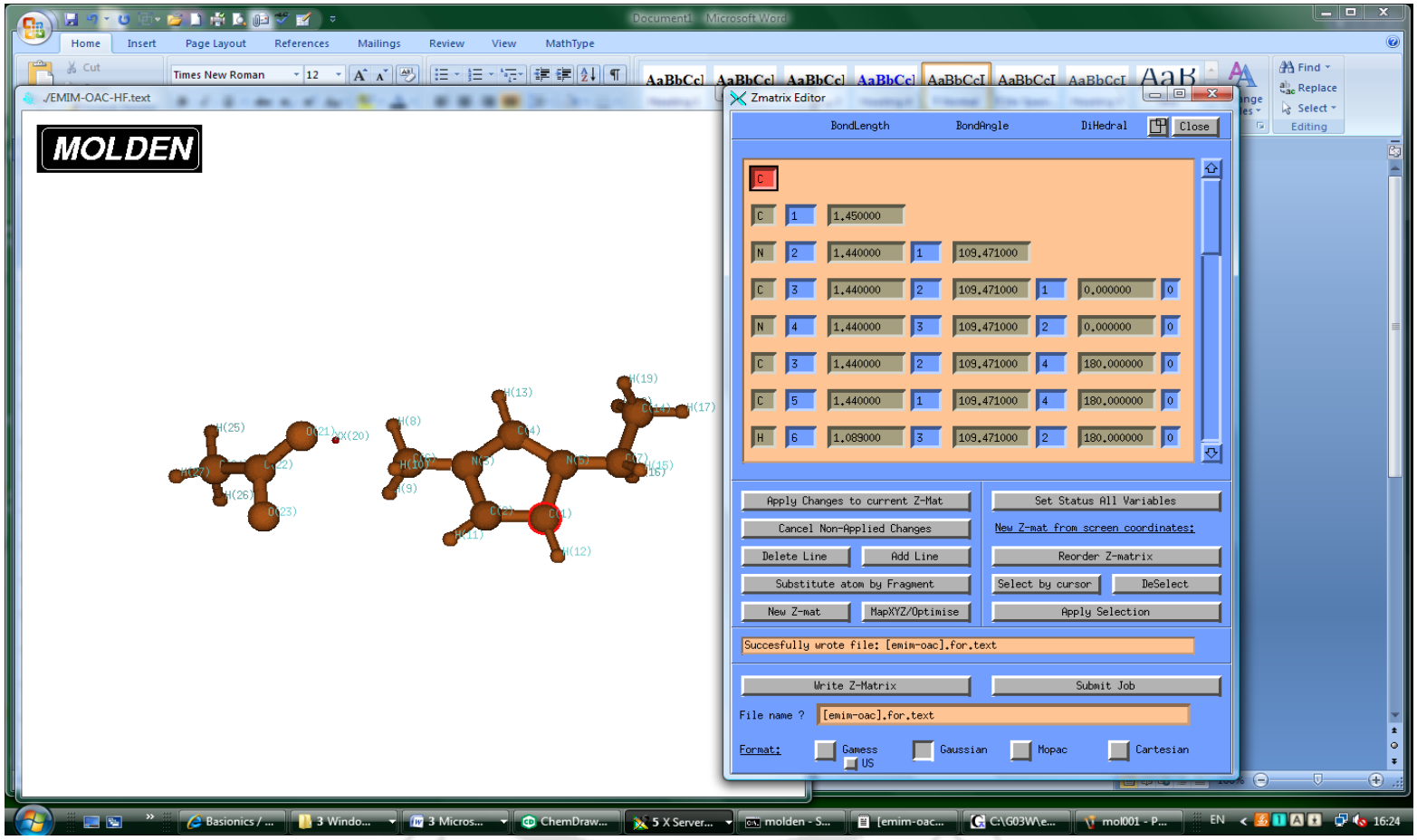

Figure 2.9: A screen shot of MOLDEN showing the final optimized [EMIM][OAc] structure and the partial Z-matrix

Frequency calculations were then done at the same level of theory using the same basis sets. No imaginary frequencies were observed that is no saddle points exist. So the obtained structure was a global minimum. The output file was viewed in MOLDEN and the final optimized structure is shown as a snapshot in Figure 2.9 along with the partial Z-matrix.

Table 2.3: Cartesian coordinates of atoms for optimized structure of [EMIM][OAc]

Atom	x	y	z
C (1)	-0.039357	-0.03044	-0.020092
C (2)	-0.0859	-0.03289	1.388942
N(3)	1.243303	-0.00024	1.899075
C(4)	2.140272	0.022678	0.83027
N(5)	1.437423	0.00616	-0.378597
C(6)	1.278697	-0.00058	3.351372
C(7)	1.637688	0.01221	-1.812038
H(8)	2.308892	0.02545	3.694964
H(9)	0.753511	0.874794	3.722236
H(10)	0.799059	-0.89887	3.727312
H(11)	-0.812832	-0.05172	2.191963
H(12)	-1.028003	-0.0545	-0.464239
C(13)	3.16641	0.047765	1.178224
H(14)	3.089622	0.013335	-2.110664
H(15)	1.179938	-0.87391	-2.238107
H(16)	1.607645	1.041793	-2.161518
H(17)	3.239048	0.014891	-3.187692
H(18)	3.553567	0.900723	-1.685674
O(19)	3.567876	-0.87039	-1.689549
C(20)	1.768956	-0.51291	6.019173
O(21)	1.134642	0.2511	6.938985
O(22)	-0.208468	0.083912	6.929742
C(23)	1.512264	1.229413	7.959299
H(24)	2.592731	1.370373	7.972284
H(25)	1.029307	2.178026	7.740669
H(26)	1.185242	0.874007	8.932601

Table 2.4: Optimized values of bond lengths, bond angles, and dihedral angles for [EMIM][OAc]

Atom		bond length		bond angle		d i h e d r a l angle
n						
c	1	1.384731				
c	2	1.342782	1	107.597		
n	3	1.374789	2	106.406	1	0.771
c	4	1.310672	3	108.829	2	-0.875
c	4	1.469552	3	125.237	2	-177.436
c	1	1.464906	2	124.29	3	179.739
c	7	1.520599	1	113.622	2	-176.166
o	3	2.928604	2	152.845	1	-162.651
o	9	1.248483	3	94.879	2	86.399
c	10	1.529802	9	115.843	3	-161.838
c	11	1.235313	10	126.14	9	17.96
h	6	1.081928	4	108.377	3	-144.458
h	6	1.076198	4	107.424	3	-23.94
h	6	1.076019	4	108.943	3	93.114
h	3	1.076578	2	134.245	1	-177.464
h	2	1.067441	3	130.926	4	179.787
h	5	1.066941	4	124.63	3	-179.394
h	7	1.081696	1	107	2	-54.331
h	7	1.082278	1	107.479	2	61.443
h	8	1.083231	7	108.639	1	179.035
h	8	1.084391	7	111.873	1	-62.328
h	8	1.084166	7	111.682	1	60.297
h	12	1.082814	11	111.516	13	1.958
h	12	1.085977	11	109.639	13	123.687
h	12	1.08625	11	109.44	13	-119.372

Zero-point correction	=0.236312(Hartree/Particle)
Thermal correction to Energy	=0.249995
Thermal correction to Enthalpy	=0.250939
Thermal correction to Gibbs Free Energy	=0.192277
Sum of electronic and zero-point Energies =	-569.446423

Figure 2.10: The results of the interact action energy appear in the regular *Gaussian* output file (red line indicates the total energy of the optimized [EMIM][OAc] structure)

The electronic state is 1-A.				
Alpha occ. eigenvalues --	-0.52036	-0.51583	-0.47158	-0.45700
Alpha occ. eigenvalues --	-0.38997	-0.35578	-0.29085	-0.24645
Alpha occ. eigenvalues --	-0.23764			
Alpha virt. eigenvalues --	0.03571	0.09744	0.12803	0.14608
Alpha virt. eigenvalues --	0.21782	0.22413	0.23087	0.24265

Figure 2.11: The results of the HOMO and LUMO energy appear in the regular *Gaussian* output file (red line indicates the HOMO values of the optimized [EMIM][OAc] structure) (blue line indicates the LUMO of the optimized [EMIM][OAc] structure)

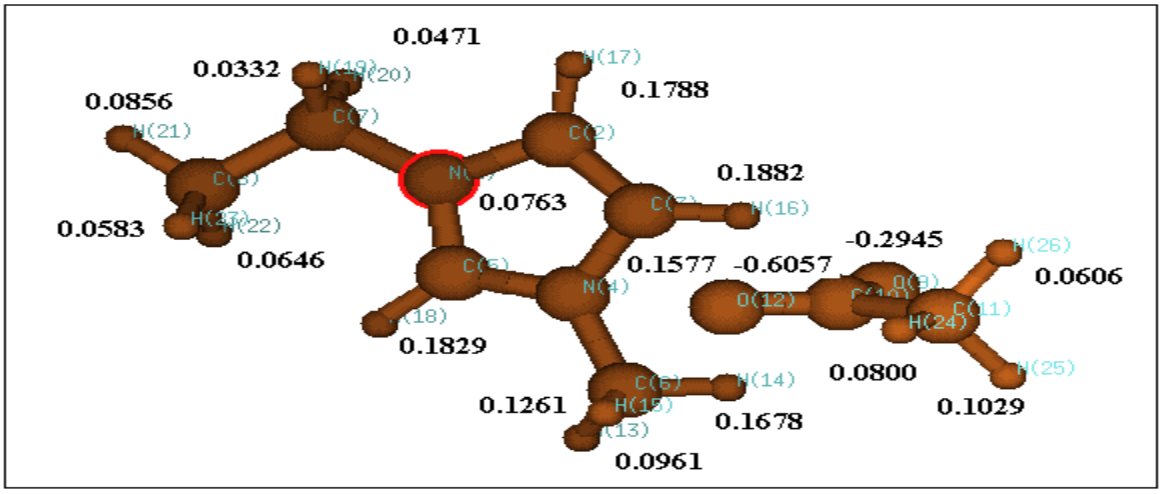

Figure 2.12: The optimized geometry with partial charge of [EMIM][OAc]

2.13 Results and Discussion

The optimized geometry of [EMIM][OAc] is shown in Figure. 2.9. The coordinates for the optimized structure are presented in Table 2.3. The optimized bond lengths, angles and dihedrals are tabulated in Table 2.4. The total energy of this stable structure is HF=-569.4464 Hartrees (Figure 2.10). The gas phase molecular structures of the ion pair [EMIM] and [OAc] are stabilized by hydrogen bonds between the O atoms in anion and various H atoms on cation. The HOMO and LUMO energy of [EMIM] is -0.23764 eV and 0.03571 eV (Figure 2.11), respectively. The other solvent properties can be calculated with the help of HOMO and LUMO energies (Figure 2.11), such as HOMO-LUMO energy gap, chemical potential, chemical softness, chemical hardness, electronegativity and electrophilicity index. These properties helps us in the understanding of the structural

properties of ionic liquid qualitatively and thus minimize the experimental cost .Furthermore, the partial charges of atom in [EMIM][OAc] are also calculated using B3LYP/6-31G* basis function (Figure 2.12).

Nomenclature

C	molecular orbital expansion coefficient
D	Slater determinant of orbitals
E	Energy
$E_{xc}[\rho]$	exchange correlation energy
E	electronic charge
	Fock operator
	Kohn-Sham operator
	One-electron operator
	Two-electron operator
	Hamiltonian operator
J_{ij}	Coulomb integral
	Coulomb operator
K_{ij}	exchange integral
	exchange operator
L	angular momentum
m_e	mass of electron
N	normalization constant
R	radial location of electron, separation distance
U	spin orbital
V	Potential
V_{xc}	exchange correlation potential
x, y, z	Coordinates
Z	nuclear charge

Greek symbols

A	Atom

E	orbital energy
P	electron probability density
Σ	Exponent
	Laplacian
Φ	basis function, orbital, electrostatic potential
Ψ	wave function

REFERENCES

Becke, A. D.Density functional calculations of molecular bond energies. *J.Chem.Phys.,* **1986,** 84, 4524-4529.

Binkley, J. Stephen; Pople, John A.; Hehre, Warren J. Self-consistent molecular orbital methods. 21. Small split-valence basis sets for first-row elements. *J.Am.Chem.Soc* **1980,**102, 939-947.

Bondi, A. van der Waals volumes and radii. *J. Phys. Chem*. **1964,** 68 ,441-451.

Born, M. Volumes and heats of hydration of ions.*Zeitschrift fuer Physik* 1 45, 1920.

Born, M.; Oppenheimer, R. Quantum theory of the molecules. *Annalen der Physik* **1927**,84, 457-484.

Boys, S. F. Electronic wave functions. I. A general method of calculation for the stationary states of any molecular system. *Proc. Roy. Soc.* **1950,** A200, 542-554.

Breneman,C.M.; Wiberg,K.B. Determining atom-centered monopoles from molecular electrostatic potentials. The need for high sampling density in formamide conformational analysis.*J. Comp. Chem.* **1990**, *11*, 361-373.

Clark,T. A Handbook of Computational Chemistry, John Wiley and Sons, New York, **1985**.

Collins, J. B.; Schleyer, P. V. R.; Binkley J. S.; Pople, J. A. Self-Consistent Molecular Orbital Methods. 17. Geometries and binding energies of second-row molecules. A comparison of three basis sets. *J.Chem.Phys*. **1976,** 64, 5142.

Cramer, C. J.; Truhlar, D.G. in: Lipkowitz, K. B.; Boyd, D.B. Reviews in Computational Chemistry vol. 6 VCH Publishers, New York, **1995.**

Ditchfield, R.; Hehre, W. J.; Pople, J. A. Self-consistent molecular-orbital methods. IX. Extended Gaussian-type basis for molecular-orbital studies of organic molecules. *J.Chem.Phys*. **1971**, 54, 724-728.

Dobbs, K. D.; Hehre, W. J. Molecular orbital theory of the properties of inorganic and organometallic compounds. 6. Extended basis sets for second-row transition metals. *J.Comp.Chem.* **1987**, 8, 880-893.

Dobbs, K. D.; Hehre, W. J. Molecular orbital theory of the properties of inorganic and organometallic compounds. 4. Extended basis sets for third- and fourth-row, main-group elements. *J.Comp.Chem.* **1986**, 7, 359-378.

Dobbs, K. D.; Hehre, W. J. Molecular orbital theory of the properties of inorganic and organometallic compounds. 5. Extended basis sets for first-row transition metals. *J.Comp.Chem.* **1987**, 8, 861-879.

Foresman, J. B.; Frisch, Æ. Exploring Chemistry with Electronic Structure Methods, 2nd edition. Gaussian Inc., Pittsburgh, **1996**.

Frisch, Æ.; Frisch, M. J. Gaussian 98 User's Reference, 2nd edition, Gaussian, Inc. Pittsburgh, **1999.**

Frisch.J.M, G. W. Trucks, H. B. Schlegel, G. E. Scuseria, M. A. Robb, J. R. Cheeseman, J. A. Montgomery, Jr., T. Vreven, K. N. Kudin, J. C. Burant, J. M. Millam, S. S. Iyengar, J. Tomasi,V. Barone, B. Mennucci, M. Cossi, G. Scalmani, N. Rega,G. A. Petersson, H. Nakatsuji, M. Hada, M. Ehara, K. Toyota,R. Fukuda, J. Hasegawa, M. Ishida, T. Nakajima, Y. Honda, O. Kitao, H. Nakai, M. Klene, X. Li, J. E. Knox, H. P. Hratchian, J. B. Cross,C. Adamo, J. Jaramillo, R. Gomperts, R. E. Stratmann, O. Yazyev, A. J. Austin, R. Cammi, C. Pomelli, J. W. Ochterski, P. Y. Ayala,K. Morokuma, G. A. Voth, P. Salvador, J. J. Dannenberg,V. G. Zakrzewski, S. Dapprich, A. D. Daniels, M. C. Strain, O. Farkas, D. K. Malick, A. D. Rabuck, K. Raghavachari,J. B. Foresman, J. V. Ortiz, Q. Cui, A. G. Baboul, S. Clifford,J. Cioslowski, B. B. Stefanov, G. Liu, A. Liashenko, P. Piskorz, I. Komaromi, R. L. Martin, D. J. Fox, T. Keith, M. A. Al-Laham,C. Y. Peng, A. Nanayakkara, M. Challacombe, P. M. W. Gill, B. Johnson, W. Chen, M. W. Wong, C. Gonzalez, and J. A. Pople, Gaussian, Inc., Wallingford CT, Gaussian 03, Revision C.02, **2004**.

Geerlings,P.; Proft,F.; Langenaeker,W. Conceptual Density Functional Theory. *Chemical Reviews*, **2003**,103, 1793-1873.

Gordon, M.S.; Stephen,B.J.; Pople, J.A.; Pietro, W.J.; Hehre, W.J. Self-consistent molecular-orbital methods. 22. Small split-valence basis sets for second-row elements.*J.Am.Chem.Soc.***1982,** 104, 2797-2803.

Guner, V.; Khuong, K. S.; Leach, A. G.; Lee, P. S.; Bartberger, M. D.; Houk, K. **N.**A Standard Set of Pericyclic Reactions of Hydrocarbons for the Benchmarking of Computational Methods: The Performance of ab Initio, Density Functional, CASSCF, CASPT2, and CBS-QB3 Methods for the Prediction of Activation Barriers, Reaction Energetics, and Transition State Geometries *J. Phys. Chem. A.* **2003**,*107*, 11445-11459.

Hariharan, P. C.; Pople, J. A. Accuracy of AHn equilibrium geometries by single determinant molecular orbital theory. *Mol. Phys.***1974,** 27, 209-214 .

Hehre, W. J.; Ditchfield, R.; Pople, J. A. Self-consistent molecular orbital methods. XII. Further extensions of Gaussian-type basis sets for use in molecular orbital studies of organic molecules.*J.Chem.Phys*. **1972**, 56, 2257-2261.

Hehre, W. J.; Stewart, R. F.; Pople, J. A. Self-consistent molecular-orbital methods. I. Use of Gaussian expansions of Slater-type atomic orbitals. *J.Chem.Phys*. **1969**, 51, 2657-2664.

Heyman, A.; Musgrave, CB .A quantum chemical study of the atomic layer deposition of Al_2O_3 using $AlCl_3$ and H_2O as precursors , *J. Phys. Chem. B* **2004**,108,5718-5725.

Hohenberg P.; Kohn, W. Inhomogeneous Electron Gas. *Physical Review.* **136**, B864, **1964**.

Höltje, Hans-Dieter; Folkerts, G. Molecular Modeling: Basic Principles and Applications, VCH, **1996.**

Hunt, P.A.; Gould,I.R. The structure of imidazolium-based ionic liquids: Insights from ion-pair interactions. Aust.J.Chem. 2007, 60, 9-14.

Irfan,a.; Cui,R.; Zhang,J.Explaining the HOMO and LUMO distribution on individual ligands in mer-Alq3 and its "CH"/N substituted derivatives.*J.Mol.Structure.THEOCHEM* **2008**,850,79-83.

Jurecka.P.;Nachtigall.P.;Hobza.P.RI-MP2 calculations with extended basis sets — a promising tool for study of H-bonded and stacked DNA base pairs *Phys. Chem. Chem. Phys.*, **2001**, 3, 4578-4582.

Kohn, W.; Sham, L. Self-Consistent Equations Including Exchange and Correlation Effects. *Physical Review.***1965,** 140, A1133-A1138.

Koopmans, T. Über die Zuordnung von Wellenfunktionen und Eigenwerten zu den Einzelnen Elektronen Eines Atoms. *Physica* (Elsevier), **1934**, **1**, 104–113.

Lee,C.;Yang, W.; Parr, R. G. Development of the Colle-Salvetti correlation-energy formula into a functional of the electron density. *Phys. Rev. B,* **1988,** 37, 785-789.

Levine, I. N. Quantum Chemistry, 4th ed., Prentice Hall, New Jersey, **1991.**

Liu.T,Gu.J.D.;Tan.X.J.;Zhu.W.L.;Luo.X.M.;Jiang.H.L.;Ji.R.Y.;Chen.K.X.;Silman.I.; Sussman.J.L. Theoretical insight into the interactions of TMA-benzene and TMA-pyrrole with B3LYP density-functional theory (DFT) and *ab initio* second order Moller-Plesset perturbation theory (MP2) calculations *J. Phys. Chem. A*, **2001**, 105, 5431-5437.

Meng.J.; Dolle.A.; Carper. R.W. Gas Phase Model of an Ionic Liquid: semi-empirical and ab-initio bonding and molecular structure, *J. Mol. Struct. (Theochem)* **2002**, 585,119–125.

Moller, Chr.; Plesset, M. S. Note on the approximation treatment for many-electron systems.*Physical Review* **1934,**46, 618-622.

Paulechka, Y. U.; Kabo, G. J.; Blokhin, A. V.; Vydrov, O. A.; Magee, J. W.; Frenkel, M. Thermodynamic properties of 1-butyl-3methylimidazolium hexafluorophosphate in the ideal gas state. *J. Chem. Eng. Data* **2003**,48, 457-462.

Pejov.L. A gradient-corrected density functional and MP2 study of phenol-ammonia and phenol-ammonia + hydrogen-bonded complexes .*Chem. Phys.* **2002**, 285, 177-193.

Perdew, J. P., Burke, K., Enzerhof, M**.** Generalized Gradient Approximation Made Simple: Errata *Phys. Rev. Lett.,***1997**,78, 1396.

Perdew, J. P., Burke, K., Enzerhof, M. Generalized Gradient Approximation Made Simple. *Phys. Rev. Lett.,* **1996** 77, 3865-3868.

Perdew, J. P.;Wang, Y. Accurate and simple analytic representation of the electron-gas correlation energy **1992,***Phys. Rev. B,* 45, 13244-13249.

Perdew,J. P.; Wang, Y. Accurate and simple density functional for the electronic exchange energy: Generalized gradient approximation *Phys. Rev. B,* **1986**, 33, 8800-8802.

Perdew.J. P. Density-functional approximation for the correlation energy of the inhomogeneous electron gas, *Phys. Rev. B* **1986** ,33, 8822-8824.

Pietro, W. J.; Francl, M. M.; Hehre, W. J.; DeFrees, D. J.; Pople, J. A.; Binkley, J. S. Self-consistent molecular orbital methods. 24. Supplemented small split-valence basis sets for second-row elements.*J.Am.Chem.Soc.***1982,** 104, 5039-5048.

Safi.B.;Choho.K.; Proft.F.; Geerlings.P.Theoretical Study of the methylamines basicity in vacuo and in different solvents : a DFT study. *Chem. Phys. Lett.***1999** 300, 85-92.

Sancho-Garcia, J. C**.**Assessment of Recently Developed Multicoefficient Strategies for the Treatment of π**-Conjugated Molecules .**J. Phys. Chem. A. ***2005*****, 109**, *3470-3475.*

Schäfer.A.;Huber.C.;Ahlrichs.R., Fully optimized contracted Gaussian basis sets of triple zeta valence quality for atoms Li to Kr, *J. Chem. Phys.***1994**,100, 5829-5835.

Schaftenaar, G.; Noordik, J.H. Molden: a pre- and post-processing program for molecular and electronic structures. *J. Comput.-Aided Mol. Design* **2000**,14, 123-134.

Shaabani,A.Frontier Orbitals Aromaticity:A Simple Approach to the analysis of Pericyclci Reactions.*J.Iran.Chem.Soc*.**2008**,47-53.

Shah, J. K.; Brennecke, J. F.; Maginn, E. J. Thermodynamic properties of the liquid 1-n-butyl-3-methylimidazolium hexafluorophosphate from Monte Carlo simulations. *Green Chemistry,* 2002, 4, 112-118.
Slater, J. C. Atomic Shielding Constants. *Physical Review* **1930,**36, 57-64.

Sosa.C, J.; Andzelm, B. C. Elkin, E. Wimmer, K. D. Dobbs.; Dixon D. A., A local density functional study of the structure and vibrational frequencies of molecular transition-metal compounds, *J. Phys. Chem.* **1992**, 96, 6630-6636.

Tomasi, J.; Persico, M. Molecular Interactions in Solution: An Overview of Methods Based on Continuous Distributions of the Solvent. *Chem. Rev*. **1994,**94, 2027-2094.

Turner. A. E.; Pye. C. C.; Singer. D. R., Use of ab initio Calculations toward the Rational Design of Room Temperature Ionic Liquids, *J. Phys. Chem. A,* **2003,** 107, 2277-2288.

Varganov.S.A.; Avramov.P.V.; Ovchinnikov.S.G.;Gordon.M.S. A study of the isomers of C36 fullerene using single and multireference MP2 perturbation theory. *Chem. Phys. Lett.* **2002**, 362, 380-386.

Wolfsberg, M.; Helmholz, L. The spectra and electronic structure of the tetrahedral ions MnO_4^-, CrO_4^{--}, and ClO_4^-. *J.Chem.Phys*. **1952**, 20, 837-843.

Yu E.Zevatski, Y.E.; Samoilov, D.V.Some Modern Methods for Estimation of Reactivity of Organic Compounds. Russian *J.Orga.Chemistry*.**2007**,43,487-504.

Zhou, J.; Mao, J.; Zhang, S. Ab initio calculations of the interaction between thiophene and ionic liquids. J.Fuel Proc.Tech. 2008, 89, 1456-1460.

3.1 Introduction

To study chemical process involving ionic liquid with other compounds it is necessary to understand reactivity and stability of the interacting system via HOMO/LUMO energies with its energy gap. However till date an approach based on simultaneous interaction has not been attempted.

Table 3.1.Ionic Liquids used in this work.

Ionic Liquid	Cation	Anion
[BUMPYR][BF_4]		
[BUMPYR][PF_6]		
[BeMIM][BF_4]		

[BUMPY][BF_4]		
[BUMPY][PF_6]		

In the present work, we have investigated the scalar quantities at micro level for the cations namely: 1-Butyl-1-Methylpyrrolidinium ([BUMPYR]),1-Butyl-4-Methylpyridinium ([BUMPY]) and 1-Benzyl-3-Methylimidazolium ([BeMIM]) combined with inorganic anions: (tetrafluoroborate ([BF_4]) and hexafluorophosphate ([PF_6]))(Table 3.1).Our aim is to determine the scalar quantities with respect to the simultaneous removal of thiophene (TS) and pyridine(PY)(Table 3.2).In subsequent sections the scalar parameters will be determined for clusters consisting of IL-thiophene, IL-pyridine and IL-thiophene-pyridine. However the present study is the first attempt to study the simultaneous removal of both pyridine and thiophene on a quantum chemical scale. Further for the first time the effect of other cations namely the pyridinium, pyrrolidinium and benzylimidazolium have also been taken up.

Table 3.2: Sulfur and Nitrogen based component used in this work.

Thiophene[TS]	Pyridine[PY]

3.2 Theoretical background

A chemical system can be of several molecules in a state of interaction, which includes hydrogen-bond interaction, electrostatic interaction, and LUMO-HOMO interaction. In quantum chemistry methods there are seven basic parameters of importance such as LUMO energy, HOMO energy, LUMO-HOMO energy gap, chemical potential ( ), electro negativity ( ), global or absolute chemical hardness ( ), chemical softness (S) and electrophlicity index ( ). Chattaraj et al [1991,2006] studied the electronic structure principles in static and dynamic situations, which gave a more theoretical basis for electro negativity, chemical hardness and electrophilicity. The definitions and nomenclature for the entire scalar quantities are given in Table 2.2.We will briefly discuss the scalar properties in the subsequent sub-sections.

3.2.1 LUMO and HOMO energies

The energy of the LUMO is directly related to the electron affinity and characterizes the susceptibility of the molecule toward attack by nucleophiles [Karelson et al., 1996]. An electron affinity (EA) refers to the capability of a ligand to accept precisely one electron from a donor. However, to influence the interacting systems, covalent or hydrogen bonding may take place which can result in a partial charge transfer [Thankaivelan et al., 2000].

A current approximation is to use Koopmans' theorem to express these quantities in terms of the frontier one electron energy levels : HOMO and LUMO [Fuentealba et al.,2000,2002].The energy of the HOMO is directly related to the ionization potential (IP) and characterizes the susceptibility of the molecules toward attack by electrophiles. Hard nucleophiles have a low HOMO energy while hard electrophiles have a high LUMO energy. The operational definition of LUMO and HOMO in the context of DFT can be written as:

(3.1)

(3.2)

Where and correspond to the Kohn–Sham [1965] one electron eigenvalues associated to the frontier molecular orbitals: HOMO and LUMO, respectively. IP and EA refers to ionization potential and electron affinity of the system respectively.

3.2.2 HOMO-LUMO energy gap

HOMO-LUMO energy gap are used as a quantum chemical descriptor in establishing correlations for chemical and biochemical systems [Francisco et al., 2008].A large HOMO-LUMO gap implies high stability for the molecules in the sense of its lower charge transfer in complexes. Polarizability is another characteristic property which is related to HOMO-LUMO energy gap. Soft molecules, with small energy gap will be more polarizable than hard molecules. Their mathematical expression can be defined as

(3.3)

3.2.3 Chemical potential ( ) and Electro negativity ( )

Chemical potential measures the escaping tendency of an electron cloud and is termed as a global property at the ground state as it characterizes the species as a whole. Pauling [1960] introduced the concept of electronegativity as the power of an atom in a molecule to attract electrons to itself. For atomic species, the chemical potential is simply the negative of Muilliken electro negativity (χ), also called as absolute electro negativity.

3.2.4 .Global hardness ( ) and global softness(S)

Roy et al.,[1998] have used hardness as a tool to understand charge transfer and other properties on a molecular system. It was found that stability of the interacting molecules is related to hardness. The global hardness can be seen as the resistance for a chemical species for charge transfer. Palke and Pearson [1992] provided the analytical definition of global hardness as given in Table 2.2. Softness is a property of molecules that measures the extent of charge transfer. It is the reciprocal of hardness [Kolandaivel et al., 1996].

3.2.5 Electrophilicity index ( )

Parr et al.[1999] proposed electrophilicity index as a measure of energy lowering due to the electron flow between donor and acceptor. The mathematical expression is given in Table 2.3. For DFT within the Koopmans theorem [1934] for closed shell species, the ionization energy(IP) and electron affinity (EA) can be approximately expressed as given in equation 3.1 and 3.2. Schematic representations of all these parameters are given in terms of total orbital energy or relative energy diagram (Figure 3.1). It offers a concise way of defining electro negativity and chemical hardness. LUMO-HOMO energy gap are also termed as the anti bonding and bonding molecular orbitals of molecules. In a recent work soft x-ray emission spectra concluded that the imidazolium based cations occupies the HOMO states [Kanai et al.,2008] .Thus all the scalar properties are global properties in the sense that they characterize the complex species such as IL, IL-thiophene, IL-pyridine and IL-thiophene-pyridine.

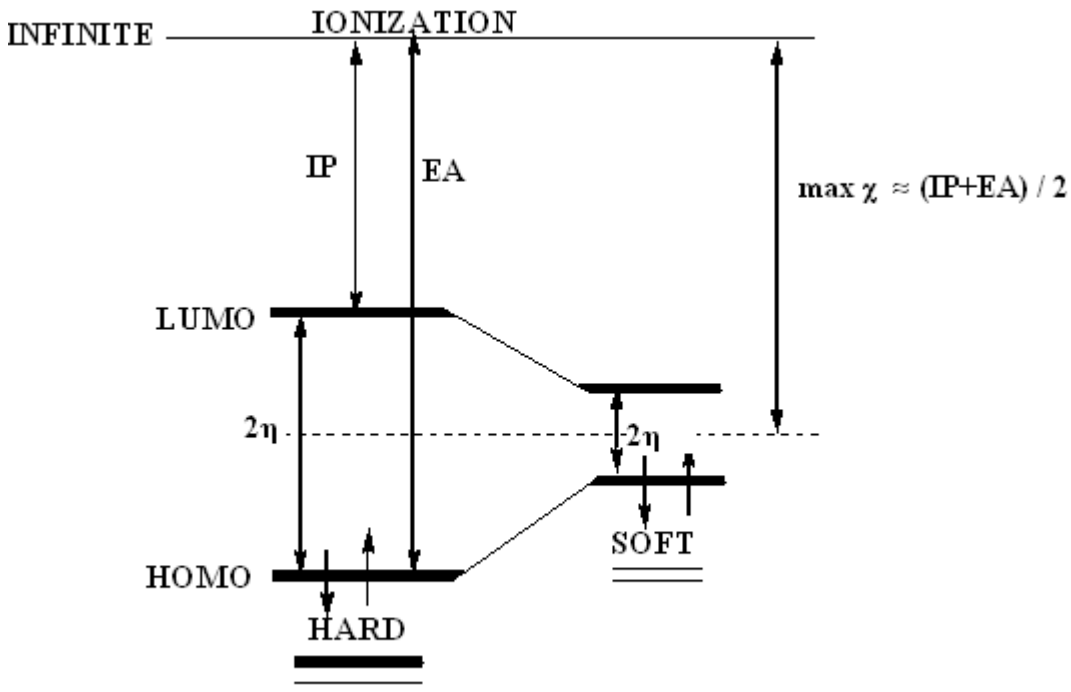

Figure 3.1: Diagram of the molecular orbital energy of molecules.

3.3 Global Scalar Properties

The initial structures of thiophene, pyridine, cations, anions and clusters containing ionic liquid were drawn by MOLDEN [Schaftenaar et al.,2000] visualization package. Dummy atoms have been used for interconnecting molecules thereby making clusters. The concept has been used earlier by Meng et al., [2002] and Turner et al [2003] for ab-initio

density functional theory calculations on ionic liquids. The optimized geometry of the studied systems were performed using Hartree-Fock theory (HF) with 6-31G* basis set. The density functional theory of Becke's three parameter exact exchange functional together with the gradient corrected correlation functional of Lee, Yang and Parr represented as B3LYP [Becke et al.,1986] were used to compute the partial charges of each atom along with the CHELPG scheme[Breneman et al.,1990] via ESP fit at 6-311+G* basis set. For example, the optimized structure with partial charges of [BeMIM][BF_4]-TS-PY is shown in Figure 3.2.

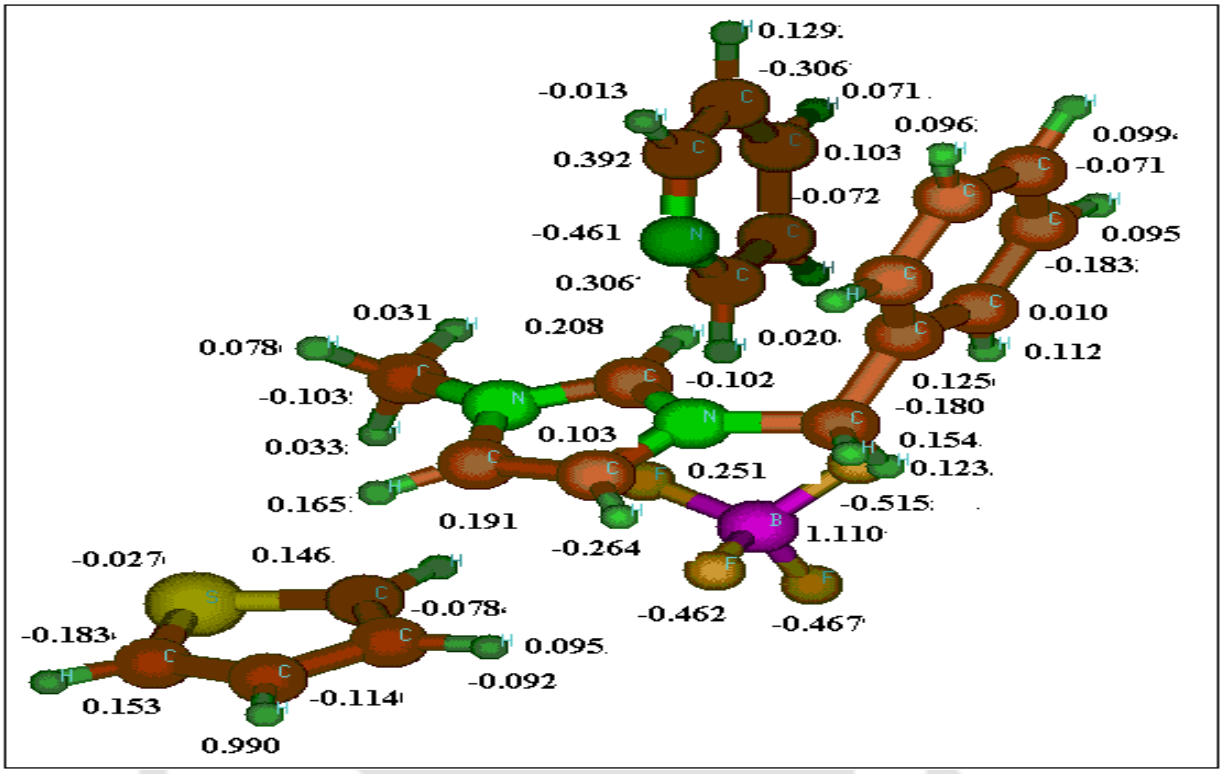

Figure 3.2: Optimized geometries and partial charges for [BeMIM][BF_4]-Thiophene-Pyridine

Thereafter the chemical potential (μ), electro negativity (χ), global hardness (η), global softness(S) and electrophilicity index (ώ) have been determined for the optimized structures as discussed in Table 2.2. The chemical hardness have been calculated at the Hatree Fock level theory, since the LUMO/HOMO energies or orbital energies calculated by

this level is more meaningful and accurate [Nirmala et al.,2006]. The highest occupied orbital (HOMO) and lowest unoccupied (LUMO) orbital energies were found at HF/6-31G* level. Diffuse functions are added in the basis set for studying the inter- and intra-molecular interactions [Selvarengan et al., 2002]. All the calculations were performed with the GAUSSIAN03 computational package [Frisch et al., 2003]. It should be noted that the quantum chemistry calculations is done on the similar lines as per earlier authors [Hernandez et al., 2009; Yu et al., 2007; Cruz et al., 2008]. Thus the calculations are done is vacuum and no packing effects within the liquids are assumed.

3.4 Result and Discussion

3.4.1 HOMO/LUMO energies

The highest occupied molecular orbital (HOMO) and lowest unoccupied molecular orbital (LUMO) are the most important aspects for the simultaneous removal of thiophene and pyridine. HOMO and LUMO are the likely locations where the external network or connectivity occurs through cation and anion of ionic liquid [Lacrama et al., 2007; Nishi et al., 2008]. The external connectivity is due to the electrons in the HOMO, which has the highest energy and therefore willing to make external interaction with thiophene and pyridine. Thus the HOMO energies are important to predict the stability of the molecules. The LUMO is a likely location for a bond to occur as incoming electrons from other molecules will fill into the LUMO orbital.

The cations and anions are listed in Table 3.1.The HOMO and LUMO energies of thiophene, pyridine, anions and cations are predicted and shown in Figure 3.3. A slight difference in HOMO and LUMO energies are observed between thiophene and pyridine. The HOMO energy of thiophene is -0.30439 Hartrees, which is slightly lesser than that of pyridine (-0.32104 Hartrees).The LUMO energy of thiophene is 0.13298 while LUMO of pyridine is 0.11255.This indicates that thiophene is slightly more stable than pyridine because lower the LUMO energy, more stable the molecule [Karelson et al.,1996].

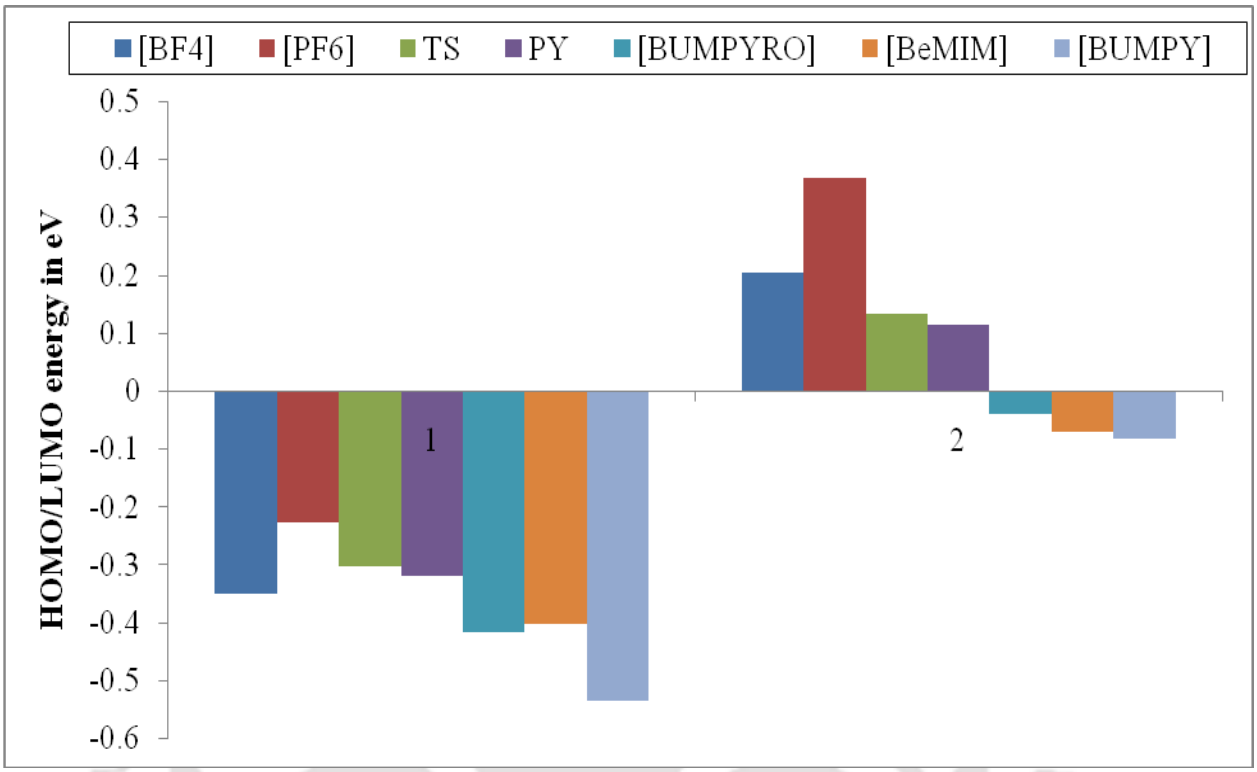

Figure 3.3: HOMO and LUMO energies for thiophene, pyridine, anions and cations

Among the anions the most stable anion was BF_4. BF_4 had HOMO energy of -0.35084 Hartree and LUMO energy of 0.2039 Hartree while PF_6 had a HOMO energy of -0.22893 Hartree and LUMO energy of 0.36732 Hartree. Based on the HOMO energies BF_4

is less reactive than PF_6. This is again in agreement with the overall energy of the BF_4 (-422.737128 hartrees) which is less than that of PF_6 (-937.611463 hartrees).Similar results were obtained from Zhao et al. [2008] in their study on IL-thiophene interaction. Among the cations the HOMO energy followed the order : [BUMPY] > [BeMIM] > [BUMPYR]. All cations possessed negative HOMO energies of -0.5362 -0.40364 and -0.41771 Hartrees and LUMO energies of -0.08242, -0.07163 and -0.03998 Hartrees respectively. Cations having electron donor tendency, is able to form external connectivity with other molecules via CH-π bonds. This agrees well with the findings of Geerlings et al.[2003]. It should be noted that thiophene and pyridine requires electron acceptors because of its positive HOMO energies. Thus thiophene and pyridine will interact with the LUMO of cations enabling better separation (Figure 3.4). This is consistent with the work of Nishi et al.,[2008] where it was found that HOMO energy of IL is derived from the anion while the LUMO comes from cation. Thus the top part of occupied states and the bottom part of the unoccupied states for ionic liquids correspond to anions and cations respectively. This implies that the incoming thiophene and pyridine molecule occupies the unoccupied states of the ionic liquid i.e cation resulting in CH-π bonds.

The ionic liquids possessed different values of HOMO and LUMO energies, which decreases in the order (in terms of HOMO) (Table 3.3): [BUMPY][PF_6] > [BeMIM][BF_4] > [BUMPY][BF_4],[BUMPYR][PF_6] > [BUMPYR][BF_4] (HOMO: -0.32952 >-0.32067 > -0.31079 >-0.27403 > -0.2656).The corresponding LUMO values are -0.0226, 0.00735, 0.00602, 0.02273, and 0.00608 respectively. Based on the HOMO/LUMO energies [BUMPY][PF_6] posses lesser stability among the ILs. It should be noted that higher negative values of LUMO or HOMO energies indicates less stability and more reactivity respectively. This is consistent with the work of Vektariene et al. [2009], where chemical stability of aromatic compounds was obtained using HOMO/LUMO energies. However for complexes involving ionic liquids, the LUMO energies are more important since the LUMO sites leads

to the overlapping of the incoming HOMO orbitals of thiophene or pyridine molecules as previously discussed. Thus chemical stability of ionic liquid via LUMO and its external interacting connectivity are prominent factors for the simultaneous removal of thiophene and pyridine with ionic liquids.

The HOMO and LUMO energies are significant not only in ionic liquid but in other complexes also as charge distribution are likely to be more significant than other interaction forces [Thanikaivelan et al.,2000]. With respect to LUMO energies the most favorable IL for the removal of thiophene follows the order : [BUMPY][BF_4] >[BUMPYR][PF_6]> [BUMPY][PF_6] > [BUMPYR][BF_4] > [BeMIM][BF_4], while for pyridine removal it follows: [BUMPYR][BF_4] >[BeMIM][BF_4]> [BUMPY][PF_6] >[BUMPY][BF_4] > [BUMPYR] [PF_6]. The effect of HOMO and LUMO energies are given in Table 3.3 for the simultaneous cluster: IL-TS-PY. Increasing size of cation leads to a lowering of positive charges of cation thereby increasing chemical polarizibility or decreasing stability. Thus for the simultaneous removal it follows the order:[BeMIM][BF_4] >[BUMPYR][BF_4] > [BUMPY][PF_6] >[BUMPY][BF_4] >[BUMPYR][PF_6]. Here the size of [BeMIM] is largest among all the cations studied.

Figure 3.4: Schematic diagram of HOMO-LUMO interaction energy of molecules

3.4.2 HOMO-LUMO energy gap

High chemical polarizability is a characteristic property attributed to ionic liquid due to their charge–ordering structures [Thanikaivelan et al., 2000]. Our results show that a similar HOMO-LUMO gap energy exist between cations and anions of different ionic liquids (Table 3.3). This implies that the investigated ionic liquids ([BUMPY][PF_6], [BeMIM][BF_4] [BUMPY][BF_4],[BUMPYR][PF_6] and [BUMPYR][BF_4]) have a small HOMO-LUMO gap. Thus the ionic liquids are more reactive, less stable and have a higher tendency to attract thiophene and pyridine. Based on the HOMO-LUMO gap the interaction of ILs towards

thiophene and pyridine followed the order: [BeMIM][BF_4] > [BUMPY][BF_4] > [BUMPY][PF_6] > [BUMPYR][PF_6] > [BUMPYR][BF_4].

The HOMO-LUMO energy gap in IL–thiophene and IL - pyridine could also induce a variation in their complex cluster. The LUMO values of ILs corresponding to the cation(s) are overlapped by the HOMO of thiophene and pyridine, as the two components posses a higher HOMO than those of [BF_4] and [PF_6]. Additionally the high LUMO values of the anions are not sufficiently lowered by the cation of the HOMO, which are having negative values. Thus the lower HOMO energy of thiophene/pyridine combined with higher LUMO energy of the ILs provides a pathway for the simultaneous removal of thiophene and pyridine molecules. The results for IL-thiophene,IL-pyridine and IL-thiophene-pyridine complexes are given in Table 3.3, which follows the order: [BUMPY][BF_4] > [BUMPYR][PF_6] > [BUMPYR][BF_4] > [BeMIM][BF_4] >[BUMPY][PF_6] for IL-TS, [BUMPYR][BF_4] > [BUMPYR][PF_6] > [BeMIM][BF_4] > [BUMPY][BF_4] > [BUMPY][PF_6] for IL-PY and [BeMIM][BF_4] > [BUMPYR][BF_4] > [BUMPYR][PF_6] > [BUMPY][BF_4] > [BUMPY][PF_6] for IL-thiophene-pyridine.

3.4.3 Global hardness and Global softness

Global hardness and global softness for [BUMPYRO][BF_4], [BUMPYRO][PF_6], [BeMIM][BF_4], [BUMPY][BF_4], [BUMPY][PF_6] ionic liquids are given in Table 3.4. The qualitative definition of hardness is closely related to the polarizability while softness is directly related to electron affinity [Pearson et al., 1992; Kolandaivel et al., 1996]. Thiophene, pyridine, anions and cations posses more softness and less hardness. The resistances of studied molecules are very less due to the electron transfer from electron donor to acceptor and vice versa. The maximum softness is favorable which can result in an

extended molecular interaction through H-bond network or increasing π density in aromatic compounds such as thiophene and pyridine [Lacrama et al., 2007].

Table 3.3: The HOMO/LUMO and HOMO-LUMO energy gap for structure and its cluster

S.No	Name	HOMO	LUMO	HOMO-LUMO energy gap
01	TS	-0.304	0.133	0.437
02	PY	-0.321	0.113	0.434
03	$[BF_4]$	-0.351	0.204	0.555
04	$[PF_6]$	-0.229	0.367	0.596
05	[BUMPYR]	-0.418	-0.039	0.378
06	[BeMIM]	-0.404	-0.072	0.332
07	[BUMPY]	-0.536	-0.082	0.454
08	[BUMPYR]$[BF_4]$	-0.265	0.006	0.271
09	[BUMPYR]$[PF_6]$	-0.274	0.023	0.297
10	[BeMIM]$[BF_4]$	-0.321	0.007	0.321
11	[BUMPY]$[BF_4]$	-0.311	0.006	0.310
12	[BUMPY]$[PF_6]$	-0.329	-0.023	0.329
13	[BUMPYR]$[BF_4]$-TS	-0.237	0.011	0.247
14	[BUMPYR]$[PF_6]$-TS	-0.259	-0.023	0.237
15	[BeMIM]$[BF_4]$-TS	-0.261	0.019	0.279
16	[BUMPY]$[BF_4]$-TS	-0.229	-0.031	0.199
17	[BUMPY]$[PF_6]$-TS	-0.329	-0.023	0.307
18	[BUMPYR]$[BF_4]$-PY	-0.191	-0.012	0.179
19	[BUMPYR]$[PF_6]$-PY	-0.202	0.059	0.261
20	[BeMIM]$[BF_4]$-PY	-0.308	0.011	0.319
21	[BUMPY]$[BF_4]$-PY	-0.328	0.049	0.049
22	[BUMPY]$[PF_6]$-PY	-0.319	0.031	0.351
23	[BUMPYR]$[BF_4]$-TS-PY	-0.194	0.012	0.205

24	[BUMPYR][PF_6]-TS-PY	-0.222	0.071	0.293
25	[BeMIM][BF_4]-TS-PY	-0.233	-0.044	0.188
26	[BUMPY][BF_4]-TS-PY	-0.306	0.056	0.362
27	[BUMPY][PF_6]-TS-PY	-0.306	0.048	0.354

Table 3.4: Global softness and hardness for the studied complexes calculated at B3LYP/6-31G* level theory.

S.No	ILs Name	Global softness (S)	Global hardness (η)
1	[BUMPYRO][BF_4]	7.37246	0.12956
2	[BUMPYRO][PF_6]	6.73945	0.13398
3	[BeMIM][BF_4]	6.09719	0.16401
4	[BUMPY][BF_4]	6.31293	0.15841
5	[BUMPY][PF_6]	6.51636	0.15346
6	[BUMPYRO][BF_4]-TS	8.07624	0.12382
7	[BUMPYRO][PF_6]-TS	8.43989	0.11849
8	[BeMIM][BF_4]-TS	7.1605	0.13966
9	[BUMPY][BF_4]-TS	10.0462	0.09954
10	[BUMPY][PF_6]-TS	6.15636	0.15346
11	[BUMPYRO][BF_4]-PY	11.1589	0.08962
12	[BUMPYRO][PF_6]-PY	7.65902	0.13057
13	[BeMIM][BF_4]-PY	6.2690	0.15952
14	[BUMPY][BF_4]-PY	5.30532	0.18849
15	[BUMPY][PF_6]-PY	5.69605	0.17556

The global softness and hardness of ILs and IL -thiophene/pyridine was determined and shown in Figure 3.5. The global softness of ILs increases with reducing global hardness because ILs are chemically less stable owing to their HOMO-LUMO gap. Increasing global softness and decreasing hardness are related phenomena as it leads to strengthening the interaction towards thiophene and pyridine molecules via HOMO/LUMO interaction. However, for (ILs - thiophene/pyridine) the global softness and global hardness shows a similar trend with respect to IL's profile. Therefore, the (softness/hardness) differences indicate that the combination of anion and cation is important for the simultaneous interaction of ILs with thiophene and pyridine. The cations with high softness provide a media to form CH-π interaction between cation-pyridine and cation-thiophene .This agrees well with our earlier findings reported in section 3.4.1 where the overlap of LUMO (cations) is seen with HOMO (thiophene/pyridine). Thus based on global softness for ILs- thiophene separation, [BUMPY][BF_4] has the highest softness and posses the highest separation ability for thiophene. Similarly [BUMPYR][BF_4] has the highest affinity for pyridine and [BeMIM][BF_4] for IL- thiophene-pyridine (Figure 3.2). The results exactly match the order as mentioned in section 3.4.1 and 3.4.2 while discussing LUMO energies and HOMO-LUMO energy gap respectively.

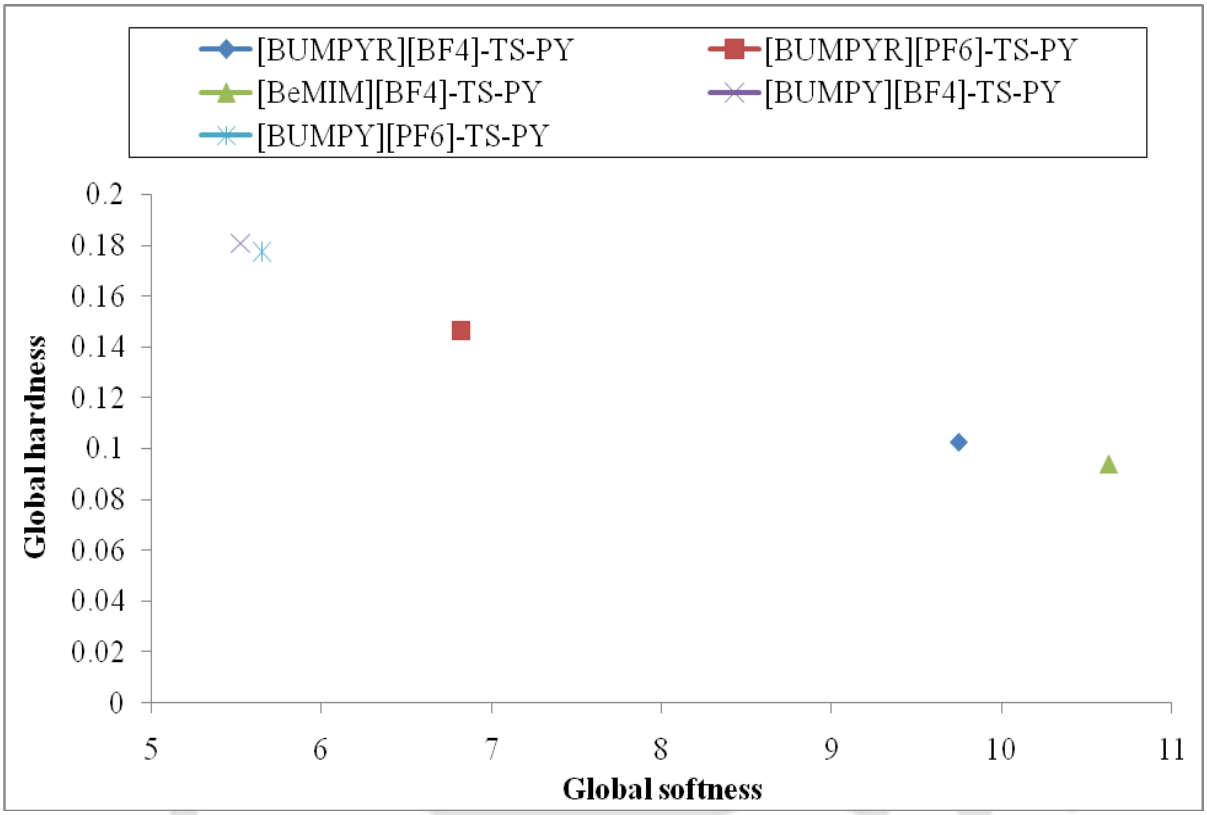

Figure 3.5: Global softness and Hardness for studied Ionic Liquid + thiophene + pyridine

3.4.4. Electrophilicity index and Electro negativity

Table 3. 5 show the measured electrophilicity and electro negativity for the studied ILs and its complexes. It can be seen that electrophilicity increases with increasing electronegativity. This is evident from the fact that a nucleophile can donate maximum number of electrons while for an electrophile it is the reverse. This trend can be explained in the ionic liquid and its complex behavior with thiophene and pyridine.Figure.3.6 shows the calculated electrophilicity and electro negativity of complexes with thiophene and pyridine respectively. The plot being linear proves that there is a possibility of strong interaction via both electrophilic and nucleophilic attack.

ILs has both electro negativity and electrophilicity, but in combination with thiophene the electro negativity decreases, due to the transfer of electrons donated from anions ($[BF_4]$ and $[PF_6]$) to thiophene molecules. This suggests that the charge of fluorine atoms of anions might contribute to thiophene via strong electron affinity. The ILs with pyridine posses less electronegativity than ILs with thiophene due to the role of cation. Pyridine, which is a good electron acceptor, have larger HOMO over lapped by LUMO of cation in the ILs. Thus it may be concluded that the thiophene extraction takes place mainly via anion-thiophene interaction while the pyridine gets extracted via CH-π interaction. This agrees well with our earlier work on predictions of desulphurization using Ionic Liquids [Kumar et al., 2009]. The simultaneous interaction of ILs with thiophene and pyridine also shows similar effect (Figure 3.2).The electro negativity and electrophilicity values of complex cluster (ILs-thiophene-pyridine) decreases as follows: $[BeMIM][BF_4]$ > $[BUMPY][PF_6]$ > $[BUMPY][BF_4]$ > $[BUMPYR][BF_4]$ > $[BUMPYR][PF_6]$. The stabilization of this complex is mainly due to the electrophilicity and electro negativity effects provided via structure of ILs - thiophene/pyridine and the compactness of the cation and anions.

Table 3.5: Eelectrophilicity (ώ) and electronegativity (χ) for the studied complexes calculated at B3LYP/6-31G* level theory.

S.No	ILs Name	Eelectrophilicity (ώ)	Electronegativity (χ)
1	[BUMPYRO][BF_4]	0.13564	0.12956
2	[BUMPYRO][PF_6]	0.48380	0.12565
3	[BeMIM][BF_4]	0.07482	0.15666
4	[BUMPY][BF_4]	0.07330	0.15239
5	[BUMPY][PF_6]	0.10099	0.17606
6	[BUMPYRO][BF_4]-TS	0.05181	0.11327
7	[BUMPYRO][PF_6]-TS	0.08450	0.14151
8	[BeMIM][BF_4]-TS	0.05239	0.12097
9	[BUMPY][BF_4]-TS	0.08536	0.13036
10	[BUMPY][PF_6]-TS	0.10099	0.17606
11	[BUMPYRO][BF_4]-PY	0.05783	0.10181
12	[BUMPYRO][PF_6]-PY	0.01968	0.07169
13	[BeMIM][BF_4]-PY	0.06931	0.14871
14	[BUMPY][BF_4]-PY	0.05181	0.13975
15	[BUMPY][PF_6]-PY	0.05921	0.14419

3.4.5 Combination of Parameters

The scalar quantities discussed above cannot be related to each other. However based on the simultaneous removal of thiophene and pyridine, the Ionic Liquids have been classified through four scalar parameters: HOMO/LUMO energies, HOMO-LUMO gap,

global softness and electrophilicity (Table3.4 to 3.6). [BeMIM][BF_4] was found to be the most effective IL based on all four scalar parameters. This is mainly due to the high number of electron donors transferred from LUMO of the ILs to the HOMO (electron acceptors) of the pyridine. Additionally the HOMO/LUMO energy of thiophene interacts strongly with the HOMO/LUMO of the fluorine based anions as discussed previously. The overall order after taking into considerations all the factors are as follows: [BeMIM][BF_4] > [BUMPYR][BF_4]> [BUMPY][PF_6]> [BUMPY][BF_4]> [BUMPYR][PF_6].

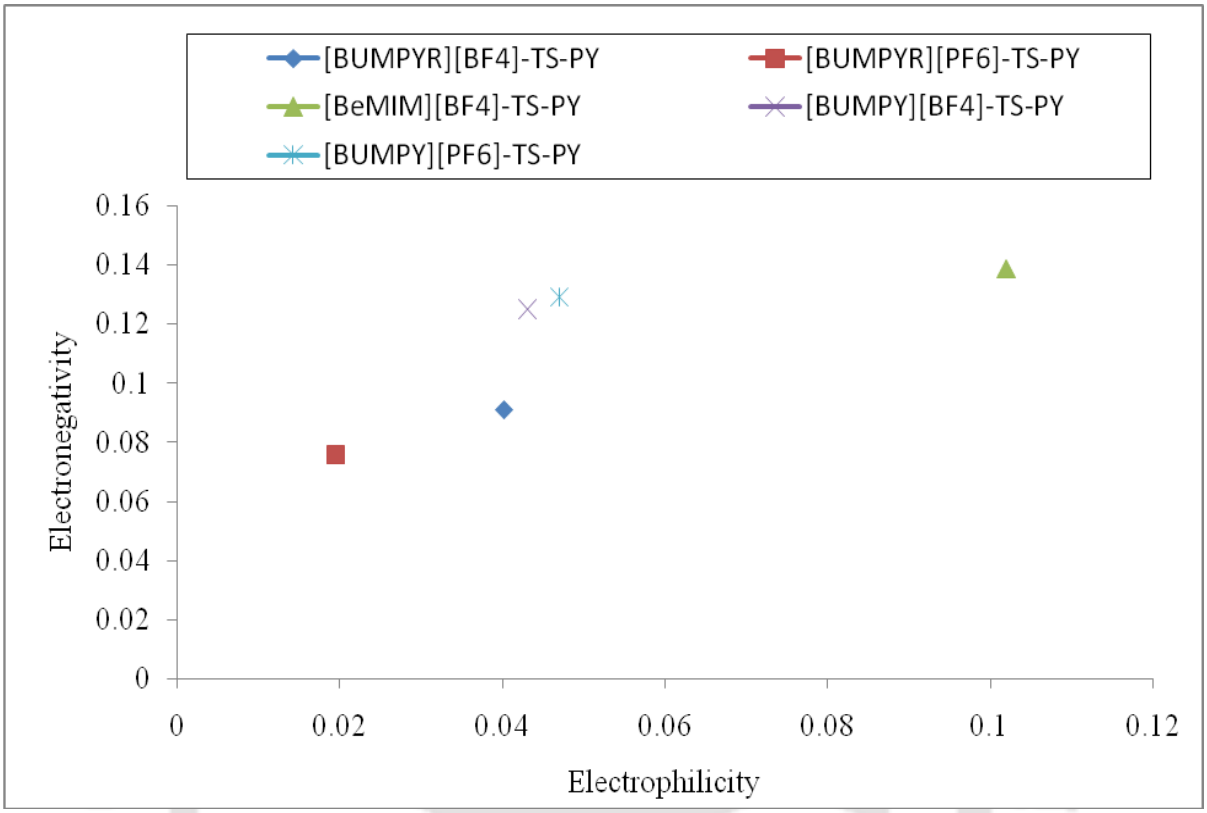

Figure 3.6: Electrophilicities and Electronegativities for Ionic Liquid –thiophene-pyridine.

Table 3.6: Comparative study for IL-TS-PY based on scalar quantities

Rank		**1**	**2**	**3**	**4**	**5**
Parameter	**Objective**					
Based on HOMO / LUMO energy values	More LUMO (higher negative)	[BeMIM][BF_4]	[BUMPYR][BF_4]	[BUMPY][PF_6]	[BUMPY][BF_4]	[BUMPYR][PF_6]
Based on HOMO-LUMO energy gap	Small Gap	[BeMIM][BF_4]	[BUMPYR][BF_4]	[BUMPY][PF_6]	[BUMPY][BF_4]	[BUMPYR][PF_6]
Based on Global softness	Higher Global Softness	[BeMIM][BF_4]	[BUMPYR][BF_4]	[BUMPYR][PF_6]	[BUMPY][PF_6]	[BUMPY][BF_4]
Based on Electrophilicity	Higher Electrophilicity	[BeMIM][BF_4]	[BUMPY][PF_6]	[BUMPY][BF_4]	[BUMPYR][BF_4]	[BUMPYR][PF_6]
Overall Rank		[BeMIM][BF_4]	[BUMPYR][BF_4]	[BUMPY][PF_6]	[BUMPY][BF_4]	[BUMPYR][PF_6]

3.5 Effect of Molecular interaction

On a quantum scale the interactions of IL-thiophene/pyridine depend on the π - π interaction, CH- π interaction and the hydrogen bonding interactions [Su et al.,2004]. π-π interactions act strongly on flat polycyclic aromatic hydrocarbons such as anthracene, triphenylene and coronene because of the presence of many delocalized π-electrons. A recent work carried out on a double concave hydrocarbon buckycatcher [Sygula et al., 2007] had an association constant of 8600 M^{-1}. This interaction, which is stronger than other noncovalent interactions (hydrogen bonds, van der Waals forces, etc) plays an important role.

Cation-π interaction energies are of the same order of magnitude as hydrogen bonds and play an important role in molecular recognition [Anslyn et al.,2004] This interaction, known as "π-cation interaction", plays a dominant role in both chemical and biological recognition[Reddy et al.,2005]. π-cation interaction has been experimentally evidenced by mass spectrometry and NMR spectroscopy[Inokuchi et al.,1995;Loach et al.,1993;Masci et al.,1995]. Smaller and more positively charged cations lead to larger electrostatic attraction. The electronic properties of the substituents on the π system also have an influence on the strength of the attraction. Electron withdrawing groups decrease the amount of negative charge in the π system and thus weaken the interaction while electron donating groups such as $-NH_2$ increase the amount of negative charge in the π system. Thus the partial charge on the nitrogen /sulphur atom of pyridine/thiophene will play an important role in increasing or decreasing the negative charge in the π system.

Often the molecular structure orientation is involved in the separation of organic /inorganic compounds through multiple interactions by CH- π bond [Suezawa et al.,2004]. The CH- π bond is strongly responsible for the simultaneous interaction by tuning the donor and acceptor ligand properties of the interacting molecules [Hirota et al., 2000]. Though the CH- π bond is weak, still it is known to lie within the lower end of the hydrogen bonding regime [Suezawa et al.,2000]. The electron withdrawing tendency of CH carbon and electron donating tendency of π aromatic system are known to play a significant role in multiple interactions [Hirota et al., 2000]. Suezawa et al.,[2004] studied the importance and

effectiveness of the aromatic CH-π hydrogen bond for complex cluster formation. Moreover the aromatic ring current in thiophene is stronger than that of ionic liquid. This is due to the fact that the bulky anions such as PF_6 prevent BMIM cation to come close and thus reduces its aromatic current effect.The thiophene molecules are tightly packed giving rise to high aromatic current density. Because of this the π- π interaction between cation and thiophene/pyridine is greatly reduced and the CH- π interaction takes over. In a recent work by Cassol et al.,[2007] the high affinity of the IL for aromatics (with and without sulfur), were experimentally found to be due to CH- π interactions between the hydrogens of the IL ring and those of the aromatic compounds. The above study implies that the CH- π bond plays a considerable role within the π group of thiophene /pyridine and CH group of ILs. The hydrogen bonding effect due to the H-bond donor of cation to the sulfur/nitrogen atom of thiophene/pyridine will be taken up later using COSMO theory.

3.6 Effect of Partial Charges

Recent studies [Zhou et al., 2008; Song et al., 2009; Kartrizky et al., 1996] showed that the NBO (Normal Bonded Orbital) analysis is used as an excellent tool for the investigation of partial charge transfer interaction within the parent compounds. Further the chemical reactivity is also explained on the basis of the partial charges [Nishi et al., 2008; Vektariene et al., 2009]. Based on these partial charges, difference in the hydrogen-bonding, electrostatic interaction and CH-π bonding interaction is considered. Therefore, based on the quantum chemical investigation, the CH groups can participate and play an important role in the simultaneous interaction of π bases compounds such as thiophene and pyridine [Cassol et al., 2007].

Table 3.7 shows the number of stable sites (i.e hydrogen atom) having positive charges on the cation. The number of '+ ve' charged hydrogen atom increases from [BPYRO](19) > [BPY] (16) > [BeMIM] (13). It should be noted that the rear hydrogen atoms of the cation are unlikely to form CH-π interaction with thiophene/ pyridine [Zhou et

al.,2008;Hunt et al.,2007] . The two H-atom of 'CH_2'group cannot be occupied at the same time due to coulombic repulsion. Thus there is a limit on the maximum number of site that can be occupied at a time. The electrostatic field effect within the IL is also important when electrons surrounding the resonating nucleus of the cation are displaced with a chemical bonded polar atom such as fluorine (F-H interaction), which is present in both anions. An individual cation or anion does not give much information about the interaction of IL with thiophene/pyridine. For favorable interaction the pryridine/thiophene molecule should be able to overcome the F-H interaction and form cation- π or hydrogen bonds. In our further discussion we will focus our attention on the partial charge of nitrogen and sulphur atom when they are in a complex consisting of ionic liquid. The partial charge of sulphur atom in thiophene is -0.06 [Zhou et al., 2008].The "electron pairs" on sulphur atom are significantly delocalized in the π electron system. The nitrogen atom on pyridine having a partial charge of –0.679 (Figure 3.7) can act as a basic lone pair of electrons. Because this lone pair is not delocalized into the aromatic π -system, it is therefore basic in nature. For efficient CH- π interaction, the aromatic π density needs to increased. A decrease in the partial charge of nitrogen or sulphur atom will result in the increase in the density of the π system thereby promoting cation- π interaction.

Pyrolidinium based ionic liquid: Table 3.8 presents the partial charges derived for sulphur and nitrogen in various complexes. The partial charge of sulphur (-0.0137) in [BPYRO][BF_4] + thiophene complex is less than that of [BPYRO][BF_4] – thiophene - pyridine (-0.037). Thus CH-π bond interaction will be weaker for the simultaneous removal when compared with the removal of thiophene alone. For the case of pyridine the partial charge decreases from –0.681([BPYRO][BF_4] -pyridine) to –0.382([BPYRO][BF_4]-pyridine-thiophene) indicating stronger CH-π interaction for simultaneous removal. Thus for the simultaneous removal, thiophene and pyridine does not compete for the same site within the ionic liquid ([BPYRO][BF_4]) since the partial charges

of either nitrogen(-0.679) or sulphur(-0.06) atom is less than that obtained in complex form. The aromatic current effects in pyridine and thiophene will be stronger and thus they will be able to form CH-π bonds. For [BPYRO][PF_6], a similar effect was observed. The partial charge of sulphur (0.1631) in [BPYRO][PF_6]-thiophene complex is positive as compared to [BPYRO][BF_4] –thiophene-pyridine (-0.035). It indicates that the CH-π bond formation is not favorable in [BPYRO][PF_6]-thiophene complex. For the case of pyridine the partial charge on nitrogen reduces from –0.697 ([BPYRO][PF_6]-pyridine) to –0.391 ([BPYRO][PF_6]-pyridine-thiophene), which is again less than that of either nitrogen (-0.679) or sulphur(-0.06) atom indicating strong simultaneous removal. However for [BPYRO][PF_6]-pyridine CH-π is not favorable as its partial charge of nitrogen (-0.697) is greater than –0.679 indicating less delocalization.

Table 3.7: The H-bond donor /acceptor of different cations

S.No	Objective	[BPYRO]	[BPY]	[BeMIM]
1	An available H-bond donor/acceptor of cation to sulphur and nitrogen	H 0.059221 H 0.058873 H 0.061347 H 0.086002 H 0.114472 H 0.111414 H 0.018728 H 0.004660 H -0.006327 H 0.007086 H 0.081874 H 0.049630 H 0.038720 H 0.064410 H 0.080052 H 0.157920 H 0.163081 H 0.169325 H 0.037685 H 0.087232	H 0.172946 H 0.129888 H 0.129239 H 0.129084 H 0.172899 H 0.173994 H 0.133369 H 0.176477 H 0.134885 H -0.020758 H -0.021695 H -0.022032 H -0.022610 H 0.093133 H 0.070041 H 0.070294	H 0.152042 H 0.209860 H 0.207561 H 0.123234 H 0.121577 H 0.121796 H 0.109687 H 0.119711 H 0.117665 H 0.119809 H 0.127274 H 0.130990 H 0.128220

2	Number of positive sites available	19	16	13
3	Number of negative sites available	01	Nil	Nil

Pyridinium based ionic liquid: For [BPY][BF_4] the partial charge on nitrogen decreases from –0.6809 ([BPY][BF_4]-pyridine) to –0.435 ([BPY][BF_4]–pyridine-thiophene) while for thiophene the partial charge on sulphur increases from +0.091 ([BPY][BF_4]–thiophene) to –0.0348 ([BPY][BF_4]–pyridine-thiophene) thus improving the CH-π interaction when they are considered simultaneously. It indicates that [BPY][BF_4] cannot be a good solvent for the removal of thiophene or pyridine individually. The trend was similar for [BPY][PF_6] where the partial charge on nitrogen decreased from –0.687 ([BPY][PF_6]-pyridine) to –0.348 ([BPY][PF_6]–pyridine-thiophene) while for thiophene the partial charge on sulphur remained stationary ~ -0.029 for both complexes ([BPYR][PF_6]–thiophene and ([BPYR][PF_6]–pyridine-thiophene).

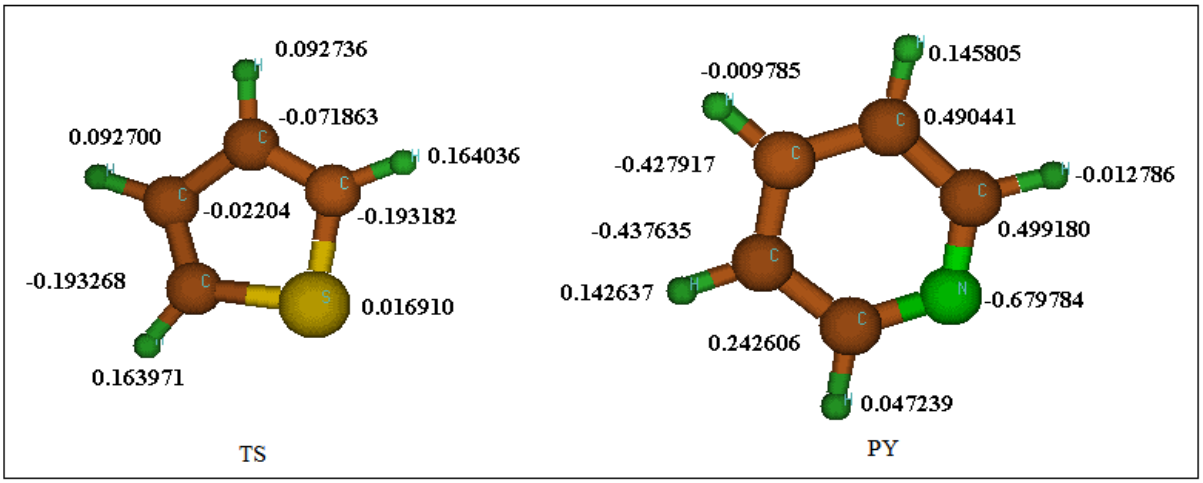

Figure 3.7: Optimized structure of thiophene and pyridine

Benzylimidazolium based ionic liquid: The CH-π bonds interactions are seen to be dominant for both [BeMIM][BF_4]-thiophene and [BeMIM][BF_4] –pyridine complex. For the case of pyridine the partial charge on nitrogen increases from –0.3788([BeMIM][BF_4]–pyridine) to –0.461([BeMIM][BF_4]–pyridine-thiophene) while for thiophene the partial charge on sulphur increases from –0.023 ([BeMIM][BF_4] – thiophene) to –0.027 ([BeMIM][BF_4]–pyridine-thiophene).For the simultaneous removal, the partial charges of nitrogen decreases from –0.679 to –0.461 while for sulphur it decreases from –0.06 to –0.027 indicating greater aromatic π density in thiophene and pyridine respectively. It can be seen that the partial charges of nitrogen and sulphur in all the ionic liquids for the simultaneous complex is less than the partial charge of nitrogen (-0.679) and sulphur (-0.06) in thiophene and pyridine respectively. This indicates all the ionic liquids have a favorable CH-π interaction with both thiophene and pyridine.

Table 3.8: The partial charge of sulphur and nitrogen on complexes involving Ionic Liquids

S.No	ILs Name	Thiophene	Pyridine	Thiophene + pyridine	
		S atom	N atom	S atom	N atom
1	[BPYRO][BF_4]	-0.0136	-0.68063	-0.03659	-0.382102
2	[BPYRO][PF_6]	0.161	-0.69785	-0.03505	-0.39108
3	[BPY][BF_4]	0.091	-0.6809	-0.03489	-0.43567
4	[BPY][PF_6]	-0.029	-0.68766	-0.02714	-0.34085
5	[BeMIM][BF_4]	-0.02355	-0.37886	-0.027697	-0.46125

3.8 Effect of Interaction Energies

In this section interaction of thiophene/pyridine with cation, anion and IL (cation + anion) have been studied explicitly and simultaneously. Figure 3.8,3.9 (a) to 3.9 (c) shows the optimized structures of anions and cations respectively while Figure 3.9 shows the optimized structure of pyridine and thiophene. The many body analysis were performed for the simultaneous removal of complexes consisting of thiophene and pyridine and the calculation of the interaction energy was done by the following expression:

(3.22)

Where

: Interaction energy (ILs –Thiophene (TS)-Pyridine (PY)) of the whole complex in KJ/mole.

= total energies for the complex system in KJ/mole.

, , **: are the individual energies of the ILs, thiophene (TS) and Pyridine** (PY) respectively in KJ/mole.

The optimized structure of thiophene has been referred form previous work [Zhou et al.,2008]. Figure 3.10(a) to 3.10(b) and 3.11(a) to 3.11(c) presents the optimization results for two anions ([PF_6] and [BF_4]) and three cations ([BPYRO],[BPY] and [BeMIM]) and their interaction with thiophene. Both anions i.e. [BF_4] and [PF_6] are situated outside the ring plane of thiophene respectively, and the fluorine atoms were found to interact with the hydrogen atoms of the thiophene through F-H interaction. This shows that the F–H interaction is important in the system. Such structure produces a maximal Columbian effect [Zhou et al., 2008] with the same charge repelling each other and the opposite charges

attracting each other. In the case of the octahedral [PF_6] anion the equatorial flourine atoms participate preferentially in hydrogen bond network, whereas for tetrahedral [BF_4] anions only three of the atoms are usually involved in the linkage. This reasonably agrees with the prediction of Zhang et.al.,[2008]. For the cations the optimized structure were obtained using the same procedure as outlined by Zhang et.al [2008]. The optimized structure indicates that the thiophene is located aside the aromatic ring of the cation with its aromatic ring being perpendicular to the aromatic ring of the cation. With this structure, the positively charged atoms of the [BPYRO],[BPY] and [BeMIM] cation are the most approachable by the negatively charged atoms of thiophene, producing a maximal columbian attraction. This agrees well with the partial charges giving the number of stable hydrogen sites (Table 3.7) in the cations. These strongest hydrogen bond always involves the most acidic hydrogen of [BPYRO], [BPY] and [BeMIM] based cation followed by the other hydrogens of the [BPYRO],[BPY] and [BeMIM] nucleus and/ or the hydrogens of the N-alkyl radicals. These bonds possess properties of weak to moderate hydrogen bonds and are mostly electrostatic in nature .The H-F bond lengths were found to be greater than 2.2Å; while the C-H…F bond angles were between 100°-180°. It should be noted that the origin of long range cation liquid crystalline properties [Freire et al.,2008] is due to the formation of domain of "coulombic layers". The cationic head groups (i.e. alkyl group) interact with the counter ions, and the "van der Waals" layers built from (anti) parallel stacking of the alkyl chains.

Figure 3.12(a) to 3.12 (b) and 3.13(a) to 3.13(c) shows the optimized geometry of two anions ([PF_6] and [BF_4]) and three cations based ([BPYRO], [BPY] and [BeMIM]) and their interaction with pyridine. Both anions i.e. [BF_4] and [PF_6] are situated outside the ring plane of the pyridine, and the fluorine atoms interact with the hydrogen atoms of the pyridine. Such structure again produces a maximal Columbian effect with the same charge repelling each other and the opposite charges attracting each other. For the cations, the interaction was found to be preferentially through N (heteroaromatic)-H(imidazolium) hydrogen bonds.

Previous work suggests that this is largely controlled by the nitrogen heterocyclic pKa value [Cassol et al., 2007]. It is clear that interaction of pyridine with the cations increases the π density as the partial charge of nitrogen on pyridine molecule (Figure 3.13 (a) to 3.13 (c)) decreases from –0.679 to –0.307 and -0.297 while interacting with [BeMIM] and [BPY] respectively, while it remains constant with [BeMIM] i.e –0.684.

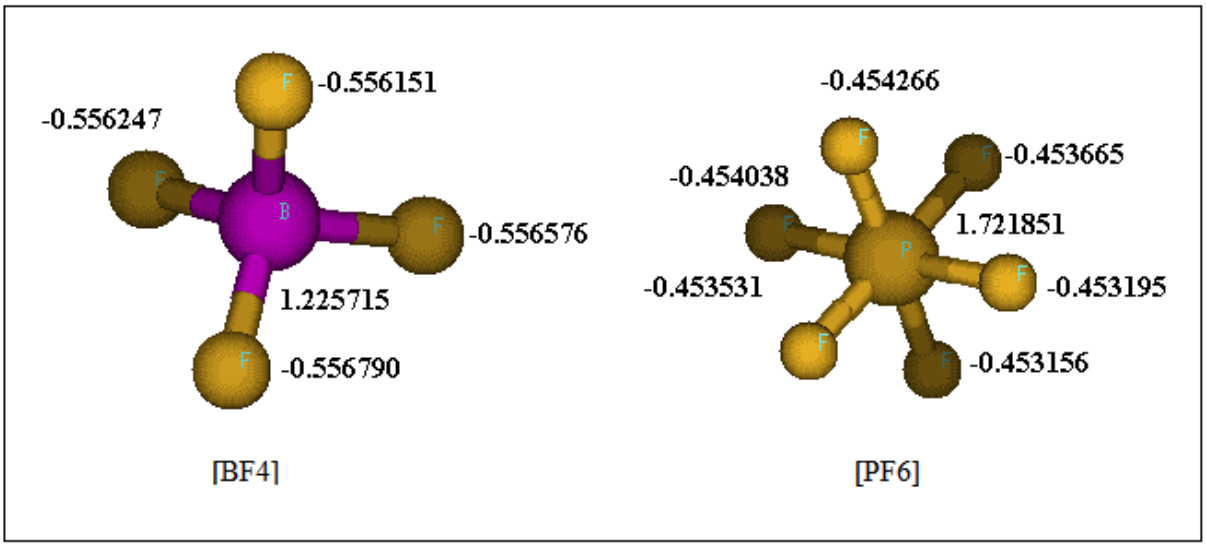

Figure 3.8: Optimized geometries of Anions ([BF_4] and [PF_6])

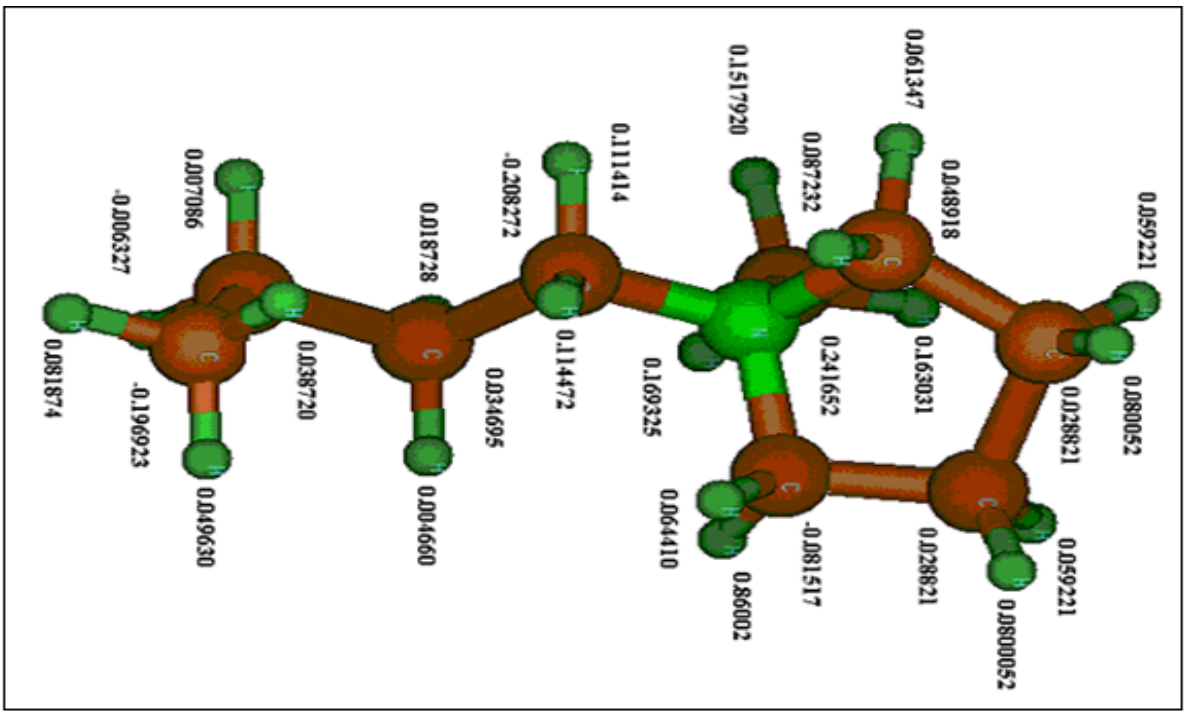

Figure 3.9 (a): Optimized structure of 1-Butyl-1-methylpyrolidinium ([BUMPYR])

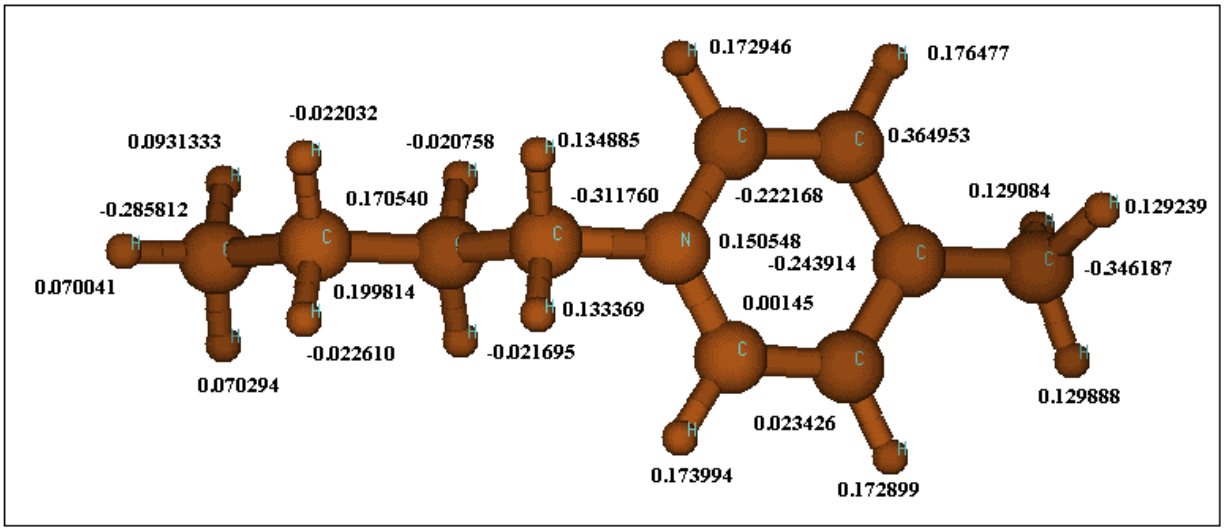

Figure 3.9(b): Optimized structure of 1-Butyl-4-methylpyridinium ([BUMPY])

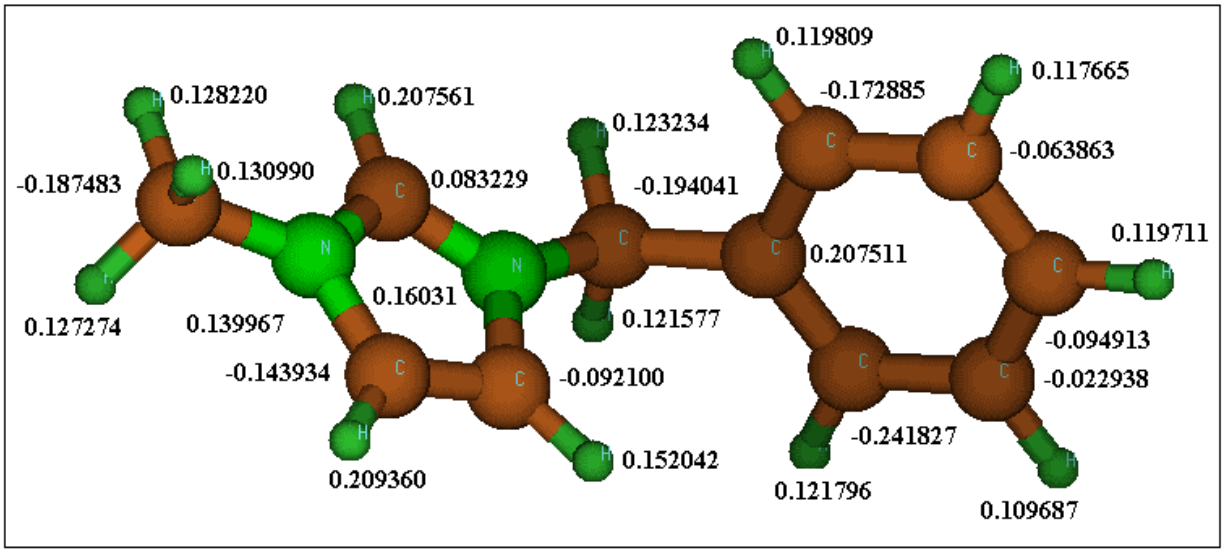

Figure 3.9(c): Optimized structure of 1-Benzyl-3-methylimidazolium ([BeMIM])

The optimized energies between thiophene with ionic liquids are given in Table 3.9. The interaction of thiophene with the different ionic liquids is preferentially through CH-π bonds and the quantity of thiophene with ionic liquid pair increases with the increase of the π-density [Eber et al.,2004]. Based on their interaction energies the ILs follow the order:

[BeMIM][BF_4] > [BPYRO][BF_4] >[BPY][BF_4] > [BPY][PF_6] > [BPYRO][PF_6] (Table 3.9). It should be noted that negative interaction energy is favorable since it means extra amount of energy (positive in nature) is required for disassembling the system/complex. It can be seen that there is a qualitative relation between the partial charges and interaction energies. [BPYRO][PF_6]-thiophene complex having interaction energy of +25.30 kJ/mol has a partial charge of +0.161 on the sulphur atom. The positive sign of partial charge is contrary of what was observed for sulphur in thiophene alone (i.e -0.06). The positive charge results in very less delocalization and ultimately leads to a positive value of interaction energy. In the same manner [BPY][BF_4]-thiophene complex having interaction energy of 10.53 kJ/mol has a partial charge of 0.091 on the sulphur atom contrary to the partial charge of sulphur in thiophene(-0.06). The optimized energies of the IL with pyridine are given in Table 3.9. The interaction of pyridine with the different ionic liquids again occurs through N (heteroaromatic)-H (cation) hydrogen bonds as previously reported [Sygula et al.,2007].The interaction energies followed the order: [BPY][PF_6] >[BeMIM][BF_4] > [BPYRO][BF_4] > [BPY][BF_4] > [BPYRO][PF_6] (Table 3.9). For [BPYRO][PF_6]-pyridine complex the positive interaction energy (88.40 kJ/mol) is due to the partial charge of nitrogen, which is –0.697. This is more than the partial charge of nitrogen in pyridine alone (-0.679). This leads to lesser delocalization and subsequently less aromatic π density in the pyridine molecule.

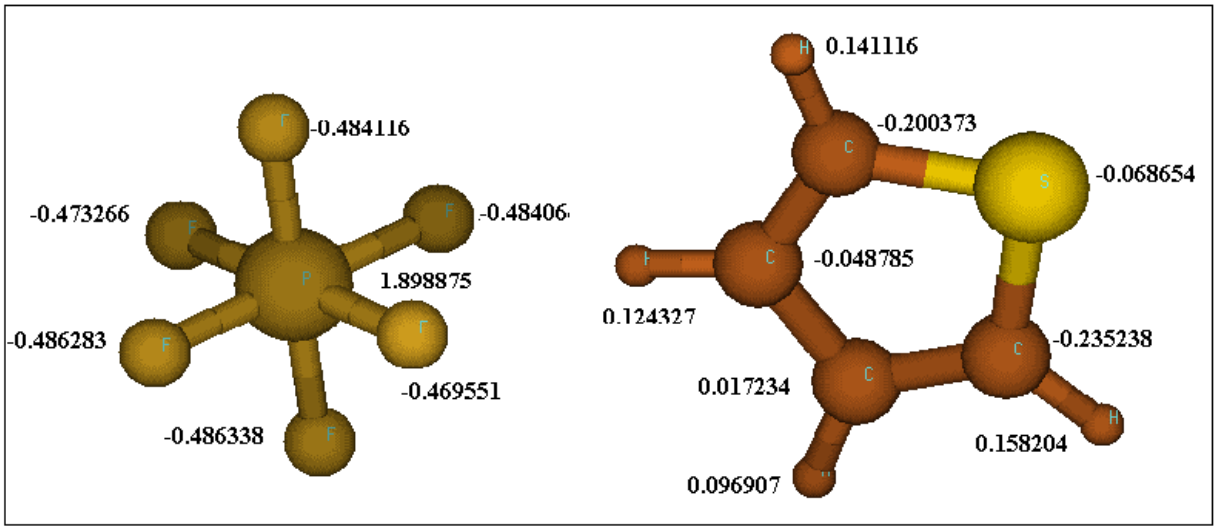

Figure 3.10 (a): Optimized geometries of [BF_4] with Thiophene.

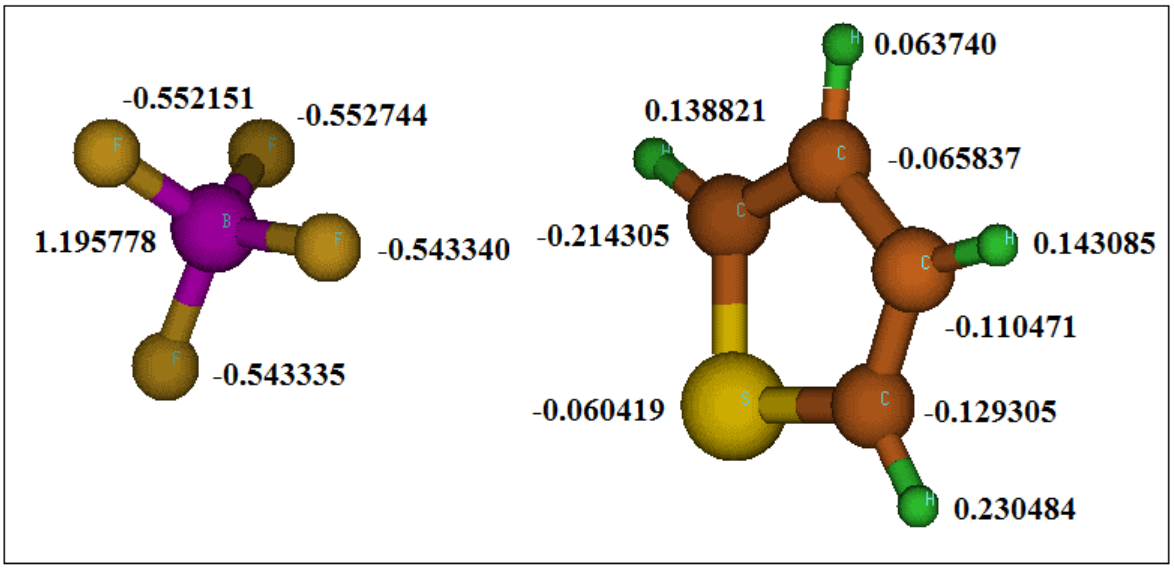

Figure 3.10(b): Optimized geometries of [PF_6] with Thiophene.

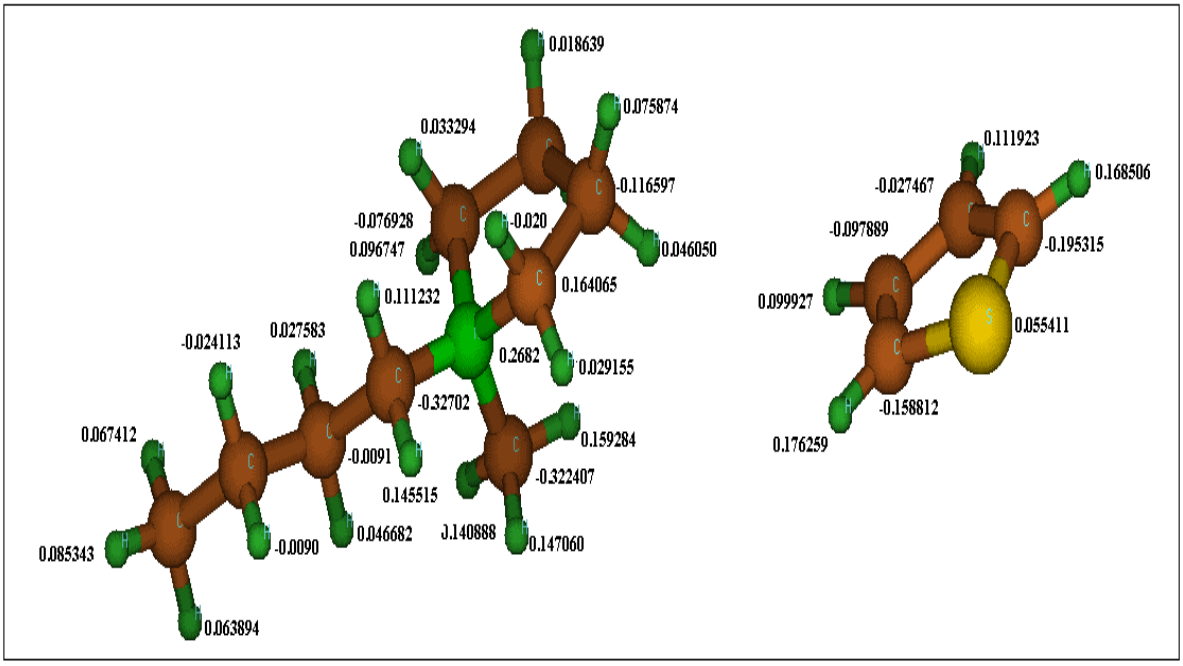

Figure 3.11(a): Optimized geometries of [BUMPYR] with Thiophene.

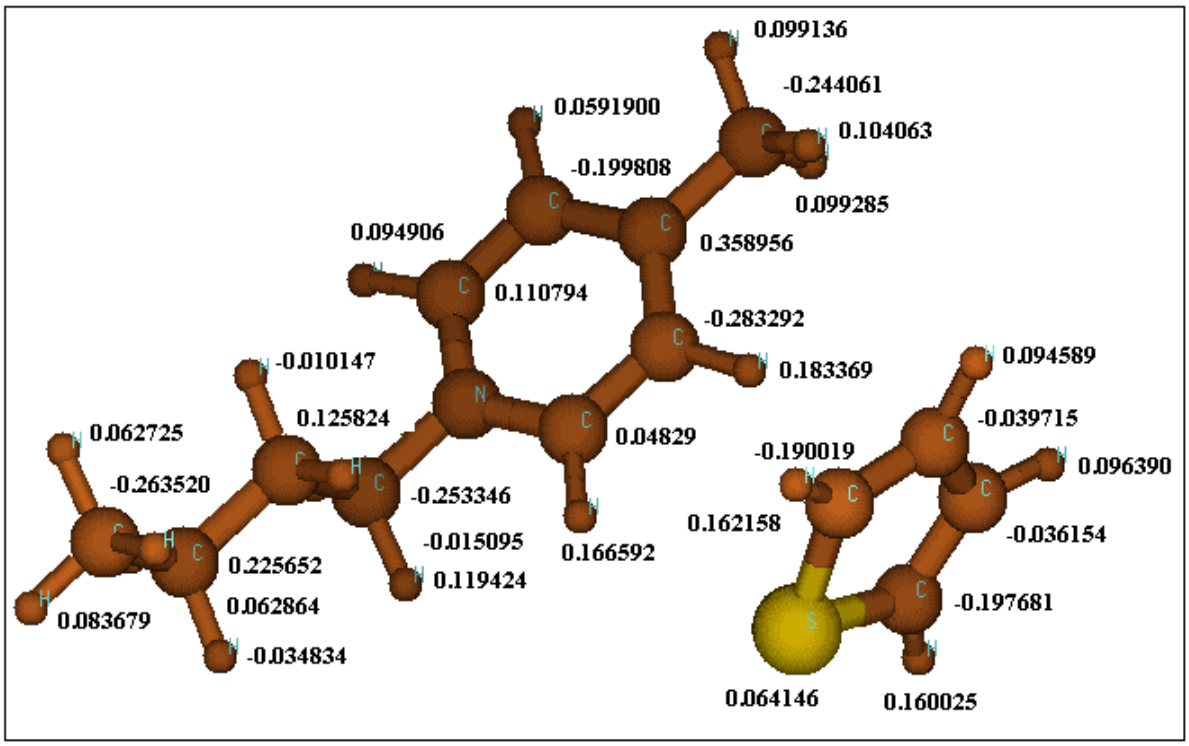

Figure 3.11 (b): Optimized geometries of [BUMPY] with Thiophene.

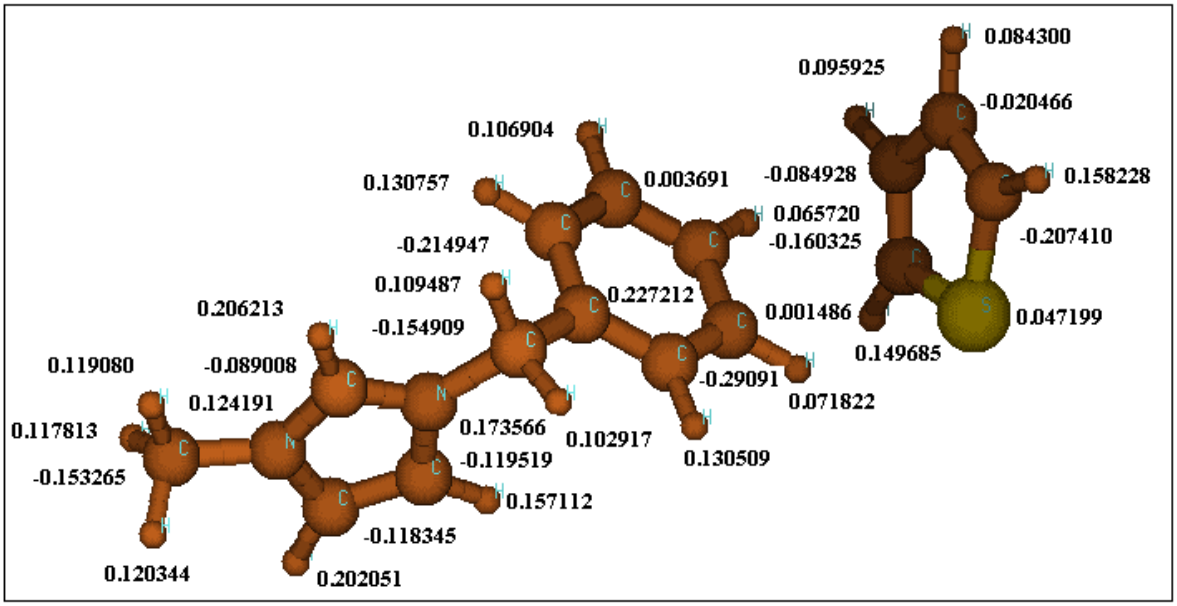

Figure 3.11(c): Optimized geometries of [BeMIM] with Thiophene.

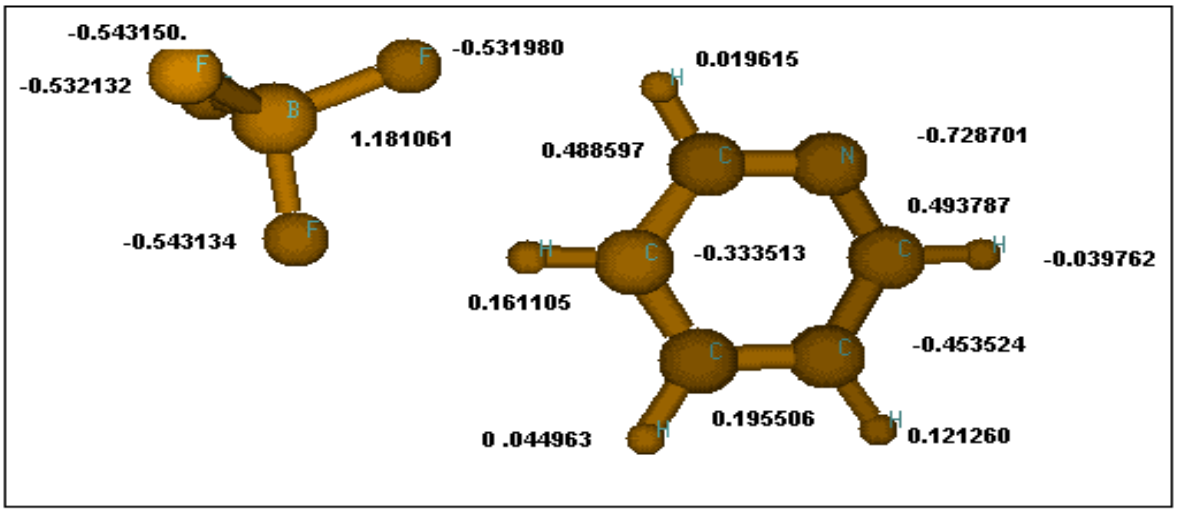

Figure 3.12 (a): Optimized geometries of [BF_4] with pyridine.

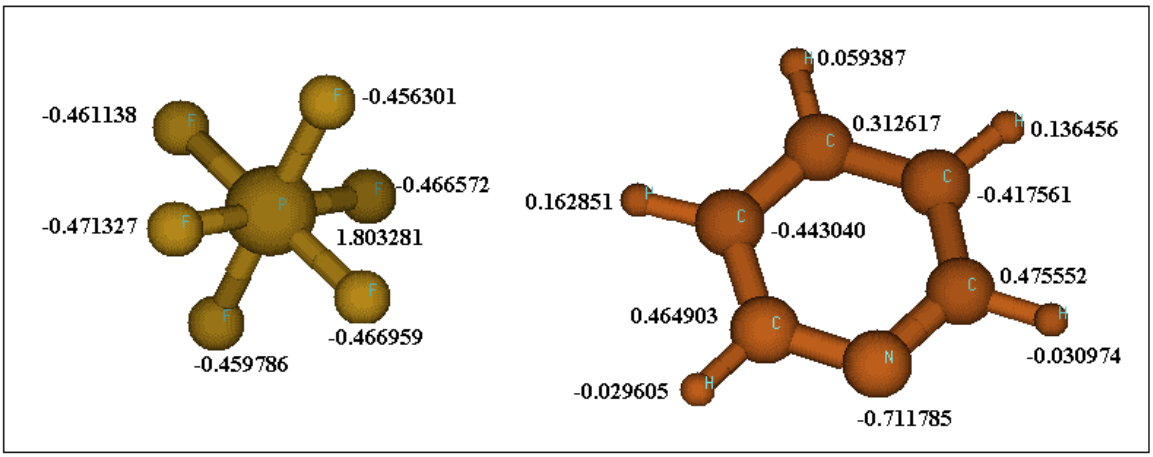

Figure 3.12 (b): Optimized geometries of [PF_6] with pyridine.

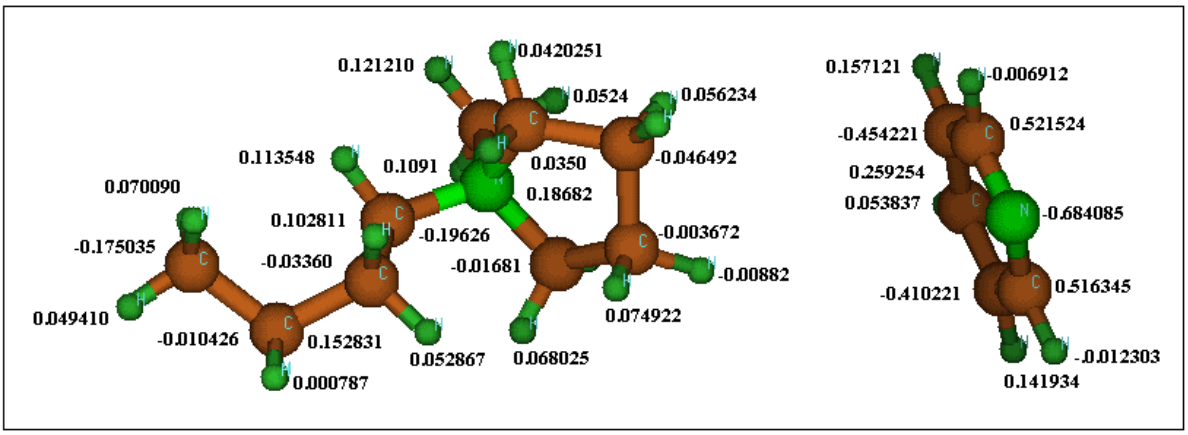

Figure 3.13 (a): Optimized geometries of [BUMPYR] with pyridine.

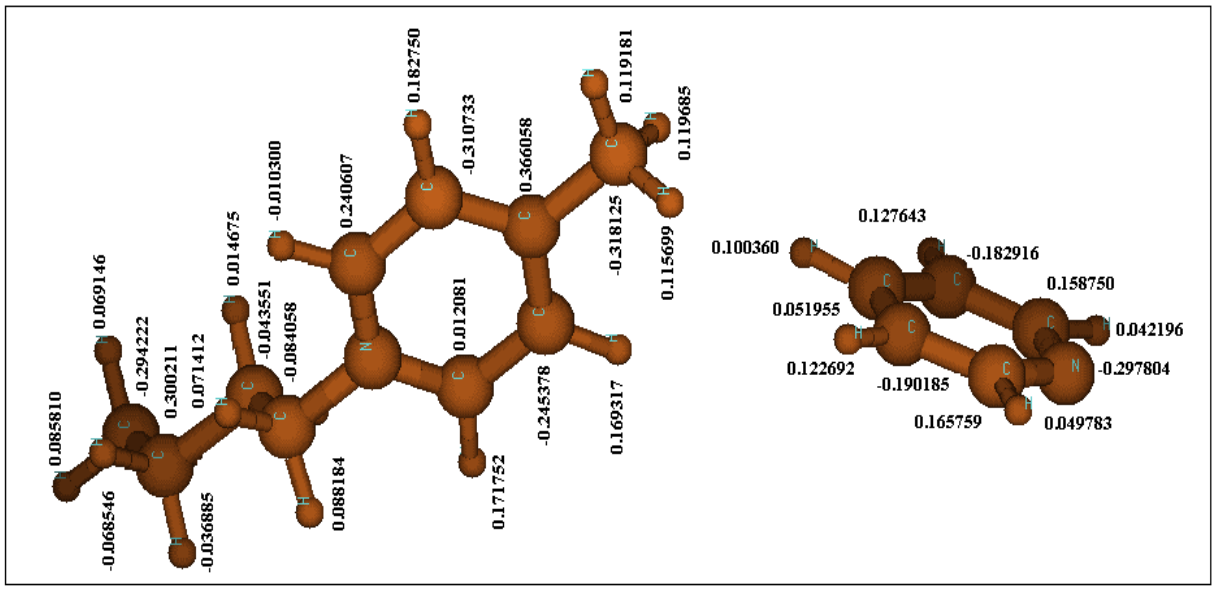

Figure 3.13 (b): Optimized geometries of [BUMPY] with pyridine.

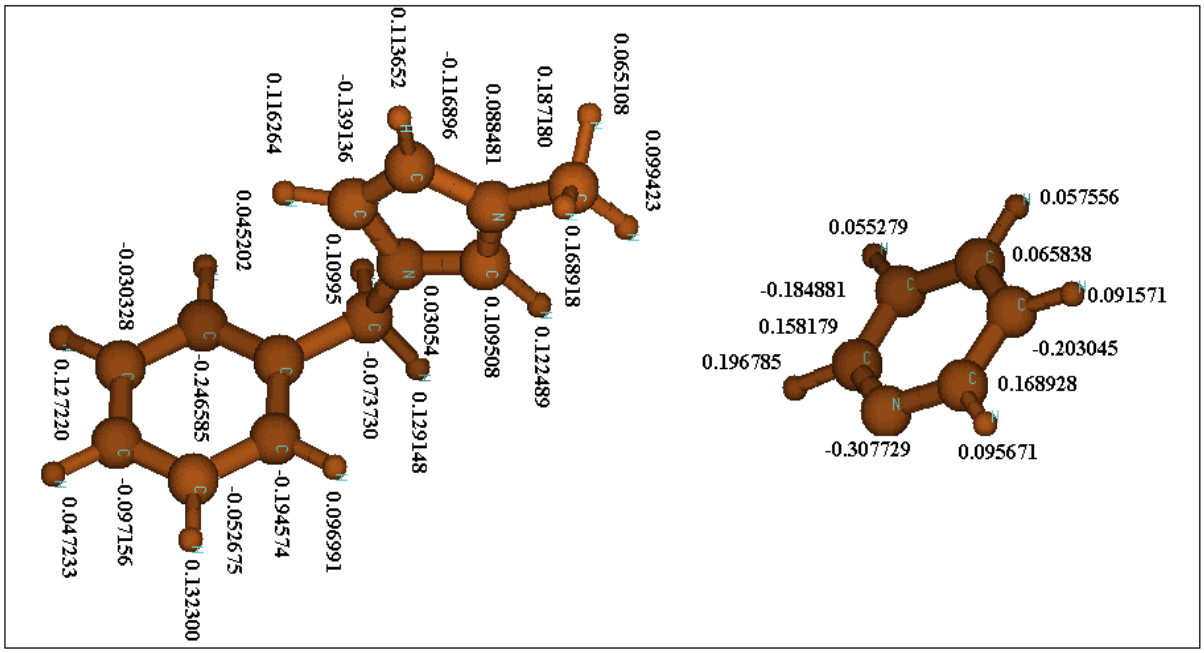

Figure 3.13 (c): Optimized geometries of [BeMIM] with pyridine.

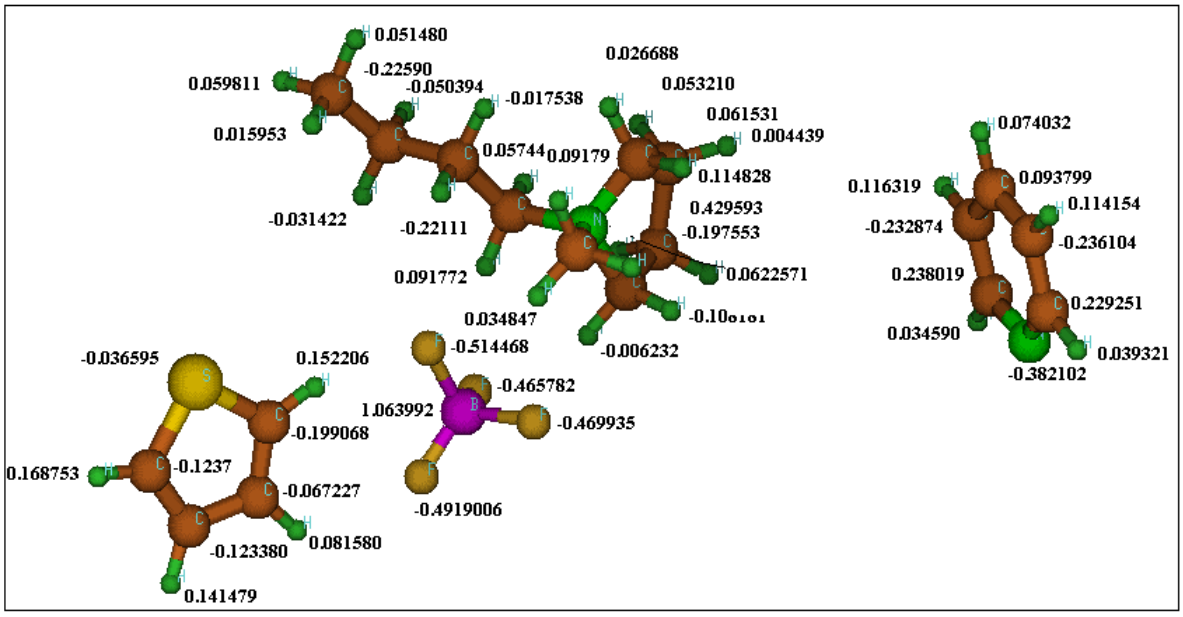

Figure 3.14 (a): Optimized geometries of [BUMPYR][BF_4] with thiophene and pyridine.

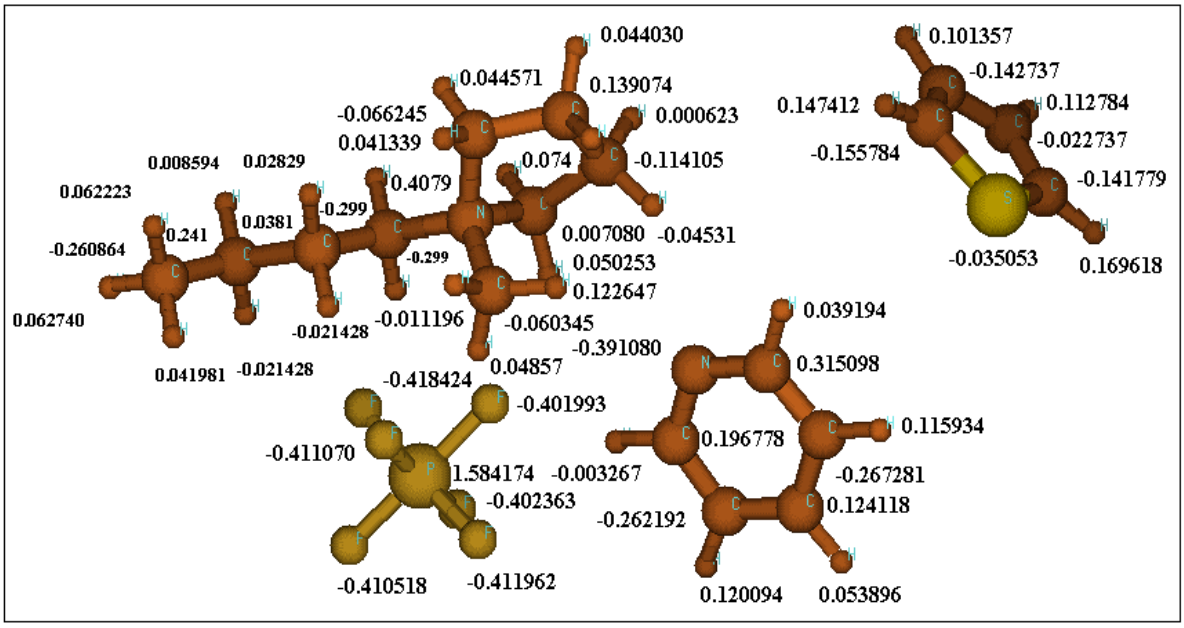

Figure 3.14 (b): Optimized geometries of [BUMPYR][PF_6] with thiophene and pyridine.

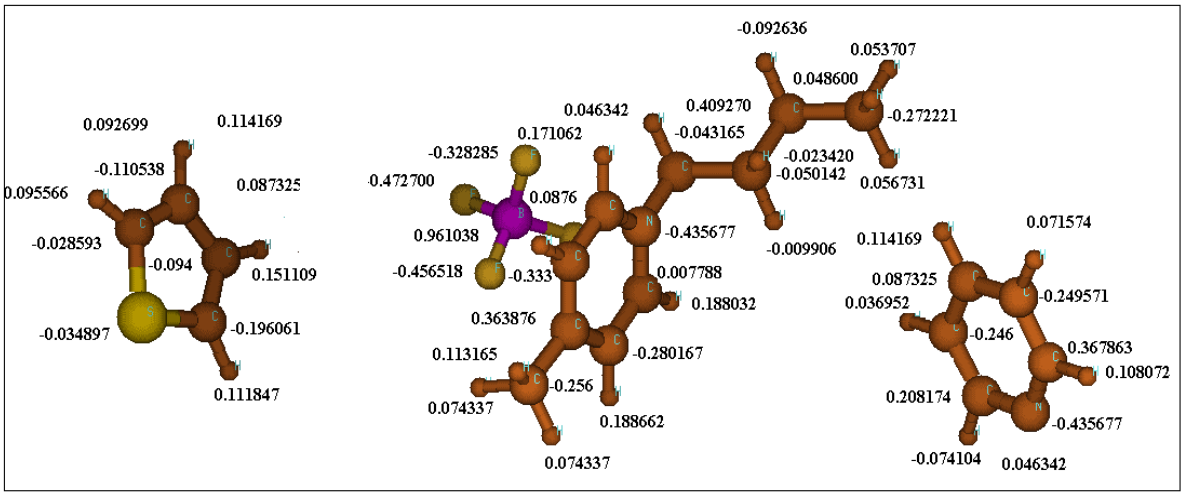

Figure 3.14 (c): Optimized geometries of [BUMPY][BF_4] with thiophene and pyridine.

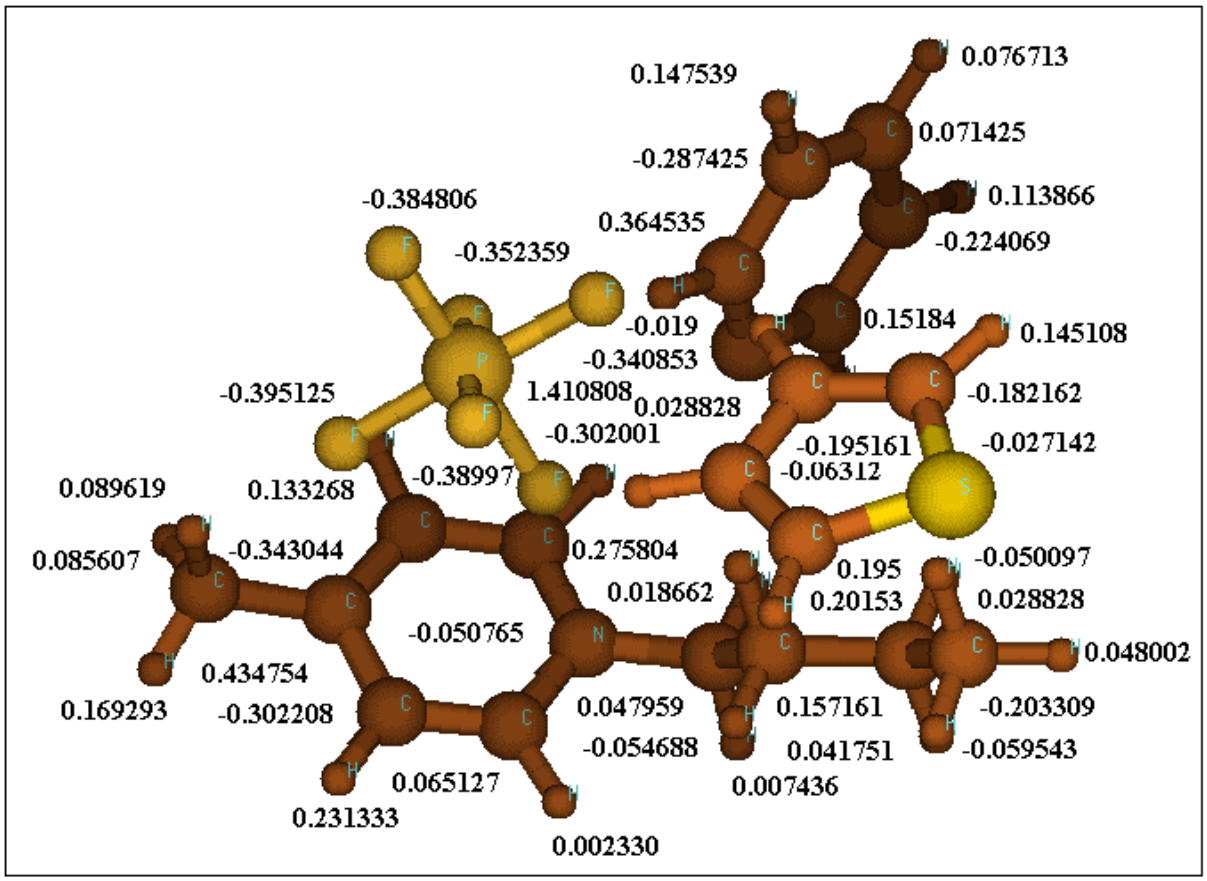

Figure 3.14 (d): Optimized geometries of [BUMPY][PF_6] with thiophene and pyridine.

Table 3.9: Interaction Energy for Ionic Liquids complexes

S.No	ILs Name	Interaction energy (KJ.mole^{-1})		
		Thiophene	Pyridine	Thiophene + Pyridine
1	[BPYRO][BF_4]	-4.37	-27.17	-23.39
2	[BPYRO][PF_6]	2.275	3.975	-33.95
3	[BPY][BF_4]	-10.53	-15.40	-48.50
4	[BPY][PF_6]	-3.43	-79.06	-27.37

5	[BeMIM][BF_4]	-20.48	-27.26	-30.29

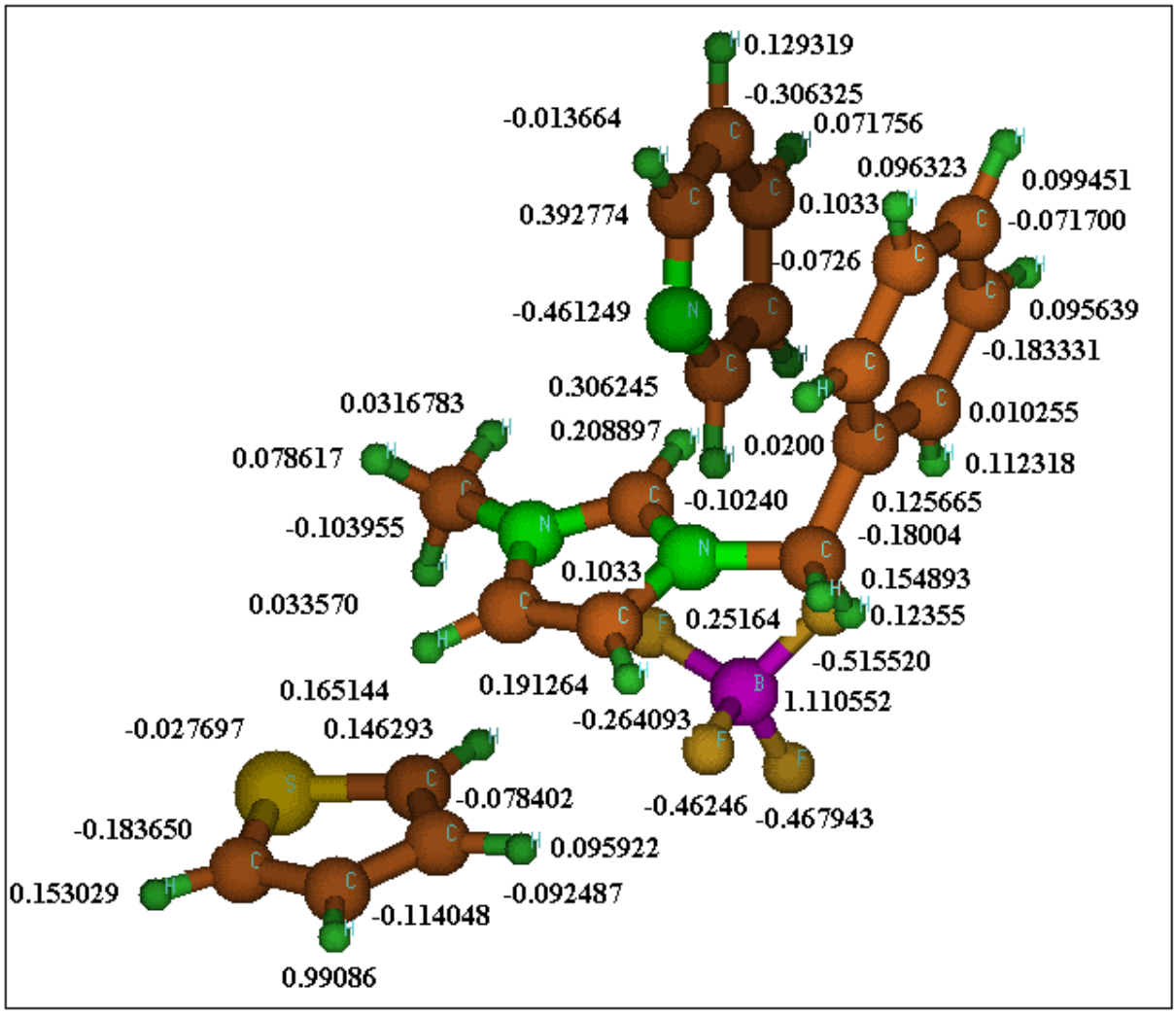

Figure 3.14 (e): Optimized geometries of [BeMIM][BF_4] with thiophene and pyridine.

Figure 3.14 (a) to 3.14 (e) shows the optimized geometry of ionic liquid –thiophene-pyridine complex along with their partial charges. It is seen that the interaction is

mainly through cation-thiophene-pyridine contacts (CH-π bond). Based on the interaction energies the degree of extraction follows the order [BPY][BF_4] > [BPYRO][PF_6] > [BeMIM][BF_4] > [BPY][PF_6] > [BPYRO][BF_4]. The result is contrary of what was obtained for IL-thiophene/pyridine. However the variation in interaction energies are very small i.e –23.39 KJ/mole [BPYRO][BF_4] to – 48.50 KJ/mole [BPY][BF_4] (Table 3.9)

Nomenclature

[BeMIM]	1-Benzyl-3-methylimidazolium
[BUMPYR]	1-Butyl-1-methylpyrrolidinium
[BUMPY]	1-Butyl-4-methylpyridinium
[BF_4]	Tetrafluoroborate
[PF_6]	Hexafluorophosphate
[BeMIM] [BF_4]	1-Benzyl-3-methylimidazolium tetrafluoroborate
[BUMPYR] [BF_4]	1-Butyl-1-methylpyrrolidinium tetrafuloroborate
[BUMPYR] [PF_6]	1- Butyl-1-methylpyrrolidinium hexafluorophosphate
[BUMPY] [BF_4]	1-Butyl-4-methylpyridinium tetrafluoroborate
[BUMPYR] [PF_6]	1-Butyl-4-methylpyridinium hexafluorophosphate
Thio	Thiophene
Pyri	Pyridine
HOMO	Higher occupied molecular orbital in Hartrees
LUMO	Lower unoccupied molecular orbital in Hartrees
IP	ionization polarizability
EA	Electron affinity

REFERENCES

Angueira, E.J.; White. M.G. Super acidic ionic liquids for arene carbonylation derived from dialkylimidazolium chlorides and MCl_3 (M = Al, Ga, or In). *J. Mol. Cat A: Chem*.**2007**, 277, 164-170.

Anslyn, E.V.; Dougherty, D. A. Modern Physical Organic Chemistry. University Science Books.

Avent, A.G.; Chaloner, P.A.;Day, M.P.; Seddon, K.R, Welton, T. Evidence for hydrogen bonding in solutions of 1-ethyl-3-methylimidazolium halides, and its implications for room-temperature halogenoaluminate(III) ionic liquids**.** *J.Chem.Soc. Dalton Trans*. **1994**,3405-3413.

Becke, A. D.Density functional calculations of molecular bond energies. *J.Chem.Phys.,* **1986,** 84, 4524-4529.

Cassol, C.C.; Umpierre ,A.P. On the extraction of Aromatic compounds from hydrocarbons by imidazolium ionic liquids. *Int.J.Mol.Sci*. **2007**, 8, 593-605.

Chattaraj, P. K. ; Sarkar, U.; Roy. D. R. Electrophilicity index. *Chem. Rev*.**2006**,106,2065-2091.

Cruz IG, Valencia D, Klimova T, Roa RO, Magadan JM, Balderas RD, Illas F. Proton affinity of S-containing compounds: Implications for crude oil hydrodesulphurization. *J.Mol.Cat A: Chem*. **2008**, 281, 79-84.

Francisco, N. Ricardo. V. Ab initio study of luminescent substituted 8-hydroxyquinoline metal complexes with application in organic light emitting diodes.*J. Mol. Struct. (Theo).***2008**,850 127-134.

Freire, M.G.; Santos, M.N..; Marrucho, I.M.; Coutinho, J.A.P. Evaluation of COSMO-RS for the prediction of LLE and VLE of alcohols + ionic liquids. *Fluid. Phase. Equilibria*.**2007**, 255, 167–178.

Frisch, M. J.; Trucks, G. W.; Schlegel, H. B.; Scuseria, G. E.; Robb, M. A.; Cheeseman,J. R.; Zakrzewski, V. G.; Montgomery, J. A., Jr., Stratmann, R. E.; Burant, J. C.; Dapprich, S.;

Millam, J. M.; Daniels, A. D.; Kudin, K. N.; Strain, M. C.; Farkas, O.; Tomasi, J.; Barone, V.; Cossi, M.; Cammi, R.; Mennucci, B.; Pomelli, C.; Adamo, C.; Clifford, S.; Ochterski, J.; Petersson, G. A.; Ayala, P. Y.; Cui, Q.; Morokuma, K.; Salvador, P.; Dannenberg, J. J.; Malick, D. K.; Rabuck, A. D.; Raghavachari, K.; Foresman, J. B.; Cioslowski, J.; Ortiz, J. V.; Baboul, A. G.; Stefanov, B. B.; Liu, G.; Liashenko, A.; Piskorz, P.; Komaromi, I.; Gomperts, R.; Martin, R. L.; Fox, D. J.; Keith, T.; Al-Laham, M. A.; Peng, C. Y.; Nanayakkara, A.; Challacombe, M.; Gill, P. M. W.; Johnson, B.; Chen, W.; Wong, M. W.; Andres, J. L.; Gonzalez, C.; Head-Gordon, M.; Replogle, E. S. and Pople, J. A. Gaussian 03, Revision B.05, Gaussian, Inc., Pittsburgh PA, **2003.**

Fuentealba , P. ; Contreras. R. Sen, I. K.D. Reviews of Modern Quantum Chemistry vol. II, World Scientific, Singapore .**2002**, 1013.

Fuentealba, P.; Perez, P.; Contreras. R. On the condensed Fukui function. *J. Chem. Phys*.**2000**, 113,2544-2551.

Geerlings.P.; Proft.F.; Langenaeker.W.; Conceptual Density Functional Theory. *Chem.Reviews*, **2003**,103, 1793-1873.

Heintz,A. Recent developments in thermodynamics and thermophysics of non -aqueous mixtures containing ionic liquids. A review, *J.Chem. Thermodyn*, **2005,** 37, 525-535.

Hernández, J. A. M.; Ramirez, S. l.; Domínguez, J. M.; Valencia, C. D.; Cruz,I.; Guevara, J. A. Survey on ionic liquids effect based on metal anions over the thermal stability of heavy oil.***J. Ther. Anal. Cal*,** 2009, **95,173-179.**

Hirota, M.;Sakaibara, K.;Suezawa, H.;Yuzuri, T.;Ankai, E.;Nishio, M.Intramolecular CH-π interaction substituent effect as a probe for hydrogen bond like character. *J.Phys.Org. Chem*. **2000**,13, 620–623.

Hunt, P.A.; Kirchner, B.; Welton. T. Characterising the electronic structure of ionic liquids: An examination of the 1- butyl-3-methylimidazolium chloride ion pair. *Chem. Eur. J*.**2006a**, 12,6762-6775.

Hunt. P.A. The Simulation of Imidazolium-Based Ionic Liquids.Mol. Simul.**2006b**,32,1-10.

Inokuchi, F.; Miyahara, Y.; Inazu, Y.; Shinkai, S. Metal-Metal Multiple Bonds Formed Across Two Tungsten-Calix[4]arenes by a Reductive Coupling Reaction. *Angew. Chem., Int. Ed*. **1995**, 34, 1364–1366.

Kanai, K.; Nishi, T.; Iwahashi, T. ; Ouchi, Y.; Seki, K.; Harada, Y.; Shin,S. Anomalous electronic structure of ionic liquids determined by soft x-ray emission spectroscopy: contributions from the cations and anions to the occupied electronic structure. *J. Chem. Phys*.**2008**, 129, 224507-224512.

Karelson, M.; Lobanov, V.S. Quantum-Chemical Descriptors in QSAR/QSPR Studies. *Chem.Rev*. **1996**,96,1027-1043.

Katritzky, A .R. Quantum–Chemical Descriptors in QSAR/QSPR studies. *Chem. Rev*. **1996**, 96, 1027-1043.

Kim.K.; Park.S.; Choi.S.; Lee.H. Vapor Pressures of the 1-Butyl-3-methylimidazolium Bromide +Water, 1-Butyl-3-methylimidazolium Tetrafluoro borate + Water, and 1-(2-Hydroxyethyl)-3-methylimidazolium Tetrafluoroborate ++ Water Systems *J. Chem. Eng. Data* **2004,** 49*,* 1550-1553.

Klamt, A.; Schüürmann, G. COSMO: A New Approach to Dielectric Screening in Solvents with Explicit Expressions for the Screening Energy and its Gradient. *J. Chem. Soc. Perkin Trans.* **1993,2,** 799-805.

Kohn, W.; Sham, L. Self-Consistent Equations Including Exchange and Correlation Effects. *Physical Review.***1965,** 140, A1133.

Kolandaivel, P. ; Arulmozhiraja, S.; Bhuvaneswari. R. Hybridization effect on chemical potential and hardness — a quantum chemical study.Chem. Phy. Lett.**1996**, 259,138-141.

Kumar, A.P.; Banerjee, T. Thiophene Separation with Ionic Liquids for Desulphurization: A Quantum Chemical Approach. *Fluid Phase Equilibria*. **2009**, 278, 1-8.

Koopmans, T. Über die Zuordnung von Wellenfunktionen und Eigenwerten zu den Einzelnen Elektronen Eines Atoms. *Physica* (Elsevier) 1, **1934**, 104–113.

Lacrama.;Putz, M.V.; Ostafe. V. A spectral-SAR model for the anionic-cationic interaction in ionic liquids: Application to Vibrio fischeri ecotoxicity. *Int.J.Mol.Sci.***2007**,8,842-863.

Lozach, L.G, Dutasta, B.; Collet, J.P. A. Remarkable effect of the receptor size in the binding of acetylcholine and related ammonium ions to water-soluble cryptophanes. *J.Am.Chem.Soc*. **1993**, 115, 11652–11653.

Masci, B. Homooxacalixarenes. 3. Complexation of quaternary ammonium ions by parent homooxacalixarenes in $CDCl_3$ solution. *Tetr. Lett*. **1995**, 51, 5459–5464.

Meng.J.; Dolle.A.; Carper. R.W. Gas Phase Model of an Ionic Liquid: semi-empirical and ab-initio bonding and molecular structure, *J. Mol. Struct. (Theochem)* **2002**, 585,119–125.

Nirmala, V.; Kolandaivel. P. Molecular interaction of H_2 and H_2O molecules with the boron nitride $(BN)_{n=3-5}$ clusters: A theoretical study**.** *J. Mol. Struct. (Theo)*. **2006**,758,9-15.

Nishi, T.; Iwahashi, T.; Yamane, H.; Ouchi ,Y.; Kanai, K.; Seki. K. Electronic structures of ionic liquid $[C_nmim]^+$ BF_4 and $[C_nmim]^+$ PF_6 studied by ultraviolet photoemission inverse photoemission, and near edge X-ray absorption fine structure spectroscopies. *Chem. Phy. Lett*. **2008**, 455,213-217.

Parr, R. G.; Yang, W. Density-Functional Theory of Atoms and Molecules; Oxford University Press: New York, **1989**.

Pauling. The Nature of the Chemical Bond, 3rd edn, Cornell University Press, Ithaca, NY, **1960**.

Pearson, R.G.; Palke. W.E. Support for a principle of maximum hardness.*J. Phys. Chem*. **1992**,96,3283-3285.

Reddy, A.S.; Sastry, G.N. Density-Functional exchange – energy approximation with correct asymmetric behavior. *J. Phys. Chem. B*. **2005**,109,8893–8903.

Reid.R.C.;Prausnitz.J.M.;Poling.B.E. *The Properties of Gases and Liquids*, 4th Edition, McGraw-Hill, New York, **1987**.

Roy, R.K.; Krishnamurti, S.; Geerlings, P.; Pal.S. Local softness and hardness based reactivity descriptors for predicting intra and intermolecular reactivity sequences: Carbonyl compounds.*J. Phys. Chem. A*. **1998**, 132,3746-3755.

Schaftenaar, G.; Noordik, J.H. Molden: a pre- and post-processing program for molecular and electronic structures. *J. Comput.-Aided Mol. Design* **2000,** 14, 123-134.

Selvarengan, P.; Kolandaivel. P. Studies of solvent effects on conformers of glycine molecule. *J. Mol. Struct. (Theo*).**2002**, 617, 99-106.

Song, Y.;Cushman, M.J. The Binding Orientation of a Norindenoisoquinoline in the Topoisomerase I-DNA Cleavage Complex Is Primarily Governed by π-π Stacking Interactions. *J. Phys.Chem B*. **2009** ,112,9484-9489.

Su,B.M.; Zhang, S.; Zhang, Z.C. Structural Elucidation of Thiophene interaction with Ionic Liquids by Multinuclear NMR Spectroscopy. *J.Phys.Chem*. **2004**, 108, 19510-19517.

Suezawa, H.; Hashimoto, T.;Tsuchinaga, Yoshida,K.; Yuzuri,T.; Sakakibara, T.; Hirota, K.; Nishio, M.; *J.Chem.Soc. Perkin Trans*. **2000**,2, 1-9.

Suezawa, H.; Ishihara, S.;Umezaw, Y.;Tsuboyam, S.;Nishio, M. The Aromatic CH/π Hydrogen Bond as an Important Factor in Determining the Relative Stability of Diastereomeric Salts Relevant to Enantiomeric Resolution - A Crystallographic Database Study. *Eur. J.Org.Chem.* **2004**, 4816-4822.

Sygula, A.; Fronczek, F.R.; Sygula. R.; Rabideau, P.W, Olmstead, M.M. J. Am. Chem.Soc. 2007,129,3842–3843

T. Koopman. Über die Zuordnung von Wellenfunktionen und Eigenwerten zu den Einzelnen Elektronen Eines Atoms. *Physica*. **1934**,1,104-113.

Thanikaivelan, P. ; Subramanian, V.; Raghava, V.R.; Unni. B.N. Application of quantum chemical descriptor in quantitative structure activity and structure property relationship. *Chem. Phy. Lett*. **2000**,323,59–70.

Turner. A. E.; Pye. C. C.; Singer. D. R. Use of ab initio Calculations toward the Rational Design of Room Temperature Ionic Liquids, *J. Phys. Chem. A,* **2003,** 107, 2277-2288.

Turner. A. E.; Pye. C. C.; Singer. D. R., Use of ab initio Calculations toward the Rational Design of Room Temperature Ionic Liquids, *J. Phys. Chem. A,* **2003,** 107, 2277-2288.

Vektariene, A.; Vektaris, G.; Svoboda, J.A theoretical approach to the nucleophilic behavior of benzofused thieno [3, 2-b]furans using DFT and HF based reactivity descriptors. *ARKTVOC*. **2009**, 311-329.

Wilkes J.S. A short history of ionic liquids from molten salts to neoteric solvents. *Green Chem*.**2002**,4,73-80.

Yu, G. ; Zhang, S. ; Yao, X. ; Zhang, J.; Dong, K.; Dai, W.; Mori. R. Design of Task-Specific Ionic Liquids for Capturing CO_2: A Molecular Orbital Study. Ind. Eng. Chem. *Res*.**2006**, 45, 2875-2880.

Yu, G.; Zhang. S. Insight into the cation–anion interaction in 1,1,3,3-tetramethylguanidinium lactate ionic liquid. *Fluid Phase Equilibria*.**2007**, 255,86–92.

Zhou, J.; Mao, J.; Zhang, S. Ab initio calculations of the interaction between thiophene and ionic liquids. *Fuel.Proc.Tech*. **2008**, 89, 1456-1460.

4.1 Introduction

The aim of this chapter is to screen the potential ionic liquids for the removal of aromatic sulphur and nitrogen species by tuning the cation and anion combination. This tuning is very difficult to perform experimentally since limited data are available in literature with respect to imidazolium, pyridinium and other classes of cations. It should be noted that without the screening of potential ILs, experimental studies are not possible because of the high cost and time involved. It is a well known fact that the most challenging and difficult part are in removing the last traces of sulphur/nitrogen species from diesel oil. The infinite dilution activity coefficient (IDAC) is an important indicator which quantifies this very phenomenon [Kumar et al.,2009]. Lesser the IDAC values from unity, greater are the tendency for the ionic liquid to remove aromatic sulphur and nitrogen species. The selectivity and capacity at infinite dilution which are function of IDAC values, quantifies and screens the potential ionic liquids. Quantum chemical based approaches such as COSMO (**C**onductor **L**ike **S**creening **M**odel)[22] along with its extension to RS (**R**eal **S**olvent)[23-27] clearly demonstrates the rapid progress in this area. An important advantage of the COSMO-RS model is that it predicts *a-priori* the liquid phase non-ideal activity coefficient of any component in a mixture without using any experimental data. It uses the molecular structure of the solute/component as the only initial input [Klamt et al.,1993,1995,2000,2005].Thus it directly predicts the IDAC values which are measurable and thereby used to calculate the selectivity (S), capacity (C) and performance index (PI) at infinite dilution. Therefore, in this work we have used the COSMO-RS model for the *a-priori* prediction of activity coefficient at infinite dilution of aromatic sulphur and nitrogen species in ionic liquid and diesel oil.

4.2 Conductor-like Screening Model (COSMO)

Quantum chemical methods originally have been developed for isolated molecules, i.e. for molecules in vacuum or, at best, in the gas phase. But due to the importance of solvents in biochemical, catalytic and separation processes, attempts have been made for the last two to three decades to combine the quantum chemical description

of a molecule with an approximate continuum description of the surrounding solvent. In order to describe the electrostatic behavior of solvents, dielectric models have been chosen, following the early ideas of [Born 1920]. Reviews on such *continuum solvation models* CSMs have been given by [Tomasi and Persico, 1994] and [Cramer et al., 1995]. The Conductor-like Screening Model COSMO introduced by [Klamt and Schüürmann, 1993], is in principle a more efficient variant of these CSMs. It avoids the complicated solution of the dielectric boundary conditions by approximating the screening charges of a dielectric medium of permeability ε with scaled screening charges of a conductor, where the scaling factor is given by

(4.1)

Thus the simpler boundary condition of a conductor appears in the equation (Eq. 4.1). The COSMO approximation is exact in the limit of $\varepsilon = \infty$ and it is within 0.5% accuracy for strong dielectrics like water with a permeability of ($\varepsilon = 80$). Even in the lower dielectric limit of solvents of $\varepsilon = 2$, COSMO coincides with the exact dielectric model within 10%. Hence the COSMO approach is becoming the standard CSM in quantum chemical codes.

The basic steps in COSMO calculation are:

1. For a given molecular geometry, a molecular cavity is constructed using element specific radii which are 1.2 times Bondi radii [Bondi 1964].
2. The cavity is discretized in m small segments, so that on each segment i, a constant screening charge density σ_i can be assumed, so that screening charge $q_i = a_i\sigma_i$, where a_i is the area of the segment; the Coulomb interaction matrix $\boldsymbol{A}$ of the segments is then calculated.
3. For each molecular charge distribution, i.e. nuclear charges and electronic density of the solute, the set of ideal screening charges $q^* = (q_1^*, \ldots, q_m^*)^T$ are calculated from the conductor condition of vanishing potential:

(4.2)

where vector is the electrostatic potential generated by the solute X *on the* m segments.

4. The screening charges q of the solvent medium are then calculated by scaling q* so that $q = f(\varepsilon)\, q^*$, where $f(\varepsilon)$ is the scaling factor given by Eqn 4.1
5. These screening charges of the solvent medium are then resubstituted as an external field into the quantum formalism.

The matrix $\boldsymbol{A}$ (which itself is a function of cavity surface) and its *Cholesky factorization* [Press et al., 1992] is needed for an efficient solution of Eq. 4.2.These have to be calculated once for each geometry so the additional computational costs of COSMO in the quantum chemical algorithms are small. In addition, COSMO may even slightly speed up the quantum chemical self-consistency part. Thus, COSMO calculations are usually no more expensive than gas phase quantum chemistry. At the end of the quantum chemical *self-consistency* and *geometry optimization* loops, a self-consistent state is reached, i.e. energy, density, and geometry of the solute X are as if embedded in a dielectric of strengths ε. In addition, the screening charge density σ supplied by the continuum on each position of the molecular contact surface and the dielectric interaction energy of the solute with the continuum is known now. The dielectric energy is an excellent measure for the polarity of molecules, much better than dipole moment, because it subsumes all ways of electrostatic interactions of a molecule with its surrounding.

The generation of the COSMO files although time consuming has to be done once for each compound. The COSMO file implementation is available on quantum mechanical packages like TURBOMOLE [Schäfer et al., 2000], $DMOL_3$ [Andzelm et al., 1995] and GAUSSIAN 03 [Frisch et al., 2003].

4.3 Generation of COSMO File by Gaussian03

The Quantum Chemistry Package of Gaussian 03 has been used to compute the COSMO files. The equilibrium geometry of the molecules in the ideal gas phase is first

obtained using the density functional theory of P BVP86 [Perdew.J. P, 1986]. The Triple Zeta Valence Potential (TZVP) [Schäfer et al., 1994] basis set has been used in combination with the density fitting basis set of DGA1 [Sosa et al., 1992]. The ideal screening charges on the molecular surface are then computed using the same level of theory i.e P BV86 [Perdew.J. P, 1986].For ionic liquids the cation and anion pair are together minimized using Hartree Fock theory. Then the optimized cation and anion combination is used to generate COSMO file using the implementation available in *Gaussian03*.The radii of the nine elements are used to define the cavity for the molecule. The radii of the nine components are taken from [Klamt et al., 1995] and are reported in Table 4.1. For phosphorous a default value of 1.17 R_{Bondii} has been used.A typical implementation of COSMO File Generation in *GAUSSIAN03* is shown in Figure 4.1. The keyword *SCRF=COSMORS* generates the COSMO file of the desired molecule of interest.

Table 4.1: Cavity Radii values considered for our work

Element	**Radius in A^o**
H	1.30
C	2.00
N	1.83
O	1.72
F	1.72
S	2.16
Cl	2.05
Br	1.85
I	1.98
P	1.80*

* Default radii of [Bondi ,1964]

```
%mem=540MW
%chk= emimac
#P BVP86/svp/DGA1 scf=tight
Comment Line
0     1                          (Charge              and
Multiplicity)
Z-Matrix
--link1--
%chk=emimac
#P  BVP86/svp/DGA1  scf=(tight,novaracc)  SCRF=COSMORS
guess=read geom=checkpoint

Comment line

0    1                   (Charge and Multiplicity)

emimac.cosmo       (The   COSMO   file   which   will   be
created)
```

Figure 4.1: Input file for COSMO File generation in Gaussian 03

The various terms and its meaning are as follows:

1. % mem = 540 MW

   This gives the total amount of internal memory needed for this calculation.

2. # P BVP86/SVP/DGA1

   This indicates the DFT Theory being used (i..e P BVP86),the basis set (SVP) and the density fitting function. The SVP orbital coefficients and its expansion can be obtained by the *GFprint* and *GFInput* command in Gaussian 03

   The DGA1 or the Density Gradient Approximation expands the electron density in a set of atom-centered functions when computing the Coulomb interaction instead of computing all the two-electron integrals. It provides significant performance gains for pure DFT calculations on medium sized systems too small to take advantage of the linear scaling algorithms without a significant degradation in the accuracy of predicted structures, relative energies and molecular properties

3. SCF = tight

This indicates a full convergence of energy.

A typical Illustration of a COSMO implementation is shown in Figure 4.2 where the screening charge densities have been shown on thiophene molecule.

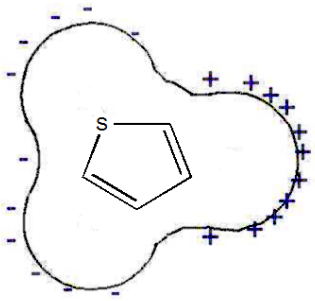

Figure 4.2: Screening Charge Distribution σ for thiophene

4.4 σ-profiles and its Algorithm

The most important descriptor used in COSMO-RS is the local screening charge density σ, which would be induced on the molecular surface if the molecule would be embedded in a virtual conductor. This descriptor, which can be calculated at reasonable cost by quantum chemical programs using the continuum solvation model CSM, COSMO [Klamt and Schüürmann, 1993], is extremely valuable for the local polarity of molecular surface. This single-molecule ideal solvation calculation needs to be done only once for each molecule, regardless of the mixture in which the molecule appears. The screening charge density σ is the only descriptor determining the interaction energies. Thus, the ensemble of surface pieces characterizing a pure compound (or a mixture *S*) is sufficiently described by the distribution function , which describes the relative amount of surface in the ensemble having a screening charge density between σ and σ+dσ. The notation "σ-profile" is used for this distribution function. The procedure for σ-profile is as follows:

1. The initial file i.e COSMO file as discussed earlier contains the ideal screening charge densities on surface segments along with the coordinates of the segments. The screening charge densities σ* from the COSMO output are averaged to give the

"apparent" charge density σ on a standard surface segment using the following expression:

(4.3)

where Å, the averaging radius of the standard surface segment,

is the radius of segment n, and d_{mn} is the distance between segments m and n. The COSMO file generated for water is given in Appendix 4.1.

2. For most compounds, the ideal screening charge density falls within the range of -0.03 to 0.03 e/Å^2. This interval is partitioned in 60 parts, and the histogram (weighted by the area of each segment) of the averaged charge density is computed at each 0.001 e/Å^2 increment. This gives the σ profile for the pure compound.

A program has been written in MATLAB which takes the name of the molecule and a_{eff} as the input and writes the σ-profile as an output file.The only parameter that appears in computation of σ-profiles is the effective area of a contact segment.

4.5 COSMO-RS vs Excess Energy Models

UNIQUAC is one of the classical models for modelling of activity coefficients where the activity coefficients are related to excess Gibbs free energy g^E :

(4.4)

The g^E consists of a combinatorial term which is derived from the pure component properties and a residual term which consists of fitted interaction parameters .These parameters are related to the interaction energies between neighbouring molecules.Thus the expression for molecular interaction energy is given by:

(4.5)

The interaction energies u_{ij} and u_{ji} are fitted to experimental data. Derivation of UNIQUAC model assumes only binary interactions in a liquid. When fitted to experimental data it is likely that the energy parameters will also capture these long-range energy contributions; but these contributions do not have the same dependency on concentrations as assumed in UNIQUAC. In UNIQUAC the local concentration (x_{ji}) of molecules of different species around a molecule of one species (x_{ji} – local concentration of particles *j* around species *i*):

(4.6)

According to this equation the probability that atoms of type *i* are interacting with molecules of type *j* is independent of the interaction between molecules of type *j* (u_{jj}). If molecules of type *j* interacted strongly with each other they would be less likely to interact with molecules of type *i* and the assumption is therefore wrong.

UNIFAC is based on the same model as in UNIQUAC i.e it views molecules as a set of groups.Here the residual part of excess Gibbs free energy is a summation over the individual contributions of the groups. This leads to group energy interaction parameters. The combinatorial energy is calculated using the same method as in UNIQUAC, molecular volumes and surfaces being sums of group volumes and surfaces.An assumption in UNIFAC [Fredensland et al., 1977] is that each contact between two groups *m* and *n* is associated with a specific group interaction energy, a_{mn} i.e any kind of contact between the groups will have same energy. This does not differentiate between vdW interactions and hydrogen bonding. Thus an average energy is provided between the two interacting groups. Intramoecular energy is completely neglected (e.g intramolecular hydrogen bonds).Also the energy of molecular conformers in the solvent phase can vary by several kcal/mol, especially for large flexible molecules the orientation of the molecule is important. This kind of energy contribution cannot be easily included in a group contribution model; this is one serious short-coming of group contribution models.

In COSMO-RS the interaction energies of the contact segments are specific contributions from electrostatic misfit, vdW and hydrogen bonding interactions. In COSMO-RS the screening charge density σ is the relevant property for interaction energy, while in UNIFAC the relevant group numbers *i* and *j* determine the interaction energy. Thus an analog of the sigma profile (i.e the probability distribution of screening charges) for UNIFAC is the normalized group constitution function:

(4.7)

in which the is the number of groups of type k *in compound* i *and* denotes the relative surface area of group *k*.

4.6 COSMO-RS Methodology

In COSMO-RS a liquid is considered to be an ensemble of almost closely packed ideally screened molecules (Figure 4.3). Each surface contact has a direct partner. In reality, there is no conducting medium between them and the energy difference between the real situation of such contact and the ideally screened situation is defined as a local electrostatic interaction energy. Considering a contact on a region of molecular surface of area a_{eff} (effective contact area), and that the two neighboring contacting surfaces have average ideal screening charge densities σ and σ′, the interaction energy is the energy which is necessary to remove the residual screening charge density σ + σ′ from the contact. In the special situation of σ = - σ′, there is nothing to remove and hence, the interaction energy is zero. Such a contact here is called ‘‘ideal electrostatic contact’’ (Figure 4.4).

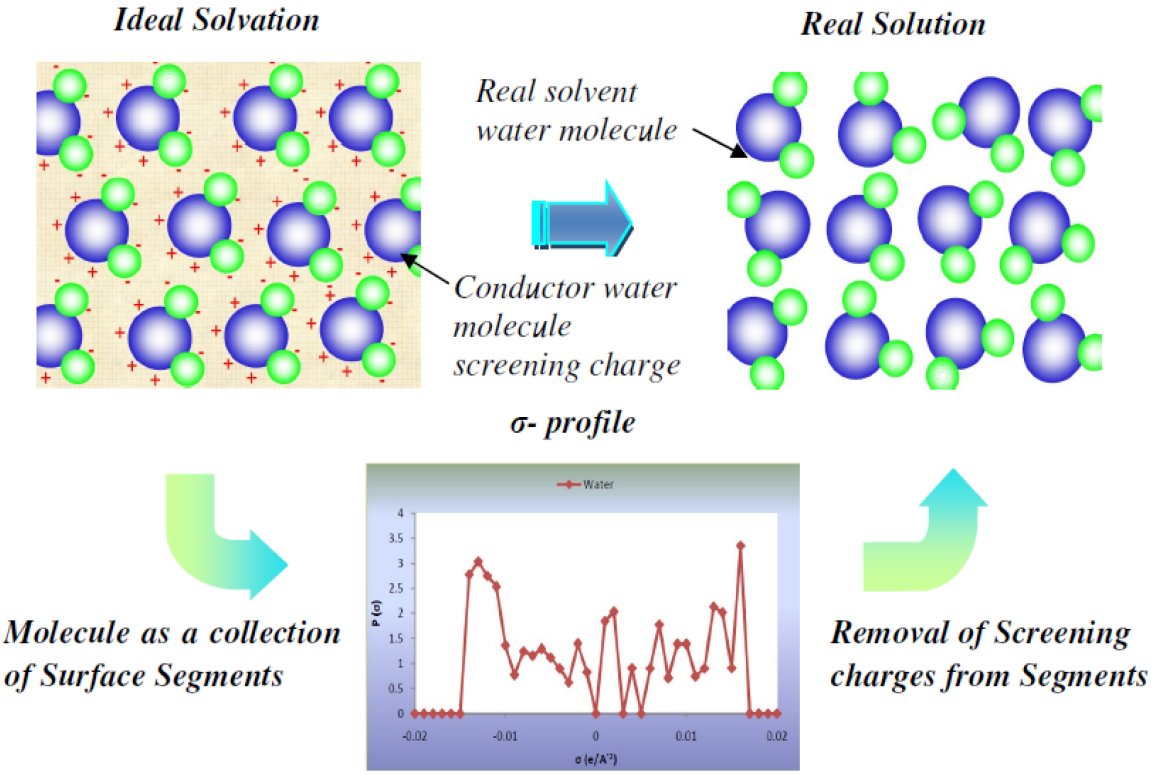

Figure 4.3: Difference between Ideal and Real Solution

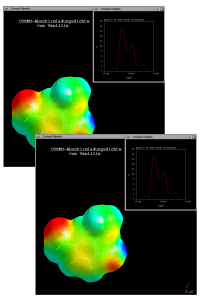

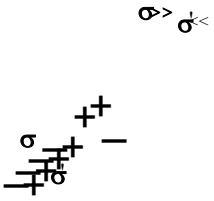

Figure 4.4: Contact Interactions between adjacent segments

The various interaction energy terms are: the misfit (Eqn 4.8), hydrogen bonding (Eqn 4.9) and the van der Waals (Eqn 4.10).

(4.8)

where $\alpha' = (0.64 \times 0.3 \times$ $)/\varepsilon 0$ and $\varepsilon 0 = 2.395 \times 10\text{-}4$ $(e_2$ mol)/(kcal Å) is the permittivity in free space. The misfit of the partners arises, when $\sigma + \sigma'$ does not vanish.

(4.9)

The hydrogen bonding term (E_{hb}) comes into play only if two sufficiently polar pieces of surface of opposite polarity are in contact, and becomes important with increasing polarity. Taking the screening charge density σ as a local measure of polarity, E_{hb} is not zero when either is less than and is greater than the threshold value

.The hydrogen bonding energy is proportional to the product of the excess screening charge densities, i.e. $(\sigma_{donor} + \sigma_{hb})$ $(\sigma_{acceptor} - \sigma_{hb})$.

(4.10)

The van der Waals (vdW) energy contribution is expressed by element-specific dispersion coefficient parameters $\tau(e)$, which have to be fitted to experimental data. The vdW energy is gained by a molecule *X* during the transfer from the gas phase to any liquid phase.This contribution is not a interaction term but a state of the molecule embedded with vdW interacting surface species. This so called 'reference state' does not contribute to the prediction of liquid phase activity coefficients and is important only for liquid-gas transfer processes e.g vapor pressure data.

The interactions of molecular surfaces in COSMO-RS are given by an interaction energy functional $e(\sigma,\sigma') = e_{misfit}(\sigma,\sigma') + e_{hb}(\sigma,\sigma')$, which depends only on the screening charge densities.

(4.11)

The vdW contribution is subsumed in the reference state energy. The generic interaction functional $e(\sigma,\sigma')$ has three adjustable parameters, α', σ_{hb}, and c_{hb} ; while the vdW term has the dispersion coefficient $\tau(e)$ as adjustable parameter per element. In addition to these explicit parameters, the screening charge densities also depend on the element-specific radii which are used in the cavity construction and roughly fixed by the rule 1.2 R_{Bondi}. Thus there are three general parameters plus two element specific parameters per element. For the nine elements H, C, N, O, F, S, Cl, Br, and I, we have

altogether 21 parameters. Details of COSMO-RS can be found in [Klamt 1995;Klamt et al.,2000,2002; Klamt, 2005]

If the liquid system under consideration is a pure liquid *X*, then the σ-profile of the system is identical with the σ-profile of the pure compound. In general, a system may be a mixture consisting of several compounds *X* with molar concentrations x_i. Then the σ-profile of the system (Eqn 4.12) is given by the weighted sum of the σ-profiles of the components, i.e.,

(4.12)

The screening charge densities σ* from the COSMO output are averaged to give the "apparent" charge density σ on a standard surface segment using Equation 3.6. An exact expression for the sigma potential of these segments based on rigorous statistical mechanical argument is given by:

(4.13)

where is the chemical potential of a surface segment with charge density in a solution *S*. This distribution has been termed as *σ-potential* by [Klamt, 1995] and it describes the affinity of the solvent for a molecular surface of polarity σ. The activity coefficient of a segment i.e and sigma potential are connected through the following relation:

(4.14)

The activity coefficient of segment in the mixture and in the pure liquid, and are determined from :

(4.15)

Activity coefficient of a species in a mixture is then calculated from:

(4.16)

where) is given by Eqn 4.11. Molecular volumes and areas from COSMO calculation are normalized by a standard volume (66.69 $Å^3$) and surface area (79.53 $Å^2$) to yield the *r* and *q* parameters which are used for computing the Staverman-Guggenheim term:

(4.17)

It is interesting to note that the activity coefficient of a species in a mixture is obtained as a function of composition without specifying a priori the form of this composition dependence. For solving Eq. (4.15) numerically, an iterative procedure is required because appears on both sides. Starting from the iteration turns out to converge rapidly, if after each iteration step the average of the old and the new chemical potentials is used for the next step in order to avoid numerical oscillations.

4.7 COSMO-RS predictions

Till now we have discussed the scalar properties as outlined in chapter 3 (Table 3.6), which cannot be measured experimentally. However an attempt is made where the scalar properties can be correlated with experimental measurements. The activity coefficient at infinite dilution can be measured via gas –liquid chromatography and gives

us an important descriptor for the effectiveness of a solvent to remove the last trace of impurity (i.e thiophene and pyridine in our case). Till date there are no experimental values available to prove our findings. However we have compared the activity coefficient at infinite dilution activity coefficients (IDAC) in our previous work [Banerjee et al., 2006b] for ionic liquids successfully. Thus we predicted the IDAC values in Table 4.2 which can be treated at par with experimental values and will serve as a test for my computational chemistry basis.

For this purpose COSMO-RS based approach was used to determine the activity co-efficient at infinite dilution for thiophene and pyridine mixture in ionic liquids .In our earlier work we have successfully reported the COSMO-RS predictions based on vapor-liquid equilibria [Banerjee et al.,2006a] and liquid-liquid equilibria [Banerjee et al.,2008] for ionic liquid based systems. For the prediction, the complete dissociation of ionic liquid is taken to be equal to the dissociation of cation and anion [Banerjee et al., 2008].The sigma profile (charge distribution of screening charge densities) [Banerjee et al., 2006a, 2006b, 2008] of ionic liquid is simply the algebraic sum of the sigma profile of cation and anion (Eqn 4.18).

(4.18)

Where and are the sigma profiles for cation and anion respectively. An equimolar concentration of cation and anion has been assumed [Banerjee et al.,2008] in the prediction. In the prediction of simultaneous removal we have assumed a pseudo binary component i.e taking thiophene and pyridine as a single entity. Sigma profiles of thiophene and pyridine are calculated and further linearly added as:

(4.19)

Thus represents the sigma profile of pseudo component (thiophene + pyridine) and will be used in our predictions. An equimolar concentration of thiophene and pyridine has been assumed in this case. The activity coefficient at infinite dilution for pyridine + thiophene in IL is presented in Table 4.2.An activity coefficient greater than one signifies that the pseudo component compound is relatively dissimilar in nature with ionic liquid and vice versa. This implies that the compound will partition less into the ionic liquid phase as compared to other ionic liquids. It is evident from Table 4.2 that [BeMIM][BF_4] with an activity coefficient of 0.9727 at infinite dilution stands out as the most effective IL.It can be seen that the ranking of ionic liquids with activity coefficient at infinite dilution (Table 4.2) exactly matches the ranking given by the combination of all parameters (Table 3.6). (i.e [BeMIM][BF_4] > [BUMPYR][BF_4]> [BUMPY][PF_6]> [BUMPY][BF_4]> [BUMPYR][PF_6]).Thus we can conclude that the correlation between quantum chemistry method and predictions using COSMO-RS (at par with experimental values) is directly related. This proves that quantum chemistry methods can provide qualitative pathways for selecting potential solvents like ionic liquids.

4.8 Infinite Dilution Activity Coefficient (IDAC) Predictions

We have discussed the interaction energies in chapter 3 (Table 3.9) and saw that it cannot be measured experimentally. However an attempt is made where the interactions energies can be correlated to experimental measurements. The infinite dilution activity coefficient (IDAC) is an important indicator which quantifies this very phenomenon. Further, the activity coefficient at infinite dilution can be measured via gas –liquid chromatography and gives us an important descriptor for the effectiveness of a solvent to remove the last trace of impurity (i.e thiophene or pyridine in our case).Lesser the IDAC

values from unity, greater is the tendency for the ionic liquid to remove nitrogen/sulphur species. We have predicted the IDAC values of pyridine and thiophene in Ionic Liquids (Table 4.3) which can be treated as close to experimental values and serve as a test for our computational chemistry basis. For the prediction of IDAC values we have used the COSMO-RS parameters are: a_{eff} = 6.25 $Å^2$ (surface area of a standard segment), α' = 8896 kcal $Å^4$ mol^{-1} e^{-2} (misfit energy constant) for misfit energy interaction, c_{hb}= 54874 kcal $Å^4$ mol^{-1} e^{-2} (hydrogen bonding energy constant) and σ_{hb}=0.0085 e $Å^{-2}$ (hydrogen bonding cutoff) [Banerjee et al.,2008].It can be seen from Table 4.3 that interaction energies of pyridine are higher than that of thiophene. However the activity coefficient at infinite dilution of pyridine is lower than that of thiophene. Thus an inverse relation between activity coefficient at infinite dilution and interaction energies is obtained. Smaller values of interaction energies indicate higher activity coefficient thereby lesser solubility with the solvent.The only anamoly in this complex is the one with the complex: [BPYRO][PF_6]-thiophene and [BPYRO][PF_6]-pyridine (Table 4.3). The interaction energies are positive in this case as the IL is solid at room temperature. The positive interaction energies implies that the columbic interactions are very high as compared to π-π interaction.

Table 4.2: Comparative study for IL-TS-PY based on scalar quantities

Rank		**1**	**2**	**3**	**4**	**5**
Parameter	**Objective**					
Based on HOMO / LUMO energy values	More LUM (higher negative)	[BeMIM][BF_4]	[BUMPYR][BF_4]	[BUMPY][PF_6]	[BUMPY][BF_4]	[BUMPYR][PF_6]
Based on HOMO-LUMO energy gap	Small Gap	[BeMIM][BF_4]	[BUMPYR][BF_4]	[BUMPY][PF_6]	[BUMPY][BF_4]	[BUMPYR][PF_6]
Based on Global softness	Higher Global Softness	[BeMIM][BF_4]	[BUMPYR][BF_4]	[BUMPYR][PF_6]	[BUMPY][PF_6]	[BUMPY][BF_4]
Based on Electrophilicity	Higher Electrophilicity	[BeMIM][BF_4]	[BUMPY][PF_6]	[BUMPY][BF_4]	[BUMPYR][BF_4]	[BUMPYR][PF_6]
Overall		[BeMIM][BF_4]	[BUMPYR][BF_4]	[BUMPY][PF_6]	[BUMPY][BF_4]	[BUMPYR][PF_6]
COSMO-RS Predictions		0.9727	1.1792	1.7864	2.5928	3.8473
Rank based on COSMO-RS		[BeMIM][BF_4]	[BUMPYR][BF_4]	[BUMPY][PF_6]	[BUMPY][BF_4]	[BUMPYR][PF_6]

Table 4.3: Interaction Energy and at Infinite Dilution Activity Coefficient (IDAC) for Ionic Liquids complexes

S.No	ILs Name	Interaction energy (KJ.mole^{-1})			Infinite dilution activity coefficient (IDAC) via COSMO-RS model	
		Thiophene	Pyridine	Thiophene + Pyridine	Thiophene	Pyridine
1	[BPYRO][BF_4]	-4.37	-27.17	-23.39	2.8272	0.359
2	[BPYRO][PF_6]	2.275	3.975	-33.95	6.6307	1.6136
3	[BPY][BF_4]	-10.53	-15.40	-48.50	1.7964	1.4571
4	[BPY][PF_6]	-3.43	-79.06	-27.37	3.0726	0.0561
5	[BeMIM][BF_4]	-20.48	-27.26	-30.29	1.3013	1.1829

4.9 Effect of Sigma Profile

In the COSMO scheme, sigma profile is the only descriptor, which describes the local polarity of molecular surface and determines the interaction energies, replacing the empirical interaction parameters usually used in chemical engineering models like UNIQUAC and UNIFAC. This further shows the polarity of the components in a mixture or within itself. The most important descriptor used in sigma profile is the local screening charge density σ, which would be induced on the molecular surface if the molecule would be embedded in a virtual conductor. This descriptor, which can be calculated at reasonable cost by quantum chemical programs using the continuum solvation model COSMO [Klamt et al.,1993] is an extremely valuable tool for the local polarity of molecular surface. This single-molecule ideal solvation calculation needs to be done only once for each molecule, regardless of the mixture in which the molecule appears. The screening charge density σ is the only descriptor determining the interaction energies. Thus, the ensemble of surface pieces characterizing a pure compound (or a mixture *S*) is sufficiently described by the distribution function , which describes the relative amount of surface in the ensemble having a screening charge density between σ and

σ+dσ. The notation "σ-profile" is used for this distribution function. For most compounds, the ideal screening charge density falls within the range of -0.03 to 0.03 e/Å^2. This interval is partitioned in 60 parts, and the histogram (weighted by the area of each segment) of the averaged charge density is computed at each 0.001 e/Å^2 increment. This gives the σ profile for the pure compound. Here we will consider the Ionic Liquids as discussed in chapter 3.The sigma profile for the combination of cation and anions of the ionic liquids:([BPYRO][PF_6], [BPY][PF_6], [BPYRO][BF_4], [BPY][BF_4] and [BeMIM][BF_4]) along with thiophene and pyridine will be considered here.The sigma profile for the different combination of cation and anions of the ionic liquids ,thiophene and pyridine are given in Figures 4.5(a) to 4.5 (c).

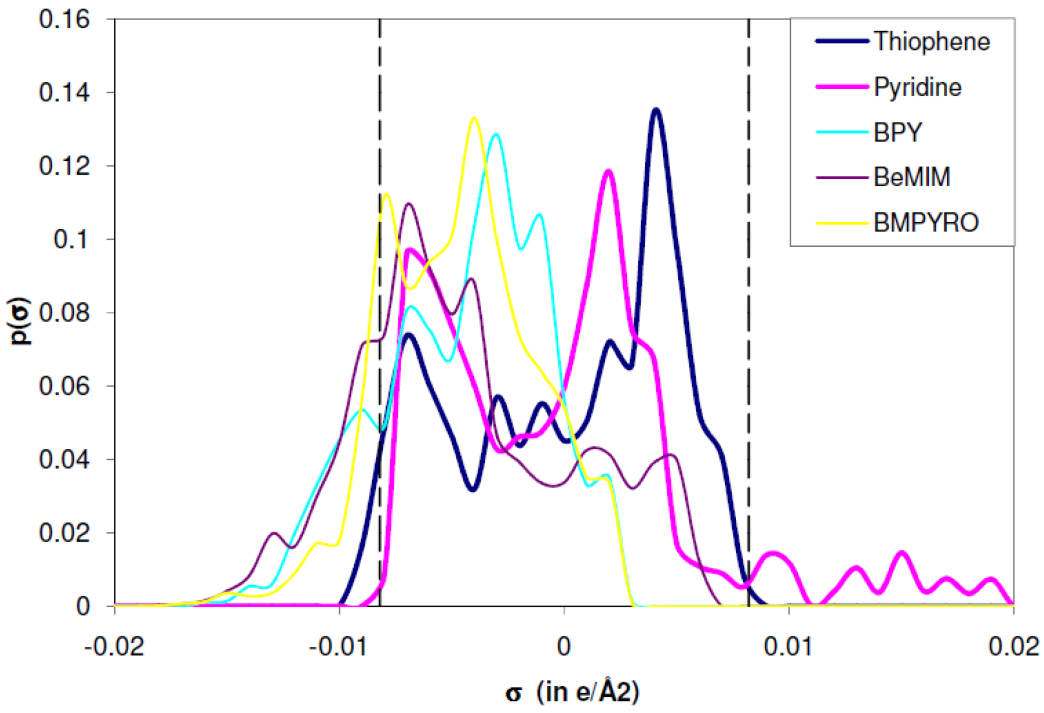

Figure 4.5(a): Sigma profiles for cations,thiophene and pyridine.(The dashed line indictate the cut off surface charge density for hydrogen bonding i.e σ_{hb}= e/Å^2)

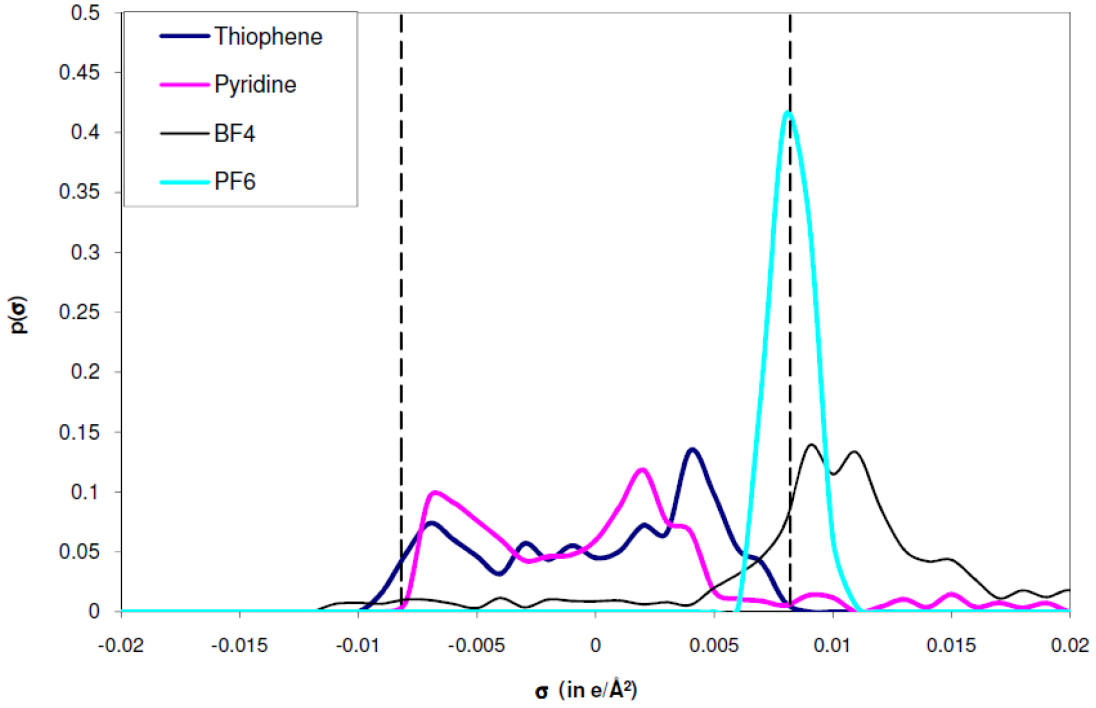

Figure 4.5(b): Sigma profiles for anions,thiophene and pyridine.(The dashed line indictate the cut off surface charge density for hydrogen bonding i.e. σ_{hb}= e/Å2)

Figure 4.5(a) shows the sigma profiles for three different cations i.e.[BMPYRO],[BMPY] and [BeMIM] and two solute compounds i.e. thiophene and pyridine, The two vertical dashed lines in Figure 4.5(a) to 4.5(c) are the locations of the cutoff values for the hydrogen bond donor (σ_{hb} < -0.0082 e/A^2) and acceptor(σ_{hb}>0.0082 e/A^2).The importance of this cut-off value lies in the fact that profile lying in the left side of σ_{hb} = -0.0082 e/A^2 will have high donator ability and right side of σ_{hb} =+0.0082 e/A^2 will have high acceptor ability. Profiles lying in the negative region are due to inherent positive charge of the atom/molecule and vice versa for the positive region of profile. The sigma profile for [BMPYRO],[BMPY] and [BeMIM], are of the similar nature while the prominent peaks of thiophene and pyridine molecules lie on the positive side of the sigma profile ,which is due to the negative charge on sulphur and nitrogen. Overlapping of the sigma profiles of thiophene and

pyridine indicates high immiscibility, which proves they do not like each other. The negative screening charges of the all three cations are due to the positive charge residing inside the aromatic ring of the cations. The three cations show peak at the outer most position in the negative direction. It can be seen that for the cations and thiophene/pyridine a very small fraction of the profile lies in the donating or acceptor region. Thus weak hydrogen bond is favored between the acidic hydrogen of [BMPYRO], [BMPY] and [BeMIM] cation with thiophene/pyridine. It should also be noted that the aromatic ring on the cation offers the H-bond interaction potential with thiophene and pyridine owing to its negative charge. The strength of the cations with thiophene/pyridine will depend on the hydrogen bond donor or acceptor availability. The cations have a better donating ability since part of the profile lies to the left of cut-off zone i.e. $\sigma_{hb} < -0.0082$ e/A^2 while the acceptor side is almost nonexistent i.e right of cut-off zone i.e. $\sigma_{hb} > +0.0082$ e/A^2. This is expected as cations carry '+ ve' charge. On looking at the sigma profiles it is clear that the sigma profiles of cations and thiophene/pyridine are complimentary, thus they like each other, which confirms the presence of CH-π bonding.

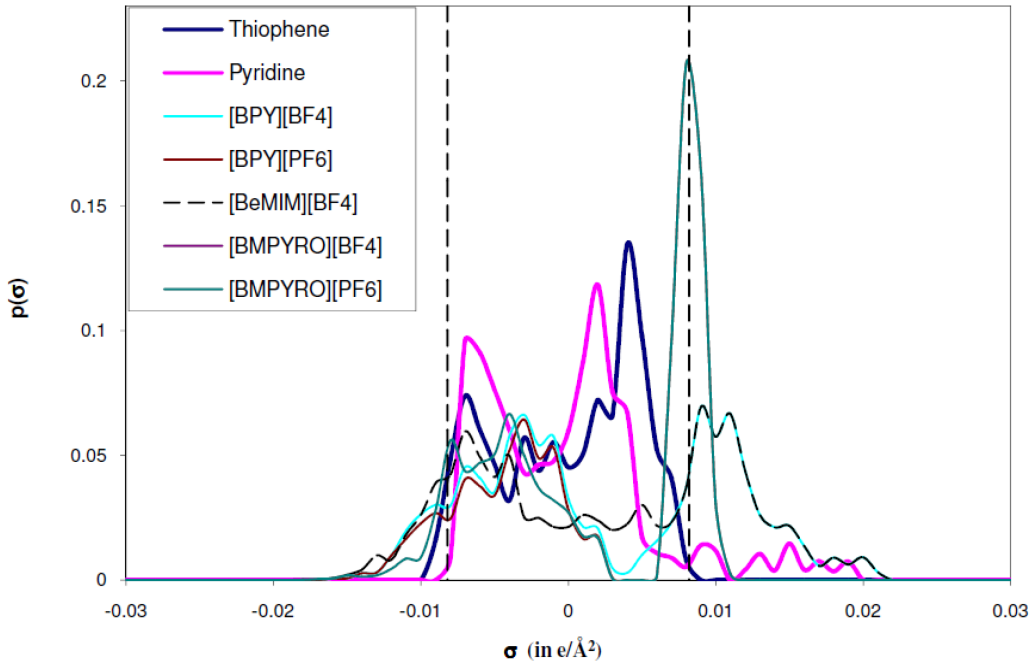

Figure 4.5(c): Sigma profiles for ILs,thiophene and pyridine.(The dashed line indictate the cut off surface charge density for hydrogen bonding i.e $\sigma_{hb}=$ e/Å$^{2)}$

The sigma profiles of anions along with thiophene and pyridine are shown in Figure 4.5(b). For the anions i.e.[BF_4] and [PF_6],peaks lie on the right of the cutoff zone for hydrogen bonding ,which is due to the inherent negative charges of the anions. However, thiophene and pyridine shows peaks at the outmost position in the negative direction. These negative positions of the screening charges are due to the positive charge residing outside the thiophene and pyridine molecules. The profiles being complimentary, again confirm the attraction of anions with the aromatic compounds. The sigma profile of

five ionic liquids i.e. [BPYRO][PF_6], [BPY][PF_6], [BPYRO][BF_4], [BPY][BF_4] and [BeMIM][BF_4] along with thiophene and pyridine molecules have been shown in Figure 4.5(c). The profiles of the cation and anion have been added to get the profile for an Ionic Liquid. The profiles being complimentary show the same information as that of cations and anions explicitly. In other words very few polar surface segments of thiophene and pyridine molecules can make energetically acceptable pairs with non-polar cation on the ionic liquid surface. Thus it can be concluded that CH-π interaction dominate over the hydrogen bonding effect of sulphur/nitrogen atom with cation.

4.10 Solvent selction paprameters

After the discussion of sigma profile, we will now proceed with the screening of cation and anion combination.For this we define two parameters namely solvent selectyivity and capacity.

Selectivity measures the composition of sulphur/nitogen species in IL rich phase and in model diesel rich phase. It is given by the relation:

(4.20)

Here ’1’ and ’2’ represents the sulphur /nitogen compound and pseudo diesel component respectively. *The* ***capacity*** of ILs is defined as the amount of sulphur/nitogen species accumulated in an IL rich phase. It can be calculated as

(4.21)

Where C_{12} is the capacity of ILs at infinite dilution.In order to judge the effectiveness of a solvent.

The **overall performance** of the ILs is given by performance index and is given below.

(4.22)

Table 4.4: Investigated Cations used in this study

	S N o Name of cation(s)	Acronym	Structure
1	1-ethyl-3-methylimidazolium	[EMIM]	
2	1-ethylpyridinium	[EPY]	
3	1-Ethyl-1-methylpyrrolidinium	[EPYRO]	
4	1-Ethyl-1-methylpiperidinium	[EPIP]	
5	4-Ethyl-4-methylmorpholinium	[EMMOR]	
6	1,2,4-Trimethylpyrazolium	[TMPYZO]	

Table 4.5: List of Anions studied in this work

S.No	Name of Anion	Acronym	Structure
1	Chlorine	[Cl]	Cl^-
2	Bromide	[Br]	
3	Nitrate	$[NO_3]$	
4	Thiocyanate	[SCN]	
5	Acetate	$[CH_3COO]$	
6	Bisulphate	$[HSO_4]$	
7	Tetrafluoroborate	$[BF_4]$	
8	methylsulphonate	$[CH_3SO_3]$	
9	trifluoroacetate	$[CF_3COO]$	

10	Methyl sulphate	$[CH_3SO_4]$	
11	Hexafluorophosphate	$[PF_6]$	
12	Triflate or Trifluoromethane sulphonate	$[CF_3SO_3]$	
13	Ethyl sulphate	$[C_2H_5SO_4]$	
14	Dimethylphosphate	$[(CH_3)_2PO_4]$	
15	Methylsulfonylacetamide	$[C_3H_7NO_3S]$	
16	Tetracyanoborate	$[B(CN)_4]$	
17	Salicylate	$[C_7H_5O_3]$	
18	Bis(methylsulphonyl) amide	$[(CH_3SO_2)_2N]$	

19	Bi-oxaloborate	$[BHO_4]$	
20	Diethyl phosphate	$[C_4H_{10}O_4P]$	
21	Tosylate	$[C7H_7SO_3]$	
22	P-Toluene sulphonate	$[C_7H_7SO_3]$	
23	Trifluoromethanesulphinate	$[CF_3SO_2]$	
24	Bis(trifluoromethylsulphonyl)amide	$[(CF_3SO_2)_2N]$	
25	2-(2-Methoxyethoxy) ethyl sulphate	$[C_5H_{11}SO_6]$	
26	Decanoate	$[C_{10}H_{19}O_2]$	

27	Octylsulphate	$[C_8H_{18}\ SO_4]$	
28	Heptyl Sulphate	$[C_7H_{15}O_4S]$	

S.No	Name	Structure	Acronym	Properties					Appearance
01	Thiophene		TS	Mole. for	Mol.wt g.mole^{-1}	B.Point K	M.Point K	Density g.cm^{-3}	
				C_4H_4S	84	357.37	234.65	1.05	Colorless liquid
02	Benzothiophene		BTS	C_9H_8S	116.	472.85	305.15	1.342	White solid
03	Dibenzothiophene		DBTS	$C_{12}H_8S$	184	588.33	415.2	1.252	White to pale yellow crystalline powder

Table 4.6: Heterocyclic acidic sulfur species in Diesel oil

4.11 ILs for Desulphurization Studies

In this study, we have taken the smaller size cations such as [EMIM], [EPY], [EMMOR], [EPYRO], [EMPIP], and [TMPYZO] (Table 4.4) along with 28 polynuclear and/or mononuclear anions (Table 4.5) for the ablation of aromatic sulphur species from model diesel oil. The refractory sulphur species such as TS, BT and DBT are given in Table 4.6. In our earlier study we have taken the influence of thiophene only, however in diesel all the compounds such as TS, BTS, and DBTS are present simultaneously. This prompted us to study the prediction of selectivity and capacity at infinite dilution for the simultaneous removal of TS, BTS, and DBTS from diesel oil (Table 4.7).The diesel oil composition is given in Table 4.7.The sigma profile of diesel component will be taken as per the equation;

(4.23)

Where i reprents all the diesel components as in Table 4.7.

4.11.1 Benchmarking the Predictions

In order to validate our findings we have already compared the infinite dilution activity coefficients of several compounds in ionic liquids successfully [Kumar et al.,2009].Additionally we have compared and predicted the infinite dilution activity coefficients (IDAC) of solutes in ionic liquids in our earlier work [Banerjee et al.,2007]. IDAC values comprising of eight ionic liquids namely: [BMIM][BF_4], [BMIM][OSu], [BMIM][SCN], [OMIM][BF_4], [OMIM][Tf_2N], [BMIM][CF_3SO_3], [BMIM][PF_6] and [EMIM][TOS] are predicted and reported in Table 4.8 for various temperatures. The average root mean square deviation (RMS) for all 20 points is equal to 0.11 *ln* units or 11%. This agrees well with the infinite dilution activity coefficient predictions of ionic liquids by Diedenhofen et al.,[2003] . Additionally in our previous work [Banerjee et al.,

2007] we have successfully compared and predicted the ternary LLE of 15 thiophene based ionic liquids systems with an average absolute deviation in root mean square deviation of 10%.With the combined benchmarking we will now proceed in the screening of other potential ionic liquids.

Table 4.7: Composition of artificial simulated Diesel [Webe et al., 2006]

PIONA series	C_5 wt %	C_6 wt %	C_7 wt %	C_8 wt %	C_9 wt %	C_{10} wt %	C_{11} wt %
Paraffins (C_nH_{2n+2})	6.7	1.32	0.41	2.5	-	-	0.06
Isoparaffins (C_nH_{2n+2})	10.9	5.62	1.81	17	1.3	-	0.3
Aromatics(C_nH_{2n-6})	-	0.32	36.71	0.3	0.3	0.6	0.4
Naphthenes(C_nH_{2n})	0.4	1.62	1.1	1.2	-	-	-
Olefins (C_nH_{2n})	6.7	1.62	0.51	0.1	0.2	-	-

4.11.2 Effect of Ionic Liquid Selectivity

The selectivity at infinite dilution (using equation 4.20) for TS, BT and DBT with [EMIM],[EPY],[EMMOR],[EPYRO],[EMPIP] and [TMPYZO] based cations along with 28 polynuclear and/or mononuclear anions are predicted with COSMO-RS .The selectivities at infinite dilution are shown in Figure 4.5,4. 6 and 4.7 for TS, BTS and DBTS respectively. The selectivity of the ILs at infinite dilution towards TS, BT, and DBT are observed to follow the order:

Thiophene: [EMMOR] > [TMPYZO] > [EMIM] > [EPY] > [EMPYRO] > [EPIP]

Benzothiophene: [EMMOR] > [EPYRO] > [EMPIP] > [TMPYZO] > [EMIM] > [EPY]

Dibenzothiophene: [EMMOR] > [EPYRO] > [EMPIP] > [EPY] > [EMIM] > [TMPYZO]

The observed maximum and minimum values with each component are given in Table 4.9. It is a well known fact that ILs are involved in the structural orientation with similar structure of organic and/or inorganic molecules through: (a) hydrogen bonding effect due to electrophilic attack, (b) CH- - π bond interaction [Gutel et al.,2009]

involving the electron withdrawing nature of heteroatom of sulphur species with the electron donating nature of cations /vice versa and (c) Aromatic ring current effect (i.e. π - π interaction with similar structure of compounds) [Suezawa et al.,2004]. Except TS, the aromatic ring current effect does not involve intra molecular interaction between lesser delocalized π-electron density of BT and DBT with ILs. The presence of an additional aromatic ring in BT and DBT hinders the π - π interaction. Thus the interaction mainly occurs via CH- π bond and H-bond formation.

Further Castro et al [2007] has reported that the cation and anion structure orientation and the compactness between cation and anion plays an important role in the selectivity of ILs at infinite dilution. It is evident that a five and/or six member ring aromatic compound with one heteroatom such as sulphur posses higher delocalized π-electron density than that of the five and /or six member ring compounds without heteroatom such as benzene. Thus the sulphur compounds due to their greater demand of inductive effect, easily gets involved in an aromatic sextet with the respective cation without having any steric hindrance [Joule et al.,2007;Gupta et al.,2005;Bansal et al.,2005]. Thus the refractory sulphur species such as TS, BT and DBT posses π– excessive electrons leading to high aromaticity.

In the aromatic sextet formation, each carbon atom donates one electron, while pair of electrons are donated by sulphur atom to its aromatic ring [Gupta et al.,2005]. These highly delocalized π- electron densities are readily polarized through intra molecular interaction with cations. Thus, the polarized compounds are able to form CH- π stacking by occupying minimum energy configuration [Su et al.,2004]. In general, the aromaticity of the sulphur species follows the order : TS > BT > DBT .The additional aromatic ring in BT and DBT decreases the aromaticity than that possessed by TS.

Among the cations the [EMMOR] possessed the highest selectivity. This is due to the fact that the positions of hetero atom like O, N and S within the cation posses appreciable influence on the selectivity of the ILs at infinite dilution. Dissimilar heteroatom (O, N) on [EMMOR] leads to higher charge sharing in the cation [Cassol et

al.,2007]. Thus the other cations having nitrogen atoms are connected to alkyl groups which are known to reduce the charge density in the cation structure. [EMMOR] because of its dissimilar heteroatom has higher charge sharing thereby increasing selectivity significantly. With this charge sharing the acidic hydrogen -X hydrogen bonding (X=Anion) is disrupted in [EMMOR] and this enhances the inclusion of aromatic compounds through CH- π bonds. With the same reason the similar structures of cations such as [EMIM] and [TMPYZO] posses greater selectivity at infinite dilution as compared to [EPYRO], [EMPIP] and [EPY] cations.

Within the anions it is clear that a linear chain in the anion of the ILs and anions having aromatic ring structure does not affect the selectivity due to its higher steric hindrance. Highly electronegative anions like the halogens (Cl and Br) gave very high values of selectivity (Figure 4.6) as compared to other anions. This is consistent with the recent work of Xie et al**.** [2008,2009] in which it was observed that [BMIM][Cl] and [OPY][Cl] provide better selectivity for the removal of neutral nitrogen (non-basic) compounds from straight run diesel during extraction process. The favorable anions are those where no sterical shielding effect around their charge centers exists, e.g. [SCN],[CH_3SO_3], [CH_3COO], [Cl], and [Br]. On the contrary, the unfavorable anions are those where sterical shielding effect around their charge centers exist, e.g. [PF_6], [BOB], [$B(CN)_4$], [TFI] etc. This is consistent with the work of Lei et al.[2006] and Kumar et al.,[2009] where the influence of hexane-hexene and thiophene-diesel were obtained respectively. It is clear from the Figure 4.6, 4.7 and 4.8 that the selectivities decrease with Thiophene (4-24) > Benzothiophene (2-12) > Dibenzothiophene (1-7). This is true since steric hindrance increases with the additional aromatic ring in the sulphur compounds.

4.11.3 Effect of Ionic Liquid Capacity

Figure 4.9, 4.10 and 4.11 shows the capacity at infinite dilution for [EMIM], [EPY], [EMMOR], [EMPYRO], [EMPIP] and [TMPYZO] based cations with 28 anions

respectively. In general it can be seen than the capacity (Equation 4.21) for any component decreases in the order:

[EMPIP] > [EPYRO] > [EPY] > [EMIM] > [EMMOR] > [TMPYZ]

The [EPYRO] and [EMPIP] based ILs show moderate capacity at infinite dilution for TS, BT, and DBT.It can be seen that the capacity of the ILs strongly depends on the heteroatom (i.e. O and N) and its site of location in the aromatic structure of the cations. The cation structure with different hetero atom such as [EMMOR] possesses higher selectivity but lower capacity towards TS, BT and DBT. This is becasue [EMMOR] posses two different heteroatoms located at opposite direction in the aromatic ring structure of the cation [Suezawa et al., 2004]. In general the capacity of the ILs decreases with increase in the number of hetero atoms located in the cation structure. Thus [EMPIP] and [EPYRO] have the highest capacity among the cations. Similar heteroatoms located on aromatic ring structure of the cation are considered to play both inductive and mesomeric effect [Joule et al., 2007; Gupta et al., 2005; Bansal et al., 2005]. An inductive effect is due to greater electronegative heteroatom repulsion whereas a mesomeric effect occurs as the result of aromaticity involving π electron density.

However, for anions an absence of elements such as carbon (C) and hydrogen (H) provides less capacity for TS, BT and DBT because of weak H bonds between anion and sulphur compound. Therefore a smaller size cation with a smaller size anion and /or longer chain of anion possesses high capacity for TS, BT and DBT. Barring Cl and Br, anions such as decanoate, heptylsulphate and octylsuphate shows the highest capacity among the anions because of its long chain. On the other hand, a smaller size cation with anion having one or two different hetero atom provides a higher capacity at infinite dilution, irrespective of TS, BT and DBT.

4.11.4 Ionic Liquid Performance Index

The performance index (Equation 4.22) for [EMIM], [EPY], [EMMOR], [EMPYRO], [EMPIP] and, [TMPYZO] based cations of ILs are presented in Figures 4.12, 4.13 and 4.14 for TS,BT and DBT respectively. [EMIM], [EPY], [EMMOR],

[EMPYRO], [EMPIP] and [TMPYZO] based cations exhibit appreciable performance index for the removal of TS, BT and DBT. Hence, a smaller ring cation with one heteroatom and anion consisting of minimum number of hetero atoms are recommended as potential ionic liquids. The heteroatom with lone pair of electron is involved in the aromatic sextet, which are delocalized over the aromatic ring of TS, BT, and DBT. The ring carbons posses' only one electron whereas the heteroatom in [EMIM], [EPY], [EMMOR], [EMPYRO], [EMPIP], [TMPYZO] cations and /or in TS, BT, and DBT contribute a pair of electrons during interaction. It is observed that in cations without aromatic ring a hetero atom provides appreciable rate of selectivity and capacity. Thus [EMMOR],[EPIP] and [EPYRO] having one hetero atom gave high performance index.

Ionic Liquid	System	Reported Selectivity (S^{∞})	Predicted Selectivity (S^{∞})	Temperature (K)
[BMIM][BF_4]	Hexane/Thiophene	85.8	70.8	313.15
	Cyclohexane/Thiophene	31.8	25.6	313.15
[BMIM][OSu]	Hexane/Thiophene	6.5	7.35	313.15
	Cyclohexane/Thiophene	3.9	4.61	313.15
[BMIM][SCN]	Hexane/Thiophene	186.2	165.3	298.15
	Heptane/Thiophene	231.5	200.8	298.15
	Decane/Thiophene	517.3	468.4	298.15
[OMIM][BF_4]	Hexane/Thiophene	18.9	11.4	298.15
[OMIM][Tf_2N]	Hexane/Thiophene	7.55	6.2	298.15
	Benzene/Thiophene	1.0	1.5	298.15
[BMIM][CF_3SO_3]	Hexane/Thiophene	36.5	30.5	298.15
[BMIM][PF_6]	Hexane/Thiophene	6.1	8.1	298.15
	Cyclohexane/Thiophene	3.4	4.7	298.15
	Benzene/Thiophene	1.0	1.517	298.15
[BMIM][OSu]	Hexane/Thiophene	6.1	7.351	298.15
	Cyclohexane/Thiophene	3.4	4.61	298.15
	Benzene/Thiophene	1	1.41	298.15
[EMIM][TOS]	Hexane/Thiophene	10.1	13.32	323.15
	Cyclohexane/Thiophene	27.3	34.2	323.15
	Benzene/Thiophene	1.8	1.5277	323.15

Table 4.8: Benchmarking of Selectivity at infinite dilution for ILs with aliphatic/thiophene mixture (Revelli et al.,2009).

Table 4.9: Maximum and minimum values of selectivity, capacity and Performance Index (PI) at infinite dilution

Sulphur species	**Limitation**	**Selectivity**	**Capacity**	**P.I**	**Better ILs for Desulfurization**		
					Selectivity	**Capacity**	**P.I**
Thiophene (TS)	Maximum	25.2	0.978569	4.203447	[EMMOR][SCN]	[EPYRO][Cl]	[EPYRO][Cl]
	Minimum	3.84772	0.009536	0.2119	[EPY][DEC]	[EMMOR][PF_6]	[EMMOR][PF_6]
Benzothiophene (BT)	Maximum	11.763006	0.978569	5.50055	[EMMOR][SCN]	[EPYRO][Cl]	[EPYRO][Cl]
	Minimum	1.86569	0.009539	0.059838	[TMPYZO][DEC]	[EMMOR][PF_6]	[EMMOR][PF_6]
Dibenzathiophene (DBT)	Maximum	6.780209	0.978569	5.32198	[EMMOR][Cl]	[EPYRO][Cl]	[EPYRO][Cl]
	Minimum	1.075724	0.009530	0.013875	[EMIM][PF_6]	[EMMOR][PF_6]	[TMPYZO][PF_6]

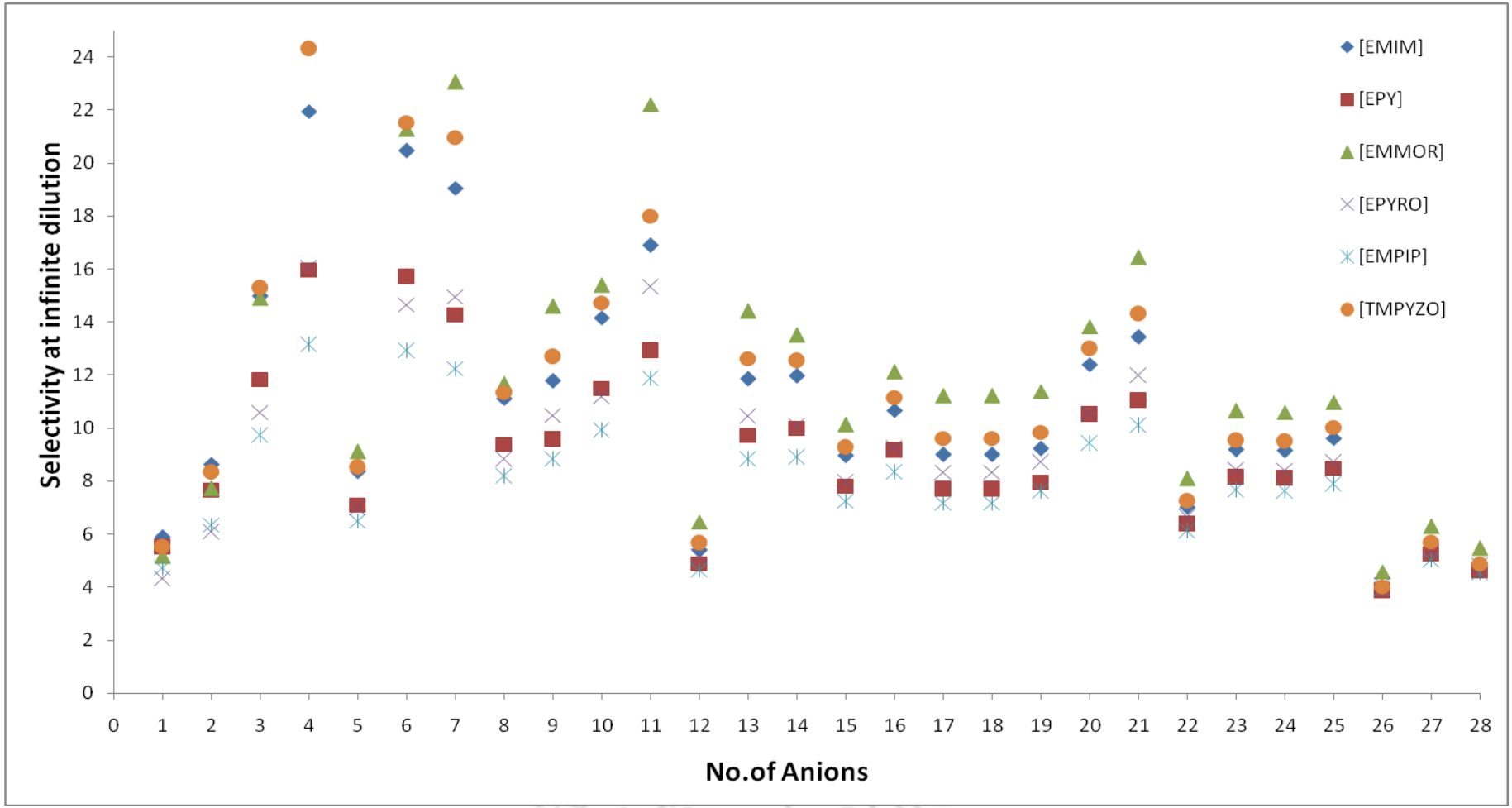

Figure 4.6: Selectivity at infinite dilution for thiophene at 298.15 K (Anion Number as given in Table 4.5)

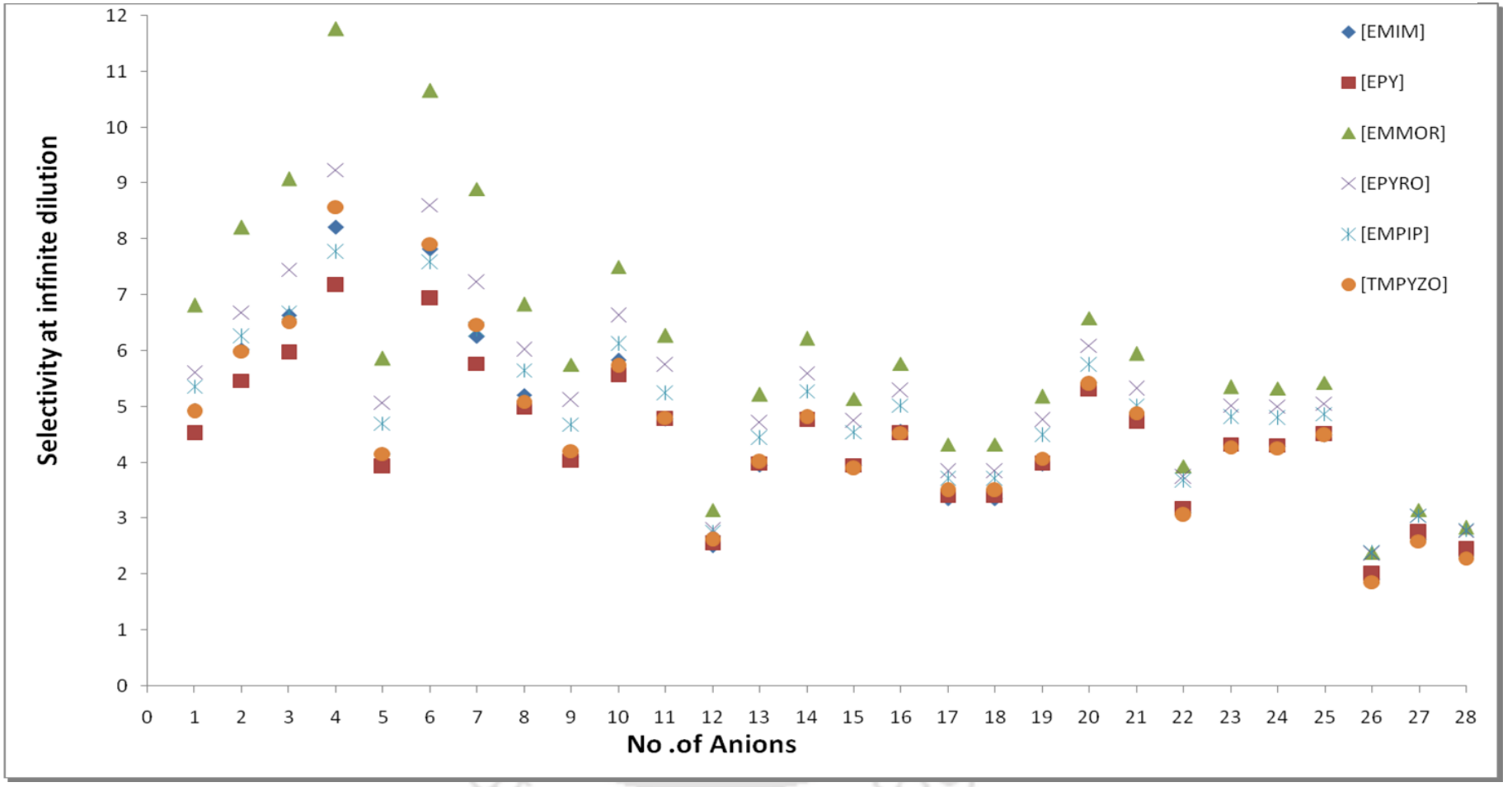

Figure 4.7: Selectivity at infinite dilution for Benzothiophene at 298.15 K (Anion Number as given in Table 4.5)

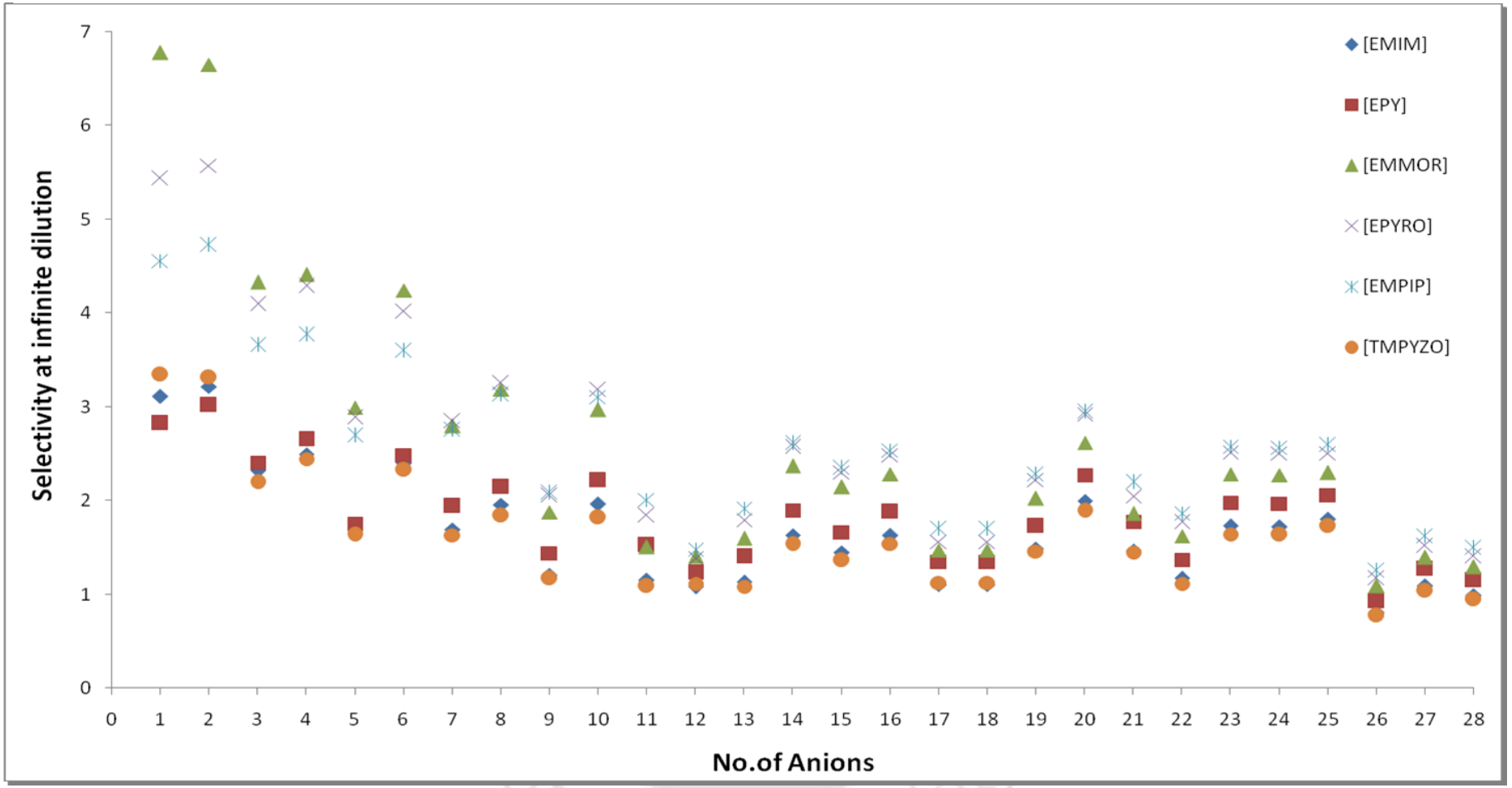

Figure 4.8: Selectivity at infinite dilution for Dibenzothiophene at 298.15 K (Anion Number as given in Table 4.5)

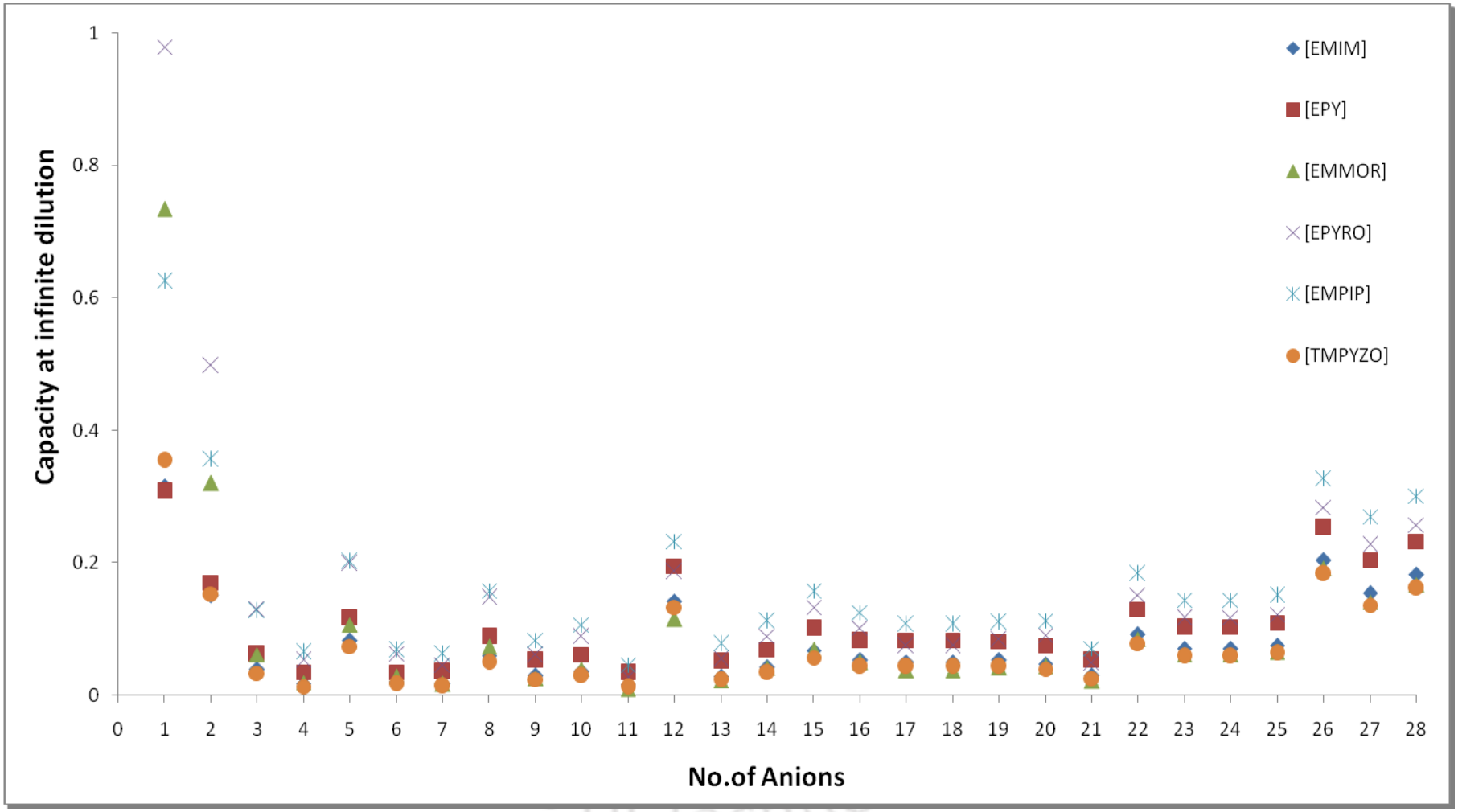

Figure 4.9: Solvent capacity at infinite dilution for thiophene at 298.15 K (Anion Number as given in Table 4.5)

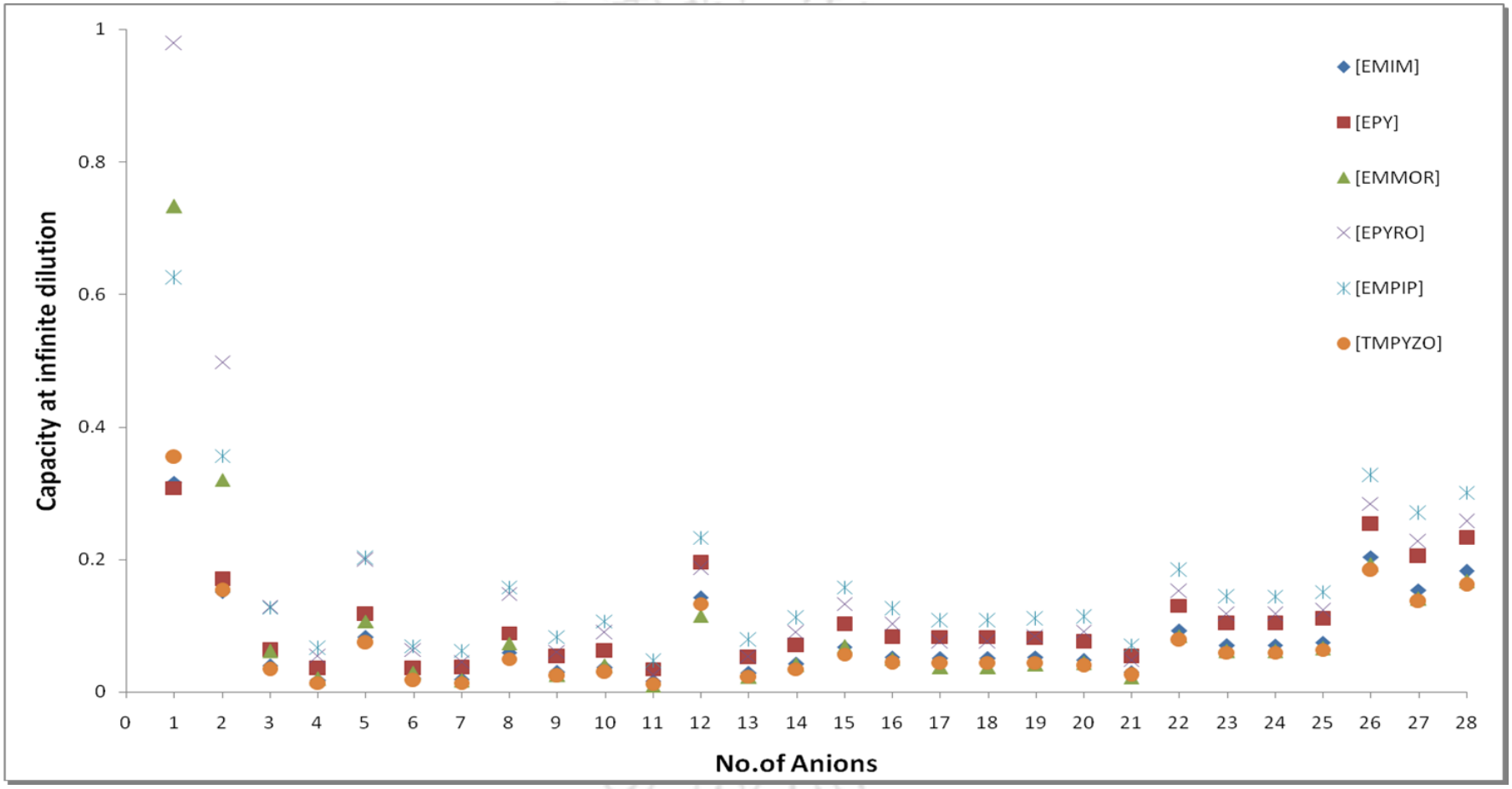

Figure 4.10: Solvent capacity at infinite dilution for Benzothiophene at 298.15 K (Anion Number as given in Table 4.5)

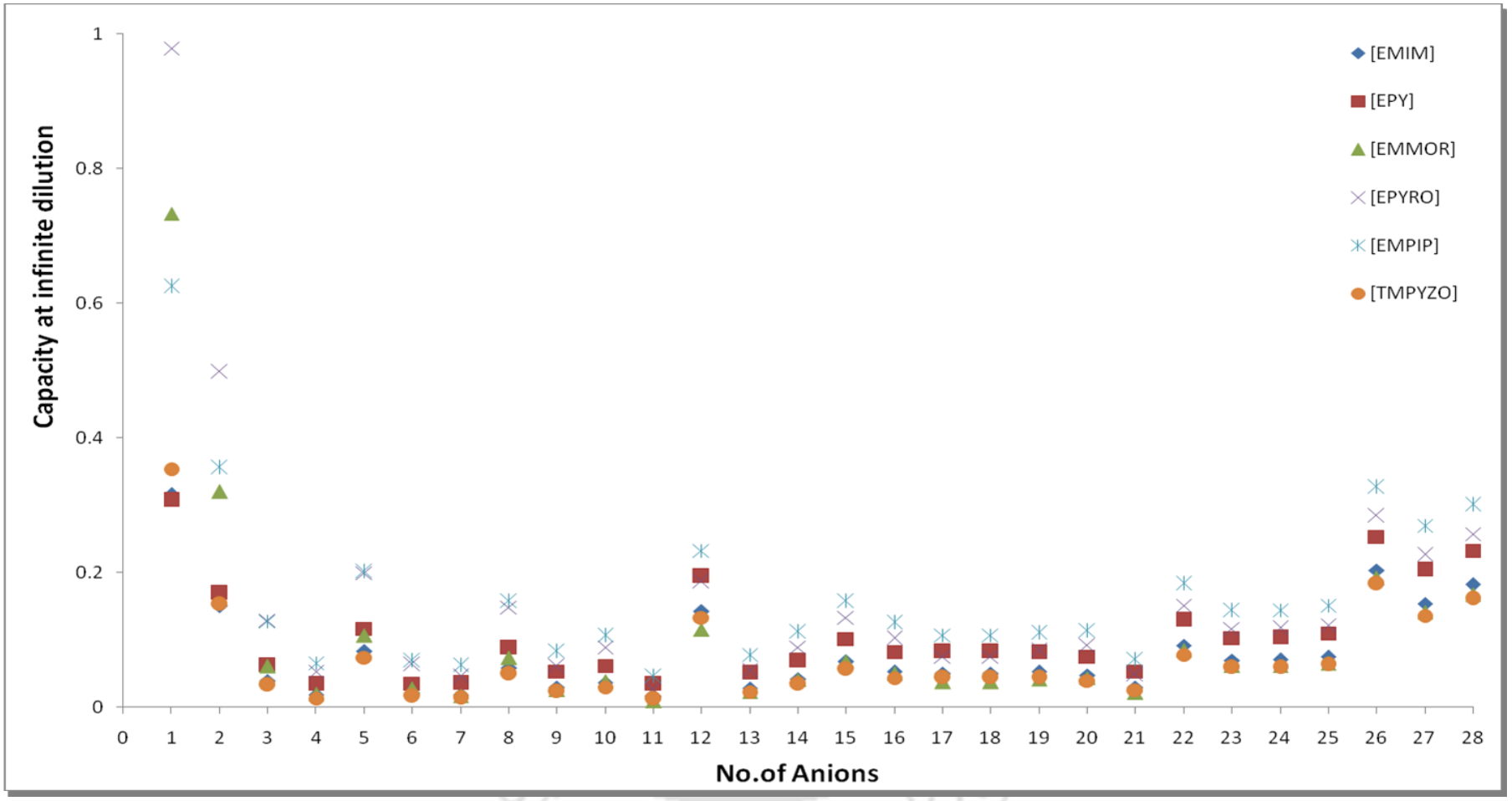

Figure 4.11: Solvent capacity at infinite dilution for Dibenzothiophene at 298.15 K (Anion Number as given in Table 4.5)

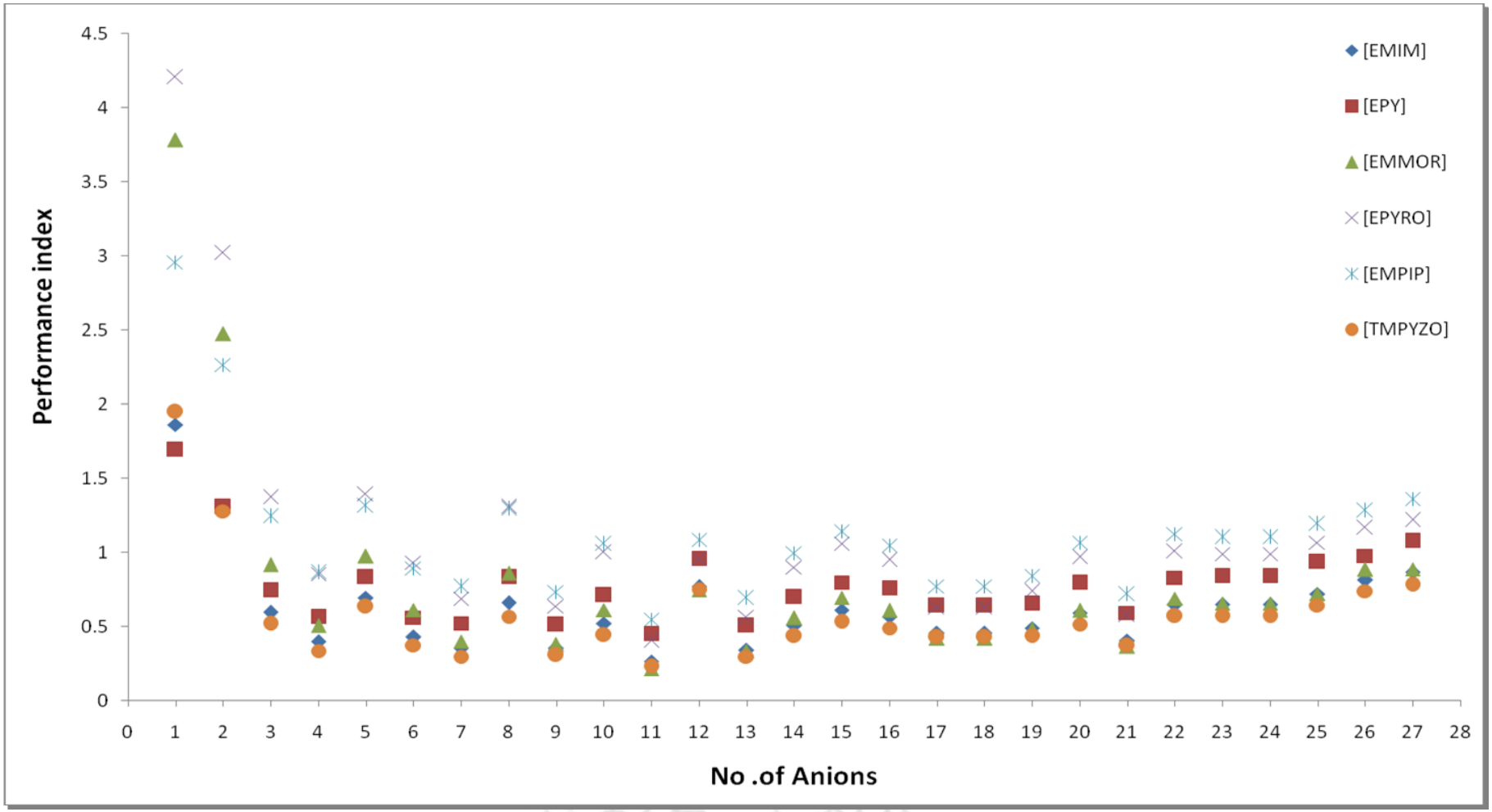

Figure 4.12: Performance index values at infinite dilution for thiophene at 298.15 K (Anion Number as given in Table 4.5)

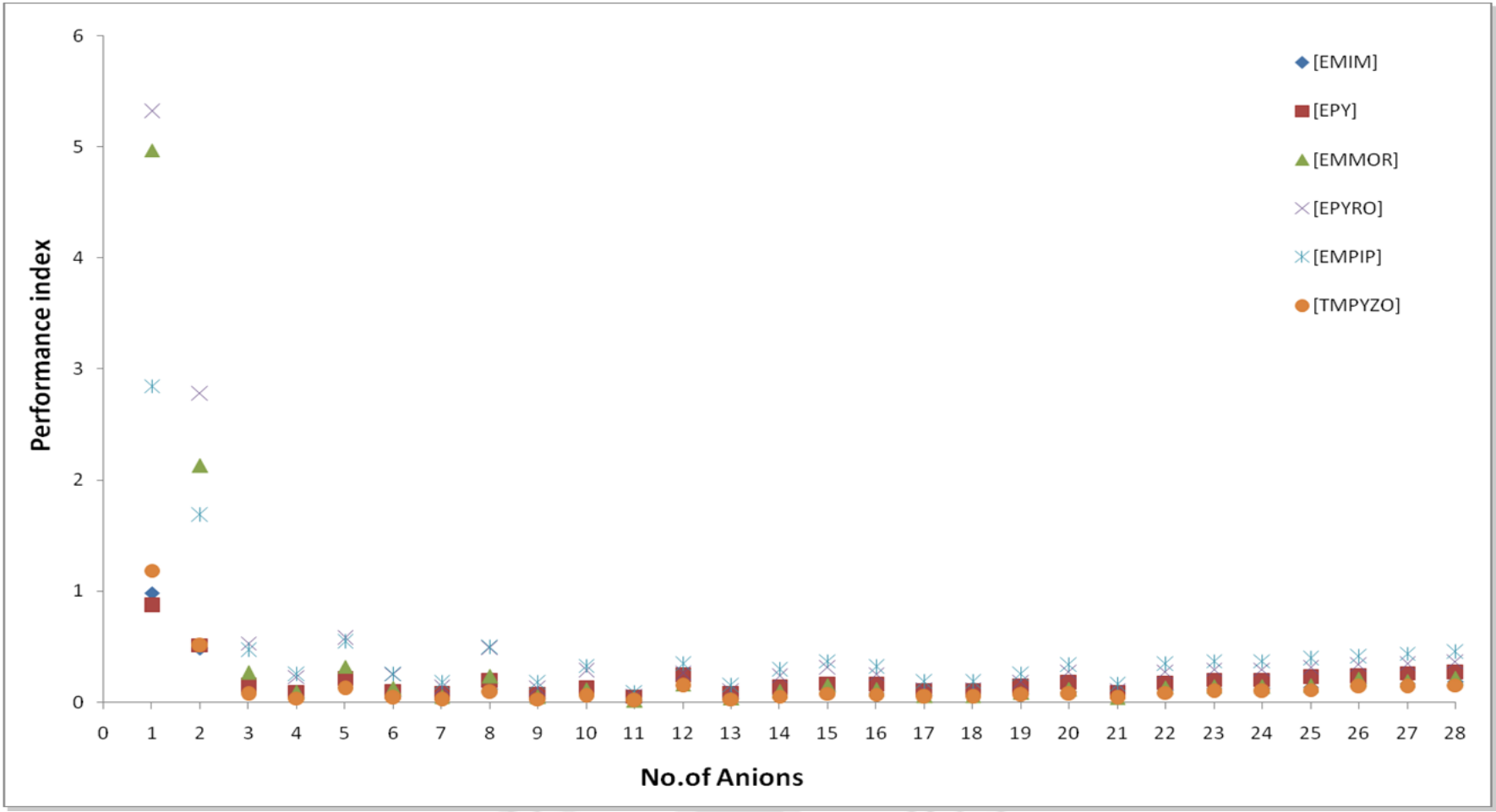

Figure 4.13: Performance index values at infinite dilution for Benzothiophene at 298.15 K (Anion Number as given in Table 4.5)

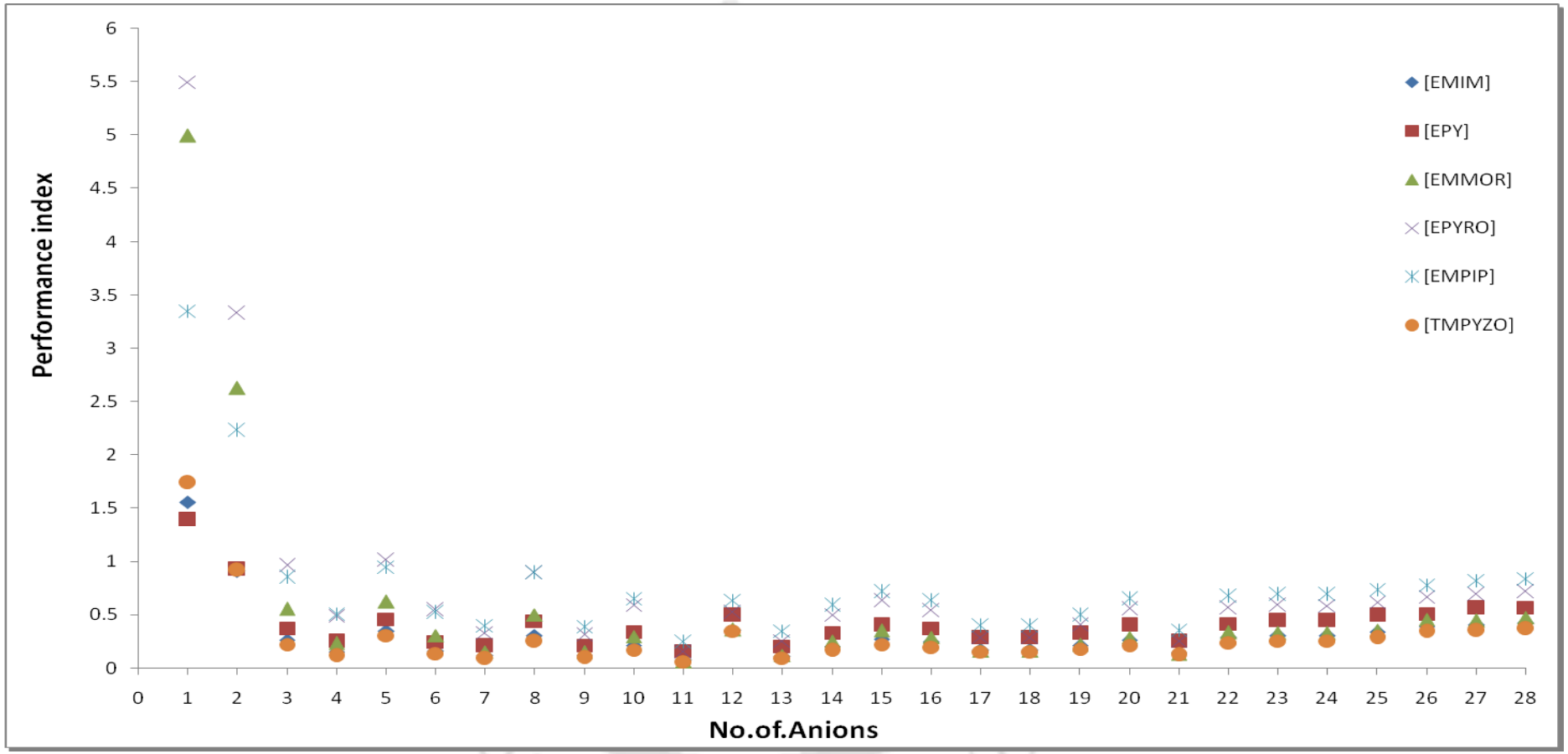

Figure 4.14: Performance index at infinite dilution for Dibenzothiophene at 298.15 K (Anion Number as given in Table 4.5)

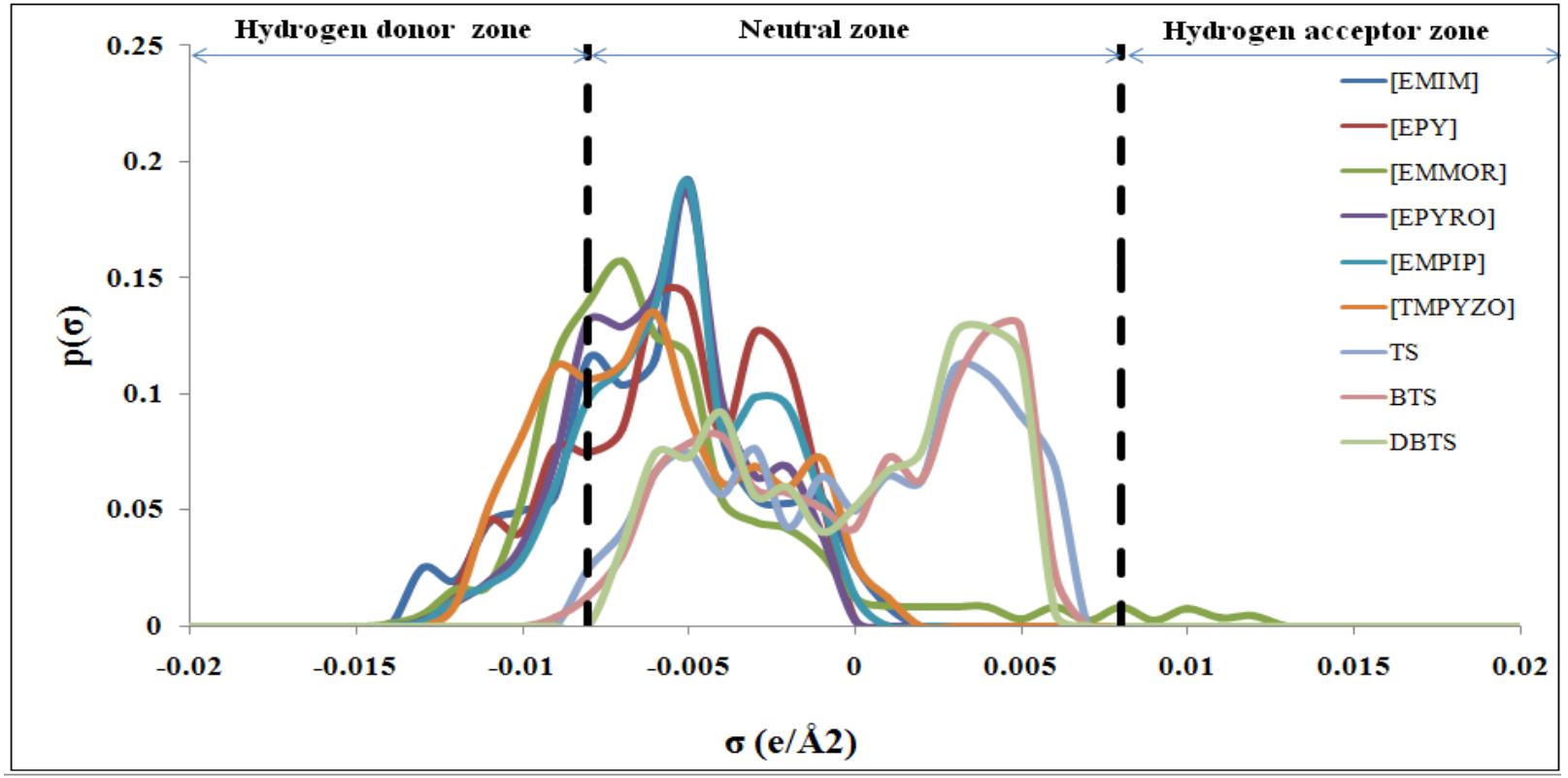

Figure 4.15: Sigma profile for [EMIM],[EPY],[EPYRO],[EMPIP], [EMMOR],[TMPYZO] ,TS,BTS, and DBTS.

4.11.5 Sigma Profiles of Cations with Sulphur Compound

In the COSMO scheme, sigma profile is the only descriptor, which describes the local polarity of molecular surface and determines the interaction energies.This further indicates the polarity of the components in a mixture or within itself. Figure 4.15 shows the sigma profiles for the six cations and the three sulphur compounds. The two vertical dashed lines in Figure 10 are the locations of the cutoff values for the hydrogen bond donor (σ_{hb} < -0.0082 e/A^2) and acceptor(σ_{hb}>0.0082 e/A^2)[16-19].The importance of this cut-off value lies in the fact that profile lying in the left side of σ_{hb} = -0.0082 e/A^2 will have high hydrogen bond donator ability and right side of σ_{hb} =+0.0082 e/A^2 will have high hydrogen bond acceptor ability[Klamt et al.,1995,2005;Lin et al.,2002;Grenseman et al.,2005]. Profiles lying in the negative region are due to inherent positive charge of the atom/molecule and vice versa for the positive region of profile.

The sigma profiles of all the cations are similar in nature. The prominent peaks of the sulphur compounds lie on the positive side of the profile, which is due to the negative charge on sulphur atom. Overlapping of the sigma profiles of all the three sulphur compounds indicates high immiscibility [Klamt et al.,1995,2005;Lin et al.,2002;Grenseman et al.,2005], which proves they do not like each other. The negative screening charges of all three cations are due to the positive charge residing inside the aromatic ring of the cations. All cations shows peak at the outer most position in the negative direction. It can be seen that for the cations and sulphur compound a very small fraction of the profile lies in the donating or acceptor region. Thus a weak hydrogen bond is favored between the acidic hydrogen of [BMPYRO], [BMPY] and [BeMIM] cation with sulphur compound. The hydrogen bond interaction of the cations with sulphur compound will depend on the hydrogen bond donor or acceptor availability which is negligible. The cations still have a better donating ability since

part of the profile lies to the left of cut-off zone i.e. $\sigma_{hb} < -0.0082$ e/A^2 while the acceptor side is almost nonexistent i.e right of cut-off zone i.e. $\sigma_{hb} > +0.0082$ e/A^2. This is expected as cations carry '+ ve' charge. In other words very few polar surface segments of sulphur molecules can make energetically acceptable pairs with non-polar cation on the ionic liquid surface. On looking at the sigma profiles it is clear that the sigma profiles of cations and sulphur compounds are complimentary in nature which indicates high miscibility via CH-π bonding.

4.12 ILs for Denitrification studies

4.12.1 Benchmarking Using Liquid-Liquid Equilibria Predictions

Till date Won et al.,[2002] reported the only ternary LLE data containing: aromatic nitrogen species + methanol + hydrocarbons. For the prediction of LLE of nitrogen containing systems, COSMO-RS parameters as used earlier in our work on aromatic extraction of multi-component systems [Kumar et al., 2009; Banerjee et al., 2007, 2006a, 2006b, 2008] have been adopted. The COSMO-RS model predicts the mole fractions of the ternary system both methanol rich phase and the hydrocarbon rich phase. These mole fractions are then compared with the reported mole fractions [Won et al., 2002]. A comparison of the mole fractions in both the phases is shown by a ternary plot for the system: methanol –hexadecane-pyridine (Figure 4.16). Additionally Table 4.10 shows the reported and predicted mole fractions in both phases. Table 4.11 shows the LLE for the four ternary systems containing aromatic nitrogen species as one of the nitrogen derivative. The goodness of fit for the prediction is usually gauged by Root Mean Square Deviation (RMSD), which is defined as:

(4.24)

where '*m*' refers to the number of tie lines, '*c*' the number of components and '2'is the number of phases. The results of all the reported ionic liquid ternary systems are given in Table 4.11. The average per cent deviation in rmsd for all the systems is ~10% (Table 4.9) which is quite good considering our method to be *a–priori*. Additionally in our previous work [Kumar et al., 2009; Banerjee et al., 2007, 2006a, 2006b, 2008] we have successfully compared our predictions with the literature data of other species in ionic liquids.

Table 4.10: Experimental and COSMO-RS Predicted Tie lines for Methanol + Pyridine+ Hexadecane at T=298.15 K.

Experimental Tie Lines					
Methanol Rich Phase			**Hexadecane Rich Phase**		
Methanol	Pyridine	Hexadecane	Methanol	Pyridine	Hexadecane
0.8199	0.152	0.0283	0.0108	0.0122	0.977
0.674	0.282	0.0435	0.0106	0.0267	0.9627
0.5253	0.413	0.0613	0.0196	0.0519	0.9285
0.4188	0.505	0.0764	0.0275	0.0857	0.8868
0.3028	0.581	0.1158	0.0306	0.1268	0.8426
0.2173	0.620	0.1629	0.0281	0.1877	0.7842
COSMO-RS model predicted Tie Lines					
Methanol Rich Phase			**Hexadecane Rich Phase**		

Methanol	Pyridine	Hexadecane	Methanol	Pyridine	Hexadecane
0.808	0.145	0.0462	0.022	0.01	0.968
0.654	0.275	0.071	0.024	0.022	0.954
0.505	0.394	0.101	0.036	0.05	0.914
0.402	0.495	0.103	0.0562	0.0758	0.868
0.292	0.561	0.147	0.071	0.105	0.824
0.208	0.578	0.214	0.047	0.178	0.775

Table 4.11: Comparison of RMSD's for Nitrogen Heterocycle containing Ternary Systems with COSMO-RS Predictions (Pererio et al., 2008)

S.No	Temp	**System Name**	**RMSD**
1	298.15	Methanol –hexadecane- quinoline	13.65
2	298.15	Methanol –hexadecane-pyridine	9.63
3	298.15	Methanol –hexadecane-indole	7.80
4	298.15	Methanol –hexadecane-pyrrole	10.50
Average RMSD deviation			**10.4**

Figure 4.16: Experimental and COSMO-RS model predicted tie-lines for the LLE of the ternary system of methanol + Hexadecane + Pyridine at 298.15 K.

4.12.2 Benchmarking using Infinite Dilution Activity Coefficient Predictions

In order to validate our findings with experimental results we have compared the Infinite Dilution Activity Coefficients (IDAC) of pyridine in IL which has been reported in literature. It should be noted that the selectivity and capacity are functions of IDAC (Eqn 4.21,Eqn 4.22).So a comparison of IDAC values serves as the validation for selectivity and capacity at infinite dilution. Recently IDAC values of pyridine in IL have been reported [Revelli et al., 2009; Mutlet et al., 2006]. For validation purpose, the IDAC values of pyridine in (1-butyl-3-methylimidazoloium tetrafluoroborate) [BMIM][BF_4] [Revelli et al.,

2009] at 303.35, 312.55,322.55 and 332.55 K and in (1-ethyl-3-methylimidazolium tosylate)[EMIM][TOS][Mutlet et al., 2006] at 323.15K have been predicted. Compared to literature data, the predicted values are comparable for pyridine in [BMIM][BF_4] at 303.35, 312.55,322.55 and 332.55K, but very close to pyridine in [EMIM][TOS] at 323.15K (Table 4.8). The root mean square is a usual way to compare deviations in IDAC values [Diedenhofen et al., 2003]· The average root mean square deviation (RMS) for all 5 points is equal to 15% for [BMIM][BF_4] and 0.85% for [EMIM][TOS].This agrees well with the infinite dilution activity coefficient predictions of ionic liquids by Diedenhofen et al.,[2003]. Thus the predicted values serve as benchmark for screening other potential ionic liquids. This will further lead to the calculation which includes selectivity (section 4.12.3), capacity (section 4.12.4) and performance index (section 4.12.5) at several temperature and atmospheric pressure, to find potential ionic liquid as a green solvent for denitrification process.

2.1.3 Selectivity at Infinite Dilution

Figures 4.17(a) to 4.17(h) shows the selectivity at infinite dilution for the nitrogen heterocyles with [EMIM], [EPY], [EMMOR], [EPYRO], [EMPIP] and [TMPYZO] cations along with 26 anions (fluorous and nonfluorous). The corresponding selectivity at infinite dilution for pyrrole, indole, indoline, carbazole, benzocarbazole, pyridine, quinoline and benzoquinoline are shown from Figures 4.17(a) to 4.17(h) respectively. The various factors on which the selectivity at infinite dilution for nitrogen species depends are as follows :(a) N (heteroaromatic)-H (imidazolium) hydrogen bonds[Cassol et al.,2007], (b) X (heteroatom of the anion)-H (NH) interaction[Zhou et al.,2008], (c) length and place of the alkyl group[Kumar et al.,2009;Alonso et al.,2008] within the aromatic ring structure of cation, (d) smaller volume of anion structure due to high sterical shielding effect at the anion charge center[Lei et al.,2006] (Figure 4.18), (e) CH(cation)-π(nitrogen species) interaction [Suezawa et al.,2000] and (f) compactness [Lei et al.,2006; Suezawa et al.,2000;Su et al.,2004;Fraser et

al.,2007] between cation and anion. In the subsequent sections we have tried to incorporate the factors (a) to (e) to explain the selectivity phenomena. The compactness between cation and anion is not explained since it requires the knowledge of interaction energies between cation and anion which is not studied here.

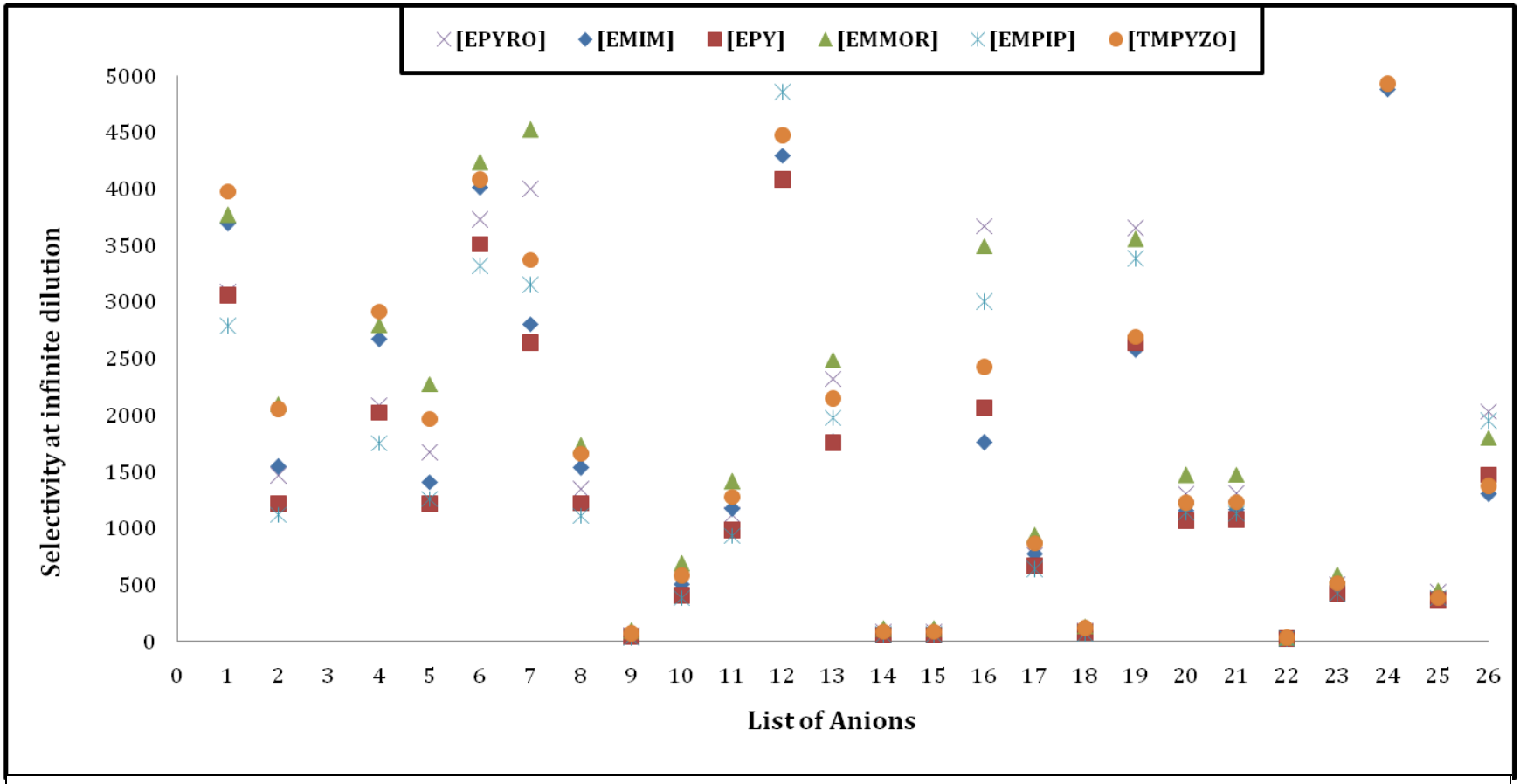

1. [Br], 2. [NO_3], 3. [SCN], 4. [CH_3COO], 5. [HSO_4], 6. [BF_4], 7. [CH_3SO_3], 8. [CF_3COO], 9. [CH_3SO_4], 10. [PF_6], 11. [CF_3SO_3], 12. [$C_2H_5SO_4$], 13. [$(CH_3)_2PO_4$], 14. [$C_3H_7NO_3S$], 15. [$B(CN)_4$], 16. [$C_7H_5O_3$], 17. [$(CH_3SO_2)_2N$], 18.

Figure 4.17 (a): Selectivity at infinite dilution for pyrrole at ambient temperature (T= 298.15K)

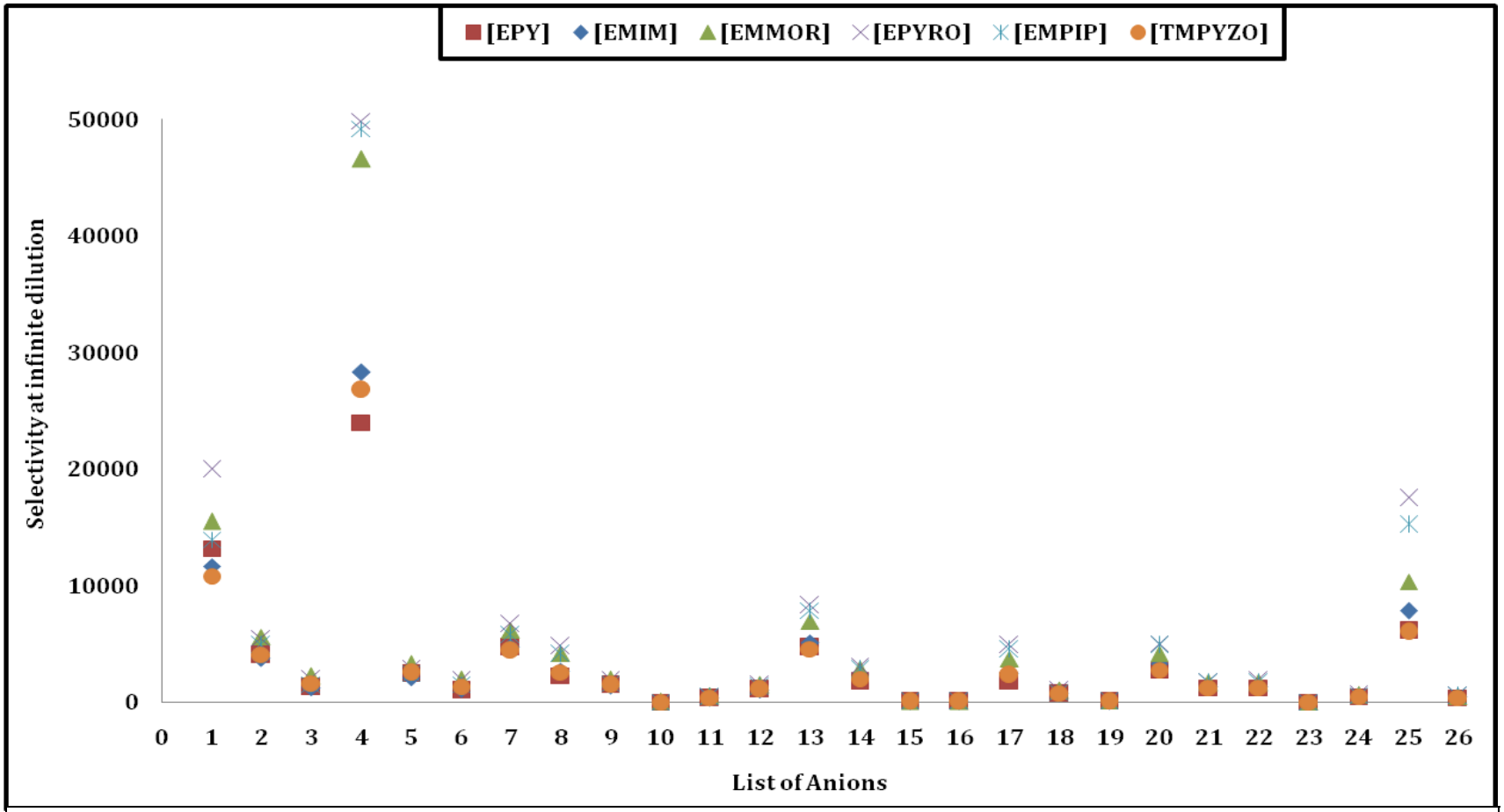

1. [Br], 2. [NO_3], 3. [SCN], 4. [CH_3COO], 5. [HSO_4], 6. [BF_4], 7. [CH_3SO_3], 8. [CF_3COO], 9. [CH_3SO_4], 10. [PF_6], 11. [CF_3SO_3], 12. [$C_2H_5SO_4$], 13. [$(CH_3)_2PO_4$], 14. [$C_3H_7NO_3S$], 15. [$B(CN)_4$], 16. [$C_7H_5O_3$], 17. [$(CH_3SO_2)_2N$], 18.

Figure 4.17 (b): Selectivity at infinite dilution for indole at ambient temperature (T=298.15K)

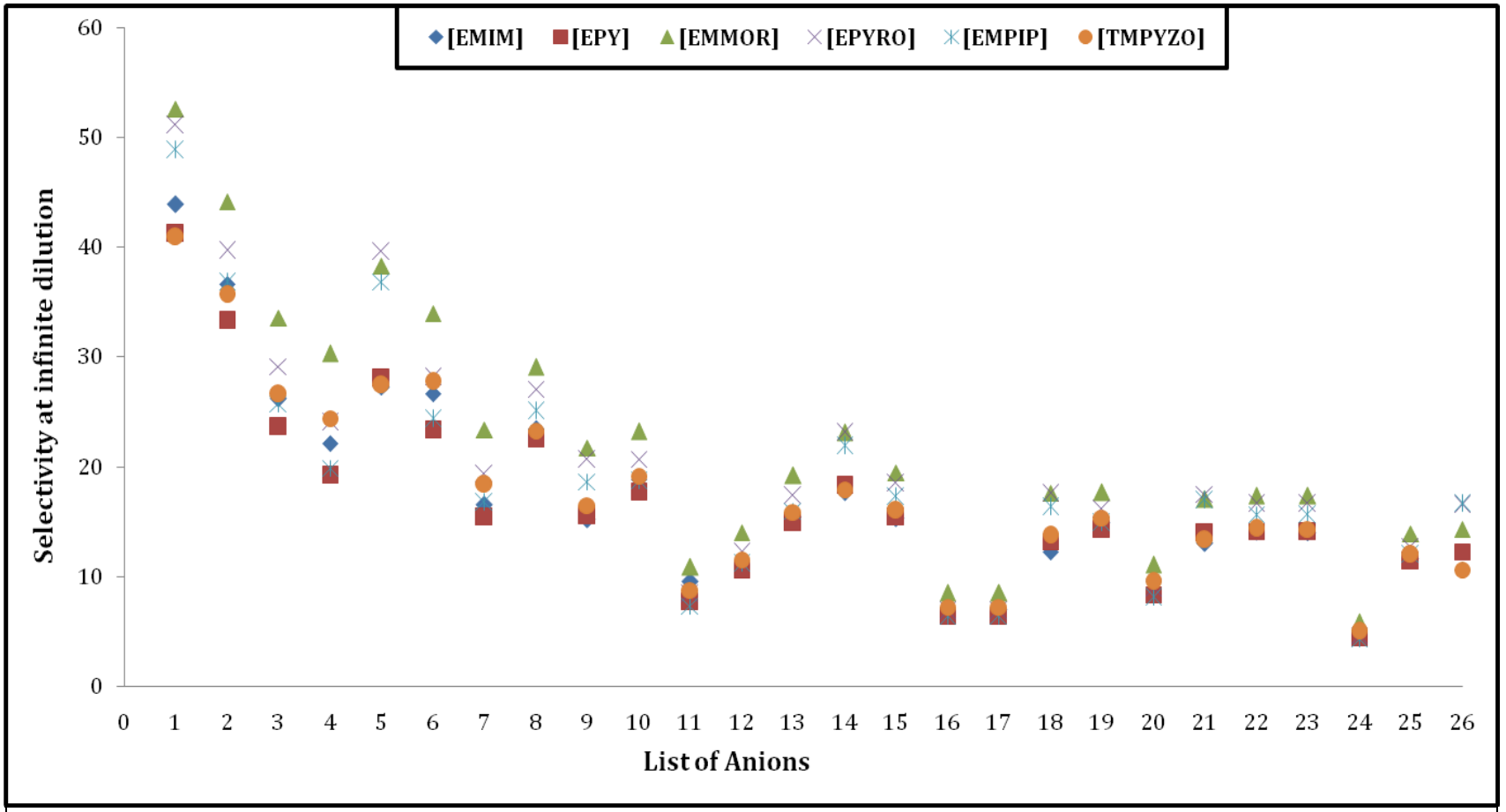

1. [Br], 2. [NO_3], 3. [SCN], 4. [CH_3COO], 5. [HSO_4], 6. [BF_4], 7. [CH_3SO_3], 8. [CF_3COO], 9. [CH_3SO_4], 10. [PF_6], 11. [CF_3SO_3], 12. [$C_2H_5SO_4$], 13. [$(CH_3)_2PO_4$], 14. [$C_3H_7NO_3S$], 15. [$B(CN)_4$], 16. [$C_7H_5O_3$], 17. [$(CH_3SO_2)_2N$], 18.

Figure 4.17 (c): Selectivity at infinite dilution for indoline at ambient temperature (T=298.15K)

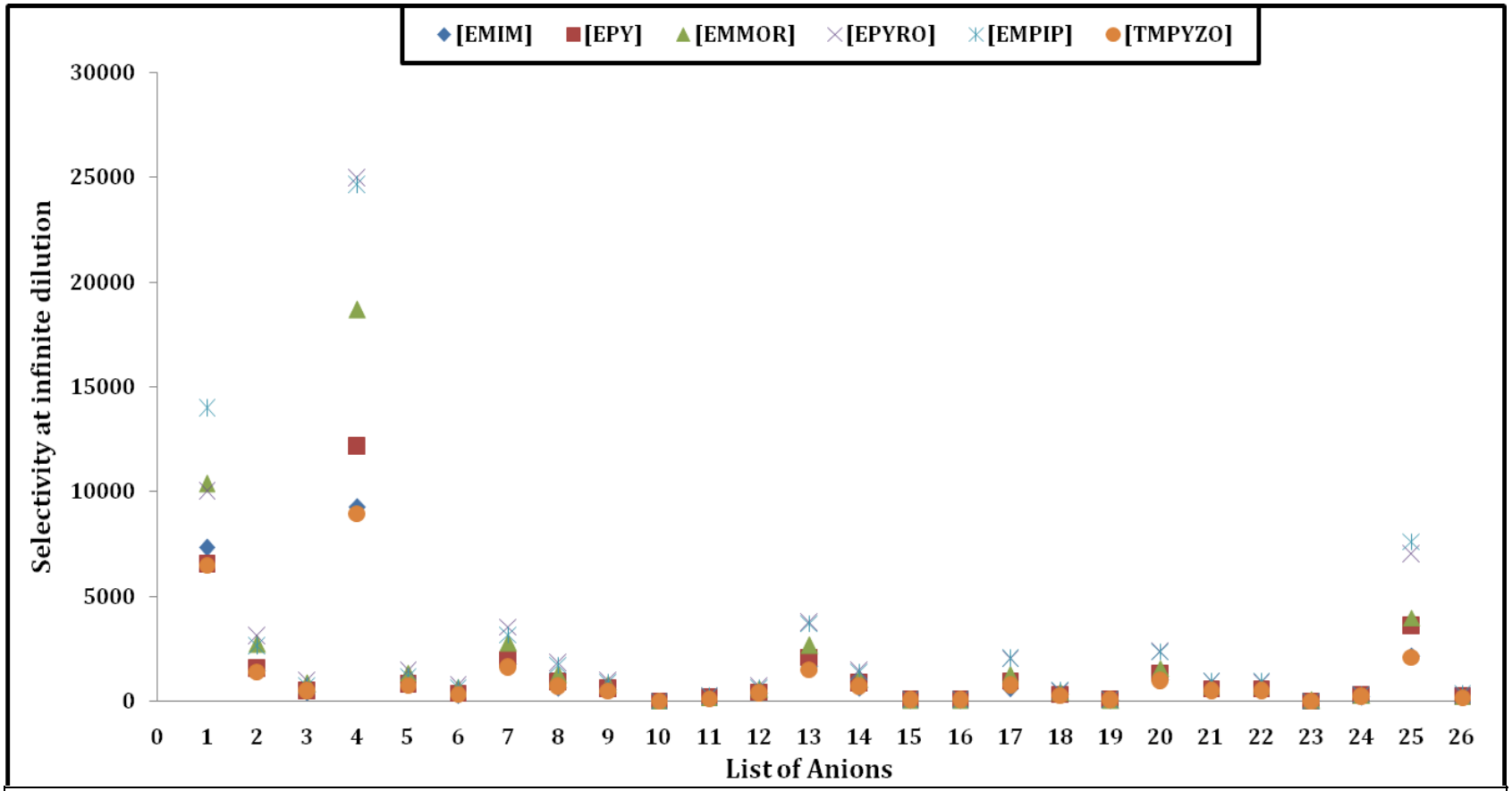

1. [Br], 2. [NO_3], 3. [SCN], 4. [CH_3COO], 5. [HSO_4], 6. [BF_4], 7. [CH_3SO_3], 8. [CF_3COO], 9. [CH_3SO_4], 10. [PF_6], 11. [CF_3SO_3], 12. [$C_2H_5SO_4$], 13. [$(CH_3)_2PO_4$], 14. [$C_3H_7NO_3S$], 15. [$B(CN)_4$], 16. [$C_7H_5O_3$], 17. [$(CH_3SO_2)_2N$], 18.

Figure 4.17 (d): Selectivity at infinite dilution carbazole at ambient temperature (T=298.15K)

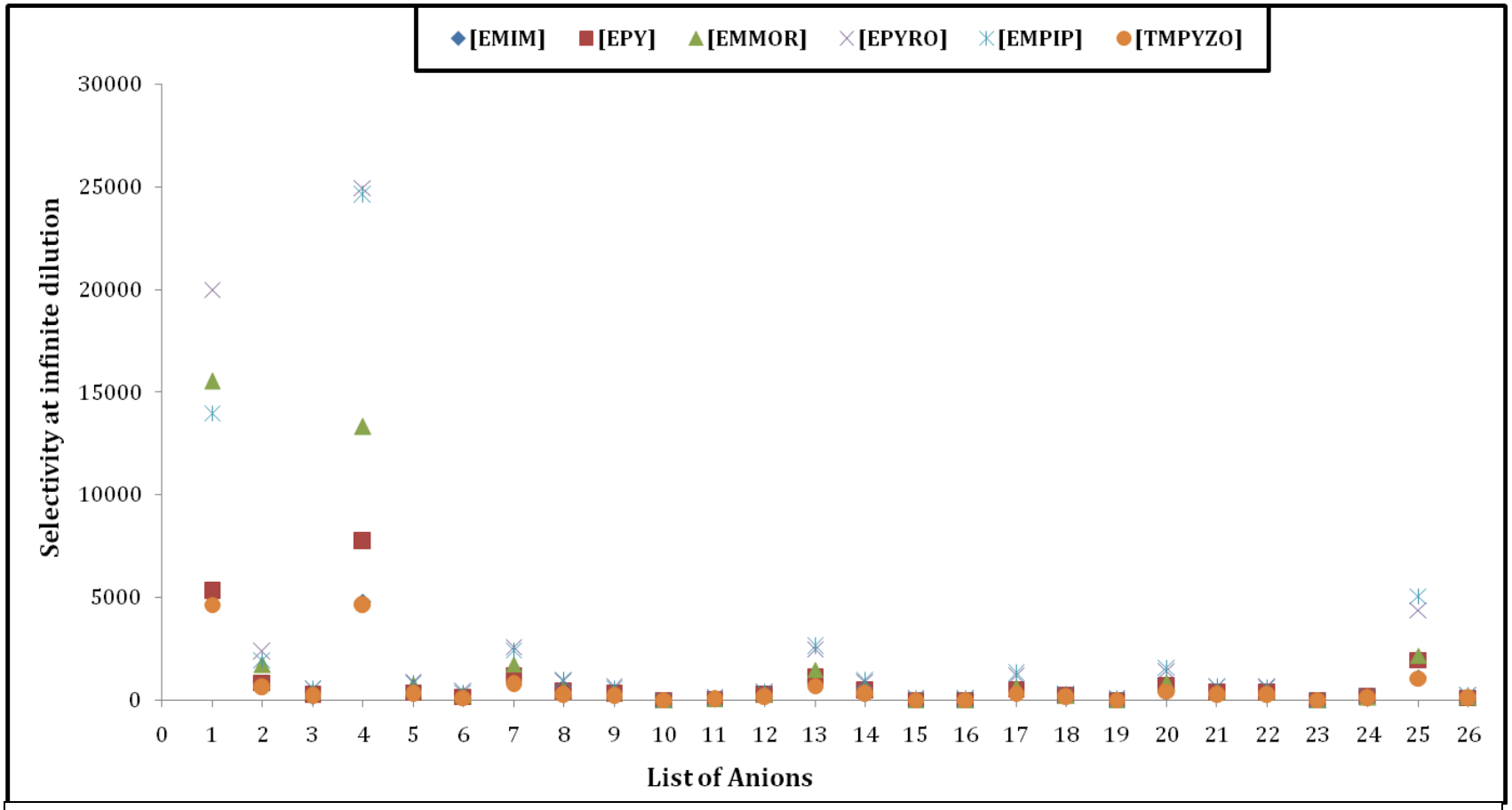

1. [Br], 2. [NO_3], 3. [SCN], 4. [CH_3COO], 5. [HSO_4], 6. [BF_4], 7. [CH_3SO_3], 8. [CF_3COO], 9. [CH_3SO_4], 10. [PF_6], 11. [CF_3SO_3], 12. [$C_2H_5SO_4$], 13. [$(CH_3)_2PO_4$], 14. [$C_3H_7NO_3S$], 15. [$B(CN)_4$], 16. [$C_7H_5O_3$], 17. [$(CH_3SO_2)_2N$], 18.

Figure 4.17 (e): Selectivity at infinite dilution benzacarbazole at ambient temperature (T=298.15K)

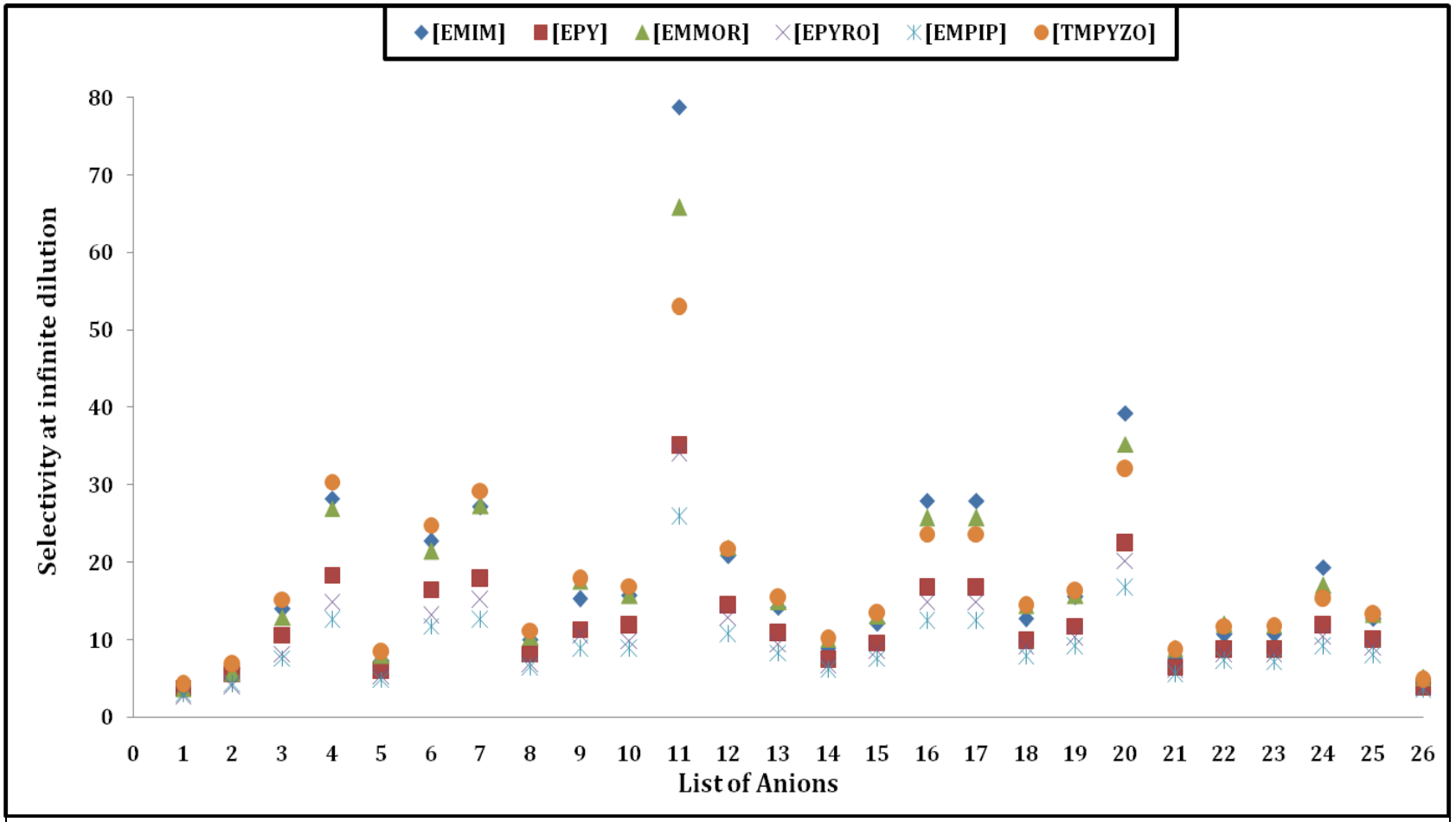

1. [Br], 2. [NO_3], 3. [SCN], 4. [CH_3COO], 5. [HSO_4], 6. [BF_4], 7. [CH_3SO_3], 8. [CF_3COO], 9. [CH_3SO_4], 10. [PF_6], 11. [CF_3SO_3], 12. [$C_2H_5SO_4$], 13. [$(CH_3)_2PO_4$], 14. [$C_3H_7NO_3S$], 15. [$B(CN)_4$], 16. [$C_7H_5O_3$], 17. [$(CH_3SO_2)_2N$], 18.

Figure 4.17 (f): Selectivity at infinite dilution pyridine at ambient temperature (T=298.15K)

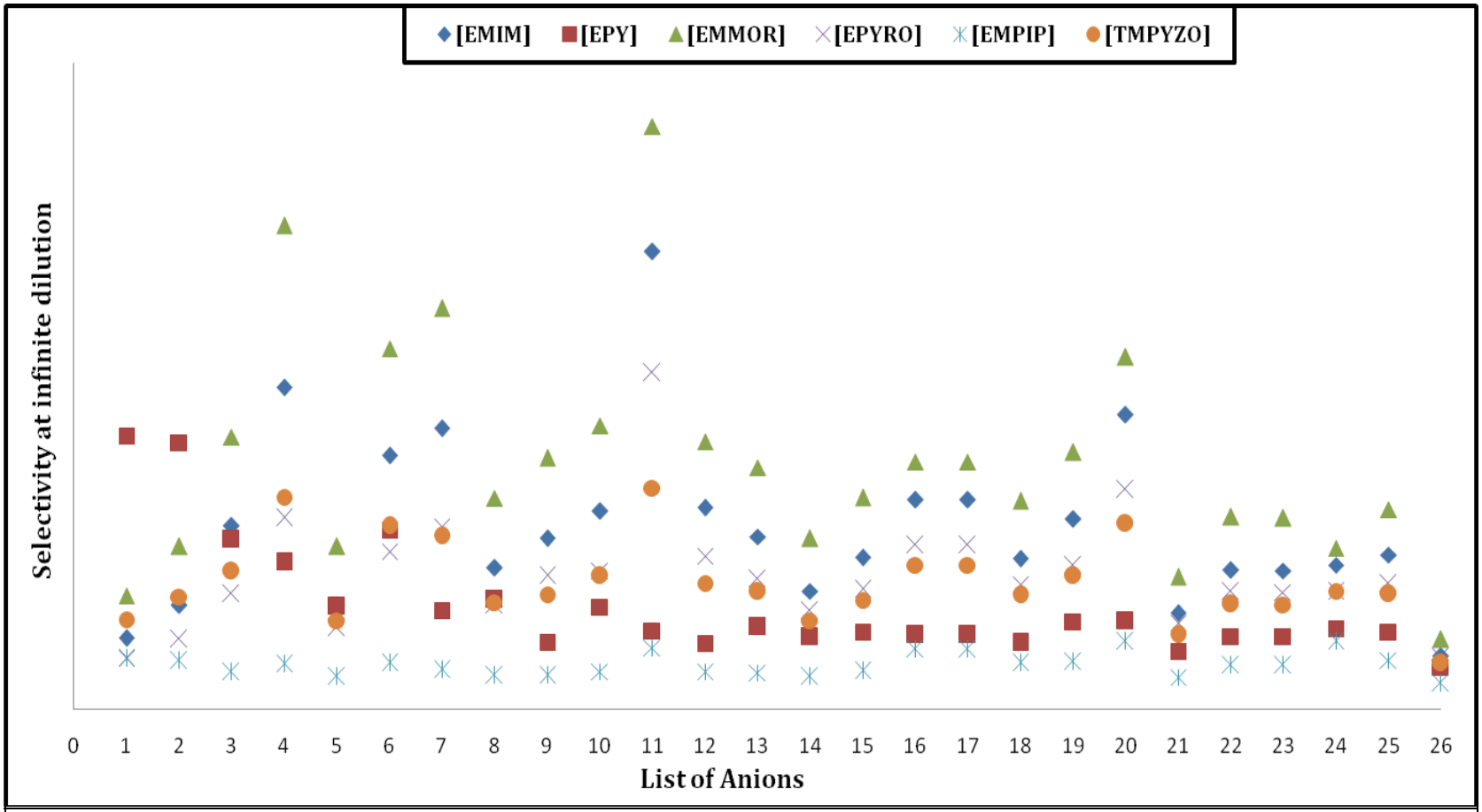

1. [Br], 2. [NO_3], 3. [SCN], 4. [CH_3COO], 5. [HSO_4], 6. [BF_4], 7. [CH_3SO_3], 8. [CF_3COO], 9. [CH_3SO_4], 10. [PF_6], 11. [CF_3SO_3], 12. [$C_2H_5SO_4$], 13. [$(CH_3)_2PO_4$], 14. [$C_3H_7NO_3S$], 15. [$B(CN)_4$], 16. [$C_7H_5O_3$], 17. [$(CH_3SO_2)_2N$], 18.

Figure 4.17(g): Selectivity at infinite dilution quinoline at ambient temperature (T=298.15K)

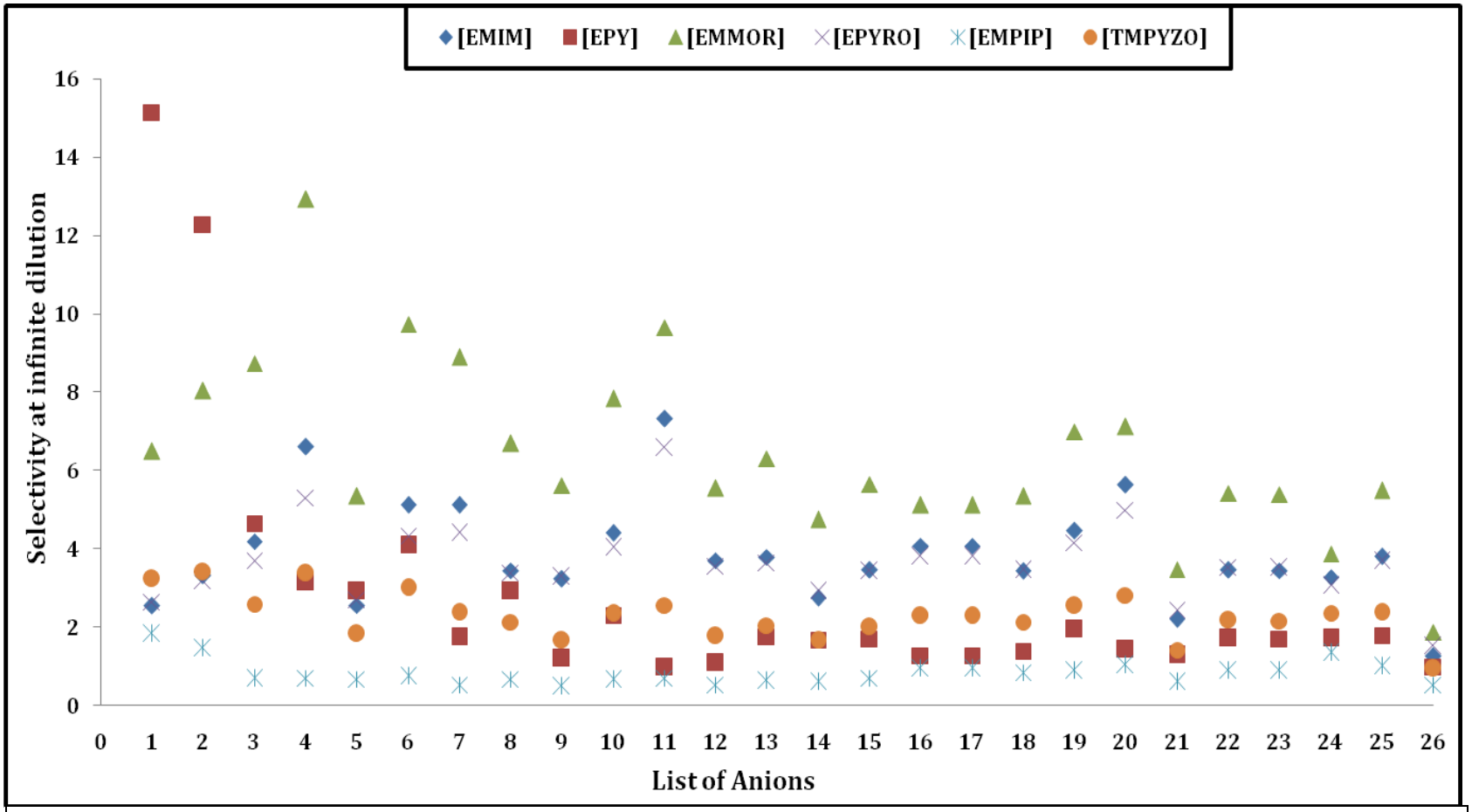

1. [Br], 2. [NO_3], 3. [SCN], 4. [CH_3COO], 5. [HSO_4], 6. [BF_4], 7. [CH_3SO_3], 8. [CF_3COO], 9. [CH_3SO_4], 10. [PF_6], 11. [CF_3SO_3], 12. [$C_2H_5SO_4$], 13. [$(CH_3)_2PO_4$], 14. [$C_3H_7NO_3S$], 15. [$B(CN)_4$], 16. [$C_7H_5O_3$], 17. [$(CH_3SO_2)_2N$], 18.

Figure 4.17 (h): Selectivity at infinite dilution benzaquinoline at ambient temperature (T=298.15K)

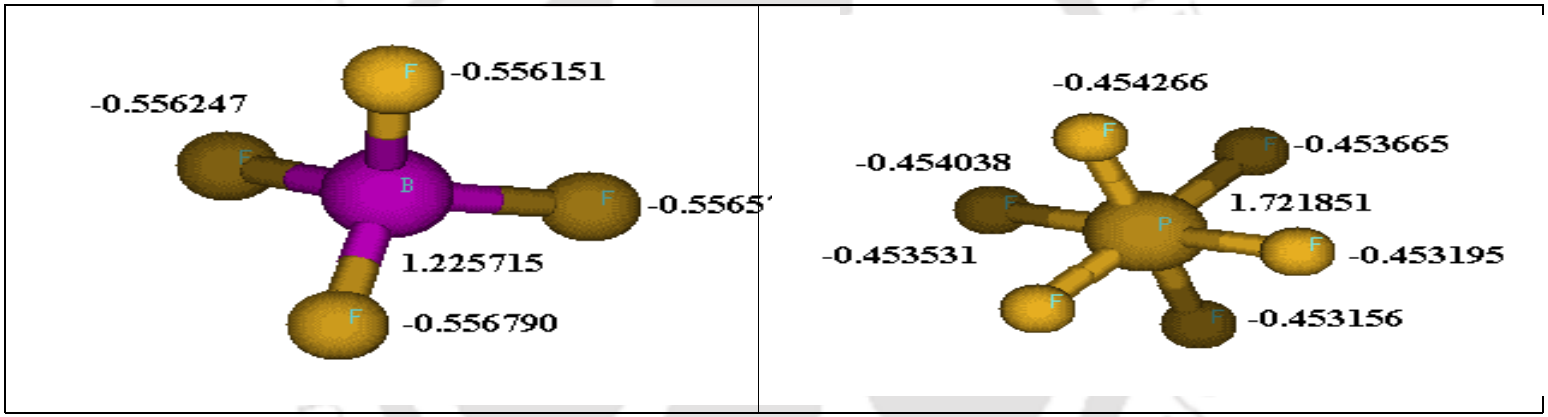

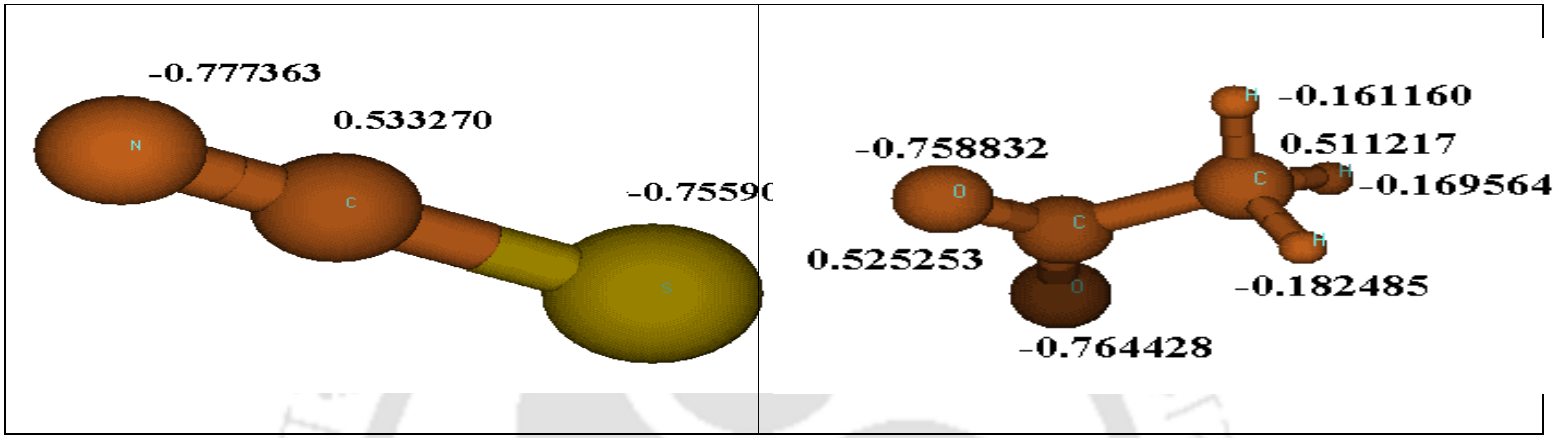

Figure 4.18: Partial charges of selected anions obtained via CHELPG scheme

4.12.4 Effect of Anion Structure

In general increasing COSMO volume of anions leads to an increase in selectivity of ILs for the nitrogen species [Alonso et al., 2008]. However the trend is somewhat different as the increase also depends on the number of heteroatom such as fluorine, sulfur, nitrogen and oxygen which are present in most of the anions [Zhou et al., 2008]. Petrukhin et al.,[2002] pointed out that the halide anions (Cl.Br, I) and the heteroatom (N, O, S, and F) present in the anions leads to an external connectivity with the hydrogen atom of the nitrogen species. This connectivity or interaction is called the X (heteroatom of the anion)-H (NH) interaction [Zhou et al.,2008] (X=heteroatom of anion, H=hydrogen atom of nitrogen species).The strength of this interaction defines the magnitude of the selectivity of the studied compounds.

It was found that for the same number of heteroatoms in the anion, a higher charge on the heteroatom leads to a higher selectivity (Figures 4.17(a)-4.17(h)). A minimum number of heteroatoms in anions such as [Ac] and [SCN] led to higher selectivity.[Ac] anion gave very high selectivites for pyrrole(Figure 4.17(a)),indole(Figure 4.17(b)),indoline (Figure 4.17(c)) and carbazole (Figure 4.17(d)) irrespective of cations. Similarly [SCN] and [PF_6] gave high selectivities for benzocarbazole(Figure 4.17(e)), pyridine(Figure 4.17(f)) ,quinoline (Figure 4. 17(g)) and benzoquinoline(Figure 4.17(h)).This is consistent with the experimental results obtained using [SCN] as an anion [Domanska et al.,2008,2009]. Additionally strong chemical effects were observed for the removal of carbon dioxide using [Ac] anion [Shiflett et al.,2009]. However irrespective of the nitrogen compound, [BF_4],[PF_6] has a comparatively lower selectivity than [SCN] and [Ac]. The partial charges of the heteroatom in [Ac],[SCN], [BF_4] and [PF_6] were obtained by B3LYP/6-31G++(d,p) by using the ESP fit as given in CHELPG scheme [Breneman et al.,1990]. Each fluorine atom in [BF_4] and [PF_6] has a charge of -0.56 and -0.45 respectively, whereas [Ac] and [SCN] have charges of -0.77 and -0.75 on the heteroatoms (Figure 4.17). Thus the higher negative charge on the heteroatom

enables the hydrogen bonding between X (heteroatom of anion)-H (NH) thereby providing higher selectivity.

4.12.5 Effect of Cation Structure

For cations the interaction mainly takes via N (heteroaromatic)-H (cation) hydrogen bonds [Cassol et al.,2007] where N and H refers to the atom present in nitrogen compound and the cation respectively. Additionally the interaction also takes via CH (cation)-π(nitrogen species) interaction[Joule et al.,2007]. The pyrrolidinium [EPYRO], piperidininum [EPIP] and morpholinium [EMMOR] based ionic liquids showed higher selectivity irrespective of nitrogen compounds as compared to imidazolium [EMIM], pyridinium [EPY] and pyrazolinium [TMPYZO] based ILs. This is due to the fact that the imidazolium, pyridinium and pyrazolium cations consist of aromatic rings which possess steric hindrance towards nitrogen species. This steric hindrance lowers the strength of N (heteroaromatic)-H (cation) hydrogen bond which ultimately decreases the selectivity. Additionally the electron donating tendency through alkyl substitution in [EMIM],[TMPYZO],[EPY] decreases the delocalized π electron density within the cations thereby providing lesser selectivity for the removal of nitrogen species.

Due to this very reason, cations such as [EPYRO] and [EMPIP] shows higher selectivity for the removal of indole (Figure 4.17(b)).The same explanation also holds true for indoline (Figure 4.17(c)), carbazole (Figure4.17(d)) and benzocarbazole (Figure 4.17(e)). [EMMOR] cation because its two heteroatoms (O and N) within its structure (Table 4.17) contributes an additional interaction based on H (heteroaromatic)-O (cation) bonds [Joule et al.,2007;Gupta et al.,2005;Bansal et al.,2005] where H and O refers to the atom present in nitrogen compound and the cation respectively. Thus [EMMOR] based ionic liquids shows the highest selectivity for quinoline (Figure 4.17(g)) and benzoquinoline (Figure 4.17(h)). The only anomaly in the trend is that present in pyrrole (Figure 4.17(a)) and pyridine (Figure

4.17(f)). It should be noted that the two nitrogen heterocycle posses a similar π-delocalized electron density due to the presence of nitrogen heteroatom in its structure.

Thus [EMIM] cation having a similar structure like pyrrole surprisingly shows lower selectivity than [EPYRO] based cations (Figure 4.17(a)). Thus is due to the increase of the cation size by the alkyl substitution on the aromatic ring in [EMIM]. It is a well known fact that by increasing the cation size, the coulombic interaction between anion and cation increases[Zhou et al.,2008], which finally leads to the decrease of the CH (cation)-π (nitrogen species) interaction [Gupta et al.,2005;Bansal et al.,2005;Gutel et al.,2009;Suezawa et al.,2004]. The COSMO-RS model does not quantify CH-π interaction by definition, but a probable answer or explanation lies in the fact that CH groups of ionic liquids can participate simultaneously [Suezawa et al.,2004] in the interaction with nitrogen species leading to higher selectivity and capacity at infinite dilution. The maximum and minimum selectivity values of ILs for the five and six membered ring compounds are given in Table 4.12. It is a known fact that five membered compounds posses hydrogen donor which can interact with electronegative atom of the cation which do not contain aromatic ring [Joule et al.,2007;Gupta et al.,2005;Bansal et al.,2005]. Thus as compared to pyridine, pyrrole and its homologues like indole, carbazole and benzocarbazole have higher selectivity and capacity with cations such as [EMMOR],[EMPIP] and [EMPYRO] (Figure 4.17(a) -4.17(h)).

We have observed that the cations without aromatic structure have significant influence on the selectivity. This is consistent with the COSMO-RS predicted selectivity of hexene/hexane system using ionic liquids [Won et al.,2002] .Thus aromatic structure of the cation without aromatic ring tends to give higher selectivity because of lower sterical hindrance. Therefore pyrrolidinium, piperidinium and morpholinium based cations have showed higher selectivity, capacity and performance index for all studied nitrogen species when compared to other cations such as imidazolium, pyridininum, pyrazolium. Further the pyrrolidinium, piperidinium, and morpholinium based cations having two electro negative

atoms in its ring pose a significant influence [Adebahr et al., 2005;Lava et al.,2009] on the selectivity and capacity of the ionic liquid. It should be noted that the pyrrolidinium, piperidinium, and morpholinium based cations have similar electronegative atom on its structure such as nitrogen and oxygen (Table 4.12).Due to this the electrostatic interaction between the cation and anion is generally weak. So the cation can form hydrogen bonding via hydrogen atom with the aromatic nitrogen ring. Thus the three cations have a very small difference with regards to selectivity, so a thumb rule for selecting the cation would be to choose cations which do not have aromatic ring.

Table 4.12: Summary of results obtained for studied aromatic Nitrogen species

Nitrogen species	**Range**			**Prospective Ionic Liquid Based on**		
				Selectivity	***Capacity***	***P.I=***
Pyrrole	Max	24956	5000	[EPYRO][Ac]	[EPYRO][Ac]	[EPYRO][Ac]
	Min	21	3.0	[EPY][$(CF_3SO_2)_2N$]	[EMMOR][DEP]	[EMPIP][PF_6]
Indole	Max	49872	10000	[EPYRO][Ac]	[EPYRO][Ac]	[EPYRO][Ac]
	Min	24	0.4	[EPY][PF_6]	[EMMOR][PF_6]	[TMPYZO][PF_6]
Indoline	Max	39.5	7.9	[EPYRO][Ac]	[EPYRO][Ac]	[EPYRO][Ac]
	Min	4.4	0.1	[EPY][$(CF_3SO_2)_2N$]	[TMPYZO][PF_6]	[EMMOR][PF_6]
Carbazole	Max	24936	5000	[EPYRO][Ac]	[EPYRO][SCN]	[EPYRO][SCN]
	Min	0.8	0.1	[TMPYZO][CH_3SO_4]	[TMPYZO][MeSu]	[TMPYZO][MeSu]
Benzacarbazole	Max	24857	10000	[EPYRO][SCN]	[EPYRO][Br]	[EPYRO][SCN]
	Min	2.3	0.03	[TMPYZO][PF_6]	[TMPYZO][PF_6]	[TMPYZO][PF_6]
Pyridine	Max	78.7	2.7	[EMIM][PF_6]	[EMIM][$(CF_3SO_2)_2$N]	[EMIM][PF_6]
	Min	8.0	0.4	[EMPIP][$(CF_3SO_2)_2$N]	[TMPYZO][BF_6]	[TMPYZO][DeCa]
Quinoline	Max	27.0	2.4	[EMMOR][PF_6]	[EMMOR][Br]	[EPY][Br]
	Min	1.2	0.1	[EMPIP][OcSu]	[TMPYZO][BF_4]	[EMPIP][CF_3COO]

Benzaquinoline	Max	12.3	2.5	[EMIM][SCN]	[EMMOR][Br]	[EPY][Br]
	Min	0.5	0.03	[EMPIP][PF_6]	[TMPYZO][PF_6]	[EMPIP][BF_4]

4.12.6 Effect of Heterocyclic Structure

In general five membered rings have greater selectivity, because of the higher electro negativity of the heteroatom [Won et al.,2002]. It is reported that the lone-pair of electrons on the nitrogen atom of five membered compounds are not tied up in the π-cloud of heterocyclic ring whereas the lone-pair electrons on the nitrogen atom of the six membered compounds, in contrast, are delocalized around the aromatic ring [Won et al.,2002].. This enables inductive effect to be more pronounced than the commonly occurring mesomeric effect involving π electrons. Thus the interaction of nitrogen heterocycle is both through cation and anion. While the cation contributes through CH(cation)-π(nitrogen species) interaction[Shiflet et al.,2009], the anion participates in the hydrogen bonding between nitrogen heretoatom and the heteroatom of anion. Indoline has a fairly low selectivity (39.5)(Figure 4.17(c)) as compared to other five membered rings such as pyrrole (24936)(Figure 4.17(a)), indole (49872)(Figure 4.17(b)) or carbazole (24936)(Figure 4.17(d)).This can be attributed to the absence of aromatic ring in its structure which prevents the delocalization of π electrons inside the rings [Domanska et al.,2008,2009;Shiflett et al.,2009]. Due to this reason, there is a absence of X (heteroatom of anion)-H(NH) interaction thereby providing low selectivity. Pyrrole and carbazole have similar order of selectivity (Figure 4.17(a), Figure 4.17(d)) because of their similar π electron density.

In the case of five membered rings, the selectivity for pyrrole varies from 24936 ([EPYRO][Ac]) to 421 ([EPY][Tf_2N](Figure 4.17(a)); indole: 49872 ([EPYRO][Ac]) - 24 ([EPY][PF_6]) (Figure 4.17(b)) ; indoline: 39.5 ([EPYRO][Ac]) - 4.4 ([EPY][Tf_2N]) (Figure

4.17(c)); carbazole: 24936 ([EPYRO][Ac]) - 0.8 ([TMPYZO][EtSu]) (Figure 4.17(d)) and benzacarbazole: 24936 ([EPYRO][SCN]) to 2.3 ([TMPYZO][PF_6]) (Figure 4.17(e)). For six memebered rings, the maximum selectivity varies for pyridine: 78.7 ([EMIM][PF6]) - 8 ([EMPIP][Tf_2N]) (Figure 4.17(f));quinoline:27 ([EMMOR][PF_6]) - 1.2 ([EMPIP][OcSu]) (Figure 4.17(g)) and benzaquionoline: 12.2 ([EMIM][SCN]) - 0.5 ([EMPIP][PF_6]) (Figure 4.17(h)).

The six membered ringed nitrogen compounds possess higher steric hindrance as compared to five membered rings [Joule et al.,2007;Gupta et al.,2005;Bansal et al.,2005]. The selectivity varies with the steric hindrance of the benzene rings and follows the order: pyridine (Figure 4.17(f)) > quinoline (Figure 4.17(g)) > benzoquinoline (Figure 4.17(h)). Further, the inductive effect is quite low as compared to five membered rings [Joule et al.,2007;Gupta et al.,2005;Bansal et al.,2005]. This lowers the ability of hydrogen bond between nitrogen heteroatom and the heteroatom of anion and the interaction is mainly via CH- π interaction. It should be noted that the hydrogen bond interaction is significantly higher in magnitude than CH- π interaction [Gutel et al., 2009; Suezawa et al., 2004]. Figure 4.19 shows the schematic diagram of various types of interaction [Cassol et al., 2007;Zhou et al.,2008;Fraser et al.,2007]which are present between the ionic liquid (e.g., [EMIM][Ac]) and five and/or six membered ring of nitrogen compounds. The ionic liquid [EMIM][Ac]) has been chosen since the [Ac] anion gave the highest selectivity among the anions.

Figure 4.19: Schematic diagram of interactions between ionic liquid (e.g., [EMIM][Ac]) and five and/or six membered nitrogen compounds.

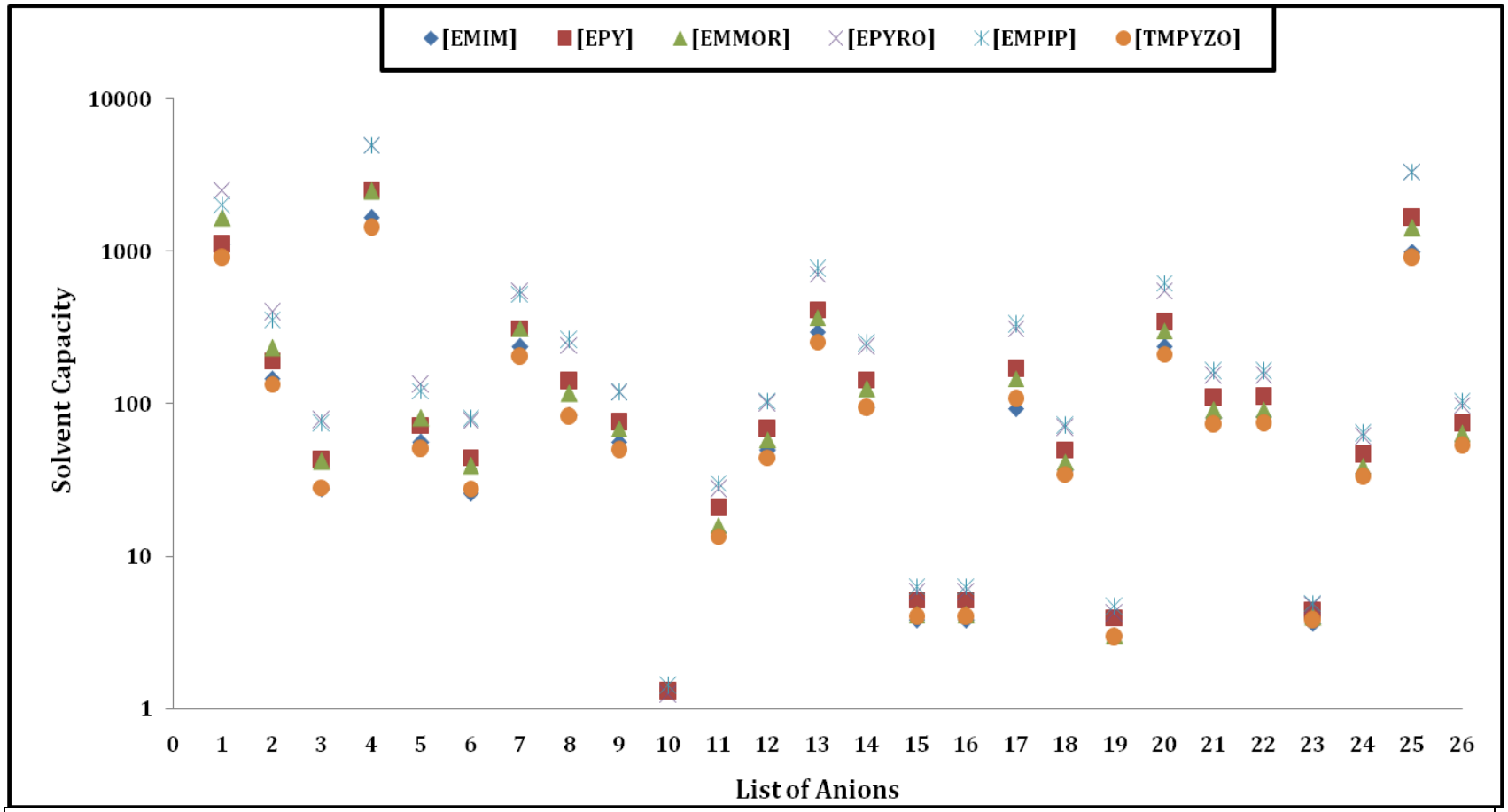

1. [Br], 2. [NO_3], 3. [SCN], 4. [CH_3COO], 5. [HSO_4], 6. [BF_4], 7. [CH_3SO_3], 8. [CF_3COO], 9. [CH_3SO_4], 10. [PF_6], 11. [CF_3SO_3], 12. [$C_2H_5SO_4$], 13. [$(CH_3)_2PO_4$], 14. [$C_3H_7NO_3S$], 15. [$B(CN)_4$], 16. [$C_7H_5O_3$], 17. [$(CH_3SO_2)_2N$], 18.

Figure 4.20 (a): Solvent capacity at infinite dilution for pyrrole at ambient temperature (T=298.155K)

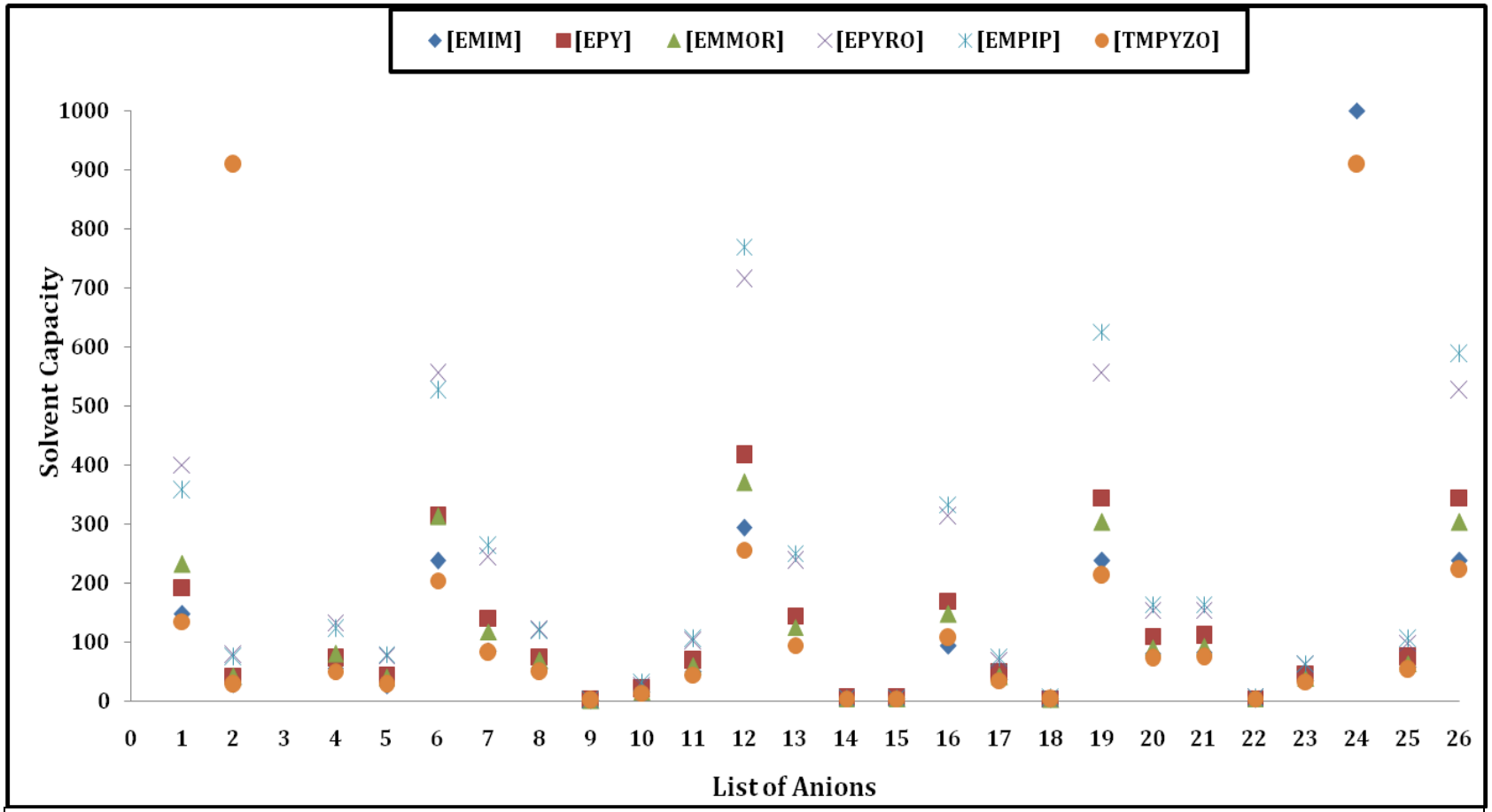

1. [Br], 2. [NO_3], 3. [SCN], 4. [CH_3COO], 5. [HSO_4], 6. [BF_4], 7. [CH_3SO_3], 8. [CF_3COO], 9. [CH_3SO_4], 10. [PF_6], 11. [CF_3SO_3], 12. [$C_2H_5SO_4$], 13. [$(CH_3)_2PO_4$], 14. [$C_3H_7NO_3S$], 15. [$B(CN)_4$], 16. [$C_7H_5O_3$], 17. [$(CH_3SO_2)_2N$], 18.

Figure 4.20 (b): Solvent capacity at infinite dilution for indole at ambient temperature (T=298.15K)

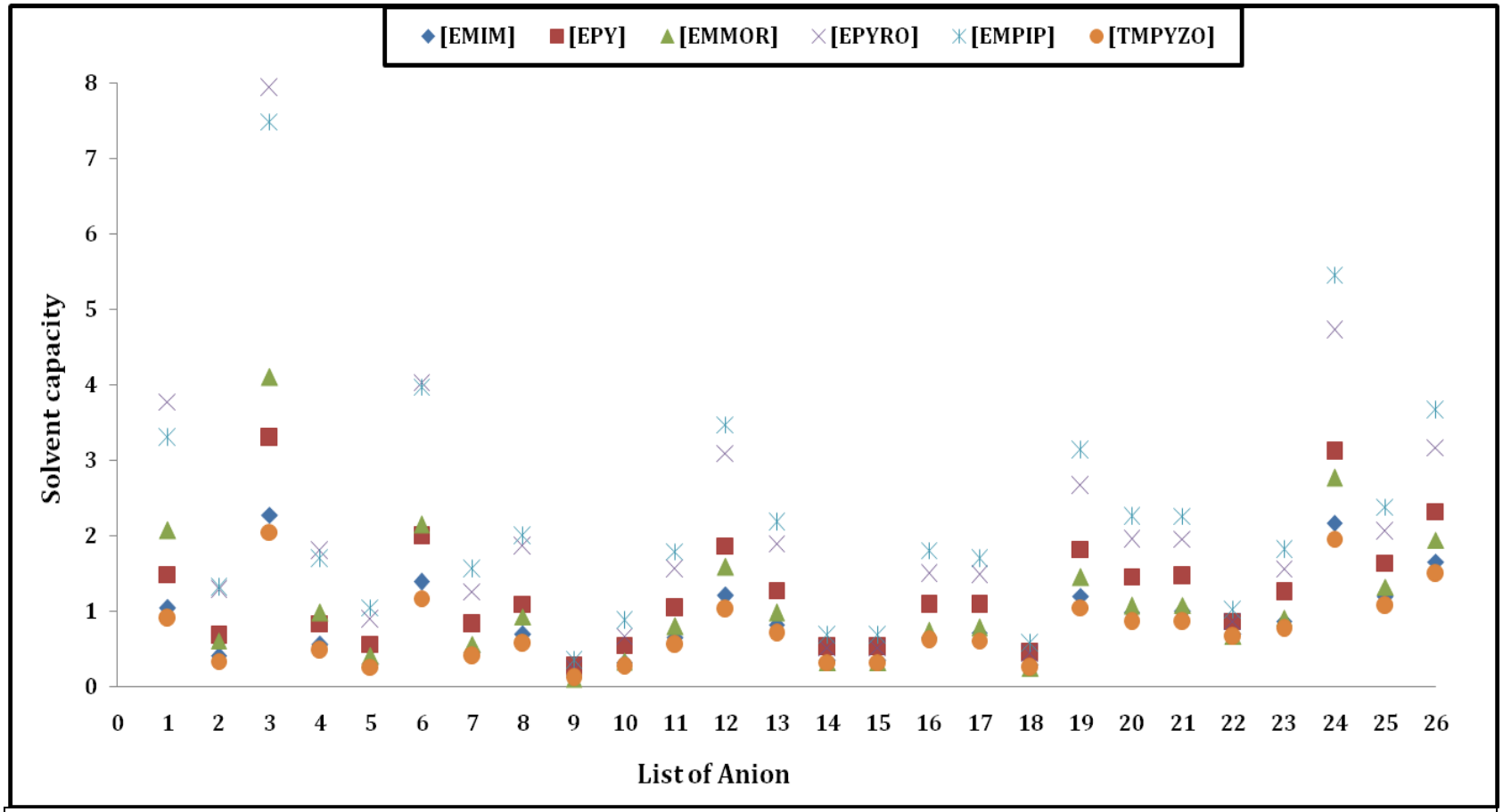

1. [Br], 2. [NO_3], 3. [SCN], 4. [CH_3COO], 5. [HSO_4], 6. [BF_4], 7. [CH_3SO_3], 8. [CF_3COO], 9. [CH_3SO_4], 10. [PF_6], 11. [CF_3SO_3], 12. [$C_2H_5SO_4$], 13. [$(CH_3)_2PO_4$], 14. [$C_3H_7NO_3S$], 15. [$B(CN)_4$], 16. [$C_7H_5O_3$], 17. [$(CH_3SO_2)_2N$], 18.

Figure 4.20(c): Solvent capacity at infinite dilution for indoline at ambient temperature (T=298.15K)

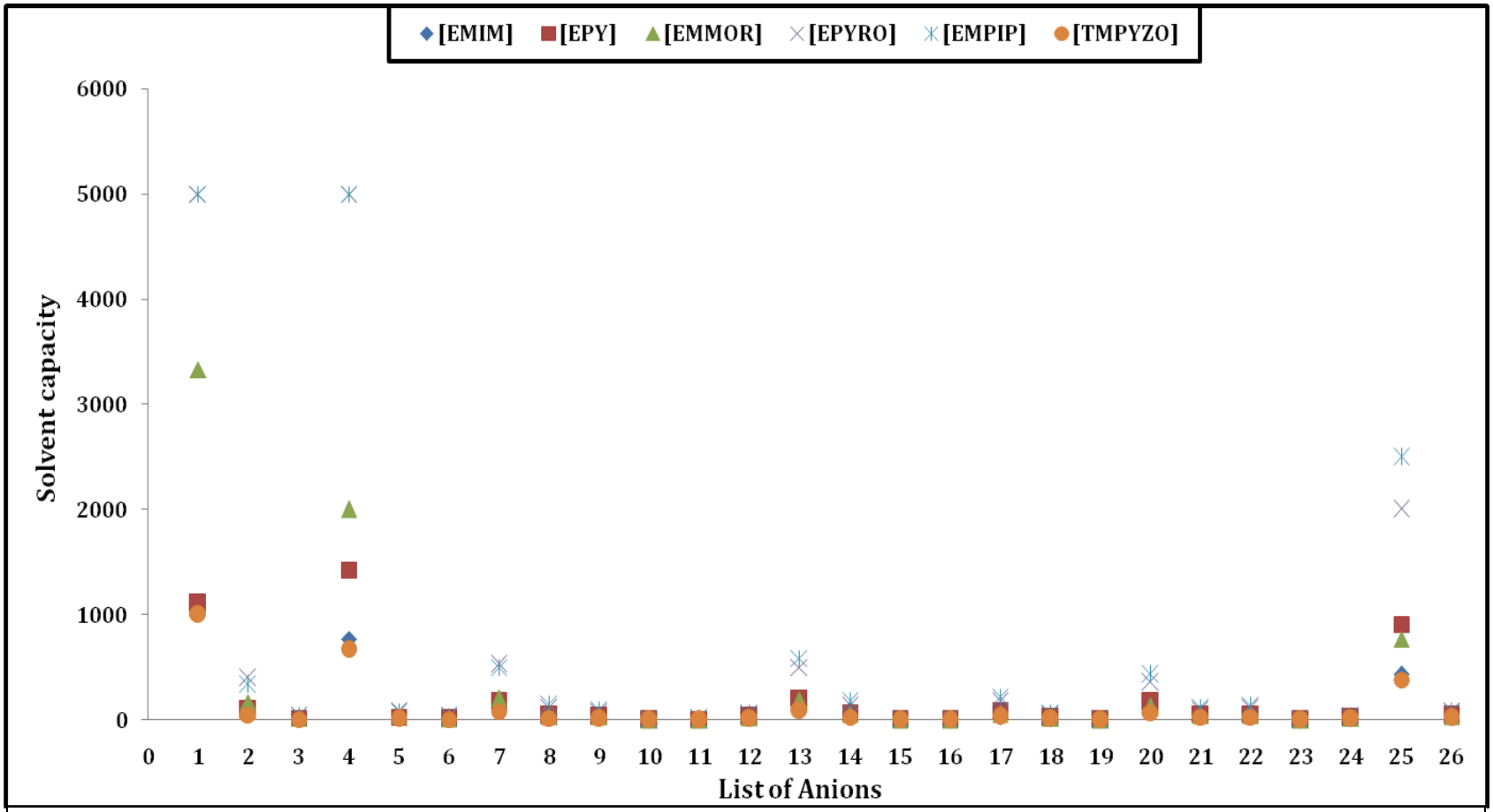

1. [Br], 2. [NO_3], 3. [SCN], 4. [CH_3COO], 5. [HSO_4], 6. [BF_4], 7. [CH_3SO_3], 8. [CF_3COO], 9. [CH_3SO_4], 10. [PF_6], 11. [CF_3SO_3], 12. [$C_2H_5SO_4$], 13. [$(CH_3)_2PO_4$], 14. [$C_3H_7NO_3S$], 15. [$B(CN)_4$], 16. [$C_7H_5O_3$], 17. [$(CH_3SO_2)_2N$], 18.

Figure 4.20 (d): Solvent capacity at infinite dilution for carbazole at ambient temperature (T=298.15)

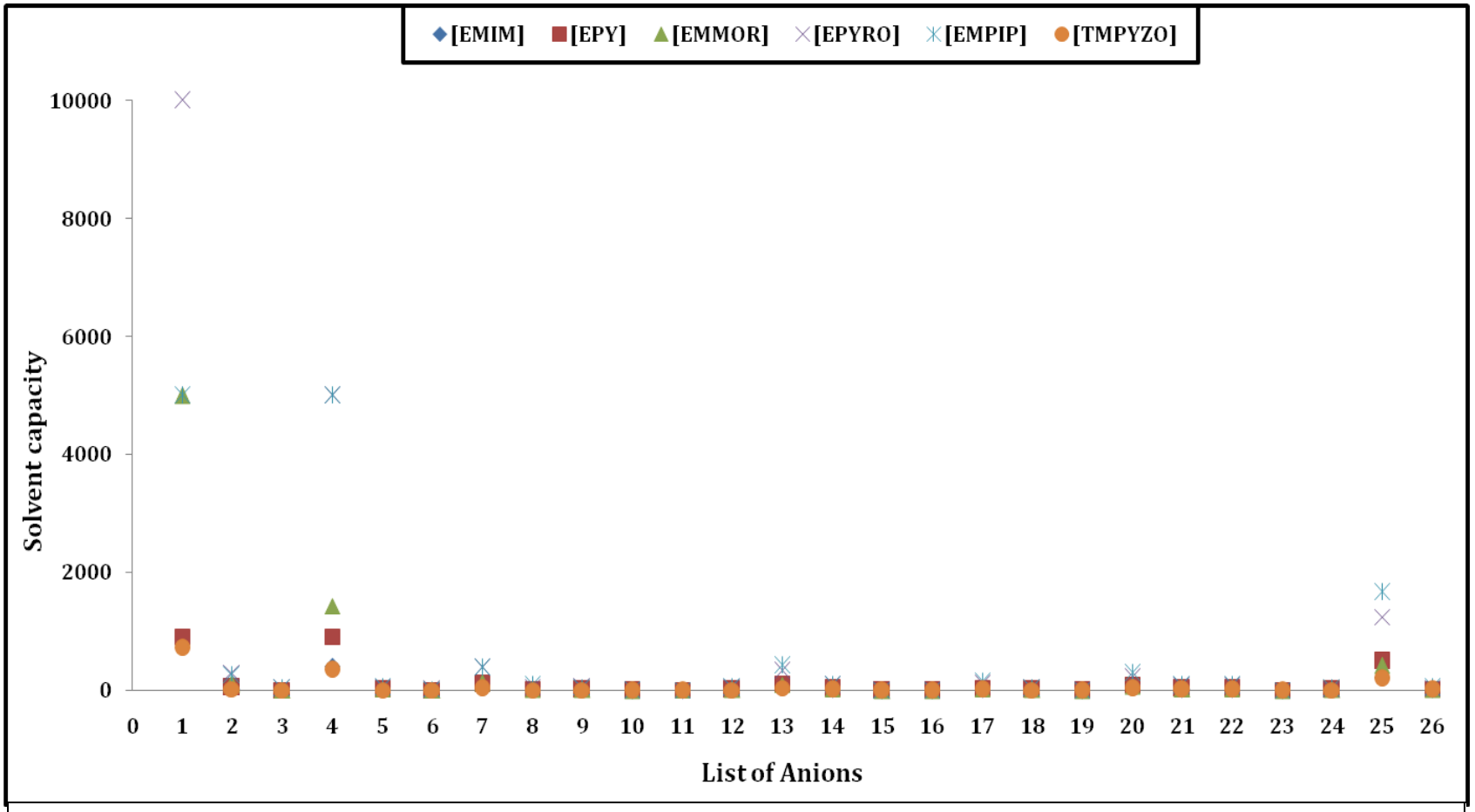

1. [Br], 2. [NO_3], 3. [SCN], 4. [CH_3COO], 5. [HSO_4], 6. [BF_4], 7. [CH_3SO_3], 8. [CF_3COO], 9. [CH_3SO_4], 10. [PF_6], 11. [CF_3SO_3], 12. [$C_2H_5SO_4$], 13. [$(CH_3)_2PO_4$], 14. [$C_3H_7NO_3S$], 15. [$B(CN)_4$], 16. [$C_7H_5O_3$], 17. [$(CH_3SO_2)_2N$], 18.

Figure 4.20 (e): solvent capacity at infinite dilution for benzacarbazole at ambient temperature (T=298.15K)

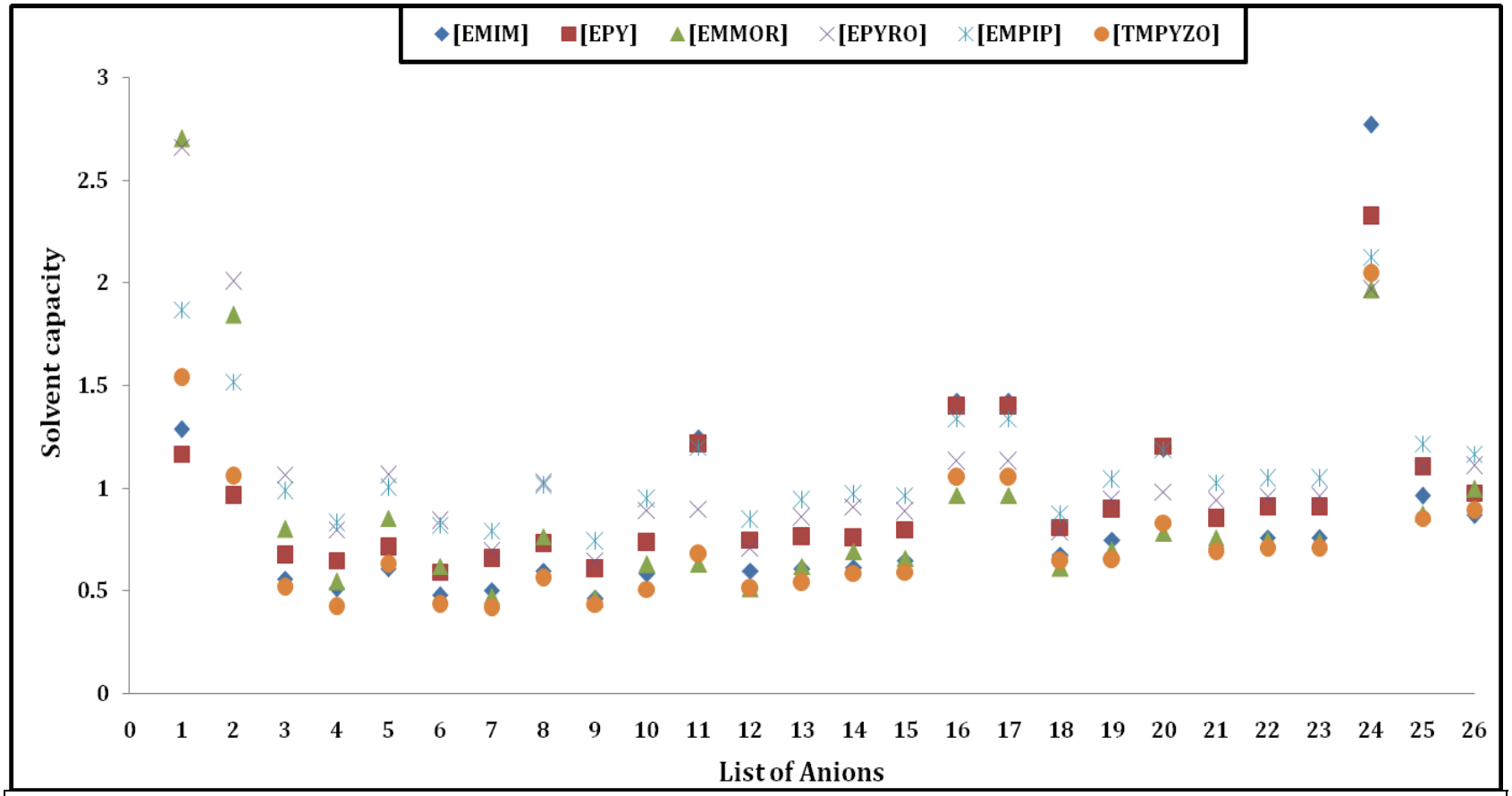

1. [Br], 2. [NO_3], 3. [SCN], 4. [CH_3COO], 5. [HSO_4], 6. [BF_4], 7. [CH_3SO_3], 8. [CF_3COO], 9. [CH_3SO_4], 10. [PF_6], 11. [CF_3SO_3], 12. [$C_2H_5SO_4$], 13. [$(CH_3)_2PO_4$], 14. [$C_3H_7NO_3S$], 15. [$B(CN)_4$], 16. [$C_7H_5O_3$], 17. [$(CH_3SO_2)_2N$], 18.

Figure 4.20 (f): Solvent capacity at infinite dilution for pyridine at ambient temperature (T=298.15)

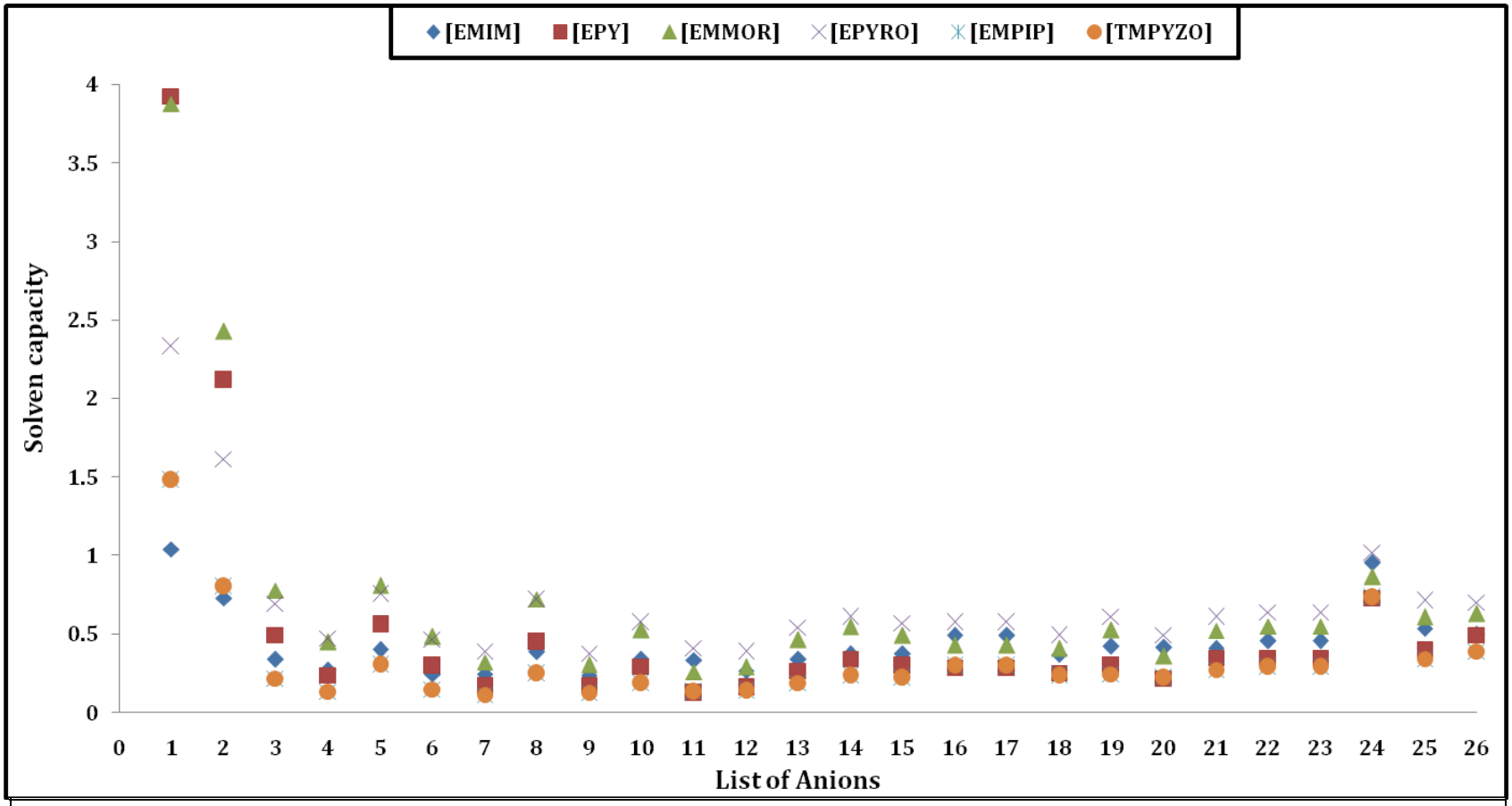

1. [Br], 2. [NO_3], 3. [SCN], 4. [CH_3COO], 5. [HSO_4], 6. [BF_4], 7. [CH_3SO_3], 8. [CF_3COO], 9. [CH_3SO_4], 10. [PF_6], 11. [CF_3SO_3], 12. [$C_2H_5SO_4$], 13. [$(CH_3)_2PO_4$], 14. [$C_3H_7NO_3S$], 15. [$B(CN)_4$], 16. [$C_7H_5O_3$], 17. [$(CH_3SO_2)_2N$], 18.

Figure 4.20(g): Solvent capacity at infinite dilution for quinoline at ambient temperature (T=298.15K)

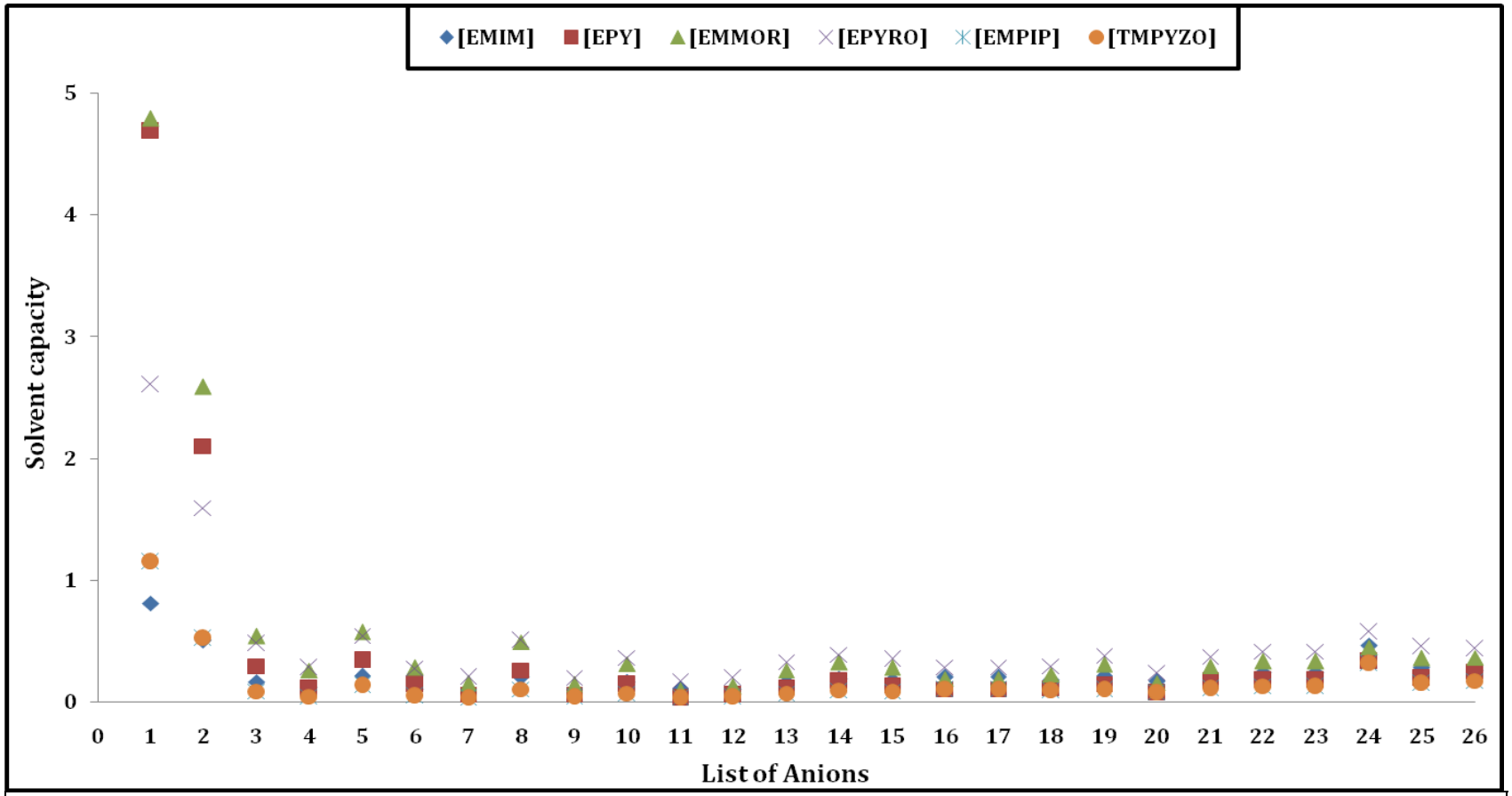

1. [Br], 2. [NO_3], 3. [SCN], 4. [CH_3COO], 5. [HSO_4], 6. [BF_4], 7. [CH_3SO_3], 8. [CF_3COO], 9. [CH_3SO_4], 10. [PF_6], 11. [CF_3SO_3], 12. [$C_2H_5SO_4$], 13. [$(CH_3)_2PO_4$], 14. [$C_3H_7NO_3S$], 15. [$B(CN)_4$], 16. [$C_7H_5O_3$], 17. [$(CH_3SO_2)_2N$], 18.

Figure 4.20 (h): Solvent capacity at infinite dilution for benzaquinoline at ambient temperature (T=298.15K)

4.12.7 Capacity at Infinite Dilution

The capacity of ILs for removal of nitrogen species were also predicted using COSMO-RS model. The predicted values are shown in Figures 4.19(a)-4.19(h) for all the nitrogen species. As with selectivity the capacity at infinite dilution did not gave us any trend within the cations or anions. The cations possessing delocalized electron density such as [EMIM], [EPY], [TMPZO] posses higher steric hindrance than [EMMOR], [EPYRO], [EMPIP], cations as reported previously. Thus [EPYRO], [EMPIP],[EMMOR] cations possess more capacity for the removal of five membered compounds (Figure 4.20(a) -4.20(e)), as well as for six member ringed nitrogen species (Figure 4.19(f)-4.19(h)). The maximum extraction capacity was as high as 10000 for pyrrole using [EPYRO][Br] as ionic liquid(Figure 4.20(a)). On the contrary the lowest value of 0.125 was encountered for quinoline (Figure 4.20(g)) on account of its two aromatic rings.

4.12.8 Performance index at Infinite Dilution

Figure 4.20(a) to 4.20(h) shows the values of performance index (PI) for [EMIM], [EPY], [EMMOR], [EPYRO], [EMPIP] and [TMPYZO] cations with 26 anions predicted by COSMO-RS model. It can be seen that the the [EPYRO], [EMPIP] and [EMMOR] cations have higher PI for five member structures of nitrogen species(Figure 4.21(a)-4.21(e)) on account of its higher selectivity and capacity. In the same manner, for the six member ring compounds the PI for [EPYRO], [EMPIP], [EMMOR] posses high values of PI. These results clearly points out to the fact that the structural feature of ILs play an important role in the extraction of both the classes of nitrogen species. The overall results are summarized in Table 4.12 with respect to maximum and minimum selectivity and capacity of each nitrogen heterocycle. It provides an excellent indicator in the judicious selection of cation and anion. It can be seen that the [EPYRO] cation is the most effective cation for the removal of both five and six membered nitrogen heterocycle.

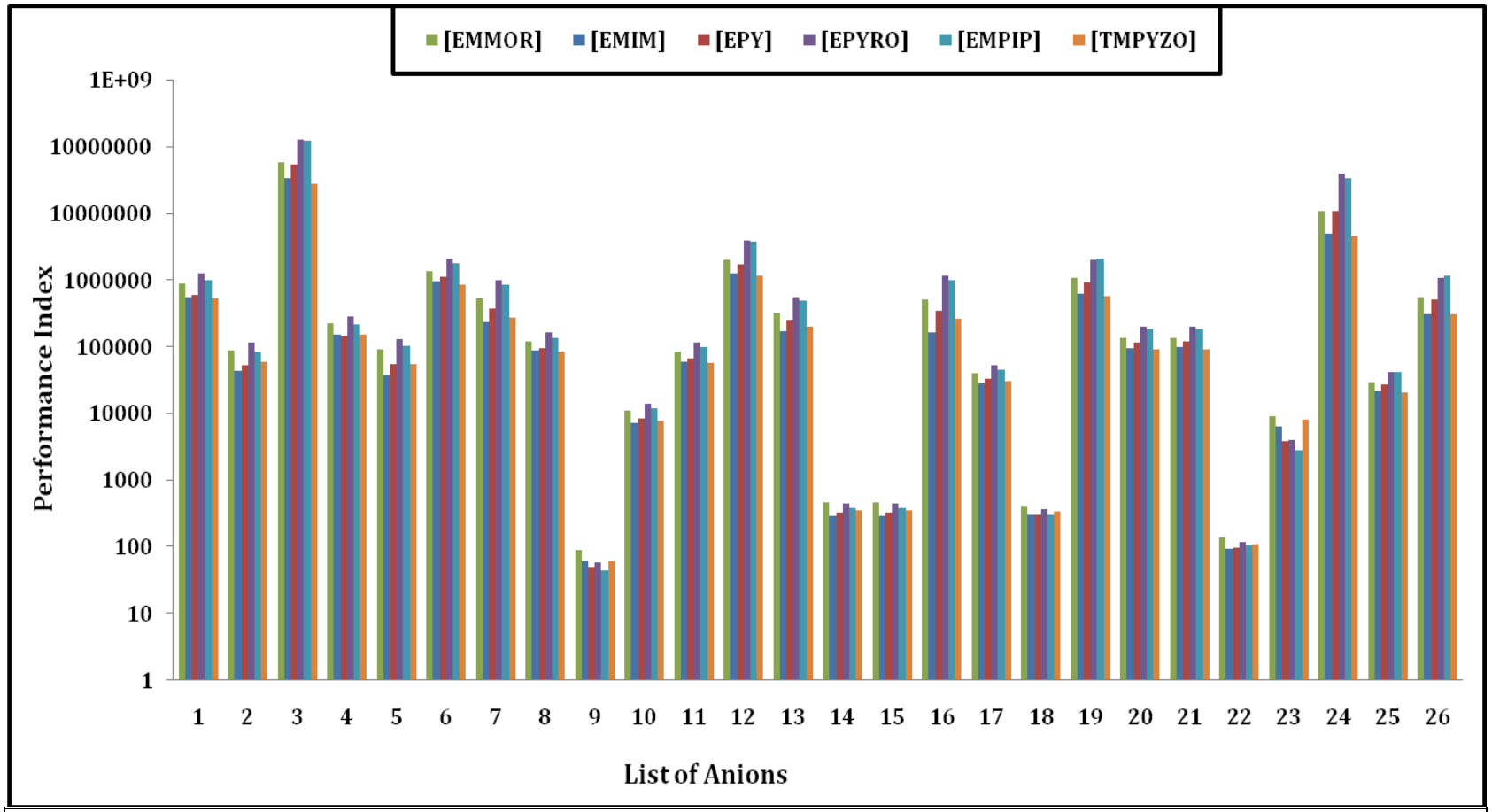

1. [Br], 2. [NO_3], 3. [SCN], 4. [CH_3COO], 5. [HSO_4], 6. [BF_4], 7. [CH_3SO_3], 8. [CF_3COO], 9. [CH_3SO_4], 10. [PF_6], 11. [CF_3SO_3], 12. [$C_2H_5SO_4$], 13. [$(CH_3)_2PO_4$], 14. [$C_3H_7NO_3S$], 15. [$B(CN)_4$], 16. [$C_7H_5O_3$], 17. [$(CH_3SO_2)_2N$], 18.

Figure 4.21(a): Performance index values at infinite dilution for pyrrole at ambient temperature (T=298.15K).

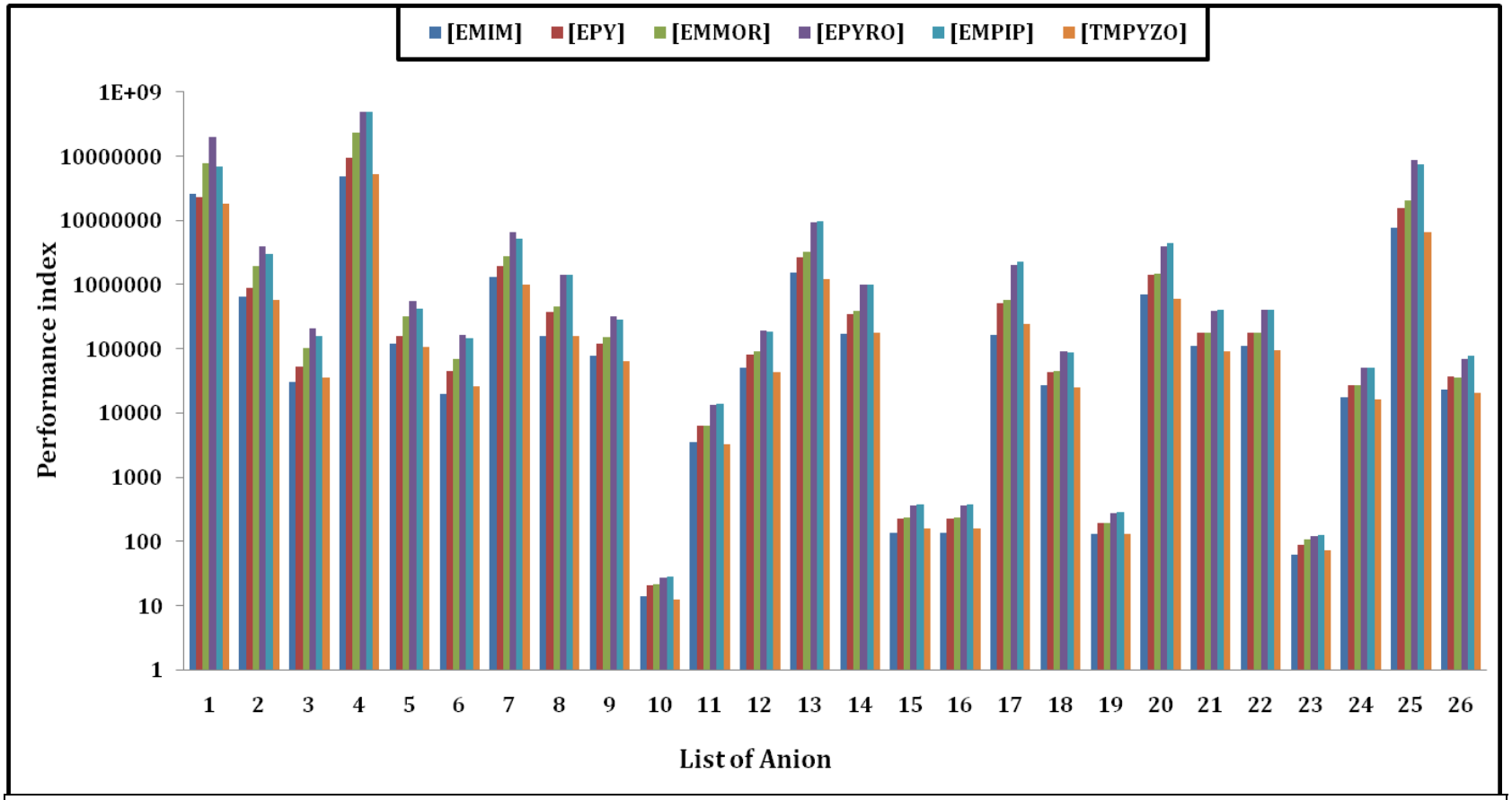

1. [Br], 2. [NO_3], 3. [SCN], 4. [CH_3COO], 5. [HSO_4], 6. [BF_4], 7. [CH_3SO_3], 8. [CF_3COO], 9. [CH_3SO_4], 10. [PF_6], 11. [CF_3SO_3], 12. [$C_2H_5SO_4$], 13. [$(CH_3)_2PO_4$], 14. [$C_3H_7NO_3S$], 15. [$B(CN)_4$], 16. [$C_7H_5O_3$], 17. [$(CH_3SO_2)_2N$], 18.

Figure 4.21 (b): Performance index values at infinite dilution for indole at ambient temperature (T=298.15K)

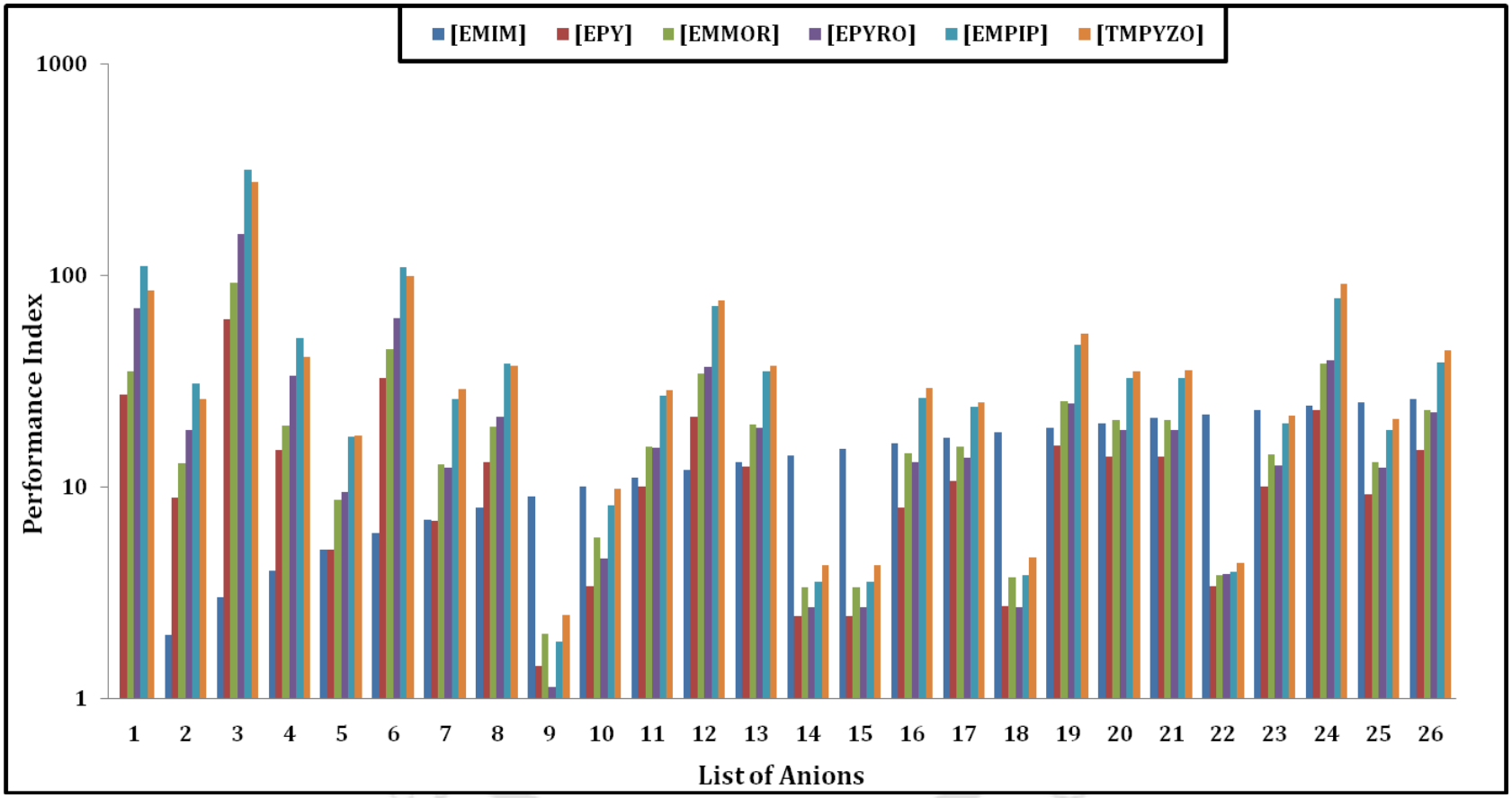

1. [Br], 2. [NO_3], 3. [SCN], 4. [CH_3COO], 5. [HSO_4], 6. [BF_4], 7. [CH_3SO_3], 8. [CF_3COO], 9. [CH_3SO_4], 10. [PF_6], 11. [CF_3SO_3], 12. [$C_2H_5SO_4$], 13. [$(CH_3)_2PO_4$], 14. [$C_3H_7NO_3S$], 15. [$B(CN)_4$], 16. [$C_7H_5O_3$], 17. [$(CH_3SO_2)_2N$], 18.

Figure 4.21(c): Performance index values at infinite dilution for indoline at ambient temperature (T=298.15K)

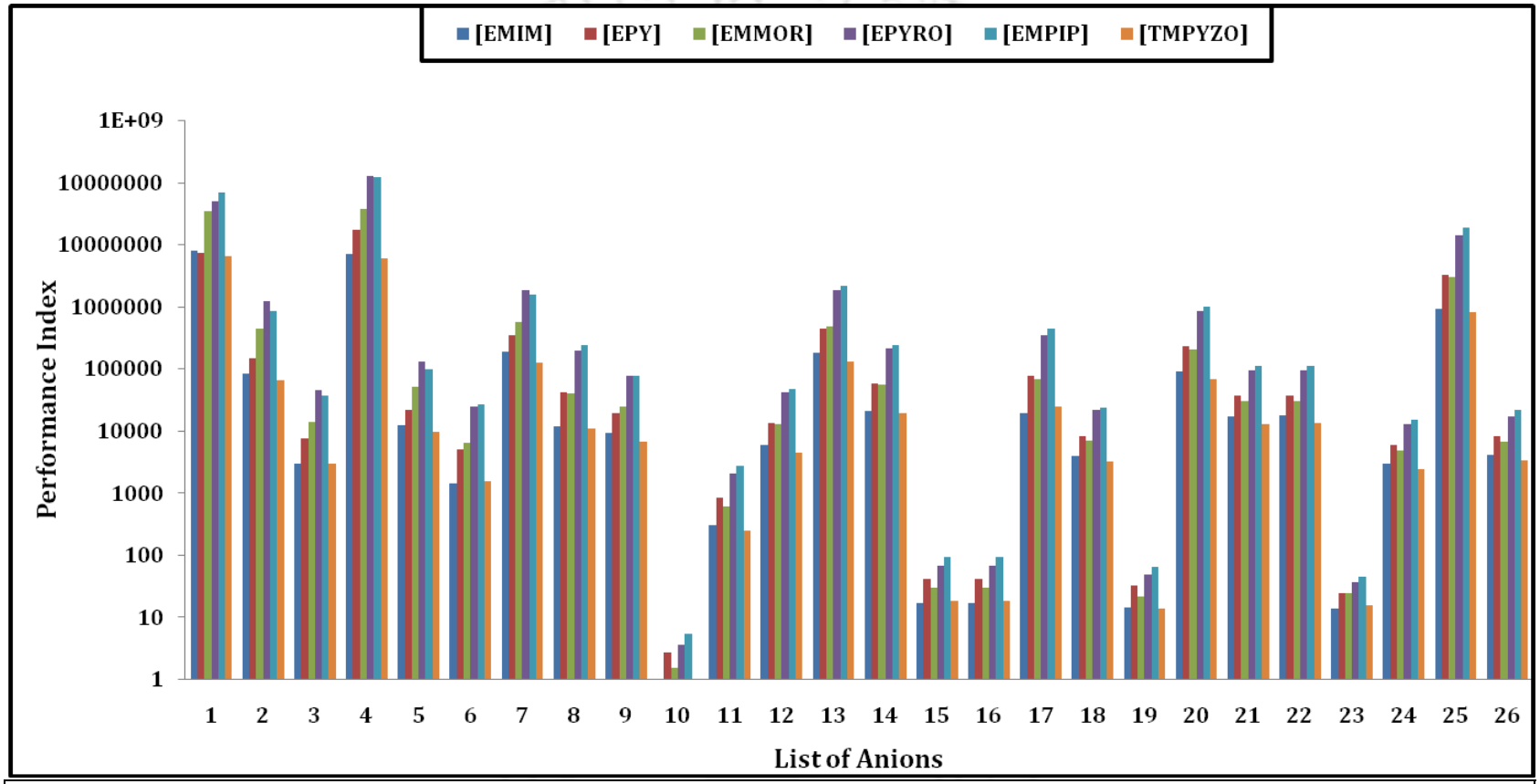

1. [Br], 2. [NO_3], 3. [SCN], 4. [CH_3COO], 5. [HSO_4], 6. [BF_4], 7. [CH_3SO_3], 8. [CF_3COO], 9. [CH_3SO_4], 10. [PF_6], 11. [CF_3SO_3], 12. [$C_2H_5SO_4$], 13. [$(CH_3)_2PO_4$], 14. [$C_3H_7NO_3S$], 15. [$B(CN)_4$], 16. [$C_7H_5O_3$], 17. [$(CH_3SO_2)_2N$], 18.

Figure 4.21(d): Performance index values at infinite dilution for carbazole at ambient temperature (T=298.15K)

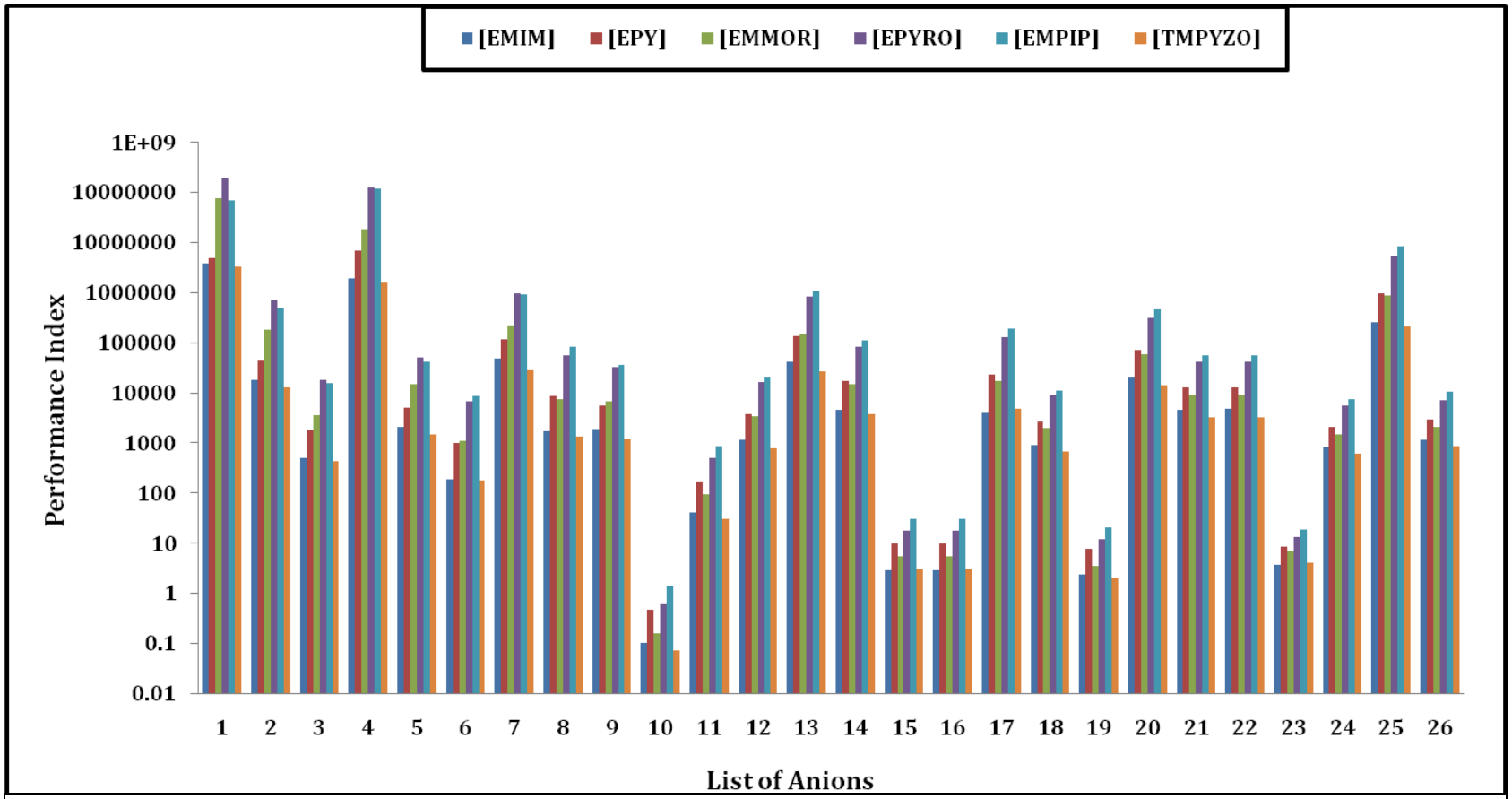

1. [Br], 2. [NO_3], 3. [SCN], 4. [CH_3COO], 5. [HSO_4], 6. [BF_4], 7. [CH_3SO_3], 8. [CF_3COO], 9. [CH_3SO_4], 10. [PF_6], 11. [CF_3SO_3], 12. [$C_2H_5SO_4$], 13. [$(CH_3)_2PO_4$], 14. [$C_3H_7NO_3S$], 15. [$B(CN)_4$], 16. [$C_7H_5O_3$], 17. [$(CH_3SO_2)_2N$], 18.

Figure 4.21(e): Performance index values at infinite dilution for benzacarbazole at ambient temperature (T=298.15K)

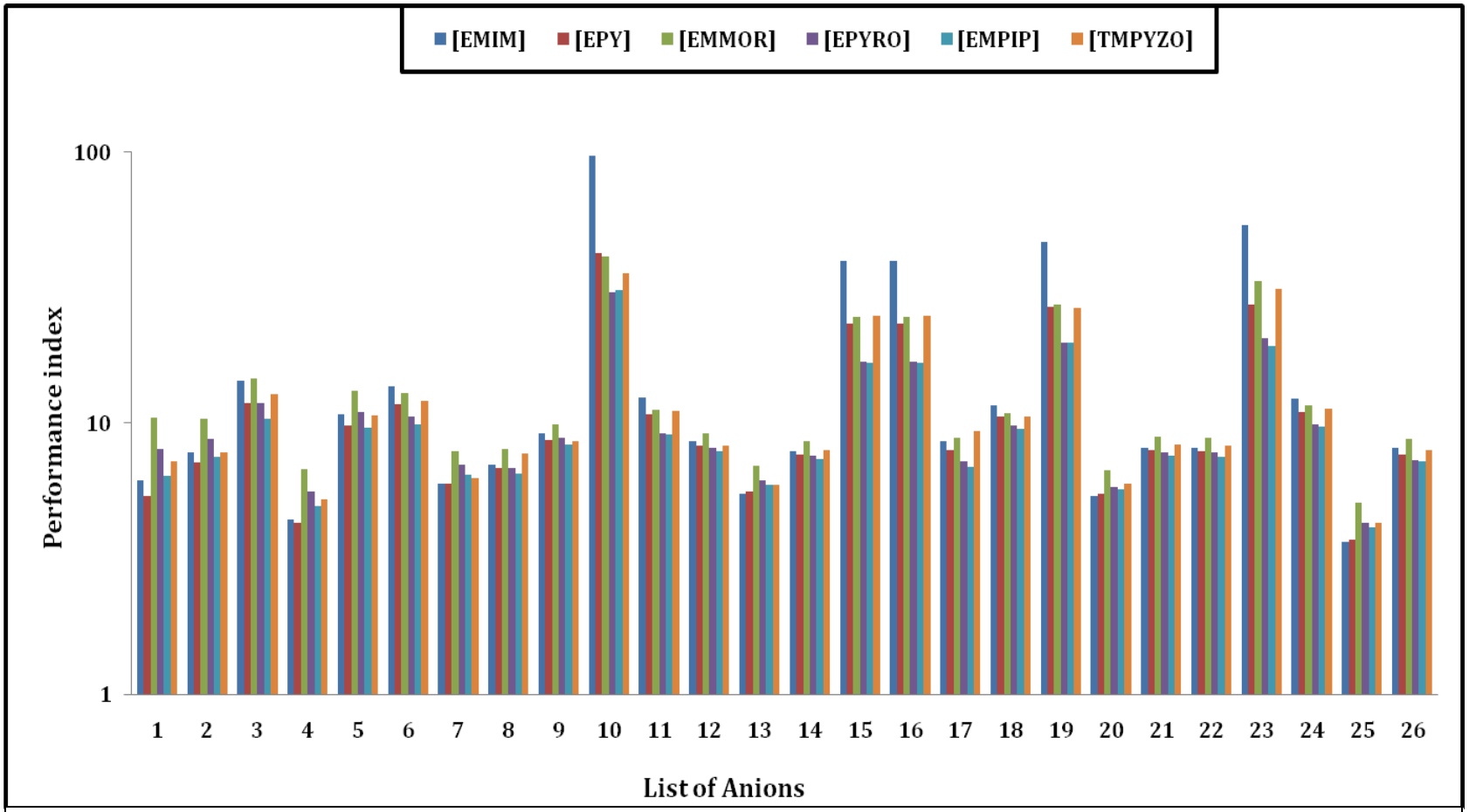

1. [Br], 2. [NO_3], 3. [SCN], 4. [CH_3COO], 5. [HSO_4], 6. [BF_4], 7. [CH_3SO_3], 8. [CF_3COO], 9. [CH_3SO_4], 10. [PF_6], 11. [CF_3SO_3], 12. [$C_2H_5SO_4$], 13. [$(CH_3)_2PO_4$], 14. [$C_3H_7NO_3S$], 15. [$B(CN)_4$], 16. [$C_7H_5O_3$], 17. [$(CH_3SO_2)_2N$], 18.

Figure 4.21(f): Performance index values at infinite dilution for pyridine at ambient temperature (T=298.15K)

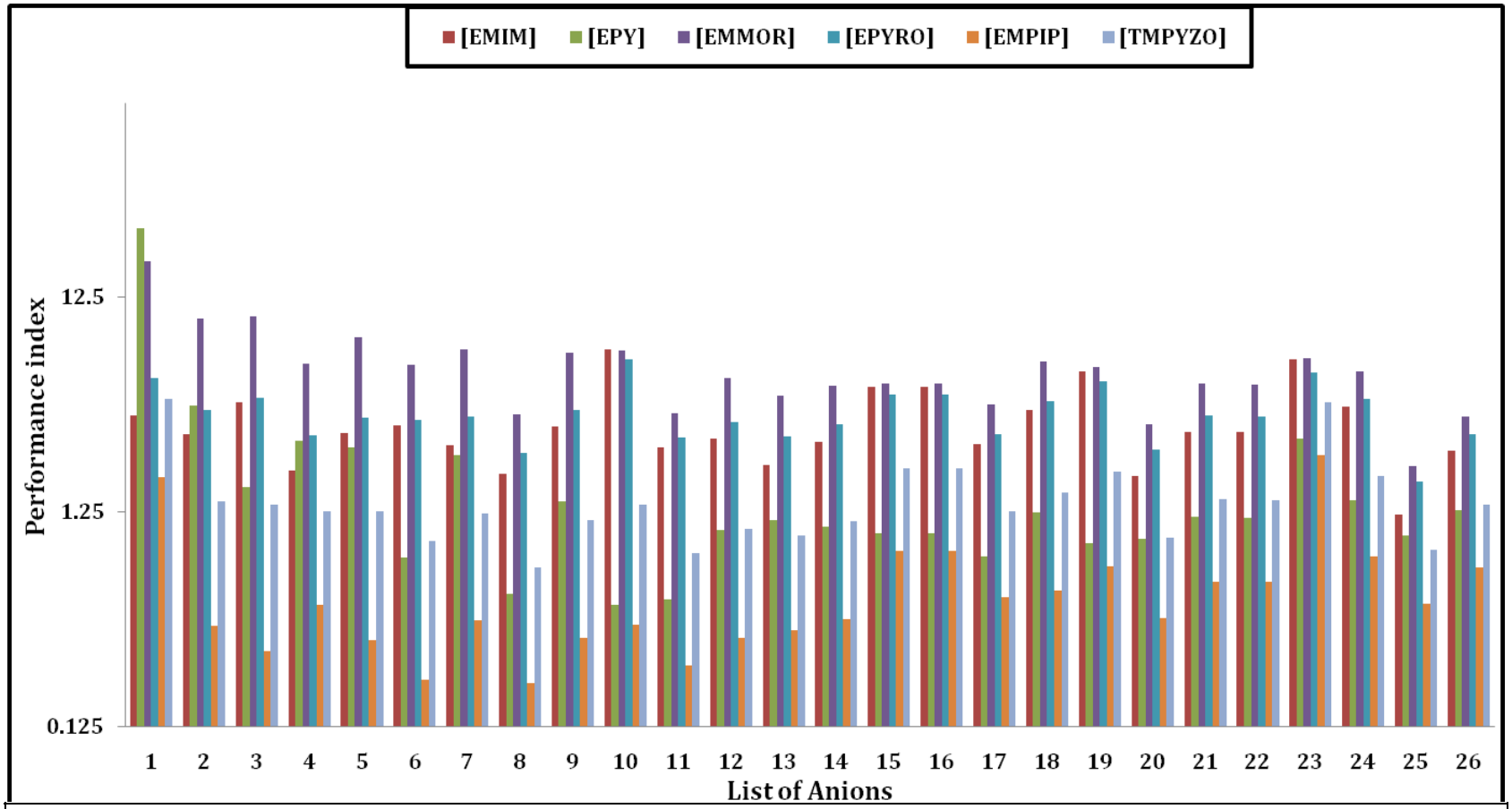

1. [Br], 2. [NO_3], 3. [SCN], 4. [CH_3COO], 5. [HSO_4], 6. [BF_4], 7. [CH_3SO_3], 8. [CF_3COO], 9. [CH_3SO_4], 10. [PF_6], 11. [CF_3SO_3], 12. [$C_2H_5SO_4$], 13. [$(CH_3)_2PO_4$], 14. [$C_3H_7NO_3S$], 15. [$B(CN)_4$], 16. [$C_7H_5O_3$], 17. [$(CH_3SO_2)_2N$], 18.

Figure 4.21 (g): Performance index values at infinite dilution for quinoline at ambient temperature (T=298.15K)

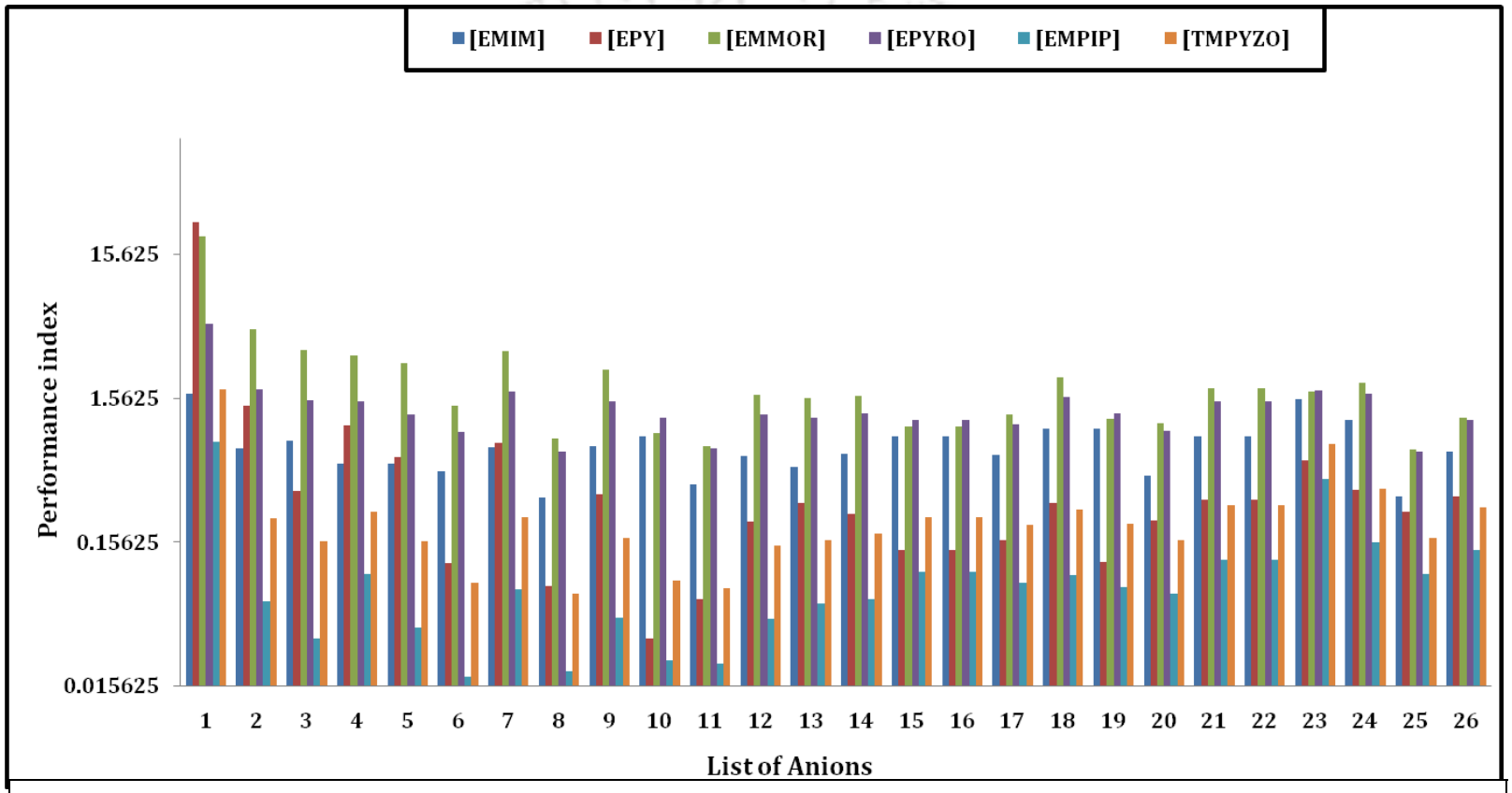

1. [Br], 2. [NO_3], 3. [SCN], 4. [CH_3COO], 5. [HSO_4], 6. [BF_4], 7. [CH_3SO_3], 8. [CF_3COO], 9. [CH_3SO_4], 10. [PF_6], 11. [CF_3SO_3], 12. [$C_2H_5SO_4$], 13. [$(CH_3)_2PO_4$], 14. [$C_3H_7NO_3S$], 15. [$B(CN)_4$], 16. [$C_7H_5O_3$], 17. [$(CH_3SO_2)_2N$], 18. [BH_2O_4], 19. [$C_4H_{11}O_4P$], 20. [$C_7H_8O_3P$], 21. [$C_7H_7SO_3$], 22. [CF_3SO_2], 23. [$CF_3SO_2)_2N$], 24. [$C_5H_{11}SO_6$],

Figure 4.21(h): Performance index values at infinite dilution for benzoquinoline at ambient temperature (T=298.15K)

Table 4.13: Mole fraction of diesel (PIONA series), sulphur and nitrogen compounds

Simulated Diesel oil composition	Until C_5	C_6	C_7	C_8	C_9	C_{10}	C_{11}^+
n-Paraffins (C_nH_{2n+2})	0.0032 Pentane	0.006 Hexane	0.003 Heptane	0.004 Octane	-	-	0.3663 Undecane
Isoparaffins (C_nH_{2n+2})	0.003 Isopentane	0.0181 Isohexane	0.0562 Isoheptanes	0.013 Isooctane	0.17 Iso nonane	-	0.109 Iso undecane
Olefins (C_nH_{2n})	0.003 Pentene	0.011 Hexane	0.0162 Heptene	0.012 Octane	0.004 Nonene	-	-
Naphthenes (C_nH_{2n})	0.0051 Cyclopentane	0.0162 Cyclohexane	0.002 Cycloheptane	0.001 Cyclooctane	-	-	-
Aromatics (C_nH_{2n-6})	–	0.067 Benzene	0.0041 Toluene	0.0132 Ethylbenzene	0.025 Probylbenzene	0.067 Butylbenzene	0.0006 Pentaylbenzene
Non-basic nitrogen species	0.001 Pyrrole	-	-	0.001,0.001 Indole,Indoline	-	-	0.001,0.001 Carbazole, Benzocarbazole
Basic nitrogen	0.001 Pyridine	-	-	-	0.001 Quinoline	-	0.001 Benzoquinoline

species							
Acidic sulphur species	0.001 Thiophene	-	-	-	0.001 Benzothiophene	-	0.001 Dibenzothiophene

4.13 Simultaneousl Desulphurization and Denitrification

4.13.1 Effect of selectivity at infinite dilution

Cation Influence: The selectivity at infinite dilution of unsaturated acidic sulphur and basic /non-basic nitrogen compounds in [EMIM](Figure 4.22(a)),[EPY] (Figure 4.22(b)),[EMMOR](Figure 4.22(c)),[EPYRO] (Figure 4.22(d)),[EMPIP] (Figure 4.22(e)) and [TMPYZO] (Figure 4.22(f)) with 25 anions were calculated using Eq 4.20.The selectivity at infinite dilution was determined from the IDAC values of studied sulphur and nitrogen compounds in simulated diesel (Table 4.13) as well as ionic liquids respectively. We have chosen a smaller cation in our predictions, since these are proven to give high values of selectivity [Kumar et al., 2009; Bansal et al., 2005].

It has been realized that variation of the cationic core is a very valuable approach for tuning the behaviour and structural phenomena of these compounds in liquid mixture. In general [EMMOR], [EPYRO], [EMPIP] based ILs gave lesser IDAC values as compared to [EMIM], [EPY], and [TMPYZO] based cation when compared with 25 anions (Figures 4.22(a) to 4.22(f)). This is due to the fact that [EMIM], [EPY], and [TMPYZO] cations consist of aromatic rings which possess aromatic steric hindrance towards similar aromatic ring structure of nitrogen species[Anantharaj et al.,2011;Joule et al.,2007;Gupta et al.,2005].Because the cations having higher π electron density as well as the positive charge of nitrogen atom is delocalized over the aromatic ring whereas the lone pair electron on the nitrogen atom is localized around their aromatic ring (pyridine)[Lava et al.,2009] and therefore when these two molecules comes close together then the higher π electron density of the cation resist the aromatic nitrogen species. This steric hindrance lowers the strength of N (heteroaromatic)-H (cation) hydrogen bond which ultimately decreases the selectivity. A steric hindrance arise from contribution ascribed to strain as the sum of (1) same charges repelling each other,(2) π--π stretches or compression and (3) maximum Columbian effect[Zhou et al.,2008]. Further the electron donating tendency through alkyl substitution in [EMIM],[TMPYZO],[EPY] decreases the delocalized π electron density within the cations thereby providing lesser selectivity for the removal of nitrogen species.Thus as discussed earlier the factors such as (a) electron

donor tendency of [EMMOR], [EPYRO], [EMPIP], [EMIM], [EPY], and [TMPYZO] cations, (b) the aromatic structure of the cation without heteroring, and (c) the number of electro negative atom (N,O and S) (similar or different) located on the aromatic structure of the cation are the deciding factors for IDAC values.

[EMIM], [EPY] or [TMPYZO] cations do exhibit higher aromaticity around their heterocyclic structure, however the positive charges are spread over the aromatic ring [Joule et al., 2007; Lava et al., 2009] From our previous work [Anantharaj et al., 20011b] the NBO (Normal Bonded Orbital) analysis is used as an excellent tool for the investigation of partial charge transfer interaction within the parent compounds. Based on these partial charges, difference in the hydrogen-bonding, electrostatic interaction and CH-π bonding interaction is considered. Therefore, based on the quantum chemical investigation, the CH groups can participate and play an important role in the simultaneous interaction of π bases compounds such as thiophene and pyridine. The number of stable sites (i.e hydrogen atom) having positive charges on the cation is 19, 16 and 13 for 1-butyl-4-methylpyridinium [BUMPY], 1-butyl-1-methylpyrolidinium [BUMPYR] and 1-benzyl-3-methylimidazolium [BeMIM] cations respectively.

[EPYRO] and [EPIP] cations do not exhibit high aromaticity due to the absence of heteroring, but the positive e charge is localized on the nitrogen atom of the five and/or six membered heterocyclic [EPYRO] and [EPIP] ring respectively. [EMMOR] has a similar trend as [EPYRO] and [EPIP] but there are two different electronegative atoms (N and O) located over the six membered heterocyclic morpholinium ring [Joule et al.,2007;Gupta et al.,2005]. Hence the nitrogen atom has positive charge (+0.656750) which is localized over the aromatic ring, while the oxygen atom poses negative charges (-0.353425) which is not delocalized over the aromatic ring as much as. Therefore [EMMOR](Figure 4.21(c)), [EPYRO](Figure 4.22(d)), and [EMPIP](Figure 4.22(e)) based ionic liquids gave lower IDAC values, while higher IDAC values was observed by [EMIM](Figure (4.22 (a)) , [EPY] (Figure 4.22(b)) , and [TMPYZO] (Figure 4.22(f)) based cation. Thus [EMMOR], [EPYRO], [EMPIP] based ionic liquid are the best choice for the removal of all kind of aromatic nitrogen and sulphur compounds from diesel oil.

Anion Influence: The anion also plays an important role in increasing the selectivity and capacity of the ionic liquids. There are several types of anions investigated in this work, such as halogenated, fluorinated, alkyl sulphonates, organo borates, alkyl sulphates and heterocyclic (Table 4. 5). It was found that the anion not only affects the selectivity but also affects the capacity of the ionic liquids. It can be seen that the selectivity increases with increasing capacity (Figure 4.22(a)-4.22(f)) by a given cation with all anions irrespective of nitrogen and sulphur compounds. The favourable anions are those having (a) highly electronegative nature, (b) different number of electronegative atom at anion structure and (c) symmetry with high negative charges or higher basicity. Additional factors such as anion structure with longer alkyl substitution and higher sterical shielding effect around the anion charge centre are also pivotal in the anion performance [Lei et al.,2006]. Anions such as [SCN],[BF_4], [PF_6], [BiSu], [Ac], [MeSu] (Figure 4.22(a)-4.22(f)) increases the hydrogen bond acceptors, though not significantly. Tosylate [TSy] and salicyclate [SCy] anions having alkyl substitution at aromatic anion structure which in principle should be favourable for increasing the overall performance of the ionic liquid. Because the addition of methyl group at tosylate and salycilate anions structure posses higher van der Waals repulsive force in which the interaction between cation and anion decreased, while the hydrogen atom of anion interact with nitrogen atom of pyridine and with sulphur atom of thiophene molecules. Further the partial charge of hydrogen atom is delocalized over the aromatic ring structure of tosylate and salycilate anions which leads to increase the possibility of π--π stacking or interaction between similar structures of anion (tosylate and salycilate) with thiophene / pyridine molecules. It is observed that the methyl group substitution at anion structure has significant influence on the overall performance of the ionic liquids which is well agree with the study of Lei et al.,[2006]. However the effect of aromaticity is higher in IL with similar structure of pyridine/thiophene molecules and the partial charge of hydrogen, sulphur, oxygen atoms are not completely delocalized over the anion structure and thereby it reduces the interactions between cation/anion with sulphur/nitrogen species and thereby decreases the selectivity and capacity for these anions.

The selectivity at infinite dilution of five member ring of sulphur and nitrogen species in ILs strongly depends on charges centre of the anion. The anion charge centre is known to exhibit higher sterical shielding effect [Lei et al.,2006]. The shielding effect of anion decreases in the following order [Anantharaj et al.,2010]: [Br] > [NT] > [TFO] > [MSACN] > [BMA] > [Tfi] > [Me-Et-EtSu] > [DeC] > [OcSu]. It is noted that the halogenated IL's gave the highest selectivity. However the fluorinated Ionic Liquids produce HF at moderate temperature when in contact with water or moisture. This limits their application in processes which uses high temperature or in aqueous solution. So we would not recommend such an IL for desulphurization or denitrification

In the nitrate ([NT]) anion, the central atom of nitrogen has a charge of + 1.272 (obtained via ESP or CHELPG fit via HF/6-31G* theory) while the oxygen has a charge of -0.757 each oxygen atom. This is higher than that of fluorine atom in [BF_4] (B = 1.356, F = -0.535) and [PF_6] (P = 2.21, F = -0.589) [Zhou et al., 2008]. The charges of the side atom also decide the selectivity of the anions. For e.g. in case of oxygen the negative charge is higher than that of fluorine atom in [BF_4] and [PF_6] anions. Thus a higher negative charge on the oxygen atom leads to increased interaction with the hydrogen atoms of nitrogen/sulphur species. Additionally a higher charge on the central atom like boron in [BF_4] and phosphorous in [PF_6] leads to a decrease in shielding effect, which causes a decrease in selectivity of anion. However a positive charge (+1.272) of nitrogen atom in [NT] causes higher sterical shielding as compared to [BF_4] and [PF_6]. Further, the positive charges of nitrogen atom in [NT] is delocalized with three oxygen atom and therefore the negative charge of oxygen atom has -0.757 as compared to fluorine atom in [BF_4] and [PF_6]. Due to this very fact cations with [NT] posses higher selectivity as compared to cations with [BF_4] or [PF_6](Figure 4.22(a)-4.22(f)).

Based on the above factors, anions such as [Br],[NT], [TFO], [MSACN], [BMA], [Tfi], [Me-Et-EtSu], [Dec], and [OcSu] gave high values of selectivity and capacity

irrespective of cations. In order to compare the performance, the selectivity and capacity has been plotted with respect to the potential cation i.e [EMMOR] cation as obtained earlier (Figure 4.23). It can be seen that the selectivity/capacity increases from [Br] to [TfO] due to the shielding effect of the anions which decreases via [Br] > [NT] > [TFO] (refer Figure 4.24). However for $[C_3H_7NO_3S]$ ([MSACN]) and $[(CH_3SO_2)_2N]$([BMA]) the selectivity increases since extra alkyl group is added which increases the shielding effect or increases the electronegativity. Similarly for $[(CF_3SO_2)_2N]$([BTA]) and $[C_5H_{11}SO_6]$ ([Me-Et-EtSu]) the alkyl group vanishes and the selectivity again is lowered because of decrease in shielding effect. The only exception is [OcSu] having higher alkyl substitution, thus contributes to higher selectivity via dominant H-bonding.

Heterocyclic Structure Influence: Unsaturated nonbasic nitrogen compounds (Figure 4.22(a)-4.22(f)) gave higher selectivity at infinite dilution as compared to unsaturated acidic (benzothiophene) and basic (benzoquinoline) compounds. It can also be observed that sulphur compounds having similar structure with heterocyclic cations like [EMIM] and [EPYRO] does not show any significant increase in selectivity with sulphur or nitrogen compounds. The anion selection plays a significant role within the cation e.g the maximum selectivity at infinite dilution of pyrrole is 44651 in [EMIM][Br] whereas the minimum value of pyrrole is 63 in [EMIM][BTA] (Table 4.14). The maximum and minimum values of selectivity for all the sulphur/nitrogen species are summarized in Table 4.14. In all the Figures(4.22(a)-4.22(f)) it is seen that the selectivity of non basic nitrogen such as indoline, pyrrole, carbazole and benzocarbazole is quite higher than that of the six membered nitrogen ring such as pyridine, quinoline and benzoquinoline. The suphur species in general show a lesser selectivity as compared to six or five membered nitrogen species.

Basic nitrogen compounds like pyridine (PY), structurally related to benzene has a lesser π- delocalized electron density where the negative charge is localized on the nitrogen atom. Therefore, high IDAC values were observed as compared to the non basic nitrogen compounds irrespective of the size of the cation and anion (Figure 4.22(a) to

4.22(f)). It was noted that [DMP],[BTA], [OcSu] and [MSACN] anion having different electronegative atom such as N (Nitrogen),O (Oxygen) and S (Sulphur) and therefore the anions play a significant role in increasing the selectivity. This is because of their ability in forming different hydrogen bond such as N-H and O-H between the nitrogen heterocyclic and the anion, especially when the cation structure (cation-anion interaction) influence is weak (Figure 23). Table 4.14 shows that [EMIM] based cation gave higher selectivity for pyridine (PY) as compared to other cations, while [EMMOR] cation shows higher selectivity for quinoline (QU),benzoquinoline (BQU),thiophene (TS),benzothiophene (BTS) and dibenzothiophene (DBTS).Their maximum selectivity values are: S_{QU} = 56 ,S_{BQU} =56, S_{TS} = 66 ,S_{BTS} =70, ,S_{DBTS} =58.The minimum selectivity values are as follows: S_{QU} = 3 ([EPYRO][TfO]),S_{BQU} =2 ([EMIM][TfO]), S_{TS} = 10 ([EMIM][TfO]) ,S_{BTS} =5 ([EPY][Dec], ,S_{DBTS} =2 ([EMPIP][Dec]).

4.13.2 Effect of ILs capacity at infinite dilution

The ionic liquid capacity at infinite dilution was compared among [EMIM](figure 4.25(a)), [EPY] (Figure 4.25(b), [EMMOR] (Figure 4.25(c)),[EPYRO] (Figure 4.25(d)),[EMPIP] (Figure 4.25(e)) and [TMPYZO] (Figure 4.25(f)) based cations with 25 anions. The capacities at infinite dilution were predicted using equation 4.21 and the results are shown in Figures 4.25(a) to 4.25(f). Evidently, [EMMOR](Figure 4.25(c)) and [EPYRO](Figure 4.25(d)) have higher solvent capacity at infinite dilution irrespective of the aromatic nitrogen and sulphur compounds. It should be noted that [EPYRO](Figure 4.25(d)) consist of low π -delocalized electron clouds with positive charge localized on the nitrogen atom of the five membered heterocyclic pyrrolidinium ring. This enables to retain a significant amount of sulphur/nitrogen species within its interstitial volume. In a similar manner,[EMMOR] (Figure 4.25(c)) has a low π-delocalized electron clouds as well as the positive charge localized on both the nitrogen and oxygen atom of the six membered heterocyclic morpholinium ring. Thus it can easily form weak hydrogen bond interaction as well as CH – π bond interaction between cation and different aromatic ring of nitrogen and sulphur compounds.

It can be seen that under a given anion the capacity decreases in the order of: [EPYRO] ≈ [EMMOR] < [EMPIP] < [EMIM] < [TMPYZO] < [EPY]. However, it can be seen that the favourable anions are those having more electron acceptor tendency and highly electronegative nature such as halogenated ions :[Br] and [NT].On the other hand, the unfavourable anions are those where sterical shielding effect around their charge centers do not exist or is very less for e.g [TFO], [MSACN], [BMA], [BTA], [Me-Et-EtSu], [Dec] and [OcSu].However, the cation without hetero ring such as [Dec] and [OcSu] increases the capacity (Figure 4.26 and 4.27) irrespective of the nitrogen and sulphur compounds. This is due to the fact that they inhibit the positive charges of cation to approach the negative charges of anions in the IL itself. They allow the negative charges of anion to approach the positive charge centre of the six membered benzene ring which is fused either with pyrrole/pyridine/thiophene. Additionally salicylate [Scy] and tosylate [TSy] anions which are aromatic in nature, is too long and posses branched alkyl chain which is unfavourable in increasing the capacity.

The results obtained for removal of aromatic nitrogen and sulphur from model diesel oil are given in Table 4.14. [EMMOR][Br] and [EPYRO][Br] ionic liquid shows the maximum capacity for all the studied compounds. Figure 4.27 shows that the comparison between capacity and selectivity of the potential cation i.e [EPYRO] () when combined with potential anions such as [Br],[NT], [TfO], [MSACN], [BMA], [BTA], [Me-Et-EtSu], [Dec] and [OcSu] anions. All the effective cation and anion combination of ionic liquids shows a linear trend, which indicates that for ionic liquid identification requires knowledge of structural phenomena as well as place of alkyl substitution at the cations or anions. Thus [EPYRO][Br] is the best among all the solvents investigated from the viewpoint of capacity but there is not much difference between[EPYRO], [EMMOR] and [EMPIP] based ionic liquids for the simultaneous removal of sulphur and nitrogen.

4.13.3 Effect of hetero atom of pyrrole, thiophene and pyridine

It was found that among all the three compounds, pyrrole has higher interaction with all studied ionic liquids because of its hydrogen bond donor tendency towards the aprotic anions and comfortable packing with the polar or protic cation of an ionic liquid.

It should be noted that the lone pair of electrons of the nitrogen atom is delocalized and is contributed over the whole aromatic ring. For thiophene, the lone pair of electron is delocalized over the five membered thiophene ring and it's responsible for higher acidity of these homologues species. For pyridine, the lone pair of electrons is localized on the nitrogen atom of the six membered pyridinium ring and can extend in the plane of the ring. This delocalized electron is responsible for the basicity of these nitrogenous bases. Like thiophene, pyridine can also form hydrogen bonding, CH--- π bonding and π --- π interaction. But when thiophene and pyridine molecules are compared with pyrrole, the interactions are very less in magnitude. For e.g the selectivity of pyrrole is higher for with cations having lower steric hindrance namely [EPYRO](Figure 4.21(d)),[EMPIP](Figure 4.21(e)) and [EMMOR](Figure 4.21(c)).

Addition of one or two six membered benzene rings fused on either side of pyrrole or thiophene and/or pyridine ring induce more sterical hindrance due to the additional π delocalized electron clouds. The higher sterical hindrance of the substituted six membered ring is a disadvantage over their structural relationship with heterocyclic ring cations such as [EMIM], [EPY], [TMPYZO], [EPYRO], [EPIP] and [EMMOR]. These planar fused structures reduce the highly localized electron tendency on nitrogen atom and/or sulphur atom of the six membered pyridine and five membered thiophene ring. Thus a combination of weak structural and intramolecular interaction results in lower selectivity and capacity at infinite dilution of ionic liquid (Figure 4.21(a)-4.21(f))(Figure 4.21(a)-4.21(f)). For example, quinoline, benzoquinoline, benzothiophene and dibenzothiophene with higher steric hindrance and highly delocalized π electron clouds have low IDAC values when compared with cations such as [EPYRO](Figure 4.21(d)), [EPIP](Figure 4.21(e)) and [EMMOR](Figure 4.21(c)). It was found that the non substituted hetero ring i.e [EPYRO], [EPIP] and [EMMOR] cations shows strong interaction since the positive charge of the cation is more localized on the nitrogen and /or oxygen atom of the five/six membered ring of [EPYRO], [EPIP] and [EMMOR] cations.

Table 4.14: Maximum and/or minimum selectivity and capacity for studied ILs

Name	Limitation	Selectivity (S)	Capacity (C)	Better ILs for aromatic nitrogen and refractory sulfur species ablation in single step	
				Selectivity (S)	Capacity (C)
Pyrrole	Maximum	44651	1667	[EMIM][Br]	[EMMOR][Br]
	Minimum	63	4	[EMIM][BTA]	[EMIM][BTA]
Indole	Maximum	46639	10000	[EMPIP][Br]	[EPYRO][Br]
	Minimum	69	3	[EMPIP][BTA]	[EMIM][BTA]
Indoline	Maximum	380	14	[EMMOR][Br]	[EMMOR][Br]
	Minimum	7	1	[EMIM][TfO]	[TMPYZO][BTA]
Carbazole	Maximum	89303	5000	[EMMOR][Br]	[EPYRO][Br]
	Minimum	41	2	[EMPIP][BTA]	[EMIM][BTA]
Benzocarbazole	Maximum	133955	10000	[EMMOR][Br]	[EPYRO][Br]
	Minimum	24	1	[TMPYZO][TfO]	[EMIM][BTA]
Pyridine	Maximum	97	3	[EMIM][BTA]	[EMIM][BTA]
	Minimum	8	0.21	[EMPIP][TfO]	[EMIM][NT]
Quinoline	Maximum	56	3	[EMMOR][Br]	[EPYRO][Br]
	Minimum	3	0.10	[EPYRO][TfO]	[EMIM][NT]

Benzoquinoline	Maximum	56	3	[EMMOR][Br]	[EPYRO][Br]
	Minimum	2	0.21	[EMIM][TfO]	[EMIM][NT]
Thiophene	Maximum	66	3	[EMMOR][Br]	[EPYRO][Br]
	Minimum	10	0.53	[EMPIP][TfO]	[TMPYZO][BMA]
Benzothiophene	Maximum	70	3.5	[EMMOR][Br]	[EPYRO][Br]
	Minimum	5	0.21	[EPY][Dec]	[EMIM][BMA]
Dibenzothiophene	Maximum	58	3	[EMMOR][Br]	[EPYRO][Br]
	Minimum	2	0.07	[EMPIP][Dec]	[EMIM][BMA]

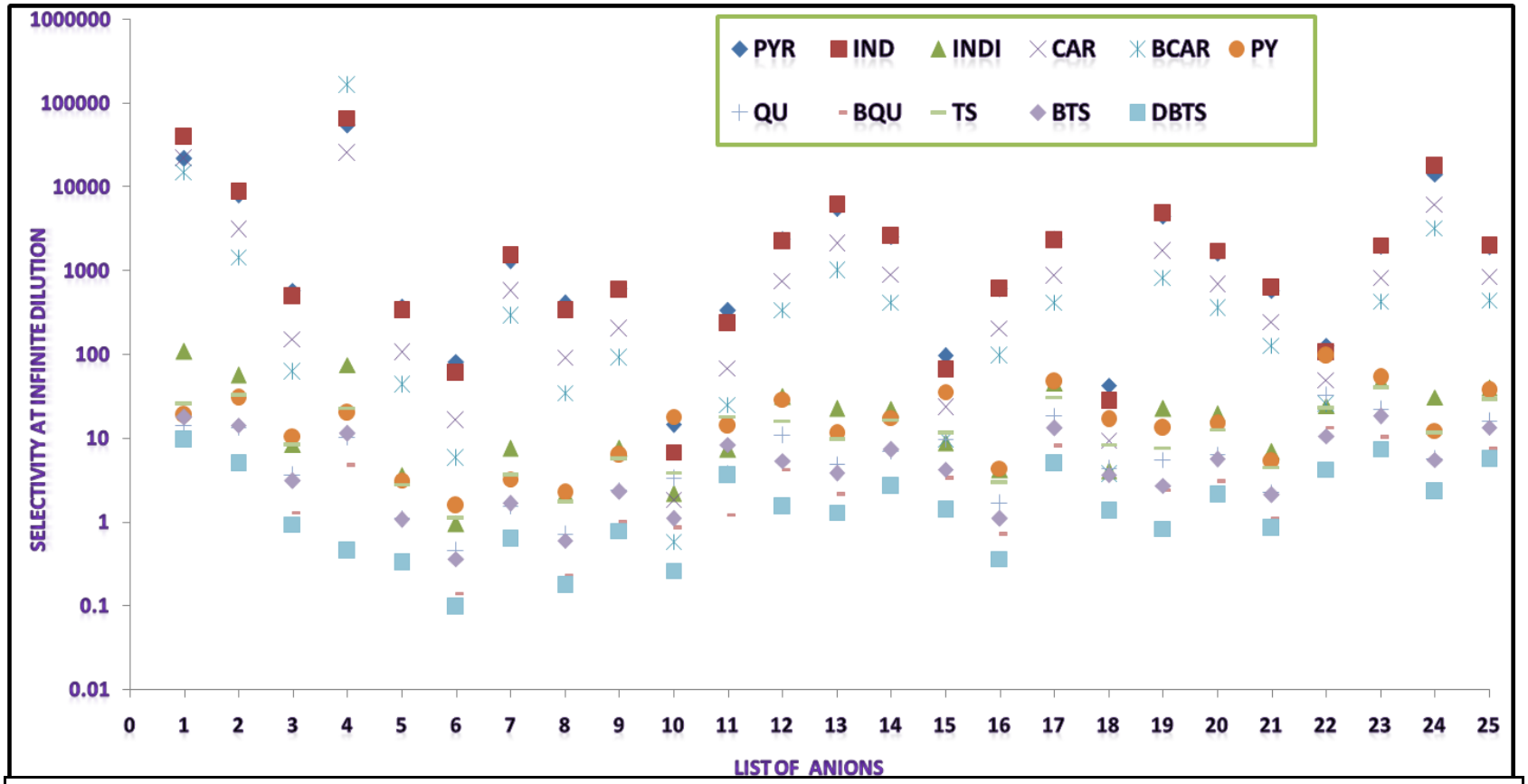

1. [Br], 2. [NO_3], 3. [SCN], 4. [CH_3COO], 5. [HSO_4], 6. [BF_4], 7. [CH_3SO_3], 8. [CF_3COO], 9. [CH_3SO_4], 10. [PF_6], 11. [CF_3SO_3], 12. [$C_2H_5SO_4$], 13. [$(CH_3)_2PO_4$], 14. [$C_3H_7NO_3S$], 15. [$B(CN)_4$], 16. [$C_7H_5O_3$], 17. [$(CH_3SO_2)_2N$], 18.

Figure 4.22(a): Selectivity at infinite dilution of aromatic nitrogen and refractory sulfur species in [EMIM] cation based ILs (X-axis legend :Anion no's mentioned are as per Table 4 .5)

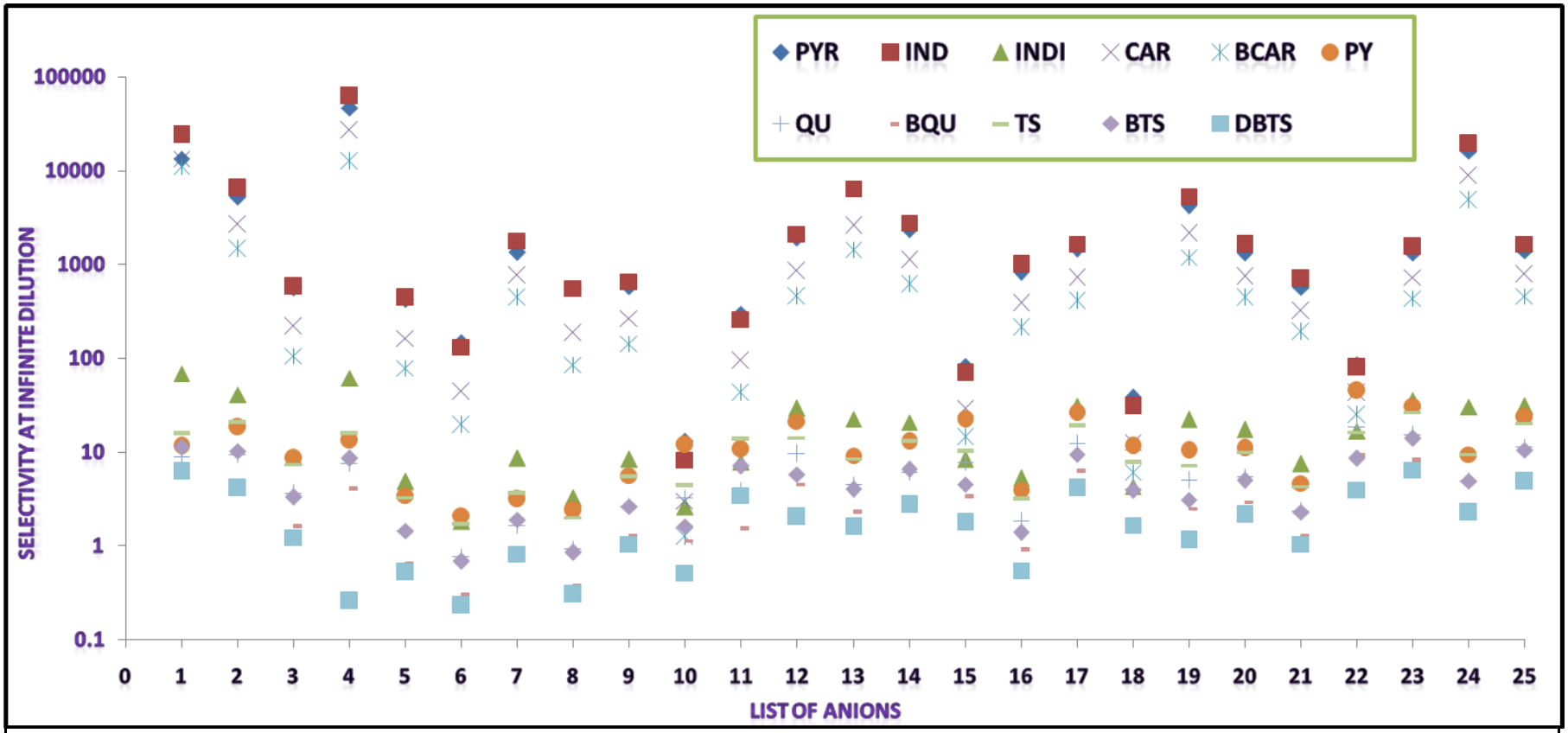

1. [Br], 2. [NO_3], 3. [SCN], 4. [CH_3COO], 5. [HSO_4], 6. [BF_4], 7. [CH_3SO_3], 8. [CF_3COO], 9. [CH_3SO_4], 10. [PF_6], 11. [CF_3SO_3], 12. [$C_2H_5SO_4$], 13. [$(CH_3)_2PO_4$], 14. [$C_3H_7NO_3S$], 15. [$B(CN)_4$], 16. [$C_7H_5O_3$], 17. [$(CH_3SO_2)_2N$], 18. [BC_2O_4], 19.

Figure 4.22 (b): Selectivity at infinite dilution of aromatic nitrogen and refractory sulfur species in [EPY] cation based ILs(X-axis legend :Anion no's mentioned are as per Table 4 .5)

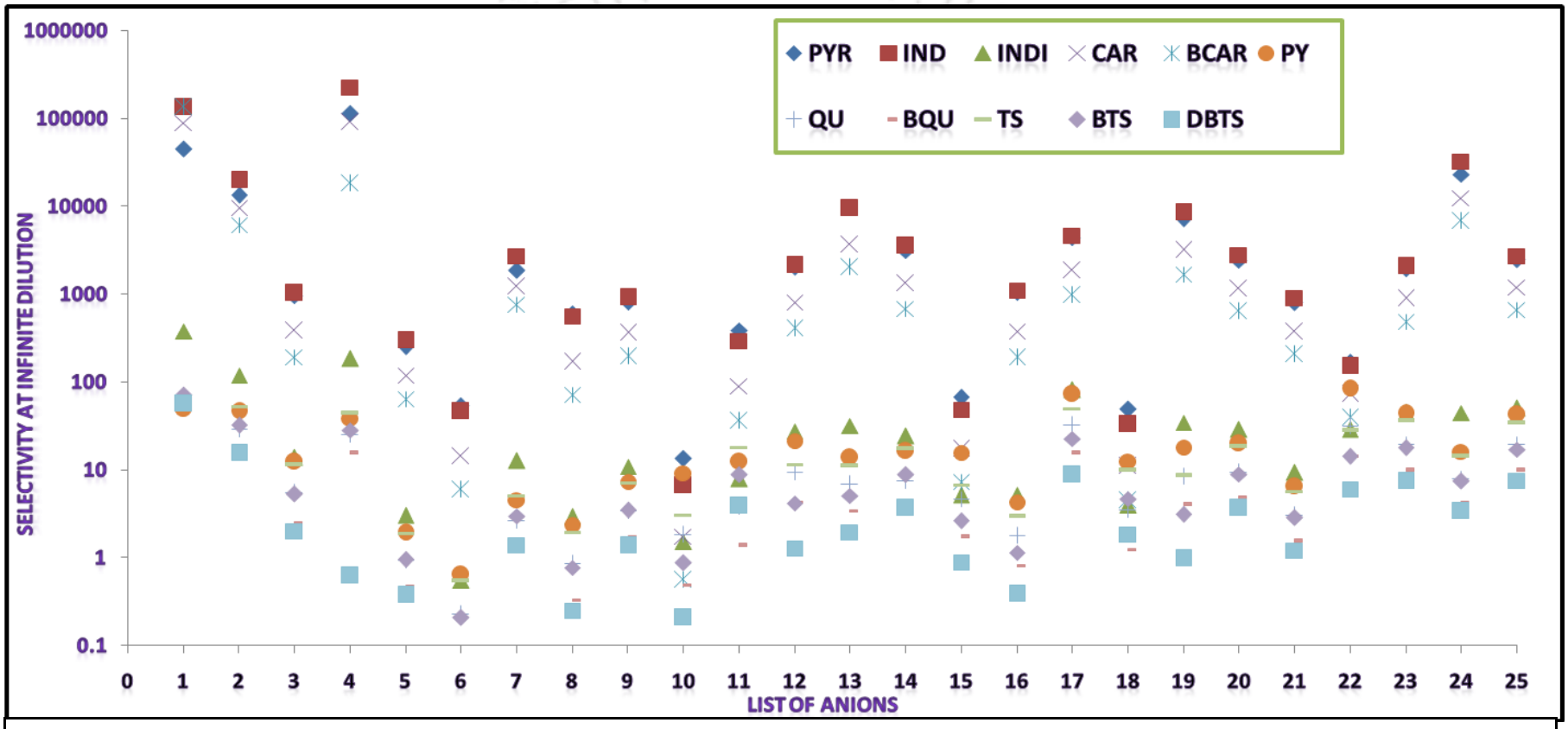

1. [Br], 2. [NO_3], 3. [SCN], 4. [CH_3COO], 5. [HSO_4], 6. [BF_4], 7. [CH_3SO_3], 8. [CF_3COO], 9. [CH_3SO_4], 10. [PF_6], 11. [CF_3SO_3], 12. [$C_2H_5SO_4$], 13. [$(CH_3)_2PO_4$], 14. [$C_3H_7NO_3S$], 15. [$B(CN)_4$], 16. [$C_7H_5O_3$], 17. [$(CH_3SO_2)_2N$], 18. [BC_2O_4], 19.

Figure 4.22(c): Selectivity at infinite dilution of basic/nonbasic nitrogen and acidic sulfur species in [EMMOR] cation based ILs(X-axis legend :Anion no's mentioned are as per Table 4 .5)

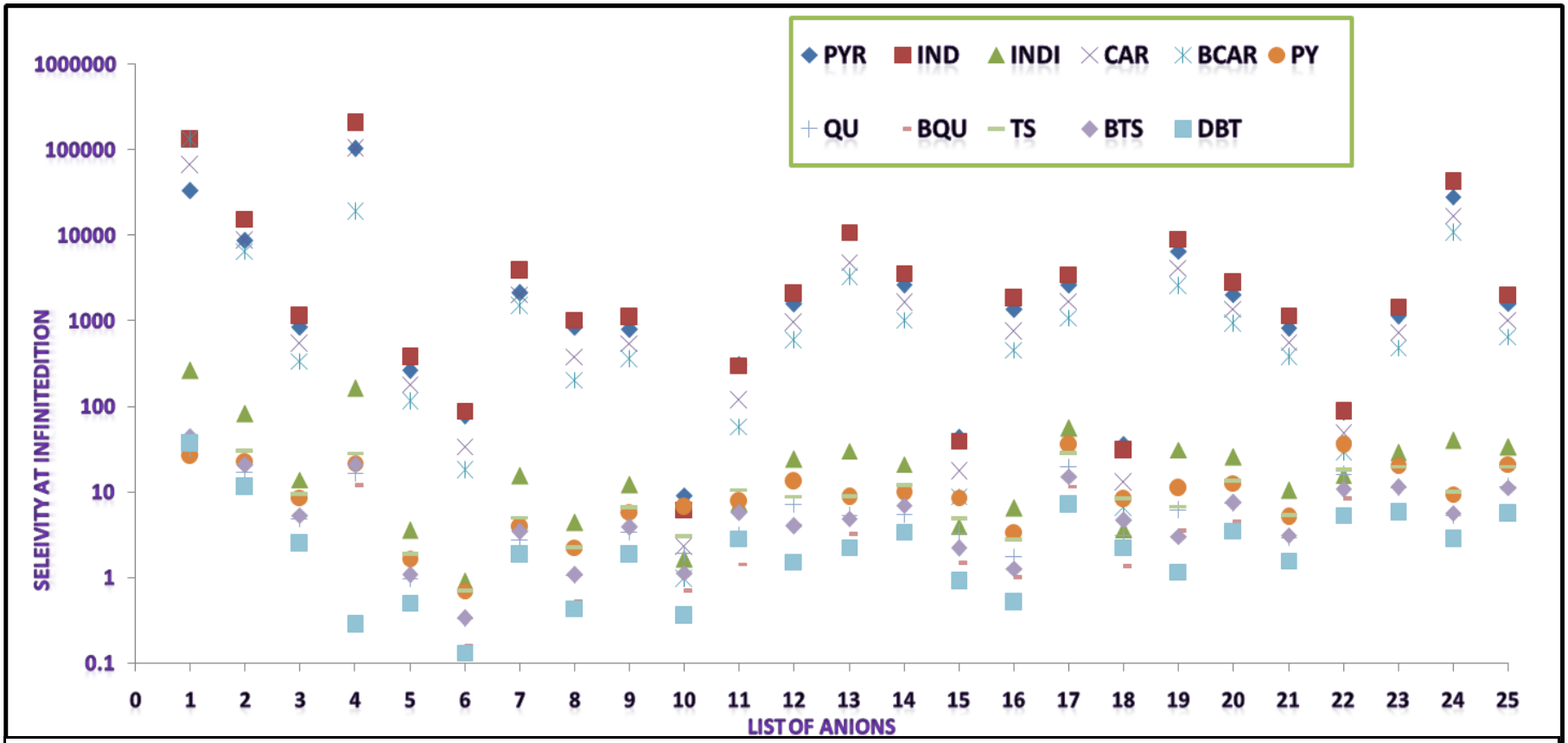

1. [Br], 2. [NO_3], 3. [SCN], 4. [CH_3COO], 5. [HSO_4], 6. [BF_4], 7. [CH_3SO_3], 8. [CF_3COO], 9. [CH_3SO_4], 10. [PF_6], 11. [CF_3SO_3], 12. [$C_2H_5SO_4$], 13. [$(CH_3)_2PO_4$], 14. [$C_3H_7NO_3S$], 15. [$B(CN)_4$], 16. [$C_7H_5O_3$], 17. [$(CH_3SO_2)_2N$], 18. [BC_2O_4], 19.

Figure 4.22(d): Selectivity at infinite dilution of aromatic nitrogen and refractory sulfur species in [EPYRO] cation based ILs(X-axis legend :Anion no's mentioned are as per Table 4 .5)

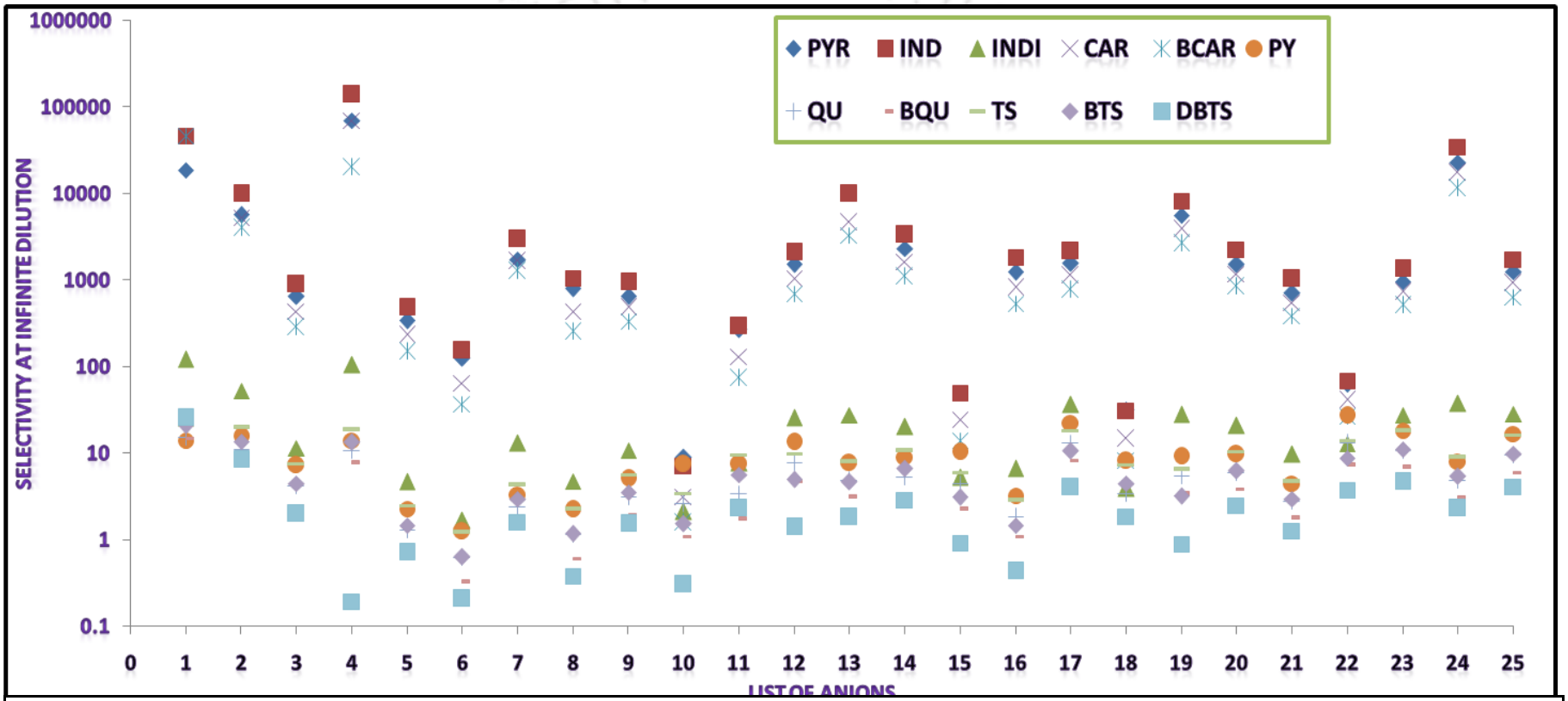

1. [Br], 2. [NO_3], 3. [SCN], 4. [CH_3COO], 5. [HSO_4], 6. [BF_4], 7. [CH_3SO_3], 8. [CF_3COO], 9. [CH_3SO_4], 10. [PF_6], 11. [CF_3SO_3], 12. [$C_2H_5SO_4$], 13. [$(CH_3)_2PO_4$], 14. [$C_3H_7NO_3S$], 15. [$B(CN)_4$], 16. [$C_7H_5O_3$], 17. [$(CH_3SO_2)_2N$], 18. [BC_2O_4], 19. [$C_4H_{10}O_4P$],

Figure 4.22(e): Selectivity at infinite dilution of aromatic nitrogen and refractory sulfur species in [EMPIP] cation based ILs(X-axis legend :Anion no's mentioned are as per Table 4 .5)

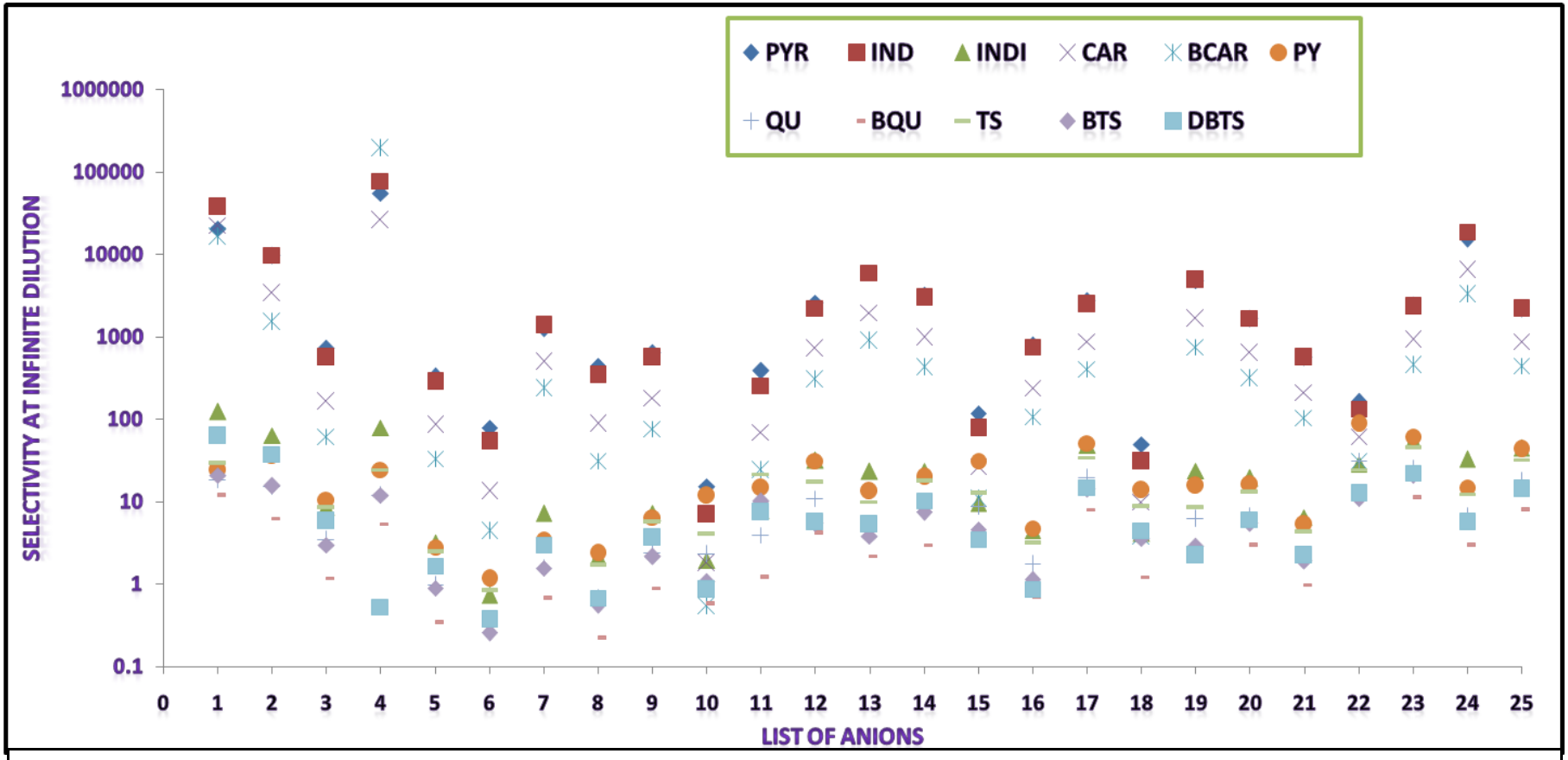

1. [Br], 2. [NO_3], 3. [SCN], 4. [CH_3COO], 5. [HSO_4], 6. [BF_4], 7. [CH_3SO_3], 8. [CF_3COO], 9. [CH_3SO_4], 10. [PF_6], 11. [CF_3SO_3], 12. [$C_2H_5SO_4$], 13. [$(CH_3)_2PO_4$], 14. [$C_3H_7NO_3S$], 15. [$B(CN)_4$], 16. [$C_7H_5O_3$], 17. [$(CH_3SO_2)_2N$], 18. [BC_2O_4], 19.

Figure 4.22 (f): Selectivity at infinite dilution of aromatic nitrogen and refractory sulfur species in [TMPYZO] cation based ILs(X-axis legend :Anion no's mentioned are as per Table 4 .5)

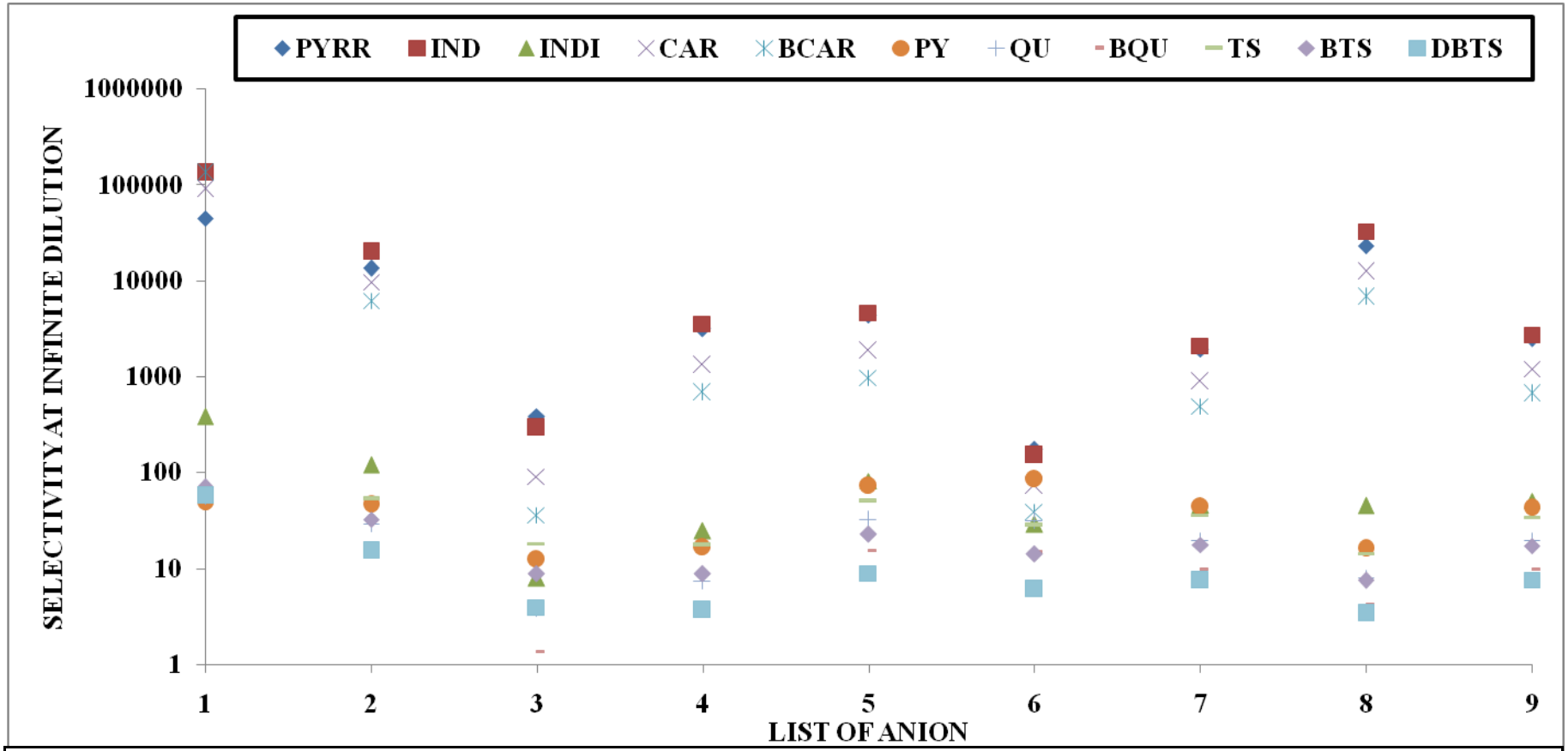

1. [Br], 2. [NO_3], 3. [CF_3SO_3], 4. [$C_3H_7NO_3S$], 5. [$(CH_3SO_2)_2N$], 6. [$CF_3SO_2)_2N$], 7. [$C_5H_{11}SO_6$], 8. [$C_{10}H_{19}O_2$], 9. [$C_8H_{18}O_4S$].

Figure 4.23: Selectivity at infinite dilution of aromatic nitrogen species and refractory sulfur species in [EPYRO] based ILs

Figure 4.24: Schematic representation of specific interaction forces between ionic liquid ([EMIM][NT]) and acidic sulphur or basic and /or non basic nitrogen compounds (thiophene,pyrrole,pyridine) and the arrow denotes the direction of electron cloud transfer.[Anantharaj et al.,2010,2011a].

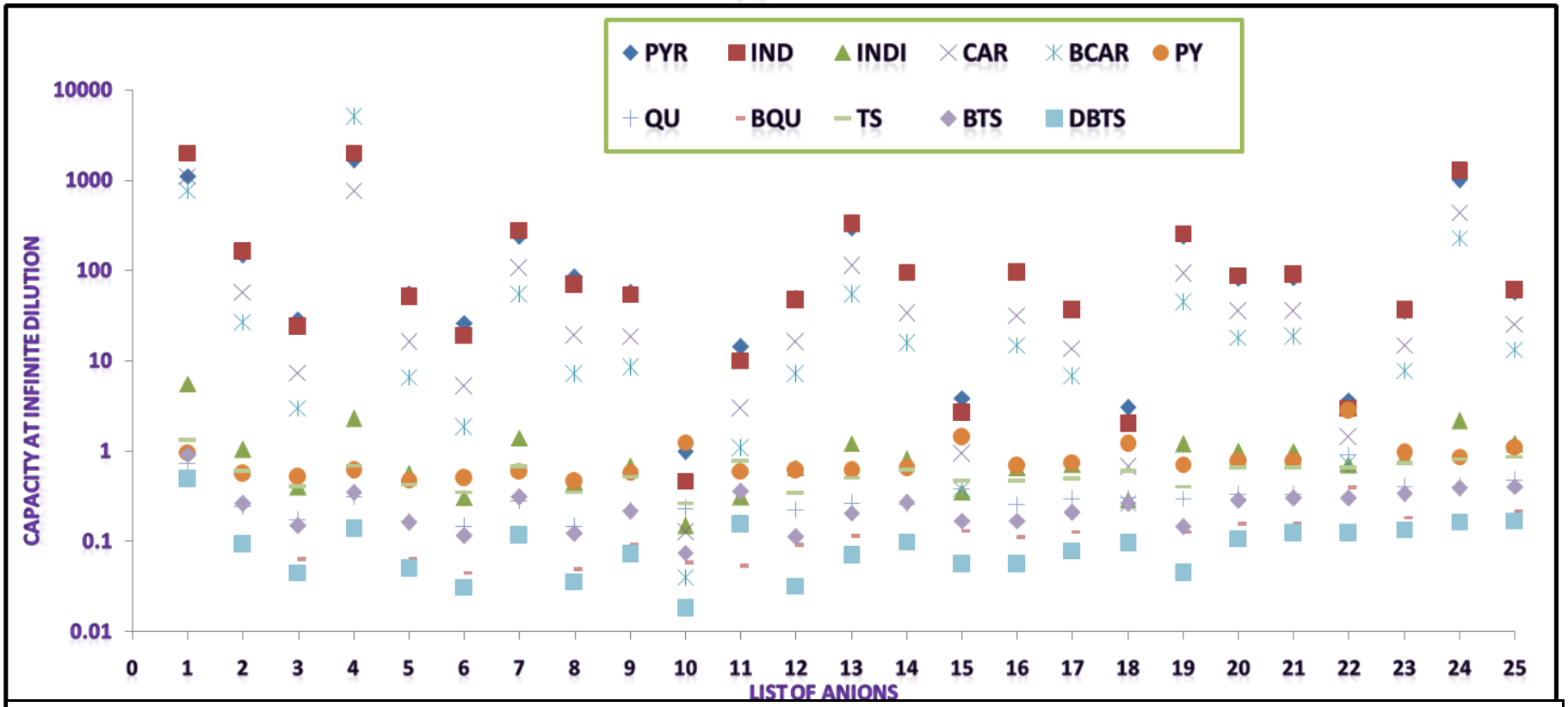

1. [Br], 2. [NO_3], 3. [SCN], 4. [CH_3COO], 5. [HSO_4], 6. [BF_4], 7. [CH_3SO_3], 8. [CF_3COO], 9. [CH_3SO_4], 10. [PF_6], 11. [CF_3SO_3], 12. [$C_2H_5SO_4$], 13. [$(CH_3)_2PO_4$], 14. [$C_3H_7NO_3S$], 15. [$B(CN)_4$], 16. [$C_7H_5O_3$], 17. [$(CH_3SO_2)_2N$], 18. [BC_2O_4], 19. [$C_4H_{10}O_4P$],

Figure 4.25(a): Capacity of [EMIM] cation based ILs for ablation of aromatic nitrogen and refractory sulfur species at infinite dilution(X-axis legend :Anion no's mentioned are as per Table 4 .5)

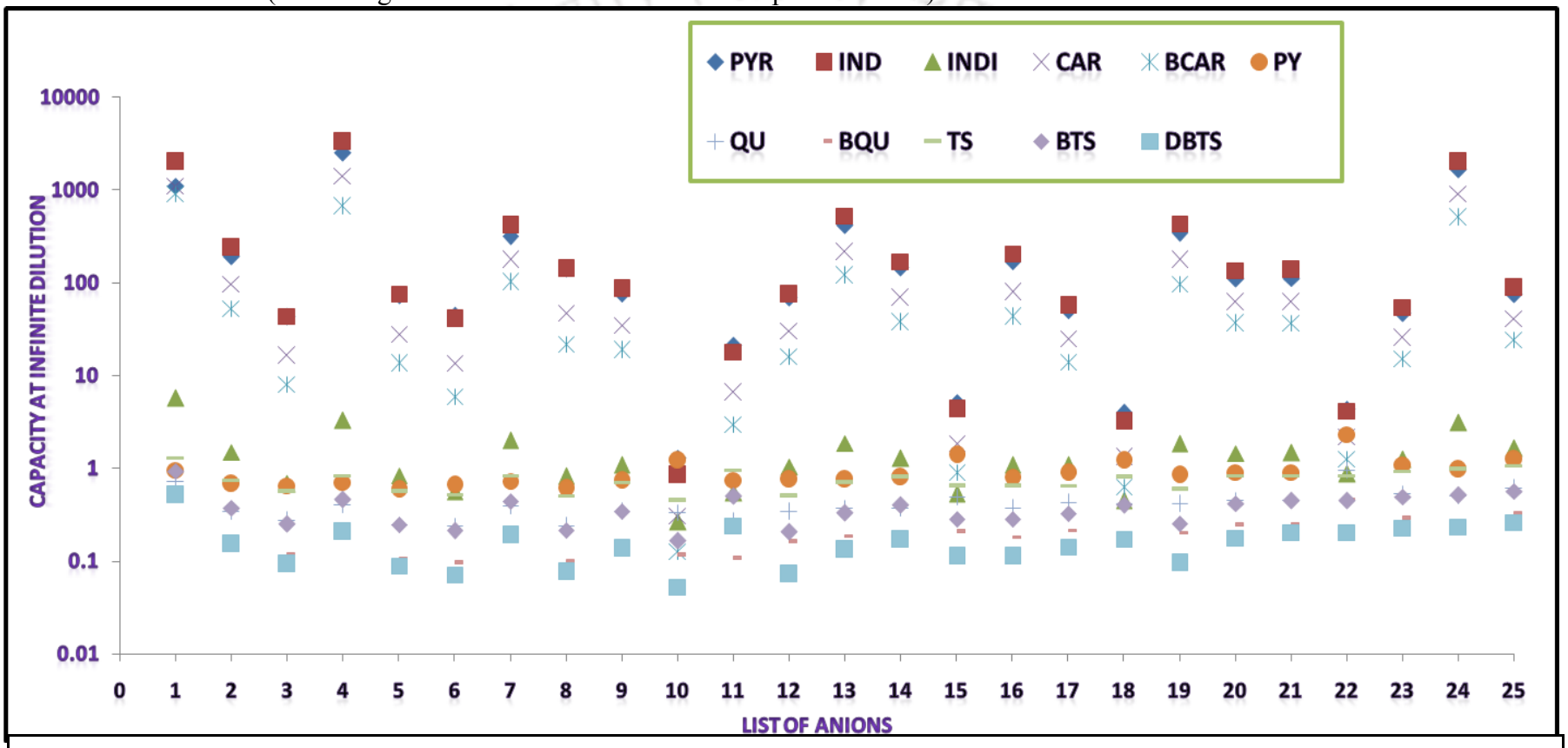

1. [Br], 2. [NO_3], 3. [SCN], 4. [CH_3COO], 5. [HSO_4], 6. [BF_4], 7. [CH_3SO_3], 8. [CF_3COO], 9. [CH_3SO_4], 10. [PF_6], 11. [CF_3SO_3], 12. [$C_2H_5SO_4$], 13. [$(CH_3)_2PO_4$], 14. [$C_3H_7NO_3S$], 15. [$B(CN)_4$], 16. [$C_7H_5O_3$], 17. [$(CH_3SO_2)_2N$], 18. [BC_2O_4], 19.

Figure 4.25(b): Capacity of [EPY] cation based ILs for ablation of aromatic nitrogen and refractory sulfur species at infinite dilution(X-axis legend :Anion no's mentioned are as per Table 4 .5)

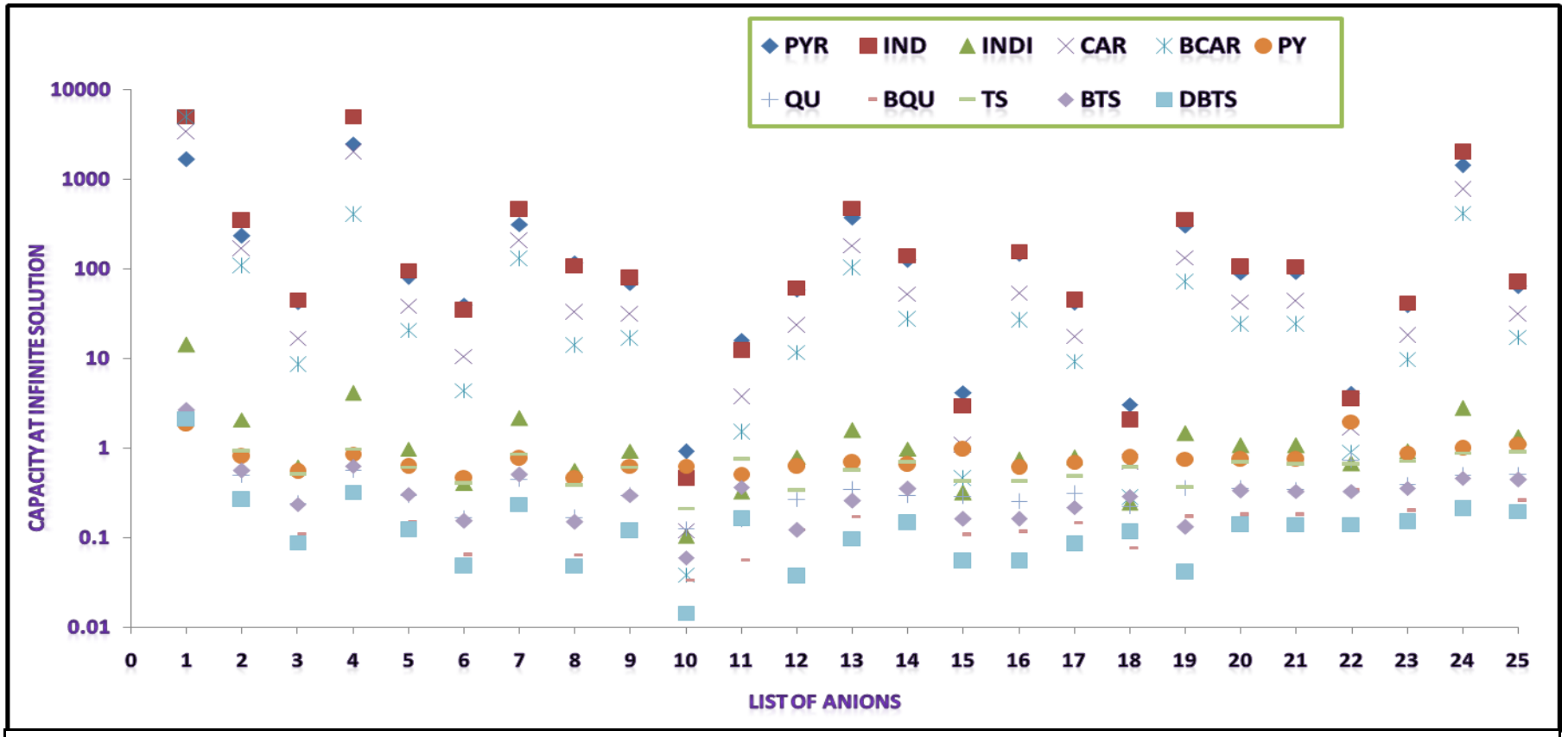

1. [Br], 2. [NO_3], 3. [SCN], 4. [CH_3COO], 5. [HSO_4], 6. [BF_4], 7. [CH_3SO_3], 8. [CF_3COO], 9. [CH_3SO_4], 10. [PF_6], 11. [CF_3SO_3], 12. [$C_2H_5SO_4$], 13. [$(CH_3)_2PO_4$], 14. [$C_3H_7NO_3S$], 15. [$B(CN)_4$], 16. [$C_7H_5O_3$], 17. [$(CH_3SO_2)_2N$], 18. [BC_2O_4], 19.

Figure 4.25(c): Capacity of [EMMOR] cation based ILs for ablation of aromatic nitrogen and refractory sulfur species at infinite dilution(X-axis legend :Anion no's mentioned are as per Table 4 .5)

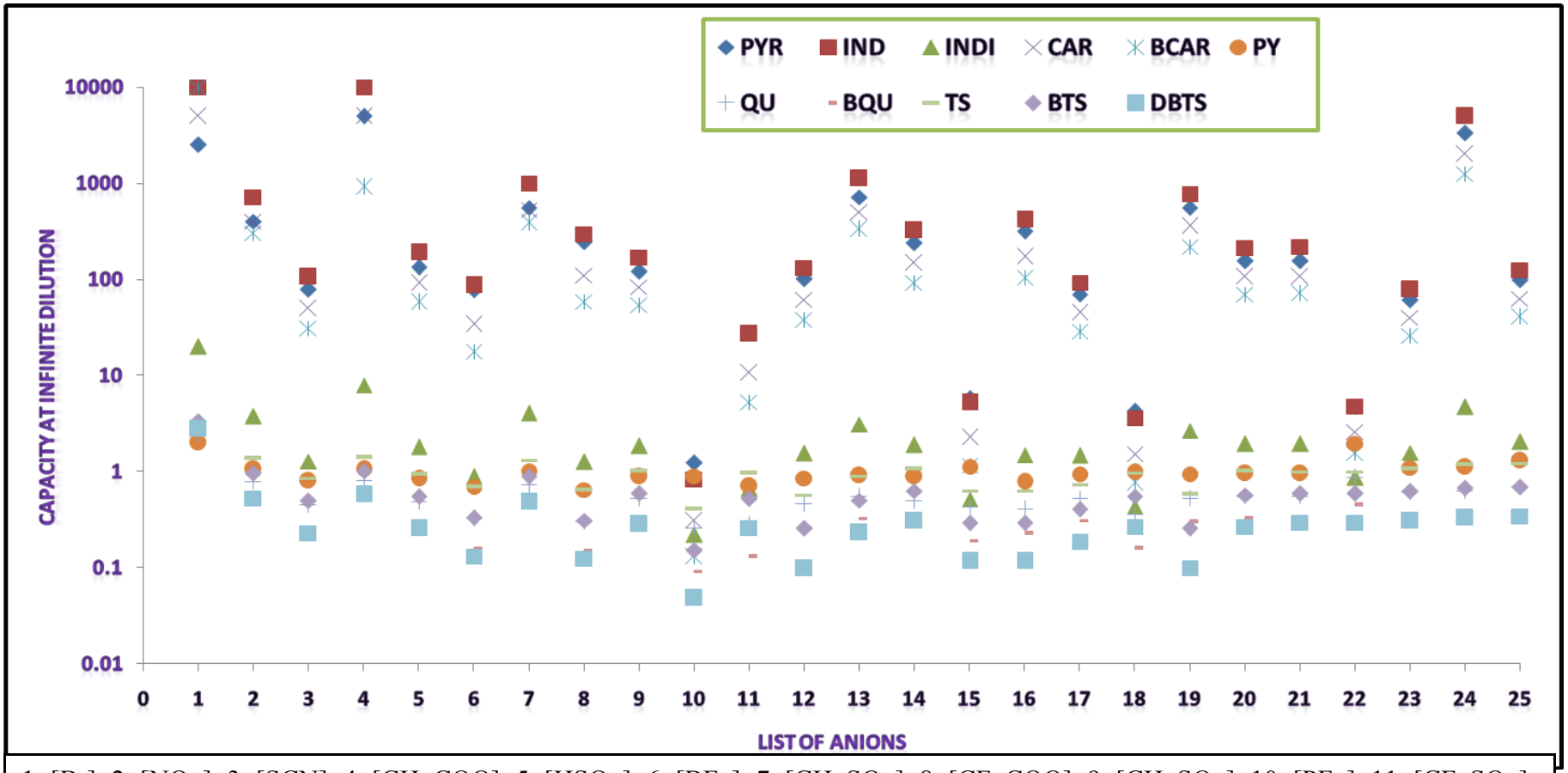

1. [Br], 2. [NO_3], 3. [SCN], 4. [CH_3COO], 5. [HSO_4], 6. [BF_4], 7. [CH_3SO_3], 8. [CF_3COO], 9. [CH_3SO_4], 10. [PF_6], 11. [CF_3SO_3], 12. [$C_2H_5SO_4$], 13. [$(CH_3)_2PO_4$], 14. [$C_3H_7NO_3S$], 15. [$B(CN)_4$], 16. [$C_7H_5O_3$], 17. [$(CH_3SO_2)_2N$], 18. [BC_2O_4], 19.

Figure 4.25(d): Capacity of [EPYRO] cation based ILs for ablation of aromatic nitrogen and refractory sulfur species at infinite dilution(X-axis legend :Anion no's mentioned are as per Table 4 .5)

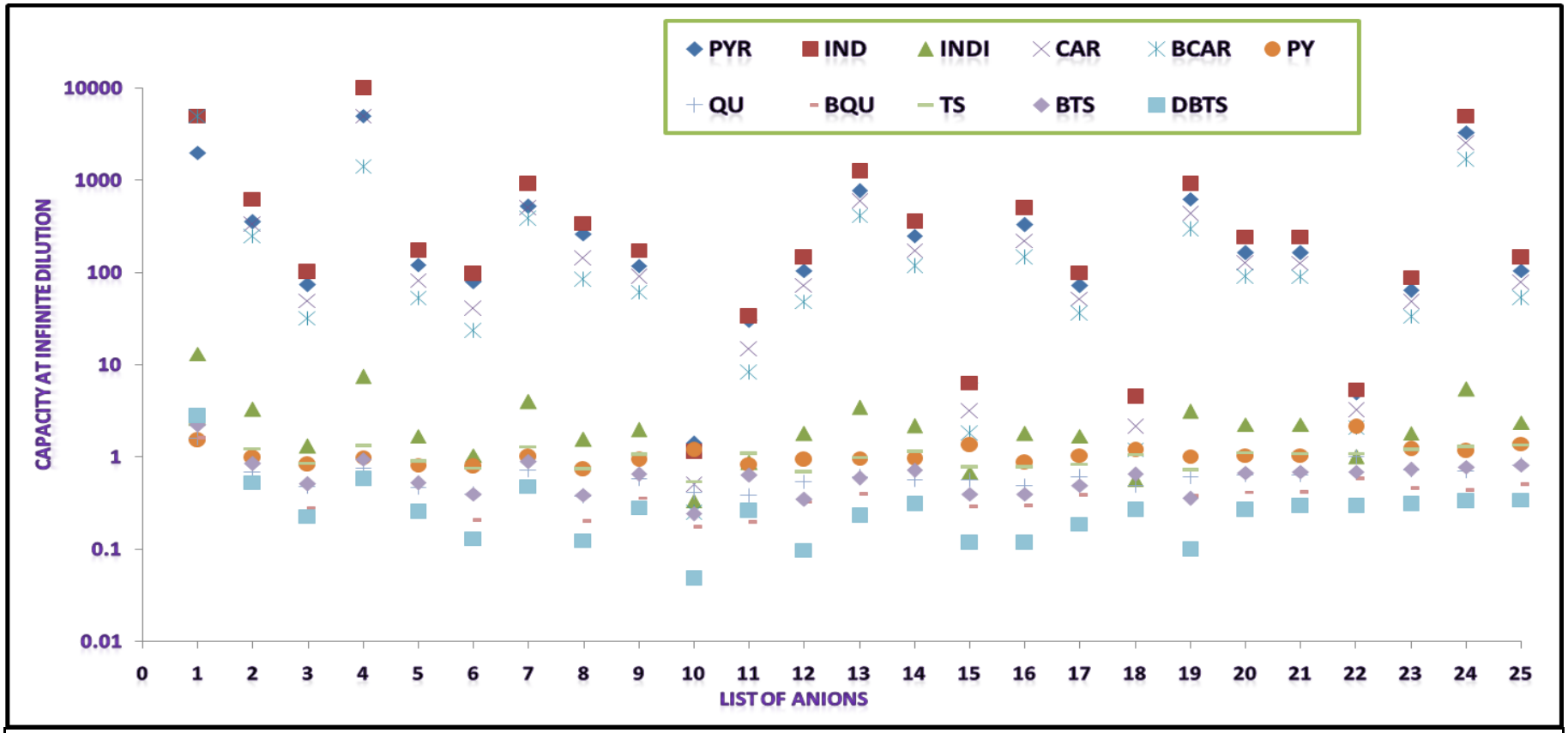

1. [Br], 2. [NO_3], 3. [SCN], 4. [CH_3COO], 5. [HSO_4], 6. [BF_4], 7. [CH_3SO_3], 8. [CF_3COO], 9. [CH_3SO_4], 10. [PF_6], 11. [CF_3SO_3], 12. [$C_2H_5SO_4$], 13. [$(CH_3)_2PO_4$], 14. [$C_3H_7NO_3S$], 15. [$B(CN)_4$], 16. [$C_7H_5O_3$], 17. [$(CH_3SO_2)_2N$], 18. [BC_2O_4], 19. [$C_4H_{10}O_4P$],

Figure 4.25(e): Capacity of [EMPIP] cation based ILs for ablation of aromatic nitrogen and refractory sulfur species at infinite dilution(X-axis legend :Anion no's mentioned are as per Table 4 .5)

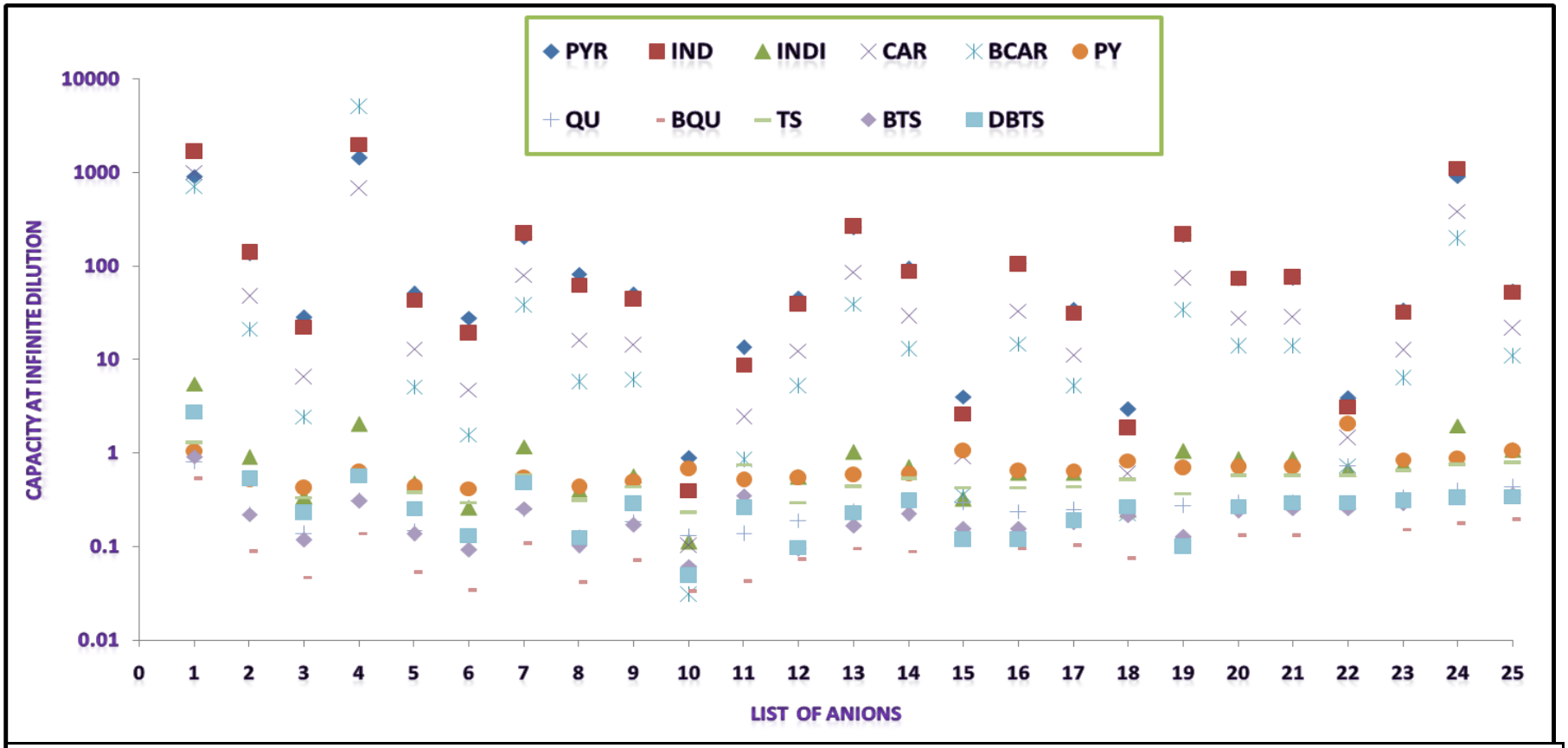

1. [Br], 2. [NO_3], 3. [SCN], 4. [CH_3COO], 5. [HSO_4], 6. [BF_4], 7. [CH_3SO_3], 8. [CF_3COO], 9. [CH_3SO_4], 10. [PF_6], 11. [CF_3SO_3], 12. [$C_2H_5SO_4$], 13. [$(CH_3)_2PO_4$], 14. [$C_3H_7NO_3S$], 15. [$B(CN)_4$], 16. [$C_7H_5O_3$], 17. [$(CH_3SO_2)_2N$], 18. [BC_2O_4], 19.

Figure 4.25(f): Capacity of [TMPYZO] cation based ILs for ablation of aromatic nitrogen and refractory sulfur species at infinite dilution.

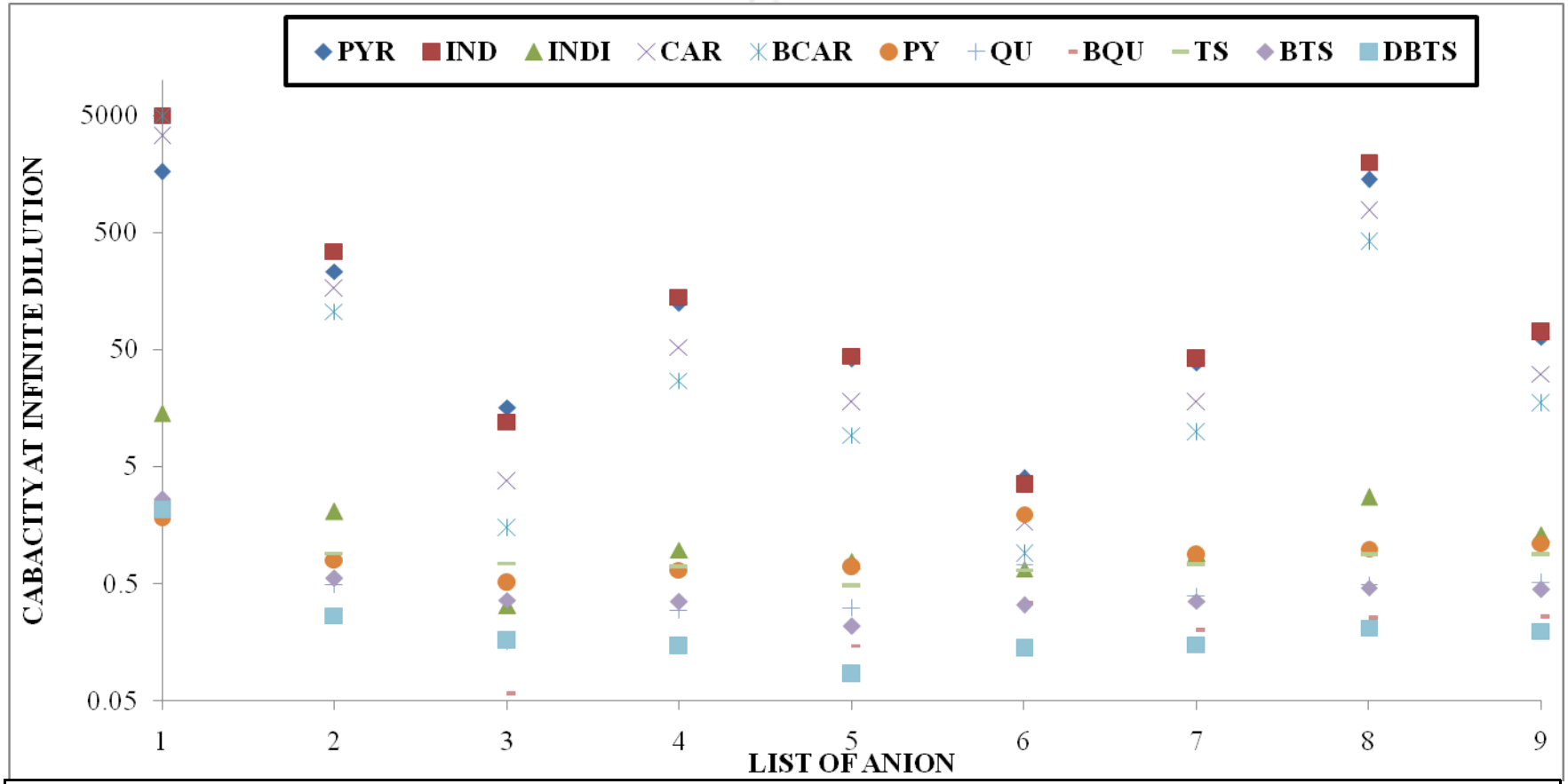

1. [Br], 2. [NO_3], 3. [CF_3SO_3], 4. [$C_3H_7NO_3S$], 5. [$(CH_3SO_2)_2N$], 6. [$CF_3SO_2)_2N$], 7. [$C_5H_{11}SO_6$], 8. [$C_{10}H_{19}O_2$], 9.

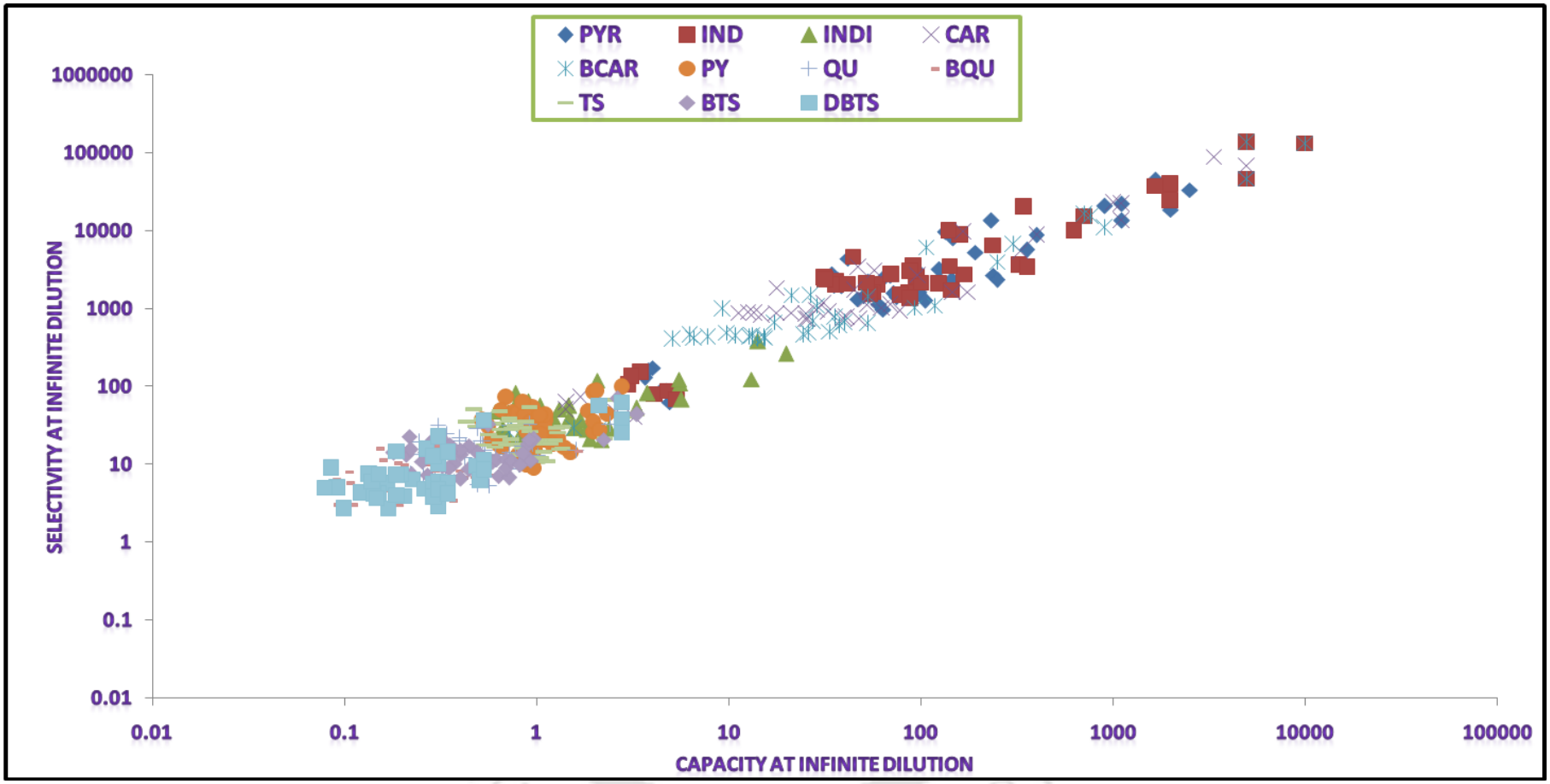

Figure 4.27: Selectivity verses solvent capacity at infinite dilution for [EMIM], [EPY], [EMMOR], [EPYRO], [EMPIP], and [TMPYZO] based cations with the combination of [Br], [NT], [TfO], [MSACN], [BMA], [BTA], [Me-Et-EtSu], [Dec], and [OcSu] based anions.

Nomenclature

List of symbols

[EMIM]	1-Ethyl-1-Methylimidazolim
[EPY]	1-Ethylpyridinium
[EPYRO]	1-Ethylpyrrolidinium
[EMMOR]	4-Ethyl-4-Methylmorpholinium
[EMPIP]	1-Ethyl-1-Methylpiperidinium
[TMPYZO]	1, 2, 4-Trimethylpyrazolium
TS	Thiophene
BT	Benzothiophene
DBT	Dibenzothiophene
C	Solvent capacity
S	Solvent Selectivity
PI	Performance index

Symbols:

	Chemical potential
	Electro negativity
	Global hardness
S	Global softness
	Electrophilicity index
x	Mole fraction in liquid phase
σ	Screening charge density in e/ $Å^2$
	Effective Contact Surface area of a segment in $Å^2$
	Molecular surface on atom ‘α’
	Hydrogen Bonding coefficient in (kcal $Å^4$)/ (mol e^2)
d_{mn}	Distance between the ‘m^{th}’ and ‘n^{th}’ segment
	Misfit Interaction Energy in Kcal/mole

	Hydrogen Bonding Interaction Energy in Kcal/mole
	van der Waal (vdW) Interaction Energy in Kcal/mole
k	Boltzmann Constant
m	Number of tie lines
c	Number of components
n_i	Contribution of molecule 'i' to the surface segments in the solution
	Probabilistic surface charge distribution for pure component(i)
	Probabilistic surface charge distribution for mixture(s)
	Normalized area parameter
r	Normalized volume parameter
	Averaging Radius in Å
	Radius of the 'n^{th}' segment in Å
R	Universal gas constant in Kcal/mol K
SG	Staverman Guggenheim Term
T	Temperature in K
	Misfit Constant in (kcal $Å^4$)/ (mol e^2)
	Cut-off screening charge density for hydrogen bonding in e/ $Å^2$
	Screening charge density for hydrogen bond donor in e/ $Å^2$
	Screening charge density for hydrogen bond acceptor in e/ $Å^2$
	Dispersion Coefficient for element 'α'
	Sigma potential for a surface segment in solution 'S'
	Segment Activity Coefficient for pure component (i)
	Segment activity coefficient for mixture (S)

Component activity coefficient in the mixture(S)

REFERENCES

Alonso, L.; Arce, A.; Francisco, M.; Soto, A. Liquid-liquid equilibria of [C_8mim][NTf_2] ionic liquid with a sulfur-compounent and hydrocarbons.*J.Chem.Thermodynamics*.**2008**,40,265-270.

Anantharaj, R.; Banerjee,T. COSMO-RS based Predictions for the Desulphurization of Diesel oil using Ionic Liquids: Effect of Cation and Anion combination, *Fuel. Proc. Tech***. 2011a**, 92, 39-52.

Anantharaj, R.; Banerjee,T. COSMO-RS-Based Screening of Ionic Liquids as Green Solvents in Denitrification Studies.*Ind.Eng.Chem.Res***. 2010,** 49, 8705-8725.

Anantharaj, R.; Banerjee,T. Quantum Chemical Studies on the Simultaneous Interaction of Thiophene and Pyridine with Ionic Liquid, *AIChEJ*. **2011b**. 57,749-764.

Andzelm. J.; Kolmet.C.; Klamt.A. Incorporation of Solvent into Density Functional Calculations of Molecular Energies and Geometries. *J.Chem.Phys.***1995,** 103**,** 9312-9320

Banerjee, T, Verma, K.K, Khanna, A. Liquid Liquid Equilibria for Ionic Liquid based systems using COSMO-RS: Effect of Cation and Anion combination. AIChE J. **2008**, 54,1874-1885.

Banerjee, T.; Khanna, A. Infinite Dilution Activity Coefficients for Trihexyltetradecyl Phosphonium Ionic Liquids: Measurements and COSMO-RS Prediction. J.Chem.Eng.Data. **2006a**, 51, 2170-2177.

Banerjee, T.; Singh, M.K.; Khanna, A. Prediction of Binary VLE for Imidazolium Based Ionic Liquid Systems Using COSMO-RS.Ind. Eng. Chem. Res.**2006b**, 45, 3207-3219.

Banerjee, T; Khanna, A. Infinite Dilution Activity Coefficients for Trihexyltetradecyl Phosphonium Ionic Liquids: Measurements and COSMO-RS Prediction *J. Chem. Engg. Data* **2006c**, 51, 2170-2177.

Banerjee.T.; Singh.M.K.; Khanna. A. Prediction of Binary VLE for Imidazolium Based Ionic Liquid Systems Using COSMO–RS, *Ind. Engg. Chem. Res.* **2006**, 45, 3207-3219.

Bansal, R.K.Heterocyclic chemistry, Fourth Edition, New Age International Publishers. **2005**.

Bondi, A. van der Waals volumes and radii. *J. Phys. Chem*. **1964**, 68, 441-451.

Born. M. Volumes and heats of hydration of ions. *Zeitschrift fuer Physik* **1920**,1**,** 45.

Breneman,C.M.; Wiberg,K.B. Determining atom-centered monopoles from molecular electrostatic potentials. The need for high sampling density in formamide conformational analysis.J. Comp. Chem. **1990**, *11*, 361-373.

Burger, T. J.; Klamt, A.; Eckert, F.; Hornig, M.; Beck, M. E. Prediction of Aqueous Solubility of Drugs and Pesticides with COSMO-RS, *J. Compt. Chem.* **2002a**, 23, 275.

Cassol, C.C.; Umpierre, A.P.; Ebeling, G.; Ferrera, B.; Sandra, S.; Chiaro, S.X.; Dupont, J. On the Extraction of Aromatic Compounds from Hydrocarbons by Imidazolium Ionic Liquids. *Int.J.Mol.Sci*.**2007**, 8, 593-605.

Castro, C.R.; Tormo, A.L.; Vega. L.F. Effect of flexibility and the anion in the structura and transport properties of ethyl-methyl-imidazolium ionic liquids. *Fluid Phase Equilib*ria.**2007**, 256, 62-69.

Contreras, R.; Fuentealba, P.; Galvan, M.; Perez, P. A direct evaluation of regional Fukui functions in molecules. *Chem Phys Lett*,**1999**, 304,405–413.

Cramer, C. J.; Truhlar, D.G.; Lipkowitz, K. B.; Boyd, D.B.; Eds., *Reviews in Computational Chemistry* vol. 6 VCH Publishers, New York, **1995.**

Delly B. DMol, Biosym Technologies, San Diego, California, 1995.

Diedenhofen, M.; Eckert, F. ; Klamt. A. Prediction of Infinite Dilution Activity Coefficients of Organic Compounds in Ionic Liquids Using COSMO-RS. *J. Chem. Eng. Data*.**2003**, 48, 475–479.

Doker.M.; Gmehling J., Measurement and prediction of vapor–liquid equilibria of ternary systems containing ionic liquids. *Fluid Phase Equilib.* **2005**,225, 255-266.

Domanska, U.; Krolikowski, M.; Slesinska, K. Phase equilibria study of the binary systems (ionic liquid + thiophene): Desulphurization process. *J.Chem.Thermodynamics*. **2009,** 41, 1303-1311.

Domanska,U.;Marciniak,A.Measurement of activity coefficient at infinite dilution of aromatic and aliphatic hydrocarbons,alcohols,and water in the new ionic liquid [EMIM][SCN] using GLC. *J.Chem.Thermodynamics* **.2008**,40,860-866.

Domańska.U.; Pobudkowska.A.; Eckert .F. Liquid–liquid equilibria in the binary systems (1,3-dimethylimidazolium, or 1-butyl-3-methylimidazolium methyl sulfate + hydrocarbons) *Green Chem.* **2006**, 3, 268-276.

Eber J, Wasserchied P,Jess A. Deep Desulfurization of Oil Refinery Streams by Extraction with Ionic Liquids. *Green Chem*. **2004**, 6,316-322.

Fleming, I. Frontier Orbitals and Organic Chemical Reactions, John Wiley and Sons, New York, **1976**.

Fraser, K.J.; Izgorodina, E.I.; Forsyth, M.; Scott, J.I.;.MacFarlane, D.R. Liquid ion pairs (LIPS): inonic liquids that exhibit poor ion mobility. *J.Chem.Comm*.**2007**, 3817-3817.

Fredenslund. A; Jones, R. L.; Prausnitz, J. M. Group-Contribution Estimation of Activity Coefficients in Non-ideal Liquid Mixtures. *AIChE J.* **1975**,21 **,** 1086.

Frisch, M. J.;Gordon. M.; Pople. A.J. Semidirect Algorithms for the MP2 Energy and Gradient. *Chem. Phys.Letters.1990,* **166** , 281.

Giles, N.; Wilson, G. Phase Equilibria on Seven Binary Mixtures. *J. Chem. Eng. Data*. **2000,** 45, 146-153.

Gmehling, J; Li, J. D.; Schiller, M. A. Modified UNIFAC Model. 2. Present Parameter Matrix and Results for Different Thermodynamic Properties. *Ind. Eng. Chem. Res.***1993***,* **32** 178.

Gong, L.; Guo, W.; Xiaong, J.; Li, R.; Wu, X.; Li. X. Structures and stability of ionic liquid model with imidazole and hydrogen fluorides chains: Density functional theory study. *Chem. Phy. Lett*.**2006**, 425,167-178.

Grenseman, H.; Gmehling, J. Performance of a Conductor Like Screening Model for Real Solvents Model in Comparison to Classical Group Contribution Methods. *Ind.Eng.Chem.Res.***2005**, 44, 1610-1624.

Gupta, R.R.; Kumar, M.; Gupta, V. Heterocyclic Chemistry –II, Five – Membered Heterocyclic, Springer.**2005**.

Gutel, T.; Santini, C.C.; Padua, A.A.; Fenet, B.; Chauvin, Y.; Lopes, Y.C.; Bayard, F.; Costa, F.; Pensado. A.S. Interaction between the π- system of toluene and the imidazolium ring of ionic liquids: combined NMR and molecular simulation study. *J. Phys. Chem. B*.**2009**, 113,170-177.

Hunt, P.A.; Gould, I.R.; Kirchner, B. The structure of imidazolium-based ionic liquids: Insights from ion-pair interactions. *Aust.J.Chem*. **2007**, 60,9-14.

Jork.C.;Kristen.D.; Pieraccini, D., Stark.A.; Chiappe.C.;Beste.A.Y.; Arlt.W. Tailor-made ionic liquids **.** *J.Chem. Thermodynamics*. **2005**,37, 537-558.

Joule, J.A.; Mills. K. Heterocyclic chemistry, Fourth Edition, Blackwell Publishing (OXFORD).**2007**.

Kato,R; Gmehling, J. Activity coefficients at infinite dilution of various solutes in the ionic liquids $[MMIM]^+$ $[CH_3SO_4]^-$,$[MMIM]^+$ $[CH_3OC_2H_4SO_4]^-$,$[MMIM]^+[(CH_3)_2PO_4]^-$$[C_5H_5NC_2H_5]^+[(CF_3SO_2)_2N]^-and[C_5H_5NH]^+[C_2H_5OC_2H_4OSO_3]^-$.*Fluid Phase Equilibria.* **2004**, 226, 37-44.

Kato. R.; Krummen. M.; Gmehling. J. Measurement and correlation of vapor–liquid equilibria and excess enthalpies of binary systems containing ionic liquids and hydrocarbons, *Fluid Phase Equilibria.* **2004**,224, 47-54

Kato.R.; Gmehling.J.; Measurement and correlation of vapor liquid equilibria of binary systems containing the ionic liquids $[EMIM][(CF_3SO_2)_2N]$, $[BMIM][(CF_3SO_2)_2N]$, $[MMIM][(CH_3)_2PO_4]$ and oxygentated organic compounds respectively water, *Fluid Phase Equili*bria. **2005**,231, 38-43.

Kim.K.; Shin.B.; Lee.H.;Ziegler.F. Refractive index and heat capacity of 1-butyl-3-methylimidazoliumbromide and 1-butyl-3-methylimidazolium tetrafluoroborate, and vapor pressure of binary systems for 1-butyl-3-methylimidazolium bromide + trifluoroethanol and 1-butyl-3-methylimidazolium tetrafluoroborate + trifluoroethanol *Fluid Phase Equilib.* **2004**,218, 215–220

Klamt, A. Conductor Like Screening Model for Real Solvents: A new Approach to the quantitative calculation of solvation phenemona. J.Phy.Chem.**1995**, 99, 2224-2235.

Klamt, A. COSMO-RS: From Quantum Chemistry to Fluid Phase Thermodynamics and Drug Design (1st Edition). Amsterdam: Elsevier. **2005.**

Klamt, A.; Eckert, F. COSMO-RS: a novel and efficient method for the a priori prediction of thermophysical data of liquids. *Fluid Phase Equilibria.* **2000,** 172, 43-72.

Klamt, A.; Eckert, F. Fast solvent screening via quantum chemistry: COSMO-RS approach. *AIChEJ*. **2002**, 48, 369-385.

Klamt, A.; Jonas, V.; Buerger, T.; Lohrenz, J. C. W. Refinement and Parameterization of COSMO-RS. *J. P. Chem. A* **1998,** 102, 5074-5085.

Klamt, A.; Schüürmann, G. COSMO: A New Approach to Dielectric Screening in Solvents with Explicit Expressions for the Screening Energy and its Gradient. *J. Chem. Soc. Perkin Trans*. **1993.2,**799-805.

Klamt. A. Mutual solubilities of hydrocarbons and water with COSMO-RS. *Fluid Phase Equilibria.* **2003,** 206, 223-235.

Klamt. A.; Eckert. F. Validation of the COSMO-RS Method: Six Binary Systems. *Ind. Engg. Chem. Res.* **2001**, 40, 2371-2378.

Klamt.A., Conductor Like Screening Model for Real Solvents: A new Approach to the quantitative calculation of solvation phenemona. *J.Phy.Chem. ,***1995**, 99, 2224-2235.

Kumar, A.A.P.; Banerjee, T.Thiophene separation with ionic liquids for Desulfurization: A quantum chemical approach. *Fluid phase equlibria*.**2009,** 278,1-8.

Lava, K.; Binnemans, K.; Cardinaels, T. Piperidinium, Piperazinium and Morpholinium Ionic Liquid Crystals. *J. Phys. Chem. B*, **200**9, 113, 9506–9511.

Lei, Z. ; Arlt, W.; Wasserscheid. P. Selection of entrainers in the 1-hexene/n-hexane system with a limited solubility. *Fluid Phase Equilibria*. **2006**, 241,290–299.

Letcher,T.M.;Ramjugernath,D.; Laskowska,M.; Krolikowski,M.; Naidoo,P.; Domanska,U. Activity coefficients at infinite dilution measurements for organic solutes in the ionic liquid trihexytetradecylphosphonium-bis-(2,4,4-trmethylpentyl)-phosphinate using g.l.c at (303.15, 308.15, 313.15, and 318.15). *J.Chem.Thermodynamics*.**2008**, 40, 1243-1247.

Lin, S.T.; Sandler, S.I. A Priori Phase Equilibrium Prediction from a Segment Contribution Solvation Model. *Ind. Engg. Chem. Res*. **2002**, 41, 899-913.

Maginn. E.; Brennecke. F. J. Ionic Liquids: Innovative Fluids for Chemical Processing *AIChE J* **2001**,47,2384-2389.

Magnussen.T.; Rasmussen.P.; Fredenslund.A.; UNIFAC Parameter Table for Prediction of Liquid-Liquid Equilibri. *Ind. Eng. Chem. Process Des. Dev.* **1981**, 20, 331-339

Marsh.N.K.; Boxall.A.J.; Lichtenthaler.R. Room temperature ionic liquids and their mixtures—a review.*Fluid Phase Equilibria.* **2004**, 219, 93-98.

Marsh.N.K.; Deev.A.; Wu.A.C.;, Emma.T.; Klamt.A. Room Temperature Ionic Liquids as Replacements for Conventional Solvents - A Review .*Korean J. Chem. Eng*.Res. **2002**, 19, 357-362.

Meindersma .G.W.; Podt. A.; Haan. B. A. Selection of ionic liquids for the extraction of aromatic hydrocarbons from aromatic/aliphatic mixtures. *Fuel Proc. Tech.* **2005**, 87, 59–70.

Morrow.T.I.; Maginn. E. J.; Molecular Dynamics of the ionic liquid 1-n-Butyl-methylimidazolium Hexafluorophosphate. *J.Phy.Chem B.* **2002** 106, 12807-12813.

Natalia, V.P.; Seddon, K.R. Applications of ionic liquids in the chemical industry. *Chem. Soc. Rev*.2**008**,37,123-150.

Paulechka.U.Y.; Zaitsau. H. D.; Kabo. J. B.; Strechan. A. Vapor pressure and thermal stability of ionic liquid 1-butyl-3-methylimidazolium Bis(trifluoromethylsulfonyl) amide *Thermochimica Acta*, **2005**,439, 158-160.

Perdew. J. P., Density-functional approximation for the correlation energy of the inhomogeneous electron gas. *Phys. Rev. B* ,**1986 ,**33, 8822-8824.

Petrukhin, O.M. Coordination chemistry and analytical methods of metal separation, *J.Coordination.Chemi*.**2002**, 28, 681-696.

Press.H.W., Teukolsky.S.A.; Vetterling.W.T.; Flannery.B.P. Numerical Recipes in FORTRAN, Cambridge University Press, New York, 2nd edn., **1992**, 89-91.

Putnam.R.; Taylor.R.; Klamt.A.; Eckert.F.; Schiller.M. Prediction of Infinite Dilution Activity Coefficients Using COSMO-RS. *Ind. Eng. Chem. Res.* **2003**, *42,* 3635-3641.

Schäfer.A.; Klamt.A.; Sattel,D.; Lohrenz.W.C.J.; Eckert.F. COSMO implementation in TURBOMOLE :Extension of an Efficient Quantum Chemical Code Towards Liquid systems. *Phys.Chem.Chem.Phys*.**2000**, 2, 2187.

Schäfer.A.;Huber.C.;Ahlrichs.R., Fully optimized contracted Gaussian basis sets of triple zeta valence quality for atoms Li to Kr, *J. Chem. Phys.***1994**,100, 5829-5835.

Seader, J.D.; Henley, E. J. Separation Process Principles, John Wiley, New York, NY, **1998 ,** 196.

Shah.K.J., Maginn. J.E., Brennecke.F.J., "Monte Carlo Simulation of the ionic liquid 1-n-Butyl-methyli Sørenson, J. M.; Arlt, W. Liquid-Liquid equilibrium data collection. *DECHEMA*. Chemistry Data Series V, Part 2 & 3, Frankfurt am Main, **1980.**

Shiflett, M. B.; Shiflett, A.; Yokozeki. Phase behavior of carbon dioxide in ionic Liquid: [emim][Acetat],[emim][Trifluoroacetate],and [emim][Acetate] + [emim][Trifluoroacetate]mixture. *J. Chem. Eng. Data.***2009**, 54,108-114.

Sosa, C.;Andzelm, J.; Elkin, B.C.; Wimmer, E.; Dobbs, K.D.; Dixon,D.A. A local density functional study of the structure and vibrational frequencies of molecular transition-metal compounds. *J. Phys. Chem*. **1992**, 96, 6630-6636.

Spuhl.O.; Arlt. W. COSMO - RS Predictions in Chemical Engineering- A Study of the Applicability to Binary VLE. *Ind. Engg. Chem. Res.* **2004**, 43, 852-861.

Su, B.M.; Zhang, S.; Zhang, C. Structural elucidation of thiophene interaction with ionic liquids by Multinuclear NMR spectroscopy. *J. Phys. Chem. B*.**2004**, 108, 19510-19517.

Suezawa, H.; Hashimoto, T.; Tsuchinaga, K.; Yoshida, T.; Yuzuri, T.; Sakakibara, K.; Hirota, M.; Nishio. M. Electronic substituent effect on intramolecular CH/π interaction as evidenced by NOE experiments. *J. Chem. Soc. Perkin Trans*.**2000**, 2, 1-9.

Suezawa, H.; Ishihara, S.; Umezawa, Y.; Tsuboyama, S.; Nishio, S. The aromatic CH/π bond as an important factor in determining the relative stability of diastereomeric salts relevant to enantiomeric resolution –A Crystallographic Database study, *Eur.J. Org. Chem*, **2004**, 4816-4822.

Tai, L. S.; Sandler, S.I.A priori Phase Equilibrium Prediction from a segment Contribution Solvation Model. *Ind. Eng. Chem. Res* **2002**, 41,899-913.

Tomasi, J.; Persico, M. Molecular Interactions in Solution: An Overview of Methods Based on Continuous Distributions of the Solvent. *Chem. Rev*. 94, **1994**, 2027-2094

Webe, M.E.; Cataluna, R.; Samios, D.; Silva,R.D Addition of an azeotropic ETBE/ethanol mixture in eurosuper-type gasolines. *Fuel*. **2006**,85,2567-2577.

Won, B.D.; Park, S.; Han, K.; Kim, C. Liquid-liquid equlibria for Methanol + hexadecane + heterocyclic nitrogen-containing compounds at298.15K. *Fluid phase Equilibria*.**2002**, 193,217-227.

Xie, M.L.L.; .Reguillon, A.F.; Wang, X.X.;.Fu, X.; Vrinat, M.; Lemaire, M. Selective Extraction of Neutral Nitrogen-Containing Compounds from Straight-Run Diesel Feed Using Polymer-Supported Ionic Liquid Moieties. *Ind. Eng. Chem. Res*. **2009**,48,3973-3977.

Xie, M.L.L.; Reguillon, A.F.; Rostaing, S.P.; Wang, X.X.; Fu, X.; Estager, J.; Vrinat, M.; Lemaire, M. Selective Extraction and Identification of Neutral Nitrogen Compounds Contained in Straight-Run Diesel Feed Using Chloride Based Ionic Liquid. *Ind. Eng. Chem. Res*.**2008**, 47 8801-8807.

Zhou, J.; Mao, J.; Zhang, S. Ab initio calculations of the interaction between thiophene and ionic liquids. *Fuel Proc.Tech*. 2**008**, 89, 1456-1460.

Appendix 4.1
List of COSMO Files included in the CD

List of Cation and Anions

Cations:

1. 1-ethyl-3-methylimidazolium
2. 1-ethylpyridinium

3. 1-Ethyl-1-methylpyrrolidinium
4. 1-Ethyl-1-methylpiperidinium
5. 4-Ethyl-4-methylmorpholinium
6. 1,2,4-Trimethylpyrazolium

Anions:

1. Chlorine
2. Bromide
3. Nitrate
4. Thiocyanate
5. Acetate
6. Bisulphate
7. Tetrafluoroborate
8. Methylsulphonate
9. Trifluoroacetate
10. methyl sulphate
11. Hexafluorophosphate
12. Trifluoromethane sulphonate
13. Ethyl sulphate
14. Dimethylphosphate
15. Methylsulfonylacetamide
16. Tetracyanoborate
17. Salicylate
18. Bis(methylsulphonyl)amide
19. Bi-oxaloborate
20. Diethyl phosphate
21. Tosylate
22. P-Toluene sulphonate
23. Trifluoromethanesulphinate
24. Bis(trifluoromethylsulphonyl)amide
25. 2-(2-Methoxyethoxy)ethyl sulphate
26. Decanoate
27. Octylsulphate
28. Heptyl Sulphate

Appendix 4.1(Continued)

List of Aromatic Sulphur and Nitrogen Compounds

Aromatic Sulphur:

1. Thiophene
2. Benzothiophene
3. Dibenzothiophene

Aromatic Nitrogen

1. Pyrrole
2. Indole
3. Indoline
4. Carbazole
5. Benzocarbazole
6. Pyridine
7. Quinoline
8. Benzoquinoline

APPENDIX 4.2

Matlab Script for calculating Segment Activity Coefficient

```
function [area, volume, marea, molprofile] = readcosmo(molname, a_eff, flag)
```

```
% this m-file reads the cosmo file corresponding to molname and extracts the necessary information (cosmo
area, volume) and generates the sigma-profiles
% in this m-file cosmo data from two sources – Gaussian03

fid=fopen(['../database/g03/',char(molname),'.cosmo']);

% get the number of segments
while 1
   tline = fgetl(fid);
   %     if findstr(tline, 'nsph') >= 1
   if findstr(tline, 'fepsi') >= 1  % comment this if you wish to read Turbomole file
      numseg = fscanf(fid, '%s', [1, 1]);
      numseg = fscanf(fid, '%s', [1, 1]);% comment this if you wish to read Turbomole file
      numseg = fscanf(fid, '%d', [1, 1]);

      area = fscanf(fid, '%s', [1,1]);
      area = fscanf(fid, '%s', [1,1]);
      area = fscanf(fid, '%f', [1,1]);
      volume = fscanf(fid, '%s', [1,1]);
     volume = fscanf(fid, '%f', [1,1]);

      break;
   end
end

if flag == 0 % do not compute the profiles, read them
   fid=fopen([char(molname),'.prof'], 'r');
   molprofile = fscanf(fid,'%f',[2, 61]);
   molprofile = molprofile';
   molprofile = molprofile(:,2);
   marea = sum(molprofile);
   fclose(fid);

else    % recompute the profiles

   % read the information for all the segments into a matrix.
   while 1
      tline = fgetl(fid);
      if findstr(tline, '$segment_information')>=1
         for i=1:1:10
            tline = fgetl(fid);
         end
         A = fscanf(fid,'%f', [9, numseg]);
         A=A';
         %the real thing
         break;
      end
      if ~ischar(tline), break, end
   end
   fclose(fid);

   % prune first two columns from the matrix A
   for i=1:1:2
      A(:,1)=[];

   end
```

```
% now extract the coordinates (position) of the segments
coords = A;
for i=1:1:4
   coords(:,4)=[];
end
coords;
% now extract the areas of the segments
areas = A;
for i=1:1:4
   areas(:,1)=[];
end
areas(:,3)=[];
sigmaid = areas;
areas(:,2)=[];

% the "ideal" screening charge densities
sigmaid(:,1)=[];

% now compute the profiles
%~~~~~~~~~~~~~~~~~~~~~~~~~~~~~~~~~~~~~~~~~~~~~~~~~~~~~~~~~~~~~~~~~~~~~~~~~~~~
r_effsq=0.81;% averaging radius
sigma = []; % this will hold the SCDs neded to generate profiles
% ---------------------------------------------------------------
% Compute the radii^2 of the segments
risq = areas./pi;

% ---------------------------------------------------------------

% Compute the SCD for each segment
for i=1:numseg     % for each element
   %     elem_m = coords(i,:); % store the ith element coords
   %     elem_msig = sigmaid(i); % store the ideal screening charge of this element

   % compute all the d_ij
   d_ij = [];
   for ctr1 = 1:numseg
      d_ij=[d_ij ; norm(coords(i,:)-coords(ctr1,:))];
   end
   avgtemp = (r_effsq*risq./(risq+r_effsq)).*exp((-d_ij.^2)./(risq+r_effsq));

   numer = sigmaid.*avgtemp;
   sigma = [sigma; sum(numer)/sum(avgtemp)];
   %sigma = [sigma; (sum(numer)-numer(i))/(sum(avgtemp)-avgtemp(i))];
end
   % ---------------------------------------------------------------

% at this point we have SCDs and areas
% Now assuming : SCD range between -0.03 to 0.03

lowlim = -0.0305;
interwid = 0.001;
areanew = [];
for j=1:61
   upperlim = lowlim + interwid;
   areaelem = 0; % juz a reinitialization
```

```
        for i = 1:numseg
            if sigma(i) <= upperlim & sigma(i) > lowlim
                areaelem = areaelem + areas(i);
            end
        end
        areanew = [areanew; areaelem];
        lowlim = lowlim + interwid;
    end
    % areanew has the required histogram (profile)
    sigprof = -0.03:0.001:0.03;
    sigprof = [sigprof', areanew];
    marea = sum(sigprof(:,2));
    molprofile = sigprof(:,2);
    % This is to show the profile as a plot

    % axis([-0.03 0.03 0 25]);
    % hold on;
    % plot(sigprof(:,1),sigprof(:,2));
    %~~~~~~~~~~~~~~~~~~~~~~~~~~~~~~~~~~~~~~~~~~~~~~~~~~~~~~~~~~~~~~~~~~~~~~~~

    % now write the profile to a file
    fid=fopen([char(molname),'.prof'], 'w');
    fprintf(fid,'%6.3f  %12.8f\n',sigprof');
    fclose(fid);
end
```

APPENDIX4.3

Matlab Script for calculating Activity Coefficient

```
function f = activity(prof, molfr, marea, area, volume, T, aeff, flag)
% prof contains augmented profiles 'non-normalized' profiles
% Returns the activity coefficients
% flag = 0 if pure comp segact have not been computed
%      = 1 otherwise

sigmas = prof(:,1);
prof(:,1) = [];

% store prof in a temprof var
temprof = prof;

% get the number of components by the size of prof matrix
[cols,numcomps]=size(prof);

% ------------------------------------------------
% compute the profile for mixture (profmix)
% ------------------------------------------------
for i=1:numcomps
   prof(:,i)=prof(:,i).*molfr(i);
end
sumprof = zeros(61,1);
for i=1:numcomps
   sumprof = sumprof + prof(:,i);
end
numr = sumprof;
denr = sum(molfr.*marea');
profmix = [sigmas numr./denr];

% ------------------------------------------------------------
% Call segact to compute the segment activities for mixture
% ------------------------------------------------------------

lngammamix = segact(profmix, T);

% restore prof
prof = temprof;

% ------------------------------------------------------------
% Call segact to compute the segment activities for pure ones
% ------------------------------------------------------------
% check if these have already been computed
if flag==0
   lngamma = [];
   for i=1:numcomps
      lngamma = [lngamma segact([sigmas prof(:,i)./marea(i)], T)];
   end
   fid1=fopen('tempp.bin','w');
   fwrite(fid1, lngamma, 'real*4');
   fclose(fid1);
elseif flag == 1
   % read them from the file
   fidtemp = fopen('tempp.bin', 'r');
```

```
    lngamma = fread(fidtemp,[61, 2*numcomps], 'real*4');
    fclose(fidtemp);
end


lngami = zeros(numcomps,1);
for i=1:numcomps
    lngammaone = zeros(61,1);
    for j=1:61
        lngammaone(j) = (prof(j,i)/marea(i))*(lngammamix(j,2)-lngamma(j,2*i));
    end
    lngami(i) = marea(i)*sum(lngammaone)/aeff;

end
lngami;
% get the Stavermann-Guggenheim term
r = volume./66.69;
q = area./79.53;
lnsg = sg(molfr', r, q);

f = exp(lngami'+lnsg);
```

5.1 Introduction

In our earlier Chapter 4 using **CO**nductor **L**ike **S**creening **M**odel for **R**eal **S**olvent (**COSMO-RS**) [Anantharaj et al.,2010b,2011a] prediction, we found that a smaller cation with acetate anion have significant influence on catalytic deactivated compounds when it is investigated in terms of selectivity, capacity and performance index. Keeping the predictions in mind,we have chosen the four Ionic Liquids namely [EMIM][OAc], [EMIM][$EtSO_4$], [EMIM][$MeSO_3$] and [EMIM][SCN] for binary studies (Table 5.1). Bowron et al.,[2010] reported that the [EMIMI][OAc] ionic liquid have effective ionic charges in liquid phase at 323K via molecular dynamics and neutron diffraction studies. [EMIMI][OAc] is also a good candidate for biomass dissolution and also has a potential to absorb CO_2 from different resources [Dhumal et al., 2009]. Although experimental data are available for imidazolium based cation with organic /inorganic species at several temperatures [Garcia et al., 2010; Arce et al., 2006], however the desired physiochemical data with [EMIMI][OAc] ionic liquid is unavailable.

In the following section we have measured the densities, surface tension and refractive index of pure IL pyrrole (PYRR), pyridine(PY), indoline (INDO), quinoline(QU), thiophene(TS), and water over the whole mole fraction of IL. Further binary mixture of IL with catalyst deactivated compounds such as: IL (1) + PY(2), IL(1) + PYRR(2), IL (1) + QU(2), IL (1) + INDO (2) , IL(1) + TS (2), IL (1) + Water (2) has also been studied over the entire mole fraction of IL (1) at T = (298.15- 323.15) K and atmospheric pressure. The excess molar volumes for similar systems are calculated from measured densities values at temperatures (298.15 to 323.15) K. In a similar fashion surface tension and refractive index deviation have been calculated from measured values over the entire mole fraction of IL at T=298.15K .

5.2 Experimental section

5.2.1 Materials

1-ethyl-3-methylimidazolium acetate [EMIM][OAc] ($C_8H_{16}N_2O_3S$), 1-ethyl-3-methylimidazolium ethylsulphate [EMIM][$EtSo_4$] ($C_8H_{16}N_2O_4S$),

1-ethyl-3-methylimidazolium methanesulphonate [EMIM][$MeSO_3$] ($C_8H_{16}N_2O_3S$) and1-ethyl-3-methylimidazolium thiocyanate [EMIM][SCN] ($C_7H_{11}N_3S$) ionic liquid were purchased from Fluka with a purity of > 95 % . A water content of 0.044% in [EMIM][OAc] , 0.058% in [EMIM][$EtSO_4$], 0.078% in [EMIM][$MeSO_3$] and 0.044% in [EMIM][SCN] were assessed by Karl Fischer titrator (KF 787,Metrohm) . Pyrrole (C_4H_5N) and indoline (C_8H_9N) were supplied from Spectrochem, India with mass fractions of 99 % each. Pyridine (C_5H_5N), quinoline (C_9H_7N) and thiophene (C_4H_4S) were received from Sigma Aldrich with mass fractions greater than 98%, and were used without further purification.

5.2.2. Apparatus and procedure

Densities of the pure components and binary mixture were measured at atmospheric pressure with Anton Paar DSA-4500MA digital vibrating U-tube densimeter. The densitometer has thermoelectric temperature control system. The uncertainty in the density measurement is ± 0.0011 $g.cm^{-3}$.The apparatus was calibrated by measuring the density of Millipore quality water and ambient air. The surface tension of the pure components and binary mixtures were measured with a tensiometer by plate type method (Hanging drop tensiometer method, kruss k9, Germany) with a precision of 0.01mN/m.The apparatus was calibrated by measuring the surface tension of Millipore quality water at ambient temperature.Refractive index of the pure components and binary mixtures were determined at ambient temperature using an automatic refractometer AD-13 model (ABBEMAT-WR Dr.Kernchen), with an uncertainty of ± 0.00004.

Samples were prepared by transferring known mass of the pure liquids into stoppered bottles via syringe. The stoppered bottles are closed with screw caps to seal and prevent evaporation. All weighing was carried out in a balance (Mettler Toledo AT 261) with an accuracy of ± 10^{-4} gm. Previous experiments [Kumar et al., 2009] showed that equilibrium was attained after 6 hours of stirring at100 rpm at temperature at 298.15 K, using circulating water bath along with automatic controller. Equilibrium was attained by keeping the mixture settled for 12 hours during which good contact was obtained between

two pure components .Samples from the homogeneous mixture was withdrawn using syringes for the thermodynamic phase behavior studies. All the samples were prepared immediately prior to performing density, surface tension and refractive index measurements so as to prevent variation in composition due to water/air retention via the hygroscopic IL.

Table 5.1: Name and structure of the studied ionic liquid

S.No	Name	Structure	Acronym	Mole. for	Mol.wt (g/mole)	CASRN[a]	Density (g/cm^3)	Appearance
01	1-Ethyl-3-methylimidazolium acetate		[EMIM][OAc]	$C_8H_{14}N_2O_2$	170.11	143314-17-4	1.027	liquid
02	1-Ethyl-3-methylimidazolium ethylsulphate		[EMIM][$EtSO_4$]	$C_8H_{16}N_2O_4S$	236.29	342573-75-5	1.24	liquid
03	1-Ethyl-3-methylimidazolium methanesulfonate		[EMIM][$MeSO_3$]	$C_7H_{14}N_2O_3S$	206.26	145022-45-2	1.247	liquid
04	1-Ethyl-3-methylimidazolium thiocyanate		[EMIM][SCN]	$C_7H_{11}N_3S$	169.25	143314-17-4	1.027	liquid

[a] CASRN, Chemical Abstracts Service Registry Number

Table 5.2: Comparison of measured Density ρ as a function of temperature with reported data

	T (K) 298.15	303.15	308.15	313.15	318.15	323.15
	ρ (g cm^{-3})					
[EMIM][OAc]						
Measured	1.0974	1.0946	1.0916	1.0886	1.0855	1.0825
Reported	NA	NA	NA	NA	NA	NA
[EMIM][$EtSO_4$]						
Measured	1.2345	1.2313	1.2279	1.2246	1.2213	1.2179
Reported	1.2423[a]	1.2388[a]	1.2354[a]	1.2319[a]	1.2285[a]	1.2251[a]
[EMIM][$MeSO_3$]						
Measured	1.2345	1.2313	1.2279	1.2246	1.2213	1.2179
Reported	1.2437[b]	NA	NA	NA	NA	NA
[EMIM][SCN]						
Measured	1.2345	1.2313	1.2279	1.2246	1.2213	1.2179
Reported	NA	NA	NA	NA	NA	NA
Pyridine (PY)						
Measured	0.9783	0.9732	0.9682	0.9631	0.9581	0.9581
Reported	0.9780[c]	NA	NA	NA	NA	NA
Pyrrole (PYRR)						
Measured	0.9655	0.9611	0.9568	0.9524	0.9479	0.9436
Reported	0.9733[c]	NA	NA	NA	NA	NA
Quinoline (Qu)						
Measured	1.0883	1.0843	1.0804	1.0764	1.0724	1.0685
Reported	1.0929[c]	NA	NA	NA	NA	NA
Indoline (INDO)						
Measured	1.0883	1.0843	1.0804	1.0764	1.0724	1.0685
Reported	NA	NA	NA	NA	NA	NA
Thiophene (TS)						
Measured	1.0584	1.0525	1.0465	1.0405	1.0344	1.0284
Reported	1.0585[d]	NA	NA	NA	NA	NA
Water						
Measured	0.9971	0.9957	0.9939	0.9918	0.9879	0.9849

Reported	0.9971[e]	0.9956[f]	0.9941[f]	0.9922[f]	0.9902[f]	NA

[a]Ref.[Krummen et al.,2002]; [b] Ref. [Alonso et al.,2006]; [c]Ref. [Won et al., 2000]; [d]Ref.[Yanfang et al.,2008]; [e]Ref. [Gomez et al., 2006];[f]Ref.[Kell et al.,1967]; NA-Not Available

Table 5.3: Surface tension σ and Refractive index *nD* for pure compounds of the binary system studied in this work at 298.15K and atmospheric pressure

	σ(mN.m^{-1})		*nD*	
	Present study	Literature value	Present study	Literature value
[EMIM][OAc]	36.5	NA	1.4771	NA
[EMIM][$EtSO_4$]	48.4	46.96[a]	1.4771	1.4794[a]
[EMIM][$MeSO_3$]	45.1	NA	1.4771	1.4955[a]
[EMIM][SCN]	43.1	NA	1.5377	NA
Pyridine (PY)	37.5	NA	1.5013	NA
Pyrrole (PYRR)	41.7	NA	1.4884	NA
Quinoline (QU)	46.5	NA	1.4997	NA
Indoline (INDO)	32.6	NA	1.5867	NA
Thiophene (TS)	31.7	NA	1.5271	1.5255[c,e]
Water	72.1	71.1[b]	1.3357	NA

[a]Ref.[Gomez et al.,2006]; [b]Ref.[Alonso et al.,2006]; [c]Ref. [Sapi et al., 2006a]; [e]Ref. [Sapi et al., 2006b]; NA-Not available

5.3. Results and Discussion

Experimental densities of pure IL aromatic nitrogen, aromatic sulphur species and water have been measured and benchmarked at different temperatures (Table 5.2). Beside the effect of temperature and experimental method, the presence of trace amount of impurities such as water or ions can have a remarkable effect on thermodynamic properties [Yangfang et al.,2008].Table 5.2 shows the comparison of measured densities for pure [EMIM][OAc] with temperature. This agrees well with the reported values [Sapi et al., 2006a, 2006b; Won et al., 2002]. Table 5.2 shows the comparison between experimental and literature data of the pure aromatic nitrogen/ sulphur, and water at 298.15 K. A comparison with the ILs could not be made because of the absence of experimental data. The density ρ of pure ionic liquid is higher than that of water, and also than that of aromatic nitrogen/sulphur compounds. Table 5.3 shows a comparison of

surface tension σ and refractive index nD of pure components with literature data at 298.15 K. The difference between experimental and literature data for pure [EMIM][OAc] can be explained by the thermodynamic properties which strongly depends on water and other impurities[Gonzalez et al.,2006]. Now let us discuses the binary properties of IL's one by one in the subsequent sections.

5.3.1 1-Ethyl-3-Methylimidazolium Acetate {[EMIM][OAc]}

5.3.1.1 Experimental Data

Experimental densities over the entire composition range for [EMIM][OAc] (1) + PY(2)(Table 5.4(a)), [EMIM][OAc] (1) + PYRR(2) (Table 5.4(b)), [EMIM][OAc] (1) + QU(2) (Table 5.4(c)), [EMIM][OAc] (1) + INDO(2) (Table 5.4(d)), [EMIM][OAc] (1) + TS(2) (Table 5.4(e)) and [EMIM][OAc] (1) + water(2) (Table 5.4(f)) have been determined at temperature T =(298.15 to 323.15) K. The surface tension σ, and refractive index nD of the pure component and its mixtures were determined at 298.15 K over the entire composition range of [EMIM][OAc] (1). Additionally we have studied the binary mixtures of [EMIM][OAc] (1) + water (2) over the entire mole fraction of ILs, which is more helpful in the purification and regeneration of [EMIM][OAc].

Table 5.4(a): Experimental Density ρ and Excess molar volume V_m^E for the binary system [EMIM][OAc] (1) + Pyridine (2)

x_{IL}	ρ g cm^{-3}	V_m^E cm^3 mol^{-1}	ρ g cm^{-3}	V_m^E cm^3 mol^{-1}	ρ g cm^{-3}	V_m^E cm^3 mol^{-1}
	T= 298.15K		T=303.15K		T= 308.15K	
0.2	1.0309	-0.0300	1.0268	-0.0260	1.0226	-0.0220
0.3	1.0470	-0.0455	1.0431	-0.0417	1.0393	-0.0380
0.4	1.0561	-0.0545	1.0524	-0.0509	1.0488	-0.0473
0.5	1.0643	-0.0627	1.0608	-0.0593	1.0573	-0.0558
0.6	1.0751	-0.0733	1.0718	-0.0701	1.0685	-0.0668
0.7	1.0819	-0.0804	1.0787	-0.0772	1.0755	-0.0740
0.8	1.0872	-0.0861	1.0844	-0.0833	1.0813	-0.0802

	T=313.15K		*T*= 318.15K		*T*=323.15K	
0.2	1.0186	-0.0180	1.0145	-0.0141	1.0104	-0.0101
0.3	1.0354	-0.0343	1.0316	-0.0305	1.0278	-0.0268
0.4	1.0452	-0.0438	1.0415	-0.0402	1.0379	-0.0367
0.5	1.0538	-0.0524	1.0503	-0.0489	1.0468	-0.0455
0.6	1.0652	-0.0635	1.0618	-0.0603	1.0586	-0.0570
0.7	1.0723	-0.0709	1.0691	-0.0677	1.0659	-0.0645
0.8	1.0781	-0.0771	1.0750	-0.0739	1.0719	-0.0708

Table 5.4(b): Experimental Density ρ and Excess molar volume V_m^E for the binary system [EMIM][OAc] (1) + Pyrrole (2)

x_{IL}	ρ g cm^{-3}	V_m^E cm^{3}mol^{-1}	ρ g cm^{-3}	V_m^E cm^3 mol^{-1}	ρ g cm^{-3}	V_m^E cm^{3}mol^{-1}
	T= 298.15K		*T*=303.15K		*T*= 308.15K	
0.2	1.0226	-0.0219	1.0190	-0.0184	1.0154	-0.0149
0.3	1.0415	-0.0399	1.0380	-0.0366	1.0345	-0.0332
0.4	1.0532	-0.0512	1.0499	-0.0482	1.0464	-0.0449
0.5	1.0638	-0.0615	1.0607	-0.0588	1.0574	-0.0556
0.6	1.0733	-0.0708	1.0704	-0.0685	1.0673	-0.0655
0.7	1.0812	-0.0789	1.0783	-0.0766	1.0752	-0.0735
0.8	1.0842	-0.0832	1.0811	-0.0801	1.0780	-0.0770
	T=313.15K		*T*= 318.15K		*T*=323.15K	
0.2	1.0117	-0.0114	1.0081	-0.0078	1.0045	-0.00438
0.3	1.0310	-0.0299	1.0275	-0.0265	1.0241	-0.02319
0.4	1.0430	-0.0415	1.0396	-0.0382	1.0363	-0.035
0.5	1.0541	-0.0524	1.0509	-0.0492	1.0476	-0.04608
0.6	1.0642	-0.0624	1.0610	-0.0592	1.0578	-0.05615
0.7	1.0721	-0.0704	1.0689	-0.0673	1.0945	-0.08989
0.8	1.0749	-0.0739	1.0718	-0.0709	1.0687	-0.06783

Table 5.4(c): Experimental Density ρ and Excess molar volume V_m^E for the binary system [EMIM][OAc] (1) + Quinoline (2)

x_{IL}	ρ	V_m^E	ρ	V_m^E	ρ	V_m^E
	g cm^{-3}	cm^3 mol^{-1}	g cm^{-3}	cm^{3}mol^{-1}	g cm^{-3}	cm^{3}mol^{-1}
	T= 298.15K		*T*=303.15K		*T*= 308.15K	
0.2	1.0771	-0.0780	1.0734	-0.0743	1.0697	-0.0705
0.3	1.0844	-0.0849	1.0810	-0.0815	1.0775	-0.0779
0.4	1.0873	-0.0877	1.0840	-0.0844	1.0807	-0.0810
0.5	1.0913	-0.0914	1.0880	-0.0881	1.0847	-0.0848
0.6	1.0923	-0.0924	1.0892	-0.0893	1.0861	-0.0861
0.7	1.0945	-0.0945	1.0915	-0.0915	1.0884	-0.0884
0.8	1.0955	-0.0955	1.0925	-0.0925	1.0894	-0.0894
	T=313.15K		*T*= 318.15K		*T*=323.15K	
0.2	1.0660	-0.0668	1.0622	-0.0630	1.0585	-0.0592
0.3	1.0740	-0.0744	1.0705	-0.0709	1.0670	-0.0674
0.4	1.0773	-0.0776	1.0739	-0.0742	1.0705	-0.0708
0.5	1.0813	-0.0814	1.0779	-0.0780	1.0746	-0.0746
0.6	1.0829	-0.0830	1.0797	-0.0798	1.0766	-0.0766
0.7	1.0853	-0.0852	1.0822	-0.0821	1.0791	-0.0790
0.8	1.0864	-0.0863	1.0833	-0.0833	1.0802	-0.0802

Table 5.4(d): Experimental Density ρ and Excess molar volume V_m^E for the binary system [EMIM][OAc] (1) + Indoline (2)

x_{IL}	ρ	V_m^E	ρ	V_m^E	ρ	V_m^E
	g cm^{-3}	cm^{3}mol^{-1}	g cm^{-3}	cm^{3}mol^{-1}	g cm^{-3}	cm^{3}mol^{-1}
	T= 298.15K		*T*=303.15K		*T*= 308.15K	
0.2	1.0960	-0.0955	1.0923	-0.0918	1.0886	-0.0881
0.3	1.0966	-0.0961	1.0930	-0.0925	1.0894	-0.0889
0.4	1.0998	-0.0991	1.0964	-0.0957	1.0929	-0.0922
0.5	1.1011	-0.1004	1.0978	-0.0970	1.0944	-0.0937
0.6	1.0009	-0.0010	1.0976	-0.0970	1.0943	-0.0937
0.7	1.1010	-0.1005	1.0979	-0.0973	1.0946	-0.0941
0.8	1.1000	-0.0996	1.0970	-0.0966	1.0938	-0.0934
	T=313.15K		*T*= 318.15K		*T*=323.15K	

0.2	1.0850	-0.0845	1.0813	-0.0808	1.0777	-0.0772
0.3	1.0858	-0.0854	1.0823	-0.0818	1.0787	-0.0783
0.4	1.0894	-0.0888	1.0860	-0.0853	1.0825	-0.0819
0.5	1.0910	-0.0903	1.08773	-0.0870	1.0843	-0.0837
0.6	1.0910	-0.0904	1.08771	-0.0871	1.0844	-0.0838
0.7	1.0914	-0.0909	1.08826	-0.0877	1.0850	-0.0845
0.8	1.0907	-0.0903	1.08756	-0.0871	1.0844	-0.0840

Table 5 .4(e): Experimental Density ρ and Excess molar volume V_m^E for the binary system [EMIM][OAc] (1) + Thiophene (2)

x_{IL}	ρ	V_m^E	ρ	V_m^E	ρ	V_m^E
	g cm^{-3}	cm^{3}mol^{-1}	g cm^{-3}	cm^{3}mol^{-1}	g cm^{-3}	cm^{3}mol^{-1}
	T= 298.15K		T=303.15K		T= 308.15K	
0.2	1.0865	-0.0849	1.0847	-0.0829	1.0804	-0.0785
0.3	1.0976	-0.0951	1.0937	-0.0912	1.0897	-0.0872
0.4	1.1016	-0.0990	1.0980	-0.0954	1.0943	-0.0918
0.5	1.1027	-0.1004	1.0992	-0.0969	1.0957	-0.0933
0.6	1.0993	-0.0977	1.0960	-0.0944	1.0927	-0.0911
0.7	1.0986	-0.0975	1.0954	-0.0942	1.0921	-0.0909
0.8	1.0981	-0.0974	1.0951	-0.0943	1.0919	-0.0911
	T=313.15K		T= 318.15K		T=323.15K	
0.2	1.0761	-0.0742	1.0718	-0.0699	1.0675	-0.0657
0.3	1.0857	-0.0832	1.0817	-0.0793	1.0777	-0.0753
0.4	1.0907	-0.0881	1.0871	-0.0845	1.0834	-0.0809
0.5	1.0921	-0.0898	1.0886	-0.0863	1.0850	-0.0827
0.6	1.0894	-0.0878	1.0861	-0.0844	1.0828	-0.0811
0.7	1.0888	-0.0876	1.0855	-0.0843	1.0823	-0.0810
0.8	1.0886	-0.0879	1.0854	-0.0846	1.0823	-0.0815

Table 5. 4(f): Experimental Density ρ and Excess molar volume V_m^E for the binary system [EMIM][OAc] (1) + water (2)

x_{IL}	ρ	V_m^E	ρ	V_m^E	ρ	V_m^E
	g cm^{-3}	cm^{3}mol^{-1}	g cm^{-3}	cm^{3}mol^{-1}	g cm^{-3}	

	cm^3mol^{-1}					
	T= 298.15K		*T*=303.15K		*T*= 308.15K	
0.2	1.0038	-0.0038	1.0659	-0.0627	1.0623	-0.0594
0.3	1.1002	-0.0936	1.0970	-0.0906	1.0937	-0.0876
0.4	1.1009	-0.0950	1.0978	-0.0923	1.0948	-0.0895
0.5	1.1050	-0.0995	1.1020	-0.0968	1.0990	-0.0939
0.6	1.1041	-0.0997	1.1012	-0.0969	1.0982	-0.0941
0.7	1.1033	-0.0999	1.1004	-0.0972	1.0976	-0.0944
0.8	1.1020	-0.0998	1.0992	-0.0970	1.0962	-0.0941
	T=313.15K		*T*= 318.15K		*T*=323.15K	
0.2	1.0591	-0.0564	1.0583	-0.0555	1.0581	-0.0551
0.3	1.0904	-0.0846	1.0870	-0.0814	1.0837	-0.0783
0.4	1.0916	-0.0865	1.0884	-0.0834	1.0852	-0.0804
0.5	1.0959	-0.0910	1.0928	-0.0880	1.0897	-0.0851
0.6	1.0953	-0.0913	1.0923	-0.0884	1.0893	-0.0855
0.7	1.0946	-0.0915	1.0916	-0.0886	1.0885	-0.0857
0.8	1.0932	-0.0911	1.0900	-0.0880	1.0872	-0.0853

5.3.1.2 Volume Expansivity " α"

The coefficient of thermal expansion of the [EMIM][OAc] $\boldsymbol{\alpha}$ is shown in Figure 1.The densities of pure [EMIM][OAc], which decreases linearly (R^2=0.999) while the densities of water increases linearly (R^2 = 0.965) with increasing temperature. The value of $\boldsymbol{\alpha}$ = 0.097K^{-1} (ionic liquid) and $\boldsymbol{\alpha}$ = 0.004K^{-1} for water was calculated from Equation 5.1.

(5.1)

Where V is the molar volume of the pure fluid, ρ is the density of the pure fluid and subscript P indicates constant pressure. The volume expansivity of [EMIM][OAc] and water was calculated using the measured density observed at different temperatures. As compared to water, the volume expansivity of [EMIM][OAc] was found to be independent of temperature (Figure 5.1). These observations are more consistent with the

reports of Rodriguez et al.[2006], Wandschneider et al.[2008] and Pererio et al.[2006,2007].

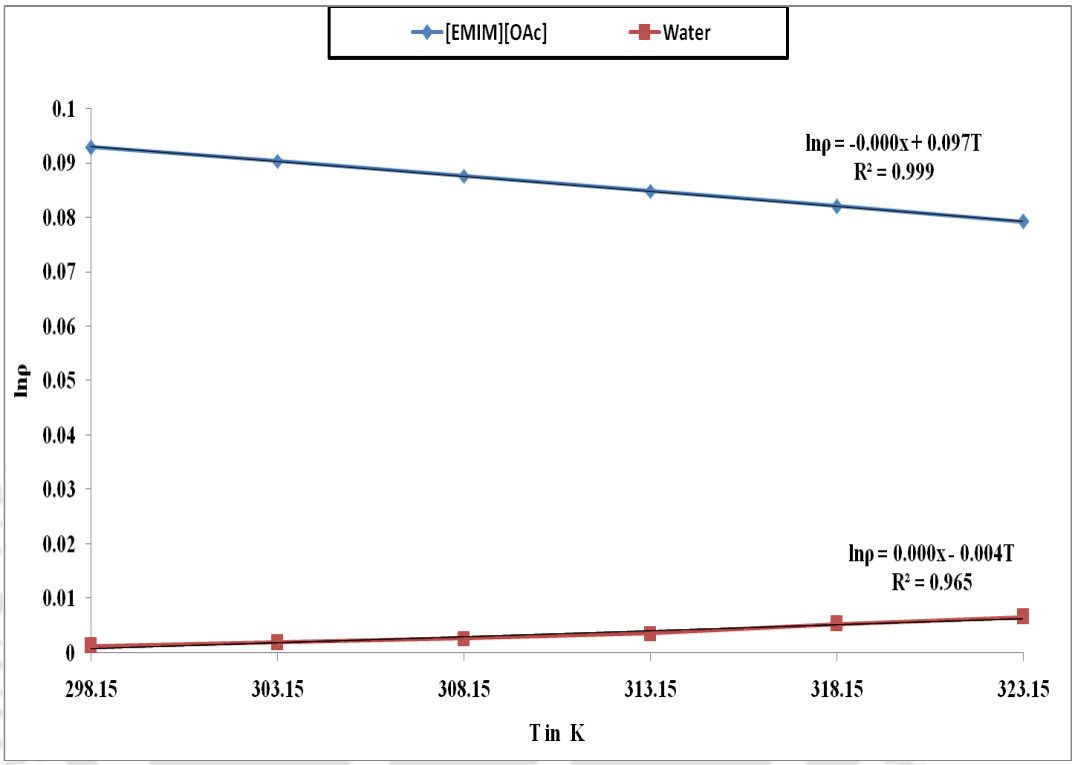

Figure 5.1: Plot of experimental values of lnρ of the pure [EMIM][OAc] ionic liquid Vs temperature of (298.15 to 323.15) K

5.3.1.3 Effect of Density

Figure 5.2 shows the experimental densities of pure [EMIM][OAc], aromatic nitrogen, aromatic sulphur and water at temperatures of T = (298.15to 323.15) K. It can be seen that the density of all the pure components including ionic liquid decreases linearly with increasing temperature. Table 5.4(a) to 5.4(f) shows the experimental densities for six binary systems studied as a function of temperature over the entire mole fraction of [EMIM][OAc]. For all the compounds with ILs, the density varies linearly with an increasing temperature over the whole composition range. This behavior can be explained by the efficient structural interaction of [EMIM][OAc] with aromatic structure of nitrogen/sulphur and water via packing effects[Domanska et al.,2007,2008]. It can also be a result of the smaller size of cation [Kumar et al., 2009] and anion, thereby providing better interaction with aromatic structure of nitrogen/sulphur and water. A small size of IL molecule is known to have a significant influence in changing densities of the mixture with increasing temperature for entire mole fraction of IL [Kumar et al., 2009]. Besides that the hydrogen bond strongly depends on the temperature [Yanfang et al., 2008] as compared to CH---π bond interaction [Acharya et al., 2003;Suezawa et al.,2000,2003] and π---π stacking [Domanska et al.,2007,2008].These behaviors are consistent with the studies carried out by Rodriguez et al. [2006] and Domanska et al., [2007,2008].

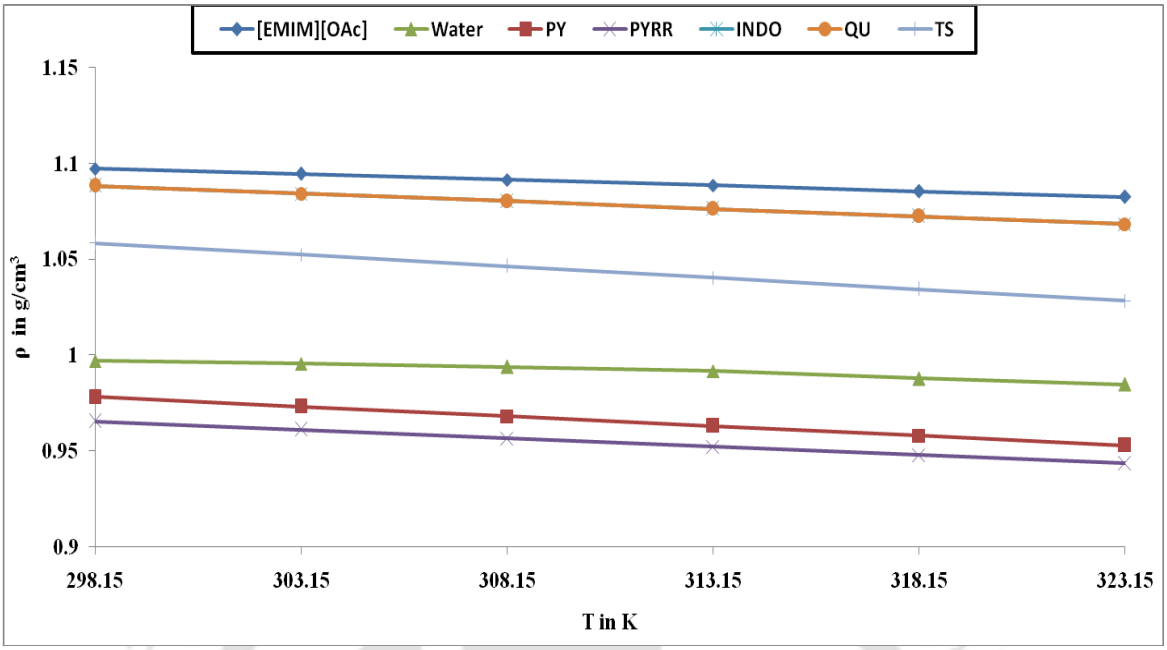

Figure 5.2: Density ρ of pure [EMIM][OAc], water , aromatic nitrogen (pyridine, pyrrole, indoline, quinoline) and aromatic sulphur (thiophene) at T = (298.15 to 323.15) K

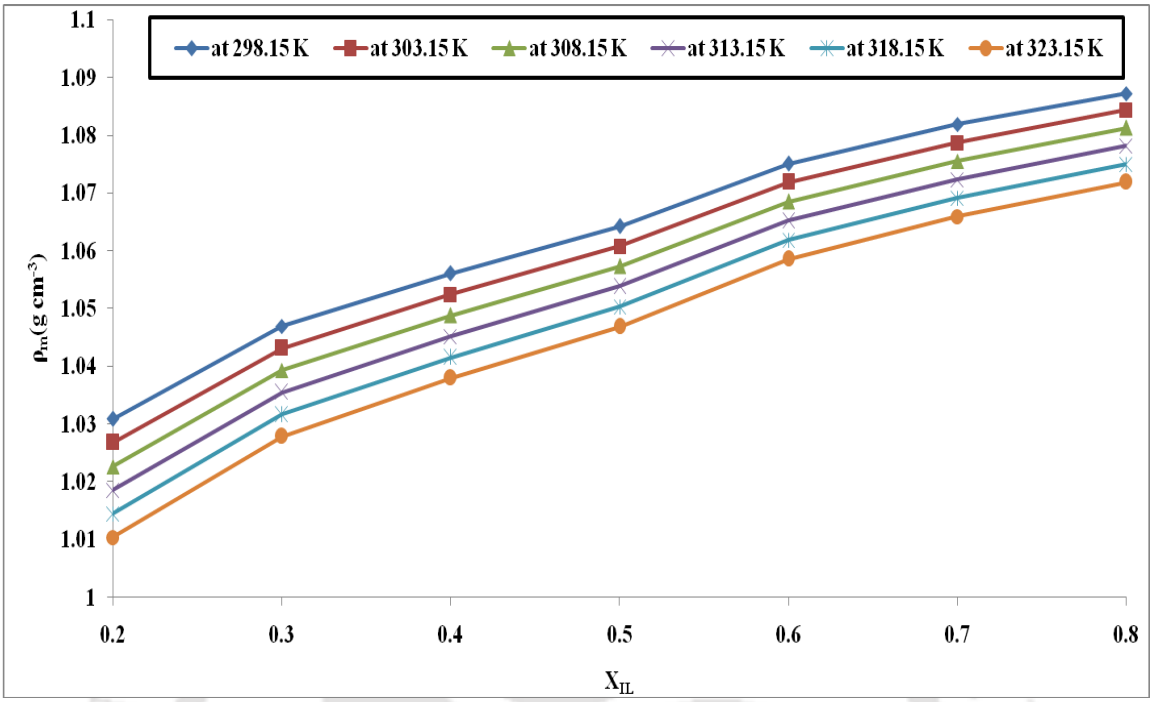

Figure 5.3: Experimental density for the binary system {[EMIM][OAc] (1) + Pyridine (2)} as a function of mole fraction of the IL at different temperature

The measured density of binary mixtures over the entire mole fraction of [EMIM][OAc] at several temperature are presented in Tables 5.4(a) to 5.4(f) . The binary mixture of [EMIM][OAc](1)+pyrridine(2) systems shows (Figure 5.3) that with increasing mole fraction of [EMIM][OAc](1), the density increases upon mixing because of the stronger association between the similar aromatic structure of molecules in liquid phase. On the other hand there are many possibilities in [EMIM][OAc] to interact with aromatic or non aromatic structure compounds such as: 1).CH- - -π bond interaction [Anantharaj et al., 2010a, 2011b; Acharya et al., 2003;Suezawa et al.,2000,2003]; 2).π---π stacking [Anantharaj et al., 2010a, 2011b;Domanska et al.,2010]; and 3). n--π bond interaction [Anantharaj et al., 2010a, 2011b], where n =N, O, F and S element or atom which are related to aromatic/non aromatic structure of nitrogen/sulphur and/or ionic liquid structure. Therefore the measured density of binary mixture for all the systems (Tables 5.4(a) to 5.4(f)) shows similar trend upon mixing including water (Table

5.4(f)).However for [EMIM][OAc] (1)+ thiophene (2) system, a similar trend from x_{IL} =0.2 to x_{IL} =0.5 is seen which remains constant (up to x_{IL} =0.8) while increasing the mole fraction of [EMIM][OAc]. It can be easily observed that the ratio of ILs and aromatic/non aromatic structure of molecules are important for the effective removal of such compounds using [EMIM][OAc].

5.3.1.4 Effect of Surface tension

The measured surface tension data for all the studied systems are listed in Table 6 and are shown in Table 5.5. At x_{IL} =0.2 the surface tension of [EMIM][OAc] (1) + pyrrole is highest as compared to [EMIM][OAc] (1)+pyridine, [EMIM][OAc](1) + thiophene, [EMIM][OAc](1) + indoline (2) and [EMIM][OAc](1) + quinoline (2).Besides that the strong association or interaction, other interactions namely CH---π bond interaction [Anantharaj et al., 2010a, 2011b; Acharya et al., 2003;Suezawa et al.,2000,2003],electrostatic force, π---π stacking [Anantharaj et al., 2010a, 2010b,2011b;Domanska et al.,2010], n--π bond interaction [Anantharaj et al., 2010a, 2010b,2011b], hydrogen bond and van der Walls force also plays an important role in deciding the extraction capacity. The strength of van der Waals force is also effective in deciding the surface tension.

From Table 5.5, it is clear that the addition of the fused ring to nitrogen heterocyclic results in a lower value of surface tension as compared to pyrrole (indoline) or pyridine (quinoline). It is a well known fact that the strength of CH--π bond interaction and hydrogen bond interaction increases upon mixing with increasing mole fraction of [EMIM][OAc] at T=298.15K .For [EMIM][OAc] (1) + pyridine(2), [EMIM][OAc] (1) + indoline(2), [EMIM][OAc] (1) + quinoline(2) and [EMIM][OAc] (1) + thiophene(2) shows a linear increase in surface tension with increasing mole fraction of IL. Among the five systems the [EMIM][OAc] (1) + thiophene (2) mixture has higher surface tension because the structure of thiophene is similar to [EMIM] cations in which the sulphur atom is located in the thiophene structure having more acidity [Joule et al.,2007]. The dissimilar structure of pyridine, indoline and quinoline with [EMIM][OAc] have higher

surface tension as compared to water. This is due to lone pair of nitrogen atom is completely delocalized around the aromatic structure of π electron cloud which has a significant influence upon mixing. It can be seen in Table 5.5, the surface tension increases in the order of:

Thiophene > Pyridine > Quinoline > Pyrrole > Indoline > Water

It means that the increasing the mole fraction of [EMIM][OAc] causes to decrease the strength of sterical hindrance possed by either dissimilar molecules or addition of benzene ring in pyrrole or pyridine structure. It can be seen that the six membered hetercycle posses higher surface tension as compared to five membered heterocycle.Thus from a separation point of view thiophene will be the most easiest to remove from the IL phase. The van der Waals force between the ethyl substitution on the [EMIM] and the aromatic structure of nitrogen/sulphur is negligible when compared to CH--π bond interaction, π--π stacking and other specific interactions. Further the similar or dissimilar aromatic structures of molecules when mixed together, decreases the interaction between [EMIM] cation and [OAc] anion while the CH--π bond, π--π stacking and dispersion forces dominates the systems having similar or dissimilar aromatic structure of molecules [Gupta et al.,2005].

Table 5.5: Experimental surface tension σ and deviation of surface tension for the Binary systems: (a). [EMIM][OAc]+ Pyridine, (b). [EMIM][OAc]+ Pyrrole, (c). [EMIM][OAc]+ Indoline, (d). [EMIM][OAc]+ Quinoline, (e). [EMIM][OAc]+ Thiophene, and (f) .[EMIM][OAc]+ Water at 298.15K.

x_{IL}	[EMIM] [OAc]+ PY		[EMIM] [OAc]+ PYRR		[EMIM] [OAc]+ QU	
	σ (mN m^{-1})	$\Delta\sigma$ (mN m^{-1})	σ (mN m^{-1})	$\Delta\sigma$ (mN m^{-1})	σ (mN m^{-1})	$\Delta\sigma$ (mN m^{-1})
0.2	29.9	-7.4	34.2	-6.46	34.2	-10.3
0.3	31.2	-6	34.2	-5.94	36.2	-7.3
0.4	37	-0.1	38.2	-1.42	37.3	-5.2
0.5	41.8	4.8	39.1	0	39.5	-2
0.6	42.4	5.5	39.9	1.32	41	0.5
0.7	43	6.2	40.8	2.74	41.7	2.2
0.8	45.8	9.1	41.7	4.16	42.9	4.4
	[EMIM] [OAc]+ INDO		[EMIM] [OAc]+ TS		[EMIM] [OAc]+ WATER	

x_{IL}	σ (mN m^{-1})	$\Delta\sigma$ (mN m^{-1})	σ (mN m^{-1})	$\Delta\sigma$ (mN m^{-1})	σ (mN m^{-1})	$\Delta\sigma$ (mN m^{-1})
0.2	31.2	-2.18	32.6	-0.06	32.6	-31.5
0.3	36.8	3.03	38.1	4.96	32.9	-22.3
0.4	37.7	3.54	43.1	9.48	35.8	-19.3
0.5	37.7	3.15	44	9.9	36.5	-16.3
0.6	40.3	5.36	44.6	10.02	36.5	-10.9
0.7	41.9	6.57	44.8	9.74	37.5	-8
0.8	42.4	6.68	45.1	9.56	41.9	-5

Table 5.6: Experimental refractive index nD and deviation of refractive index ΔnD for the Binary systems: (a). [EMIM][OAc]+ Pyridine, (b). [EMIM][OAc] + Pyrrole, (c). [EMIM][OAc]+ Indoline, (d). [EMIM][OAc]+ Quinoline, (e). [EMIM][OAc]+ Thiophene, and (f). [EMIM][OAc] + Water at 298.15K.

	[EMIM] [OAc]+ PY		[EMIM] [OAc]+ PYRR		[EMIM] [OAc]+ QU	
x_{IL}	*nD*	*ΔnD*	*nD*	*ΔnD*	*nD*	*ΔnD*
0.2	1.5000	-0.0020	1.4917	2E-05	1.5823	0.0815
0.3	1.4920	-0.0103	1.4870	-0.0063	1.5960	0.0810
0.4	1.3971	-0.1056	1.4869	-0.0080	1.5643	0.0942
0.5	1.3928	-0.1102	1.4862	-0.0104	1.5553	0.0620
0.6	1.3821	-0.1213	1.4860	-0.0122	1.5474	0.0525
0.7	1.2721	-0.2316	1.4838	-0.0160	1.5329	0.0441
0.8	1.1943	-0.3098	1.4800	-0.0215	1.5190	0.0291
	[EMIM] [OAc]+ INDO		[EMIM] [OAc]+ TS		[EMIM] [OAc]+ WATER	
x_{IL}	*nD*	*ΔnD*	*nD*	*ΔnD*	*nD*	*ΔnD*
0.2	1.5586	-0.0117	1.5241	0.0848	1.4517	0.0947
0.3	1.5464	-0.0157	1.4906	-0.0672	1.4518	0.0763
0.4	1.5399	-0.0140	1.4822	-0.0835	1.4675	0.0735
0.5	1.5250	-0.0207	1.5841	-0.0934	1.4745	0.0621
0.6	1.5166	-0.0209	1.4889	-0.1012	1.4848	0.0539
0.7	1.5143	-0.0150	1.4933	-0.1022	1.4787	0.0293
0.8	1.5061	-0.0150	1.4965	-0.1136	1.4816	0.0137

5.3.1.5 Refractive index of mixture

Table 5.6 shows the composition dependence of refractive index for the above mentioned binary systems. Refractive index for [EMIM][OAc](1) + pyrrole (2) decreases linearly with increasing mole fraction of [EMIM][OAc] because there is no mobility of ion upon mixing over entire mole fraction of [EMIM][OAc] at *T*=298.15K.In case of

[EMIM][OAc](1) + thiophene(2), [EMIM][OAc](1) + pyridine(2),[EMIM][OAc](1) + indoline(2) , [EMIM][OAc] (1)+ quinoline(2) systems, a little variation is seen with increasing mole fraction of [EMIM][OAc].This is due to the interaction between dissimilar aromatic structure of molecules via CH---π bond interaction [2,3,5,26-28] and π---π stacking [Anantharaj et al., 2010a, 2010b,2011b;Domanska et al.,2010]. The refractive index for [EMIM][OAc] + water system slightly increases with increasing mole fraction. This can be attributed to the strength of mobility of ions. It is clear from Table 5.6 that for the binary mixture under study, the refractive index increasingly in the order:

[EMIM][OAc]: Pyridine < Water < Pyrrole < Thiophene < Indoline < Quinoline.

The observed trend and magnitudes of refractive index indicates a presence of significant interaction for [EMIM][OAc] + catalytic deactivated compounds due to the similar molecular structure and its chemical nature (e.g acidic, basic and neutral molecules).

5.3.1.6 Derived thermodynamic properties of mixture

The excess molar volume for above mentioned systems was calculated from experimental data at temperature from (298.15 to 323.15) K according to the following equations [Gomez et al., 2006;Rodriguez et al.,2006]:

(5.2)

Where V is the molar volume of the pure fluid, ρ is the density of the pure fluid and subscript P indicates constant pressure. V_m^E is the excess molar volume of the binary mixture, ρ_{mix} is density of the mixture, and density of the pure components denoted as ρ_1

and ρ_2 respectively. x_1 and x_2 are the mole fraction of component 1 and 2 .M_1, M_2 are the molecular weight of the component 1 and 2 respectively.

The calculated excess molar volume values are listed in Table 5.4(a) to 5.4(f). [EMIM][OAc] (1) +pyridine(2) (Figure 5.4) and [EMIM][OAc] (1) +pyridine(2) (Figure 5.5) system exhibit a linear decreases over the entire mole fraction of [EMIM][OAc](1) at all studied temperatures. In general the excess molar volume can be used to identify the molecular interaction between similar size and shape of the component in the binary mixture. There are three different routes of identifications such as: (a)the positive sign and its magnitude are indication of physical interaction which is due to the dispersion forces or weak dipole-dipole interaction,(b) the negative sign and its magnitude are indication of chemical or specific interaction which is due to the charge transfer,CH---π bond interaction, hydrogen bond formation or other interactions and (c)the minimum positive and maximum negative sign and its magnitude are the indication of stronger association and π---π stacking between similar size and shape of molecules in a mixtures[Omrani et al.,2010]. At temperature T=298.15K, the excess molar volume is negative as compared to temperature above T=298.15K. This is due to the fact that the specific interactions in the mixture typically: weak H- bonds are easily broken when the temperature is increased but at the same time other interactions are (i.e.CH - - π bond, π---π bond and n---π bond) have negligible effect. These similar tendencies have been observed for all other studied systems. This is explained by the stronger association between similar or dissimilar aromatic structure of molecules in liquid phase at any composition/temperature. It is observed for [EMIM][OAc] (1) +thiophene (2) system, from x_{IL} =0.2 to x_{IL} =0.4 the excess molar volume decreases linearly with increasing mole fraction(Table 5. 4(e)). After x_{IL} =0.4 the excess molar volume is constant over the remaining mole fraction of all temperatures. In case of IL-water, a sudden decrease is noticed; thereafter a further linear decrease occurs when the composition is increased.

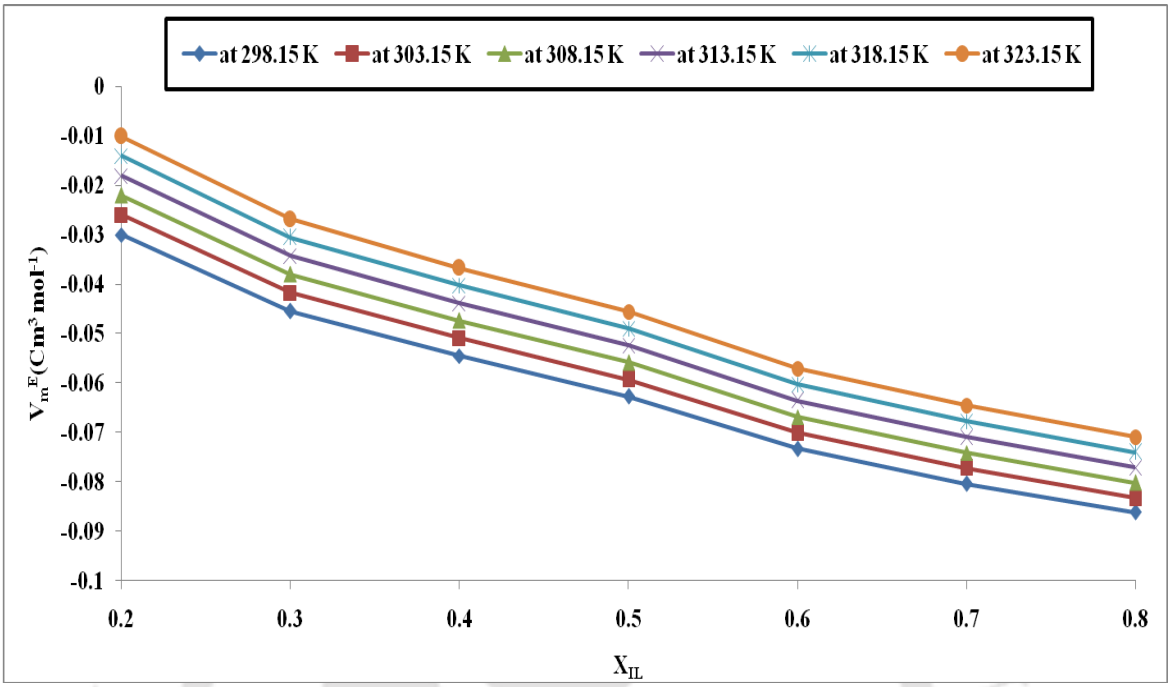

Figure 5.4: Excess molar volume V_m^E for the system of [EMIM][OAc] (1) + pyridine (2) at different temperatures

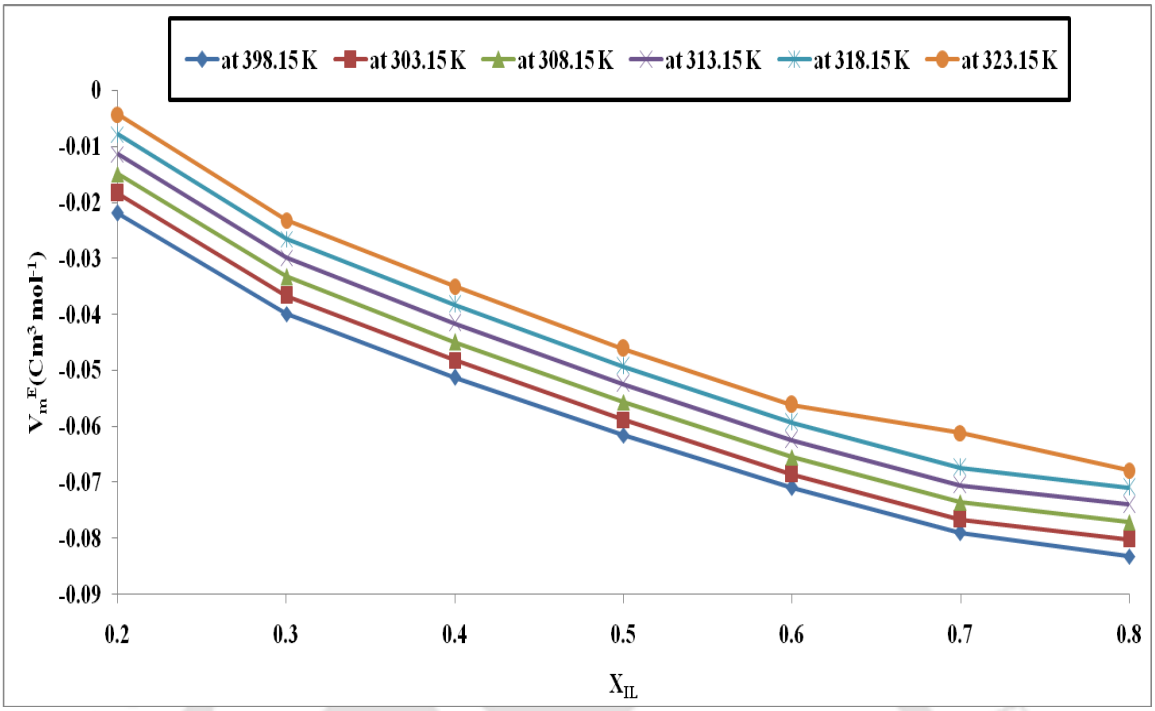

Figure 5.5: Excess molar volume V_m^E for the system of [EMIM][OAc] (1) + pyrrole (2) at different temperatures

The deviation of surface tension (Table 5.5) and refractive index (Table 5.6) were calculated from experimental data according to the following equation [Gomez et al., 2006; Rodriguez et al., 2006]:

(5.3)

(5.4)

Where, Δσ and ΔnD are the deviation of surface tension and refractive index. The surface tension and refractive index of the binary mixture is denoted as σ_{mix} and nD_{mix} respectively. The x_1 and x_2 are the mole fraction of the component 1 and 2 respectively. The deviation of surface tension and refractive index are presented in Table 5.6 and

5.7.The deviation of surface tension for [EMIM][OAc] (1) + pyrrole (2) exhibit linear increasing trend with increasing mole fraction of [EMIM][OAc] while the refractive index deviation decreases at T=298.15K.It can be observed that the strong electrostatic interaction take place between the two aromatic structure(IL-N/S heterocycle) of the molecules upon mixing ,even if it has similar or dissimilar structure. The deviation of surface tension is inversely proportional to deviation of refractive index at T=298.15K. When [EMIM][OAc] mixes with water molecules the deviation of surface tension increases linearly with composition (Table 5.5) , while the deviation of refractive index decreases slightly (Table 5.6). The molecular interaction is very strong between similar and dissimilar aromatic structure [Domanska et al.,2010a,2010b;Mottar et al.,2007] of sulphur/nitrogen compounds and [EMIM] cation, however the mobility of ions is weakened upon mixing, but still [EMIM][OAc] can interact with these compounds via n -- H bonding (where n:N,O from both either molecules).

It can be observed that a minimum amount of [EMIM][OAc] ionic liquid is enough for separation of pyrrole and thiophene while for pyridine,indoline and quinoline it is vice versa.[EMIM][OAc] ionic liquid can be easily regenerated by simple distillation or evaporation. The water molecules have a crucial role upon properties of mixture whenever ionic liquid is used as a solvent in the separation process. Therefore their behavior exhibits mostly negative over the mole fraction of IL at temperature from (298.15 to 323.15)K for excess molar volume studies. The deviation of surface tension and refractive index studies also shows similar trend.

5.3.2 1-Ethyl-3-Methylimidazolium Ethylsulphate {[EMIM][$EtSO_4$]}

5.3.2.1 Pure components

Experimental densities of pure [EMIM][$EtSO_4$], aromatic nitrogen, and aromatic sulphur species are measured and benchmarked at different temperatures (Table 5.2). Table 5.3 shows the comparison of measured densities for pure [EMIM][$EtSO_4$] with temperature. Beside the effect of temperature and experimental method, the presence of

trace amount of impurities such as water or ions can have a remarkable effect on thermodynamic properties [Yanfang et al., 2008]. Due to this very reason the % deviation in the density values is 6% when compared to the literature values. Table 5.2 also shows the comparison between experimental and literature data of the pure aromatic nitrogen/ sulphur, and water at 298.15 K. The density ρ of pure ionic liquid is higher than that of water and aromatic nitrogen/sulphur compounds. Table 5.3 show a comparison of surface tension σ and refractive index *nD* of pure components with literature data at 298.15 K. As compared to densities, the deviation in surface tension and refractive index for [EMIM][$EtSO_4$] was equal to 3% and 0.15% respectively. Thus a small impurity such as water or other ions has marked difference in density when compared to surface tension or refractive index.

5.3.2.2 Binary mixtures

Experimental densities over the entire composition range for [EMIM][$EtSO_4$] (1) + PY(2)(Table 5.7), [EMIM][$EtSO_4$] (1) + PYRR(2) (Table 5.8), [EMIM][$EtSO_4$] (1) + QU(2) (Table 5.9), [EMIM][$EtSO_4$] (1) + INDO(2) (Table 5.10), [EMIM][$EtSO_4$] (1) + TS(2) (Table 5.11), and [EMIM][$EtSO_4$] (1) + water(2) (Table 5.12) have been determined at temperature of (298.15 to 323.15) K and at atmospheric pressure. As expected the density was found to decrease with increasing temperature. In order to compare the properties such as refractive index and surface tension, we will concentrate our study at room temperature i.e *T*=298.15 K. Thereafter the surface tension σ and refractive index *nD* of the pure component and its binary mixtures i.e [EMIM][$EtSO_4$] (1) + PY(2), [EMIM][$EtSO_4$] (1) + PYRR(2), [EMIM][$EtSO_4$] (1) + QU(2), [EMIM][$EtSO_4$] (1) + INDO(2), and [EMIM][$EtSO_4$] (1) + TS(2) were determined at *T*=298.15 K over the entire composition range of [EMIM][$EtSO_4$] (1). The refractive index was found to decrease, while the surface tension increased with increasing mole fraction of [EMIM][$EtSO_4$]. Further, measurements of the physiochemical properties of

mixtures: [EMIM][$EtSO_4$] (1) + water (2) were also carried out, which is helpful for the purification and regeneration of [EMIM][$EtSO_4$][Gonzalez et al.,2006].

Table 5.7: Experimental Density ρ *and* Excess molar volume V_m^E for the binary system [EMIM][$EtSO_4$] (1) + Pyridine (2)

x_{IL}	ρ	V_m^E	ρ	V_m^E	ρ	V_m^E
	g.cm^{-3}	cm^3.mol^{-1}	g.cm^{-3}	cm^3.mol^{-1}	g.cm^{-3}	cm^3.mol^{-1}
	T=298.15K		T=303.15K		T= 308.15K	
0.2	1.0900	-1.5561	1.0860	-1.6160	1.0838	-1.8536
0.3	1.1299	-2.2786	1.1259	-2.3311	1.1220	-2.3957
0.4	1.1586	-2.5356	1.1549	-2.6002	1.1511	-2.6546
0.5	1.1731	-1.7004	1.1729	-2.1481	1.1703	-2.3102
0.6	1.1914	-1.6230	1.1878	-1.6640	1.1844	-1.7185
0.7	1.2067	-1.5063	1.2033	-1.5300	1.1998	-1.5702
0.8	1.2184	-1.1659	1.2149	-1.1669	1.2115	-1.1903
	T=313.15K		T=318.15K		T=323.15K	
0.2	1.0799	-1.9346	1.0758	-1.9970	1.0717	-2.0625
0.3	1.1182	-2.4623	1.11428	-2.5300	1.1104	-2.5998
0.4	1.1476	-2.7460	1.14395	-2.8194	1.1403	-2.8958
0.5	1.1671	-2.4201	1.16367	-2.5060	1.1527	-1.7096
0.6	1.1809	-1.7724	1.17738	-1.8247	1.1738	-1.8797
0.7	1.1963	-1.6118	1.19289	-1.6541	1.1894	-1.6988
0.8	1.2081	-1.2173	1.20464	-1.2434	1.2012	-1.2717

Table 5.8: Experimental Density ρ and Excess molar volume V_m^E for the binary system [EMIM][$EtSO_4$] (1) + Pyrrole (2)

x_{IL}	ρ	V_m^E	ρ	V_m^E	ρ	V_m^E
	g.cm^{-3}	cm^3.mol^{-1}	g.cm^{-3}	cm^3.mol^{-1}	g.cm^{-3}	cm^3.mol^{-1}
	T=298.15K		T=303.15K		T= 308.15K	
0.2	1.0955	-1.7383	1.0920	-1.7969	1.0883	-1.8385
0.3	1.0963	1.4405	1.0931	1.3789	1.0894	1.3664
0.4	1.1085	3.3324	1.1047	3.3566	1.1009	3.3686
0.5	1.1095	6.2719	1.1092	5.9001	1.1088	5.5279
0.6	1.1080	9.5403	1.1079	9.1236	1.1075	8.7333
0.7	1.1094	12.414	1.1089	12.027	1.1086	11.621
0.8	1.1103	15.326	1.1099	14.925	1.1095	14.502
	T=313.15K		T=318.15K		T=323.15K	
0.2	1.0845	-1.8768	1.0807	-1.9164	1.0768	1.9547
0.3	1.0856	1.3624	1.0818	1.3591	1.0779	-1.3551
0.4	1.0955	3.5758	1.0935	3.3931	1.0898	-3.6002
0.5	1.1085	5.1509	1.1081	4.7705	1.1077	-4.3935
0.6	1.1072	8.3432	1.1068	7.9409	1.1064	-7.5508
0.7	1.1082	11.2132	1.1078	10.8025	1.1075	-10.3946
0.8	1.1091	14.0779	1.1088	13.6512	1.1084	-13.2270

Table 5.9: Experimental Density ρ and Excess molar volume V_m^E for the binary system [EMIM][$EtSO_4$] (1) + Quinoline (2)

x_{IL}	ρ	V_m^E	ρ	V_m^E	ρ	V_m^E
	g.cm^{-3}	cm^3.mol^{-1}	g.cm^{-3}	cm^3.mol^{-1}	g.cm^{-3}	cm^3.mol^{-1}
	T=298.15K		T=303.15K		T= 308.15K	
0.2	1.1373	-0.8139	1.1334	-0.8054	1.1296	-0.8204
0.3	1.1388	1.14189	1.1353	1.1327	1.1316	1.1313
0.4	1.1342	3.89602	1.1313	3.8265	1.1274	3.8725
0.5	1.1780	0.06978	1.1762	-0.1535	1.1731	-0.2196
0.6	1.2034	-1.5676	1.1947	-0.8666	1.1939	-1.2486
0.7	1.2234	-2.7068	1.2207	-2.8231	1.2177	-2.9089

0.8	1.2305	-2.2468	1.2273	-2.2721	1.2239	-2.3007
		T=313.15K		*T*=318.15K	*T*=323.15K	
0.2	1.1260	-0.8525	1.1223	-0.8657	1.1185	-0.8793
0.3	1.1278	1.1408	1.1241	1.1494	1.1203	1.1577
0.4	1.1269	3.4589	1.1232	3.4875	1.1195	3.5157
0.5	1.1697	-0.2619	1.1664	-0.2947	1.1631	-0.3448
0.6	1.1912	-1.3799	1.1882	-1.4611	1.1849	-1.5165
0.7	1.2145	-2.9731	1.2113	-3.0258	1.2079	-3.0690
0.8	1.2206	-2.3295	1.2173	-2.3602	1.2139	-2.3924

Table 5.10: Experimental Density ρ and Excess molar volume V_m^E for the binary system [EMIM][$EtSO_4$] (1) + Indoline (2)

x_{IL}	ρ	V_m^E	ρ	V_m^E	ρ	V_m^E
	g.cm^{-3}	cm^3.mol^{-1}	g.cm^{-3}	cm^3.mol^{-1}	g.cm^{-3}	cm^3.mol^{-1}
		T=298.15K		*T*=303.15K	*T*= 308.15K	
0.2	1.1329	-0.0172	1.1292	-0.0269	1.1255	-0.0410
0.3	1.1339	2.0031	1.1303	2.0157	1.1266	2.0214
0.4	1.1619	0.6270	1.1584	0.6174	1.1548	0.6119
0.5	1.1723	1.1524	1.1685	1.1981	1.1590	1.9779
0.6	1.1874	0.8990	1.1839	0.9101	1.1804	0.9066
0.7	1.1976	1.1281	1.1942	1.1446	1.1907	1.1439
0.8	1.2088	1.0822	1.2053	1.1021	1.2019	1.1067
		T=313.15K		*T*=318.15K	*T*=323.15K	
0.2	1.1212	0.0209	1.1182	-0.0716	1.1145	-0.0865
0.3	1.1229	2.0263	1.1193	2.0312	1.1156	2.0355
0.4	1.1512	0.5993	1.1477	0.5877	1.1442	0.5727
0.5	1.1542	2.1489	1.1486	2.4399	1.1439	2.6034
0.6	1.1769	0.8998	1.1735	0.8942	1.1701	0.8848
0.7	1.1873	1.1428	1.1839	1.1417	1.1804	1.1379
0.8	1.1985	1.1096	1.1951	1.1095	1.1917	1.1126

Table 5.11: Experimental Density ρ and Excess molar volume V_m^E for the binary system [EMIM][$EtSO_4$] (1) + Thiophene (2)

x_{IL}	ρ	V_m^E	ρ	V_m^E	ρ	V_m^E

	g.cm^{-3}	cm^3.mol^{-1}	g.cm^{-3}	cm^3.mol^{-1}	g.cm^{-3}	cm^3.mol^{-1}
	T=298.15K		*T*=303.15K		*T*= 308.15K	
0.2	1.1598	52.8065	1.1577	54.1409	1.1531	68.7926
0.3	1.1679	65.7820	1.1654	64.9267	1.1615	51.8879
0.4	1.1889	42.5225	1.1851	36.4262	1.1811	34.8293
0.5	1.1943	19.7579	1.1905	20.8277	1.1866	13.4028
0.6	1.2079	-1.3906	1.2042	-13.4828	1.2005	-16.7099
0.7	1.2127	-5.0043	1.2092	-15.6031	1.2056	-16.4008
0.8	1.2199	-4.6987	1.2164	-8.3316	1.2129	-20.7794
	T=313.15K		*T*=318.15K		*T*=323.15K	
0.2	1.1488	53.3051	1.1442	59.7818	1.1396	60.8412
0.3	1.1573	61.0223	1.1527	52.3702	1.1471	60.8360
0.4	1.1771	36.1422	1.1732	37.8967	1.1692	33.6579
0.5	1.1828	16.3931	1.1789	15.5642	1.1751	17.4040
0.6	1.1968	-19.9785	1.1931	-24.2541	1.1895	-22.6699
0.7	1.2024	-20.7949	1.1985	-25.3382	1.1949	-36.2777
0.8	1.2094	-27.2300	1.2059	-27.0188	1.2024	-23.0099

Table 5.12: Experimental Density ρ and Excess molar volume V_m^E for the binary system [EMIM][EtSO$_4$] (1) + water (2)

x_{IL}	ρ	V_m^E	ρ	V_m^E	ρ	V_m^E
	g.cm^{-3}	cm^3.mol^{-1}	g.cm^{-3}	cm^3.mol^{-1}	g.cm^{-3}	cm^3.mol^{-1}
	T=298.15K		*T*=303.15K		*T*= 308.15K	
0.2	1.1773	-0.3474	1.1739	-0.3179	1.1689	-0.2282
0.3	1.1886	0.1805	1.1857	0.2208	1.1816	0.2527
0.4	1.2004	0.3416	1.1947	0.3714	1.1936	0.3995
0.5	1.1989	1.3230	1.1954	1.3729	1.1919	1.4068
0.6	1.2054	1.5315	1.2019	1.5756	1.1985	1.6067
0.7	1.2135	1.3619	1.2101	1.4004	1.2065	1.4351
0.8	1.2275	0.1941	1.2243	0.2051	1.2209	0.2052
	T=313.15K		*T*=318.15K		*T*=323.15K	
0.2	1.1685	-0.3429	1.1673	-0.4496	1.1669	-0.5882
0.3	1.1780	0.2814	1.1744	0.2884	1.1709	0.3079
0.4	1.1901	0.4261	1.1866	0.4341	1.1830	0.4529
0.5	1.1884	1.4413	1.1848	1.4599	1.1824	1.3913

0.6	1.1949	1.6365	1.1915	1.6559	1.1879	1.6839
0.7	1.2033	1.4387	1.1999	1.4474	1.1965	1.4652
0.8	1.2177	0.2079	1.2143	0.2076	1.2109	0.2097

5.3.2.3 The coefficient of thermal expansion of the [EMIM][EtSO$_4$] α.

Figure 5.6 shows the densities of pure [EMIM][EtSO$_4$], which decreases linearly (R^2=0.999) while the densities of water increases linearly (R^2 = 0.965) with temperature.The value of **α** = 0.097 K^{-1}([EMIM][EtSO$_4$]) and **α** = 0.004 K^{-1} (water) was calculated from Equation 5.1. The volume expansivity of [EMIM][EtSO$_4$] and water was calculated using the measured density observed at different temperatures. As compared to water, the volume expansivity of [EMIM][EtSO$_4$] was found to be independent of temperature (Figure 5.6). These observations are consistent with the observations by Rodriguez et al.,[2006], Wandschneider et al., [2008] and Pererio et al.,[2006,2007].

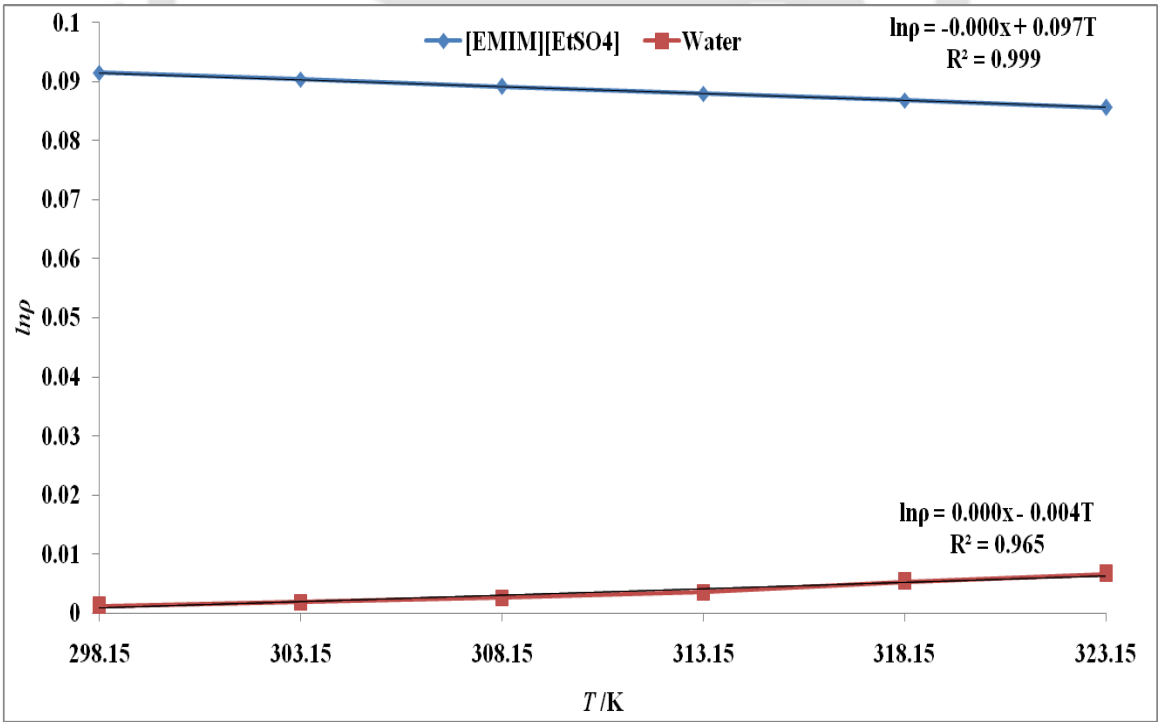

Figure 5.6: Plot of experimental values of *ln* ρ of the pure [EMIM][$EtSO_4$] ionic liquid and water Vs temperature (298.15, 303.15, 308.15, 313.15,318.15,and 323.15) K

5.3.2.4 Effect of temperature on density

Table 5.2 shows the experimental densities of pure [EMIM][$EtSO_4$], aromatic nitrogen, aromatic sulphur and water at temperatures : (298.15 to 323.15) K. It can be seen that the density of all the pure components including ionic liquid decreases linearly with temperature. Table 5.7 to 5.12 shows the experimental densities for six binary systems studied as a function of temperature over the entire mole fraction of [EMIM][$EtSO_4$]. For all the compounds with ILs the densities varied linearly in the entire mole fraction with increasing temperature. This behavior can be explained by the efficient structural interaction of [EMIM][$EtSO_4$] with aromatic nitrogen/aromatic sulphur via packing effects[Domanska et al.,2007,2008]. Additionally it can be a result of the smaller size of cation and anion providing better interaction with aromatic nitrogen/sulphur and water. A smaller size of IL molecule was found to have a significant influence on the densities of the mixture with increasing temperature. These behaviors strongly agree with the studies carried out be Rodriguez et al.,[2006] and Domanska et al.,[2007,2008]. A similar trend was observed by Gonzalez et al., [2007] and Gomez et al., [2006], which reported the experimental data for densities of binary mixture [EMIM][$EtSO_4$] with ethanol and water at several temperatures. This is also consistent with the measurements of Garcia et al.,[2010] which reported the effect of [EMIM][$EtSO_4$] and [EMIM][$EtSO_4$] with aliphatic and aromatic hydrocarbons in the binary systems.

5.3.2.5 Effect of composition on density

The experimental values of densities for [EMIM][$EtSO_4$] with aromatic nitrogen/sulphur and water are given from Tables 5.7 to 5.12. As expected density of mixture increases with increasing mole fraction of [EMIM][$EtSO_4$]. The densities for [EMIM][$EtSO_4$] with PY,TS and water increases with increasing mole fraction of

[EMIM][$EtSO_4$] at different temperature. Besides that the n- π interaction (n = H(CH), O, N, F)[34], weak hydrogen bond interaction[Alonso et al.,2008;Garcia et al.,2010], van der waals interaction[Alonsa et al.,2008;Garcia et al.,2010], CH-π bond interaction[Cassol et al.,2007;Anantharaj et al.,2010b] and π - -π interaction[Domanska et al.,2010] plays a significant role when aromatic nitrogen/sulphur is mixed with [EMIM][$EtSO_4$]. The nitrogen and sulphur atom of aromatic compounds forms hydrogen bond with hydrogen in imidazolium ring or with the hydrogen located on the alkyl group of the imidazolium cation. It should be noted that the electrostatic interaction is mostly weaker between [EMIM] and [$EtSO_4$] due to the ethyl substitution on the anion structure. Due to this very fact, the density of mixture increases with increasing mole fraction of [EMIM][$EtSo_4$] at different temperatures. On the other hand, it is observed that the influence of composition have an important role on the interaction between [EMIM][$EtSO_4$] and neutral aromatic species like pyrrole and water. Therefore, the probable explanation lies in the fact that [EMIM][$EtSO_4$] have stronger interaction with similar molecules like pyrrole than dissimilar molecules such as pyridine, indoline, quinoline, and water. Similar and dissimilar compounds imply a similarity in their structure. For e.g pyrrole or thiophene has a similar five member ring structure as compared to the imidazolium ring. Thus IL and pyrrole/thiophene possessing different electro negative atom within their structure is known to play a significant role in enhancing the solubility.

But at the same time [EMIM][$EtSO_4$] posses excellent structural orientation with dissimilar structure molecules like indoline, pyridine, quinoline and water, since there is an enormous possibility to interact with each other via n- π interaction (n = H(CH), O, N, F)[Domanska et al.,2007], weak hydrogen bond interaction[Garcia et al.,2010], CH-π bond interaction[Cassol et al.,2007;Anantharaj et al.,2010b] and π - -π interaction[Domanska et al.,2010]. These similar trends are observed for systems such as: [EMIM][$EtSO_4$] (1) + PYRR(2), [EMIM][$EtSO_4$] (1) + QU(2), and [EMIM][$EtSO_4$] (1) + INDO(2).

5.3.2.6 Effect of composition on surface tension

Table 5.13 present the variation of surface tension with mole fraction for all the studied binary systems. The values of surface tension exhibit a linear increase with increasing mole fraction of [EMIM][$EtSO_4$] except for water.The fusion of benzene ring or addition of benzene ring with nitrogen species have significant influence on the surface tension. Thus quinoline and indoline (Table 5.13) posses higher surface tension as compared to those compounds without additional benzene ring such as pyrrole, thiophene, pyridine and water. For [EMIM][$EtSO_4$]-water mixture, the surface tension linearly decreases with an increasing mole fraction due to the decreasing strength of hydrogen bond coupled with the high difference in their surface tensions(72.1mN.m^{-1} for water and 48.4 mN.m^{-1} for [EMIM][$EtSO_4$]). Although the nature of alkyl substitution at [EMIM][$EtSO_4$] dominate the surface tension and can define the trend of surface tension, still the ratio of van der Waals interaction[Pereiro et al.,2007] and columbic interaction[Alonso et al.,2008;Garcia et al.,2010;Lei et al.,2006] plays an important part upon mixing. The observed trend and values are consistent with those reported by Gomez et al.,[2006] and Wandschneider et al., [2008].The surface tension of aromatic nitrogen and sulphur are lower than [EMIM][$EtSO_4$], however a comparison could not be done because of the scarcity of literature data. [EMIM][$EtSO_4$] with aromatic nitrogen/sulphur are highly governed by the nature of their structure as well as the electro negative atom located on the studied compound and [EMIM][$EtSO_4$] structures. The observed values decreases in the order: [EMIM][$EtSO_4$] < quinoline < pyrrole < pyridine < indoline < thiophene i.e. 48.4 < 46.5 < 41.7 < 37.5 < 32.6 < 31.7. Thus trace of water and other impurities play an important role on surface tension of [EMIM][$EtSO_4$] upon mixing. Thus by adjusting the ratio of van der Waals interaction to columbic interaction [Kilaru et al.,2007] one can promote higher solvation capability of [EMIM][$EtSO_4$][Ghatee et al.,2008].

Table 5.13: Experimental surface tension σ, Refractive Index nD for the Binary systems: (a) [EMIM][$EtSO_4$] + PY, (b).[EMIM][$EtSO_4$] + PYRR, (c).[EMIM][$EtSO_4$] + QU, (d). [eEMIM][$EtSO_4$] + INDO, (e) [EMIM][$EtSO_4$] + TS, and (f) [EMIM][$EtSO_4$] + Water at 298.15K.

	[EMIM][$EtSO_4$] + PY		[EMIM][$EtSO_4$] + PYRR		[EMIM][$EtSO_4$]+ QU	
x_{IL}	σ /mN.m^{-1}	*nD*	σ /mN.m^{-1}	*nD*	σ /mN.m^{-1}	
0.2	37.2	1.4893	39.3	1.4972	41.2	1.5356
0.3	38.1	1.4867	39.9	1.4904	41.4	1.5318
0.4	39.1	1.4852	40.3	1.4867	42.5	1.5237
0.5	39.6	1.4826	40.6	1.4849	42.9	1.5003
0.6	42.4	1.4808	41.8	1.4845	43.1	1.5000
0.7	46.7	1.4799	41.9	1.4779	43.7	1.4989
0.8	47.1	1.4721	42.6	1.45779	44.5	1.4928
	[EMIM][$EtSO_4$] + INDO		[EMIM][$EtSO_4$] + TS		[EMIM][$EtSO_4$]+ Water	
x_{IL}	σ /mN.m^{-1}	*nD*	σ /mN.m^{-1}	*nD*	σ /mN.m^{-1}	
0.2	41.4	1.5774	31.5	1.4736	52.6	1.4356
0.3	43.1	1.5761	36.4	1.4662	51.5	1.4516
0.4	43.6	1.5584	37.1	1.4624	50.4	1.4524
0.5	44.2	1.5581	45.6	1.4608	49.2	1.4537
0.6	44.5	1.5418	47.2	1.459	47.8	1.4562
0.7	45.2	1.5022	48.4	1.4524	47.8	1.4569
0.8	47.1	1.5006	49.0	1.443	46.2	1.4660

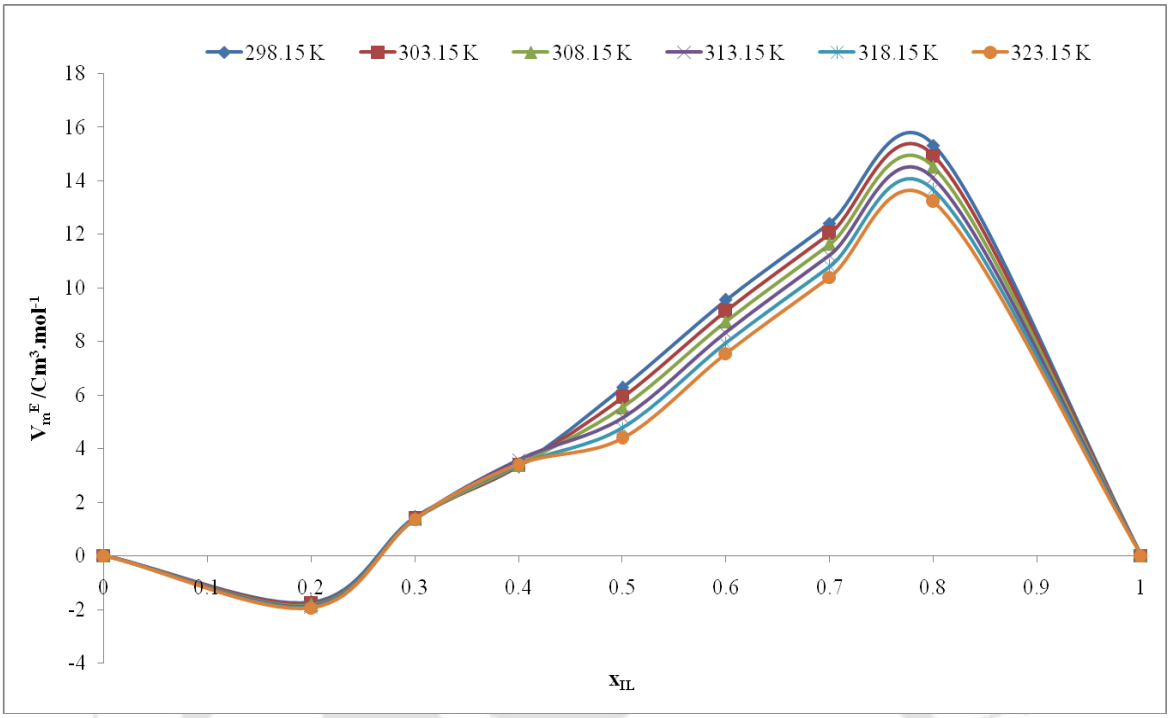

Figure 5.7: Excess molar volume for {[EMIM][$EtSO_4$] (1) + Pyrrole (2)} as a function of {[EMIM][$EtSO_4$] (1) mole fraction composition at different temperature.

5.3.2.7 Effect of Composition on Refractive index

Table 5.13 shows the experimental refractive index over the whole composition range of [EMIM][$EtSO_4$] . The refractive index decreases over the mole fraction of [EMIM][$EtSO_4$] except for water mixture, where the refractive index increases with increasing mole fraction of [EMIM][$EtSO_4$]. This behaviour can be explained by an efficient packing in the [EMIM][$EtSO_4$]-nitrogen/sulphur mixture as compared to [EMIM][$EtSO_4$] -water mixture system. Among the six binary systems, the higher refractive index was observed for [EMIM][$EtSO_4$] with quinoline which indicates an increased interaction with [EMIM][$EtSO_4$].The influence of an increasing mole fraction of [EMIM][$EtSO_4$] on the mixture refractive index has shown that except for [emim][$EtSO_4$] + water system, refractive index increases in the order: [EMIM][$EtSO_4$]

+ quinoline > [EMIM][$EtSO_4$] + indoline > [EMIM][$EtSO_4$] + pyrrole > [EMIM][$EtSO_4$] + pyridine > [EMIM][$EtSO_4$] + thiophene. The ratio of van der Waals and coulombic force [Kilaru et al.,2007] again causes the refractive index of the mixture to decrease with increasing mole fraction of [EMIM][$EtSO_4$]. Therefore, these results suggest that [EMIM][$EtSO_4$] have more influence on the separation of aromatic nitrogen/sulphur rather than water. Besides, the ability of [EMIM][$EtSO_4$] to create a favorable hydrogen bond with aromatic nitrogen/sulphur, significantly increases the solubility of [EMIM][$EtSO_4$] in aromatic nitrogen/sulphur.

5.3.2.8 Effect of Composition on Excess molar volume

The excess molar volume V_m^E gives information over the net destruction of interactions and packing phenomena that appears in the mixing process [Seddon et al., 2000; Huo et al., 2007]. The excess molar volume V_m^E was calculated from experimental density data for all studied systems according to equation 2. These calculated values are given in Table 5.7 to 5.12. The excess molar volume V_m^E of [EMIM][$EtSO_4$] + pyrrole systems (Figure 5.7) system exhibits a linear trend with increasing mole fraction of [EMIM][$EtSO_4$] due to insufficient amount of pyrrole in the liquid phase. Therefore it does not cause a volume contraction upon mixing with [emim][$EtSO_4$] at different temperatures. It can be observed from Tables 5.7-5.12 that the excess molar volume strongly depends on composition than temperature. A similar phenomena has been observed for [BMIM][BF_4] +water system by Seddon et al.,[2000] and [BMIM][PF_6]+ [BMIM][BF_4] with benzene, acetonitrile, and 1-propanol at by Huo et al., [2007]. It should be noted that [EMIM][$EtSO_4$] produces another IL i.e.[EMIM][HSo_4] when in contact with water molecules due to the high dissociation of ions [Moattar et al.,2007;Su et al.,2004].

Thus the Ionic Liquid in a mixture can be explained by two different types of interactions:(1) if the sign and magnitude of the excess molar volume is positive implies physical interaction mainly via dispersion forces or weak dipole-dipole interaction ;(2) negative values refers to the chemical or specific interaction which includes charges transfer, CH---π bond interaction--- n---π interactions, formation of hydrogen bond etc. The sign and magnitude of the excess molar volume is negative upon mixing with two similar aromatic structure of molecules indicates a strong π---π stacking [Wankhede et al., 2006; Omrani et al., 2010].

5.3.2.9 Combined Effect of Temperature and Composition on transport properties

The trend in the performance of experimental data for density (Table 5.7 to 5.12) of the studied binary systems has been presented as a function of temperature and mole fraction of [EMIM][$EtSO_4$].In general for all the systems other than water, densities were found to decrease with increasing temperature. It can be seen that the variation of the thermodynamic property is much dependent on composition as compared to temperature. This can be explained by the composition of [EMIM][$EtSO_4$],which plays a significant role upon mixing than temperature over the transport properties of mixtures. Water molecules are influenced by hydrogen bonding upon mixing, which is more temperature dependent therefore the columbic force [Garcia et al., 2010] and other interaction parameters [Alonso et al., 2008; Domanska et al., 2010] are negligible. The aromatic nitrogen/sulphur with [EMIM][$EtSO_4$] is influenced by composition and by nature of species which are strongly recognized with several possible interaction parameters as discussed earlier and also due to the effective structural orientation of similar molecules. This behaviour is more consistent with information available in the literature [Kilaru et al., 2007]. Thus it is observed that the mole fraction of [EMIM][$EtSO_4$] has significant influence on the separation of aromatic nitrogen and sulphur.

5.3.2.10 Combined Effect of Temperature and Composition on thermodynamic properties

The combined effect of temperature and composition gives the information about the net destruction of interaction and packing effect for all the studied systems. The excess molar volume is negative for [EMIM][$EtSO_4$] (1) + PY(2)(Table 5.7) mixture over the entire mole fraction of [EMIM][$EtSO_4$] as the temperature is raised, however, the maximum interaction occurs between $0.4 < x_{IL} < 0.5$. For the system [EMIM][$EtSO_4$] (1) + TS(2)(Table 5.11), a negative excess molar volume is seen when $x_{IL} > 0.5$ irrespective of temperature. The excess molar volume and density is seen to vary linearly with respect to temperature and mole fraction for all the systems. It was thus observed that the size and shape of the components in mixture and the nature of electro negative atom located on the structure of the compounds greatly affect the thermodynamic properties.

5.3.3 1-Ethyl-3-Methylimidazolium Methylsulphonate {[EMIM][$MeSO_3$]}

5.3.3.1 Pure component

Experimental densities of pure [EMIM][$MeSO_3$], aromatic nitrogen, and aromatic sulphur species have been measured and benchmarked at different temperatures (Table 5.2). Beside the effect of temperature and experimental method, the presence of trace amount of impurities such as water or ions does have a remarkable effect on thermodynamic properties[Yanfang et al.,2008].Table 5.2 shows the comparison of measured densities for pure [EMIM][$MeSO_3$] with temperature. This agrees well with the reported values at 298.15 K [Alonso et al.,2006]. Table 5.2 shows the comparison between experimental and literature data of the pure aromatic nitrogen/ sulphur, and water at 298.15 K. The density ρ of pure ionic liquid is higher than that of water, and also than that of aromatic nitrogen/sulphur compounds. Table 5.3 show a comparison for the surface tension σ and refractive index nD of pure components with literature data at 298.15 K[Sapi et al.,2006a.2006b]. The difference between experimental and literature data for pure [EMIM][$MeSO_3$] can be explained by the thermodynamic properties which strongly depends on water and other impurities[Yanfang et al.,2008].

5.3.3.2 Binary mixture

Experimental densities over the entire composition range for [EMIM][$MeSO_3$] (1) + PY(2)(Table 5.14(a)), [EMIM][$MeSO_3$] (1) + PYRR(2) (Table 5.14(b)), [EMIM][$MeSO_3$] (1) + QU(2) (Table 5.14(c)), [EMIM][$MeSO_3$] (1) + INDO(2) (Table 5.14(d)), [EMIM][$MeSO_3$] (1) + TS(2) (Table 5.14(e)), and [EMIM][$MeSO_3$] (1) + water(2) (Table 5.14(f)) have been determined at temperature of T =(298.15 to 323.15) K and atmospheric pressure. As expected the density decreases with increasing temperature. The refractive index decreases, while the surface tension increases with increasing mole fraction of [EMIM][$MeSO_3$]. The surface tension σ, and refractive index nD of the pure component and its binary mixtures i.e. [EMIM][$MeSO_3$] (1) + PY(2), [EMIM][$MeSO_3$] (1) + PYRR(2), [EMIM][$MeSO_3$] (1) + QU(2), [EMIM][$MeSO_3$] (1) + INDO(2), and [EMIM][$MeSO_3$] (1) + TS(2) were determined at 298.15 K over the entire composition range of [EMIM][$MeSO_3$] (1). Further, measurements of the physiochemical properties of mixtures [EMIM][$MeSO_3$] (1) + water (2) were also carried out, which is helpful in the purification and regeneration of [EMIM][$MeSO_3$].

Table 5.14(a): Experimental Density ρ and Excess molar volume V_m^E for the binary system [EMIM][$MeSO_3$] (1) + Pyridine (2)

x_{IL}	ρ	V_m^E		ρ	V_m^E		ρ	V_m^E	
	g.cm^{-3}	cm^3.mol^{-1}		g.cm^{-3}	cm^3.mol^{-1}		g.cm^{-3}	cm^3.mol^{-1}	
	T= 298.15K			T=303.15K			T= 308.15K		
0.2	1.093	-0.0879	1.3881	1.081	-0.0831	1.387	1.0840	-0.0791	1.3857
0.3	1.124	-0.1165	1.5894	1.120	-0.1128	1.5898	1.1161	-0.1090	1.5896
0.4	1.148	-0.1399	1.7370	1.147	-0.1363	1.7399	1.1410	-0.1327	1.7424
0.5	1.170	-0.1619	1.8244	1.163	-0.1584	1.8313	1.1637	-0.1548	1.838
0.6	1.187	-0.1793	1.8583	1.180	-0.1758	1.8695	1.1840	-0.1751	1.8807
0.7	1.203	-0.1964	1.8496	1.201	-0.1930	1.8653	1.1966	-0.1895	1.8808
0.8	1.216	-0.2115	1.8101	1.214	-0.2082	1.8298	1.2100	-0.2048	1.8486
	T=313.15K			T= 318.15K			T=323.15K		
0.2	1.079	-0.0752	1.3844	1.078	-0.0713	1.3829	1.0717	-0.0673	1.3814
0.3	1.112	-0.1053	1.5895	1.103	-0.1015	1.5888	1.1044	-0.0978	1.5882

0.4	1.137	-0.1291	1.7449	1.135	-0.1255	1.7465	1.1298	-0.1219	1.7482
0.5	1.160	-0.1513	1.8436	1.155	-0.1478	1.8492	1.1529	-0.1443	1.8537
0.6	1.176	-0.1688	1.8904	1.174	-0.1653	1.9000	1.1699	-0.1619	1.9082
0.7	1.193	-0.1861	1.8947	1.187	-0.1827	1.9077	1.1862	-0.1793	1.9206
0.8	1.206	-0.2014	1.8663	1.203	-0.1981	1.884	1.1982	-0.1933	1.8999

Table 5.14(b): Experimental Density ρ and Excess molar volume V_m^E for the binary system [EMIM][$MeSO_3$] (1) + Pyrrole (2)

x_{IL}	ρ		V_m^E	ρ		V_m^E	ρ		V_m^E
	g.cm^{-3}		cm^3.mol^{-1}	g.cm^{-3}		cm^3.mol^{-1}	g.cm^{-3}		cm^3.mol^{-1}
	T= 298.15K			T=303.15K			T= 308.15K		
0.2	1.0787	-0.0744	0.0744	1.0751	-0.0708	0.0796	1.0713	-0.0673	0.0850
0.3	1.1108	-0.1043	0.0339	1.1072	-0.1010	0.0370	1.1036	-0.0975	0.0401
0.4	1.1351	-0.1273	0.0205	1.1315	-0.1245	0.0225	1.1279	-0.1210	0.0247
0.5	1.1662	-0.1562	0.0140	1.1629	-0.1539	0.0155	1.1594	-0.1505	0.0171
0.6	1.1793	-0.1707	0.0102	1.1785	-0.1706	0.0114	1.1723	-0.1650	0.0126
0.7	1.1963	-0.1888	0.0078	1.1929	-0.1866	0.0088	1.1895	-0.1832	0.0098
0.8	1.2129	-0.2081	0.0062	1.2095	-0.2046	0.0070	1.2061	-0.2012	0.0078
	T=313.15K			T= 318.15K					T=323.15K
0.2	1.0675	-0.0638	0.0905	1.0639	-0.0602	0.0962	1.0601	-0.0566	0.1020
0.3	1.0999	-0.0941	0.0435	1.0963	-0.0906	0.0469	1.0601	-0.0872	0.0505
0.4	1.1244	-0.1176	0.0270	1.1208	-0.1141	0.0294	1.0927	-0.1108	0.0320
0.5	1.1559	-0.1471	0.0188	1.1524	-0.1438	0.0206	1.1173	-0.1404	0.0226
0.6	1.1689	-0.1616	0.0140	1.1654	-0.1582	0.0154	1.1489	-0.1549	0.0170
0.7	1.1860	-0.1798	0.0109	1.1827	-0.1764	0.0120	1.1619	-0.1730	0.0133
0.8	1.2027	-0.1979	0.0087	1.1993	-0.1945	0.0097	1.1792	-0.1911	0.0107

Table 5.14(c): Experimental Density ρ and Excess molar volume V_m^E for the binary system [EMIM][$MeSO_3$] (1) + Quinoline (2)

x_{IL}	ρ		V_m^E	ρ		V_m^E	ρ		V_m^E
	g.cm^{-3}		cm^3.mol^{-1}	g.cm^{-3}		cm^3.mol^{-1}	g.cm^{-3}		cm^3.mol^{-1}
	T= 298.15K			T=303.15K			T= 308.15K		
0.2	IM	IM	1.6435	IM	IM	1.6391	IM	IM	1.6346
0.3	1.1500	-0.1478	2.1415	1.1465	-0.1444	2.137	1.142	-0.1408	2.1325
0.4	1.1673	-0.1646	2.6676	1.1637	-0.1611	2.6672	1.160	-0.1576	2.666

0.5	1.1835	-0.1805	3.1509	1.1807	-0.1776	3.1614	1.176	-0.1737	3.1695
0.6	1.1889	-0.1874	3.5309	1.1855	-0.1839	3.5564	1.180	-0.1792	3.5795
0.7	1.2051	-0.2033	3.7652	1.2016	-0.1997	3.8109	1.198	-0.1963	3.8538
0.8	1.2200	-0.2181	3.8419	1.2166	-0.2148	3.9118	1.213	-0.2114	3.9763
T=313.15K				*T*= 318.15			*T*=323.15K		
0.2	IM	IM	1.6302	IM	IM	1.6258	IM	IM	1.6211
0.3	1.139	-0.1372	2.1274	1.1356	-0.1336	2.1224	1.131	-0.1299	2.1168
0.4	1.156	-0.154	2.6647	1.1529	-0.1504	2.6621	1.149	-0.1469	2.6594
0.5	1.173	-0.1703	3.1762	1.1698	-0.1668	3.1826	1.166	-0.1634	3.1867
0.6	1.178	-0.177	3.6021	1.1751	-0.1736	3.6212	1.171	-0.1701	3.6397
0.7	1.194	-0.1928	3.8959	1.1909	-0.1892	3.9333	1.187	-0.1857	3.9682
0.8	1.209	-0.208	4.0377	1.2065	-0.2047	4.0985	1.203	-0.2013	4.1539

IM-Immiscible

Table 5.14(d): Experimental Density ρ and Excess molar volume V_m^E for the binary system [EMIM][$MeSO_3$] (1) + Indoline (2)

x_{IL}	ρ	V_m^E		ρ	V_m^E		ρ	V_m^E	
	g.cm^{-3}	cm^3.mol^{-1}		g.cm^{-3}	cm^3.mol^{-1}		g.cm^{-3}	cm^3.mol^{-1}	
T= 298.15K				*T*=303.15K			*T*= 308.15K		
0.2	1.0825	-0.0853	0.9225	1.0787	-0.0813	0.9657	1.0748	-0.0773	1.0084
0.3	1.1351	-0.1350	1.0036	1.1316	-0.1314	1.0433	1.1280	-0.1278	1.0831
0.4	1.1497	-0.1496	1.056	1.1463	-0.1461	1.091	1.1431	-0.1429	1.1256
0.5	1.1681	-0.1675	1.0703	1.1648	-0.1642	1.0998	1.1614	-0.1608	1.1285
0.6	1.1883	-0.1868	1.0457	1.185	-0.1835	1.069	1.1816	-0.1801	1.0917
0.7	1.2014	-0.2002	0.9926	1.1981	-0.1969	1.0103	1.1947	-0.1935	1.0274
0.8	1.2146	-0.2137	0.938	1.2114	-0.2105	0.9505	1.2081	-0.2072	0.9625
T=313.15K				*T*=318.15K			*T*=323.15K		
0.2	1.0709	-0.0733	1.6302	1.067	-0.0693	1.6258	1.0631	-0.0653	1.6211
0.3	1.1244	-0.1242	2.1274	1.1209	-0.1206	2.1224	1.1173	-0.1171	2.1168
0.4	1.1399	-0.1397	2.6647	1.1365	-0.1362	2.6621	1.1330	-0.1326	2.6594
0.5	1.1580	-0.1573	3.1762	1.1546	-0.1539	3.1826	1.1511	-0.1504	3.1867
0.6	1.1783	-0.1768	3.6021	1.175	-0.1735	3.6212	1.1717	-0.1701	3.6397
0.7	1.1914	-0.1901	3.8959	1.188	-0.1868	3.9333	1.1847	-0.1835	3.9682
0.8	1.2048	-0.2038	4.0377	1.2014	-0.2004	4.0985	1.1981	-0.1971	4.1539

Table 5.14(e): Experimental Density ρ and Excess molar volume V_m^E for the binary system [EMIM][$MeSO_3$] (1) +Thiophene (2)

x_{IL}	ρ g.cm^{-3}	V_m^E cm^3.mol^{-1}		ρ g.cm^{-3}	V_m^E cm^3.mol^{-1}		ρ g.cm^{-3}	V_m^E cm^3.mol^{-1}	
	T= 298.15K			T=303.15K			T= 308.15K		
0.2	1.182	-0.1685	1.7825	1.180	-0.1662	1.8181	1.174	-0.1608	1.8524
0.3	1.191	-0.1791	1.9024	1.188	-0.1752	1.9339	1.184	-0.1714	1.9634
0.4	1.200	-0.1964	1.9969	1.196	-0.1926	2.0214	1.193	-0.1887	2.0445
0.5	1.210	-0.1919	2.0413	1.206	-0.1882	2.0581	1.202	-0.1845	2.0736
0.6	1.213	-0.2051	2.0072	1.209	-0.2014	2.0162	1.206	-0.1978	2.024
0.7	1.218	-0.2124	1.8693	1.214	-0.2089	1.8712	1.211	-0.2053	1.8725
0.8	1.225	-0.2217	1.6207	1.222	-0.2182	1.6186	1.218	-0.2147	1.6162
	T=313.15K			T= 318.15K			T=323.15K		
0.2	1.1719	-0.1582	1.8863	1.169	-0.1552	1.9182	1.168	-0.1537	1.9488
0.3	1.1803	-0.1676	1.9916	1.176	-0.1637	2.0192	1.172	-0.1599	2.0449
0.4	1.1894	-0.1848	2.067	1.185	-0.1809	2.0876	1.182	-0.1770	2.107
0.5	1.1985	-0.1807	2.0886	1.194	-0.1770	2.1019	1.190	-0.1733	2.1147
0.6	1.2024	-0.1942	2.0312	1.198	-0.1906	2.0374	1.195	-0.1870	2.0427
0.7	1.2078	-0.2018	1.8734	1.204	-0.1982	1.8737	1.200	-0.1947	1.8736
0.8	1.2154	-0.2112	1.6137	1.212	-0.2077	1.6109	1.208	-0.2043	1.6081

Table 5.14(f): Experimental Density ρ and Excess molar volume V_m^E for the binary system [EMIM][$MeSO_3$] (1) + water (2)

x_{IL}	ρ g.cm^{-3}	V_m^E cm^3.mol^{-1}		ρ g.cm^{-3}	V_m^E cm^3.mol^{-1}		ρ g.cm^{-3}	V_m^E cm^3.mol^{-1}	
	T= 298.15K			T=303.15K			T= 308.15K		
0.2	1.046	-0.0463	0.0701	1.0438	-0.0439	0.0733	1.032	-0.0332	0.0766
0.3	1.190	-0.1709	0.0826	1.1870	-0.1682	0.0863	1.183	-0.1654	0.0900
0.4	1.211	-0.1912	0.1002	1.2085	-0.1884	0.1045	1.205	-0.1855	0.1088
0.5	1.218	-0.2006	0.1263	1.2152	-0.1977	0.1314	1.211	-0.1947	0.1364
0.6	1.221	-0.2072	0.1682	1.2180	-0.2041	0.1743	1.214	-0.2011	0.1804
0.7	1.224	-0.2137	0.2426	1.2208	-0.2106	0.2499	1.217	-0.2075	0.2573
0.8	1.231	-0.2239	0.3911	1.2280	-0.2207	0.3996	1.224	-0.2175	0.4079
	T=313.15K			T= 318.15K			T=323.15K		
0.2	1.029	-0.0300	0.0799	1.0214	-0.0218	0.0833	1.0205	-0.0208	0.0866
0.3	1.180	-0.1624	0.0938	1.1769	-0.1593	0.0976	1.1735	-0.1562	0.1014
0.4	1.201	-0.1826	0.1131	1.1985	-0.1794	0.1175	1.1951	-0.1764	0.1219
0.5	1.208	-0.1917	0.1415	1.2053	-0.1886	0.1466	1.2020	-0.1856	0.1517

0.6	1.211	-0.1980	0.1864	1.2080	-0.1948	0.1925	1.2047	-0.1917	0.1986
0.7	1.214	-0.2044	0.2646	1.2109	-0.2011	0.2718	1.2075	-0.1980	0.2790
0.8	1.221	-0.2143	0.416	1.2180	-0.2110	0.4241	1.2147	-0.2078	0.4320

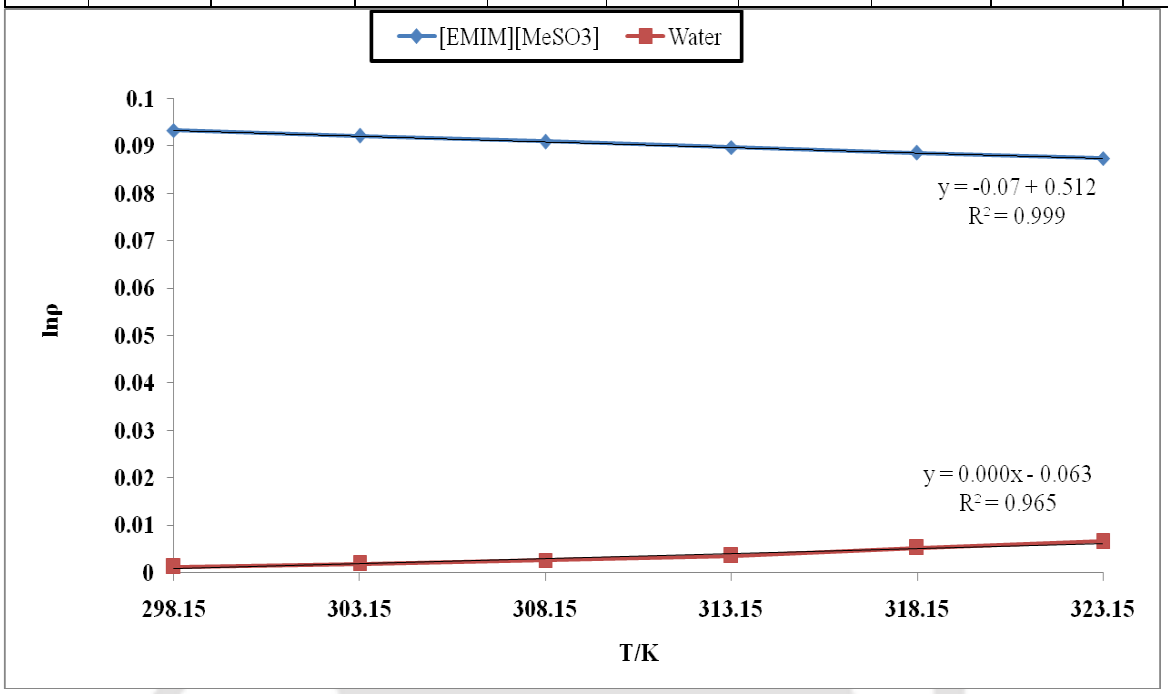

Figure 5.8: Plot of experimental values of *ln* ρ of the pure [EMIM][$MeSO_3$] ionic liquid Vs temperature of (298.15, 303.15,308.15,313.15,318.15,and 323.15) K

5.3.3.3 The coefficient of thermal expansion of {[EMIM][$MeSO_3$]}

Figure 5.8 shows the densities of pure [EMIM][$MeSO_3$], which decreases linearly (R^2=0.999) while the densities of water increases linearly (R^2 = 0.965) with increasing temperature. The value of α = 0.512K^{-1} (ionic liquid) and α = 0.004K^{-1} (water) was calculated from Equation 5.1. The volume expansivity of [EMIM][$MeSO_3$] and water was calculated using the measured density observed at different temperatures. As compared to water, the volume expansivity of [EMIM][$MeSO_3$] was found to be independent of temperature (Figure 2). These observations are consistent with the pure IL as measured by Rodriguez et al.,[2006], Wandschneider et al.,[2008], Pererio et al.,[2006, 2007].

5.3.3.4 Effect of temperature on density

Figure 5.9 shows the experimental densities of pure [EMIM][$MeSO_3$], aromatic nitrogen, aromatic sulphur, and water at temperatures of T = (298.15to 323.15) K. It can be seen that the density of all the pure components including ionic liquid decreases linearly with increasing temperature. Table 5.14(a) to 5.14(f) shows the experimental densities for six binary systems studied as a function of temperature over the entire mole fraction of [EMIM][$MeSO_3$]. For all the compounds with ILs, the densities varied linearly in the entire mole fraction with increasing temperature. This behavior can be explained by the efficient structural interaction of [EMIM][$MeSO_3$] with aromatic nitrogen/aromatic sulphur and water via packing effects [Domanska et al.,2007,2008]. Additionally it can be a result of the smaller size of cation and anion providing better interaction with aromatic nitrogen/sulphur, and water. A smaller size of IL molecule has a significant influence on densities with increasing temperature for entire mole fraction of IL. These behaviors strongly agree with the studies carried out by Rodriguez et al.,[2006], Domanska et al.,[2007, 2008].

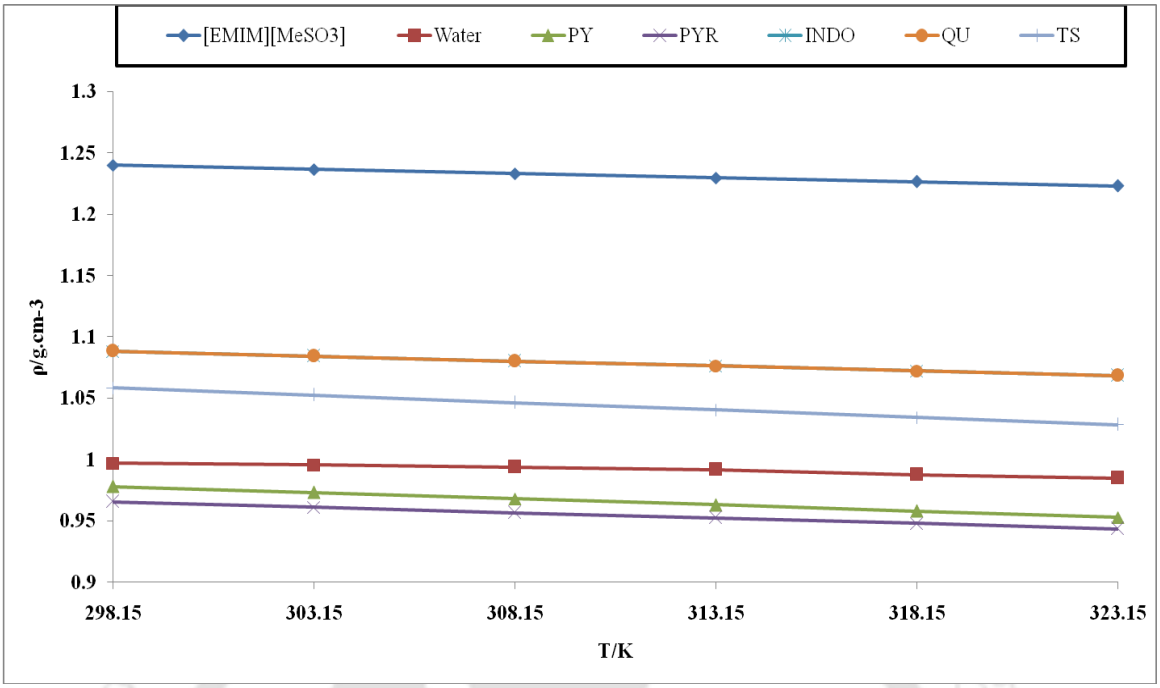

Figure 5.9: Density ρ of pure [EMIM][$MeSO_3$] ionic liquid, water , aromatic nitrogen (pyridine, pyrrole, indoline, quinoline) and aromatic sulphur (thiophene) at T = (298.15 to 323.15) K

5.3.3.5 Effect of composition on density

The experimental values of densities for [EMIM][$MeSO_3$] with aromatic nitrogen/sulphur and water with mole fraction of [EMIM][$MeSO_3$] are given in Table 5.14(a) to 5.14(f). As expected, density of mixture increases with increasing mole fraction of [EMIM][$MeSO_3$]. The densities for [EMIM][$MeSO_3$] with PY, PYR,INDO,QU, TS and water increases with increasing mole fraction of [EMIM][$MeSO_3$] at different temperature(Figure 5.10 and Table 5.14(b), 5.14(c), 5.14(d) ,5.14(e)). The n- π interaction (n = H(CH), O, N, F)[Domanska et al.,2007] weak hydrogen bond interaction [Alonso et al.,2008, Gomez et al.,2007], van der Waals [Alonso et al.,2008, Gomez et al.,2007,Lei et al.,2006] interaction, CH-π bond interaction [Cassol et al.,2007,Anantharaj at al.,2011,2010a,2010b] and π - -π interaction [Domanska et al.,2010] plays a significant

role when aromatic nitrogen/sulphur is mixed with [EMIM][$MeSO_3$]. The nitrogen and sulphur atom of aromatic compounds forms hydrogen bond with hydrogen in imidazolium ring or with the hydrogen located on the alkyl group of the imidazolium cation. It should be noted that the electrostatic interaction is mostly weaker between [EMIM] and [$MeSO_3$] due to the methyl substitution on the anion structure. Due to this very fact, the density of mixture increases with increasing mole fraction of [EMIM][$MeSO_3$] at different temperature.

On the other hand, it is observed that the influence of composition has a important role on the interaction between [EMIM][$MeSO_3$] and neutral aromatic species like pyrrole and thiophene as compared to other aromatic nitrogen compounds with basic and acidic nature such as pyridine, indoline, quinoline and water. Therefore, the probable explanation lies in the fact that [EMIM][$MeSO_3$] have stronger interaction with similar molecules like pyrrole and thiophene (both five membered) than dissimilar molecules such as pyridine, indoline, quinoline, and water. Similar structures of IL and pyrrole/thiophene possessing different electro negative atom within their structure is known to play a crucial role in increasing the interaction. But at the same time [EMIM][$MeSO_3$] has excellent structural orientation with dissimilar structure molecules like pyridine, indoline, quinoline and water, since there is an enormous possibility to interact with each other via n- π interaction (n = H(CH), O, N, F)[Domanska et al.,2007], weak hydrogen bond interaction [Gomez et al.,2007], CH-π bond interaction[Cassol et al.,2007,Anantharaj at al.,2011,2010a,2010b] and π - -π interaction [Anantharaj at al.,2010b].However these interaction are less when compared with pyrrole or thiophene. This results in the increasing trend of density with increasing mole fraction of [EMIM][$MeSO_3$].This is evident from IL-pyridine (Figure 5.10), IL-indoline (Table 5.14(c)), IL-thiophene (Table 5.14(e)) and IL-water (Table 5.14(f)) mixtures where the densities increases with increasing mole fraction of IL.

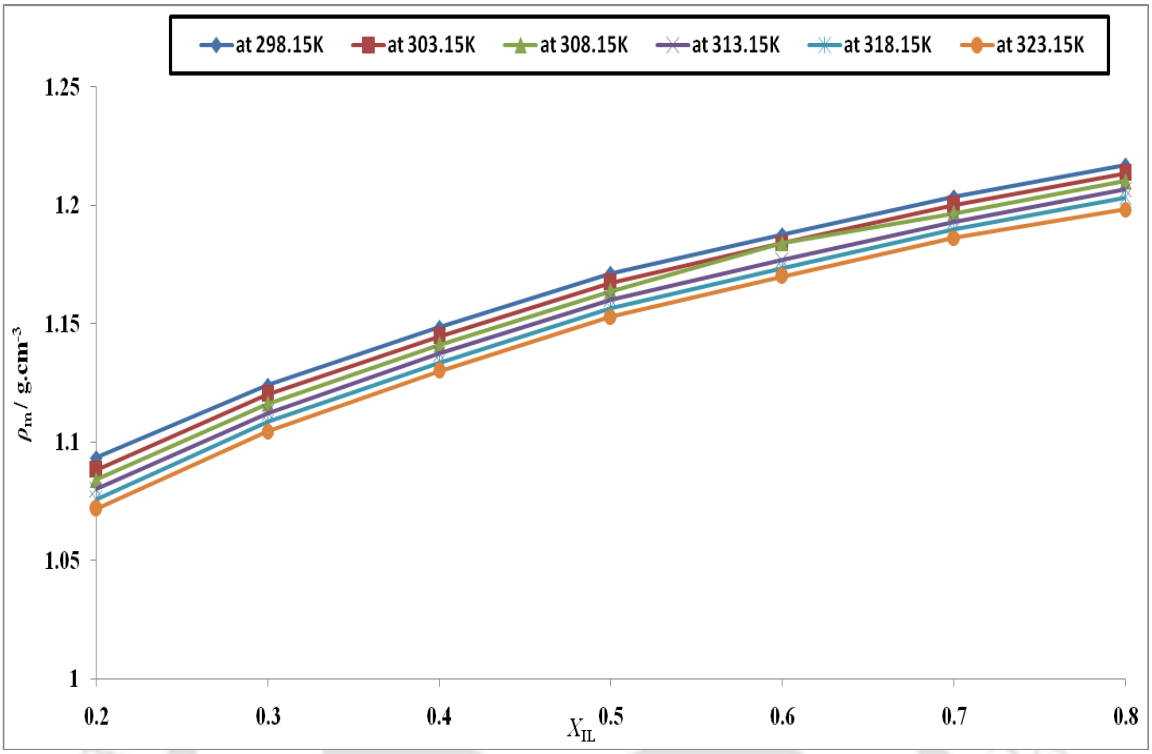

Figure 5.10: Experimental density for the binary system {[EMIM][$MeSO_3$] (1) + pyridine (2)} as a function of mole fraction of the IL at different temperature

5.3.3.6 Effect of composition on surface tension

Table 5.15 present the variation of surface tension with mole fraction for all the studied binary systems. The values of surface tension for all studied systems exhibit a linear increase with increasing mole fraction of [EMIM][$MeSO_3$].The fusion of benzene ring or addition of benzene ring with nitrogen species have significant influence on the surface tension upon mixing with [EMIM][$MeSO_3$]. Thus pyrrole, thiophene and water (Table 5.15) have higher surface tension as compared to those compounds with additional benzene ring such as quinoline,indoline and pyridine. For [EMIM][$MeSO_3$] -water mixture, the surface tension linearly increases with an increasing mole fraction due to the increasing strength of hydrogen bond upon mixing (72.1mN.m^{-1} for water and 48.4

$mN.m^{-1}$ for [EMIM][$EtSO_4$]). The nature of alkyl substitution at [EMIM][$MeSO_3$] dominates the surface tension and can define the trend of surface tension. The observed trend and values are consistent with those reported by Gomez et al.,[2006], Wandschneider et al.,[2008].

The surface tension of aromatic nitrogen and sulphur are lower than [EMIM][$MeSO_3$] ionic liquid, however a comparison could not be done because of the scarcity of literature data. [EMIM][$MeSO_3$] with aromatic nitrogen/sulphur are highly governed by the nature of their structure as well as the electro negative atom located on the studied compounds. The observed surface tension values decreases in the order: [EMIM][$MeSO_3$] +water < [EMIM][$MeSO_3$] +QU <[EMIM][$MeSO_3$] + PYRR < [EMIM][$MeSO_3$] + INDO < [EMIM][$MeSO_3$] + TS< [EMIM][$MeSO_3$] + PY. Thus trace of water and other impurities play an important role on surface tension of [EMIM][$MeSO_3$] upon mixing. Thus by adjusting the ratio of van der Waals interaction to coulumbic interaction [Kilaru et al., 2007] one can promote higher solvation capability of [EMIM][$MeSO_3$] [Ghatee et al.,2008].

5.3.3.7 Effect of composition on refractive index

Table 5.16 shows the experimental refractive index over the entire composition range of [EMIM][$MeSO_3$]. The refractive index decreases over the mole fraction of [EMIM][$MeSO_3$] for all systems except for [EMIM][$MeSO_3$] + water mixture where the refractive index increases with increasing mole fraction of [EMIM][$MeSO_3$]. This behavior can be explained by an efficient packing in the [EMIM][$MeSO_3$] -nitrogen/sulphur mixture as compared to [EMIM][$MeSO_3$] -water mixture system. Among the six binary systems, the higher refractive index was observed for [EMIM][$MeSO_3$] with quinoline which indicates an increased interaction with [EMIM][$MeSO_3$].The influence of an increasing mole fraction of [EMIM][$MeSO_3$] on

the mixture refractive index has shown that except for [EMIM][$MeSO_3$] + water system, refractive index decreases in the order: [EMIM][$MeSO_3$] + thiophene < [EMIM][$MeSO_3$] + quinoline < [EMIM][$MeSO_3$] + indoline < [EMIM][$MeSO_3$] + pyrrole < [EMIM][$MeSO_3$] + pyridine. The ratio of van der Waals and coulombic force [Kilaru et al., 2007] again causes the refractive index of the mixture to decrease with increasing mole fraction of [EMIM][$MeSO_3$] due to the difference in shape and size of the molecules .Therefore, these results suggest that [EMIM][$MeSO_3$] have more influence on the separation of aromatic nitrogen/sulphur rather than water. Besides, the ability of [EMIM][$MeSO_3$] to create a favorable hydrogen bond with aromatic nitrogen/sulphur significantly increases the solubility of [EMIM][$MeSO_3$] in aromatic nitrogen/sulphur.

Table 5.15: Experimental surface tension σ and deviation of surface tension $\Delta\sigma$ for the Binary systems: (a) [EMIM][$MeSO_3$] + Pyridine, (b). [EMIM][$MeSO_3$]+ Pyrrole, (c).[EMIM][$MeSO_3$] + Indoline, (d). [EMIM][$MeSO_3$] + Quinoline, (e) [EMIM][$MeSO_3$] + Thiophene, and (f) [EMIM][$MeSO_3$] + Water.

[EMIM][$MeSO_3$] + PY		[EMIM][$MeSO_3$] + PYRR		[EMIM][$MeSO_3$] + QU	
x_{IL}	σ /mN.m^{-1}	$\Delta\sigma$ /mN.m^{-1}	σ /mN.m^{-1}	$\Delta\sigma$ /mN.m^{-1}	σ mN.m^{-1}	$\Delta\sigma$ /mN.m^{-1}
0.2	26.8	-12.22	34.4	-7.98	IM	IM
0.3	28.2	-11.58	35.1	-7.62	39.1	-6.98
0.4	33.2	-7.34	36.0	-7.06	40.6	-5.34
0.5	36.2	-5.1	37.4	-6	40.6	-5.2
0.6	38.2	-3.86	39.0	-4.74	40.7	-4.96
0.7	39.5	-3.32	40.8	-3.28	42.1	-3.42
0.8	40.2	-3.38	42.4	-2.02	42.6	-2.78
[EMIM][$MeSO_3$] + INDO		[EMIM][$MeSO_3$] + TS		[EMIM][$EtSO_3$]+ WATER	
x_{IL}	σ /mN.m^{-1}	$\Delta\sigma$ /mN.m^{-1}	σ /mN.m^{-1}	$\Delta\sigma$ /mN.m^{-1}	σ mN.m^{-1}	$\Delta\sigma$ /mN.m^{-1}
0.2	30.8	-4.3	30.8	-3.58	33.6	-31.5
0.3	32.5	-3.85	33.0	-2.72	40.3	-22.3
0.4	34.2	-3.4	34.4	-2.66	40.8	-19.3
0.5	36.0	-2.85	36.8	-1.6	41.3	-16.3

0.6	38.1	-2	38.6	-1.14	44.2	-10.9
0.7	40.0	-1.35	40.0	-1.08	44.6	-8
0.8	42.4	-0.2	41.7	-0.72	45.1	-5

IM-Immiscible

5.3.3.8 Combined effect of temperature and composition on density properties

The trend in the performance of experimental data for density (Figure 5.10 and Table 5.14(b)) to 5.14(f)) of the studied binary systems has been presented as a function of temperature and mole fraction of [EMIM][$MeSO_3$]. In general for all the systems, an increase in property in seen with composition, and decrease with temperature. However the variation of the thermodynamic property is much dependent on composition as compared to temperature. This can be explained by the composition of [EMIM][$MeSO_3$],which plays a significant role upon mixing than temperature over the transport properties of mixtures. Water molecules are influenced by hydrogen bonding upon mixing, which is more temperature dependent therefore the columbic force [Gomez et al.,2007] and other interaction parameters[Alonso et al.,2008, Domanska et al.,2007, Domanska et al.,2008, Cassol et al.,2007,Anantharaj at al.,2011,2010a,2010b] are negligible. The aromatic nitrogen/sulphur compound with [EMIM][$MeSO_3$] is influenced by composition and by nature of species and are strongly recognized with several possible interaction parameters as discussed earlier and also due to the effective structural orientation of similar molecules (Figure 5.13(a) to 5.13(e),Table 5.14(f)). This behavior is more consistent with information available in the literature [Kilaru et al., 2007]. Thus it can be observed that the mole fraction of [EMIM][$MeSO_3$] has significant influence on the separation of aromatic nitrogen and sulphur compound .

5.3.3.9 Effect of composition on excess molar volume

The excess molar volume V_m^E gives information over the net destruction of interactions and packing phenomena that appears in the mixing process [Seddon et al., 2000, Huo et al., 2007]. The excess molar volume V_m^E were calculated from

experimental density data for all studied systems according to equation 5.2. These calculated values are given in Table 5.14(a) to 5.14(f). For [EMIM][$MeSO_3$] + pyridine mixture (Figure 5.11)exhibit negative deviation from ideality. It is readily observed that the pyridine has stronger interaction with [EMIM][$MeSO_3$]. A similar phenomena has been observed for other studied system including water and it is more consistent with [BMIM][BF_4] +water system as reported by Seddon et al.,2000.This behaviour is explained in terms of dissociation of ions or the association of similar molecules with [EMIM][$MeSO_3$], in which they can form another IL namely: [EMIM][HSO_4] due to the hydrophilic nature of [EMIM][$MeSO_3$] .It should be noted that [EMIM][$MeSO_3$] have the ability to form hydrogen bonds or other specific interaction with basic, acidic and neutral molecules .

Table 5.16: Experimental refractive index *nD* and deviation of refractive index *ΔnD* for the Binary systems: (a) [EMIM][$MeSO_3$] + Pyridine, (b). [EMIM][$MeSO_3$]+ Pyrrole, (c).[EMIM][$MeSO_3$] + Indoline, (d). [EMIM][$MeSO_3$] + Quinoline, (e) [EMIM][$MeSO_3$] + Thiophene, and (f) [EMIM][$MeSO_3$] + Water.

[EMIM][$MeSO_3$] + PY			[EMIM][$MeSO_3$] + PYRR		[EMIM][$MeSO_3$] + QU	
x_{IL}	*nD*	*ΔnD*	*nD*	*ΔnD*	*nD*	*ΔnD*
0.2	1.4893	-0.03254	1.5003	-0.01452	IM	IM
0.3	1.4867	-0.04666	1.4935	-0.03453	1.5651	0.03642
0.4	1.4852	-0.06758	1.4880	-0.05324	1.5506	0.01708
0.5	1.4826	-0.0807	1.4871	-0.06735	1.5395	-0.0095
0.6	1.4808	-0.09382	1.4870	-0.08066	1.5264	-0.03268
0.7	1.4799	-0.10664	1.4784	-0.11047	1.5176	-0.05786
0.8	1.4721	-0.11866	1.4783	-0.11578	1.5030	-0.07874
[EMIM][$MeSO_3$] + INDO			[EMIM][$MeSO_3$] + TS		[EMIM][$EtSo_4$]+ WATER	
x_{IL}	*nD*	*ΔnD*	*nD*	*ΔnD*	*nD*	*ΔnD*
0.2	1.5771	-0.01636	1.6306	0.08482	1.4544	0.0743
0.3	1.5539	-0.04294	1.4879	-0.06722	1.4427	0.03255

0.4	1.5305	-0.06972	1.4809	-0.08356	1.4416	0.0014
0.5	1.5231	-0.0805	1.4804	-0.0934	1.4659	-0.00435
0.6	1.5163	-0.09068	1.4819	-0.10124	1.4680	-0.0323
0.7	1.5101	-0.10026	1.4902	-0.10228	1.4767	-0.05365
0.8	1.4977	-0.11604	1.4882	-0.11362	1.4808	-0.0796

IM-Immiscible

5.3.3.10 Effect of composition on deviation of surface tension

The deviations of surface tension of above mentioned system were calculated from their experimental data at 298.15K via equation 5.3 The dependence of the surface tension deviations on mole fraction of IL is displayed in Table 5.15.The values of surface tension deviations for all the systems were negative over the whole range of compositions at 298.15K. The deviation of surface tension increases as in the following order: [EMIM][$MeSO_3$] (1) + QU(2)< [EMIM][$MeSO_3$] (1) + INDO(2)< [EMIM][$MeSO_3$] (1) + PY(2)< [EMIM][$MeSO_3$] (1) + PYRR(2)< [EMIM][$MeSO_3$] (1) + TS(2) < [EMIM][$MeSO_3$] (1) + water(2).It can be observed that similar molecules (pyrrole and thiophene) and hydrophilic nature of ILs has significant role as compared to dissimilar molecules (pyridine, quinoline and indoline)., except water molecules

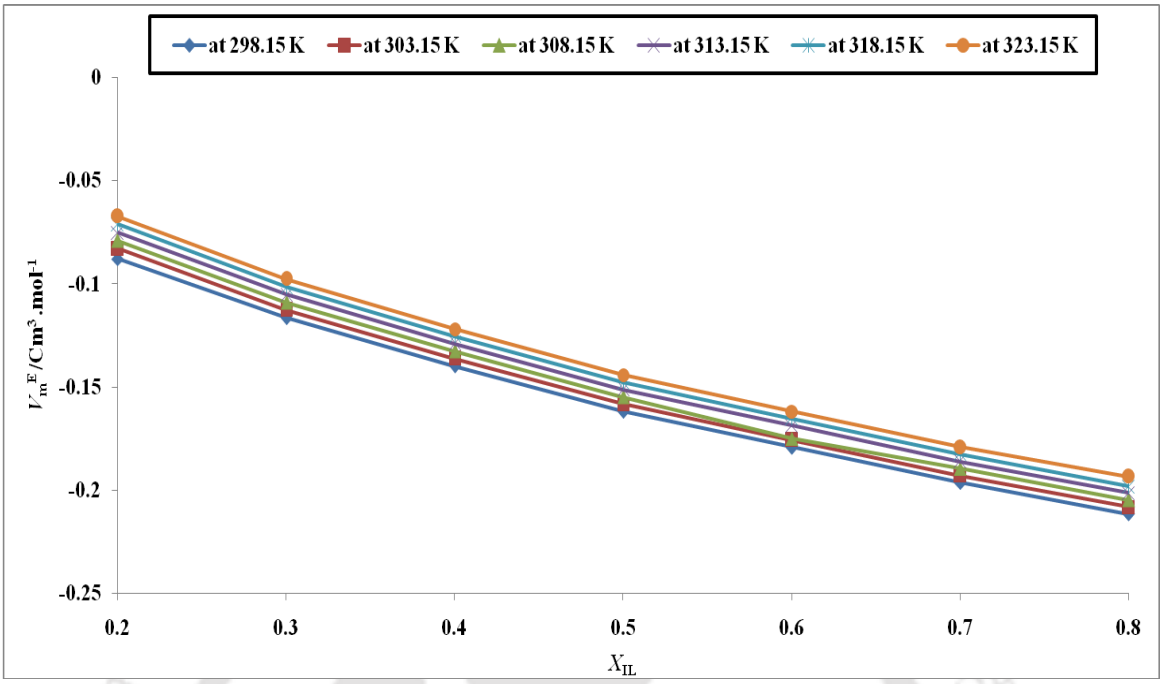

Figure 5.11: Excess molar volume V_m^E for the system of [EMIM][$MeSO_3$] (1) + pyridine (2) at different temperatures

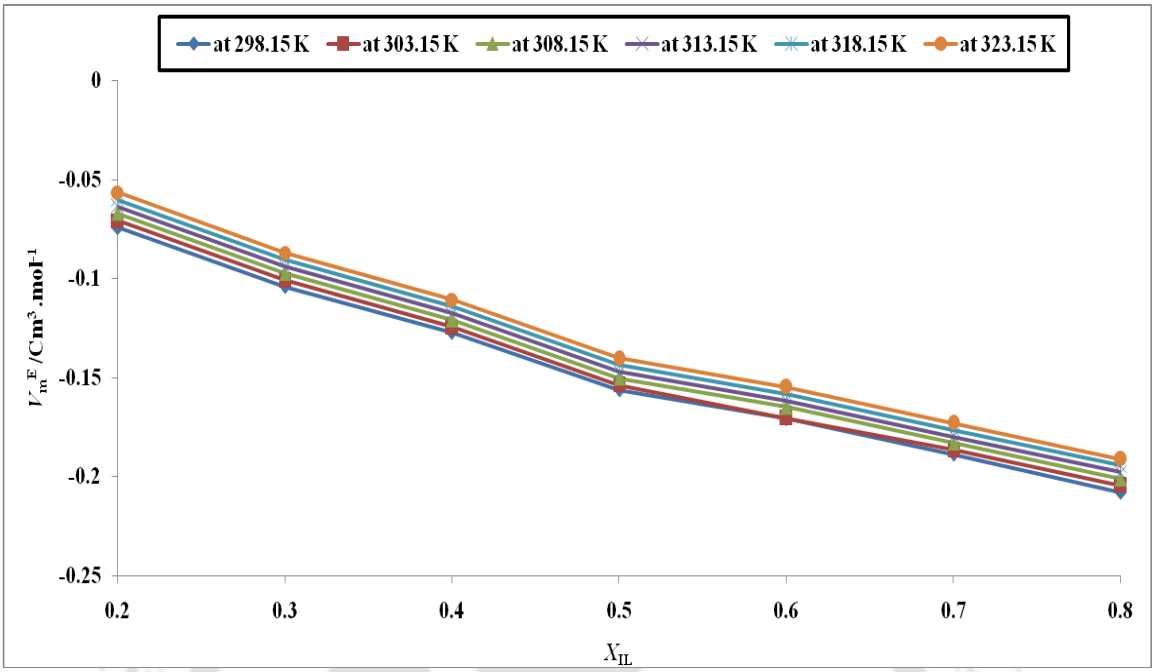

Figure 5.12: Excess molar volume V_m^E for the system of [EMIM][$MeSO_3$] (1) + pyrrole (2) at different temperatures

5.3.3.11 Effect of composition on deviation of refractive index

Table 5.16 shows the deviation of refractive index for [EMIM][$MeSO_3$] (1) + PY(2), [EMIM][$MeSO_3$] (1) + PYRR(2), [EMIM][$MeSO_3$] (1) + QU(2), [EMIM][$MeSO_3$] (1) + INDO(2), [EMIM][$MeSO_3$] (1) + TS(2) and [EMIM][$MeSO_3$] (1) + water(2) system as a function of composition of [EMIM][$MeSO_3$] at 298.15K.The deviation of refractive index were calculated from our experimental data according to equation 5.4.The values of deviation of refractive index for [EMIM][$MeSO_3$] (1) + PY(2), [EMIM][$MeSO_3$] (1) + PYRR(2), [EMIM][$MeSO_3$] (1) + INDO(2) and [EMIM][$MeSO_3$] (1) + TS(2) system exhibit more negative values, ~ - 0.1.The decrease in refractive index deviation is in the order: [EMIM][$MeSO_3$] (1) + water(2) >

[EMIM][$MeSO_3$] (1) + QU(2)> [EMIM][$MeSO_3$] (1) + INDO(2)> [EMIM][$MeSO_3$] (1) + PYRR(2)> [EMIM][$MeSO_3$] (1) + PY(2)>[EMIM][$MeSO_3$] (1) + TS(2).

5.3.3.12 Combined effect of temperature and composition on thermodynamic properties

The combined effect of temperature and composition gives more information about the net destruction of interaction and packing effect for [EMIM][$MeSO_3$] (1) + PY(2), [EMIM][$MeSO_3$] (1) + PYRR(2), [EMIM][$MeSO_3$] (1) + QU(2), [EMIM][$MeSO_3$] (1) + INDO(2), [EMIM][$MeSO_3$] (1) + TS(2) and [EMIM][$MeSO_3$] (1) + water(2) system as a function of temperature and composition of [EMIM][$MeSO_3$] (Table 5.14(a) to 5.14(f)).The excess molar volume is negative for all the studied systems over the whole mole fraction of [EMIM][$MeSO_3$] as the temperature is raised. This indicates that the mixtures are non-ideal, and the IL – IL or component – component interaction is lesser as compared to IL – component interaction. Thus IL can be used as a solvent for desulphurization and denitrification. However, the maximum interaction occurs when approximately $x_{IL} < 0.5$ is reached for all the systems. The excess molar volume and density is seen to vary linearly with respect to temperature and mole fraction for all the systems. On the other hand, the surface tension and refractive index deviation for the above mentioned system has a negative deviation for entire mole fraction of [EMIM][$MeSO_3$] at T=298.15K .Therefore, it is clear that the mole fraction or composition of [EMIM][$MeSO_3$] has an important role as compared to temperature on thermodynamic properties of all the systems.

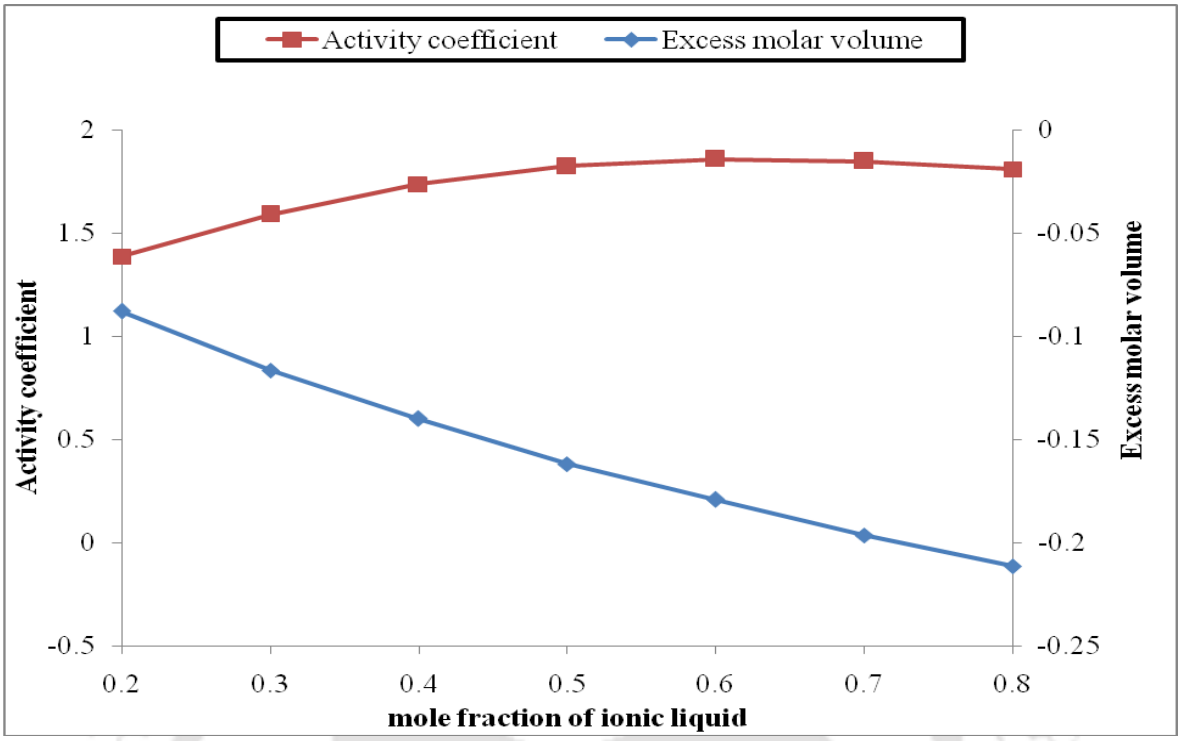

Figure 5.13: Relation of activity coefficient with excess molar volume as a function of mole fraction of [EMIM][$MeSO_3$] at T=298.15K.

5.3.3.13 Comparison of activity coefficient with excess molar volume

The activity coefficient values predicted via COSMO-RS for the all the studied systems are given in Table 5.14(a) to 5.14(f). Figure 5.13 shows a comparison of predicted activity coefficient and excess volume for IL-pyridine mixture. The computational details are given in our earlier published articles [Anantharaj et.al., 20l0a, Anantharaj et.al., 20l1b]. The predicted activity coefficient increases with increasing mole fraction of ionic liquid in the mixture, except for [EMIM][$MeSO_3$] + water systems. However the excess molar volumes are seen to decrease with mole fraction. Thus it is fair to say that the activity coefficient is inversely proportional to excess volume.

It is observed that the properties of mixture are influenced by the aromatic ring structure of thiophene, pyridine, pyrrole, indoline and quinoline (Table 5.14(a) to 5.14(f)

).The activity coefficient also gives us an indication of the strength of solubility.For example, [EMIM][$MESO_3$] + pyrrole system (Table 5.14(b)) shows low activity coefficient (i.e,.high solubility with mole fraction of IL) as compared to [EMIM][$MESO_3$] + thiophene(Table 5.14(e)) which implies that the solubility of pyrrole in [EMIM][$MeSO_3$] is higher than thiophene. In case of excess molar volume both the systems shows an increasing excess molar volume with increasing mole fraction of IL. Here the possible specific interactions may be π--π stacking, CH -- π interaction, N (nitrogen compounds) -- H and S (sulphur compounds) -- H interaction.

5. 3.4 1-Ethyl-3-Methylimidazolium Thiocyanate {[EMIM][SCN] }

5.3.4.1 Pure components

Experimental densities of pure **[**EMIM][SCN], aromatic nitrogen, aromatic sulphur species and water have been measured and benchmarked at different temperatures (Table 5.2). Beside the effect of temperature and experimental method, the presence of trace amount of impurities such as water or ions provides a remarkable effect on thermodynamic properties [Yanfang et al.,2008].Table 5.2 shows the comparison of measured densities for pure **[**EMIM][SCN] with temperature. Table 5.2 shows the comparison between experimental and literature data of the pure aromatic nitrogen/ sulphur, and water at 298.15 K. This agrees will with data reported for pyridine, pyrrole and quinoline [Sapi et al.,2006a].This also matches with the experimental data obtained earlier for thiophene [Sapi et al.,2006b] and water [Gomez et al.,2006]. The density ρ of pure ionic liquid is higher than that of water, and also than that of aromatic nitrogen/sulphur compounds. Table 5.3 shows a comparison for the surface tension σ and refractive index *nD* of pure components with literature data at 298.15 K. The surface tension and refractive index were compared successfully against the known value of water [Sapi et al.,2006a] and thiophene [Sapi et al.,2006b] respectively. The difference between experimental and literature data for pure **[**EMIM][SCN] can be explained by the thermodynamic properties which strongly depends on water and other impurities.

Table 5.17(a): Experimental Density ρ and Excess molar volume V_m^E, for the binary system [EMIM][SCN] (1) + Pyridine (2)

x_{IL}	ρ g cm^{-3}	V_m^E cm^3 mol^{-1}		ρ g cm^{-3}	Vm_E cm^3 mol^{-1}		ρ g cm^{-3}	VmE cm^3 mol^{-1}	
	T= 298.15K			T=303.15K			T= 308.15K		
0.2	1.0452	-0.0434	1.1988	1.0412	-0.0396	1.2007	1.0372	-0.0357	1.2025
0.3	1.0601	-0.0578	1.3841	1.0563	-0.0541	1.3874	1.0525	-0.0504	1.3900
0.4	1.0726	-0.0699	1.5733	1.0691	-0.0664	1.5788	1.0655	-0.0630	1.5833
0.5	1.0823	-0.0795	1.7402	1.0788	-0.0762	1.7493	1.0754	-0.0728	1.7570
0.6	1.0928	-0.0900	1.8689	1.0895	-0.0868	1.8822	1.0862	-0.0836	1.8950
0.7	1.0965	-0.0945	1.9504	1.0933	-0.0913	1.9694	1.0900	-0.0881	1.9879
0.8	1.1021	-0.1007	1.9863	1.0989	-0.0975	2.0117	1.0957	-0.0944	2.0362
	T=313.15K			T= 318.15K			T=323.15K		
0.2	1.0332	-0.0319	1.2039	1.0293	-0.0281	1.2053	1.0253	-0.0242	1.2066
0.3	1.0488	-0.0468	1.3923	1.0450	-0.0431	1.3946	1.0412	-0.0395	1.3965
0.4	1.0620	-0.0596	1.5877	1.0585	-0.0562	1.5911	1.0550	-0.0528	1.5944
0.5	1.0720	-0.0695	1.7645	1.0686	-0.0662	1.7706	1.0653	-0.0629	1.7765
0.6	1.0830	-0.0803	1.9061	1.0797	-0.0771	1.9169	1.0765	-0.0739	1.9259
0.7	1.0868	-0.0849	2.0042	1.0836	-0.0817	2.0201	1.0804	-0.0785	2.0339
0.8	1.0925	-0.0912	2.0591	1.0894	-0.0881	2.0799	1.0862	-0.0850	2.1000

Table 5.17(b): Experimental Density ρ and Excess molar volume V_m^E, for the binary system [EMIM][SCN] (1) + Pyrrole (2)

x_{IL}	ρ g cm^{-3}	V_m^E cm^3 mol^{-1}		ρ g cm^{-3}	Vm_E cm^3 mol^{-1}		ρ g cm^{-3}	VmE cm^3 mol^{-1}	
	T= 298.15K			T=303.15K			T= 308.15K		
0.2	1.0284	-0.0275	0.3445	1.0247	-0.0239	0.3552	1.0210	-0.0203	0.3659
0.3	1.0492	-0.0472	0.2176	1.0457	-0.0440	0.2271	1.0422	-0.0406	0.2367

0.4	1.0562	-0.0543	0.1522	1.0528	-0.0512	0.1604	1.0493	-0.0478	0.1687
0.5	1.0736	-0.0708	0.1124	1.0703	-0.0680	0.1194	1.0669	-0.0648	0.1266
0.6	1.0886	-0.0853	0.0858	1.0854	-0.0827	0.0919	1.0822	-0.0796	0.0981
0.7	1.0945	-0.0918	0.0671	1.0913	-0.0893	0.0723	1.0882	-0.0861	0.0777
0.8	1.1035	-0.1018	0.0535	1.1003	-0.0986	0.058	1.0972	-0.0955	0.0626
		T=313.15K			*T*= 318.15K			*T*=323.15K	
0.2	1.0174	-0.0168	0.3764	1.0137	-0.0133	0.3869	1.0101	-0.0097	0.3973
0.3	1.0388	-0.0373	0.2464	1.0353	-0.0339	0.256	1.0319	-0.0306	0.2657
0.4	1.0458	-0.0444	0.1771	1.0424	-0.0411	0.1857	1.0390	-0.0377	0.1942
0.5	1.0636	-0.0616	0.134	1.0604	-0.0584	0.1415	1.0571	-0.0552	0.1491
0.6	1.0790	-0.0764	0.1045	1.0758	-0.0733	0.111	1.0726	-0.0702	0.1177
0.7	1.0850	-0.0830	0.0832	1.0819	-0.0800	0.089	1.0788	-0.0769	0.0948
0.8	1.0941	-0.0925	0.0675	1.0910	-0.0894	0.0725	1.0879	-0.0864	0.0777

Table 5.17(c): Experimental Density ρ and Excess molar volume V_m^E for the binary system [EMIM][SCN] (1) + Quinoline (2)

x_{IL}	ρ	V_m^E		ρ	Vm_E		ρ	VmE	
	g cm^{-3}	cm^3 mol^{-1}		g cm^{-3}	cm^3 mol^{-1}		g cm^{-3}	cm^3 mol^{-1}	
	T= 298.15K			T=303.15K			T= 308.15K		
0.2	1.1084	-0.1070	1.4345	1.1049	-0.1034	1.4326	1.1012	-0.0998	1.4307
0.3	1.1122	-0.1106	1.9141	1.1087	-0.1071	1.9102	1.1053	-0.1037	1.9062
0.4	1.1140	-0.1125	2.5577	1.1106	-0.1090	2.5528	1.1071	-0.1056	2.5477
0.5	1.1163	-0.1148	3.3339	1.1131	-0.1116	3.3324	1.1098	-0.1083	3.3304
0.6	1.1170	-0.1157	4.1652	1.1138	-0.1125	4.1776	1.1106	-0.1093	4.1854
0.7	1.1172	-0.1161	4.9321	1.1141	-0.1130	4.9702	1.1109	-0.1098	5.0011
0.8	1.1173	-0.1165	5.5048	1.1141	-0.1133	5.5815	1.1110	-0.1102	5.6486
	T=313.15K			T= 318.15K			T=323.15K		
0.2	1.0976	-0.0963	1.4285	1.0940	-0.0927	1.4264	1.0904	-0.0891	1.424
0.3	1.1018	-0.1003	1.9016	1.0983	-0.0968	1.897	1.0948	-0.0934	1.8918
0.4	1.1037	-0.1022	2.5414	1.1002	-0.0988	2.535	1.0968	-0.0954	2.5274
0.5	1.1065	-0.1050	3.3258	1.1033	-0.1018	3.321	1.1000	-0.0986	3.3139
0.6	1.1074	-0.1061	4.1923	1.1042	-0.1029	4.1949	1.1010	-0.0997	4.1969
0.7	1.1077	-0.1067	5.0304	1.1045	-0.1035	5.0529	1.1014	-0.1004	5.0742
0.8	1.1079	-0.1071	5.7135	1.1047	-0.1040	5.7725	1.1016	-0.1009	5.8225

Table 5.17(d): Experimental Density ρ and Excess molar volume V_m^E for the binary system [EMIM][SCN] (1) + Indoline (2)

x_{IL}	ρ	V_m^E		ρ	Vm_E		ρ	VmE	
	g cm^{-3}	cm^3 mol^{-1}		g cm^{-3}	cm^3 mol^{-1}		g cm^{-3}	cm^3 mol^{-1}	
	T= 298.15K			T=303.15K			T= 308.15K		
0.2	1.0838	-0.0846	1.2640	1.0802	-0.0809	1.2659	1.0765	-0.0772	1.2675
0.3	1.0927	-0.0930	1.5451	1.0893	-0.0896	1.5484	1.0858	-0.0861	1.5511
0.4	1.0992	-0.0991	1.8866	1.0959	-0.0959	1.8931	1.0926	-0.0925	1.8987
0.5	1.1041	-0.1039	2.2431	1.1009	-0.1006	2.2568	1.0976	-0.0973	2.2687
0.6	1.1061	-0.1059	2.5539	1.1029	-0.1027	2.5800	1.0997	-0.0995	2.6033
0.7	1.1093	-0.1090	2.7565	1.1061	-0.1059	2.8004	1.1030	-0.1027	2.8406
0.8	1.1131	-0.1127	2.8091	1.1100	-0.1096	2.8725	1.1069	-0.1065	2.9346
	T=313.15K			T= 318.15K			T=323.15K		
0.2	1.0729	-0.0735	1.2690	1.0693	-0.0699	1.2702	1.0656	-0.0662	1.2712
0.3	1.0824	-0.0826	1.5536	1.0789	-0.0791	1.5555	1.0754	-0.0755	1.5572
0.4	1.0892	-0.0891	1.9038	1.0859	-0.0858	1.9080	1.0826	-0.0825	1.9117
0.5	1.0944	-0.0941	2.2799	1.0911	-0.0908	2.2895	1.0879	-0.0876	2.2984
0.6	1.0965	-0.0962	2.6257	1.0933	-0.0931	2.6455	1.0901	-0.0899	2.6644
0.7	1.0999	-0.0996	2.8796	1.0967	-0.0965	2.9150	1.0936	-0.0934	2.9493
0.8	1.1038	-0.1034	2.9926	1.1008	-0.1004	3.0492	1.0977	-0.0974	3.1032

Table 5.17(e): Experimental Density ρ and Excess molar volume V_m^E, for the binary system [EMIM][SCN] (1) + Thiophene (2)

x_{IL}	ρ	V_m^E		ρ	Vm_E		ρ	VmE	
	g cm^{-3}	cm^3 mol^{-1}		g cm^{-3}	cm^3 mol^{-1}		g cm^{-3}	cm^3 mol^{-1}	
	T= 298.15K			T=303.15K			T= 308.15K		
0.2	1.1107	-0.1066	1.6572	1.1067	-0.1026	1.6502	1.1023	-0.0983	1.6432
0.3	1.1061	-0.1031	2.0822	1.1024	-0.0994	2.0738	1.0986	-0.0956	2.0654
0.4	1.1122	-0.1090	2.4632	1.1085	-0.1054	2.4581	1.1049	-0.1017	2.4518
0.5	1.1144	-0.1116	2.7427	1.1107	-0.1078	2.7449	1.1069	-0.1040	2.7464
0.6	1.1150	-0.1127	2.8916	1.1119	-0.1095	2.9055	1.1087	-0.1062	2.9184
0.7	1.1157	-0.1139	2.9142	1.1124	-0.1105	2.9428	1.1090	-0.1071	2.9688
0.8	1.1166	-0.1152	2.8414	1.1133	-0.1120	2.8824	1.1101	-0.1087	2.9211
	T=313.15K			T= 318.15K			T=323.15K		

0.2	1.0980	-0.0940	1.6362	1.0935	-0.0896	1.6292	1.0889	-0.0851	1.6222
0.3	1.0947	-0.0917	2.0566	1.0909	-0.0879	2.0477	1.0870	-0.0840	2.0384
0.4	1.1012	-0.0981	2.4452	1.0976	-0.0944	2.4376	1.0940	-0.0908	2.4298
0.5	1.1031	-0.1003	2.7459	1.0993	-0.0965	2.7449	1.0955	-0.0928	2.7421
0.6	1.1055	-0.1030	2.9285	1.1023	-0.0998	2.9376	1.0992	-0.0967	2.945
0.7	1.1056	-0.1038	2.9915	1.1023	-0.1004	3.0129	1.0990	-0.0971	3.0321
0.8	1.1069	-0.1055	2.9573	1.1037	-0.1023	2.9909	1.1005	-0.0991	3.0216

Table 5.17(f): Experimental Density ρ and Excess molar volume V_m^E, for the binary system [EMIM][SCN] (1) + water (2)

x_{IL}	ρ g cm^{-3}	V_m^E cm^3 mol^{-1}		ρ g cm^{-3}	Vm_E cm^3 mol^{-1}		ρ g cm^{-3}	VmE cm^3 mol^{-1}	
	T= 298.15K			T=303.15K			T= 308.15K		
0.2	1.0758	-0.0719	0.8053	1.0725	-0.0689	0.8106	1.0693	-0.0659	0.8157
0.3	1.0893	-0.0847	0.7201	1.0861	-0.0817	0.7261	1.0828	-0.0787	0.7319
0.4	1.0997	-0.0947	0.6502	1.0966	-0.0918	0.6565	1.0934	-0.0888	0.6624
0.5	1.1042	-0.0996	0.5916	1.1010	-0.0966	0.5978	1.0978	-0.0937	0.6038
0.6	1.1066	-0.1029	0.5417	1.1035	-0.0999	0.5477	1.1004	-0.0969	0.5537
0.7	1.1104	-0.1074	0.4987	1.1074	-0.1044	0.5045	1.1043	-0.1015	0.5104
0.8	1.1112	-0.1092	0.4612	1.1081	-0.1062	0.4670	1.1050	-0.1032	0.4725
	T=313.15K			T= 318.15K			T=323.15K		
0.2	1.0659	-0.0628	0.8206	1.0626	-0.0596	0.8254	1.0591	-0.0562	0.8299
0.3	1.0796	-0.0756	0.7376	1.0763	-0.0725	0.7431	1.0731	-0.0694	0.7483
0.4	1.0902	-0.0858	0.6683	1.0870	-0.0827	0.6740	1.0838	-0.0797	0.6794
0.5	1.0946	-0.0907	0.6097	1.0915	-0.0876	0.6153	1.0883	-0.0846	0.6208
0.6	1.0972	-0.0939	0.5594	1.0941	-0.0909	0.5650	1.0910	-0.0879	0.5704
0.7	1.1012	-0.0985	0.5159	1.0982	-0.0955	0.5214	1.0951	-0.0925	0.5266
0.8	1.1020	-0.1002	0.4779	1.0989	-0.0972	0.4833	1.0958	-0.0942	0.4884

Experimental densities over the entire composition range for [EMIM][SCN] (1) + PY(2)(Table 4a), [EMIM][SCN] (1) + PYRR(2) (Table 4b), [EMIM][SCN] (1) + QU(2) (Table 4c), [EMIM][SCN] (1) + INDO(2) (Table 4d), [EMIM][SCN] (1) + TS(2) (Table 4e) and [EMIM][SCN] (1) + water(2) (Table 4f) have been determined at temperature of T =(298.15 to 323.15) K. The surface tension σ, and refractive index nD of the pure component and its mixtures were determined at 298.15 K over the entire composition range of [EMIM][SCN] (1). Additionally we have studied the binary mixtures of [EMIM][SCN] (1) + water (2) which is more helpful in the purification and regeneration of [EMIM][SCN] [21].

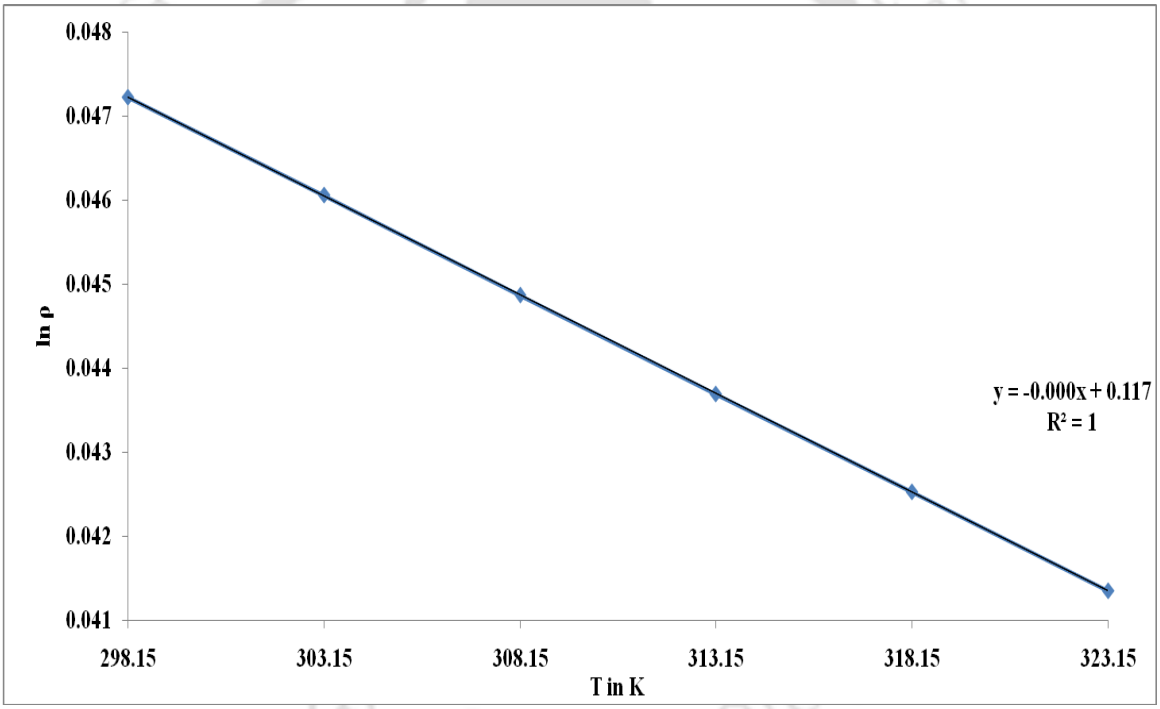

Figure 5.14: Experimental values of ln ρ of pure [EMIM][SCN] ionic liquid vs temperature of (298.15 to 323.15) K

5.3.4.2 Thermal expansion *"α"*

The coefficient of thermal expansion of the [EMIM][SCN] α is shown in Figure 5.14.The densities of pure [EMIM][SCN], decreases linearly (R^2=0.999) with increasing temperature. The value of α = 0.0117K^{-1} (ionic liquid) was calculated from Equation 5.1. The volume expansivity of [EMIM][SCN] was calculated using the measured density observed at different temperatures. The volume expansivity of [EMIM][SCN] was found to be independent of temperature (Figure 5.14). These observations are more consistent with the studies of Rodriguez et al., [2006], Wandschneider et al., [2008] and Pererio et al., [2006, 2007].

Figure 5.15: 1-ethyl-3-methylimidazolium thiocyanate with six membered ring of pyridine and five membered ring of thiophene.

5.3.4.3 Effect of composition on density and excess molar volume

Table 5.2 shows the experimental densities of pure [EMIM][SCN], aromatic nitrogen, aromatic sulphur and water at temperatures of T = (298.15to 323.15) K. It can be seen that the density of all the pure components including ionic liquid decreases linearly with increasing temperature. Table 5.17(a) to 5.17(f) shows the experimental densities for six binary systems studied as a function of temperature over the entire mole fraction of [EMIM][SCN]. For all the compounds with ILs, the densities varied linearly in the entire mole fraction with increasing temperature. This behavior can be explained by the efficient structural interaction of [EMIM][SCN] with aromatic structure of nitrogen/sulphur and water via packing effects[Anantharaj et al.,2010b,2010c,2011a,2011b,2011c],[Domanska et al.,2007,2008](Figure 5.15). Additionally it can be a result of smaller size of cation [Kumar et al., 2009] and anion providing better interaction with aromatic compounds. A small size of IL molecule has a significant influence on the changing densities of the mixture with an increase in temperature over the entire mole fraction of IL. Besides that the hydrogen bonding strongly depends on the temperature [Won et al.,2002] as compared to CH---π bond interaction [Anantharaj et al.,2010b,2010c,2011b] and π---π bond interactions[Anantharaj et al.,2010b,2010c,2011a,2011b,2011c].These similar trend often were observed for other binary systems by Rodriguez et al. [2006] and Domanska et al. [2007,2008].

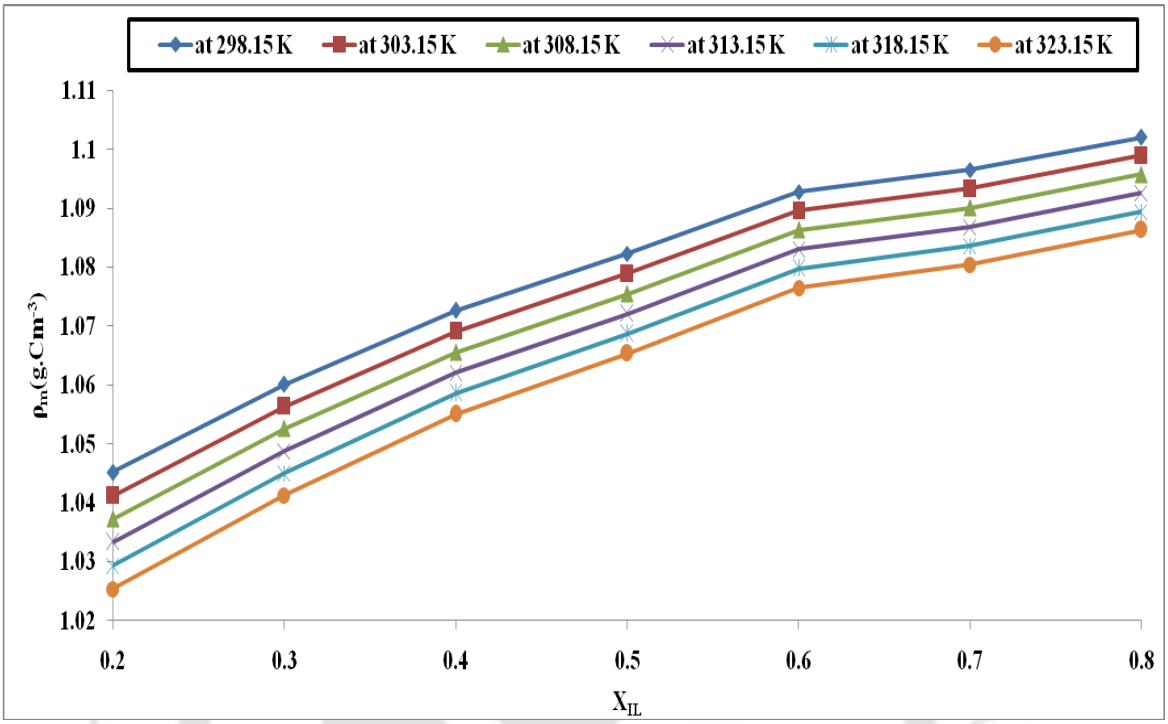

Figure 5.16: Experimental density for the binary system {[EMIM][SCN] (1) + Pyridine (2)} as a function of mole fraction of the IL at different temperature

The measured densities of binary mixtures over the entire mole fraction of [EMIM][SCN] at several temperature are reported in Tables 5.17(a) to 5.17(f). The binary mixture of [EMIM][SCN](1)+pyridine (2) (Figure 5.16)system shows that the composition or mole fraction of [EMIM][SCN](1) increases with density. This is due to the stronger association between the similar aromatic structure of molecules (i.e [EMIM] cation and pyrrole molecule). There are many possibilities in [EMIM][SCN] to interact with aromatic or non aromatic structure compounds such as: 1) CH- - -π interaction [Anantharaj et al.,2010b,,2011b;,Acharya et al.,2003;Suezawa wt al.,2000,2004],2) π---π interaction [Anantharaj et al.,2010b,2010c,2011a,2011b,2011c] and 3) n--π interaction [Anantharaj et al.,2010b,,2011b], where n =N, O, F and S atoms are located on the aromatic/non aromatic compound or ionic liquid structure(Figure 5.15). Therefore the measured densities of binary mixture for all the systems (Table 5.18(a) to 5.18(f)) shows a

similar trend in the liquid phase at all temperatures, which includes water (Figure 2f).But in case of [EMIM][SCN] (1)+ thiophene (2) system, a similar trend is observed for > x_{IL} =0.3 with increasing the mole fraction . This is due to the ratio of van der Waals force and electrostatic force which initially is very less .Further, the repulsive forces acts between two different electronegative atoms located on both the structure of the molecules in liquid phase.

5.3.4.4. Effect of composition on surface tension and refractive index

The measured surface tension data for all the studied systems are listed in table.5 and illustrated in Table 5.18. At x_{IL} =0.2 the surface tension of [EMIM][SCN] (1) + water system is higher as compared to other systems such as [EMIM][SCN] (1)+pyrrole, [EMIM][SCN] (1)+pyridine, [EMIM][SCN](1) + thiophene, [EMIM][SCN](1) + indoline (2) and [EMIM][SCN](1) + quinoline (2). It should be noted that the strength of van der Waals force is negligible as compared to the sterical hindrance provided by the addition of benzene ring [Joule et al., 2007; Gupta et al., 2005; Bansal et al., 2005] in pyrrole/pyridine structure which is accountable upon mixing. Therefore with increasing mole fraction of [EMIM][SCN], surface tension of mixture increases even if it has dissimilar molecules like indoline and quinoline (Table 5.18).

Table 5.18: Experimental surface tension σ and deviation of surface tension for the Binary systems: (a). [EMIM][SCN]+Pyridine, (b). [EMIM][SCN]+Pyrrole, (c). [EMIM][SCN]+Indoline, (d). [EMIM][SCN]+Quinoline, (e). [EMIM][SCN]+ Thiophene, and (f) .[EMIM][SCN]+ Water at 298.15K.

x_{IL}	[EMIM][SCN]+ PY		[EMIM][SCN]+ PYRR		[EMIM][SCN]+ QU	
	σ (mN.m^{-1})	$\Delta\sigma$ (mN.m^{-1})	σ (mN.m^{-1})	$\Delta\sigma$ (mN.m^{-1})	σ (mN.m^{-1})	$\Delta\sigma$ (mN.m^{-1})
0.2	37.4	-1.22	40.9	-1.08	29.5	-16.32
0.3	38.6	-0.58	41	-1.12	32.3	-13.18
0.4	38.7	-1.04	42.5	0.24	35.2	-9.94
0.5	41	0.7	42.8	0.4	39.4	-5.4
0.6	42.4	1.54	44	1.46	40.1	-4.36
0.7	45.4	3.98	46.5	3.82	40.4	-3.72
0.8	46.5	4.52	47.4	4.58	40.8	-2.98
x_{IL}	[EMIM][SCN]+ INDO		[EMIM][SCN]+ TS		[EMIM][SCN]+ Water	

	σ (mN.m^{-1})	$\Delta\sigma$ (mN.m^{-1})	σ (mN.m^{-1})	$\Delta\sigma$ (mN.m^{-1})	σ (mN.m^{-1})	$\Delta\sigma$ (mN.m^{-1})
0.2	39.9	5.2	30.8	-3.18	44.6	-20.1
0.3	40.8	5.05	31.8	-3.32	45.1	-16.9
0.4	40.9	4.1	32.1	-4.16	46.2	-13.1
0.5	41.9	4.05	33.6	-3.8	46.8	-9.8
0.6	42.4	3.5	34.1	-4.44	50.2	-3.7
0.7	43.9	3.95	38.4	-1.28	50.4	-0.8
0.8	44	3	45.5	4.68	50.4	1.9

It is well known fact that the strength of CH--π bond and hydrogen bond increases in liquid phase over the entire mole fraction of [EMIM][SCN] at T=298.15K [9-12].For [EMIM][SCN] (1) + pyridine(2), [EMIM][SCN] (1) + indoline(2), [EMIM][SCN] (1) + quinoline(2) and [EMIM][SCN] (1) + thiophene(2) systems, this trend increases linearly from x_{IL} =0.3 to x_{IL} =0.8. [EMIM][SCN] (1) + thiophene (2) mixture gave higher surface tension because of the similarity in structure of thiophene to [EMIM] cation. The dissimilar structure of pyridine, indoline and quinoline in [EMIM][SCN] gave higher surface tension as compared to water with [EMIM][SCN].It can be seen in Table 5.19 that the surface tension increases in the order of: thiophene > quinoline > pyridine > indoline > pyrrole > water. Thus a increasing mole fraction of [EMIM][SCN] causes a decrease in the strength of sterical hindrance possed by either dissimilar or addition of benzene ring in pyrrole or pyridine structure. The van der Waals force between the ethyl substitution on the [EMIM] and the aromatic structure of nitrogen/sulphur is not much significant in liquid phase. Further when the similar or dissimilar aromatic structures of molecules are mixed together then the interaction between [EMIM] cation and [SCN] anion decreases while the CH--π bond interaction, π--π stacking and dispersion forces gets increases particularly for the systems having similar or dissimilar aromatic structure of molecules [Mottar et al.,2007].

Table 5.19: Experimental refractive index nD and deviation of refractive index ΔnD for the Binary systems: (a). [EMIM][SCN] + Pyridine, (b). [EMIM][SCN] + Pyrrole, (c). [EMIM][SCN] + Indoline, (d). [EMIM][SCN] + Quinoline, (e). [EMIM][SCN] + Thiophene, and (f). [EMIM][SCN] + Water at 298.15K

x_{IL}	[EMIM] [SCN]+ PY	[EMIM] [SCN]+ PYRR	[EMIM] [SCN]+ QU

	nD	*ΔnD*	*nD*	*ΔnD*	*nD*	*ΔnD*
0.2	1.5335	0.02492	1.5214	0.02314	1.5974	0.0901
0.3	1.5326	0.02038	1.5209	0.01771	1.5968	0.0863
0.4	1.5351	0.01924	1.5187	0.01058	1.5756	0.0819
0.5	1.5302	0.0107	1.5137	0.00065	1.5746	0.0569
0.6	1.5188	-0.00434	1.5126	-0.00538	1.5727	0.0521
0.7	1.5178	-0.00898	1.5093	-0.01361	1.5675	0.0464
0.8	1.5171	-0.01332	1.5079	-0.01994	1.5587	0.0374
x_{IL}	[EMIM] [SCN]+ INDO		[EMIM] [SCN]+ TS		[EMIM] [SCN]+ WATER	
	nD	*ΔnD*	*nD*	*ΔnD*	*nD*	*ΔnD*
0.2	1.581	0.0041	1.5426	0.01338	1.4754	0.11186
0.3	1.5762	0.0042	1.5421	0.01182	1.4927	0.10739
0.4	1.5699	0.0028	1.5398	0.00846	1.5095	0.10242
0.5	1.5614	-0.0008	1.5388	0.0064	1.5186	0.08975
0.6	1.5541	-0.0032	1.5373	0.00384	1.5247	0.07408
0.7	1.5518	-0.0006	1.537	0.00248	1.5308	0.05841
0.8	1.5507	0.0032	1.5305	-0.00508	1.5314	0.03724

Table 5.19 shows the composition dependence of refractive index for the above mentioned binary systems. Refractive index for [EMIM][SCN](1) + pyrrole (2) systems decreases linearly with increasing mole fraction of [EMIM][SCN] because there is no mobility of ion upon mixing over the entire mole fraction of [EMIM][SCN] at T=298.15K.This similar behavior have been observed for other studied systems such as [EMIM][SCN](1) + thiophene(2), [EMIM][SCN](1) + pyridine(2),[EMIM][SCN](1) + indoline(2) and [EMIM][SCN] (1)+ quinoline(2).The only exception is system shows [EMIM][SCN](1) + water (2) system which shows a increasing trend with increasing mole fraction due to the increased strength of hydrogen bond. It is clear from Table 5.19 that for the binary mixture under study, the refractive index increasingly as in the order of:[EMIM][SCN]: pyrrole < Pyridine < thiophene < indoline <quinoline.Thus [EMIM][SCN] + quinoline mixture has the highest refractive index values as compared to other studied systems.

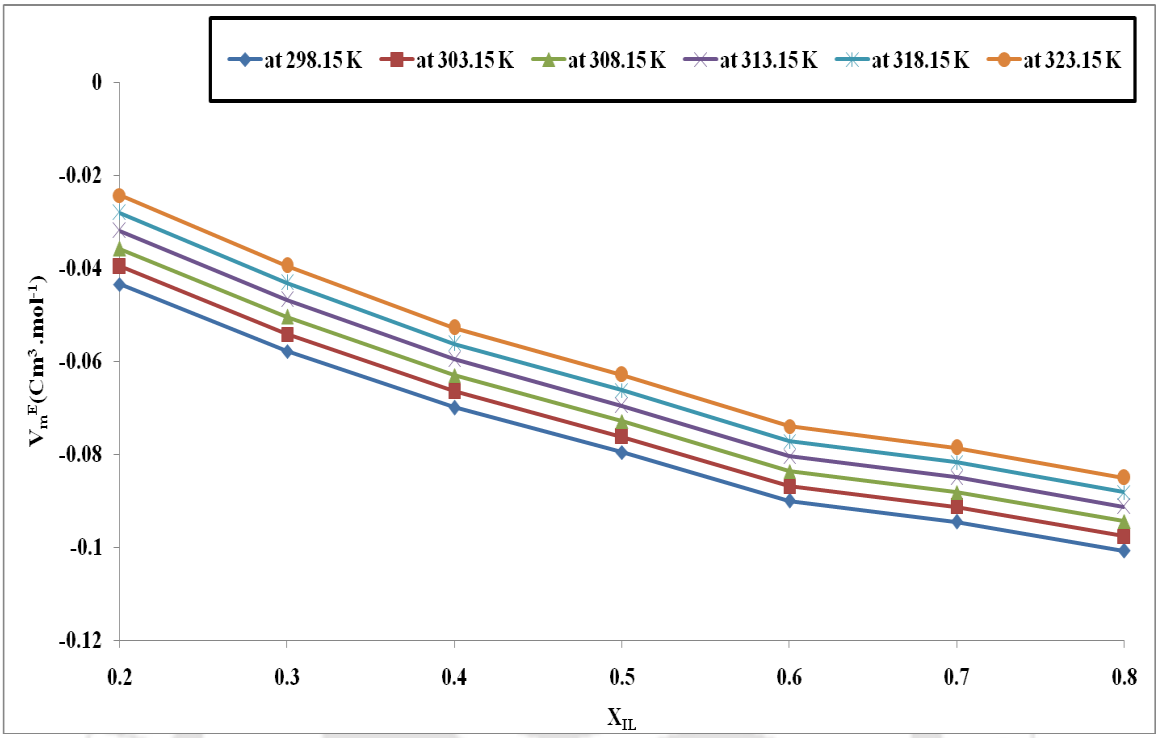

Figure 5.17: Excess molar volume V_m^E for the system of [EMIM][SCN] (1) + pyridine (2) at different temperatures

5.3.4.5. Effect of composition on excess molar volume

The calculated excess molar volume values are listed in Tables 5.17(a) to 5.17(f). [EMIM][SCN] (1) +pyridine (2) (Figure 5.17) binary mixture exhibit a linear decrease with an increase in the mole fraction of [EMIM][SCN](1) at all studied temperatures. At temperature *T*=298.15K a negative excess molar volume for all the systems are obtained over the entire mole fraction. This is due to fact that the specific interactions which includes the partial charge transfer, formation of hydrogen bond, CH - - π bond, π---π stacking and n---π bond interaction have significant influence in the binary mixture. The weak H- bonds are easily broken up when the temperature increases as compared to CH - - π bond, π---π stacking and n---π bond. This indicates that the IL-sulphur/nitrogen mixture has stronger interaction as compared to IL-IL ,thiophene-thiophene or

pyrrole-pyrrole interaction. A similar phenomenon is applicable for all other studied systems. This can also be explained by the stronger association occurring between similar or dissimilar aromatic structure of molecules in liquid phase at any composition or temperatures without any temperature and composition influence.

In case of [EMIM][SCN] (1) +water (2) mixture, a sudden decrease is seen at initial mole fraction, thereafter decreasing linearly as the composition increases. This is due to the fact that at individual concentration (higher dilution rate), the oxygen sites are stabilized be electron or partial charge transfer. Thus [EMIM][SCN] has strong attraction with water at low concentrations. Furthermore the temperature effect on the excess molar volume is negligible since the rate of kinetic energy is not enough to change the phase behavior upon mixing with aromatic structure of the nitrogen/sulphur molecules. It means that the structural effect becomes more important than the dispersion or dipolar interactions. Hence the composition has significant influence on excess molar volume of aromatic structure with multiple ring compounds like indoline and quinoline.

5.3.4.6. Effect of composition on deviation of surface tension and refractive index

The deviation of surface tension and refractive index are presented in Table 5.18 and 5.19.The deviation of surface tension for [EMIM][SCN] (1) + pyrrole (2) indicate a increasing trend with increasing mole fraction of [EMIM][SCN] while the refractive index deviation shows a decreasing trend at T=298.15K. It can be observed that the strong electrostatic interaction take place between the two similar aromatic structure of the molecules (IL-nitrogen/sulphur compound), even though molecules posses additional benzene ring such as indoline and quinoline. The deviation of surface tension was found to be inversely proportional to deviation of refractive index. It can be explained that the deviation of surface tension of the binary mixture strongly depends on the cohesive interaction at the surface level while the refractive index deviation depends on the dispersion interaction upon mixing. However both depends on the size and shape of the molecules in a liquid phase. These tendencies agree well with the reported data of Nain et al [2008] and Freire et al [2007]. In [EMIM][SCN] + Water mixture, the deviation of

surface tension increases linearly with composition (Table 5.18) while the deviation of refractive index decreases slightly (Table 5.19). The molecular interaction is very strong between similar and dissimilar aromatic structure [Zhou et al., 2006; Zhang et al., 2004] of sulphur/nitrogen compounds and [EMIM] cation while the mobility of ions is weakened upon mixing. However [EMIM][SCN] interacts with the compounds in liquid phase via n -- π bonding (where n:N,O from both the side).It can be observed that the minimum amount of [EMIM][SCN] ionic liquid is enough for separation of similar structure of pyrrole and thiophene while for pyridine, indoline and quinoline more amount is required as compared to pyrrole and thiophene. Negative deviation were observed for the entire mole fraction of IL at temperature from (298.15 to 323.15) K for both deviation in surface tension and refractive index studies. The observed trends are as follows:

For surface tension deviation:

Water > quinoline > thiophene > pyrrole > pyridine >indoline

For refractive index deviation:

Indoline > thiophene > pyrrole > pyridine > quinoline > water

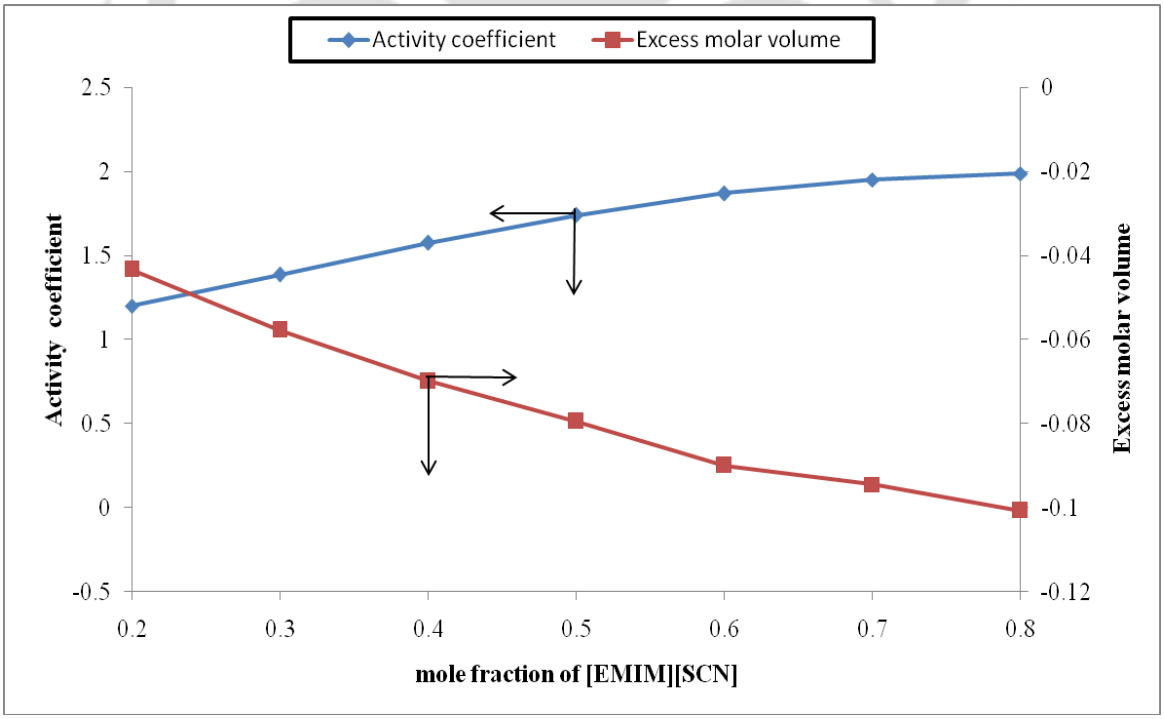

Figure 5.18: Relation of activity coefficient with excess molar volume of [EMIM][SCN] (1) + pyridine (2) systems at T=298.15K.

5.3.4.7 Relation of activity coefficient with excess molar volume

The activity coefficient values predicted via COSMO-RS for the all the studied systems are given in Table 5.17(a) to 5.17(f). Figure 5.18 shows a comparison of predicted activity coefficient and excess volume for IL-pyridine mixture. The predicted activity coefficient increases with increasing mole fraction of ionic liquid in the mixture, except for [EMIM][SCN] + water systems. However the excess molar volumes are seen to decrease with mole fraction. Thus it is fair to say that the activity coefficient is inversely proportional to excess volume.

It is observed that the properties of mixture are influenced by the aromatic ring structure of thiophene, pyridine, pyrrole, indoline and quinoline (Table 5.17(a) to 5.17(f)).The activity coefficient also gives us an indication of the strength of solubility.For example, [EMIM][SCN] (1) + Pyridine(2) system (Figure 8) shows low activity coefficient (i.e,.high solubility with mole fraction of IL) as compared to [EMIM][SCN] + thiophene(Table 5.17(e)) which implies that the solubility of pyridine in [EMIM][SCN] is higher than thiophene. In case of excess molar volume both the systems shows an increasing excess molar volume with increasing mole fraction of IL. Here the possible specific interactions may be π--π stacking, CH -- π interaction, N (nitrogen compounds) -- H and S (sulphur compounds) -- H interaction.

Nomenclature

List of Symbols

[EMIM]	-	1-Ethyl-3-Methylimidazolium
[OAc]	-	Acetate
[$EtSO_4$]	-	Ethylsulphate
[$MeSO_3$]	-	Methylsulphonate
[SCN]	-	Thiocyanate
[EMIM][OAc]	-	1-Ethyl-3-Methylimidazolium Acetate
[EMIM][$EtSO_4$]	-	1-Ethyl-3-Methylimidazolium ethylsulphate
[EMIM][$MeSO_3$]	-	1-Ethyl-3-Methylimidazolium Methylsulphonate
[EMIM][SCN]	-	1-Ethyl-3-Methylimidazolium Thiocyanate
PY	-	Pyridine
PYRR	-	Pyrrole
INDO	-	Indoline
QU	-	Quinoline
TS	-	Thiophene

REFERENCES

Acharya, P.; Plashkevych, O.; Morita, C.; Yamada, S.; Chattopadhyaya, J.A. A Repertoire of Pyridinium−Phenyl−Methyl Cross-Talk through a Cascade of Intramolecular Electrostatic Interactions. *J. Org. Chem*. **2003,** 68,1529-1538.

Alonso, L.; Arce, A.; Francisco, M.; Rodriguez, O.; Soto, A. Gasoline Desulphurization Using Extraction with [C_8mim][BF_4]ionic liquid.*AIChEJ*.**2007**, 53, 3108-3115.

Alonso, L.; Arce, A.; Francisco, M.; Soto, A.Phase behavior of 1-methyl-3-octylimidazolium bis[trifluoromethylsulfonyl]imide with thiophene and aliphatic hydrocarbons: The influence of n-alkane chain length. *Fluid Phase Equilibria*. **2008a**, 263, 176–181.

Alonso, L.; Arce. A.; Francisco. M.; Soto, A. (Liquid + liquid) equilibria of [C_8mim][NTf_2] ionic liquid with a sulfur-component and hydrocarbons. *J. Chem. Thermodynamics*.**2008b**, 40,265–270.

Alonso, L.; Rodriguez,H.M.; Soto, A. Effect of anion fluorination in 1-ethyl-3-methylimidazolium as solvent for the liquid extraction of ethanol from ethyl tert-butyl ether," *Fluid Phase Equilibria*. **2006**,242, 164–168.

Anantharaj, R .; Banerjee, T.COSMO-RS based Predictions for the Desulphurization of Diesel oil using Ionic Liquids: Effect of Cation and Anion combination. *Fuel.Proce.Tech*. **2011a**,92, 39-52.

Anantharaj, R. ; Banerjee, T. Quantum Chemical Studies on the Simultaneous Interaction of Thiophene and Pyridine with Ionic Liquid. *AIChEJ*. **2011b**. 57,749-764.

Anantharaj, R.; Banerjee, T. Evaluation and comparison of global scalar properties for the simultaneous interaction of ionic liquids with thiophene and pyridine. *Fluid Phase Equilibriaria.* **2010a**, 293, 22–31.

Anantharaj, R.; Banerjee, T. COSMO-RS based Screening of Ionic Liquids as Green Solvents in Denitrification Studies. *Ind. Eng. Chem.Res*. **2010b**, 49, 8705-8725.

Arce, A.; E.Rodil.; Soto, A. Volumetric and Viscosity Study for the Mixtures of 2-Ethoxy-2-methylpropane, Ethanol, and 1-Ethyl-3-methylimidazolium Ethyl Sulphate Ionic Liquid. *J. Chem. Eng. Data*.**2006**, 51, 1453-1457.

Banerjee,T.; Khanna, A. Infinite Dilution Activity Coefficients for Trihexyltetradecyl Phosphonium Ionic Liquids: Measurements and COSMO-RS Prediction. *J.Chem.Engg.Data*. **2006b** ,51, 2170-2177.

Banerjee,T.; Rath, S.; Sahoo. R.K.; Khanna. A. Multi-component Liquid-Liquid Equilibria prediction for Aromatic Extraction Systems using COSMO-RS. *Ind. Eng. Chem. Res*. **2007,** 46, 1292-1304.

Banerjee,T.; Singh, M.K.; Khanna,A .Prediction of Binary VLE of Imidazolium based ionic liquids by COSMO-RS. *Ind. Eng. Chem. Res*.**2006a**, 45, 3207-3219.

Banerjee,T.; Verma, K.K.; Khanna. A. Liquid Liquid Equilibria for Ionic Liquid based systems using COSMO-RS: Effect of Cation and Anion combination. *AIChE J,* **2008**, 54, 1874-1885.

Bansal, R.K.Heterocyclic chemistry; Fourth Edition. New Age International Publishers.**2005.**

Cassol, C.C.; Umpierre, A.P.On the extraction of Aromatic compounds from hydrocarbons by imidazolium ionic liquids. *Int.J.Mol.Sci*. **2007,**8, 593-605.

Domanska, U.; Krolikowski, M. Phase equilibria study of the binary systems (1-butyl-3-methylimidazolium tosylate ionic liquid +water, or organic solvent). J.Chem.Thermodyn. **2010**,42,355-362,.

Domanska, U.; Laskowska, M.Phase equilibria and volumetric properties of (1-Ethyl-3-methylimidazolium ethylsulphate + Alcohol or water systems. *J.Sol.Chem*. **2008,** 37, 1271-1287.

Domanska, U.; Tryznowska, Z.Z.; Krolikowski, M.Thermodynamic Phase behavior of ionic liquids.*J.Chem.Eng.Data*. **2007,** 52, 1872-1880.

Esperancüa, J.M.S.S.; Guede, H.J.R.; Blesic, M.; Rebelo, L.P.N. Densities and Derived Thermodynamic Properties of Ionic Liquids. 3. Phosphonium-Based Ionic Liquids over an Extended Pressure Range. *J. Chem. Eng. Data*. **2006**, 51, 237-242.

Ficke, L.E.; Rodriguez. H.; Brennecke, J.F.Heat Capacities and Excess Enthalpies of 1-Ethyl-3-methylimidazolium-Based Ionic Liquids and Water. *J. Chem. Eng. Data*. **2008**,53, 2112–2119.

Gao, H.; Li, Y. ; Wu, Y;. Luo, M.; Li, Q.; Xing , J.; Liu, H. Extractive Desulfurization of Fuel Using 3-Methylpyridinium-Based Ionic Liquids. *Energy & Fuels*. **2009**, 23, 2690–2694.

Garcia, J.; Torrecilla,J.S.; Fernández, A.; Oliet, M.; Rodrígue, F.(Liquid + liquid) equilibria in the binary systems (aliphatic or aromatic hydrocarbons + 1-ethyl-3-methylimidazolium ethylsulfate, or 1-butyl-3-methylimidazolium methylsulfate ionic liquids). *J. Chem. Thermodynamics*. **2010**,42, 144–150.

Ghatee, M.H.; Zolghadar, A.R.Surface tension measurements of imidazolium – based ionic liquids at liquid – vapor equilibrium. *Fluid Phase Equilibria*. **2008,** 263, 168-175.

Gomez, E.; Gonzalez, B.; Calvar, N.; Tojo, E.; Dominguez, A.Physical Properties of Pure 1-Ethyl-3-methylimidazolium Ethylsulfate with several alcohols at T= (298.15, 313.15, and 328.15)K and atmospheric pressure. *J. Chem. Eng. Data*. **2007**, 52, 1641-1648.

Gomez,E.; Gonzalez, B.; Calvar, N.; Tojo, E.; Dominguez, A.Physical Properties of Pure 1-Ethyl-3-methylimidazolium Ethylsulfate and Its Binary Mixtures with Ethanol and Water at Several Temperatures. *J. Chem. Eng. Data*. **2006,** 51, 2096-2102.

Gonzalez, E.J.; Alonso, L.; Dominguez, A.Physical Properties of Binary Mixtures of the Ionic Liquid 1-Methyl-3-octylimidazolium Chloride with Methanol, Ethanol, and 1-Propanol at T) (298.15, 313.15, and 328.15) K and at P) 0.1 MPa. *J. Chem. Eng. Data*. **2006**,51, 1446-1452.

Gonzalez,E.J.; Gonzalez, B.; Calvar, N.; Domınguez, A.Physical Properties of Binary Mixtures of the Ionic Liquid 1-Ethyl-3-methylimidazolium Ethylsulphate with Several Alcohols at T) (298.15, 313.15, and 328.15) K and Atmospheric Pressure. *J. Chem. Eng. Data*. **2007**,52, 1641-1648.

Gupta, R.R.; Kumar, M.; Gupta, V. Heterocyclic Chemistry –II; Five – Membered Heterocyclic. Springer.**2005**.

Huo, Y.; Xia, S.; Ma, P.;Densities of Ionic Liquids, 1-Butyl-3-methylimidazolium Hexafluorophosphate and 1-Butyl-3-methylimidazolium Tetrafluoroborate, with Benzene, Acetonitrile, and 1-Propanol at T = (293.15 to 343.15) K. *J.Chem.Engg.Data*. **2007,** 52, 2077-2082.

Hwang,I.; Park, S.; Seo, D.W.;.Han, K.J.Binary Liquid –Liquid Equilibrium (LLE) for N-Methylformaide (NMF) + Hexadecane between (288.15 and 318.15) K and Ternary LLE

for systems of NMF + Heterocyclic Nitrogen Compounds + Hexadecane at 298.15K. *J.Chem.Eng.Data*.**2009***,* 54, 78-82.

Jayaraman, A.; Yang, F.H.; Yang, T.R. Effects of Nitrogen Compounds and Polyaromatic Hydrocarbons on Desulfurization of Liquid Fuels by Adsorption via π-Complexation with Cu (I) Y Zeolite. Energy & Fuels. **2006**, 20, 909-914.

Jeon, H.J.; Ko, C.H.; Kim, S.H.; Kim, J.N.Removal of Refractory Sulfur Compounds in Diesel Using Activated Carbon with Controlled Porosity.*Energy & Fuels*. **2009**, 23, 2537-2543.

Joule, J.A.; Mills, K. K.Heterocyclic chemistry, Fourth Edition. Blackwell Publishing (OXFORD).**2007**.

Kell,G. S. Precise Representation of Volume Properties of Water at One Atmosphere. *J.Chem.Engg.Data*. **1967**, 12, 66-69.

Kilaru,P.; Baker, G.A.; Scovazzo, P. Density and surface tension measurements of Imidazolium, quaternary phosphonium, and ammonium – Based Room Temperature Ionic Liquids: Data and Correlations.*J.Chem.Eng.Data*. **2007,** 52, 2306-2314.

Kumar,A.P.; Banerjee, T. Thiophene separation with ionic liquids for desulphurization: A quantum chemical approach. *Fluid Phase Equilibria*. **2009**,278, 1–8.

Lei, Z.; Arlt. W.; Wassersched, P.Separation of 1-Hexene and n-Hexane with ionic liquids," *Fluid Phase Equilibria*. **2006,**241, 290-299.

Macaud, M.; Sevignon, M.; Reguillon, A.F.; Lemaire, M. Novel Methodology toward Deep Desulfurization of Diesel Feed Based on the Selective Elimination of Nitrogen Compounds. *Ind. Eng. Chem. Res*. **2004,** 43, 7843-7849.
Maduro, R.M.; Aznar, M. Liquid–liquid equilibrium of ternary systems 1-butyl-3-methylimidazoliumhexafluorophosphate + aromatic + aliphatic. *Fluid Phase Equilibria*. **2008,** 265, 129–138.

Moattar, M.T.Z.; Cegincara, R.M.Viscosity, Density, Speed of Sound, and Refractive Index of Binary Mixtures of Organic Solvent + Ionic Liquid, 1-Butyl-3-methylimidazolium Hexafluorophosphate at 298.15 K. *J. Chem. Eng. Data*. **2007,** 52, 2359-2364.

Motttar, M.T.Z.; Cegincara, R.M. Viscosity, Density, Speed of Sound, and Refractive Index of Binary Mixtures of Organic Solvent + Ionic Liquid, 1-Butyl-3-methylimidazolium Hexafluorophosphate at 298.15 K. *J.Chem.Eng.Data*. **2007**, 52, 2359-2364.

Nie, Y.; Li, C.; Meng, H.; Wang, Z. N, N-dialkylimidazolium dialkylphosphate ionic liquids: Their Extractive performance for thiophene series compounds from fuel oils versus the length of alkyl group. *Fuel.Proc.Tech*. **2008,** 89, 978 – 983.

Omrani, A.; Rostami, A.A.; Mokhtary, M. Density and volumetric properties of 1, 4-dioxane with ethanol,3-methyl-1-butanol,3-amino-1-propanol and 2-propanol binary mixtures at various temperatures. *J.Molecular Liquids*. **2010**, 157, 18-24.

Pereiro , A.B.; Tojo, E.; Rodriguez, A.; Canosa, J.; Tojo, J.Properties of ionic liquid $HMIMPF_6$ with carbonates, ketones and alkyl acetates. *J. Chem. Thermodynamics*. **2006,**38, 651–661.

Pereiro, A.B.; Tojo, E.; Rodriguez, A. Physical properties of ionic liquids based on 1-alkyl-3-methylimidazolium cation and hexafluorophosphate as anion and temperature dependence. *J. Chem. Thermodynamics*. **2007**,39 ,1168–1175.

Pereiroa, A.B.; Deivea, F.J.;.Esperanc, J.M.S.S.; Rodrigueza, A.Alkylsulfate-based ionic liquids to separate azeotropic mixtures. *Fluid Phase Equilibria*. **2010,** 291 ,13–17.

Ramirez, S.; Cabrera, C.; Aguilar, C.; Vaca, H.; Vega, P.; Agueda, R.; Garcia, A.; Santiago, R.; Schacht, P. Two stages light gasoil hydrotreating for low sulphur diesel production.*Catalysis Today*. **2004**,98, 323-332.

Rodrıguez, H.; Brennecke, J.F.Temperature and Composition Dependence of the Density and Viscosity of Binary Mixtures of Water + Ionic Liquid. *J. Chem. Eng. Data*. 2**006**,51, 2145-2155.

Sapi, E.; Zaytseva, A.; Kyyny, P.K.; Keskinen, K.I.; Aittamaa, J.Vapor-Liquid Equilibrium for binary system of 1-propanethiol, Thiophene and Diethylsulfide withToluene at90.03kPa.*J.Chem.Eng.Data*. **2006a,** 51, 1372-1376.

Sapi, E.; Zaytseva, A.; Kyyny, P.K.; Keskinen, K.I.; Aittamaa, J.Vapor-Liquid Equilibrium for binary system of Thiophene + n-Hexane at (338.15 and 323.15) K and Thiophene + 1-Hexane at (333.15 and 323.15) K. *J.Chem.Eng.Data*. **2006b**, 57, 2203-2208.

Seddon, K.R.; Sark, A.; Torres, M.J.Influence of chloride, water, and organic solvents on the physical properties of ionic liquids, *Pure Appl.Chem*. **2000**,72, 2275-2287.

Shan, J.H.; Liu, X.Q.; Sun, L.B.; Cui, R.Cu−Ce Bimetal Ion-Exchanged Y Zeolites for Selective Adsorption of Thiophenic Sulfur. *Energy & Fuels* . **2008**, 22, 3955–3959.

Shekaari, H.; Mousavi, S.S.Volumetric properties of ionic liquid 1,3-dimethylimidazolium methyl sulphate + molecular solvents at T = (298.15–328.15)K. *Fluid Phase Equilibria*. **2010** ,291, 201–207.

Singh**,** S. P.; Anantharaj, R.; Banerjee, T. UNIFAC Group Interaction Prediction for Ionic Liquid-Thiophene based systems using Genetic Algorithm. *LNC Science*. **2010c**,6457,195-204.

Song, T.; Zhang, Z.; Chen, J.; Ring, Z.; Yang, H.; Zheng, Y. Effect of Aromatics on Deep Hydrodesulfurization of Dibenzothiophene and 4,6-Dimethyldibenzothiophene over NiMo/Al_2O_3 Catalyst.*Energy & Fuels*. **2006**, 20,2344-2349.

Su, B.M.; Zhang, S.; Zhang, Z.C. Structural Eluicidation of Thiophene Interaction with Ionic liquids by Multinuclear NMR Spectroscopy. *J.Phys.Chem.B*. **2004**,108, 19510-19517.

Suezawa, H.; Hashimoto, T. ; Tsuchinaga, K.; Yoshida, T.; Yuzuri, T.; Sakakibara, K.; Hirota, M.; Nishio, M. Electronic substituent effect on intramolecular CH/π interaction as evidenced by NOE experience. *J. Chem. Soc., Perkin Trans*. **2000**, 2, 1243-1249,

Suezawa, H.; Ishihara, S.; Umezaw, Y.; Tsuboyam, S.; Nishio, M. The Aromatic CH/π Hydrogen Bond as an Important Factor in Determining the Relative Stability of Diastereomeric Salts Relevant to Enantiomeric Resolution - A Crystallographic Database Study. *Eur. J.Org.Chem*. **2004**,4816-4822.

Varma, N. R.; Anantharaj, R.; Banerjee, T. Experiments, correlations and COSMO-RS predictions for the extraction of benzothiophene from n-hexane using imidazolium-based ionic liquids**.** Chem.Eng.J. **2011c**. 166,30-39.

Wandschneider, A.; Lehmann, J.K.; Heintz, A.Surface Tension and Density of Pure Ionic Liquids and Some Binary Mixtures with 1-Propanol and 1-Butanol. *J. Chem. Eng. Data.* **2008**,53, 596–599.

Wankhede, N. N.; Wankhede, D.S.; Lande, M.K.; Arbad, B.R.Molecular interactions in (2,4,6-trimethyl-1,3,5-trioxane+n-alkyl acetates)at T=(298.15,303.15,and 308.15)K. *J.Chem.Thermodynamics*. **2006**, 38, 1664-1668.

Wiwel, P.; Knudsen, K.; Zeuthen, P.; Whitehurst, D.Assessing Compositional Changes of Nitrogen Compounds during Hydrotreating of Typical Diesel Range Gas Oils Using a Novel Preconcentration Technique Coupled with Gas Chromatography and Atomic Emission Detection. *Ind. Eng. Chem. Res*. **2000**,39, 533-540.

Won, D.B.; Park, S.J.; Han, K.J.; Kim, C.J.Liquid-Liquid equilibria for methanol + hexadecane + heterocyclic nitrogen containing compounds at 298.15K.*Fluid.Phase.Equilibria*. **2002**,193,217-227.

Xie,L.; Favrergillon, A.; Wang, X.; Fu, X.; Rostaing, S.P.; Toussaint, G.; Geantet, C.; Vrinat, M.; Lemaire, M.Selective extraction of neutral nitrogen compounds found in diesel oil by 1-butyl-3-methyl-imidazolium chloride. *Green Chem*. **2008**,10,524-531.

Yanfang,G.; Tengfang, W.; Dahong, Y.U.; Changjum, P.; Honglai, L.; Ting, H.U. Densities and Viscosities of the Ionic Liquid [C_4mim][PF_6] + N,N-dimethylformamide Binary Mixtures at 293.15K to 318.15K.*Chin.J.Chem.Eng*. **2008**,16,256-262.

Yang, H.; Chen, J.; Briker, Y.; Szynkarczuk, R.; Ring, Z.; Effect of nitrogen removal from light cycle oil on the hydrodesulphurization of dibenzothiophene, 4-methyldibenzothiophene and 4,6-dimethyldibenzothiophene. *Catalyst Taoday*. **2005**,109,16-23.

Zhang, S.; Zhang, Q. Zhang, Z.C. Extractive Desulfurization and Denitrogenation of Fuels Using Ionic Liquids. *Ind. Eng. Chem. Res*. **2004**,43, 614-622.

Zhang, S.; Zhang, Z.C.Novel properties of ionic liquids in selective sulphur removal from fuels at room temperature. *Green Chem*. **2002**, 4, 376-379.

Zhang,S.; Li. X.; Chen, H.; Wang, J.; Zhang, J.; Zhang, M. Determination of Physical Properties for the Binary System of 1-Ethyl-3-methylimidazolium Tetrafluoroborate + H_2O. *J. Chem. Eng. Data*. **2004**,49, 760-764.

Zhou,Q.; Wang, L.; Chen, H.Densities and Viscosities of 1-Butyl-3- methylimidazolium Tetrafluoroborate + H_2O Binary Mixtures from (303.15 to 353.15) K. *J. Chem. Eng. Data*. **2006**,51, 905-908.

6.1 Introduction

The most commonly studied ionic liquids are based on the imidazolium cation with fluorinated anions [BF_4],[PF_6].However, the instability of such anions in the presence of water is drastic since the decomposition of these fluorinated anions leads to the formation of highly toxic and corrosive HF. On the other hand ionic liquids with anions such as alkyl sulphate are free from halogen and are known to be non-toxic. They are easy to synthesis and known to have excellent purity. Additionally they posses low viscosities and low melting points [Holbrey et al.,2002]. Moreover, their affinity for aromatic sulphur compounds is very high, and they are virtually immiscible with diesel, preventing cross-contamination. Post extraction, the sulphur compounds can be easily recovered by a simple heating process [Zhang et al.,2002]. Moreover, due to the abundance of cations and anions, many combinations are possible, allowing one to fine tune the various physical and chemical properties depending on the extraction process.

Over the past few years, considerable amount of experimental and modeling work have been done using imidazolium-based ionic liquids with different alkyl groups substituted on the ring, which has yielded positive results for the extraction of the various aromatic sulphur compounds. Most of the research has been concentrated on the recovery of thiophene from model fuels like *n*-hexane, toluene, cyclohexane etc. In a recent study, the potential of polysubstituted pyridinium-based ionic liquids for the extraction of thiophene from different model fuels was studied [Arce et al.,2010]. Pyridinium based ionic liquids also showed potential in removing sulphur with a high sulphur removal after multiple extraction cycles [Wang et al.,2007]. The ionic liquid [OMIM][BF_4] used for extracting thiophene from *i*-octane yielded selectivities upto 27.62, and a high solubility of thiophene in the IL-phase, which establishes the high affinity of aromatic compounds for the ionic liquids [Arce et al.,2007,2008a]. In a separate study, the ionic liquid [OMIM][NtF_2] was used to analyze the effect of the *n*-alkane on the extraction process [Arce et al., 2008b]. Ionic liquids with an

alkyl substituted imidazolium group as cation and different anions were used for the extraction of thiophene and its derivatives from model fuels [Eber et al.,2004].A comprehensive analysis of the performance of alkylimidazolium-based ionic liquids with BF_4 and PF_6 as the anions was done by Zhang et al. [2004], which showed an improvement in performance when the latter anion was used. This also illustrated the use of $AlCl_3$-TMAC ionic liquid, which was lauded for its ease of preparation and highly effective sulphur removal, but at the cost of demerits like moisture sensitivity and colour formation. Domanska et al. [2009] studied the LLE and SLE (Solid-Liquid Equilibria) of binary systems which involved an ionic liquid and thiophene. An extensive study spanning ten ionic liquids was done in the study.

Predictive analysis of the selectivities of various ionic liquids for the extraction of thiophene at infinite dilution was done using the COSMO-RS model. The novelty of COSMO-RS model is that it is independent of experimental data and the only input required is the molecular structure [Banerjee et al., 2006, 2007;Kumar et al.,2009]. It predicts the non-ideal liquid phase activity coefficient from which one can calculate phase equilibria such as LLE and SLE. From our earlier study, considerably high selectivities were achieved for acetate and ethyl sulphate based ionic liquids [Kumar et al., 2009]. It was also found that a smaller cation led to a higher selectivity. Due to this we have chosen the cation as 1-ethyl 3-methylimidazolium ([EMIM]). In the present study, the effectiveness of imidazolium-based ionic liquids with the associated anions, acetate and ethyl sulphate is studied for the extraction of benzothiophene from a model fuel, *n*-hexane.

6.2 Experimental

6.2.1 Chemicals and Materials

The ionic liquids 1-ethyl-3-methylimidazolium ethyl sulphate of purity > 95% and 1-ethyl-3-methylimidazolium acetate of purity > 98%, were supplied by Sigma Aldrich,

Germany. Benzothiophene of 95% purity was supplied by Sigma Aldrich, Germany. *n*-Hexane of 99.9% purity was supplied by Merck Specialities Private Limited, India. $CDCl_3$ of purity > 99.8%, used for the NMR analysis of the extract and raffinate phase compositions was supplied by Sigma Aldrich, Germany. All the chemicals were used without further purification. The comparisons of physical properties of the individual components have been reported in Table 6.1. Densities of the pure components were measured at atmospheric pressure with Anton Paar DSA-4500 MA digital vibrating U-tube densimeter. The uncertainty in the density measurement is ± 0.0011g.cm^{-3} .The apparatus was calibrated by measuring the density of Millipore quality water and ambient air.

Table 6. 1: Physical properties of components used in this work

Component	**CAS no.**	**M.W/g**	**ρ/g·cm^{-3}**	
			Present study	**Literature**
[EMIM][CH_3COO]	143314-17-4	206.26	1.0273	NA
[EMIM][$EtSO_4$]	342573-75-5	236.29	1.2421	1.2423[42]
Benzothiophene	110-54-3	134.20	1.1604	NA
Hexane	95-15-8	86.18	0.6596	0.6551[22]

6.2.2 Procedure

Feed mixtures of equimolar concentrations of the ionic liquid and *n*-hexane, with the benzothiophene concentrations varying from 5 to 50 % were first prepared. All weighing was carried out in a Mettler Toledo AT 261 balance with an accuracy of ± 10^{-4} gm .The total volume of all the feed mixtures were fixed at 8 ml. Capped glass bottles of a total capacity of 20 ml volume were used for holding the feed mixtures. The samples were properly sealed with parafilm tape to avoid any loss of the components due to evaporation.

The bottles were then placed inside a water-shaker bath set at 308.15 K, and allowed to shake for not less than 6 hours at 100 rpm in thermostatic shaker bath (Dailhan Lab, China). Spring clamps were used to hold the flasks on the tray. The temperature was accurate within an error of ±0.01 K, and was set to 308.15 K for all samples. The mixture was then allowed to settle for a minimum of 12 hours so that equilibrium is attained. The LLE experiment was conducted at T=308.15 K which is the melting point of benzothiophene. We selected this temperature since below this temperature benzothiophene is solid and the solubility of benzothiophene in IL or hexane is not known in literature. So in order to carry liquid-liquid equilibria we conducted the experiment at 308.15 K.

Table 6.2: NMR Peak Assignment for Quantitative Analysis in the ternary mixture

Chemical Compound and Peak Type	**Chemical Shifts in NMR Spectra (Relative to TMS)**
	a: ~ 7.8 (doublet, 2 H) b: ~ 7.4 (doublet, 4 H)
	a: ~ 0.96 (singlet,6 H) b: ~ 1.2 (doublet,8 H)
	a: ~ 3.65 (singlet, 2 H)
	a: ~ 2 (singlet, 3 H)

6.2.3 Compositional Analysis

For doing compositional analysis, samples of each phase in equilibrium were taken using syringes. A drop of each phase was dissolved in 0.5 ml of $CDCl_3$ and placed inside NMR tubes (thrift Grade), which were properly sealed. The NMR spectrometer of 11.74 Tesla (20 MHz response of ^1H) was used to conduct the ^1H NMR spectral analysis for the measurement of the peak areas of the hydrogen molecule of each component.

The aromatic sulphur compounds show a peak in the range of 7.5-7.8, the hydrocarbon (i.e. hexane) in the range of 1.1-1.3 for the $–CH_2-$ linkage, and below 1.1 for the $–CH_3$ group. The peaks of the ionic liquid are obtained in the range of 3-4, depending on the anion attached to the imidazolium ring. From these ranges, the peak areas of the individual hydrogen atoms belonging to the respective components were obtained by automatic integration of the NMR spectrogram. The equation used to calculate the concentration is given as follows,

(6.1)

where is the mole fraction of species i *and* is the peak area of a single hydrogen atom in the component *i*. The correspondence between peak assignments of both the phases in ternary mixture is shown in Table 6.2. The NMR spectra of the extract and raffinate phase of the ternary system involving [EMIM][$EtSO_4$] are given in Figures 6.1 and 6.2 respectively. Since the cation is similar for the second ternary system, the NMR spectra is

similar to the one shown except that the shift of the acetate anion is observed at around 2 ppm.For checking the accuracy we prepared some known mixtures in the homogenous region close to the binodal curve and then obtained the ^{1}H NMR. The measured results were found to be in good agreement with the actual compositions. Calibration lines corresponding to standard deviations of < 0.007 for each compound were obtained. The maximum absolute deviation was found to be 0.010 in mole fraction.

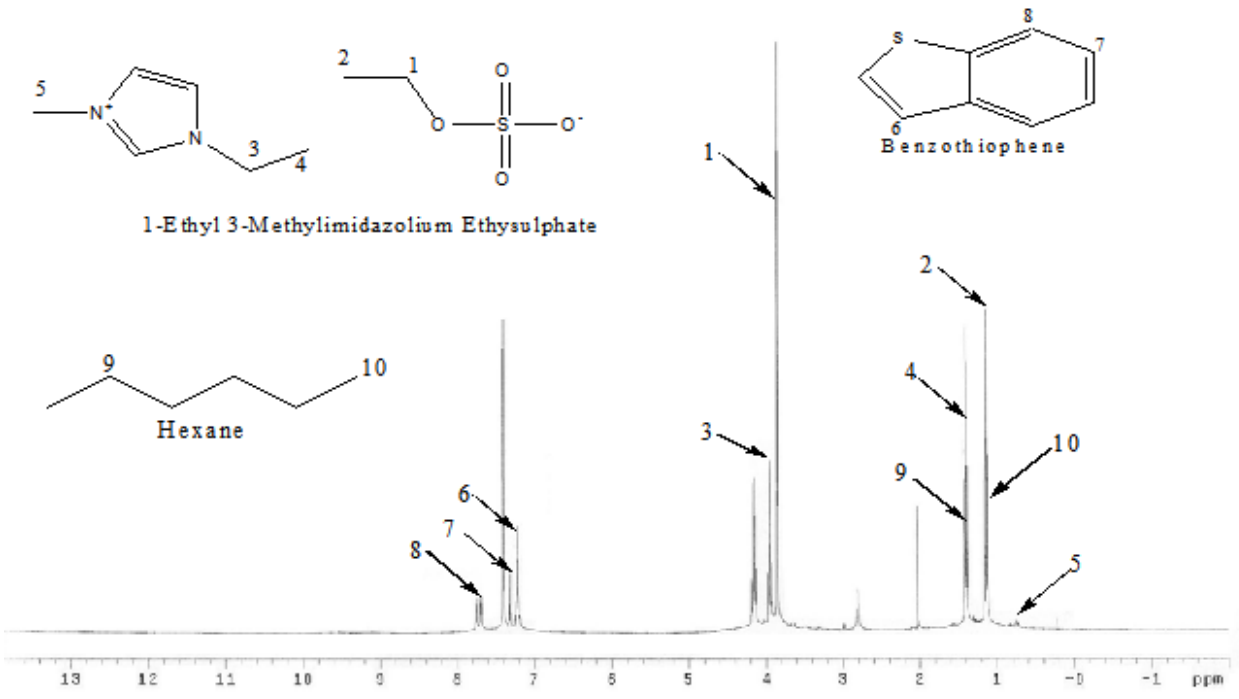

Figure 6.1: NMR spectra of the extract phase for the system [EMIM][$EtSO_4$] – Benzothiophene – *n*-Hexane

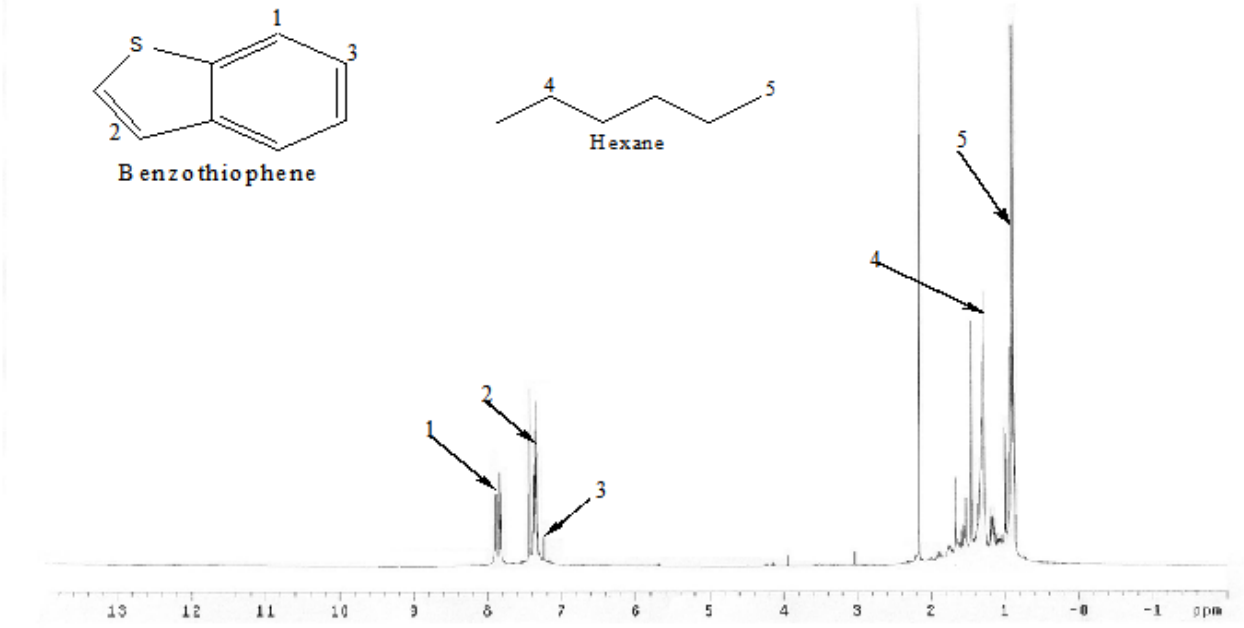

Figure 6.2: NMR spectra of the raffinate phase for the system [EMIM][$EtSO_4$] – Benzothiophene – *n*-Hexane

6.3 Results and Discussions

6.3.1 Ternary Tie-line Data

Ternary LLE experiments were done for the systems 1-ethyl 3-methylimidazolium ethyl sulphate (1)-benzothiophene (2)-hexane (3) and 1-ethyl 3-methylimidazolium acetate (1)-benzothiophene (2)-hexane (3) at 308.15 K. These experiments were done so as to compare the potential of the individual ionic liquids on their performance in the extraction of benzothiophene from hexane.

The sample tie lines range from a feed concentration of 5-50% benzothiophene (mole basis). An equimolar ratio of ionic liquid over the hydrocarbon was considered for all the samples. The tie line compositions for these systems are reported in Tables 6.3 and 6.4.The selectivity and distribution coefficient for the corresponding tie line data are calculated from equation 6.2 and 6.3 respectively.

(6.2)

(6.3)

where and denote mole fraction of benzothiophene (BT) and hexane (HX) in extract phase, and raffinate phase, respectively. For both the systems, the values of selectivity and distribution coefficient decreased as the concentration of benzothiophene in the feed increased. The distribution coefficient and selectivity is especially higher for lower concentrations of benzothiophene in the feed. Since the quantity of sulphur compounds in the actual crude is in ppm level, these results are favourable for analyzing the potential of these ionic liquids for aromatic sulphur extraction on an industrial scale.

From the analysis, it is observed that the concentration of hexane in extract phase was as high as 4.93% in [EMIM][$EtSO_4$] (Table 6.3)and 14.74% for [EMIM][CH_3COO](Table 6. 4).It should be noted that this concentration is obtained at the high concentration of benzothiophene in feed mixture. Since the quantity of benzothiophene in the actual crude is in ppm level, these results are favourable. This is of particular importance as this suggests that regeneration of the ionic liquid could be done with negligible loss of hydrocarbon at intermediate or lower concentration of benzothiophene. On the other hand, the corresponding concentration of IL in raffinate phase is zero for both ILs. Thus the ionic liquid does not remain as a impurity in the hydrocarbon or diesel rich phase. The selectivity and distribution coefficient with the concentration of benzothiophene in the hydrocarbon-rich phase has been presented in Figure 6.3 and 6.4.

Table 6.3: Experimental tie lines for the system [EMIM][$EtSO_4$](1) – Benzothiophene(2) – *n*-Hexane(3) at 308.15 K.

[EMIM][$EtSO_4$] rich phase			***n*-Hexane rich phase**			**S**	**β**
0.9287	0.0641	0.0072	0.0000	0.0350	0.9651	245.59	1.8365
0.8708	0.1203	0.0089	0.0000	0.0883	0.9117	139.57	1.3625
0.8100	0.1700	0.0200	0.0000	0.1496	0.8504	48.31	1.1362
0.7556	0.2112	0.0332	0.0000	0.2017	0.7983	25.15	1.0471
0.6986	0.2580	0.0434	0.0000	0.3429	0.6571	11.38	0.7523
0.6348	0.3171	0.0481	0.0000	0.4532	0.5468	7.95	0.6996
0.5885	0.3581	0.0534	0.0000	0.5125	0.4875	6.38	0.6988
0.5569	0.3938	0.0493	0.0000	0.5825	0.4175	5.73	0.6760

Table 6.4: Experimental tie lines and for the system [EMIM][CH_3COO](1) – Benzothiophene(2) – *n*-Hexane(3) at 308.15 K.

[EMIM][CH_3COO] rich Phase			*n*-Hexane rich Phase			S	β_{BT}
0.9054	0.0832	0.0114	0.0000	0.0346	0.9654	203.63	2.40
0.8542	0.1253	0.0205	0.0000	0.0672	0.9328	84.84	1.86
0.8133	0.1498	0.0369	0.0000	0.0959	0.9041	38.27	1.56
0.7077	0.2234	0.0689	0.0000	0.1671	0.8329	16.16	1.34
0.6542	0.2733	0.0725	0.0000	0.2278	0.7722	12.78	1.20
0.6040	0.3159	0.0801	0.0000	0.2851	0.7149	9.89	1.11
0.5288	0.3844	0.0868	0.0000	0.4250	0.5750	5.99	0.90
0.3824	0.4702	0.1474	0.0000	0.5495	0.4505	2.62	0.86

Figure 6.3: Selectivity for the ternary systems {[EMIM][OAc] + bezothiophene +hexane} and{[EMIM][$EtSO_4$]+ bezothiophene +hexane} at 308.15K,as function of mole fraction of Ionic Liquid in Hexane-rich phase.

Figure 6.4: Distribution coefficient for the ternary systems {[EMIM][OAc] + bezothiophene +hexane} and{[EMIM][$EtSO_4$]+ bezothiophene +hexane} at 308.15K,as function of mole fraction of Ionic Liquid in Hexane-rich phase.

The selectivity of [EMIM][$EtSO_4$] is higher than that for [EMIM][OAc] for lower concentration of benzothiophene in the feed. The values of selectivity for [EMIM][$EtSO_4$]

reached as high as 245.59, while that for [EMIM][OAc] went upto 203.63, indicating the increased affinity for aromatic sulphur compounds towards ionic liquids, thereby supporting the well-known fact that as the aromaticity increases, the selectivity also increases. Values as high as 162.95 were achieved by Arce et al. [2008] for the extraction of thiophene from hexane using [EMIM][$EtSO_4$]. Also, Zhang et al. [2004] revealed a direct correspondence between the aromaticity of the sulphur compound and the affinity towards the ionic liquid.

6.3.2 NRTL and UNIQUAC Correlations

According to the NRTL model [Renon et al.,1968], the non-ideal liquid phase activity coefficient ( ) of component is given by the following equation.

(6.4)

where,

(6.5)

The UNIQUAC model [Abrams at el.,1975] gives the following equation for the non-ideal activity coefficient for component .

(6.6)

where (6.7)

(6.8)

(6.9)

(6.10)

(6.11)

(6.12)

In equations 6.4 to 6.12, , and represent the area fraction, interaction parameter and segment fraction, respectively. The pure-component surface area parameter and the pure-component volume parameter in the UNIQUAC model are represented by

and , *respectively. The mole fraction in the liquid phase is represented by* , and the coordination number is represented by . We have used in our calculations. In equation 6.7, represents the average interaction energy for the interaction of molecules of component *j* with molecules of component *i*, *R* represents the gas constant and *T* represents the temperature.

The binary interaction parameters were obtained from the experimental LLE data by minimizing the objective function, which was defined as the sum of the square of errors between the experimental and calculated compositions of all the components over the entire set of tie lines as per equation 6.13. The methodology, application and the details are presented in our earlier work [Banerjee et al., 2005]. We have taken the population size, *npop* = 100, and the number of generations, *ngen* = 200 for the GA program. As the GA toolbox [MATLAB GA Toolbox, www.ise.ncsu.edu/kay/gaotv5.zip] in MATLAB is for maximization, the objective function (*F*) for minimizing the total error between the experimental and calculated mole fractions was defined as,

(6.13)

,

The goodness of the fit was measured by the root mean square deviation (RMSD) defined as in equation 4.24.The modified Rachford-Rice algorithm [Seader et al.,2005] was used to compute the tie lines (Figure 6.4). For the UNIQUAC model, the structure parameters *r* and *q* of the components were predicted using the Polarizable Continuum Model (PCM) as outlined in our previous work [Banerjee et al.,2005]. The values of *r* and *q* for the components have been presented in Table 6.5.

Figure 6.5: Modified Rashford –Rice algorithm for NRTL and UNIQUAC model.

The tie lines predicted by NRTL and UNIQUAC models are compared with the experimental tie lines in Figures 6.4-6.5 and 6.6-6.7 for the [EMIM][$EtSO_4$] and [EMIM][CH_3COO] ternary systems respectively. The NRTL and UNIQUAC interaction parameters are presented in Table 6.6. The RMSD values of 0.48% and 0.83% were obtained for [EMIM][$EtSO_4$] and [EMIM][CH_3COO] respectively, when using the NRTL model, and the corresponding RMSD values when using the UNIQUAC model were 0.693% and 1.053%.

Table 6.5: UNIQUAC structural parameters for the different compounds in the LLE system

Component	*r*	*q*
1-ethyl- 3-methylimidazolium ethyl sulphate*	8.3927	6.6260
1-ethyl-3-methylimidazolium acetate*	8.7500	5.5600
Benzothiophene	5.3803	3.4200
Hexane	4.4998	3.8560

* calculated via [Banerjee et al., 2005]

Table 6.6: NRTL and UNIQUAC interaction parameters for the two systems at T = 308.15K

	NRTL Model Parameters				**UNIQUAC Model Parameters**			
	/K	/K	*	RMSD**	/K	/K	*	RMSD**
System: [EMIM][$EtSO_4$] (1) – Benzothiophene (2) – *n*-Hexane (3)								
1-2	14.467	17.334	2.28×10^{-5}	0.48	670.98	-150.01	2.3×10^{-3}	0.693
1-3	18.151	9.507			358.05	156.55		
2-3	0.729	16.042			-9.0668	434.89		

System: [EMIM][CH_3COO] (1) – Benzothiophene (2) – *n*-Hexane (3)								
1-2	19.238	2.662	3.31×10^{-3}	0.83	-21.037	257.3	5.32×10^{-3}	1.053
1-3	19.469	12.870			406.51	8.4471		
2-3	15.948	2.469			11.131	140.03		

* Calculated using equation 6.13; **Calculated using equation 4.24.

Figure 6.6: Experimental vs. NRTL correlations for the composition tie lines of the system [EMIM][$EtSO_4$] – Benzothiophene – *n*-Hexane at 308.15 K.

Figure 6.7: Experimental vs. NRTL correlations for the composition tie lines of the system [EMIM][CH_3COO] – Benzothiophene – *n*-Hexane at 308.15 K

Figure 6.8: Experimental vs. UNIQUAC correlations for the composition tie lines of the system [EMIM][CH_3COO] – Benzothiophene – *n*-Hexane at 308 K.

Figure 6.9: Experimental vs. UNIQUAC correlations for the composition tie lines of the system [EMIM][$EtSO_4$] – Benzothiophene – *n*-Hexane at 308 K.

6.3.3 COSMO-RS Predictions

The equilibrium for ternary liquid-liquid system is defined by the equation:

(6.14)

where , the activity coefficient of component i *in a phase (*I *or* II*), is predicted using the* COSMO-RS model. and represents the mole fraction of component i in phase *I* and *II*

respectively. Most liquid-liquid equilibria are reached under adiabatic conditions, thus necessitating the consideration of an energy balance. However, if both feed *F* and solvent *S* enter the stage at identical temperatures, the only energy effect is the heat of mixing, which is often sufficiently small that only a very small temperature change occurs. Thus, we have assumed the process to occur isothermally and the compositions of the extract and raffinate phases are calculated using a flash algorithm as described by the modified Rashford-Rice Algorithm [Seader et al.,2005] (Figure 6.10). Also, the effect of pressure (*P*) on LLE calculations is assumed to be negligible. To start with, the feed concentration ( ) is calculated using the following equation,

(6.15)

The feed rate has been assumed to be unity (*F*=1). In the next step, the values of distribution coefficient (K_i, $i=1,2,3$) are calculated using the equation:

(6.16)

Here and are predicted using the COSMO-RS model. With the values of the isothermal flash equation is solved using eq 6.17,

(6.17)

subject to,

(6.18)

and,

(6.19)

Here and represents the flow rate of the extract and raffinate phases respectively. Eq 6.18 which is non-linear in nature is first solved for . Thereafter, the mole fractions in both phases are calculated via eqs 6.20 and 6.21.

(6.20)

(6.21)

The experimental data obtained for both the ionic liquid systems were used to benchmark the COSMO-RS code that we compiled in the manner represented above to predict the tieline compositions. Similar tie line prediction has been done successfully in our earlier work on Ionic Liquid based ternary system [Banerjee et al.,2008]. The results of these predictions on the ternary systems for both the predicted and experimental tie lines have been presented in Figures 6.9 and 6.10 for [EMIM][CH_3COO] and [EMIM][$EtSO_4$] based system respectively . We were able to successfully predict the result of the ternary equilibrium for the systems with fair amount of accuracy. RMSDs of 4.36% and 7.87% were obtained for the system containing the ionic liquids [EMIM][$EtSO_4$] and [EMIM][CH_3COO] respectively.

Thus, the COSMO-RS model based on the initial input of can predict the tie lines for any system whose experimental data is not known or is not practically possible due to economic or technical constraints. For the LLE prediction of any unknown ternary system we first and foremost require the COSMO file of the components in the LLE system. Thereafter based on any random feed composition ( ) one can generate the tie line data. The model will work only when equ 6.17 is solvable which in turn depends on the accuracy of predicting (equ 6.16). For a homogeneous phase, the flash algorithm will not converge,

which gives an idea that the feed composition we have chosen lies outside the immiscible region. This can therefore be used as a check to help us choose feed points that lie within the immiscible zone. Moreover, this model is not just limited to binary or ternary systems. After making necessary adjustments, the same model can be utilized to predict the results containing more than three components. This has been discussed in the next section.

Figure 6.10: Modified Rashford –Rice algorithm for COSMO-RS model.

Figure 6.11: Experimental vs. COSMO-RS predictions for the composition tie lines of the system [EMIM][CH_3COO] – Benzothiophene – *n*-Hexane at 308.15 K

Figure 6.12: Experimental vs. COSMO-RS predictions for the composition tie lines of the system [EMIM][$EtSO_4$] – Benzothiophene – *n*-Hexane at 308.15K

6.3.4 Single vs. Mixed Ionic Liquids: COSMO-RS predictions

Using the COSMO-RS model that we implemented for ternary systems, higher selectivities were obtained for the $EtSO_4^-$ anion over the CH_3COO^- anion, though this difference was not really significant. On the other hand, the distribution coefficient was higher for the CH_3COO^- anion, again the difference being insignificant. Anantharaj et al., [2011] obtained the interaction of sulphur compounds with ionic liquids and linked the solvent power to the mode of interaction that is involved. The work was done for fluorinated

anions in association with various cations, and their interaction with thiophene. It was observed that the affinity of the sulphur compounds for the anion in the ionic liquids depends on the electronegativity of the hetero atoms involved. In the case of acetate and ethyl sulphate, the difference in electronegativity is not large, which would explain the data on selectivity and distribution coefficient.

For imidazolium-based ionic liquids, the interactions between the ionic liquid and the sulphur compounds were found to mainly occur from the interactions between the –CH group in the imidazolium cation and the π-bond of the aromatic ring in the sulphur compound [Dupont et al.,2000]. Going by this observation, in the case of imidazolium-based ionic liquids, the cation must have a larger effect on the selectivity than the anion. This could explain the insignificant difference in the selectivities irrespective of whether one uses the [$EtSO_4$] anion or the [CH_3COO] anion. Since the predictions and experiments done for single ionic liquids did not show any significant difference in the selectivity or distribution coefficient, we implemented the COSMO-RS model to analyze mixed ionic liquids. The primary objective of this analysis was to observe any changes in the selectivity and distribution coefficient when mixed ionic liquids are chosen for the extraction of benzothiophene. For this purpose, we benchmarked the COSMO-RS model using the feed mixture as obtained for the system [EMIM][$EtSO_4$](1) – Benzothiophene(2) – *n*-Hexane(3).

In order to obtain a mixture of ionic liquids, the two ionic liquids, [EMIM][$EtSO_4$] and [EMIM][CH_3COO], were added in different proportions. This was done by dividing the feed concentration of the experimental data between the two ionic liquids as given by,

(6.22)

where is the total mole fraction of both the ionic liquids in the feed which is obtained from eq 6.17, is the mole fraction of [EMIM][$EtSO_4$] and is the mole fraction of [EMIM][CH_3COO]. The various mixtures of ionic liquids are obtained by varying the mole

ratio of the same in the feed, or the ratio

takes the values 1:4, 2:3, 1:1, 3:2 and 4:1 (i.e 20,40,50,60,80% respectively).

The selectivities and distribution coefficients for the various tie lines were calculated based on the equations as mentioned earlier. Figures 6.13 and 6.14 present a comparison of selectivities and distribution coefficients using the different ratios or %. From the charts, we can see that as long as [EMIM][$EtSO_4$] is the dominant ionic liquid, the selectivity is towards the higher side for all the benzothiophene feed concentrations, achieving maximum selectivity at 100% concentration of [EMIM][$EtSO_4$]. Whereas, when [EMIM][CH_3COO] is the dominant ionic liquid, the distribution coefficient is higher for all the feed concentrations of benzothiophene. For higher concentrations of benzothiophene in the raffinate, our model has predicted the selectivity to be the highest for a mixed composition of ionic liquids. Comparing Figure 6.3 with Figure 6.13 and 6.14,it is clear that the selectivity and distribution of mixed ionic liquids are very less as compared to single ionic liquid. Thus to have a better sulphur removal efficiency, it would be advisable to use a single ionic liquid. However, irrespective of the ionic liquid selected, the distribution coefficient and selectivity decreases with a rise in the feed concentration of benzothiophene. The importance of the findings is that using the COSMO-RS model, it is now possible to conduct a priori predictions for LLE systems containing mixed ionic liquids. In the present case, we have used two ionic liquids, benzothiophene and *n*-hexane as a quaternary system or pseudo ternary system. Thus using a similar approach, it is also possible to conduct predictions for systems containing any number of components. The only input required is the feed compositions and the sigma profiles of the individual components.

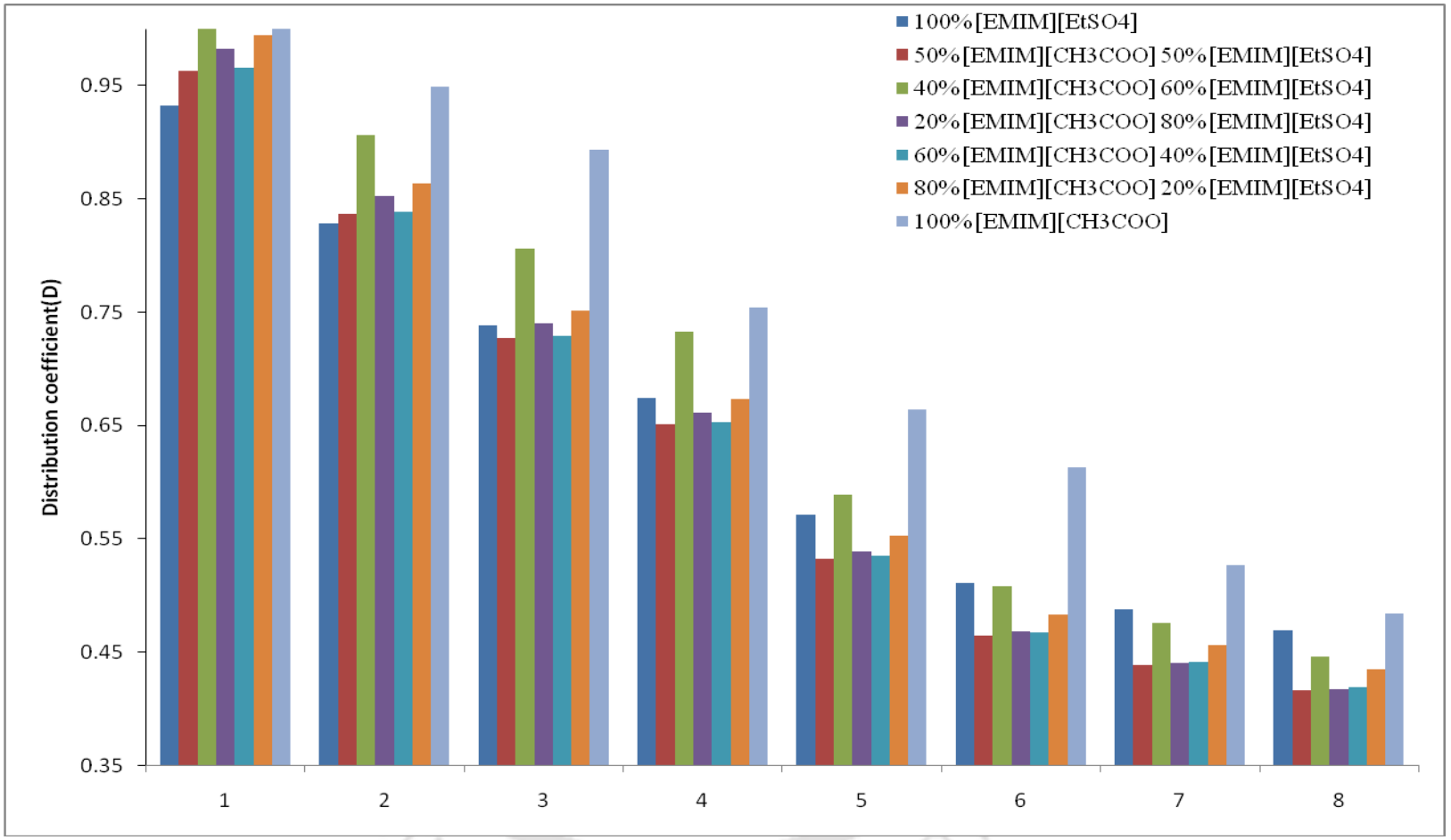

Figure 6.13: Comparison of distribution coefficients of benzothiophene in mixed ionic liquids of varying ratios vs the concentration of benzothiophene in the n-hexane rich phase at 308K (x-axis corresponds to the feed concentration of benzothiophene: 1: 5%; 2: 10%; 3: 20%; 4: 25%; 5: 30%; 6: 35%; 7: 45%; 8: 50%).

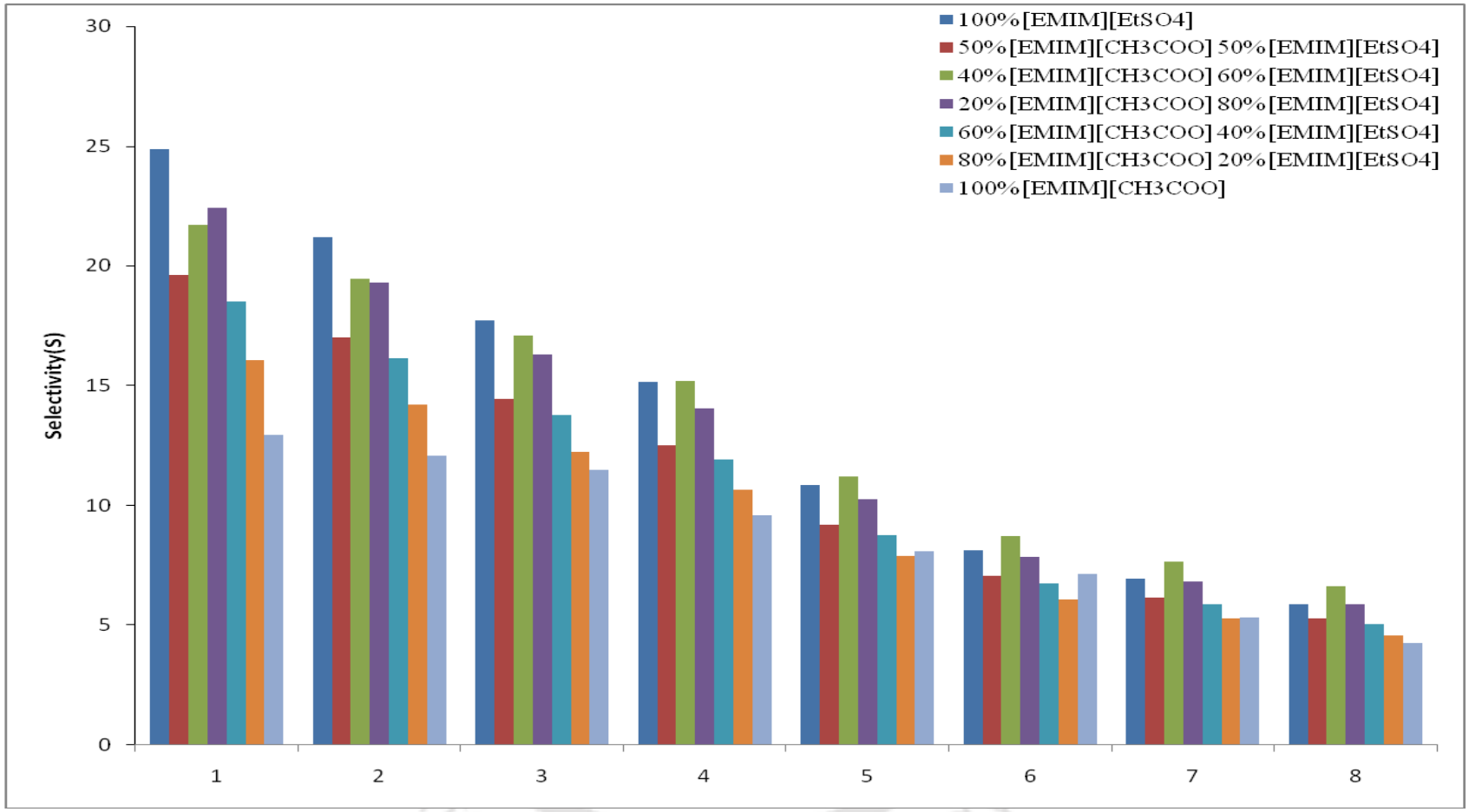

Figure 6.14: Comparison of selectivities of benzothiophene in mixed ionic liquids of varying ratios vs the concentration of benzothiophene in the n-hexane rich phase at 308K (x-axis corresponds to the feed concentration of benzothiophene: 1: 5%; 2: 10%; 3: 20%; 4: 25%; 5: 30%; 6: 35%; 7: 45%; 8: 50%).

6.4 UNIFAC Model

The original UNIFAC model combines the functional group concept with a model for activity coefficients based on an extension of the quasi-chemical theory of liquid mixtures (UNIQUAC) as proposed by Fredenslund et al., [1975]. This model can be applied at infinite dilution and finite concentrations and was the most widely used before several revisions and extensions were developed. The activity coefficient is expressed as a function of composition and temperature.

The data required for calculating activity coefficients at infinite dilution (non-ideality) using UNIFAC are two folds, first the group specific parameters – group volume and surface area parameters, and second the group interaction parameters. Although the group surface area and volume parameters are available for a large number of groups including those of ionic liquids (ILs), it is the group interaction parameter that is largely missing. Keeping this in mind this work focuses on finding the group interaction parameters for groups present in ternary mixture of IL –thiophene-diesel. Thiophene is taken as the model sulphur component and our aim in to separate it from diesel .However in our work we have taken the hydrocarbon such as hexane, heptane etc as the diesel component.

The UNIFAC model has a combinatorial contribution ( ) to the activity coefficient which is directly related to differences in size and shape of the molecules, and a residual contribution ( ) to define the energetic interactions between the molecules.

(6.23)

The combinatorial part is given by

(6.24)

(6.25)

(6.26)

The pure component parameters r_i and q_i are, respectively, related to molecular van der Waals volume and molecular surface area. They are calculated as the sum of the group volume and group area parameters, R_k and Q_k.. The mole fraction of component j in the mixture is denoted as x_j. Thus

(6.27)

(6.28)

Where , always an integer is the number of groups of type k *in molecule* i. *The* group parameters R_k and Q_k.. are normally obtained from van der Waals group volumes and surface areas, V_k and A_k.., as given below:

(6.29)

(6.30)

The residual part is given by:

(6.31)

is the group residual activity coefficient, and is the residual activity coefficient of group k in a reference solution containing only molecules of type i.

(6.32)

(6.33)

(6.34)

The surface area fraction of group *m* in the mixture is represented by ; and *is the* mole fraction of group *m* in the mixture. The group interaction parameter *is defined by*

(6.35)

The parameter *characterizes the interaction between groups* m *and* n *at* temperature *T*. For each group-group interaction, there are two parameters: . *Equations* 6.33-6.35 hold true for , except that the group composition variable , ,is now the group fraction of group *k* in pure fluid *i*. In pure fluid, which means that the activity coefficient approches unity when mole fraction approaches unity. Thus *must be* close to unity because as , and . Therefore, the group parameters (R_k, Q_k, a_{nm} and a_{mn}) should be available beforehand to solve the above equations.

6.5 Computational Details

6.5.1 Liquid - Liquid Equilibrium

Many pairs of chemical species when mixed, would not satisfy the stability criterion for single phase and thus split into two phases having different composition of different components. The equilibrium criterion for LLE is uniformity of *P*, *T* and of fugacity for each component throughout both phases (I and II refers to the two phases) .The equation 6.16 clearly shows that if we are able to predict activity coefficient of each component in both phases then it is easier to calculate distribution coefficient of components in both phases.

6.5.2 Calculation of composition

The mole fraction of all components in both phases can be calculated using distribution coefficient K at a particular temperature. This calculation has been performed using the Rachford-Rice algorithm [Seader et al., 1998] (Figure 6.15) and it is constructed by the following equations (c refers to the equilibrium condition and the number of components respectively, z being the initial molar feed fraction of mixture and $\psi=V/F$ *the* split between the two liquid phases as represented by V and L, such that $F=V+L$):

(6.36)

(6.37)

(6.38)

(6.39)

The Modified Rachford-Rice algorithm (Figure 6.15) along with UNIFAC model predicts the distribution coefficient whenever the ionic liquid is involved in the separation of thiophene from hydrocarbon. Thereafter we will extend our work to predict group interaction parameters of ionic liquids systems containing aromatic sulphur compounds.

Figure 6.15: Modified Rashford-Rice algorithm for UNIFAC model

6.5.3 Group Interaction Parameter Prediction

The group interaction parameters can be predicted by correlating large number of experimental data in combination with an objective function (Equation 6.13). The calculated mole fraction is obtained using equation 6.38 and 6.39. The global minimum of the objective function (OF) may be found until some tolerance limit is reached, which is related to accuracy of, a_{nm} and a_{mn} predicted. For this purpose we require Genetic Algorithm (GA) for regressing the experimental data. GA leads to nearly globally optimum values; it does not require any initial guess but only the upper and lower bounds of the interaction parameters. It has also been shown to perform better than inside variance estimation method (IVEM)[Vasquez et al.,2000] and the techniques used in ASPEN^R and DECHEMA^R.

We have used the Float genetic algorithm (FGA).This is better than both binary genetic algorithm (BGA) and Simulated Annealing(SA) in terms of computational efficiency and solution quality [Houck et al.,1996; MATLAB Toolbox ;www.ise.ncsu.edu/kay/gaotv5.zip]. The methodology and the operators are described by Sahoo et al., [2006]. Relationships for selection function and operators are also given in elsewhere [Sahoo et al., 2006].GA moves from generation to generation until a termination criterion is met. The most frequently used stopping criterion is a specified maximum number of generations (G_{max}) [Houck et al., 1996]. The operator values are the default values are as used in MATLAB Toolbox [www.ise.ncsu.edu/kay/gaotv5.zip]. For the regression GA is used with the objective function as given in equation 21. Prior to the optimization the lower and upper bounds for the interaction parameters were given beforehand (+1000 to -1000) based on prior literature data. Based on our earlier work on LLE [Sing et al., 2005], the number of population and generation has been kept at 100 and 200 respectively.

For this study, we considered ten two phase, three component systems with [OMIM][BF_4] and [OMIM][BTI] based ternary systems. The groups for the three component systems used in the prediction are listed in Table 6.7. The group interaction parameter was determined from the liquid liquid equilibrium (LLE) results through UNIFAC via regression of experimental data. The group volume *R* and area *Q* values are taken from literature .All the group and their parameters are listed in Table 6.7. In this case the ionic liquid [OMIM][BF_4] (Fifure 6.16) or [OMIM][BTI] (Figure 6.17) is broken in three parts i.e. one [IM][BF_4] and/or [IM][BTI] group, one octyl group and one methyl group. When these data are used simultaneously, we need to have a grand parameter matrix. A Grand Parameter Matrix (GPA) is a matrix of group interaction parameters which includes all the groups (frequency matrix) present in all the compounds as shown in Table 6.8.But it can be readily observed that the interaction parameter or group parameter matrix for ILs is still scarce. The accuracy of the new observed interaction parameters (Table 6.9) of these values can be judged by looking at RMSDs of the five groups used for the prediction (Equation. 4.24).

Table 6.7: Group volume and area parameters

Parameters	CH_2	CH_3	Thiophene	[IM][BF_4]	[IM][BTI]
R_k	0.6744	0.9011	2.8569	5.6658	7.4134
Q_k	0.540	0.848	2.140	3.1570	6.5440

The observed RMSD values for [OMIM][BF_4] and [OMIM][BTI] are quite accurate given the cumulative RMSD of ten systems (systems 1-7 and 8-14) considered simultaneously is 3.01% and 3.65% respectively. All the RMSD values are shown in Table 6.10.A further check is provided by applying the group parameters values to system which involve compounds that are not used for the prediction. Two different ternary data sets were

taken for both the ionic liquid systems to confirm the predictions. For the prediction of group interaction parameters for [OMIM][BF_4] based systems, tie lines corresponding to systems 1-5 of Table 6.10 were used for regression

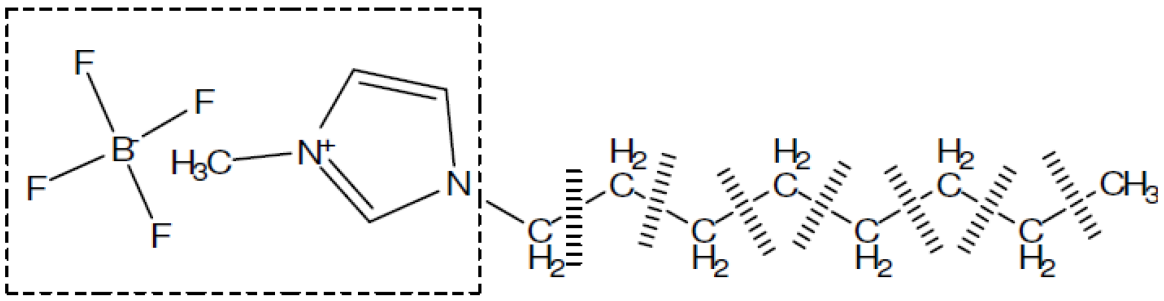

Figure 6.16: Group segmentation of 1-Octyl-3-Methylimidazolium Tetrafluoroborate {[OMIM][BF_4]} ionic liquid

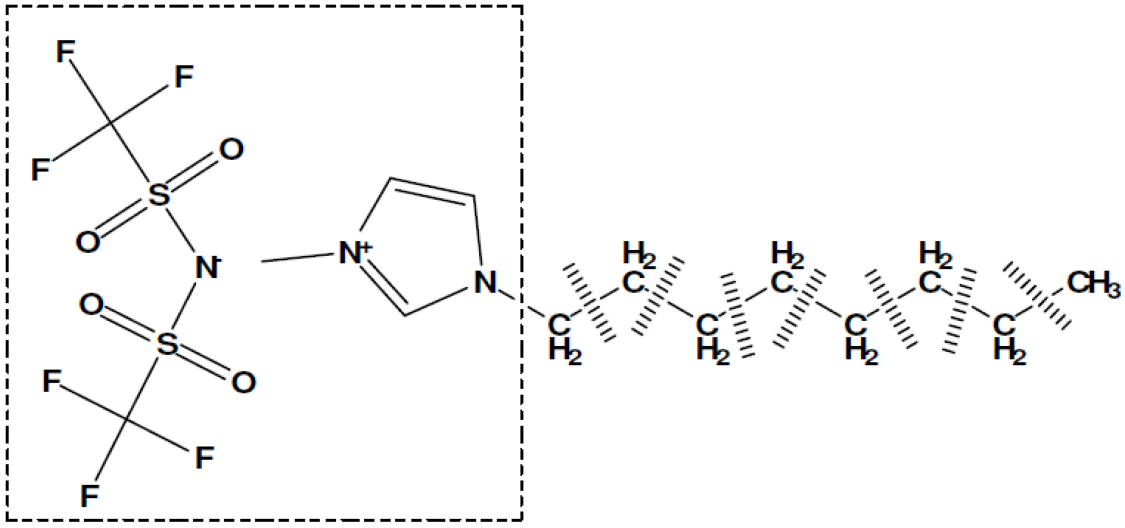

Figure6.17: Group segmentation of 1-Octyl-3-Methylimidazolium Bis-(trifluoromethylsulphonyl) amide {[OMIM][BTI]} ionic liquid.

Table 6.8: Grand Parameter matrix & Frequency matrix

Grand parameter matrix					
Name	CH_2	CH_3	Thiophene	[IM][BF_4]	[IM][BTI]
CH_2	0	0	92.99	NA	NA
CH_3	0	0	92.99	NA	NA
Thiophene	-8.479	-8.479	0	NA	NA
[IM][BF_4].	NA	NA	NA	0	-
[IM][BTI]	NA	NA	NA	-	0

Frequency matrix					
[OMIM][BF_4]	7	2	0	1	-
[OMIM][BTI]	7	2	0	-	1
Thiophene	0	0	1	0	0
Cyclohexane	6	0	0	0	0
Hexane	4	2	0	0	0
Heptane	5	2	0	0	0
Dodecane	10	2	0	0	0
Hexadecane	14	2	0	0	0

NA: not available

Table 6.9: Estimated group interaction parameters

[IM][BF_4]			
	CH	Thiophene	[IM][BF_4]
CH	0	92.99	1268.3
Thiophene	-8.479	0	679.7
[IM][BF_4]	1374.4	456.4	0
[IM][BTI]			
CH	0	92.99	313.71
Thiophene	-8.479	0	240.9
[IM][BTI]	333.81	175.06	0

Thereafter the predicted group interaction (Table 6.9) has been used in predicting the tie lines of systems: [OMIM][BF_4] + thiophene + methylcyclohexane (Figure 6.18) and [OMIM][BF_4] + thiophene + isooctane (Figure 6.19) (system 7 of Table 6.10) with RMSD of 3.99 and 2.39% respectively. For the prediction of group interaction parameters for [OMIM][BTI] based system, tie lines corresponding to systems 8-12 of Table 6.9 were used for regression. Thereafter the predicted group interaction (Table 6.9) has been used in predicting the tie lines of systems: [OMIM][BTI] + thiophene + 224trimethylpentane (Figure 6.20) and [OMIM][BTI] + thiophene + methylcyclohexane (Figure 6.21) with RMSD of 3.55 and 1.76% respectively. The data shown in above tables can also be plotted in a ternary

diagram to give a pictorial comparison of the experimental and the predicted data. Figure 6.19 shows the comparison between predicted and experimental tie lines for the system: [OMIM][BF_4]-thiophene-methylcyclohexane .It can be seen that our predicted results are in qualitative agreement with those of reported values [Alonso et al.,2007a,2007b,2007c,2008a,2008b].

Figure 6.18: Experimental and Predicted tielines for [OMIM][BF_4]-thiophene-methylcyclohexane

Table 6.10: RMSDs of the ternary systems used in the prediction

S.No	System Name	RMSD in %	Ref	T /K
1	[OMIM][BF_4]—thiophene–cyclohexane	5.85	[Alonso et al.,2007b]	298.15
2	[OMIM][BF_4]—thiophene–hexane	3.33	[Alonso et al.,2007b]	298.15
3	[OMIM][BF_4]—thiophene–heptane	1.78	[Alonso et al.,2008]	298.15
4	[OMIM][BF_4]—thiophene–dodecane	2.35	[Alonso et al.,2008]	298.15
5	[OMIM][BF_4]—thiophene–hexadecane	3.60	[Alonso et al.,2008b]	298.15
6	[OMIM][BF_4]—thiophene–isooctane	3.99	[Alonso et al.,2007c]	298.15
7	[OMIM][BF_4]—thiophene–methyl--cyclohexane	2.39	[Alonso et al.,2007a]	298.15
8	[OMIM][BTI]—thiophene–cyclohexane	2.88	[Alonso et al.,2008a]	298.15
9	[OMIM][BTI]—thiophene–hexane	2.00	[Alonso et al.,2008c]	298.15
10	[OMIM][BTI]—thiophene–heptane	2.40	[Alonso et al.,2008c]	298.15
11	[OMIM][BTI]—thiophene–dodecane	2.65	[Alonso et al.,2008a]	298.15
12	[OMIM][BTI]—thiophene–hexadecane	4.70	[Alonso et al.,2008c]	298.15
13	[OMIM][BTI]—thiophene– isooctane	3.55	[Alonso et al.,2007a]	298.15
14	[OMIM][BTI]—thiophene–methyl--cyclohexane	1.76	[Alonso et al.,2007a]	298.15

Figure 6.19: Experimental and Predicted tielines for [OMIM][BF_4]-thiophene-Isooctane

Figure 6.20: Experimental and Predicted tie lines for [OMIM][BTI]-thiophene-224trimethylpentane

Figure 6.21: Experimental and Predicted tie lines for [OMIM][BTI]-thiophene-methylcyclohexane.

Nomenclature

[EMIM]	Cation: 1-ethyl 3-methylimidazolium
[OMIM]	Cation: 1-octyl 3-methylimidazolium
[$EtSO_4$]	Anion: ethyl sulphate
[CH_3COO]	Anion: acetate
[NtF_2]	Anion: bis-(trifluoromethanesuphonyl)-imide
TMAC	Tri Methyl Aluminium Chloride
[BF_4]	Tetrafluoroborate
[BTI]	Bis [trifluoromethylsulfonyl] imide
UNIFAC	UNIQUAC functional group activity coefficient
K	Distribution coefficient
Z	Feed composition
L	Liquid Feed Rate for phase I
V	Liquid Feed Rate for phase II
S	Selectivity
F	Objective function
$RMSD$	Root mean square deviation
a_{eff}	Effective segment surface area, $Å^2$
c_{hb}	Misfit energy constant, kcal $Å^4$ mol^{-1} e^{-2}
	Sigma profile of component i i.e. probability of segment i having a charge density σ
R	Universal gas constant, J K^{-1} mol^{-1}
T	Temperature, K
r_i	Normalized volume parameter for the Staverman-Guggenheim combinatorial term, $Å^3$
q_i	Normalized surface area parameter for the Staverman-Guggenheim combinatorial term, $Å^2$
r_{std}	Standard volume parameter, 79.53 $Å^3$
q_{std}	Standard surface area area parameter, 66.69 $Å^2$
m	Number of tie lines
c	Number of components in the LLE system
x_i	Mole fraction of component i of either phase in the LLE system
n_i	Total number of segments on the surface of the molecular cavity
H_i	Peak area under NMR spectra of species i
z	Coordination number =10
l	Staverman-Guggenheim combinatorial term parameter

g_{ji}	Average interaction energy for the interaction of molecules of component j with molecules of component i

Greek Symbols

α'	Misfit energy constant, kcal $Å^4$ mol^{-1} e^{-2}
σ_{hb}	Hydrogen bonding cut-off value, 0.0084 e $Å^{-2}$
	Activity coefficient of solute i in solution S
	Segment activity coefficient of segment σ_i in pure species
H_i	Peak area under NMR spectra of species i
β	Distribution coefficient
θ	Area fraction in UNIQUAC equation
τ	NRTL/UNIQUAC interaction parameter
Φ	Segment fraction in UNIQUAC equation
α	NRTL non-randomness parameter
	Staverman-Guggenheim activity coefficient

REFERENCES

Abrams, D.S.; Prausnitz, J.M. Statistical thermodynamics of liquid mixtures: a new expression for the excess Gibbs energy of partly or completely miscible systems. *AIChE J.* **1975**, 21, 116–128.

Alonso, L.; Arce, A.; Francisco, M.; Rodriguez, O.; Soto, A. (Liquid + liquid) equilibria of [C8mim][NTf2] ionic liquid with a sulfur-component and hydrocarbons. *J. Chem. Thermodynamics*. **2008**,40, 265-270.

Alonso, L.; Arce, A.; Francisco, M.; Rodriguez, O.;Soto, A. Gasoline Desulfurizationusing Extraction with [C8min][BF4] Ionic Liquid. *AIChE J*.**2007a**, 53, 3108-3115.

Alonso, L.; Arce, A.; Francisco, M.; Rodriguez, O.;Soto, A. Liquid-Liquid Equilibria for Systems Composed by 1-Methyl-3-octylimidazolium Tetrafluoroborate Ionic Liquid, Thiophene, and *n*-Hexane or Cyclohexane. *J.Chem. Eng. Data*, **2007b**,52 1729-1732.

Alonso, L.; Arce, A.; Francisco, M.; Rodriguez,O.; Soto, A. Measurement and Correlation of Liquid-Liquid Equilibria of Two Imidazolium Ionic Liquids with Thiophene and Methylcyclohexane. *J. Chem. Eng. Data*.**2007c**, 52, 2409-2412.

Alonso, L.; Arce, A.; Francisco, M.; Soto, A. Phase behaviour of 1-methyl-3-octylimidazolium bis[trifluoromethylsulfonyl] imide with thiophene and aliphatic hydrocarbons: The influence of *n*-alkane chain length. *Fluid Phase Equilibria*. **2008a**,263, 176-18.1

Alonso, L.; Arce, A.; Francisco, M.; Soto, A. Solvent extraction of thiophene from n-alkanes (C7, C12 and C16) using the ionic liquid [C8mim][BF4].*J. Chem.Thermodynamic*s.**2008b**,40,966-972.

Anantharaj, R.; Banerjee. T. Quantum Chemical Studies on the Simultaneous Interaction of Thiophene and Pyridine with Ionic Liquid. *AIChE J*. **2011**. 57,749-764.

Arce, A.; Alonso, L. ; Francisco, M.; Soto. A. Phase behaviour of 1-methyl 3-octylimidazolium bis[trifluoromethylsulfonyl]imide with thiophene and aliphatic hydrocarbons: The influence of *n*-alkane chain length. *Fluid Phase Equilibria*. **2008a**, 263, 176-181.

Arce, A.; Alonso, L.; Francisco, M.; Rodriguez, O.; Soto, A. Gasoline desulfurization using extraction with [C_8mim][BF_4] ionic liquid. *AIChE J*. **2007,** 53,3108-3115.

Arce, A.; Alonso, L.; Francisco, M.; Soto. A. Solvent extraction of thiophene from *n*-alkanes (C_7, C_{12}, and C_{16}) using the ionic liquid [C_8mim][BF_4]. *J. Chem. Thermodynamics*. **2008b,** 40, 966-972.

Arce, A.; Alonso, L.; Francisco, M.; Soto. A. Thiophene separation from aliphatic hydrocarbons using the 1-ethyl-3-methylimidazolium ethyl sulfate ionic liquid. *Fluid Phase Equilibria*. **2008c**, 270**,** 97-102.

Arce, A.; Francisco, M.; Soto. A. Evaluation of the polysubstituted pyridinium ionic liquid [hmmpy][Ntf_2] as a suitable solvent for desulfurization: Phase equilibria. *J. Chem. Thermodyn*amics.**2010**, 42,712-718.

Banerjee, T.; Khanna, A. Infinite Dilution Activity Coefficients for Trihexyltetradecyl Phosphonium Ionic Liquids: Measurements and COSMO-RS Prediction. *J. Chem. Eng. Data*. **2006**,51, 2170-2177.

Banerjee, T.; Sahoo, R.K.; Rath, S.S.; Kumar, P.; Khanna, A. Multicomponent liquid-liquid equilibria prediction of aromatic extraction systems using COSMO-RS. *Ind. Eng. Chem. Res*. **2007**, 46, 1292-1304.

Banerjee, T.; Singh, M.K.; Khanna, A. Genetic Algorithm to Estimate Interaction Parameters of Multicomponent Systems for Liquid–Liquid Equilibria. *Comp. Chem. Engg*. **2005**, 29,1712 – 1719.

Banerjee, T.; Singh, M.K.; Khanna, A. Multicomponent Liquid-Liquid Equilibria Prediction for Aromatic Extraction Systems Using COSMO-RS. *Ind. Eng.Chem.Res*.**2006a**, 46, 1292-1304.

Banerjee, T.; Singh, M.K.; Khanna, A. Prediction of binary VLE for imidazolium based ionic liquid systems using COSMO-RS. *Ind. Eng. Chem. Res*. **2006b,** 45,3207-3219.

Banerjee, T.; Singh, M.K.; Sahoo, R.K.; Khanna, A. Volume, surface and UNIQUAC interaction parameters for imidazolium based ionic liquids via Polarizable Continuum Model. *Fluid Phase Equilibria*. **2005**, 234, 64-76.

Banerjee, T.; Verma, K.K.; Khanna, A. Liquid-Liquid Equilibrium for Ionic Liquid Systems Using COSMO-RS: Effect of Cation and Anion Dissociation. *AIChE J*. **2008**, 54, 1874-1885.

Brennecke, J. F.; Maginn, E. J. Ionic Liquids: Innovative Fluids for Chemical Processing. *AIChE J*.**2001**, 47, 2384-2389.

Domańska, U.; Królikowski, M.; Ślesińska. K. Phase equilibria study of the binary systems (ionic liquid+ thiophene): Desulphurization process. *J. Chem. Thermodynamics*. **2009**, 41, 1303-1311.

Dupont, J.; Suarez, P.A.Z.; De Souza, R.F.; Burrow, R.A.; Kintzinger, J. CH-π Interactions in 1-*n*-Butyl-3-methylimidazolium Tetraphenylborate Molten Salt: Solid and Solution Structures. *Chem Eur. J*. **2000**, 6 **,** 2377-2381.

Eβer, J.; Wasserchеid, P.; Jess A. Deep desulfurization of oil refinery streams by extraction with ionic liquids. *Green Chem*. **2004**, 6,316-322.

Fredenslund; Jones, R.L.; Prausnitz, J.M. Group contribution estimation of activity coefficients in nonideal liquid mixtures. *AIChE J*.**1975**, 21,1087-1099.

Holbrey, J.D.; Reichert, W.M.; Swatloski, R.P.; Broker, G.A.; Pitner, W.R.; Seddon K.R.; Rogers, R.D.Efficient, halide free synthesis of new, low cost ionic liquids: 1,3-dialkylimidazolium salts containing methyl- and ethyl-sulfate anions. *Green Chem.***2002**,4, 407–413

Kabe, T.; Ishihara, A.; Tajima, H. Hydrodesulfurization of Sulfur-Containing Polyaromatic Compounds in Light Oil.*Ind. Eng. Chem.Res*.**1992**, 31, 1577-1580.

Kumar, A.A.P. ; Banerjee, T. Thiophene separation with ionic liquids for desulphurization: A quantum chemical approach. *Fluid Phase Equilibria*. **2009**, 278, 1-8.

Li, Y.; Nie, C.; Sun, A.; Meng, H.; Wang, Z. Extractive Desulfurization of Gasoline Using Imidazolium-Based Phosphoric Ionic Liquids. *Energy Fuels* .**2006**, 20, 2083-2087.

Lin, S.T.; Sandler, S.I. A Priori Phase Equilibrium Prediction from a Segment Contribution Solvation Model. *Ind. Eng. Chem. Res*. **2002**, 41, 899-913.

MATLAB GA Toolbox, www.ise.ncsu.edu/kay/gaotv5.zip.
Renon, H.; Prausnitz, J.M. Local compositions in thermodynamic excess functions for liquid mixtures. *AIChE J*. **1968**, 14, 135-144.

Seader, J.D.; Henley, E.J. Separation process principles, 2nd ed.; Wiley: New York, **2005**.

Singh.M. K.; Banerjee.T.; Khanna.A. Genetic algorithm to estimate interaction parameters of multicomponent systems for liquid–liquid equilibria. *Comp. Chem. Engg.* **2005**, 29, 1712-1719.

Wang, J.; Zhao, D.; Zhou, E.; Dong, Z. Desulfurization of gasoline by extraction with N-alkyl-pyridinium-based ionic liquids. *J. Fuel Chem. Technol*.**2007**,35,293-296.

Zhang, S.; Zhang Z.C. Novel properties of ionic liquids in selective sulphur removal from fuels at room temperature.*Green Chem*.**2002**, 4, 376-379.

Zhang, S.; Zhang, Q. ; Zhang, Z.C. Extractive desulfurization and denitrogenation of fuels using ionic liquids. *Ind. Eng. Chem. Res*. **2004**,43,614-622.

7.1 Introduction

The possibility of IL as entrainer for the separation of aromatic sulphur and nitrogen compounds has already been explored earlier by experimental and computational studies [Alonso et al., 2007; Xie et al., 2008]. However ILs consisting of cation and anion is limitless in combination. Thus a judicious selection is required for its use as solvent. The quantum chemical based Conductor Like Screening Model for Real Solvent (COSMO-RS) is used for evaluating ILs as solvents in extraction process. This is a novel and efficient method for a-priori prediction of infinite dilution activity coefficient (IDAC). In our previous chapters from the IDAC values, the selectivity (S), capacity (C) and performance index (PI) of IL were calculated for desulphurization and denitrification studies. A considerably high selectivity and capacity were achieved for acetate ([OAc]), ethyl sulphate ([$EtSO_4$]) and methylsulphonate ([$MeSO_3$]) anion with [EMIM] cation. It was found that a smaller size of cation led to a higher selectivity. Thus we have chosen the ILs: 1-ethyl-3-methylimidazolium acetate ([EMIM][OAc]),1-ethyl-3methylimidazolium ethylsulphate ([EMIM][$EtSO_4$]) and 1-ethyl-3-methylimidazolium methylsulphonate ([EMIM][$MesO_3$]) for the simultaneous HDS and HDN of diesel oil at T=298.15K.

The aim of this work is to investigate the quaternary LLE phase behavior of [EMIM][OAc],[EMIM][$EtSO_4$] and [EMIM][$MesO_3$] for the simultaneous extraction of thiophene and pyridine from diesel stream (i.e.pentane,isooctane,cyclohexane and toluene). This LLE data will be essential for the design of the extraction equipment and also helps us to know the thermodynamic limit of separation. Therefore, the LLE diagram for quaternary mixture of [EMIM][OAc] + thiohphene + pyridine + pentane /isooctane /cyclohexane /toluene,[EMIM][$EtSO_4$] + thiohphene + pyridine +pentane/ isooctane/cyclohexane/toluene and [EMIM][$MesO_3$] + thiohphene + pyridine +pentane/ isooctane/cyclohexane/toluene have been determined at ambient condition i.e. at 298.15K.From the experimental data, the

extraction efficiency of thiophene and pyridine, the selectivity and the distribution coefficient were also determined.

7.2 Experimental section

7.2.1 Chemicals and Materials

The ionic liquids: 1-ethyl-3-methylimidazolium acetate [EMIM][OAc]($C_8H_{14}N_2O_2$) of purity > 98% and 1-ethyl-3-methylimidazolium ethyl sulphate [EMIM][$EtSO_4$] ($C_8H_{16}N_2O_4S$) of purity > 95% were supplied by Sigma Aldrich, Germany. 1-ethyl-3-methylimidazolium methanesulphonate [EMIM][$MeSO_3$] ($C_8H_{16}N_2O_3S$) ionic liquid was purchased from Fluka with a purity of > 95%. Pyridine (C_5H_5N) and thiophene (C_4H_4S) were received from Sigma Aldrich with mass fractions greater than 98%. Pentane (C_5H_{12}), isooctane (C_8H_{18}), cyclohexane (C_6H_{12}) and toluene (C_7H_8) were obtained from Merck with a purity of >99.5%. $CDCl_3$ of purity > 99.8%, used for the NMR analysis of the extract and raffinate phase compositions was supplied by Sigma Aldrich, Germany.

7.2.2 Experimental procedure

An equimolar concentration of the ionic liquid and hydrocarbon (pentane/isooctane/cyclohexane/toluene) with a 3:1 ratio of thiophene and pyridine was prepared as a feed mixture. The concentration of thiophene and pyridine was varied from 5% to 80%. The desired amount of individual components was transferred into the stoppered bottles using 5ml syringe. The total volume of mixtures was fixed at 8ml for all studied systems. A 15ml stopered bottle was used for holding the feed mixture. The sample bottles were properly sealed with parafilm tape to prevent any loss of the components due to evaporation. The bottles were then placed inside a water-shaker bath set at 100 rpm and at

298.15 K for not less than 6 hours in thermostatic shaker bath (Dailhan Lab, China). Spring clamps were used to hold the bottles on the tray. The temperature was accurate within the uncertainty of ±0.01 K.The mixture was then allowed to settle for a minimum of 12 hours so that equilibrium is attained.

Table 7.1: NMR Peak Assignment for Quantitative Analysis in the Quaternary mixture

Chemical Compound and Peak Type	**Chemical Shifts in NMR Spectra (Relative to TMS)**
	a: ~ 6.96 (doublet, 2 H) b: ~ 7.20 (doublet, 2 H)
	a: ~7.38 (singlet,2H) b: ~ 8.59 (singlet,2 H)
	a: ~ 1.33 (singlet, 6 H)
	a: ~ 2 (singlet, 3 H)

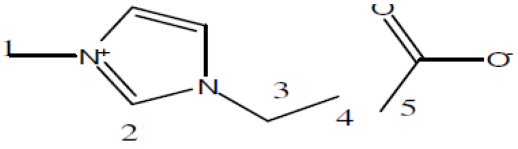

1-Ethyl-3-Methylimidazolium Acetate

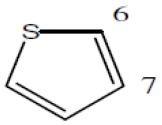

Thiophene

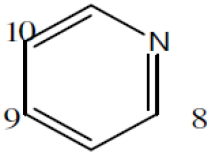

Pyridine

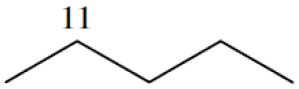

Pentane

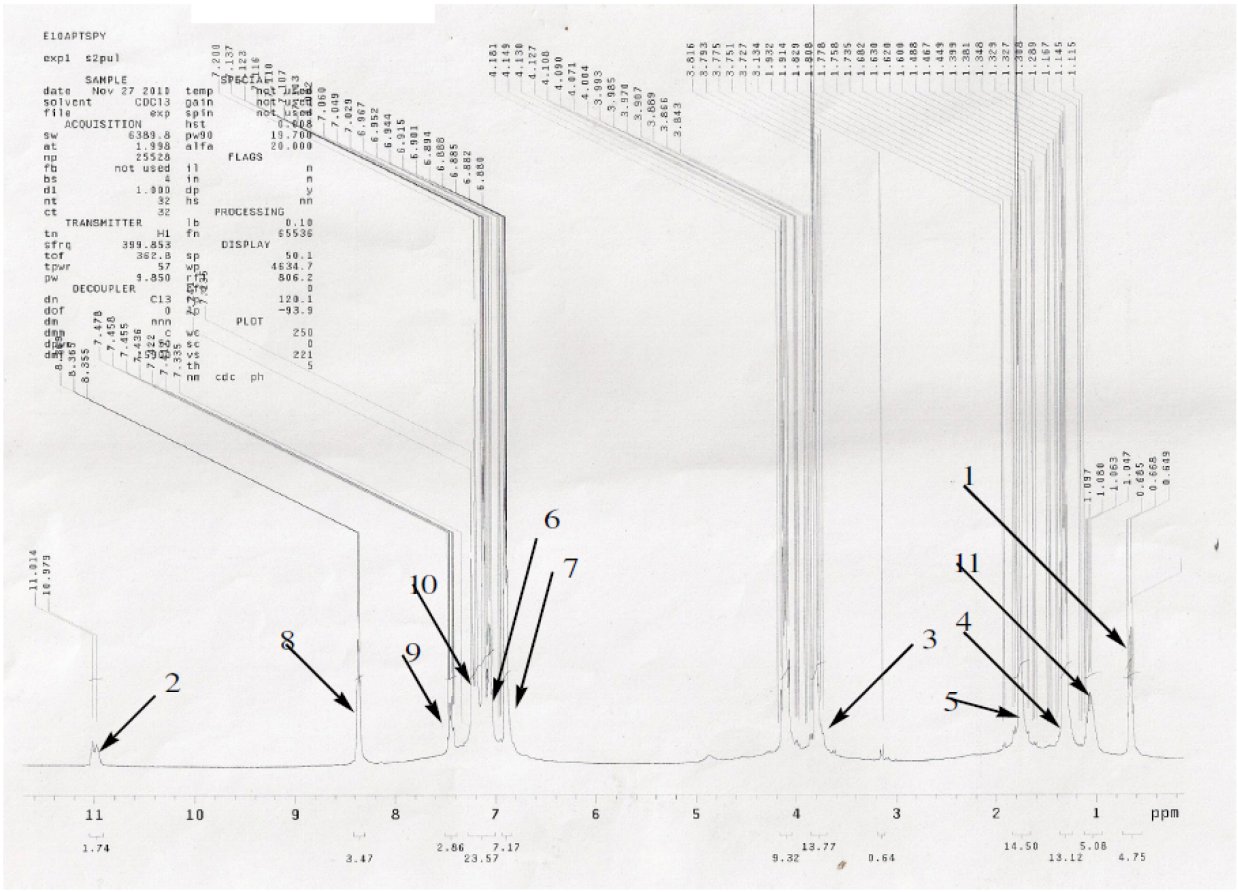

Figure 7.1: NMR spectra of the extract phase for the system [EMIM][OAc] –Thiophene-Pyridine –Pentane

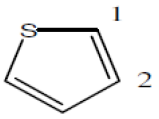

Thiophene

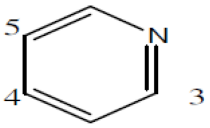

Pyridine

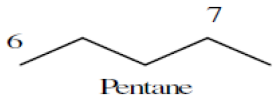

Pentane

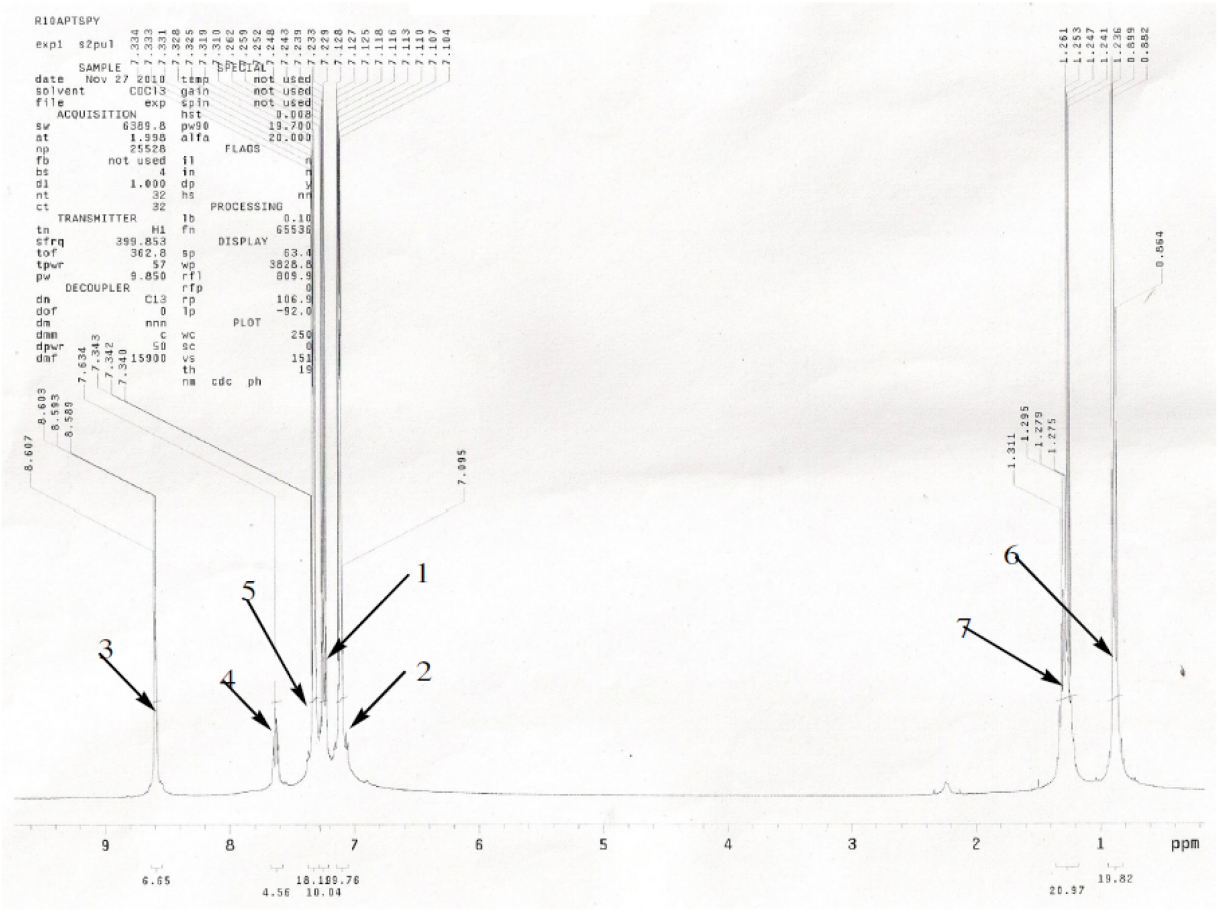

Figure 7.2: NMR spectra of the raffinate phase for the system [EMIM][OAc] – Thiophene – Pyridine -Pentane

7.2.3 Analysis

LLE data for quaternary systems were determined experimentally by an analysis of the phases at equilibrium. The composition of the equilibrium phases were analyzed using the NMR spectrometer of 11.74 Tesla (20 MHz response of ^{1}H). For this study, a small amount of each phase was dissolved in 0.5ml of $CDCl_3$ in two different NMR (thrift Grade) tubes, which were sealed properly. According to the ^{1}H NMR spectral analysis principle, we obtained the peak areas of the hydrogen molecule of each component from which we can calculate the individual composition in both the phases. The aromatic ring structure of imidazolium, thiophene and pyridine compounds shows peak in the range of 6-9.5. The hydrocarbon (i.e. pentane) shows a peak in the range of 1.1-1.5 for the $–CH_2-$ linkage, and below 1.1 for the $–CH_3$ group. The oxinate compounds like CH_3SO_3, CH_3COO and $–CH_2SO_4$ shows a peak between 2.5 to 3 which depends on the anion attached to the imidazolium cation. From these ranges, the peak areas of the individual hydrogen atoms belonging to the respective components were obtained by automatic integration of the NMR spectrogram. In order to calculate the composition of the individual component the following equation 6.1 is used.

The correspondence between peak assignments of both the phases in quaternary mixture is shown in Table 7.1. The NMR spectra of the extract and raffinate phase of the quaternary system involving [EMIM][OAc] are given in Figures 7.1, and 7.2 respectively. Since the cation is similar for the other quaternary system, the NMR spectra is similar to the one shown except that the shift of the acetate anion is observed at around 2 ppm.

7.3 Results and Discussion

7.3.1 Experimental LLE of the quaternary system of [EMIM] based ILs (1) + Thiophene (2) +Pyridine (3) +Pentane (4).

The experimental liquid-liquid equilibrium data (tie-lines) for the quaternary systems {[EMIM][OAc] (1) + Thiophene (2) +Pyridine (3) +Pentane (4)}, {[EMIM][$EtSO_4$] (1) + Thiophene (2) +Pyridine (3) + Pentane(4)} and {[EMIM][$MeSO_3$] (1) + Thiophene (2) +Pyridine (3) +Pentane (4) }at 298.15K and atmospheric pressure are given in Table 7.2 to 7.4. .The feasibility of using [EMIM][OAc], [EMIM][$EtSO_4$] and [EMIM][$MeSO_3$] as solvents was obtained using the selectivity and distribution coefficient which are calculated from the experimental composition of tie line (equation 7.1 and 7.2)

(7.1)

(7.2)

Where *x* is the mole fraction of thiophene/ pyridine and pentane in the extract (E) and raffinate (R) phase respectively. The selectivity of the studied quaternary systems is plotted in Figure 7.3(a).For the quaternary system studied in this work, the selectivity decreases with the increase in the thiophene+pyridine mixture concentration in the pentane rich phase. This agrees well with the previous work on ILs [Gomez et al., 2010; Gonaleg et al., 2010]. The selectivity decreases as the distance between IL and thiophene/pyridine becomes larger which makes the strength of CH--π and π--π stacking in the cation and anion lesser. Moreover the selectivity values are higher than unity for all the studied systems which conforms that [EMIM][OAc], [EMIM][$EtSO_4$] and [EMIM][$MeSO_3$] ionic liquid could be a choice for the simultaneous separation process. The distribution coefficient values if considered, increases with an increase in the thiophene+pyridine mixture concentration in the pentane rich phase.

This again agrees with the reported values on ILs [Garcia et al., 2010; Garcia et al., 2010]. Since β is lower than unity (Figure 7.3 (b)) implies more quantity of IL is required for the extraction. But at the same time, the ILs are totally immiscible in the pentane rich phase which could make their recovery and reuse easier and cheaper when multiple extraction steps are carried out using ILs. Therefore [EMIM][OAc], [EMIM][$EtSO_4$] and [EMIM][$MeSO_3$] ionic liquid could be considered as alternative solvents for simultaneous desulphurization and denitrification of diesel oil when the aromatic sulphur- and nitrogen concentration in the diesel oil is low i.e.ppm level.

Figure 7.3(a): Selectivity for the ternary systems {[EMIM][OAc]+thiophene+pyridine +pentane},{[EMIM][$EtSO_4$]+thiophene+ pyridine +pentane}and {[EMIM][$MeSO_3$]+ thiophene + pyridine +pentane } at 298.15K,as function of mole fraction of solute in pentane-rich phase.

Figure7.3(b): Distribution coefficient for the ternary systems {[EMIM][OAc] +thiophene + pyridine + pentane}, {[EMIM][$EtSO_4$] + thiophene + pyridine + pentane} and

{[EMIM][$MeSO_3$] + thiophene + pyridine +pentane } at 298.15K,as function of mole fraction of solute in pentane-rich phase.

7.3.2 NRTL and UNIQUAC correlations

The NRTL and UNIQUAC model were used to correlate the LLE data .It is seen that Figure 7.4 to 7.9, it has proved to adequately represent the quaternary system that contains ILs. The linearity of the plot indicates a high degree of consistency of the data. The pure component surface area and volume parameters are given in Table 7.5. The set of plot provides a clear visualization of the change in the size and shape of the immiscibility region as results of increasing mole fraction of thiophene +pyridine in pentane rich phase. It is observed that the specific molecular interaction between similar sizes of the molecules (thiophene + imidazolium cation or pyridine +imidazolium cations) strongly depends on the mole fraction of thiophene +pyridine in pentane rich phase. An interesting fact from all the triangular diagrams is that the tie lines show two different slopes: positive slope at lower part and negative slope exhibit at upper part of the triangular diagram. It is well known fact that as the amount of thiophene+pyridine increases, the distance between IL and thiophene/pyridine becomes larger and therefore the strength of interaction decreases at 298.15K.This behavior is in accordance with previous work on LLE of systems containing an n-Hexane + pyridine + [EMIM][$EtSO_4$] (tie line shows a positive slope),hexadecane +pyridine + methanol (tie line exhibits a negative slope), and Hexane + thiophene + [HMIM][NTf_2], Dodecane + thiophene + [HMIM][NTf_2] and Hexadecane + thiophene + [HMIM][NTf_2] where both positive and negative slopes are visible in the ternary plot [Won et al., 2002;Alonsa et al.,2010;Maduro et al.,2010].

Table 7.6 to 7.8 shows the values of the interaction parameters obtained using NRTL and UNIQUAC model to correlate the experimental data for the three quaternary systems. The negative objective function minimizes (Equation 6.13) the difference between the experimental and calculated mole fraction of the components in both the phases. The values of the root mean square deviation (RMSD) (Equation 4.24) for the three quaternary systems were less than unity i.e. RMSD is less than1% at 298.15K.

Table 7.2: Composition of experimental tie-lines, selectivity (S) and distribution ratio for [EMIM][OAc] (1) + Thiophene (2) +Pyridine (3) +Pentane (4) at 298.15K.

S.No	[EMIM][OAc] rich phase					Pentane rich phase					Selection parameter	
											S_{23}	β_{23}
1	0.9056	0.0572	0.0297	0.0870	0.0074	0.0000	0.0079	0.0245	0.0324	0.9676	349.3081	2.6827
2	0.8772	0.0781	0.0411	0.1193	0.0036	0.0000	0.0650	0.0208	0.0858	0.9142	357.9476	1.3907
3	0.7555	0.1882	0.0504	0.2387	0.0058	0.0000	0.1235	0.0387	0.1622	0.8378	212.0952	1.4714
4	0.6902	0.2150	0.0864	0.3013	0.0085	0.0000	0.2433	0.0937	0.3370	0.6630	69.7392	0.8942
5	0.6593	0.1585	0.1755	0.3339	0.0068	0.0000	0.3511	0.0881	0.4393	0.5607	62.5698	0.7602
6	0.5589	0.2952	0.1390	0.4342	0.0069	0.0000	0.4088	0.1368	0.5456	0.4544	52.7368	0.7958
7	0.5409	0.3407	0.1145	0.4552	0.0039	0.0000	0.4599	0.1221	0.5819	0.4181	84.0743	0.7822
8	0.4949	0.3143	0.1898	0.5041	0.0010	0.0000	0.5439	0.1951	0.7390	0.2610	174.4802	0.6821

Table 7.3: Composition of experimental tie-lines, selectivity (S) and distribution ratio for [EMIM][$EtSO_4$] (1) + Thiophene (2) +Pyridine (3) +Pentane(4) at 298.15K.

S.No	[EMIM][$EtSO_4$] rich phase					Pentane rich Phase					Selection parameter	
											S_{23}	β_{23}
1	0.9176	0.0346	0.0376	0.0722	0.0101	0.0000	0.0093	0.0184	0.0278	0.9722	249.3191	2.6002
2	0.8563	0.0674	0.0553	0.1227	0.0210	0.0000	0.0100	0.0314	0.0414	0.9586	135.6543	2.9664
3	0.8073	0.0878	0.0623	0.1501	0.0427	0.0000	0.1038	0.0329	0.1367	0.8633	22.2157	1.0980
4	0.7684	0.0945	0.0694	0.1639	0.0678	0.0000	0.1848	0.0419	0.2268	0.7732	8.2408	0.7225
5	0.7442	0.0975	0.0887	0.1863	0.0695	0.0000	0.2197	0.0566	0.2764	0.7236	7.0149	0.6740
6	0.7231	0.1060	0.0917	0.1977	0.0791	0.0000	0.3222	0.0590	0.3812	0.6188	4.0577	0.5188
7	0.6330	0.1087	0.1678	0.2766	0.0904	0.0000	0.4409	0.0753	0.5163	0.4837	2.8665	0.5357
8	0.4972	0.1642	0.1913	0.3555	0.1473	0.0000	0.4488	0.1437	0.5926	0.4074	1.6591	0.5999

Table 7.4: Composition of experimental tie-lines, selectivity (S) and distribution ratio for [EMIM][$MeSO_3$] (1) + Thiophene (2) +Pyridine (3) +Pentane (4) at 298.15K.

S.No	[EMIM][$MeSO_3$] rich phase					Pentane rich phase					Selection parameter	
											S_{23}	β_{23}
1	0.9389	0.0132	0.0474	0.0606	0.0005	0.0000	0.0205	0.0616	0.0821	0.9179	1352.0069	0.7372
2	0.8964	0.0084	0.0930	0.1014	0.0022	0.0000	0.1051	0.0306	0.1357	0.8643	296.2162	0.7472
3	0.8690	0.0016	0.1257	0.1273	0.0038	0.0000	0.1897	0.0328	0.2225	0.7775	117.7196	0.5719
4	0.7629	0.0563	0.1688	0.2251	0.0120	0.0000	0.2815	0.1497	0.4312	0.5688	12.2390	0.5292
5	0.6650	0.0678	0.2033	0.2710	0.0640	0.0000	0.3688	0.1650	0.5338	0.4662	5.6596	0.8406
6	0.5550	0.0898	0.2693	0.3590	0.0860	0.0000	0.4120	0.1830	0.5950	0.4050	5.5199	0.6280
7	0.3687	0.4135	0.0996	0.5131	0.1182	0.0000	0.5420	0.1350	0.677	0.323	3.5041	0.9274
8	0.2787	0.4899	0.1159	0.6057	0.1156	0.0000	0.5394	0.1896	0.729	0.271	2.5315	0.8984

Table 7.5: UNIQUAC structural parameters for the different compounds in the LLE system

Component	***r***	***q***
1-ethyl-3-methylimidazolium acetate	8.7500	5.5600
1-ethyl- 3-methylimidazolium ethyl sulphate	8.3927	6.6260
1-ethyl- 3-methylimidazolium methylsulphonate	8.14	6.08
Thiophene	2.8569	2.140
pyridine	2.9993	2.113
Pentane	3.8254	3.316
Isooctane	5.8478	4.932
Cyclohexane	4.0464	3.240
Toluene	3.9228	2.968

Table 7.6: NRTL and UNIQUAC interaction parameters for the [EMIM][CH_3COO] (1) + Thiophene (2) +Pyridine (3) +Pentane (4) systems at T = 298.15 K.

	NRTL Model Parameters				**UNIQUAC Model Parameters**			
	/K	/K	*	RMSD**	/K	/K	*	RMSD**
System: [EMIM][CH_3COO] (1) + Thiophene (2) +Pyridine (3) +Pentane (4)								
1-2	4901.2	4149.1	-3.4 × 10^{-3}	0.73%	197.55	994.31	-1.82 × 10^{-3}	1.69%
1-3	1468.6	-59.601			-632.88	-37.805		
1-4	4903.8	4129.8			232.31	669.61		
2-3	1852.5	1421.2			366.55	208.06		
2-4	1217.4	4567.5			-159.76	86.708		
3-4	2814.9	1612.8			961.13	-671.03		

* Calculated using equation 6.13; **Calculated using equation 4.24.

Table 7.7: NRTL and UNIQUAC interaction parameters for the [EMIM][$EtSO_4$] (1) + Thiophene (2) +Pyridine (3) +Pentane (4) systems at T = 298.15 K.

	NRTL Model Parameters				UNIQUAC Model Parameters			
	/K	/K	*	RMSD**	/K	/K	*	RMSD**
System: [EMIM][$EtSO_4$] (1) + Thiophene (2) +Pyridine (3) +Pentane (4)								
1-2	2695	1101	-6.7× 10^{-3}	1.02%	-35.853	335.64	-3.705 × 10^{-2}	2.10%
1-3	4477.7	-378.4			444.14	999.67		
1-4	5548.6	3743			139.34	631.97		
2-3	6681.9	6034.8			998.26	154.34		
2-4	5904	4367.6			457.36	-149.83		
3-4	3925	2641.5			373.74	451.28		

* Calculated using equation 6.13; **Calculated using equation 4.24.

Table 7.8: NRTL and UNIQUAC interaction parameters for the [EMIM][$MeSO_3$] (1) + Thiophene (2) +Pyridine (3) +Pentane (4) systems at T = 298.15 K

	NRTL Model Parameters				UNIQUAC Model Parameters			
	/K	/K	*	RMSD**	/K	/K	*	RMSD**
System: [EMIM][$MeSO_3$] (1) + Thiophene (2) +Pyridine (3) +Pentane (4)								
1-2	664.04	692.46	-14.25 × 10^{-3}	1.49%	2005.4	-18.062	-16.51 × 10^{-3}	1.69%
1-3	697.94	842.87			2600.8	49.031		
1-4	704.64	350			330.81	722.95		
2-3	507.05	1999.8			49.132	34.142		
2-4	716.49	418.34			567.31	1367.5		
3-4	309.01	967.29			645.45	777.07		

* Calculated using equation 6.13; **Calculated using equation 4.24.

Figure 7.4: LLE for the quaternary system [EMIM][OAc] (1) + Thiophene (2) +Pyridine (3) +Pentane(4) systems at T = 298.15 K. This is correlated with NRTL model.

Figure 7.5: LLE of the quaternary system [EMIM][$EtSO_4$] (1) + Thiophene (2) +Pyridine (3) +Isooctane (4) systems at T = 298.15 K. This is correlated with NRTL model.

Figure 7.6: LLE of the quaternary system [EMIM][$MeSO_3$] (1) + Thiophene (2) +Pyridine (3) +Pentane(4) systems at T = 298.15 K. Which is correlated with NRTL model.

Figure 7.7: Experimental tie-lines for the LLE of the quaternary system [EMIM][OAc] (1) + Thiophene (2) + Pyridine (3) +Pentane (4) systems at T = 298.15 K.Which is correlated with UNIQUAC model.

Figure 7.8: Experimental tie-lines for the LLE of the quaternary system [EMIM][$EtSO_4$] (1) + Thiophene (2) +Pyridine (3) +Isooctane (4) systems at T = 298.15 K. which is correlated with UNIQUAC model

Figure 7.9: Experimental tie-lines for the LLE of the quaternary system [EMIM][$MeSO_3$] (1) + Thiophene (2) +Pyridine (3) +Pentane (4) systems at T = 298.15 K. which is correlated with UNIQUAC model

7.3.3 LLE COSMO-RS predictions

The experimental LLE data were validated with the COSMO-RS prediction in the triangular diagram. The COSMO-RS predicted tie lines are somewhat agreeable for [EMIM][OAc] system(Figure 7.10),where the raffinate phase is correctly predicted. However there are deviations in the extract phase. For [EMIM][$EtSO_4$] (Figure 7.11) and [EMIM][$MeSO_3$] (Figure 7.12) based system, the tie lines are quantitatively matching with raffinate phase but considerable deviation is obtained in extract phase. This may be due to the several possible interactions between IL and thiophene/pyridine molecules in the mixture where the hydrogen bond interaction plays a major role. We did not intend to change the

COSMO-RS parameters in this study. The values of RMSD is 4.62% for [EMIM][OAc],5.3% for [EMIM][$EtSO_4$] and 6.07% for [EMIM][$MeSO_3$] based system. It is also observed that the predicted composition of IL in the raffinate phase is zero which provides a clear information that the IL does not make any contamination in the hydrocarbon stream.

Figure 7.10: Experimental tie lines for the LLE of the quaternary system [EMIM][OAc] (1) + Thiophene (2) +Pyridine (3) +Pentane (4) systems at T = 298.15 K.Which is correlated with COSMO-RS predictions.

Figure 7.11: Experimental tie-lines for the LLE of the quaternary system [EMIM][$EtSO_4$] (1) + Thiophene (2) +Pyridine (3) +Isooctane (4) systems at T = 298.15 K. which is correlated with COSMO-RS predictions.

Figure 7.12: Experimental tie-lines for the LLE of the quaternary system [EMIM][$MeSO_3$] (1) + Thiophene (2) +Pyridine (3) +Pentane(4) systems at T = 298.15 K. which is correlated with COSMO-RS predictions.

7.4.1 Experimental LLE of the quaternary system of [EMIM] based ILs (1) + Thiophene (2) +Pyridine (3) +Isooctane (4).

The quaternary LLE experimental data for: 1-ethyl 3-methylimidazolium acetate (1) + thiophene (2) + pyridine (3) + isooctane (4), 1-ethyl 3-methylimidazolium ethylsulphate (1) + thiophene (2) + pyridine (3) + isooctane (4) and 1-ethyl 3-methylimidazolium methylsulphonate (1) + thiophene (2) + pyridine (3) + isooctane (4) are reported in Tables 7.9 to 7.11, respectively. The values of selectivity (S) and solute distribution ratio (β) are also given. Equilateral triangular diagrams with graphical representations of the quaternary LLE are shown in Figure 7.13, 7.14 and 7.15 for [EMIM][CH_3COO], [EMIM][$ETSO_4$], and [EMIM][$MESO_3$] based system respectively. As can be seen, both pseudo-ternary systems correspond to the Type 2 category, with two of their constituent pairs exhibiting partial immiscibility and with one immiscible region. As the sulfur and nitrogen content in fuels is very low, the lowest part of the diagrams must be observed. Tie-line slopes in that region for the system with all the Ionic Liquids are parallel or negative. Thus large quantities of ILs would have to be used. However, the negligible vapor pressure of ionic liquid facilitates solvent recovery without losses. It can be seen from previous work that the sloping of the tie lines in the ternary plot for [EMIM][$EtSO_4$]-Thiophene-Isooctane is negative [Arce et al.,2007].However the counterpart ternary diagram i.e [EMIM][$EtSO_4$]-Thiophene-Hexane is positive[Gomez et al.,2010]. There is no literature data which contains the system [EMIM][$EtSO_4$]-Pyridine-Isooctane, so a comparison could not be made. Thus it can be confirmed that the selectivities and distribution coefficient in case of simultaneous removal is lesser as compared to its individual removal.

Figure 7.16(a) and 7.16(b) show the selectivity (S) and solute distribution ratio (β) as a function of mole fraction of thiophene and pyridine in isooctane rich phase at 298.15K.It is observed that the selectivity (S) decreases while solute distribution ratio (β) increases with

increasing mole fraction of thiophene and pyridine mixture in the iso-octane rich phase. This agrees well with the studies conducted on the separation of benzene from linear alkanes (C6 –C9) using ionic liquids by Gonzalez et al.[2010]. As compared to other ILs [EMIM][OAc] ionic liquid posses high selectivity at low concentration of thiophene and pyridine mixture. This is important since the diesel oil contains impurities close to ppm levels. Thus the selectivity values less than 0.1 are more important than at $x > 0.1$.However the change in selectivity and distribution ratio after 0.1 mole fraction is insignificant. This matches well with the obtained selectivity values of IL for the extraction of aromatic compounds [Garca et al., 2010; Arce et al., 2007; Gomez et al., 2010]. The distribution coefficient values (β) are lower than unity which indicates that the amount of ionic liquid required is high for the effective separation and thus implies high operating cost of the processes. It should be noted that thiophene and pyridine molecules interacts with the ionic liquid cation via CH--π and π---π interactions [Anantharaj et al., 2010, 2011a, 2011b]. As the thiophene and pyridine content increases, the distance between the thiophene and pyridine molecules with cation in IL becomes larger, and therefore the strength of interaction and consequently the solvent characterization parameters are reduced. The S and β values for three ionic liquid are almost close to each other for mole fraction less than 0.1. This indicates that the anion influence on the simultaneous separation is higher as compared to imidazolium ring of cation. The selected anions such as CH_3COO,$C_2H_5SO_4$ and CH_3SO_3 posses an electronegative atom in their molecular structure, thus it can easily interact with the hydrogen atom of thiophene and pyridine molecules. For example, the oxygen atom of acetate anion simultaneously interacts with hydrogen atom present in thiophene and pyridine molecules.

Table 7.9: Composition of experimental tie-lines, selectivity (S) and distribution ratio for [EMIM][CH_3COO] (1) + Thiophene (2) +Pyridine (3) +Isooctane (4) at 298.15K.

S.No	[EMIM][CH_3COO] rich phase					Isooctane rich phase					Selection parameter	
											S	β
1	0.8229	0.0314	0.0105	0.0419	0.1353	0.0000	0.0045	0.0091	0.0136	0.9864	22.3905	3.0704
2	0.7535	0.0562	0.0330	0.0892	0.1573	0.0000	0.0989	0.0123	0.1113	0.8887	4.5292	0.8015
3	0.6887	0.0813	0.0559	0.1372	0.1741	0.0000	0.1344	0.0206	0.1550	0.8450	4.2973	0.8855
4	0.6527	0.1015	0.0697	0.1713	0.1760	0.0000	0.1904	0.0450	0.2354	0.7646	3.1600	0.7274
5	0.5953	0.1504	0.0778	0.2282	0.1765	0.0000	0.1973	0.1571	0.3544	0.6456	2.3552	0.6439
6	0.4340	0.2742	0.1026	0.3768	0.1892	0.0000	0.2619	0.1875	0.4494	0.5506	2.4403	0.8385
7	0.3521	0.3250	0.1321	0.4572	0.1908	0.0000	0.2687	0.2624	0.5311	0.4689	2.1156	0.8607
8	0.3158	0.3288	0.1621	0.4910	0.1932	0.0000	0.2771	0.3394	0.6165	0.3835	1.5808	0.7964

Table 7.10: Composition of experimental tie-lines, selectivity (S) and distribution ratio for [EMIM][$EtSO_4$] (1) + Thiophene (2) +Pyridine (3) +Isooctane (4) at 298.15K.

S.No	[EMIM][$EtSO_4$] rich phase					Iso-octane rich phase					Ionic liquid rich phase	
											S	β
1	0.9038	0.0088	0.0183	0.0271	0.0691	0.0000	0.0140	0.1037	0.1177	0.8823	2.9378	0.2300
2	0.8060	0.0910	0.0227	0.1138	0.0802	0.0000	0.1090	0.0902	0.1993	0.8007	5.7019	0.5710
3	0.7423	0.1235	0.0459	0.1694	0.0883	0.0000	0.1545	0.1112	0.2657	0.7343	5.3046	0.6376
4	0.6971	0.1255	0.0766	0.2021	0.1008	0.0000	0.1850	0.1382	0.3232	0.6768	4.1978	0.6253
5	0.5675	0.1810	0.1451	0.3260	0.1065	0.0000	0.2838	0.1458	0.4296	0.5704	4.0653	0.7590
6	0.4772	0.2210	0.1890	0.4100	0.1128	0.0000	0.3707	0.1528	0.5235	0.4765	3.3094	0.7833
7	0.4004	0.2810	0.1994	0.4804	0.1192	0.0000	0.4368	0.1645	0.6013	0.3987	2.6728	0.7990
8	0.3522	0.3105	0.2057	0.5162	0.1316	0.0000	0.4632	0.1982	0.6614	0.3386	2.9378	0.2300

Table 7.11: Composition of experimental tie-lines, selectivity (S) and distribution ratio for [EMIM][$MeSO_3$] (1) + Thiophene (2) +Pyridine (3) +Isooctane (4) at 298.15K.

S.No	[EMIM][$MeSO_3$] rich phase					Iso-octane rich phase					Ionic liquid rich phase	
											S	β
1	0.8604	0.0265	0.0397	0.0663	0.0733	0.0000	0.1331	0.0386	0.1717	0.8283	4.3610	0.3860
2	0.7236	0.0455	0.1084	0.1540	0.1224	0.0000	0.1866	0.0707	0.2574	0.7426	3.6298	0.5983
3	0.6987	0.0503	0.1243	0.1747	0.1267	0.0000	0.2168	0.1155	0.3323	0.6677	2.7702	0.5256
4	0.5726	0.0813	0.1981	0.2793	0.1481	0.0000	0.2617	0.1205	0.3822	0.6178	3.0483	0.7308
5	0.4522	0.1715	0.2224	0.3939	0.1539	0.0000	0.3546	0.1441	0.4987	0.5013	2.5730	0.7899
6	0.3916	0.2009	0.2405	0.4414	0.1670	0.0000	0.4360	0.1635	0.5995	0.4005	1.7658	0.7363
7	0.2991	0.2457	0.2877	0.5335	0.1674	0.0000	0.6101	0.0981	0.7082	0.2918	1.3134	0.7533
8	0.2187	0.2596	0.3507	0.6103	0.1710	0.0000	0.6108	0.1462	0.7570	0.2430	1.1453	0.8062

Figure 7.13: Experimental tie lines for the LLE of the quaternary system [EMIM][OAc] (1) + Thiophene (2) +Pyridine (3) +Isooctane (4) systems at T = 298.15 K.The corresponding tie-lines correlated with NRTL (α=0.2).

Figure 7.14: Experimental tie-lines for the LLE of the quaternary system [EMIM][$EtSO_4$] (1) + Thiophene (2) +Pyridine (3) +Isooctane (4) systems at T = 298.15 K. which is correlated with NRTL model (α=0.2).

Figure 7.15: Experimental tie-lines for the LLE of the quaternary system [EMIM][$MeSO_3$] (1) + Thiophene (2) +Pyridine (3) +Isooctane (4) systems at T = 298.15 K. which is correlated with NRTL model (α=0.2)

7.4.2 NRTL and UNIQUAC Correlations

The NRTL and UNQUAC model was used to correlate the experimental tie-line data for the quaternary system. We have demonstrated that the NRTL and UNQUAC model have adequate capability in correlating the LLE data for systems containing ILs [Varma et al., 2011]. We used $\alpha_{ij}= \alpha_{ji}=0.2$ as a non-randomness factor for immiscible binaries in NRTL model. NRTL predicted tie lines are plotted in Figure 7.13 to 7.15 with respect to [EMIM][OAc],[EMIM][$EtSO_4$] and [EMIM][$MeSO_3$] based system, respectively. Similarly the UNIQUAC predicted tie lines for [EMIM][OAc] [EMIM][$EtSO_4$] and [EMIM][$MeSO_3$] based systems are illustrated in Figure 7.17 to 7.19,respectively. The deviation between the experimental and predicted tie lines can be calculated by the RMSD (Root Mean Square Deviation).The RMSD values were lesser than unity for all the cases (Table 7.12 to7.14) which indicates that a fairly good prediction is obtained with a good degree of accuracy.

Figure 7.16(a): Selectivity for the quaternary systems {[EMIM][OAc]+thiophene+pyridine +isooctnae},{[EMIM][$EtSO_4$]+thiophene+ pyridine +isooctane}and {[EMIM][$MeSO_3$]+ thiophene + pyridine +isooctane } at 298.15K,as function of mole fraction of solute in isooctane-rich phase.

The binary interaction parameters are estimated from experimental LLE data of quaternary systems via NRTL and UNIIQUAC model and these values are reported in Table 7.12 to 7.14. In UNIQUAC model, the fraction of volume *r* and surface area *q* parameter for 1-ethyl-3-methylimidazolium acetate, 1-ethyl-3-methylimidazolium ethylsulphate, 1-ethyl-3-methylimidazolium methylsulphonate, thiophene, pyridine and isooctane are reported in Table 7.5. The results of binary interaction parameters along with objective

function and RMSD values for the quaternary systems are given in Table 7.12 to 7.14. The objective function (Equation 6.13) is used to minimize the difference between the experimental and the calculated mole fraction of the components in both the phases and these values are presented in Table 7.12 to 7.14. Based on our earlier work [Xie et al.,2008], we have chosen the population size and maximum number of generation as 100 and 200 respectively. The interaction parameters are essential for the design and simulation of extraction columns for any systems. They are used in process simulations such as ASPEN^R and HYSIS^R.

Figure 7.16(b): Distribution coefficient for the quaternary systems {[EMIM][OAc]+thiophene+pyridine +isooctane},{[EMIM][$EtSO_4$]+thiophene+

pyridine +isooctane}and {[EMIM][$MeSO_3$]+ thiophene + pyridine +isooctane } at 298.15K,as function of mole fraction of solute in isooctane-rich phase.

Table 7.12: NRTL and UNIQUAC interaction parameters for the [EMIM][CH_3COO] (1) + Thiophene (2) +Pyridine (3) +Isooctane (4) systems at T = 298.15 K

	NRTL Model Parameters				**UNIQUAC Model Parameters**			
	/K	/K	*	RMSD**	/K	/K	*	RMSD**
System: [EMIM][CH_3COO] (1) + Thiophene (2) +Pyridine (3) +Isooctane (4)								
1-2	5089.4	318.78	-5.5×10^{-3}	0.92%	512.13	38.013	-6.57×10^{-3}	1.01%
1-3	5425.3	3820.5			1517.9	2977.9		
1-4	4890.2	7496.1			-84.712	403.62		
2-3	7065.6	2836.7			1042.8	362.93		
2-4	819.27	4511.6			2903.6	510.95		
3-4	7499.9	1646			1647.8	671.69		

* Calculated using equation 6.13; **Calculated using equation 4.24.

Table 7.13: NRTL and UNIQUAC interaction parameters for the [EMIM][$EtSO_4$] (1) + Thiophene (2) +Pyridine (3) +Isooctane (4) systems at T = 298.15 K

	NRTL Model Parameters				**UNIQUAC Model Parameters**			
	/K	/K	*	RMSD**	/K	/K	*	RMSD**

System: [EMIM][$EtSO_4$] (1) + Thiophene (2) +Pyridine (3) +Isooctane (4)								
1-2	4972.4	98.336	-5.3 × 10^{-3}	0.91%	745.38	-100.37	-9.1 × 10^{-3}	1.20%
1-3	6430	3518.1			852.91	8.5635		
1-4	521.31	-594.86			74.963	618.81		
2-3	5215.4	3420.9			282.15	160.73		
2-4	7585	4066.3			179.03	616		
3-4	7396.1	2766.8			849.39	68.479		

* Calculated using equation 6.13; **Calculated using equation 4.24

Table 7.14: NRTL and UNIQUAC interaction parameters for the [EMIM][$MeSO_3$] (1) + Thiophene (2) +Pyridine (3) +Isooctane (4) systems at T = 298.15 K

	NRTL Model Parameters				UNIQUAC Model Parameters			
	/K	/K	*	RMSD**	/K	/K	*	RMSD**
System: [EMIM][$MeSO_3$] (1) + Thiophene (2) +Pyridine (3) +Isooctane (4)								
1-2	6325.3	118.03	-3.6 × 10^{-3}	0.0074	372.61	257.84	-13.74 × 10^{-3}	0.014652
1-3	532.65	4103.8			1008.3	-153.37		
1-4	1030.7	3256.2			11.529	1156.1		
2-3	2366	6910			563.13	161.25		
2-4	4586	357.07			1491.1	148.44		
3-4	751.58	216.61			628.15	664.54		

* Calculated using equation 6.13; **Calculated using equation 4.24.

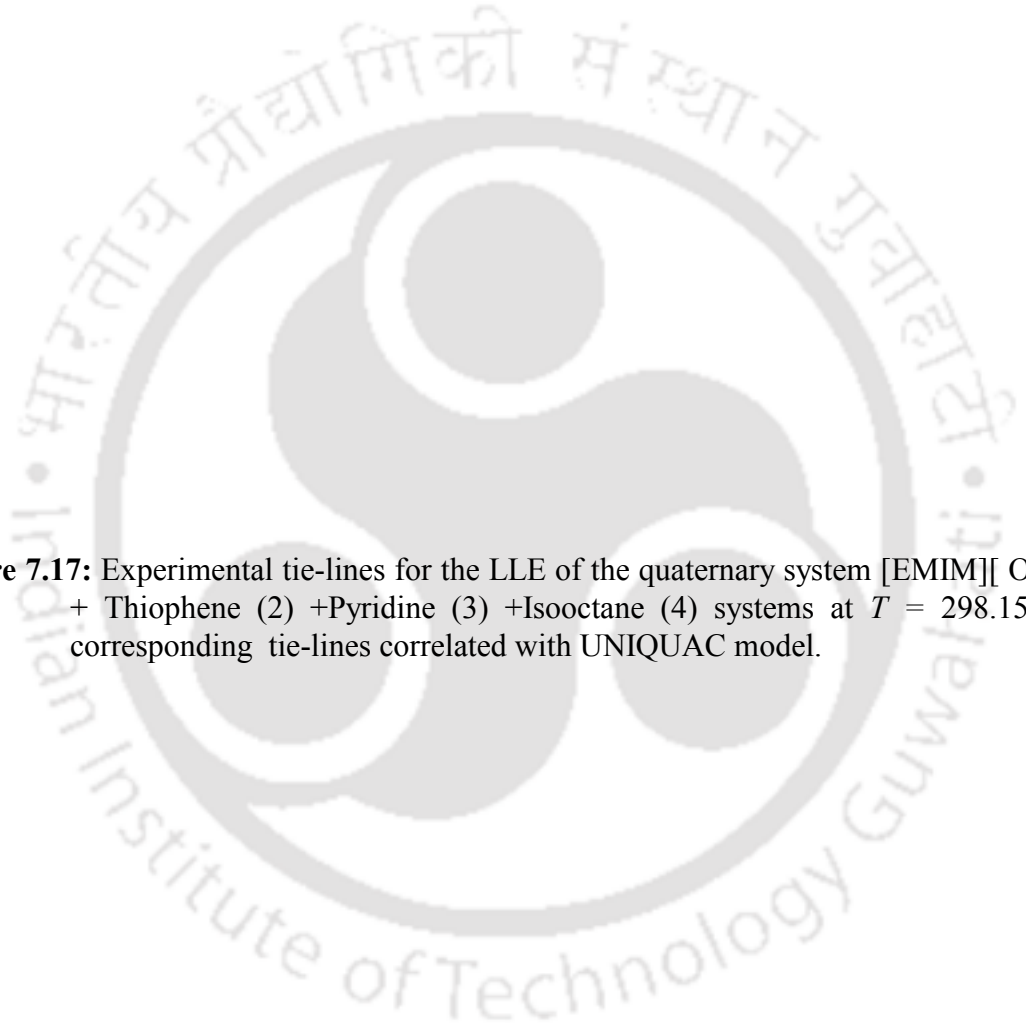

Figure 7.17: Experimental tie-lines for the LLE of the quaternary system [EMIM][OAc] (1) + Thiophene (2) +Pyridine (3) +Isooctane (4) systems at T = 298.15 K.The corresponding tie-lines correlated with UNIQUAC model.

Figure 7.18: Experimental tie-lines for the LLE of the quaternary system [EMIM][$EtSO_4$] (1) + Thiophene (2) +Pyridine (3) +Isooctane (4) systems at T = 298.15 K. which is correlated with UNIQUAC model

Figure 7.19: Experimental tie-lines for the LLE of the quaternary system [EMIM][$MeSO_3$] (1) + Thiophene (2) +Pyridine (3) +Isooctane (4) systems at T = 298.15 K. which is correlated with UNIQUAC model

7.4.3 LLE COSMO-RS predictions

The reliability of the experimentally measured LLE data for the three quaternary systems are validated with the COSMO-RS prediction, which is shown in Figure 7.20, 7.21 and 7.22 for [EMIM][OAc],[EMIM][$EtSO_4$] and [EMIM][$MeSO_3$] based system respectively. The plots provide a clear visualization of the change in the slope of the tie-line as a result of the change in the anion structure with imidazolium ring of cation in ionic liquid. The negative slope is quite visible at low concentration of thiophene and pyridine in feed mixture. However the COSMO-RS fails to reproduce the correct extract phase composition for all the ILs.However an important aspect which the COSMO-RS and experiments indicate is that the composition of IL in raffinate phase is zero (Table 7.12, 7.13, 7.14).It implies that there will be no contamination of IL in raffinate phase. The goodness of the fit was measured

by the root mean square deviation (RMSD) which provide the RMSD as 7.4% ([EMIM][OAc]),4.49% ([EMIM][$EtSO_4$]) and 8.26% ([EMIM][$MeSO_3$]).This RMSD values indicates that the high degree of consistency of the experimental LLE data are obtained for the studied systems at 298.15K. The COSMO-RS predictions are fairly good considering it to be a-priori in nature. It should also be noted that no change of COSMO-RS parameters [Banerjee et al., 2006] were made for the quaternary system. However it is competitive that NRTL and UNIQUAC model reproduce the model more efficiently.

Figure 7.20: Experimental tie lines for the LLE of the quaternary system [EMIM][OAc] (1) + Thiophene (2) +Pyridine (3) +Isooctane (4) systems at T = 298.15 K.The corresponding tie-lines correlated with COSMO-RS predictions

Figure 7.21: Experimental tie-lines for the LLE of the quaternary system [EMIM][$EtSO_4$] (1) + Thiophene (2) +Pyridine (3) +Isooctane (4) systems at T = 298.15 K. which is correlated with COSMO-RS predictions

Figure 7.22: Experimental tie-lines for the LLE of the quaternary system [EMIM][$MeSO_3$] (1) + Thiophene (2) +Pyridine (3) +Isooctane (4) systems at T = 298.15 K. which is correlated with COSMO-RS predictions.

7.5.1 Experimental LLE of the quaternary system of [EMIM] based ILs (1) + Thiophene (2) +Pyridine (3) +Cyclohexane (4).

The composition of experimental liquid-liquid equilibrium data (tie-lines) for [EMIM][OAc] (1) + Thiophene (2) +Pyridine (3) +Cyclohexane (4), [EMIM][$EtSO_4$] (1) + Thiophene (2) +Pyridine (3) + Cyclohexane (4) and [EMIM][$MeSO_3$] (1) + Thiophene (2) +Pyridine (3) +Cyclohexane (4) at 298.15K are shown in Table 7.15 to 7.17.Values of selectivity and distribution coefficient are also shown in those tables. The selectivity (S) and distribution coefficient (β) are shown in Figure 7.23 (a) and Figure 7.23(b).The selectivity decreases with increase in mole fraction of thiophene and pyridine in cyclohexane rich phase at 298.15K.It can be explained by the reduction of hydrogen bond strength between the IL and thiophene/pyridine molecules. The sulphur (S) atom in thiophene molecule interacts with

hydrogen atom of anion (acetate, ethylsulphate and methylsulphonate) whereas the hydrogen atom of cation in ILs interacts with nitrogen (N) atom in pyridine molecules. Anions possessing more number of electronegative atoms are favorable since it leads to interaction between the anion and thiophene/pyridine. Thus the lone pair of electron effect in thiophene and pyridine is very less as compared to its aromaticity. So thiophene is basic while pyridine is acidic. Due to this selectivity of [EMIM][OAc],[EMIM][$EtSO_4$] and [EMIM][$MeSO_3$] ionic liquids decreases with increasing mole fraction of thiophene and pyridine in cyclohexane rich phase. However the selectivity values are higher than unity for all the systems which indicates that the Ionic Liquid can be a choice for simultaneous separation processes at 298.15K.

Figure 7.23(a): Selectivity for the quaternary systems {[EMIM][OAc]+thiophene+pyridine +cyclohexane},{[EMIM][$EtSO_4$]+thiophene+ pyridine +cyclohexane}and

{[EMIM][$MeSO_3$]+ thiophene + pyridine +cyclohexane } at 298.15K,as function of mole fraction of solute in cyclohexane-rich phase.

The distribution coefficient values should also be considered, since the distribution coefficient is lower than unity. This is due to the higher strength of sterical hindrance coupled with weak hydrogen bond between IL and thiophene/pyridine. The distribution coefficient also strongly depends on the structural orientation through CH--π interaction and π--π stacking. Both the effects are weak, therefore the values of distribution coefficient are lower than unity with increasing mole fraction of thiophene and pyridine in cyclohexane rich phase.

Figure 7.23(b): Distribution coefficient for the quaternary systems {[EMIM][OAc] + thiophene + pyridine + cyclohexane},{[EMIM][$EtSO_4$] + thiophene + pyridine +

cyclohexane} and {[EMIM][$MeSO_3$] + thiophene + pyridine +cyclohexane } at 298.15K,as function of mole fraction of solute in cyclohexane-rich phase.

The triangular diagrams for all studied systems are presented in Figure 7.24 to 7.26.From these figures; it can be observed that, thiophene and pyridine are partially soluble in [EMIM][OAc],[EMIM][$EtSO_4$] and [EMIM][$MeSO_3$] at 298.15K.In all triangular diagrams, the size and shape of the immiscibility region and the tie line length is significantly large. This indicates that there is a significant interaction between the similar size and shape of the molecules. Further the thiophene/pyridine molecules and cations in ILs interact through CH-π interaction and π--π stacking. From the ternary plots, two different tie line slopes are visible: a positive slope in the lower part, while a negative slope in the upper part. Positive slope indicates that the ionic liquids has desirable feature for an extracting solvent whereas the negative slope implies that more quantity of ILs is required for the separation at ambient conditions. The negative slope indicates that the interaction between the thiophene/pyridine and ILs strongly depends on the composition of thiophene/pyridine in the feed mixture. The practical application of simultaneous desulphurization and denitrification of diesel oil correspond to low concentration of sulphur- and nitrogen containing compounds, therefore the lowest part (positive slope) of the diagram is important for further development of such a process.

7.5.2 NRTL and UNIQUAC correlations

The correlation of the experimental data was done with the NRTL and UNIQUAC model equations. The value of the non-randomness parameter was fixed to a 0.2 whereas the UNIQUAC structural parameters are reported in Table 7.5. The calculated tie lines from the correlation based on the NRTL and UNIQUAC models are presented in Figure 7.24 to 7.29 together with the experimental tie line data. The values of the root mean square deviation for

all the studied systems are lower than unity which indicates a good degree of accuracy in the values. The NRTL and UNIQUAC binary interaction parameters of the quaternary systems are listed in Table 7.15 to 7.17.

Table 7.15: Composition of experimental tie-lines, selectivity (S) and distribution ratio for [EMIM][OAc] (1) + Thiophene (2) +Pyridine (3) +Cyclohexane (4) at 298.15K.

S.No	[EMIM][OAc] rich phase					Cyclohexane rich phase					Selection parameter	
											S	β
1	0.9017	0.0025	0.0791	0.0816	0.0167	0.0000	0.0470	0.0788	0.1259	0.8741	33.9753	0.6486
2	0.7511	0.1007	0.1160	0.2167	0.0322	0.0000	0.1859	0.0839	0.2698	0.7302	18.1854	0.8031
3	0.6843	0.1475	0.1277	0.2752	0.0405	0.0000	0.2608	0.0919	0.3527	0.6473	12.4623	0.7803
4	0.6249	0.2295	0.0835	0.3130	0.0620	0.0000	0.4504	0.0351	0.4854	0.5146	5.3482	0.6448
5	0.4675	0.3937	0.0693	0.4631	0.0695	0.0000	0.7068	0.0160	0.7228	0.2772	2.5560	0.6406
6	0.4078	0.4277	0.0875	0.5152	0.0770	0.0000	0.7829	0.0159	0.7988	0.2012	1.6847	0.6449
7	0.3418	0.4854	0.0970	0.5824	0.0758	0.0000	0.8698	0.0235	0.8933	0.1067	0.9182	0.6520
8	0.3138	0.5447	0.1149	0.6595	0.0267	0.0000	0.9173	0.0241	0.9414	0.0586	1.5367	0.7006

Table 7.16: Composition of experimental tie-lines, selectivity (S) and distribution ratio for [EMIM][$EtSO_4$] (1) + Thiophene (2) +Pyridine (3) + Cyclohexane (4) at 298.15K.

S.No	[EMIM][$EtSO_4$] rich phase					Cyclohexane rich phase					Selection parameter	
											S	β
1	0.9197	0.0196	0.0354	0.0550	0.0253	0.0000	0.0547	0.0267	0.0815	0.9185	24.4809	0.6750
2	0.8483	0.0030	0.0818	0.0848	0.0669	0.0000	0.1102	0.0601	0.1703	0.8297	6.1731	0.4978
3	0.7374	0.0421	0.0968	0.1390	0.1236	0.0000	0.1244	0.2017	0.3261	0.6739	2.3235	0.4262
4	0.6024	0.0688	0.1731	0.2420	0.1556	0.0000	0.1261	0.2606	0.3868	0.6132	2.4650	0.6256
5	0.5498	0.1053	0.1813	0.2866	0.1637	0.0000	0.1709	0.3033	0.4742	0.5258	1.9411	0.6043
6	0.4008	0.1669	0.2369	0.4038	0.1954	0.0000	0.2180	0.3090	0.5270	0.4730	1.8541	0.7661
7	0.3459	0.2001	0.2499	0.4500	0.2041	0.0000	0.3032	0.2916	0.5948	0.4052	1.5023	0.7566
8	0.2713	0.2637	0.2608	0.5245	0.2042	0.0000	0.3511	0.3720	0.7232	0.2768	0.9835	0.7253

Table 7.17: Composition of experimental tie-lines, selectivity (S) and distribution ratio for [EMIM][$MeSO_3$] (1) + Thiophene (2) +Pyridine (3) +Cyclohexane (4) at 298.15K.

S.No	[EMIM][$MeSO_3$] rich phase					Cyclohexane rich phase					Selection parameter	
											S	β
1	0.8844	0.0220	0.0329	0.0549	0.0607	0.0000	0.0761	0.0220	0.0981	0.9019	8.3088	0.5594
2	0.7162	0.0563	0.0760	0.1323	0.1514	0.0000	0.1357	0.0497	0.1855	0.8145	3.8385	0.7135
3	0.6626	0.0810	0.0915	0.1726	0.1649	0.0000	0.1525	0.0812	0.2338	0.7662	3.4305	0.7381
4	0.6396	0.0908	0.1041	0.1949	0.1655	0.0000	0.1946	0.1314	0.3260	0.6740	2.4352	0.5979
5	0.5380	0.1807	0.1115	0.2922	0.1698	0.0000	0.2722	0.1475	0.4197	0.5803	2.3787	0.6962
6	0.4526	0.1950	0.1724	0.3674	0.1800	0.0000	0.3409	0.1780	0.5189	0.4811	1.8932	0.7081
7	0.3896	0.2273	0.1893	0.4166	0.1938	0.0000	0.3521	0.2317	0.5838	0.4162	1.5325	0.7136
8	0.3120	0.2487	0.2294	0.4782	0.2098	0.0000	0.4049	0.2738	0.6787	0.3213	1.5325	0.7136

Table 7.18: NRTL and UNIQUAC interaction parameters for the [EMIM][CH_3COO] (1) + Thiophene (2) +Pyridine (3) +Cyclohexane (4) systems at T = 298.15 K

	NRTL Model Parameters				UNIQUAC Model Parameters			
	/K	/K	*	RMSD**	/K	/K	*	RMSD**
System: [EMIM][CH_3COO] (1) + Thiophene (2) +Pyridine (3) +Cyclohexane (4)								
1-2	5874.3	599.28	-6.8×10^{-3}	1.03%	1183.9	1033.7	-18.3×10^{-3}	1.69%
1-3	6663.3	3830.5			470.43	153.24		
1-4	5322.1	4316.71			87.808	633.04		
2-3	642.67	2813.8			51.488	159.17		
2-4	4922.9	2923			800.85	476.24		
3-4	7713	6267.3			840.99	566.22		

* Calculated using equation 6.13; **Calculated using equation 4.24.

Table 7.19: NRTL and UNIQUAC interaction parameters for the [EMIM][$EtSO_4$] (1) + Thiophene (2) +Pyridine (3) +Cyclohexane (4) systems at T = 298.15 K

	NRTL Model Parameters				UNIQUAC Model Parameters			
	/K	/K	*	RMSD**	/K	/K	*	RMSD**
System: [EMIM][$EtSO_4$] (1) + Thiophene (2) +Pyridine (3) +Cyclohexane (4)								
1-2	8538.5	725.48	-10.07×10^{-3}	1.25%	1146.6	1175.3	-23.25×10^{-3}	1.9%
1-3	7499	10500			-49.993	1830.2		
1-4	5041.6	3411.2			276.07	305.57		
2-3	787.8	3880.7			-13.264	-1.4705		
2-4	260.79	560.63			101.93	576.9		
3-4	10499	6429.7			1845	-15.227		

* Calculated using equation 6.13; **Calculated using equation 4.24.

Table 7.20: NRTL and UNIQUAC interaction parameters for the [EMIM][$MeSO_3$] (1) + Thiophene (2) +Pyridine (3) +Cyclohexane(4) systems at T = 298.15 K

	NRTL Model Parameters				UNIQUAC Model Parameters			
	/K	/K	*	RMSD**	/K	/K	*	RMSD**
System: [EMIM][$MeSO_3$] (1) + Thiophene (2) +Pyridine (3) +Cyclohexane (4)								
1-2	1844.7	429.87	-7.65 × 10^{-3}	1.03%	1127.1	-172.24	-39.15 × 10^{-3}	2.47%
1-3	3207.4	7133.4			559.28	-229.46		
1-4	930.84	3332.2			208.44	1588.2		
2-3	5746.3	8736.8			-9.6083	119.47		
2-4	3940.2	1722			-738.88	372.72		
3-4	2468.4	1759.6			208.22	-693.93		

* Calculated using equation 6.13; **Calculated using equation 4.24.

Figure 7.24: Experimental tie lines for the LLE of the quaternary system [EMIM][OAc] (1) + Thiophene (2) +Pyridine (3) +Cyclohexane (4) systems at T = 298.15 K.The corresponding tie-lines correlated with NRTL (α=0.2).

Figure 7.25: Experimental tie-lines for the LLE of the quaternary system [EMIM][$EtSO_4$] (1) + Thiophene (2) +Pyridine (3) + Cyclohexane(4) systems at T = 298.15 K. which is correlated with NRTL model (α=0.2).

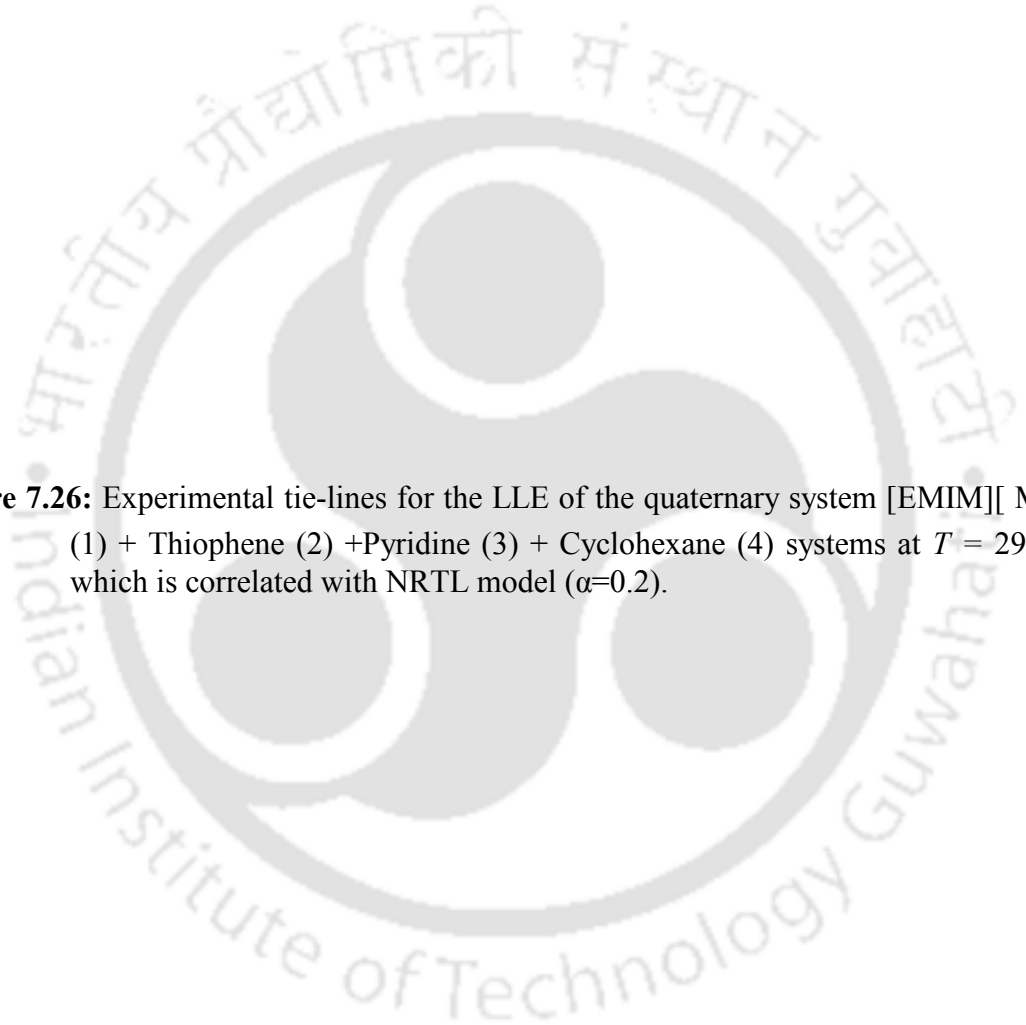

Figure 7.26: Experimental tie-lines for the LLE of the quaternary system [EMIM][$MeSO_3$] (1) + Thiophene (2) +Pyridine (3) + Cyclohexane (4) systems at T = 298.15 K. which is correlated with NRTL model (α=0.2).

Figure 7.27: Experimental tie-lines for the LLE of the quaternary system [EMIM][OAc] (1) + Thiophene (2) +Pyridine (3) + Cyclohexane (4) systems at T = 298.15 K.The corresponding tie-lines correlated with UNIQUAC model.

Figure 7.28: Experimental tie-lines for the LLE of the quaternary system [EMIM][$EtSO_4$] (1) + Thiophene (2) +Pyridine (3) + Cyclohexane (4) systems at T = 298.15 K. which is correlated with UNIQUAC model.

Figure 7.29: Experimental tie-lines for the LLE of the quaternary system [EMIM][$MeSO_3$] (1) + Thiophene (2) +Pyridine (3) + Cyclohexane (4) systems at T = 298.15 K. which is correlated with UNIQUAC model

7.5.3 LLE COSMO-RS predictions

The reliability of the experimentally measured LLE data for the three quaternary systems are validated with the COSMO-RS prediction, which is shown in Figure 7.30 and 7.32 for [EMIM][OAc],[EMIM][$EtSO_4$] and [EMIM][$MeSO_3$] respectively. The plots provide a clear visualization of the change in the slope of the tie-line as a result of the change in the anion structure with imidazolium ring of cation in ionic liquid. The negative slope is quite visible at low concentration of thiophene and pyridine in feed mixture. However the COSMO-RS fails to reproduce the correct extract phase composition for all the ILs. However an important aspect which the COSMO-RS and experiments indicate is that the composition of IL in raffinate phase is zero (Table 7.15, 7.16, 7.17).It implies that there will be no

contamination of IL in raffinate phase. The goodness of the fit was measured by the root mean square deviation (RMSD) which provide the RMSD of 7.8% ([EMIM][OAc]) ,5.93% ([EMIM][$EtSO_4$]) and 5.3% ([EMIM][$MeSO_3$]) based system. This RMSD values indicates that a high degree of consistency of the experimental LLE data are obtained for the studied systems at 298.15K. The COSMO-RS predictions are fairly good considering it to be a-priori in nature. It should also be noted that no change of COSMO-RS parameters were made for the quaternary system. However it is competitive that NRTL and UNIQUAC model reproduce the data more efficiently.

Figure 7.30: Experimental tie lines for the LLE of the quaternary system [EMIM][OAc] (1) + Thiophene (2) +Pyridine (3) + Cyclohexane (4) systems at T = 298.15 K.The corresponding tie-lines correlated with COSMO-RS predictions.

Figure 7.31: Experimental tie-lines for the LLE of the quaternary system [EMIM][$EtSO_4$] (1) + Thiophene (2) +Pyridine (3) +Cyclohexane (4) systems at T = 298.15 K. which is correlated with COSMO-RS predictions

Figure 7.32: Experimental tie-lines for the LLE of the quaternary system [EMIM][$EtSO_4$] (1) + Thiophene (2) +Pyridine (3) + Cyclohexane(4) systems at T = 298.15 K. which is correlated with COSMO-RS predictions.

Figure 7.33(a): Selectivity for the quaternary systems {[EMIM][OAc]+thiophene+pyridine +toluene},{[EMIM][$EtSO_4$]+thiophene+ pyridine +toluene}and {[EMIM][$MeSO_3$]+ thiophene + pyridine +toluene} at 298.15K,as function of mole fraction of solute in toluene-rich phase.

Figure 7.33(b): Distribution coefficient for the quaternary systems {[EMIM][OAc]+thiophene+pyridine +toluene},{[EMIM][$EtSO_4$]+thiophene+ pyridine +toluene}and {[EMIM][$MeSO_3$]+ thiophene + pyridine +toluene} at 298.15K,as function of mole fraction of solute in toluene-rich phase.

Table 7.21: Composition of experimental tie-lines, selectivity (S) and distribution ratio for [EMIM][OAc] (1) + Thiophene (2) +Pyridine (3) +Toluene (4) at 298.15K.

S.No	[EMIM][OAc] rich phase					Toluene rich phase					Selection parameter	
											S	β
1	0.9017	0.0025	0.0791	0.0816	0.0167	0.0000	0.0470	0.0788	0.1259	0.8741	33.9753	0.6486
2	0.7511	0.1007	0.1160	0.2167	0.0322	0.0000	0.1859	0.0839	0.2698	0.7302	18.1854	0.8031
3	0.6843	0.1475	0.1277	0.2752	0.0405	0.0000	0.2608	0.0919	0.3527	0.6473	12.4623	0.7803
4	0.6249	0.2295	0.0835	0.3130	0.0620	0.0000	0.4504	0.0351	0.4854	0.5146	5.3482	0.6448
5	0.4675	0.3937	0.0693	0.4631	0.0695	0.0000	0.7068	0.0160	0.7228	0.2772	2.5560	0.6406
6	0.4078	0.4277	0.0875	0.5152	0.0770	0.0000	0.7829	0.0159	0.7988	0.2012	1.6847	0.6449
7	0.3418	0.4854	0.0970	0.5824	0.0758	0.0000	0.8698	0.0235	0.8933	0.1067	0.9182	0.6520
8	0.3138	0.5447	0.1149	0.6595	0.0267	0.0000	0.9173	0.0241	0.9414	0.0586	1.5367	0.7006

Table 7.22: Composition of experimental tie-lines, selectivity (S) and distribution ratio for [EMIM][$EtSO_4$] (1) + Thiophene (2) +Pyridine (3) + Toluene (4) at 298.15K.

S.No	[EMIM][$EtSO_4$] rich phase					Toluene rich phase					Selection parameter	
											S	β
1	0.8583	0.0697	0.0066	0.0763	0.0654	0.0000	0.0288	0.0220	0.0508	0.9492	21.7861	1.5013
2	0.7527	0.1420	0.0064	0.1484	0.0988	0.0000	0.0998	0.0326	0.1324	0.8676	9.8428	1.1212
3	0.6981	0.1729	0.0110	0.1839	0.1180	0.0000	0.1631	0.0461	0.2092	0.7908	5.8922	0.8790
4	0.6676	0.1898	0.0225	0.2123	0.1200	0.0000	0.2474	0.0584	0.3059	0.6941	4.0142	0.6942
5	0.5582	0.2439	0.0565	0.3004	0.1414	0.0000	0.3079	0.0714	0.3793	0.6207	3.4763	0.7920
6	0.5019	0.2892	0.0641	0.3533	0.1447	0.0000	0.3640	0.0759	0.4398	0.5602	3.1093	0.8033
7	0.4477	0.3270	0.0776	0.4046	0.1477	0.0000	0.4175	0.1192	0.5367	0.4633	2.3636	0.7538
8	0.2869	0.4560	0.0780	0.5340	0.1791	0.0000	0.5141	0.1240	0.6381	0.3619	1.6916	0.8369

Table 7.23: Composition of experimental tie-lines, selectivity (S) and distribution ratio for [EMIM][$MeSO_3$] (1) + Thiophene (2) +Pyridine (3) +Toluene (4) at 298.15K.

S.No	[EMIM][$MeSO_3$] rich phase					Toluene rich phase					Selection parameter	
											S	β
1	0.9145	0.0375	0.0235	0.0610	0.0245	0.0000	0.1245	0.0305	0.1550	0.8450	13.5455	0.3934
2	0.7966	0.0928	0.0577	0.1505	0.0529	0.0000	0.1974	0.0915	0.2889	0.7111	7.0069	0.5209
3	0.7222	0.1131	0.0801	0.1933	0.0845	0.0000	0.2491	0.1005	0.3496	0.6504	4.2535	0.5528
4	0.6281	0.2022	0.0658	0.2681	0.1038	0.0000	0.3284	0.0986	0.4270	0.5730	3.4666	0.6278
5	0.5507	0.2382	0.0915	0.3296	0.1197	0.0000	0.4410	0.1066	0.5476	0.4524	2.2746	0.6019
6	0.4391	0.3249	0.1123	0.4372	0.1237	0.0000	0.4665	0.1292	0.5957	0.4043	2.3981	0.7339
7	0.3653	0.3706	0.1368	0.5075	0.1272	0.0000	0.5146	0.1400	0.6546	0.3454	2.1053	0.7753
8	0.3205	0.4043	0.1496	0.5539	0.1255	0.0000	0.5771	0.1487	0.7258	0.2742	1.6669	0.7632

7.6.1 Experimental LLE of the quaternary system of [EMIM] based ILs (1) + Thiophene (2) +Pyridine (3) +Toluene (4).

LLE for the quaternary systems of 1-ethyl 3-methylimidazolium acetate (1) + thiophene (2) + pyridine (3) + toluene (4), 1-ethyl 3-methylimidazolium ethylsulphate (1) + thiophene (2) + pyridine (3) + toluene (4) and 1-ethyl- 3-methylimidazolium methylsulphonate (1) + thiophene (2) + pyridine (3) + toluene (4) were experimentally determined at 298.25K.Table 7.21 to 7.23 list the composition of the experimental tie lines for the three investigated systems at 298.15K,respectively.It also shows the values of the selectivity (S) (Figure 7.33(a)) and distribution coefficient (β) (Figure 7.33(b))which are widely used parameter to characterize the suitability of a solvent in Liquid-Liquid Extraction.

Table 7.21 to 7.23 shows the experimental composition of the tie-lines of three quaternary systems at 298.15K.The evaluation of selectivity (S) and distribution coefficient (β) for each system as a function of mole fraction of the thiophene and pyridine mixture (solute) in the toluene rich phase is plotted in Figure 7.33(a) and 7.33 (b). In this figure, it can be observed that the selectivity decreases with a increase in mole fraction of solute in the toluene rich phase, whereas the distribution coefficient increases with mole fraction. This similar behaviour has been observed from various studies on the separation of aromatic and aliphatic compounds using IL [Deisenhofer et al., 2010; Lin et al., 2002; Arce et al., 2007; Gonzalez et al., 2010].This is mainly due to the fact that the aromatic ring structure of thiophene and pyridine molecules has a similar structure when compared with imidazolium ring of cation. The smaller size of imidazolium cation makes interaction through CH--π and π--π interaction with thiophene and pyridine. This statement is consistent with the reported work of Kumar et al.,[2009], and Anantharaj et.al. [2010a,2010b] The selectivity of ionic liquid strongly depends on the anion, and therefore [OAc],[$EtSO_4$] and [$MeSO_3$] posses a high selectivity for mole fraction of (TS+PY) less than 0.2. The [OAc],[$EtSO_4$] and

[$MeSO_3$] anion causes electron donating tendency towards hydrogen atom of thiophene (acidic) [Berresheim et al.,1993;Gonzalez et al.,2010] and pyridine (basic) [Anantharaj et al.,2010a].This is due to the presence of electronegative atom (**O**xygen,**N**itrogen,**S**ulphur) in the anion structure. In addition these three anions ([OAc], [$EtSO_4$] and [$MeSO_3$]) are neutral or loosely basic in nature and thereby exhibit weak electrostatic interactions with the imidazolium cations and thus impart high selectivity [Meindersma et al., 2010]. Thus the higher selectivity is due to weak electrostatic interaction between cation and anion. Further the high interaction between cation with thiophene and pyridine further causes significant attraction.

The value of the distribution coefficient for all the studied systems is between 0.5 to 2 which indicates that for the simultaneous separation more IL or solvent is required. In Figure 7.33, the distribution coefficient increases as the mixture of thiophene and pyridine concentration in the toluene rich phase decreases. The distribution coefficient is higher than unity and the corresponding tie-line of the slope is positive (Figure 7.31 to 7.33), while the values which are lower than unity show negative slope [Kumar et al., 2009]. From the thermodynamic point of view, an extracting solvent must be exhibit high selectivity and distribution coefficient, but the presence of similar structure and size of molecules in the quaternary systems has some limitations on the simultaneous interaction. However selectivity values are higher than unity and the distribution values are above 0.5 for all the studied systems at 298.15K.In diesel oil, the sulphur and nitrogen concentration is very low. Additionally the ionic liquid has higher density than thiophene and pyridine molecules, therefore it can be exist as separate phase when in contact with water. Thus it can be readily recovered and reuse for multiple extractions without additional environmental concern. Therefore [EMIM][OAc], [EMIM][$EtSO_4$] and [EMIM][$MeSO_3$] can be confirmed as a potential solvent for the simultaneous separation of thiophene and pyridine molecules from toluene at 298.15K.

7.6.2 NRTL and UNIQUAC correlations

The NRTL and UNIQUAC models were used to correlate the experimental tie line compositions. The triangular diagrams with the tie lines for each system are plotted in Figure 7.34 to 7.36 for NRTL and 7.37 to 7.38 for UNIQUAC model. The figures provide a clear visualization of the change in the size and shape of the immiscibility region as a result of the increase in solute concentration in the toluene rich phase. It is seen that the tie line length is significantly large. Therefore the immiscibility of aromatic + ILs and solute (thiophene+pyridine) + ILs pairs are very high at 298.15K. It is observed that the tie-lines show a positive slope at the bottom of triangular diagram. This is due to the fact that the distance between the aromatic solute and cation of ionic liquids becomes larger [Diedenhofen et al., 2010] as the composition of solute in the toluene rich phase increases. The sign of the tie-line slope change also depends on the molecular interaction at 298.15K. For example, the ternary system of {n-Hexane + pyridine + [EMIM][$EtSO_4$] } shows a positive slope [Ramirez et al.,2004], where as { hexadecane +pyridine + methanol}[Anantharaj et al.,2010a] exhibits a negative slope. In addition the ternary system of {Hexane + thiophene + [HMIM][NTf_2]}, {Dodecane + thiophene + [HMIM][NTf_2]} and {Hexadecane + thiophene + [HMIM][NTf_2]} shows both positive and negative slope in the triangular diagram[Zhou et al.,2008]. However it is observed that the extraction of thiophene is higher than that of pyridine. An important observation on looking at Figure 7.32 to7.34 indicates that the mole fraction of IL in raffinate phase is zero. This indicates the IL will not contaminate the diesel phase. Thus in the quaternary system, the tie lines show a positive slope till a certain concentration of solute and thereafter the sign of tie line changes, becomes negative as the mole fraction of solute becomes greater. It is also observed that the sign of tie line is directly

related to the distribution coefficient of the solute in both the phases. However, the negative slope of tie line indicates that the effective separation requires more quantity of IL, while the positive slope means desirable feature for an extracting solvent at 298.15K.It should be noted that the practical application of simultaneous desulphurization and denitrification of diesel oil corresponds to low concentration of sulphur- and nitrogen-containing compounds. Therefore, the lowest part of the triangular diagrams must be considered as a effective separation region in all the diagrams.

The difference between experimental and predicted tie line composition were minimized using objective function (Equation 6.13) and then used to calculate the root mean square deviation values (Equation 4.24).The observed RMSD values for three quaternary systems are listed in Table 7.24 to 7.26.The rmsd values are lesser than unity for all the studied system which indicates a high degree of accuracy. For UNIQUAC model prediction, *r* and *q* values are given in Table 7.4.The NRTL and UNIQUAC binary interaction parameter of the quaternary systems are listed in Tables 7.24 to 7.26 and the corresponding objective function value and RMSD are also listed. The observed interaction parameter can be used for the design and simulation of extraction column for the simultaneous separation of thiophene and pyridine from diesel oil.

Table 7.24: NRTL and UNIQUAC interaction parameters for the [EMIM][CH_3COO] (1) + Thiophene (2) +Pyridine (3) +Toluene (4) systems at T = 298.15 K

	NRTL Model Parameters				**UNIQUAC Model Parameters**			
	/K	/K	*	RMSD**	/K	/K	*	RMSD**
System: [EMIM][CH_3COO] (1) + Thiophene (2) +Pyridine (3) +Toluene (4)								

1-2	8147.2	798.5	-9.71 × 10^{-3}	0.9268%	628	567.34	-15.57 × 10^{-3}	1.5493%
1-3	1187.8	7108.1			847.04	-28.8211		
1-4	1603	369.69			271.21	1185.2		
2-3	975.68	8323.8			-34.06	149.41		
2-4	1542.7	-0.4032			947.97	211.46		
3-4	684.87	3393.2			301.23	1326.3		

* Calculated using equation 6.13; **Calculated using equation 2.40.

Table 7.25: NRTL and UNIQUAC interaction parameters for the [EMIM][$EtSO_4$] (1) + Thiophene (2) +Pyridine (3) +Toluene (4) systems at T = 298.15 K

	NRTL Model Parameters				**UNIQUAC Model Parameters**			
	/K	/K	*	RMSD**	/K	/K	*	RMSD**
System: [EMIM][$EtSO_4$] (1) + Thiophene (2) +Pyridine (3) +Toluene (4)								
1-2	8147.2	798.87	-9.71 × 10^{-3}	1.2318%	628	567.34	-15.36 × 10^{-3}	1.5493%
1-3	1187.8	7108.1			847.04	-28.821		
1-4	1603	369.69			271.21	1185.2		
2-3	975.68	8323.8			-34.06	149.41		
2-4	1542.7	-0.4032 6			947.97	211.46		
3-4	684.87	3393.2			301.23	1326.3		

* Calculated using equation 6.13; **Calculated using equation 2.40.

Table 7.26: NRTL and UNIQUAC interaction parameters for the [EMIM][$MeSO_3$] (1) + Thiophene (2) +Pyridine (3) +Toluene(4) systems at T = 298.15 K

	NRTL Model Parameters	**UNIQUAC Model Parameters**

	/K	/K	*	RMSD**	/K	/K	*	RMSD**
System: [EMIM][$MeSO_3$] (1) + Thiophene (2) +Pyridine (3) +Toluene (4)								
1-2	1087.3	7365.9	-5.63 × 10^{-3}	0.9375%	-67.256	238.13	-35.3 × 10^{-3}	2.3485%
1-3	6576.8	113.74			638.49	2710		
1-4	5714.5	12788			373.86	2668		
2-3	14999	1242.2			806.65	-57.081		
2-4	336.13	867.22			25.911	-179.68		
3-4	14938	6377			978.09	975.95		

* Calculated using equation 6.13; **Calculated using equation 2.40.

Figure 7.34: Experimental tie lines for the LLE of the quaternary system [EMIM][OAc] (1) + Thiophene (2) +Pyridine (3) +Toluene (4) at T = 298.15 K.The corresponding tie-lines are correlated with NRTL (α=0.2).

Figure 7.35: Experimental tie-lines for the LLE of the quaternary system [EMIM][$EtSO_4$] (1) + Thiophene (2) +Pyridine (3) +Toluene (4) at T = 298.15 K.

Figure 7.36: Experimental tie-lines for the LLE of the quaternary system [EMIM][$EtSO_4$] (1) + Thiophene (2) +Pyridine (3) +Toluene (4) at T = 298.15 K.

Figure 7.37: Experimental tie-lines for the LLE of the quaternary system [EMIM][OAc] (1) + Thiophene (2) +Pyridine (3) +Toluene (4) at T = 298.15 K.The corresponding tie-lines are correlated with UNIQUAC model.

Figure 7.38: Experimental tie-lines for the LLE of the quaternary system [EMIM][$EtSO_4$] (1) + Thiophene (2) +Pyridine (3) +Toluene (4) at T = 298.15 K.

Figure 7.39: Experimental tie-lines for the LLE of the quaternary system [EMIM][$EtSO_4$] (1) + Thiophene (2) +Pyridine (3) +Toluene (4) systems at T = 298.15 K. which is correlated with UNIQUAC model.

7.6.3 LLE COSMO-RS predictions

Finally the COSMO-RS model was used for the validation of experimental data. The COSMO-RS predicted tie lines are given in Figure 7.40 to 7.42. The tie lines are exactly matching each other qualitatively, whereas length and shape of the immiscible region has a bit deviation, particularly in IL rich phase. It can be explained by the presence of significant molecular interactions which is not well defined in the present COSMO-RS model. However the results are good in terms of tie line slope direction and shape of immiscibility region in all the diagrams (Figure 7.40 to 7.42). The RMSD for the systems are 8.41%, 8.74% and 6.53% for [OAc],[$EtSO_4$] and [$MeSO_3$] based system, respectively.

Figure 7.40: Experimental tie lines for the LLE of the quaternary system [EMIM][OAc] (1) + Thiophene (2) +Pyridine (3) +Toluene (4) at T = 298.15 K.The corresponding tie-lines are correlated with COSMO-RS predictions.

Figure 7.41: Experimental and COSMO-RS predicted tie-lines for the LLE of the quaternary system [EMIM][$EtSO_4$] (1) + Thiophene (2) +Pyridine (3) +Toluene(4) at T = 298.15 K.

Figure 7.42: Experimental and COSMO-RS predicted tie-lines for the LLE of the quaternary system [EMIM][$EtSO_4$] (1) + Thiophene (2) +Pyridine (3) +Toluene (4) at T = 298.15 K.

LLE data for the quaternary system containing [EMIM][OAc],[EMIM][$EtSO_4$] and [EMIM][$MeSO_3$] ionic liquid with thiophene, pyridine and ***PIONA*** series components were experimentally determined at 298.15K. It was observed that the selectivity values are higher than unity for all the studied systems whereas the distribution coefficient values are lesser than unity which indicates higher amount of ionic liquid are required for separation. However [EMIM][OAc], [EMIM][$EtSO_4$] and [EMIM][$MeSO_3$] ionic liquid are totally immiscible in ***PIONA*** component rich phase which could be make their recovery and reuse easier and cheaper. The reliability of the experimental LLE data was correlated with NRTL and UNIQUAC models. These results are very satisfactory with the root mean square deviation lower than unity for all the studied systems at 298.15K. Further these experimental tie-lines were validated with COSMO-RS model. The RMSD for the COMO-RS prediction are observed to the follow the order:

Pentane:4.62%([EMIM][OAc]) >5.3%([EMIM][$EtSO_4$]~6.07%([EMIM][$MeSO_3$])

Isooctane:4.49%([EMIM][$EtSO_4$])>7.43%([EMIM][OAc]) 8.26%([EMIM][$MeSO_3$])

Cyclohexane:5.39%([EMIM][$MeSO_3$])>5.93%([EMIM][$EtSO_4$]>7.8%([EMIM][OAc])

Toluene: 5.74%([EMIM][$EtSO_4$])>6.53%([EMIM][$MeSO_3$])>8.41%([EMIM][OAc]) .

Nomenclature

Latin Symbols

[EMIM]	Cation: 1-ethyl 3-methylimidazolium
[CH_3COO] or [OAC]	Anion: acetate
[$EtSO_4$]	Anion: ethyl sulphate
[MeSO3]	Anion: methylsulphonate
S	Selectivity
F	Objective function
$RMSD$	Root mean square deviation
a_{eff}	Effective segment surface area, $Å^2$
c_{hb}	Misfit energy constant, kcal $Å^4$ mol^{-1} e^{-2}
	Sigma profile of component i i.e. probability of segment i having a charge density σ
R	Universal gas constant, J K^{-1} mol^{-1}
T	Temperature, K
r_i	Normalized volume parameter for the Staverman-Guggenheim combinatorial term, $Å^3$
q_i	Normalized surface area parameter for the Staverman-Guggenheim combinatorial term, $Å^2$
r_{std}	Standard volume parameter, 79.53 $Å^3$
q_{std}	Standard surface area area parameter, 66.69 $Å^2$
m	Number of tie lines
c	Number of components in the LLE system
x_i	Mole fraction of component i of either phase in the LLE system

n_i	Total number of segments on the surface of the molecular cavity
H_i	Peak area under NMR spectra of species *i*
z	Coordination number =10
l	Staverman-Guggenheim combinatorial term parameter
g_{ji}	Average interaction energy for the interaction of molecules of component *j* with molecules of component *i*

Greek Symbols

α'	Misfit energy constant, kcal $Å^4$ mol^{-1} e^{-2}
σ_{hb}	Hydrogen bonding cut-off value, 0.0084 e $Å^{-2}$
	Activity coefficient of solute *i* in solution *S*
	Segment activity coefficient of segment σ_i in pure species
H_i	Peak area under NMR spectra of species *i*
β	Distribution coefficient
θ	Area fraction in UNIQUAC equation
τ	NRTL/UNIQUAC interaction parameter
Φ	Segment fraction in UNIQUAC equation
α	NRTL non-randomness parameter
	Staverman-Guggenheim activity coefficient

REFERENCES

Alonso, L.; Arce, A.; Francisco, M.; Soto, A. Extraction Ability of Nitrogen-Containing Compounds Involved in the Desulphurization of Fuels by Using Ionic Liquids.*J.Chem.Eng.Data*.**2010**,55,3262-3267.

Anantharaj,R.; Banerjee.R. Desulphurization of Diesel oil using Ionic Liquids: Effect of Cation and Anion combination. *Fuel Proc.Tech.* **2011a**, 92, 39-52.

Anantharaj, R.; Banerjee,T. COSMO-RS-Based Screening of Ionic Liquids as Green Solvents in Denitrification Studies.*Ind.Eng.Chem.Res***. 2010b,** 49, 8705-8725.

Anantharaj,R.; Banerjee.T. Evaluation and comparison of global scalar properties for the simultaneous interaction of ionic liquids with thiophene and pyridine. *Fluid Phase Equilibria*, 2010a,293, 22–31.

Anantharaj,R.; Banerjee.T. Quantum Chemical Studies on the Simultaneous Interaction of Thiophene and Pyridine with Ionic Liquid.*AIChEJ*, 2011b. 57,749-764.

Arce, A.; Earle, M.J.; Rodríguez, H.; Seddon, K.R. Separation of Benzene and Hexane by Solvent Extraction with 1-Alkyl-3-methylimidazolium

Bis{(trifluoromethyl)sulfonyl}amide Ionic Liquids: Effect of the Alkyl-Substituent Length. *J. Phys. Chem. B*. **2007,** 111, 4732–4736.

Banerjee, T.; Singh, M.K.; Sahoo, R.K.; Khanna, A. Volume, surface and UNIQUAC interaction parameters for imidazolium based ionic liquids via Polarizable Continuum Model. *Fluid Phase Equilibria*.**2005**, 234:64-76.

Francisco, M.; Arce, A.; Soto, A.Ionic Liquids on desulphurization of fuesl oils. *Fluid Phase Equilibria*.**2010**, 294: 39-48.

Garcia, J.;Garcia, S.;Torrecilla, J.S, Oliet, M.;Rodriguez, F.Liquid-Liquid Equilibria for the Ternary sytems {Heptane + Toluene +N-Butylpyridinium Tetrafluoroborate or N-Hexylpyridinium Terta fluoroborate} at T=313.2K. *J.Chem. Eng. Data*. **2010,** 55, 2862-2865.

Garcia, J.;Garcia, S.;Torrecilla, J.S.;Rodriguez, F.Solvent extraction of Toluene from Hepaten with the Ionic Liquids N-Ethylpyrinium Bis(trifluoromethylsulfonyl)imide and z-methyl-N-ethylpyriidnium Bis(trifluoromethylsulfonyl)imide (z=2,3,or 4) at T=313.2K. *J.Chem. Eng. Data*. **2010**, 55, 4937-4942.

Gomez, E.;Dominguez, I.;Gonzalez, B.;Dominguez, A.Liquid-Liquid Equilibria of the Ternary systems of Alkane + Aromatic + 1-Ethylpyriidnium Ethylsulfate Ionic Liquid at T=(283.15 and 298.15)K.*J.Chem.Eng.Data*.**2010**,55,5169-5175.

Gonzalez, E.J.; Calvar, N.; Gomez, E.; Domlnguez, A. Separation of Benzene from Linear Alkanes (C_6−C_9) Using 1-Ethyl-3-Methylimidazolium Ethylsulfate at T = 298.15 K. *J. Chem. Eng. Data*. **2010**, 55, 3422–3427.

Gonzalez, E.J.; Calvar, N.; Gomez, E.; Domlnguez. A. Liquid−Liquid Equilibria of the Ternary Systems of Alkane + Aromatic + 1-Ethylpyridinium Ethylsulfate Ionic Liquid at T = (283.15 and 298.15) K. *J. Chem. Eng. Data*.**2010**, 55: 5169-5175.

Gonzalez, E.J.; Calvar, N.; Gomez, E.; Domlnguez. A. Separation of Benzene from Linear Alkanes (C_6–C_9) Using 1-Ethyl-3-Methylimidazolium Ethylsulfate at T = 298.15 K. *J. Chem. Eng. Data*. **2010**, 55, 3422–3427.

Jeon, H.J. Ko, C.H, Kim, S.H, Kim, J.N. Refractory Sulphur Compounds in Diesel oil Using Activated compounds with Controlled Porosity. *Energy & Fules*.**2009**, 23, 2537-2543.

MacFarlane, D.R.; Pringle, J.M.; Johansson, K.M.; Forsyth, S.A.; Forsyth, M.Lewis base ionic liquids.*Chem.Commun*.**2006**, 1905-1971.

Maduro, R.M.;Aznar, M. Liquid-Liquid equilibrium of ternary systems 1-butyl-3-methylimidazolium hexafluorophosphate +aromatic +aliphatic. *Fluid Phase Equilibria*.**2010**, 265, 129-138.

Meindersma, G.W.; Hansmeier, A.R.; Haan, B. Ionic Liquids for Aromatics Extraction. Present Status and Future Outlook. *Ind. Eng. Chem. Res*.**2010**, 49: 7530–7540.

Varma,N.R.; Anantharaj.R.; Banerjee.T. Experiments, correlations and COSMO-RS predictions for the extraction of benzothiophene from n-hexane using imidazolium-based ionic liquids. *Chem. Engine. J*. 2011. 166,30-39.

Won, D.B.; Park, S.J.; Han, K.J.; Kim, C.J.Liquid-Liquid equilibria for methanol + Hexadecane +Heterocyclic nitrogen –containing compounds at 298.15K. *Fluid Phase Equilibria*.**2002**, 193,217-227.

Zhou, J.; Mao, J.; Zhang, S. Ab initio calculations of the interaction between thiophene and ionic liquids. *Fuel. Proc.Tech.***2008**, 89, 1456-1460.

A three tier approach involving Ab-intio technique, COSMO-RS predictions and subsequent experimentation was performed to evaluate the performance of Ionic Liquid(IL's) for desulphurization and denitrification studies on diesel oil. Ab initio technique was carried out for the simultaneous interaction of IL's with thiophene and pyridine. It was observed that the global scalar properties such as HOMO/LUMO energies, HOMO-LUMO energy gap, chemical hardness, chemical softness, chemical potential, electronegativity and electrophilicity index have a significant influence on the solubility of these compounds in IL. It was also observed that the simultaneous interaction of ILs with thiophene and pyridine strongly depends on the CH-π bond interaction and the partial charge transfer between ILs and thiophene/pyridine.

This was confirmed by the prediction of Infinite Dilution Activity Coefficient (IDAC) using quantum chemical based COSMO-RS (**CO**nductor **L**ike **S**creening **MO**del for **R**eal **S**olvent). A total of 28 anions and 6 cations resulting in 168 possible combinations were further screened for desulphurization, denitrification and simultaneous removal via COSMO-RS. It was found that the cation without the aromatic ring such as pyrrolidinium and morpholinium when combined with anions having sterical shielding effect such as $[CH_3SO_3]$,$[CH_3COO]$,[SCN],[Br] and [Cl] proved to be the most favourable IL. Additionally it was observed that the molecular rearrangement in the ILs strongly depends on possibility of hydrogen bond formation between the cationic rings themselves and with other heterocyclic compounds. UNIFAC model was then to used to regress the group interaction parameters for ternary mixture containing IL+ thiophene+ hydrocarbon regression from known experimental data. Further the group interaction parameters were used to predict the LLE of unknown thiophene containing systems successfully with an average root mean square deviation (RMSD) of 1.5-5%. Based on the COSMO-RS predictions, four potential ILs ([EMIM]$[CH_3COO]$, [EMIM][SCN], [EMIM]$[C_2H_5SO_4]$, [EMIM]$[CH_3SO_3]$,)were used for binary system studies where it was observed that the CH---π bond interaction and π---π stacking effects become more dominant with the difference in size and shape between two components.

Further we have studied ternary system of IL-benzothiophene-hexane at T=308.15 K. [EMIM][$C_2H_5SO_4$] and [EMIM][CH_3COO] showed high selectivity. These results were also correlated with the NRTL and UNIQUAC models with RMSD less than 1%. Further the LLE were predicted via COSMO-RS predictions with a RMSD of ~6.33%. Thus this work complimented the theoretical and experimental aspects for desulpurization and denitrification studies using IL's.

Very high selectivity values were achieved for the quaternary experiments done on the systems, ([EMIM][OAc], [EMIM][$EtSO_4$] and [EMIM][$MeSO_3$] ionic liquids with thiophene,pyridine and ***PIONA*** series components (penatne,isooctane,cyclohexane and toluene). The experimental results were correlated with the NRTL and UNIQUAC models, of which the NRTL model displayed superior accuracy in correlating the data. The experimental data so obtained was then used to validate with the COSMO-RS predictions. The deviations were found to be satisfactorily low for both the systems. From the experimental and predicted results, we conclude that the three ionic liquids, [EMIM][OAc], [EMIM][$EtSO_4$] and [EMIM][$MeSO_3$] are highly effective for the removal of thiophene and pyridine from ***PIONA*** series components. The studies also stand testimonial to the potential of imidazolium-based ionic liquids in general, for the extractive desulfurization and denitrification of diesel oil. High selectivity values with negligible cross-contamination of the ***PIONA*** series components in the ionic liquid phase were achieved, with negligible amount of ionic liquid in the ***PIONA*** series components -rich phase.

Future Work

The research presented in this thesis can be furthered in various ways that would strengthen the arguments made and conclusions reached in this thesis. In this work we have assessed only ***PIONA*** series compounds which is based on their concentration level in simulated diesel oil.

- The main challenge in this regard would be to *assess the production of zero emission of actual diesel oil* (containing 125 compounds) using Ionic Liquids at 298.15K.
- The methodology presented in this thesis can also be extended to *other aromatic sulphur, nitrogen compounds and its derivatives*.
- A *rate based model* can be proposed for the multistage extraction of these compounds from diesel oil
- *Molecular Dynamics simulations* can be applied on IL-sulphur-pyridine complexes to know important dynamic properties which affect the mass transfer rates such as diffusivity etc.

SYNOPSIS

Name of the Student**: Anantharaj R** Roll No**: 08610702**

Degree for which submitted**: PhD** Department**: Chemical Engineering**

Thesis Title**: Simultaneous Desulphurization and Denitrification of Diesel oil using Ionic Liquids: Quantum Chemical Predictions and Experiments**

Name of the Thesis Supervisor**: Dr.Tamal Banerjee**

Department of Chemical Engineering

Month and Year of Submission: **May, 2011**

The simultaneous removal of aromatic compounds of sulphur and nitrogen from diesel oil is becoming increasingly difficult because of its resistance to hydrodesulphurization (***HDS***) and hydrodenitrification ***(HDN***) .The current conventional HDS and HDN processes requires higher hydrogen consumption and high operating conditions, yet it is unable to remove all sulphur and nitrogen aromatic compound. Ionic Liquids (ILs) better known as green solvents provide an important alternative in removing such compounds by liquid liquid extraction (LLE) at room temperature and atmospheric pressure. ILs, also known as tuneable solvents or ***green solvents*** consists of an organic cation and an organic/inorganic anion. They are considered to be the most promising candidates for HDS and HDN processes.

Recently theoretical quantum chemical calculations have become complementarities for experimental methods in many fields. Therefore our objective is to apply quantum chemical calculations to investigate the fundamental nature of the IL-sulphur-nitrogen systems at atomic and molecular level. This will be helpful in understanding the nature of structural relation between molecules such as: ionic liquid + aromatic sulphur + aromatic nitrogen system(s). A three tier approach involving Ab-intio technique, ***COSMO-RS*** (***CO***nductor ***L***ike ***S***creening ***MO***del for ***R***eal ***S***olvents) predictions and subsequent experimentation was performed to evaluate the performance of Ionic Liquid(IL's) for desulphurization and denitrification studies on diesel oil. The following excerpts summarize the outline of the thesis.

1. Estimation of Higher Occupied Molecular Orbital (HOMO) and Lower Unoccupied Molecular Orbital (LUMO) Energies for the system of Ionic Liquids with thiophene and pyridine.

Ab initio studies were carried out with mixtures containing ionic liquid with thiophene and pyridine for studying the simultaneous interaction. Global scalar properties such as HOMO/LUMO energies, HOMO–LUMO energy gap, chemical hardness, chemical potential, electronegativity, global hardness, global softness and electrophilicity index were determined for clusters containing ionic liquids with thiophene and pyridine. Ionic liquids containing: 1-butyl-3-methylpyrrolidinium [BUMPYR], 1-benzyl-3-methyimidazolioum [BeMIM] and 1-butyl-3-methylpyridinium [BUMPY] cations combined with inorganic anions containing fluorine ($[BF_4]$ and $[PF_6]$) were studied in this work. [BeMIM][BF_4] (1-benzyl- 3-methyimidazolioum tetrafluoroborate) with a HOMO–LUMO energy gap of 0.1882 Hartrees was found to be the most effective IL. Further a ranking based on all the mentioned scalar parameters also pointed out [BeMIM][BF_4] to be the most desirable IL. The overall ranking after taking into considerations all factors followed: [BeMIM][BF_4] > [BUMPYR][BF_4] > [BUMPY][PF_6] > [BUMPY][BF_4] > [BUMPYR][PF_6]. To validate the findings, infinite dilution activity coefficients (IDAC) were predicted using the quantum chemical based COSMO-RS methodology which gave the same trend as observed using scalar properties.

2. Evaluation of Interaction Energy for the Simultaneous Interaction of Five-/Six-Membered Rings of Sulphur and Nitrogen Compounds with Ionic Liquids

The simultaneous interaction of thiophene and pyridine with different ionic liquids: 1-butyl-1-methylpyrrolidiniumtetrafluoroborate([BPYRO][BF_4]),1-butyl-1-ethylpyrrolidinium hexafluoro-phosphate ([BPYRO][PF_6]), 1-butyl-4-methylpyridinium tetrafluoroborate ([BPY][BF_4]), 1-butyl-4-methylpyridinium hexafluorophosphate ([BPY][PF_6]) and 1-benzyl-3-methylimidazolium tetrafluoroborate ([BeMIM][BF_4]) were investigated

using quantum chemical calculations. A three-tier approach comprising of partial charges, interaction energies and sigma profile generation using conductor-like screening model for real solvents (COSMO-RS) was chosen to study the systems. A quantitative attempt based on the CH-π interaction in ionic liquid; thiophene–pyridine complexes gave the interaction energies of ILs in the order: [BPY][BF_4] [[BPYRO][PF_6] [[BeMIM][BF_4] [[BPY][PF_6] [[BPYRO][BF_4]. An inverse relation was observed between the activity coefficient at infinite dilution predicted via COSMO-RS–based model and interaction energies. The dominance of CH-π interaction was evident from the sigma profiles of ionic liquid together with thiophene and pyridine.

3. Screening of Potential Ionic Liquids for Desulphurization and Denitrification using COnductor Like Screening MOdel for Real Solvents (COSMO-RS).

A total of 28 anions and 6 cations resulting in 168 possible combinations were screened via COSMO-RS model. Initially benchmarking was performed to predict the infinite dilution activity coefficients of thiophene in ionic liquids. Comparison with literature values involving 8 ILs with 20 points gave the average root mean square deviation (RMS) to be 11%. Thereafter artificial simulated diesel, aromatic sulphur compound and the cation and anion combination was used to predict the capacity (C) and selectivity (S) at infinite dilution. In general the selectivities were found to decrease in the following order: thiophene (4–24) > benzothiophene (2–12)> dibenzothiophene (1–7). The different hetero atom (N,S,O) and its location in the cation structure strongly influenced the selectivity and capacity at infinite dilution for all the three aromatic sulphur compounds. It was found that the cation without the aromatic ring combined with anions having sterical shielding effect such as [SCN], [$MeSO_3$], [OAc], [Cl], and [Br] proved to be the most favourable IL for desulphurization. [EMMOR][SCN] proved to be the most viable IL for the removal of all the three aromatic sulphur compounds.

The Five- and six-membered heteroaromatic nitrogen compounds play an inhibiting role in the hydrodesulfurization of diesel oil. Approximately 168 ILs comprising cations which include 1-ethyl-3- methylimidaozlium [EMIM],

1-ethylpyridinium [EPY], 1-ethyl-1-methyl pyrrolidinium [EPYRO], 1-ethyl-1-methylpiperidinium [EMPIP], 4-ethyl-4-methyl morpholinium [EMMOR], and 1,2,4-trimethylpyrazolium[TMPYZO] combined with 26 anions were investigated in this work. The infinite dilution activity coefficient (IDAC) was predicted through COSMO-RS model in order to screen the potential solvents. Initially the model was benchmarked via IDAC and LLE predictions. LLE was predicted for four reported ternary systems in which a nitrogen heterocycle was one of the compounds. The average root-mean-square deviation (rmsd) obtained was 10%. The IDAC values were predicted for pyridine in two ionic liquids, namely [BMIM][BF_4] and [EMIM][TOS], with a root-mean-square (rms) error of 8%. Thereafter the selectivity, capacity, and performance index at infinite dilution were calculated to evaluate the performance. It was found that the five-membered nitrogen species having high delocalized electron density possessed 3 orders of magnitude higher selectivity than the six-membered nitrogen species. For the fivemembered ring structures, the selectivity was found to follow the order [EPYRO] > [EMPIP] > [EPY] > [EMMOR] > [EMIM] > [TMPYZO]. For the six-membered heterocycle, it followed the order [EPY] > [EMMOR] > [EPYRO] > [EMPIP] > [EMIM] > [TMPYZO]. Irrespective of nitrogen heterocycle, anions such as thiocyanate [SCN] and acetate [Ac] gave high values of selectivity. In general cations without aromatic rings such as [EPYRO], [EMPIP], and [EMMOR] gave higher selectivity and capacity irrespective of the nitrogen heterocycle.

4. Physiochemical Properties Studies on the Hydrodesulphurization and Hydrodenitrification Inhibiting Compounds with Ionic Liquids at *T*= (298.15 to 323.15) K and *p*=1 bar.

The ability of 1-ethyl 3-methylimidazolium acetate [EMIM][OAc], 1-ethyl 3-methylimidazolium ethylsulphate [EMIM][$EtSO_4$] and 1-ethyl 3-methylimidazolium methylsulphonate [EMIM][$MeSO_3$] as a green and tuneable solvent for simultaneous desulphurization and denitrification of diesel oil has been studied in detail. Experimental density, surface tension and refractive index data have been measured for the following

systems: ILs (1) + pyridine(2), ILs (1) + pyrrole(2), ILs (1) + quinoline(2), ILs (1) + indoline(2), ILs (1) + thiophene(2) and ILs (1) + water(2) over the entire mole fraction of ILs at temperatures of (298.15 to 323.15)K and at atmospheric pressure. Further from experimental density values, coefficient of thermal expansivity and excess molar volume were also calculated. It was found that the heteroaromatic nitrogen/sulphur compounds and water are completely miscible in the ILs. The surface tension values were found to increase while the refractive index decreases with increasing mole fraction of ILs. On the other side dissimilar molecule such as water showed mobility of ions on mixing resulting in lower surface tension. The experimental values of surface tension increased in the order: thiophene > pyridine > pyrrole > indoline > quinoline and for refractive index: quinoline > indoline > pyrrole > pyridine > thiophene > water. It was found that the composition of ILs has a greater influence than temperature in deciding the densities, surface, optical and thermodynamic properties for similar molecular interaction than dissimilar molecules such as water.

5. Experimental and Computational Studies on the Phase Behaviour of Ionic Liquid with Aromatic Sulphur and Diesel Compound at 308.15 K.

Based on the COSMO-RS predictions in 3 the Ionic Liquids with the anion [OAc] and [$EtSO_4$] combined with a small cation i.e [EMIM] was chosen to evaluate the extractive ability of the ILs with the anions. The extraction of benzothiophene from *n*-hexane was then studied using 1-ethyl 3-methylimidazolium ethyl sulphate ([EMIM][$EtSO_4$]) and 1-ethyl 3-methylimidazolium acetate ([EMIM][OAc]) at 308.15 K to analyze the performance of ionic liquids in the extractive desulphurization of aromatic sulphur compounds from petroleum fuels. A comparative study was done from the perspective of selectivity and distribution coefficient of the sulphur compounds. From the ternary LLE experiments, it was found that while the selectivity was higher for the ethyl sulphate-based ionic liquids, the distribution coefficient was higher for acetatebased ionic liquids. Selectivities as high as 245 and 203 were obtained for [EMIM][$EtSO_4$] and [EMIM][OAc] with negligible loss of hydrocarbon. The experimental results were

correlated using the NRTL and UNIQUAC models. The root mean square deviation (RMSD) values of 0.48% and 0.83% were obtained for [EMIM][$EtSO_4$] and [EMIM][OAc] respectively, when using the NRTL model, and the corresponding RMSD values when using the UNIQUAC model were 0.693% and 1.053%. The quantum chemical based COSMO-RS model was then used to predict the performance of single as well as mixed ionic liquids. RMSDs of 4.36% and 7.87% were achieved for [EMIM][$EtSO_4$] and [EMIM][OAc] based system, which are satisfactory considering that the method is *a-priori*. Thus this work complimented the theoretical and experimental aspects for desulphurization and denitrification studies using IL's.

6. Quaternary Liquid-Liquid Equilibria for the Systems of Imidazolium Based Ionic Liquid + Thiophene + Pyridine + Diesel Compounds at 298.15K

In this work, 1-ethyl 3-methylimidazolium acetate [EMIM][OAc], 1-ethyl 3-methylimidazolium ethylsulphate [EMIM][$EtSO_4$] and 1-ethyl 3-methylimidazolium methylsulphonate [EMIM][$MeSO_3$] was investigated as a green solvent for the simultaneous separation of thiophene and pyridine from diesel compounds (pentane,iso-octane,cyclohexane and toluene) at 298.15K and atmospheric pressure. The liquid liquid equilibrium (LLE) data for the quaternary mixture of 1-ethyl 3-methylimidazolium acetate (1) + thiophene (2) + pyridine (3) + diesel compounds (4), 1-ethyl 3-methylimidazolium ethylsulphate (1) + thiophene (2) + pyridine (3) + diesel compounds (4) and 1-ethyl 3-methylimidazolium methylsulphonate (1) + thiophene (2) + pyridine (3) + diesel compounds (4) were experimentally determined at ambient conditions. In all the systems the tielines possessed positive slope at low concentration of thiophene and pyridine. This is beneficial since the concentration of thiophene or pyridine are usually of the order of ppm levels. The effectiveness of the simultaneous extraction of thiophene and pyridine from diesel compounds was evaluated by means of the determination of the selectivity and distribution coefficient values. The distribution values were found to be less than unity which indicates a higher consumption of Ionic Liquids. The experimental tie-line data were successfully correlated with the NonRandom Two Liquid (NRTL) and UNIversal QUAsi-Chemical (UNIQUAC) models, which gave a good

correlation of the experimental data with RMSD (root mean square deviation) values lesser than unity for all the systems. The reliability of experimental data was further ascertained by applying the COSMO-RS model to predict the tie lines giving an average RMSD of 6.33% for all the systems.

7. UNIFAC Group Interaction Prediction for Ionic Liquid-Thiophene Based Systems using Genetic Algorithm

The group interaction parameter prediction of Ionic Liquids (IL's) with thiophene (C_4H_4S) and other hydrocarbons are essential to generate (Liquid Liquid Equilibria) LLE through UNIFAC model. UNIFAC model is highly non-convex and can have several local extrema. In this work, the structural group interaction parameters have been calculated for [OMIM][BF_4] + thiophene + hydrocarbons and [OMIM] [BTI] + thiophene + hydrocarbons systems through regression using GA.The obtained LLE data has been correlated with reported values and it was observed that the cumulative RMSD(root mean square deviation) of ten ternary systems used for regression were 3.01% and 3.65% for [OMIM][BF_4] and [OMIM]BTI] based system respectively. Further, the obtained interaction parameters were used to correlate the experimental LLE data for four ternary systems which were not used for regression. These systems having a total of 40 tie lines gave a very satisfactory RMSD of 1.76 to 3.99% between reported and predicted composition.

List of Publications

Referred Journals

1. **R. Anantharaj**, T. Banerjee. Evaluation and comparison of global scalar properties for the simultaneous interaction of ionic liquids with thiophene and pyridine. ***Fluid Phase Equilibria***, **2010**,293, 22–31.
2. S. P.Singh**, R.Anantharaj**, T. Banerjee**.** UNIFAC Group Interaction Prediction for Ionic Liquid-Thiophene based systems using Genetic Algorithm**.** ***Lecture Notes in Computer Science*****. 2010,**6457,195-204.
3. **R.Anantharaj**, T. Banerjee. COSMO-RS based Screening of Ionic Liquids as Green Solvents in Denitrification Studies. ***Industrial Engineering Chemistry Research***, **2010,** 49, 8705-8725
4. **R.Anantharaj**, T. Banerjee. Desulphurization of Diesel oil using Ionic Liquids: Effect of Cation and Anion combination. ***Fuel Processing Technology***, **2011,** 92, 39-52.
5. **R. Anantharaj**, T.Banerjee. Quantum Chemical Studies on the Simultaneous Interaction of Thiophene and Pyridine with Ionic Liquid.***AIChEJ***, **2011**. 57,749-764
6. N. R.Varma**,R.Anantharaj**, T. Banerje**e.** Experiments, correlations and COSMO-RS predictions for the extraction of benzothiophene from n-hexane using imidazolium-based ionic liquid**s.** ***Chemical Engineering Journal*****. 2011**. 166,30-39.
7. **R.Anantharaj**, T. Banerjee. Phase Behaviour of Hydrodenitrification and Hydrodesulphurization inhibiting Compounds with 1-Ethyl-3-Methylimidazolium Ethylsulphate at T= (298.15 to 323.15) K and p=1 bar. ***Journal of Thermodynamics*** (**Article in Press**).
8. **R.Anantharaj**, T. Banerjee. Phase Behaviour of Catalytic Deactivated Compounds with 1-ethyl-3-methylimidazolium Acetate {[EMIM][OAc]} Ionic Liquid at Several Temperatures. ***Journal of Industrial Engineering Chemistry*** (**Article in Press**)
9. **R.Anantharaj**, T. Banerjee. Fast Solvent Screening for the Simultaneous Hydrodesulphurization and Hydrodenitrification of Diesel oil using Ionic Liquids. ***Journal of Chemical Engineering Data*****. 2011.** ID: je-2010-011289 **(Under review**)
10. **R.Anantharaj**, T.Banerjee. Phase Behaviour of 1-Ethyl-3-Methylimidazolium Thiocyanate {[EMIM][SCN} Ionic Liquid with Catalytic Deactivated Compounds and Water at Several Temperatures**.** ***International Journal of Chemical Engineering*** (**Under review**)
11. **R.Anantharaj**, T.Banerjee. Density, Surface tension, Refractive index and Thermodynamic Properties of 1-Ethyl-3-Methylimidazolium Methanesulphonate with

Aromatic Nitrogen, Aromatic Sulphur and Water at Several Temperatures and at Atmospheric Pressure. ***Canadian Journal of Chemical Engineering*** **(Under review)**

12. **R.Anantharaj**, T.Banerjee. Liquid-Liquid Equilibria for Quaternary Systems of Imidazolium based Ionic Liquid + Thiophene + Pyridine + Iso-octane at 298.15K: Experiments and Quantum Chemical Predictions. ***Fluid Phase Equilibria*** (**Under review**)

Conferences:
International

1. A. P.Kumar A, R.**Anantharaj** , T.Banerjee. Denitrification Studies on Diesel Oil Using Ionic Liquids with COSMO-RS. COSMOlogic Symposium, ***Leverkusen, Germany*** (March 31-2nd April), **2009**.
2. **R.Anantharaj**, T.Banerjee. Interaction Energies between Aromatic Nitrogen Compounds and Ionic Liquid: Ab initio and COSMO-RS based Approach*"*. Dalian Institute of Chemical Physics (DICP) Symposiyam on Applications and Industrial Processes of Ionic Liquids, ***Dalian, China***, September 5-6, **2010**.
3. **R.Anantharaj**, T.Banerjee**.** Measurement and Evaluation of Transport, Surface, Optical and Thermodynamic properties of 1-ethyl-3-methylimidazolium ethylsulphate with heteroaromatic nitrogen, heteroaromatic sulphur and water at (298.15, 303.15, 308.15, 313.15, 318.15, 323.15) K and 1 bar**.** 2nd Asia Pasicific Conference on Ionic Liquids and Green Processes,***Dalian,China***,September 7-10, **2010.**
4. S. P. Singh, **R.Anantharaj**, T. Banerjee. UNIFAC Group Interaction Prediction for Ionic Liquid-Thiophene based systems using Genetic Algorithm. Simulation Evolution And Learning (SEAL-2010), Indian Institute of Technology ***Kanpur, India***, December 01-04, **2010.**

National

1. **R.Anantharaj**, T. Banerjee**.** Surface tension and refractive index studies for the binary mixture of1-ethyl-3-methylimidazolium methylsulphonate ionic liquid with Nitrogen heteroaromatic compounds at 298.15 K and atmospheric pressure. CHEMCON-2009:63RD Annual Session of the Indian Institute of Chemical Engineers,Chidambram,***TamilNadu, India***, December 27-30,**2010**.

2. **Anantharaj R**,T.Banerjee, *Evaluation of Ionic Liquids for the Removal of Aromatic Nitrogen Species from Diesel Oil using COSMO-RS model*.CHEMCON-2009:62ND Annual Session of the Indian Institute of Chemical Engineers,Vizakhapatnam, ***Andhrapradesh, India***, December 27-30,**2009**.

Abstract of Papers Published/Accepted

Evaluation and Comparison of Global Scalar Properties for the Simultaneous Interaction of Ionic Liquids with Thiophene and Pyridine

R.Anantharaj , T. Banerjee*
Department of Chemical Engineering, Indian Institute of Technology Guwahati
Guwahati – 781039, Assam, India

Fluid Phase Equilibria, **2010**,293, 22–31

Ab-inito studies were carried out with mixtures containing ionic liquid with thiophene and pyridine for studying the simultaneous interaction. Global scalar properties such as HOMO/LUMO energies, HOMO-LUMO energy gap, chemical hardness, chemical potential, electronegativity, global hardness, global softness and electrophilicity index were determined for clusters containing ionic liquids with thiophene and pyridine. Ionic liquids containing: 1-butyl-3-methylpyrrolidinium [BUMPYR], 1-benzyl-3-methyimidazolioum [BeMIM] and 1-butyl-3-methylpyridinium [BUMPY] cations combined with inorganic anions containing fluorine ([BF_4] and [PF_6]) were studied in this work. [BeMIM][BF_4] (1-benzyl-3-methyimidazolioum tetrafluoroborate) with a HOMO-LUMO energy gap of 0.1882 eV was found to be the most effective IL. Further a ranking based on all the mentioned scalar parameters also pointed out [BeMIM][BF_4] to be the most desirable IL. The overall ranking after taking into considerations all factors followed: [BeMIM][BF_4] > [BUMPYR][BF_4] > [BUMPY][PF_6]> [BUMPY][BF_4] > [BUMPYR][PF_6]. To validate the findings, infinite dilution activity coefficients were predicted using the quantum chemical based COSMO-RS methodology which gave the same trend as observed using scalar properties.

COSMO-RS based Screening of Ionic Liquids as Green Solvents in Denitrification Studies

R.Anantharaj , T. Banerjee*
Department of Chemical Engineering, Indian Institute of Technology Guwahati
Guwahati – 781039, Assam, India

Industrial Engineering Chemistry Research, **2010,** 49, 8705-8725

Five and six membered heteroaromatic nitrogen compounds plays a inhibiting role in the hydrodesulphurization of diesel oil. In this work, the ionic liquids (IL's) are used as green solvents to remove such compounds by Liquid-Liquid Extraction (LLE).Around 168 ILs comprising cations which includes: 1-ethyl-3-methylimidaozlium [EMIM], 1-ethylpyridinium [EPY], 1-ethyl-1-methyl pyrrolidinium [EPYRO], 1-ethyl-1-methylpiperidinium [EMPIP], 4-ethyl-4-methyl morpholinium [EMMOR] and 1,2,4-Trimethylpyrazolium[TMPYZO] combined with 26 anions were investigated in this work. The infinite dilution activity coefficient(IDAC) was predicted through COSMO-RS (**CO**nductor Like **S**creening **MO**del for **R**eal **S**olvents) model in order to screen the potential solvents. Initially the model has been benchmarked via IDAC and LLE predictions.LLE was predicted for 4 reported ternary systems in which nitrogen heterocycle was one of the compound. The average root mean square deviation(RMSD) obtained was 10%. The IDAC values were predicted for pyridine in two ionic liquids namely [BMIM][BF_4] and [EMIM][TOS] with a root mean square(RMS) error of 8%. Thereafter the selectivity, capacity and performance index at infinite dilution were calculated to evaluate the performance. It was found that the five membered nitrogen species having high delocalized electron density possessed three order of magnitude higher selectivity than six membered nitrogen species. For the five membered ring structures the selectivity were found to follow the order: [EPYRO] > [EMPIP] > [EPY] > [EMMOR] > [EMIM] > [TMPYZO].For the six membered heterocycle it followed the order: [EPY] > [EMMOR] > [EPYRO] > [EMPIP] > [EMIM] > [TMPYZO]. Irrespective of nitrogen heterocycle, anions such as thiocyanate [SCN] and acetate [Ac] gave high values of selectivity. In general cations without aromatic rings such as [EPYRO], [EMPIP] and [EMMOR] gave higher selectivity and capacity irrespective of nitrogen heterocycle.

UNIFAC Group Interaction Prediction for Ionic Liquid-Thiophene based Systems using Genetic Algorithm

S.P.Singh,R.Anantharaj, T. Banerjee*
Department of Chemical Engineering, Indian Institute of Technology Guwahati
Guwahati – 781039, Assam, India

Lecture Notes in Computer Science, **2010,** 6457, 195-204.

The group interaction parameter prediction of Ionic Liquids (IL's) with thiophene (C_4H_4S) and other hydrocarbons are essential to generate (Liquid Liquid Equilibria) LLE through UNIFAC model. UNIFAC model is highly non-convex and can have several local extrema. In this work, the structural group interaction parameters have been calculated for [OMIM][BF_4] + thiophene + hydrocarbons and [OMIM] [BTI] + thiophene + hydrocarbons systems through regression using GA.The obtained LLE data has been correlated with reported values and it was observed that the cumulative RMSD(root mean square deviation) of ten ternary systems used for regression were 3.01% and 3.65% for [OMIM][BF_4] and [OMIM]BTI] based system respectively. Further, the obtained interaction parameters were used to correlate the experimental LLE data for four ternary systems which were not used for regression. These systems having a total of 40 tie lines gave a very satisfactory RMSD of 1.76 to 3.99% between reported and predicted composition.

Quantum Chemical Studies on the Simultaneous Interaction of Thiophene and Pyridine with Ionic Liquid

R.Anantharaj , T. Banerjee*
Department of Chemical Engineering, Indian Institute of Technology Guwahati
Guwahati – 781039, Assam, India

AIChEJ, **2011,** 57,749-764

The simultaneous interaction of thiophene and pyridine with different ionic liquids:1-butyl-1-methylpyrrolidiniumtrafluoroborate([BPYRO][BF_4]),1-butyl-1-methylpyrrolidinium hexafluoro-phosphate ([BPYRO][PF_6]), 1-butyl-4-methylpyridinium tetrafluoroborate ([BPY][BF_4]), 1-butyl-4-methylpyridinium hexafluorophosphate ([BPY][PF_6])and 1-benzyl-3-methylimidazolium tetrafluoroborate ([BeMIM][BF_4]) were investigated using quantum chemical calculations. A three-tier approach comprising of partial charges, interaction energies and sigma profile generation using COnductor like Screening MOdel (COSMO) was chosen to study the systems. A quantitative attempt based on the CH-π interaction in ionic liquid – thiophene- pyridine complexes gave the interaction energies of ILs in the order: [BPY][BF_4] > [BPYRO][PF_6] > [BeMIM][BF_4] > [BPY][PF_6] > [BPYRO][BF_4]. An inverse relation was observed between the activity coefficient at infinite dilution predicted via COSMO based model and interaction energies .The dominance of CH-π interaction was evident from the sigma profiles of ionic liquid together with thiophene and pyridine.

COSMO-RS based Predictions for the Desulphurization of Diesel oil using Ionic Liquids: Effect of Cation and Anion combination

R.Anantharaj , T. Banerjee*
Department of Chemical Engineering, Indian Institute of Technology Guwahati
Guwahati – 781039, Assam, India

Fuel Processing Technology, **2011,** 92, 39-52

Ionic Liquids ILs provide an important alternative in removing aromatic sulphur compounds by Liquid-Liquid Extraction (LLE). A total of 28 anions and 6 cations resulting in 168 possible combinations were screened via COSMO-RS (Conductor Like Screening Model for Real Solvents). Initially benchmarking was performed to predict the infinite dilution activity coefficients of thiophene in ionic liquids. Comparison with literature values involving 8 ILs with 20 points gave the average root mean square deviation (RMS) to be 11%. Thereafter artificial simulated diesel, aromatic sulphur compound and the cation and anion combination was used to predict the capacity (C) and selectivity (S) at infinite dilution. In general the selectivities were found to decrease in the following order: Thiophene (4-24) > Benzothiophene (2-12)> Dibenzothiophene (1-7). The different hetero atom (N,S,O) and its location in the cation structure strongly influenced the selectivity and capacity at infinite dilution for all the three aromatic sulphur compounds. It was found that the cation without aromatic ring combined with anions having sterical shielding effect such as [SCN],[CH_3SO_3], [CH_3COO], [Cl], and [Br] proved to be the most favourable IL for desulphurization. [EMMOR][SCN] proved to be the most viable IL for the removal of all the three aromatic sulphur compounds.

Experiments, Correlations and COSMO-RS Predictions for the Extraction of Benzothiophene from *n*-hexane using Imidazolium-based Ionic Liquids

N.R.Varma,R.Anantharaj , T. Banerjee*
Department of Chemical Engineering, Indian Institute of Technology Guwahati
Guwahati – 781039, Assam, India

Chemical Engineering Journal, **2011**. 166, 30-39

The extraction of benzothiophene from *n*-hexane was studied using 1-ethyl 3-methylimidazolium ethyl sulphate ([EMIM][$EtSO_4$]) and 1-ethyl 3-methylimidazolium acetate ([EMIM][CH_3COO]) at 308.15 K to analyze the performance of ionic liquids in the extractive desulphurization of aromatic sulphur compounds from petroleum fuels. A comparative study was done from the perspective of selectivity and distribution coefficient of the sulphur compounds. From the ternary LLE (Liquid-Liquid Extraction) experiments, it was found that while the selectivity was higher for the ethyl sulphate-based ionic liquids, the distribution coefficient was higher for acetate-based ionic liquids. Selectivities as high as 245 and 203 were obtained for [EMIM][$EtSO_4$] and [EMIM][CH_3COO] with negligible loss of hydrocarbon. The experimental results were correlated using the NRTL and UNIQUAC models. The root mean square deviation (RMSD) values of 0.48% and 0.83% were obtained for [EMIM][$EtSO_4$] and [EMIM][CH_3COO] respectively, when using the NRTL model, and the corresponding RMSD values when using the UNIQUAC model were 0.693% and 1.053%. The quantum chemical based **CO**nductor like **S**creening **MO**del for **R**eal **S**olvent (COSMO-RS) model was then used to predict the performance of single as well as mixed

ionic liquids. RMSDs of 4.36% and 7.87% were achieved for [EMIM][$EtSO_4$] and [EMIM][CH_3COO] based system, which are satisfactory considering that the method is *a-priori*.

Phase Behaviour of Catalytic Deactivated Compounds and Water with 1-Ethyl-3-Methylimidazolium Acetate {[EMIM][OAc]} Ionic Liquid at at *T*=(298.15 to 323.15) K and *p*=1 bar

R.Anantharaj , T. Banerjee*
Department of Chemical Engineering, Indian Institute of Technology Guwahati
Guwahati – 781039, Assam, India

Journal of Industrial Engineering Chemistry, **2011,** Article in Press

Density, surface tension and refractive index of the binary mixture of catalytic deactivated compounds with 1-ethyl-3-methylimidazolium acetate {[EMIM][OAc]} ionic liquid were measured at temperature of (298.15 to 323.15) K from which the derived thermodynamic properties including excess molar volume and deviation of surface tension and refractive index were calculated. The derived thermodynamic properties could be explained well by the interaction between similar and dissimilar aromatic structure of the molecules over the entire mole fraction of ILs. It was observed that all the catalytic deactivated compounds and water molecules have significant structural interaction with [EMIM][OAc] via CH---π bond interaction, π---π stacking and n---π interaction over the entire mole fraction of IL at T=298.15K .Further the composition of ionic liquid have significant influence on the interaction between dissimilar aromatic structure of molecules like pyridine,indoline and quinoline in liquid phase as compared to temperature. The surface tension increases in the order of: hiophene > Pyridine > Quinoline > Pyrrole > Indoline > Water ; while the refractive index increases in the order: Pyridine < Water < Pyrrole <

Thiophene < Indoline < Quinoline. The deviation of surface tension was found to be inversely proportional to the deviation of refractive index at T=298.15K. From these results it was concluded that the structure of the ionic liquids is very important for extraction processes on catalytic deactivated compounds, especially for pyridine, indoline and quinoline as compared to water molecules.

Phase Behaviour of Hydrodenitrification and Hydrodesulphurization inhibiting Compounds with 1-Ethyl-3-Methylimidazolium Ethylsulphate at *T*=(298.15 to 323.15) K and *p*=1 bar

R.Anantharaj , T. Banerjee*
Department of Chemical Engineering, Indian Institute of Technology Guwahati
Guwahati – 781039, Assam, India

Journal of Thermodynamics, **2011,** Article in Press

This work investigates the ability of 1-ethyl-3-methylimidazolium ethylsulphate ([EMIM][$EtSo_4$]) as a green and tuneable solvent for denitrification and desulphurization of diesel oil. Experimental density, surface tension and refractive index data have been measured for the following systems: [EMIM][$EtSo_4$](1) + pyridine(2), [EMIM][$EtSo_4$](1) + pyrrole(2), [EMIM][$EtSo_4$](1) + quinoline(2), [EMIM][$EtSo_4$](1) + indoline(2), [EMIM][$EtSo_4$](1) + thiophene(2) and [EMIM][$EtSo_4$](1) + water(2) over the entire mole fraction of [EMIM][$EtSo_4$] at temperatures of (298.15 to 323.15)K and at atmospheric pressure. Further from experimental density values, coefficient of thermal expansivity and excess molar volume were also calculated. It was found that the heteroaromatic nitrogen/sulphur compounds and water are completely miscible in the [EMIM][$EtSo_4$] ionic liquid. The surface tension values were found to increase while the refractive index decrease

with increasing mole fraction of [EMIM][$EtSo_4$]. On the other side dissimilar molecule such as water showed mobility of ions on mixing resulting in lower surface tension. The experimental values of surface tension increased in the order: thiophene > pyridine > pyrrole > indoline > quinoline and for refractive index: quinoline > indoline > pyrrole > pyridine > thiophene > water. It was found that the composition of [EMIM][$EtSo_4$] has a greater influence than temperature in deciding the densities, surface, optical and thermodynamic properties for similar molecular interaction than dissimilar molecules such as water.

Fast Solvent Screening for the Simultaneous Hydrodesulphurization and Hydrodenitrification of Diesel oil using Ionic Liquids

R.Anantharaj , T. Banerjee*
Department of Chemical Engineering, Indian Institute of Technology Guwahati
Guwahati – 781039, Assam, India

Journal of Chemical Engineering Data, **2011,** Manuscript under review

1-ethyl-3-methylimidazolium [EMIM], 1-ethylpyridinium [EPY], 1-ethyl-1-methylpyrrolidinium [EPYRO], 4-ethyl-4-methylmorpholium [EMMOR], 1-ethyl-1-methylpiperidinium [EMPIP] and 1,2,4-trimethylpyrazolium [TMPYZO] based cations along with 25 anions have been investigated as possible solvents for the simultaneous hydrodesulphurization and hydrodenitrification of Diesel oil at T=298.15 K. The infinite dilution activity coefficient (IDAC) of thiophene, benzothiophene, dibenzothiophene, pyrrole, indole, indoline, carbazole, benzocarbazole, pyridine, quinoline and benzoquinoline was predicted via quantum chemical based COSMO-RS (**CO**nductor like **S**creening **MO**del for **R**eal **S**olvents) model. Subsequently, the selectivity and capacity at infinite dilution were used as indicators for the possible screening of Ionic Liquids. [EMMOR], [EMPYRO],

[EMPIP] based cations gave lesser activity coefficient values at infinite dilution as compared to [EMIM], [EPY], and [TMPYZO] based cations. It was noted that [DMP],[BTA], [OcSu] and [MSACN] anion having different electronegative atom such as N (Nitrogen),O (Oxygen) and S (Sulphur) and therefore the anions play a significant role in increasing the selectivity. High activity coefficients at infinite dilution values were observed for basic nitrogen compounds as compared to the non basic nitrogen compounds irrespective of cation and anion. Evidently, [EMMOR] and [EPYRO] gave higher solvent capacity at infinite dilution irrespective of the aromatic nitrogen and sulphur compounds.

Transport and Thermodynamic Properties of 1-ethyl-3-methylimidazolium methanesulphonate with aromatic sulphur, nitrogen compounds: Experiments and COSMO-RS predictions

R.Anantharaj , T. Banerjee*
Department of Chemical Engineering, Indian Institute of Technology Guwahati
Guwahati – 781039, Assam, India

Canadian Journal of Chemical Engineering, **2011,** Manuscript under review

This work investigates the ability of 1-ethyl-3-methylimidazolium methanesulphate ([EMIM][$MeSO_3$]) as a green and tuneable solvent for denitrification and desulphurization studies. Experimental density, surface tension and refractive index data have been measured for the following systems: [EMIM][$MeSO_3$] (1) + pyridine(2), [EMIM][$MeSO_3$] (1) + pyrrole(2), [EMIM][$MeSO_3$] (1) + quinoline(2), [EMIM][$MeSO_3$] (1) + indoline(2), [EMIM][$MeSO_3$] (1) + thiophene(2) and ([EMIM][$MeSO_3$] (1) + water(2) over the entire mole fraction of [EMIM][$MeSO_3$] at T= (298.15-323.15) K and p = 1 bar. Further from experimental density, surface tension and refractive index, coefficient of thermal expansivity,

excess molar volume, deviation of surface tension and refractive index deviation were also calculated. It was found that the heteroaromatic nitrogen/sulphur compounds are completely miscible in **[**EMIM][$MeSO_3$]. The surface tension values were found to increase while the refractive index decrease with increasing mole fraction of **[**EMIM][$MeSO_3$].The experimental values for surface tension increased in the order: pyridine > thiophene > pyrrole > indoline > quinoline>water and for refractive index: pyridine > pyrrole > indoline >quinoline > thiophene> water. It was found that the composition of **[**EMIM][$MeSO_3$] has a greater influence than temperature in deciding the transport, surface, optical and thermodynamic properties for similar molecular interaction such as IL-thiophene and IL-pyrrole than dissimilar molecules such as IL-water. Further quantum chemical based COSMO-RS predictions for mixtures indicated an inverse relation between activity coefficient and excess molar volumes.

Phase Behaviour of 1-Ethyl-3-Methylimidazolium Thiocyanate {[EMIM][SCN} Ionic Liquid with Catalytic Deactivated Compounds and Water at Several Temperatures: Experiments and Theoretical Predictions

R.Anantharaj , T. Banerjee*
Department of Chemical Engineering, Indian Institute of Technology Guwahati
Guwahati – 781039, Assam, India

International Journal of Chemical Engineering, **2011,** Manuscript under review

Density, surface tension and refractive index were determined for the binary mixture of catalytic deactivated compounds with 1-ethyl-3-methylimidazolium thiocyanate {[EMIM][SCN]} at temperature of (298.15 to 323.15) K. For all the compounds with ILs, the densities varied linearly in the entire mole fraction with increasing temperature. From the obtained data, the excess molar volume and deviation of surface tension and refractive index have been calculated. A strong interaction was found between similar (cation-thiophene or

cation-pyrrole) compounds. The interaction of IL with dissimilar compounds such as indoline and quinoline and other multiple ring compounds was found to strongly depend on the composition of IL at any temperatures. For the mixtures, the surface tension decreases in the order of: thiophene > quinoline > pyridine > indoline > pyrrole > water. [EMIM][SCN] + quinoline mixture gave the highest refractive index values as compared to other studied systems. In general from the excess volume studies, the IL-sulphur/nitrogen mixture has stronger interaction as compared to IL-IL, thiophene-thiophene or pyrrole-pyrrole interaction. The deviation of surface tension was found to be inversely proportional to deviation of refractive index. However it was observed that all the deactivated compounds and water molecules have fairly good structural interaction with [EMIM][SCN] ionic liquid via CH--π bond interaction, π---π stacking and n---π interaction over the entire mole fraction of IL . The quantum chemical based COSMO-RS was used to predict the non-ideal liquid phase activity coefficient for all mixtures. It indicated an inverse relation between activity coefficient and excess molar volumes.

Liquid-Liquid Equilibria for Quaternary Systems of Imidazolium based Ionic Liquid + Thiophene + Pyridine + Iso-octane at 298.15K: Experiments and Quantum Chemical Predictions

R.Anantharaj , T. Banerjee*
Department of Chemical Engineering, Indian Institute of Technology Guwahati
Guwahati – 781039, Assam, India

Fluid Phase Equilibria, **2011**, Manuscript under review

In this work, 1-ethyl 3-methylimidazolium acetate [EMIM][OAc], 1-ethyl 3-methylimidazolium ethylsulphate [EMIM][$EtSO_4$] and 1-ethyl 3-methylimidazolium methylsulphonate [EMIM][$MeSO_3$] was investigated as green solvents for the simultaneous separation of thiophene and pyridine from iso-octane at 298.15K and atmospheric pressure. The liquid liquid equilibrium (LLE) data for the quaternary mixture of 1-ethyl 3-methylimidazolium acetate (1) + thiophene (2) + pyridine (3) + isooctane (4), 1-ethyl

3-methylimidazolium ethylsulphate (1) + thiophene (2) + pyridine (3) + isooctane (4) and 1-ethyl 3-methylimidazolium methylsulphonate (1) + thiophene (2) + pyridine (3) + isooctane (4) systems were experimentally determined at ambient conditions. The effectiveness of the simultaneous extraction of thiophene and pyridine from iso octane was evaluated by means of the determination of the selectivity and distribution coefficient values. The reliability of experimental data was ascertained by applying the Quantum chemical based COnductor like Screening MOdel for Real Solvents(COSMO-RS) model. The goodness of the fit was measured by the root mean square deviation (RMSD) which provide the RMSD: 7.4% ([EMIM][OAc]),4.49% ([EMIM][$EtSO_4$]) and 8.26% ([EMIM][$MeSO_3$]). In addition the experimental tie-line data were successfully correlated with the NonRandom Two Liquid (NRTL) and UNIversal QUAasi-Chemical (UNIQUAC) models, which provide a good correlation of the experimental data with low rmsd values such as lesser than unity for all the studied systems. These results show that [EMIM][OAc], [EMIM][$EtSO_4$] and [EMIM][$MeSO_3$] ionic liquid can be used as an alternative solvent for the simultaneous separation of thiophene and pyridine from hydrocarbon stream via LLE processes at ambient conditions.